V. Z. PARTON
I. M. MOROZOV

Elastic-plastic Fracture Mechanics

MIR PUBLISHERS · MOSCOW

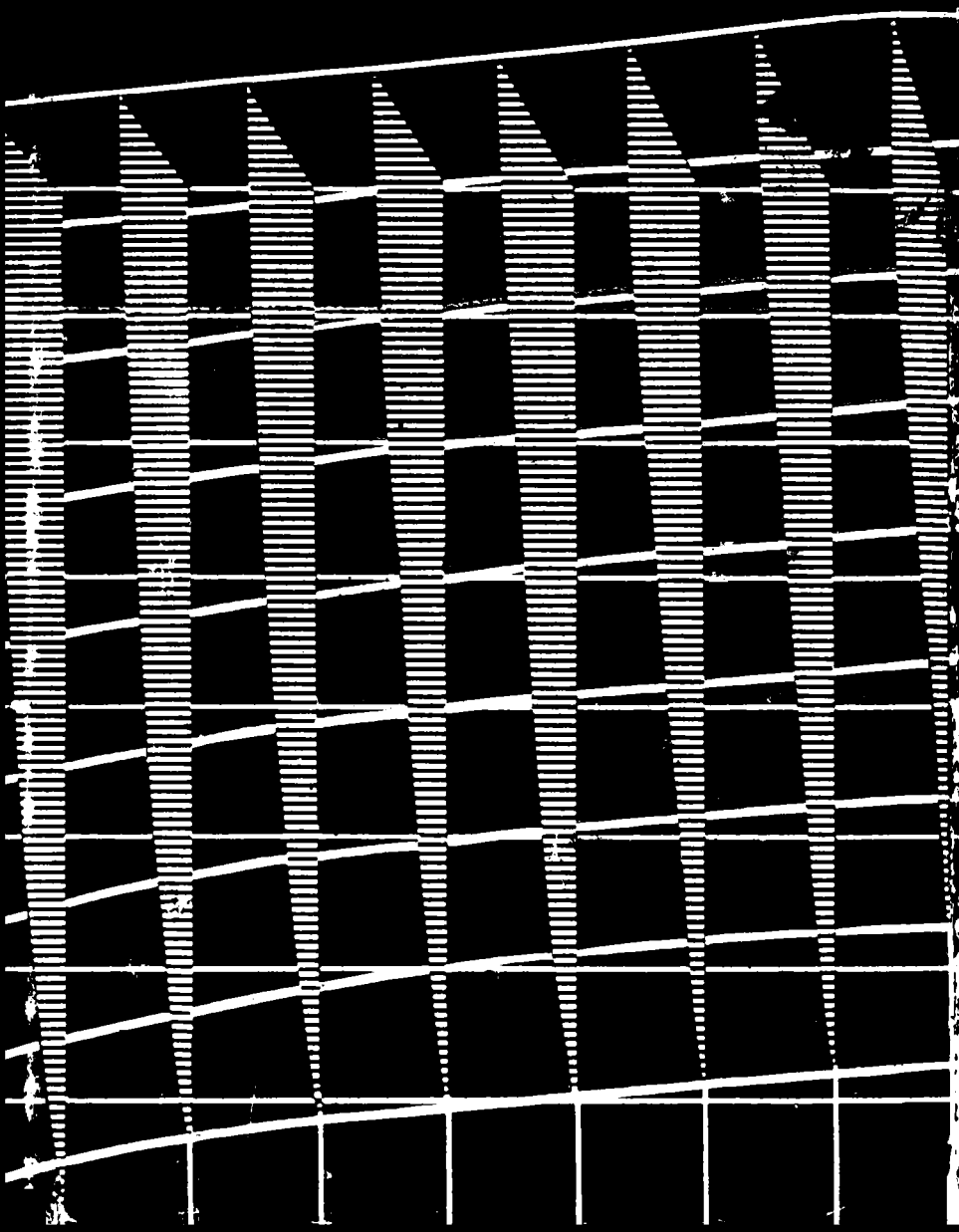

Mir Publishers of Moscow publish Soviet scientific and technical literature in sixteen languages—English, German, French, Italian, Spanish, Portuguese, Czech, Slovak, Serbo-Croat, Hungarian, Mongolian, Arabic, Persian (Farsi), Hindi, Bengal and Tamil. Titles include textbooks for higher technical schools and vocational schools, literature on the natural sciences and medicine, including textbooks for medical schools, popular science and science fiction.

The contributors to Mir Publishers' list are leading Soviet scientists and engineers in all fields of science and technology and include more than 40 Members and Corresponding Members of the USSR Academy of Sciences. Skilled translators provide a high standard of translation from the original Russian.

MIR PUBLISHERS • MOSCOW

The book presents modern concepts and the original investigations on the theory of large cracks capable of propagating in deformable solids and initiating partial or complete fracture. It covers a wide range of problems relating to the behaviour of cracked bodies, from crack extension criteria to the solution of a number of complex fracture mechanics problems. Consideration is given to limiting and sublimiting states of equilibrium under single, multiple, thermal, and dynamic loadings in elastic, viscoelastic, and elastic-plastic bodies with cracks.

The book is intended for scientific workers and practising engineers engaged in fracture mechanics and also for post-graduates and senior students specializing in solid mechanics and in strength of machine parts.

MIR PUBLISHERS • MOSCOW

ИЗДАТЕЛЬСТВО · МИР ·

В. З. ПАРТОН, Е. М. МОРОЗОВ

МЕХАНИКА УПРУГО-ПЛАСТИЧЕСКОГО РАЗРУШЕНИЯ

ИЗДАТЕЛЬСТВО «НАУКА»
МОСКВА

V. Z. PARTON
and
I. M. MOROZOV

Elastic-plastic Fracture Mechanics

MIR PUBLISHERS
MOSCOW

Translated from the Russian

First published 1978
Revised from the 1974 Russian edition

На английском языке

© Издательство «Наука», 1974
© English translation, Mir Publishers, 1978

CONTENTS

PREFACE 9

CHAPTER I. CONDITIONS FOR CRACK GROWTH 15

1. Fracture Mechanics and Strength of Solids 15
2. Stress and Displacement Fields in the Vicinity of a Crack Tip 22
3. The Griffith-Orowan-Irwin Concept. Stable and Unstable Crack Growth 30
4. The Integral Variational Principle in Crack Theory 36
5. Some Other Model Representations 50

CHAPTER II. STRESS INTENSITY FACTOR 55

6. Intensity Factor—Basic Characteristic of a Cracked Body 55
7. Basic Numerical Methods for Calculating the Stress Intensity Factor 58
8. Calculation of the Stress Intensity Factor for Double Cantilever Beam Specimens by the Finite Element Method 72
9. The Method of Sections for an Approximate Calculation of the Stress Intensity Factor 74
10. Some Material Characteristics Used for the Evaluation of Crack Propagation Resistance 80

CHAPTER III. CRACKS IN LINEARLY ELASTIC BODIES 87

11. Solution of Some Plane and Three-dimensional Problems 87
12. Constructional Crack Arrest 98
13. System of Cracks 105
14. Stress Intensity Factors for Some Practically Important Cases 121
15. Shell with a Crack 136
16. On a Method of Calculating a Crack Trajectory 142

CHAPTER IV. CRACKS IN ELASTIC-PLASTIC BODIES 151

17. Experimental Investigations of the Plastic Zone at the End of a Cut (Crack) 151
18. Calculation of the Plastic Zone 163
19. Critical State of the Plane and Space with a Crack 186
20. The Elastic-plastic Problem for a Plane with Straight Slits 197
21. Subcritical Crack Growth 205
22. Low-cycle Fatigue Life Based on the Number of Cycles 218
23. Experimental Results for Single and Cyclic Loadings 222
24. The Ultimate Fracture Strength 231
25. Design Procedure in the Presence of Cracks 234
26. Examples of Designing with Cracks 236

CHAPTER V. CRACKS IN LINEARLY VISCOELASTIC MEDIA 252

27. The Viscoelastic Analogue of the Griffith and Sack Problems 252
28. The Viscoelastic-plastic Analogue of the Griffith and Sack Problems 255
29. Allowance for Material Sensitivity to the Rate and Frequency of Loading 258

CHAPTER VI. THERMAL PROBLEMS IN FRACTURE MECHANICS 267

30. Cracks Under Thermal Loading 267
31. The Axially Symmetric Thermoelastic Problem for a Cylinder with a Cut 270
32. The Quasi-stationary Thermoelastic Problem for a Plane with a Semi-infinite Cut 277
33. Procedure for Solving Crack and Punch Problems 285

CHAPTER VII. DYNAMIC PROBLEMS IN FRACTURE MECHANICS 295

34. Velocity of Supercritical Crack Propagation 295
35. The Dynamic Problem for a Plane with a Cut 303
36. The Dynamic Problem for a Longitudinal Shear Crack 312
37. The Plane Problem of Steady-state Vibrations for a Strip with a Cut 318

38. Steady-state Vibrations of an Infinite Plane with a Periodic System of Cuts Along an Axis 326
39. Steady-state Vibrations of an Infinite Plane with a Periodic System of Cuts Along an Axis (Continued) 336
40. The Action of a Shear Wave on a Periodic System of Cracks 349
41. On Some Prospective Problems in Fracture Mechanics 361
42. Conclusion 376

APPENDIX A 378
APPENDIX B 383
APPENDIX C 404
REFERENCES 409

PREFACE

Fracture mechanics, this term still sounds strange to many people. So far it has been customary to speak of 'strength', of 'resistance of materials.' Looking after health, we have carefully avoided the word 'illness.' But to prevent a mortal disease, one must know its nature, symptoms, and the course of the illness; to ensure the strength of a structure, one must know the causes and nature of its possible failure.

The problem of fracture is the central problem of the science of resistance of materials in the true and direct meaning of this word combination. However, the mechanics of fracture as an independent branch of the mechanics of deformable solids has originated quite recently, literally before our eyes. The boundaries of this new branch of science are still not clearly defined, the need for the unification of the efforts of not only mechanicians and not only physicists and physical chemists for solving the problem of fracture is realized and admitted by almost everyone (I say 'almost,' for here, too, as everywhere, there are extremists), but the difference in the terminology usual to the representatives of different sciences, along with the natural (but making difficult the intercourse) conviction that it is precisely this part of the general problem which is the most important and gives the clue to everything else, not infrequently leads to a situation when the arguments about the concepts are replaced by the arguments about the words.

At present, when speaking of fracture mechanics one usually implies a study of the conditions under which there is a crack or a system of cracks propagating in a body. But cracks may be very different and they are considered on different scales. On the one hand, the fracture of a crystal grain begins with the formation of a submicroscopic crack,

with the separation of two atomic layers by such a distance when the forces of interaction between the atoms are negligible. The other limiting case is that of a crack in a welded turbine rotor or in a nuclear reactor, whose length and width may be estimated by the centimetre. In the first case the condition for crack propagation is determined by the configuration of atoms at the crack tip. Since we are dealing here not with a continuous medium but with a discrete crystal lattice formed by atoms, the concept of the 'crack tip' itself becomes indefinite. The study of this kind of submicroscopic cracks and of their interaction with other lattice defects relates, in fact, rather to the field of solid-state physics than mechanics, though the methods of the classical theory of elasticity are fully applicable to problems of this kind. Of course, there is no strict line of demarcation between physics and mechanics, but nevertheless we have to draw it somewhere, if only to avoid terminological confusion.

A macroscopic crack, the subject matter of mechanics proper, has dimensions exceeding by several orders the size of the largest structural element containing a sufficient number of crystal grains for its properties not to differ from the properties of any other element of the same dimensions which may be isolated from the material. It is precisely this condition that allows the crack problem to be solved within the framework of continuum mechanics. The condition formulated above refers to an ideal situation for the applicability of the theory, in actuality this requirement may be weakened, which leads to certain strained interpretations, though does not make the theory pointless. But assuming the material to be continuous, homogeneous, elastic, and using the techniques of the classical linear theory of elasticity, we necessarily come to a paradoxical conclusion that as the crack tip is approached the stresses increase indefinitely. This paradox is a payment for the simplicity associated with the extension of the linear theory of elasticity to a region where it is obviously wrong.

The so-called linear fracture mechanics assigns the reality to a physically impossible singularity. Such a situation is not so unusual for continuum mechanics, it suffices to recall, for example, vortex filaments with zero cross section

and finite circulation. It appears that the work required to propagate a crack which is done either as a result of increasing external forces or due to a reduction in the elastic energy of a body with increasing crack size is directly expressed in terms of the coefficient of the singular term in the stress formula. This coefficient is called the intensity factor and plays a fundamental role in the whole theory. The crack extension work may be associated with the overcoming of surface tension forces (Griffith's concept), with the work of plastic deformation in a small region adjacent to the crack tip, or with something else. One thing is then important: the size of the region where the relations of the linear theory of elasticity are violated in some way or other must be very small. The ability of a crack for further extension is then determined by the sole characteristic, viz. the work per unit length of the path or the critical intensity factor.

But if the size of the zone in which the relations of the linear theory of elasticity are violated is great, we enter the range of non-linear fracture mechanics. The outward, formal indifference of linear fracture mechanics to an object and a scale, the full mathematical equivalence of problems relating to entirely different physical phenomena have raised hopes at the outset that non-linear mechanics can also be constructed in a similar uniform manner. It turned out to be quite different.

The fundamental problem on which were concentrated in recent years the efforts of men of mechanics engaged in practical applications of fracture mechanics to the estimation of the strength of large-scale parts is perhaps the problem of finding the conditions for the equilibrium or propagation of a large crack in a sufficiently ductile material. The plastic zone ahead of a crack is so large that the relations of the macroscopic theory of plasticity considering the medium as continuous and homogeneous may be assumed to be valid for it. For plane stress, the Leonov-Panasyuk-Dugdale model, which replaces the plastic zone by a segment prolonging the crack and having no thickness, is found to be satisfactory. In particular, this is confirmed by an analysis presented in this book for the corresponding elastic-plastic problem which is solved numerically, viz. by the finite

element method. As the number of elements is increased, the plastic zone contracts and it may be assumed that in the limit when, with the number of elements increasing indefinitely, the solution tends to the exact solution, the plastic zone does actually degenerate into a segment. Note that in considering submicroscopic cracks at the atomic level many authors adopt the hypothesis to the effect that the non-linearity of interaction between atoms is essential only within the limits of one interatomic layer, by analogy with the way in which the so-called Pierels dislocation is calculated. Again, as in the linear theory, there is a formal analogy, but here it is of an artificial nature, and the assessments of the relative acceptability of the model in different cases are based on entirely different considerations; the degree of cogency of the argumentation in its favour is far from being the same.

Unfortunately, a state of plane stress is never realized in practice, in any case at a distance from the tip of the order of the sheet thickness the state of stress is essentially three-dimensional and is far too complicated for analysis. In the other case, in plane strain, the configuration of the plastic zone is completely different: it spreads not so much forward as sideways, and the plastic segment model adopted for plane stress does not correspond to reality in any way.

But the position of a designer is usually much worse. Typical of modern structures from modern alloys is a situation when the size of the plastic zone is of the same order as the thickness of a part and hence the state of stress in the plastic region is everywhere essentially three-dimensional. On the other hand, the most important structural materials (carbon and alloy steels) are sufficiently ductile. The propagation of a crack begins when the plastic strain near its tip becomes large, of the order of tens per cent. The tip of an originally sharp crack, say of a fatigue crack, becomes blunted, its sides, which were initially closed, separate almost parallel by a finite distance and further fracture occurs only when this separation reaches a certain critical value. Thus, the theory of crack propagation in ductile materials must include at least two elements, namely (1) the solution of an elastic-plastic problem taking account of the finiteness of plastic strain and satisfying the boundary conditions

on the deformed boundary and (2) the finding of the condition for the formation of a macrocrack in a material which has undergone a considerable plastic deformation accompanied by accumulation of microdefects.

The proposed book by V. Z. Parton and E. M. Morozov, the first Russian monograph on this subject, based mainly on the original investigations of the authors, treats the problems of non-linear fracture mechanics in the aspect mentioned above. It deals with some elastic-plastic problems for bodies containing cracks. But the principal content of the book is linear fracture mechanics and also its development which leads to constitutive equations that may be non-linear.

In spite of certain limitations of linear fracture mechanics the range of problems reliably solvable with its help is sufficiently wide. The development of this theory reduces in great part to an accumulation of the fund of solved problems of elasticity theory for cracks of different shape in various bodies. The number of the corresponding publications grows steadily both abroad and in our country, many of the results obtained by foreign authors became available thanks to translations of books and collected papers. In particular, Mir Publishers began to issue a translation of the seven-volume edition of an encyclopaedic nature published in the USA (edited by H. Liebowitz) and entitled *Fracture*.

The authors of the present book make an essential contribution to this fund. The preface must not expose the content of the book, but some results should be mentioned. This is first of all a new variational principle which enables one to solve approximately numerous problems and, in particular, to find the crack trajectory in a non-uniform stress field. Of obvious interest is a simple approximate method of finding the stress intensity factor, which makes it possible to obtain a reasonable estimate in cases where the exact solution of an elasticity problem cannot be found, while the numerical solution is extremely laborious. We also mention a series of newly solved dynamic problems for bodies subjected to periodic loads.

A natural extension of linear fracture mechanics consists in applying its basic concepts to the problems of the kinetics of crack growth in time or as a function of the number of

cycles in the case of fatigue failure. It is important that kinetics, be it linear or non-linear, is assumed to be purely local, all processes of failure of any nature are assumed to take place in the end region of very small size, the material outside this region is elastic. In all kinetic equations the only representative of the state of stress is then the stress intensity factor. The sections of the book concerned with fatigue failure, for example, are constructed in exactly this way.

In conclusion we note that the great efforts and considerable advances in the field of the mechanics of crack propagation have led to the fact that the whole fracture mechanics is often reduced to it. Actually the subject-matter of fracture mechanics is much wider. In some cases, for example in metals under load at high temperatures, the fracture is of a diffused nature, voids accumulate in the whole volume at grain boundaries, interfuse, and finally combine into a macrocrack. Here a macrocrack is merely the last, visible result of the process of damage accumulation invisible to the naked eye but well seen even through an optical microscope.

It is likely that a similar mode of fracture is observed in some polymers, but here more precise methods are needed to detect microdamages.

The significance of statistical methods for the estimation of the strength of structures is widely known. The statistical theory of fracture must also be classified under fracture mechanics, though now, perhaps, the refinement of theoretical-probabilistic analysis combines with rather primitive mechanical models, which is due to the complexity of the subject.

This enumeration may be continued, but it will be very remotely connected with the proposed book which illuminates one extremely important and interesting aspect of the problem and at the same time contains many curious remarks and considerations, at times of a tentative nature but providing food for thought and a stimulus to further work.

Academician *Yu. N. Rabotnov*

CHAPTER I

CONDITIONS FOR CRACK GROWTH

1. FRACTURE MECHANICS AND STRENGTH OF SOLIDS

The astounding growth of the relatively ancient science of strength of deformable solids in the last fifty years is associated first of all with a different view of scientists and engineers of the problem of brittle fracture whose solution, according to modern notions, may be reliable only in cases where initial cracks existing in a body are taken into account. The proposed monograph *Elastic-plastic Fracture Mechanics* is concerned with the most urgent problems of fracture mechanics.

Fracture mechanics in the broad sense of this concept includes the part of the science of strength of materials and structures which relates to a study of the carrying capacity of a body both with and without consideration of initial cracks and also to a study of various laws governing crack development. We note right away that while such sciences as the classical theory of elasticity, the theories of plasticity and creep are sufficiently clearly formulated and well studied by the present time, the mechanics of fracture is still far from its completion.

Omitting a historical review of the subject matter, we shall mention the main stages of the development of fracture mechanics.*

From ancient times the man has been confronted with the problem of strength. For a long time, however, the

* Detailed information on the problems discussed below may be found, for example, in the review by V. Z. Parton and G. P. Cherepanov *Fracture Mechanics* (in *Mechanics in the USSR for 50 years*, Nauka, Moscow, 1972).

knowledge of the strength and fracture of materials, despite the creation of magnificent architectural ensembles surprising us to the present day, was accumulated fortuitously, passed on from generation to generation, and related rather to the field of art.

The founder of fracture mechanics is rightfully considered Galileo Galilei. He stated that the breaking load is independent of the length of a tension bar and is directly proportional to its cross-sectional area (this result in slightly modified form is still used in engineering strength design in the case of a homogeneous state of stress).

In general the first stage of the investigation on fracture mechanics associated with the names of Galileo Galilei, Robert Hooke, Charles Augustin de Coulomb, Barré de Saint Venant, Otto Mohr is characterized by extensive studies of deformation properties of solids and by the development (phenomenological in nature) of various failure criteria termed strength theories. These theories state that fracture occurs at the moment when at a certain point of a body a particular combination of parameters, such as stress, strain, etc., reaches its critical value. In this approach the process of fracture propagation through the volume of the body is completely ignored, which is justified only in cases where the development of defects causing failure takes place in a small vicinity of the critical region. At present several strength criteria (the maximum principal stress theory, the maximum shearing stress theory, the distortion energy theory or the octahedral shearing stress theory, etc.) are used in strength design, depending on the type of material and service conditions. For all the importance of the investigations on strength theory carried out within the framework of this approach, they are inadequate for a number of reasons.

In the well-known work of A. F. Ioffe with collaborators [114] a series of experiments were performed to study the strength of rock-salt crystals for different surface conditions of the specimen. It was found that the strength of a crystal with a hot-water dissolved surface layer was many times higher than its engineering strength and in some cases attained the theoretical strength value. The basic idea of this work consists in the proof that structural imperfections

in a crystal are responsible for the discrepancy between the actual and theoretical strength. In the experiments of A. F. Ioffe there was an increase in strength from a few kgf/mm^2 to approximately 200 kgf/mm^2, which is close to the theoretical strength value (approximately 400 kgf/mm^2). In the thirties A. P. Aleksandrov and S. N. Zhurkov obtained a strength of 600 kgf/mm^2 with glass fibres, and 1300 kgf/mm^2 with quartz fibres. Subsequently intensive experimental investigations associated with raising the strength ceiling of various structural materials were carried out in the USSR. In the fifties filamentary crystals, 'whiskers,' with a strength of about 1000 kgf/mm^2 were studied at the A. F. Ioffe Physical-Technical Institute in the laboratory of A. V. Stepanov, and under the supervision of F. F. Vitman the strengthening of the usual window glass from about 5 kgf/mm^2 to 500 kgf/mm^2 was obtained. A high strength (up to 600 kgf/mm^2) of oriented polymers was obtained in the laboratory of S. N. Zhurkov. Thus, it was demonstrated in a vivid way that the change of defective crystal structure assists in increasing the strength of crystals by several orders and makes it approach the theoretical value.

The effect of increasing the strength of a rock-salt crystal and experimentally observed numerous cases of early failure of structures at stresses less than the yield strength $\sigma_{0.2}$ were a direct indication of the inadequacy of the developed concepts of strength as a material constant. Hence, beginning with the work of A. A. Griffith, G. I. Taylor, E. O. Orowan, G. R. Irwin, and others, a new direction has originated in strength analysis, a direction central to which is a detailed study of the fracture process itself. Since fracture results from the development of real defects existing in a body, the consideration of cracks present in a body and the determination of their effect on strength are essential in the evaluation of strength.

In this connection the problems relating to the equilibrium of elastic bodies with cracks are gaining in importance. However, the solutions of these problems, which often involve great mathematical difficulties, contain much more information than is required in this study.

The main question here is whether a body under a particular load possesses carrying capacity or not, i.e., of principal interest is not the solution itself of the complex problem concerning the equilibrium of a cracked body, but the existence or non-existence of this solution under the given loading conditions. Mathematically, therefore, fracture occurs when a situation is realized which leads to the fulfilment of some limiting conditions ensuring the non-existence of solutions of the corresponding problem concerning the equilibrium of a cracked body. These conditions are integral characteristics of the fracture process, which is in accord with the general global concept of fracture of solids [234].

Within the framework of the phenomenological approach, common to various models for crack growth in solids is the assumption that at the initial moment a certain finite disturbance in the form of inherent flaws is given, which is in good agreement with experimental data on the presence of structural imperfections in a material, no matter what the previous technological treatment may be. Hence, in deriving various strength criteria taking account of the fracture process, relations are obtained which are identical in form with the usual strength criteria, the only difference being that the constants involved are now dependent on the co-ordinates, lengths and geometry of initial cracks.

Before the forties of our century the development of the ideas in this direction was insignificant. This is mainly due to the fact that in the traditional scheme the process of crack propagation was left out of consideration. Moreover, there was an opinion that fracture occurred almost instantaneously, which pointed at once to the limitation of possible derivations of strength criteria where the constants were dependent on the size of initial cracks existing in a body. In the subsequent decades this point of view was reconsidered. It was found that the crack development takes a more or less extended time preceding complete fracture, this being true not only of fatigue and ductile fracture, but also of brittle fracture. Thus, for soda-lime silicate glasses for which the fracture process was assumed to be practically instantaneous, the crack velocity at the beginning of the process was by a factor of 10^7 to 10^8 lower than that at the final stage. At the same time the experimental evidence

points to the fact [66] that in properly (as regards fracture strength) designed and made structures the crack growth is stable over a considerable range of external loads lengthening the time for the occurrence of the critical state. Hence, the strength characteristics may be independent, within certain limits, of the initial crack lengths and are determined by some structure parameters of the material, such, for example, as the grain size [202, 43].

Thus, an approach applicable here is that associated with the possibility of using the well-known and approved strength theories after introducing one additional internal structure parameter not involved in the formulation of the rheological model. Similar ideas associated with introducing additional structure parameters into equations of state are developed extensively in the work of L. I. Sedov [249, 250].

At present the significance of investigations on fracture mechanics is far beyond the scope of the problem of carrying capacity. First of all, the study of the fracture process is of interest in its own right. Monitoring of the fracture process and a knowledge of its laws are of great importance in engineering. Thus, it is desirable to slow down the process of crack growth for structures and buildings, whereas in cutting, on the contrary, it is necessary to facilitate fracture in every possible way.

The most important aspect of crack theory is the formulation of the condition for local fracture at a particular point of the crack contour. This is as important in solving the problem of crack growth as is the correct choice of a criterion for the onset of yielding in a volume element.

The condition for local fracture is most simply formulated in the theory of so-called quasi-brittle cracks when the largest dimension of the region of irreversible strains at a particular point of the crack contour is small compared with the crack length and with the distance of this point to the nearest boundary of the body. The simplest variant of this condition was proposed by G. R. Irwin [115-119] based on the physical and mathematical ideas of A. A. Griffith [103, 104], H. Neuber [202], and H. M. Westergaard [289, 290]. It assumes that the coefficient of the stress singularity at the point under consideration at the moment

of local fracture (and crack extension at that point) is equal to a certain material constant; the stresses are then calculated on the assumption of a perfectly elastic body.

Since the above-mentioned coefficient represents a certain function of the external loads, crack length and body geometry which is found from the solution of the elastic problem as a whole, the condition for local fracture on the contour of a crack provides, in principle, a means for determining its development and, in particular, for finding a combination of external loads separating stability and instability regions (this subject will be discussed in greater detail in the next sections).

Later several models were proposed for the fracture mechanism at the tip of a quasi-brittle crack. However, all known models (there are some 10 models at present), which differ in details of the description of local rupture at the tip of a brittle crack, are equivalent in the sense that they always reduce to the Griffith-Irwin condition [47, 96].

A general approach to the description of crack extension in arbitrary continuous media was proposed by J. R. Rice [239, 241]* and G. P. Cherepanov [44]. In the latter case the approach is based on the energy concept and the concepts of a 'fine' and a 'hyperfine' structure of a crack tip introduced by G. P. Cherepanov.

We shall use the expressions 'body with a cut' and 'body with a crack' on the understanding that a cut changes to a crack only when use is made of an additional fracture condition following from physical considerations and not following from the classical equations of equilibrium and motion of elasticity theory.

In actual conditions the development of initial cracks existing in a body may depend on the following basic parameters: (1) material, (2) the shape and dimensions of the body, (3) the mode of applying an external load, (4) time, (5) the number of cycles of load, (6) temperature, (7) the degree of environmental reactivity, (8) strain rate and deformation history.

---

* Note that the expression for the path-independent integral (which is now commonly termed the Rice integral or J-integral) had been previously obtained by J. D. Eshelby [76].

We shall mention the following mathematical problems of fracture mechanics whose solution may depend on one or several of the parameters mentioned above.

(1) 'Strength of cracked bodies.' The determination of relationship between crack size and applied loads.

(2) 'Crack geometry.' The determination of the equations for the trajectories of curvilinear (surface) cracks and fracture surfaces (resulting from the development of internal cracks).

(3) 'Crack dynamics.' The determination of the laws of motion of a crack tip and of a fracture surface front for finding the velocity and acceleration of cracks.

A major portion of the material presented in the book is concerned with the problem of calculating the limiting loads for cracked bodies, i.e., with the first of the above-enumerated mathematical problems of the mechanics of brittle fracture. This is primarily due to the growth of all kinds of overloads which make it necessary to take into consideration the presence of cracks and to introduce them into analysis when evaluating the residual strength and reliability of a structure. Besides, of great importance is the progress in the development of new materials and alloys possessing increasingly higher strength ceiling. During the 19th century the ultimate strength of commercial structural iron (cast iron) increased from about 30 kgf/mm^2 to 40 kgf/mm^2, at the present time we have alloys with an ultimate strength of the order of 200 to 300 kgf/mm^2. Even now one can say with certainty that in the following decades strengths of the order of 400 to 600 kgf/mm^2 will be fully achievable. The physical theories of the causes of strength and failure, among which are first of all dislocation theory and the theory of macroscopic cracks, had an appreciable effect on the choice of means of developing stronger and stronger alloys in metallurgical engineering and physical metallurgy.

The present book *Elastic-plastic Fracture Mechanics* is concerned with a study of the equilibrium and growth of macroscopic cracks within the framework of continuum mechanics. Nature and the practical activity of men permitted of observing various modes of fracture. A special case is perfectly brittle or elastic fracture, which is not encountered in practice among metallic materials. The fracture of such

materials is accompanied by plastic deformation. There is a simple possibility of introducing into consideration a small (compared with the characteristic dimension of a crack) plastic zone due to stress concentration at the crack edge. According to Irwin, the size of this plastic zone is proportional to the square of the ratio of the stress intensity factor to the yield strength. This zone is surrounded by the field of elastic strain whose value is related directly to the stress intensity factor calculable from the solution of the elastic problem. If the plastic zone must be taken into account, its length artificially increases the extent of the crack (see Secs. 6 and 10). This formal action enables an easy analytic transition from the description of elastic fracture to that of elastic-plastic fracture, which suggested the title of the book. Thus, the determination of the stress intensity factor and its critical value includes both the above modes of fracture.

2. STRESS AND DISPLACEMENT FIELDS IN THE VICINITY OF A CRACK TIP

Before proceeding to the solution of the problem indicated in the heading of the section we recapitulate some basic relations of the theory of elasticity which will be needed in what follows.

Considerable mathematical difficulties involved in solving general equations of elasticity call for the construction of solutions for more or less wide classes of special cases. Such is, for example, the class of 'plane elasticity problems,' which incorporates two practically important cases: (a) the deformation of a long cylinder by forces, the same in all planes, applied to its lateral surface and lying in planes perpendicular to the generators of the cylinder; (b) the deformation of a plate by forces lying in its plane and applied to its perimeter.

Every elementary course in elasticity gives the derivation of the equilibrium equations for the plane elasticity problem (in this case we have three equilibrium equations, with neglect of body forces and inertial terms). We present the complete system which is closed by Hooke's law

for an isotropic body in plane strain

$$\frac{\partial\sigma_x}{\partial x}+\frac{\partial\tau_{xy}}{\partial y}=0, \quad \frac{\partial\sigma_y}{\partial y}+\frac{\partial\tau_{xy}}{\partial x}=0,$$

$$\sigma_x=\lambda\theta+2\mu\varepsilon_x, \quad \sigma_y=\lambda\theta+2\mu\varepsilon_y, \quad \tau_{xy}=\tau_{yx}=\mu\gamma_{xy}, \tag{2.1}$$

$$\varepsilon_x=\frac{\partial u}{\partial x}, \quad \varepsilon_y=\frac{\partial v}{\partial y}, \quad \gamma_{xy}=\frac{\partial u}{\partial y}+\frac{\partial v}{\partial x}$$

$$\left(\theta=\varepsilon_x+\varepsilon_y=\frac{\partial u}{\partial x}+\frac{\partial v}{\partial y}\right).$$

The last relations in (2.1) are obtained on the assumption of 'small strains,' i.e., such changes in a body when the derivatives of the displacement components with respect to x and y are so small that their squares and products may be neglected.

The system of five equations (2.1) with first-order partial derivatives in five unknown functions σ_x, σ_y, τ_{xy}, u, v is the system of basic equations in plane elasticity.*

By using the set of formulas (2.1), it is easy to derive both a system of equations containing only displacements

$$(\lambda+\mu)\frac{\partial\theta}{\partial x}+\mu\Delta u=0, \quad (\lambda+\mu)\frac{\partial\theta}{\partial y}+\mu\Delta v=0, \tag{2.2}$$

and equations involving only stresses, for which purpose to the first two relations of (2.1) must be added one more equation

$$\Delta(\sigma_x+\sigma_y)=0. \tag{2.3}$$

If use is made of the representations of stress and displacement components in terms of the stress function $U(x, y)$ introduced in 1862 by the English astronomer G. B. Airy

$$\sigma_x=\frac{\partial^2 U}{\partial y^2}, \quad \sigma_y=\frac{\partial^2 U}{\partial x^2}, \quad \tau_{xy}=-\frac{\partial^2 U}{\partial x\,\partial y},$$

* In the case of a long cylinder there is one more component present, $\sigma_z=\lambda\theta=\nu(\sigma_x+\sigma_y)$ (ν is Poisson's ratio), which is, however, at once determined after solving the system of equations as a whole. Moreover, in the case of a flat plate λ is replaced by the elastic constant

$$\lambda^*=\frac{2\lambda\mu}{\lambda+2\mu}=\frac{E\nu}{1-\nu^2}.$$

then from (2.3) it follows that $U(x, y)$ is a biharmonic function

$$\Delta^2 U = 0.$$

As far back as 1898, E. Goursat proved that every biharmonic function may be expressed in terms of analytic functions of a complex variable. In particular, he suggested the following representation of a biharmonic function in terms of two analytic functions, φ, χ, of a complex variable:

$$U = \frac{1}{2}(\bar{z}\varphi + z\bar{\varphi} + \chi + \bar{\chi}). \tag{2.4}$$

From the foregoing relations and (2.4) one obtains the complex representation of solutions of the plane elasticity problem, which underlies the methods of application of complex function theory in elasticity developed by G. V. Kolosov and N. I. Muskhelishvili.

Omitting rather simple computations, we present the expressions for the complex representation of displacements and stresses obtained by G. V. Kolosov in 1909 [137, 200]

$$\begin{gathered}
\sigma_x + \sigma_y = 2[\Phi(z) + \overline{\Phi(z)}], \quad \psi(z) = \chi'(z), \\
\sigma_y - \sigma_x + 2i\tau_{xy} = 2[\bar{z}\Phi'(z) + \Psi(z)], \quad \Phi(z) = \varphi'(z), \\
\Psi(z) = \psi'(z), \\
2\mu(u + iv) = \varkappa\varphi(z) - \overline{z\varphi'(z)} - \overline{\psi(z)}.
\end{gathered} \tag{2.5}$$

Here $\varkappa = \frac{\lambda + 3\mu}{\lambda + \mu} = 3 - 4\nu$ for plane strain, $\varkappa = \frac{\lambda^* + 3\mu}{\lambda^* + \mu} = \frac{3 - \nu}{1 + \nu}$ for plane stress.

It may be shown that for any values of $\varphi(z)$ and $\psi(z)$ the functions σ_x, σ_y, τ_{xy}, u, and v as determined from (2.5) satisfy the basic equations (2.1). In other words, (2.5) is the general solution of the plane problem (2.1) of the theory of elasticity. In solving practically important problems, however, we have to impose some additional conditions on the quantities under consideration on the boundary of the region, which leads to the so-called boundary value problems, and relations (2.5), in spite of their generality, are not a specific solution of these boundary value problems.

Two special cases of relations (2.5) are associated with the name of H. M. Westergaard [290]. Assuming, for example, that

$$\Phi(z)=\frac{1}{2}Z_1(z),\quad \Psi(z)=-\frac{1}{2}zZ_1'(z), \tag{2.6}$$

from relations (2.5) we obtain

$$\sigma_x+\sigma_y=2\operatorname{Re}Z_1,\quad \sigma_y-\sigma_x=2y\operatorname{Im}Z_1', \tag{2.7}$$
$$\tau_{xy}=-y\operatorname{Re}Z_1'.$$

The solution furnished by these equations possesses the property that when $y=0$, $\tau_{xy}=0$ and $\sigma_x=\sigma_y$.

By using Hooke's law and expressing the displacements u, v from (2.1) in terms of the stresses determined by relations (2.7), we obtain the following expressions for the case of plane strain ($\varepsilon_z=0$):

$$\begin{aligned} u&=\frac{1+\nu}{E}[(1-2\nu)\operatorname{Re}Z_1^\circ-y\operatorname{Im}Z_1]\quad\left(Z_1=\frac{dZ_1^\circ}{dz}\right),\\ v&=\frac{1+\nu}{E}[2(1-\nu)\operatorname{Im}Z_1^\circ-y\operatorname{Re}Z_1]. \end{aligned} \tag{2.8}$$

Let now

$$\Phi(z)=-\frac{1}{2}iZ_2(z),\quad \Psi(z)=\frac{1}{2}izZ_2'+iZ_2. \tag{2.9}$$

From the same relations (2.5) we then have

$$\sigma_x+\sigma_y=2\operatorname{Im}Z_2,\ \sigma_y-\sigma_x=-2\operatorname{Im}Z_2-2y\operatorname{Re}Z_2',$$
$$\tau_{xy}=\operatorname{Re}Z_2-y\operatorname{Im}Z_2'. \tag{2.10}$$

This solution possesses the property that $\sigma_y=0$ along the line $y=0$.

In a similar way we determine the displacements

$$\begin{aligned} u&=\frac{1+\nu}{E}[2(1-\nu)\operatorname{Im}Z_2^\circ+y\operatorname{Re}Z_2]\left(Z_2=\frac{dZ_2^\circ}{dz}\right),\\ v&=\frac{1+\nu}{E}[-(1-2\nu)\operatorname{Re}Z_2^\circ-y\operatorname{Im}Z_2]. \end{aligned} \tag{2.11}$$

One of the most important features in the design of structural elements with cracks is the consideration of stress redistribution resulting from the formation of slits and cracks

under the action of external loads. The crack tip is then the location of the highest stress concentration and the origin of the likeliest further fracture. The analysis of the state of stress at the crack tip therefore assumes a special importance. The most general case of strain and stress fields at the crack tip can be obtained by superimposing the stresses due to the following three particular modes of deformation

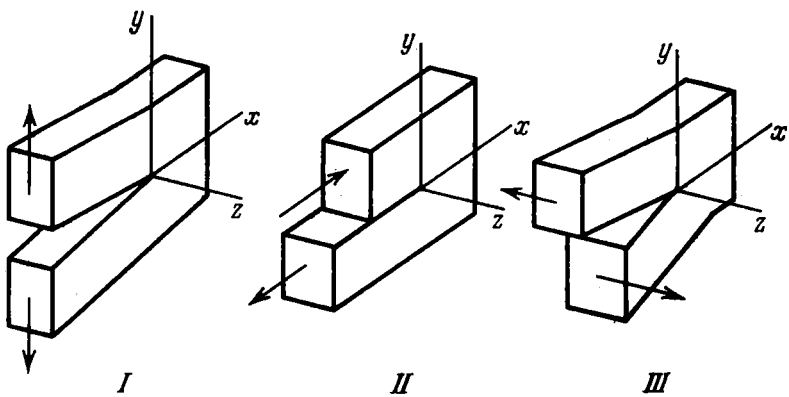

Fig. 2.1. Basic modes of deformation of crack surfaces.

(Fig. 2.1). The first mode is associated with an opening displacement in which the crack surfaces move directly apart in opposite directions (symmetrically about the xy and xz planes). The second mode corresponds to displacements in which the crack surfaces slide over one another (symmetrically about the xy plane, but skew-symmetrically about the xz plane). The third mode is connected with antiplane strain (cutting with the scissors) in which one surface slides over the other parallel to the leading edge of the crack (skew-symmetric strain about the xy and xz planes).

We now revert to Westergaard's solutions and choose the function Z_1, analytic in the entire region with the exception of some segment of the real axis, in the following form:

$$Z_1 = \frac{g(z)}{\sqrt{(z-a)(z-b)}}. \tag{2.12}$$

If $g(z)$ is a reasonably smooth function, this expression furnishes the solution of the problem of a crack situated along the real axis, $a < x < b$, $y = 0$, since $\sigma_y = \tau_{xy} = 0$ in this interval. From this it follows that

$$\operatorname{Im} g(x) = 0 \quad (a < x < b). \tag{2.13}$$

For example, the function giving the solution of the problem of a crack subjected to uniaxial tension p at infinity and

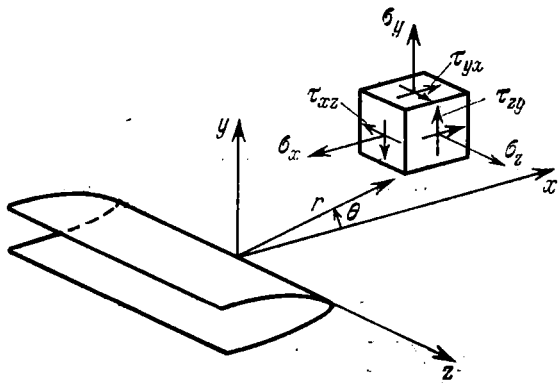

Fig. 2.2. Co-ordinate system and stress components at a crack tip.

free from stress in the interval $-l < x < l$, $y = 0$ is of the form

$$Z_1 = \frac{pz}{\sqrt{z^2 - l^2}}. \tag{2.14}$$

We now make a change of the variable $\xi = z - b$ in expression (2.12); then

$$Z_1 = f(\xi)\,(\xi)^{-1/2}. \tag{2.15}$$

In the vicinity of the crack tip $x = b$, i.e., for small values of $|\xi|$, from (2.12) and (2.13) it follows that the function $f(\xi)$ is sufficiently smooth and when $|\xi| \to 0$ it may be replaced by a real constant

$$Z_1|_{|\xi|\to 0} = \frac{K_{\mathrm{I}}}{\sqrt{2\pi\xi}} \quad \text{or} \quad K_{\mathrm{I}} = \lim_{|\xi|\to 0} \sqrt{2\pi\xi}\, Z_1. \tag{2.16}$$

We substitute (2.16) in (2.7) and transform to polar coordinates $\xi = re^{i\theta}$ in these relations (Fig. 2.2). By reject-

ing terms of higher order than r, we easily obtain formulas for stress fields giving a good approximation in a region where r is small compared, for example, with the crack length*

$$\begin{aligned}
\sigma_x &= \frac{K_{\mathrm{I}}}{\sqrt{2\pi r}} \cos\frac{\theta}{2}\left(1-\sin\frac{\theta}{2}\sin\frac{3}{2}\theta\right),\\
\sigma_y &= \frac{K_{\mathrm{I}}}{\sqrt{2\pi r}} \cos\frac{\theta}{2}\left(1+\sin\frac{\theta}{2}\sin\frac{3}{2}\theta\right),\\
\sigma_z &= \nu(\sigma_x+\sigma_y),\\
\tau_{xy} &= \frac{K_{\mathrm{I}}}{\sqrt{2\pi r}} \sin\frac{\theta}{2}\cos\frac{\theta}{2}\cos\frac{3}{2}\theta, \quad \tau_{xz}=\tau_{yz}=0.
\end{aligned} \tag{2.17}$$

The displacements in the vicinity of the crack tip are obtained by substituting (2.16) in (2.8) and transforming to polar co-ordinates

$$\begin{aligned}
u &= \frac{K_{\mathrm{I}}}{G}\sqrt{\frac{r}{2\pi}}\cos\frac{\theta}{2}\left(1-2\nu+\sin^2\frac{\theta}{2}\right),\\
v &= \frac{K_{\mathrm{I}}}{G}\sqrt{\frac{r}{2\pi}}\sin\frac{\theta}{2}\left(2-2\nu-\cos^2\frac{\theta}{2}\right).
\end{aligned} \tag{2.18}$$

Relations (2.16), (2.17), and (2.18) represent asymptotic expressions for the stress and displacement fields in the vicinity of the crack tip for the first mode of deformation associated with an opening displacement.

We now proceed to the second mode of deformation in which the crack surfaces slide over one another. Similarly to the above we conclude that as $|\xi| \to 0$ in the vicinity of the crack tip

$$Z_2\big|_{|\xi|\to 0} = \frac{K_{\mathrm{II}}}{\sqrt{2\pi\xi}}, \quad K_{\mathrm{II}} = \lim_{|\xi|\to 0}\sqrt{2\pi\xi}\, Z_2. \tag{2.19}$$

Substituting (2.19) in (2.10) and (2.11), we obtain the following asymptotic representations in polar co-ordinates

* All formulas that follow correspond to the case of plane strain ($w = 0$). In the case of plane stress ($\sigma_z = 0$) Poisson's ratio in the displacements is replaced by the appropriate quantity.

for this case of deformation:

$$\begin{aligned}
\sigma_x &= -\frac{K_{II}}{\sqrt{2\pi r}} \sin\frac{\theta}{2}\left(2+\cos\frac{\theta}{2}\cos\frac{3}{2}\theta\right),\\
\sigma_y &= \frac{K_{II}}{\sqrt{2\pi r}} \cos\frac{\theta}{2}\sin\frac{\theta}{2}\cos\frac{3}{2}\theta,\\
\sigma_z &= \nu(\sigma_x+\sigma_y),\\
\tau_{xy} &= \frac{K_{II}}{\sqrt{2\pi r}} \cos\frac{\theta}{2}\left(1-\sin\frac{\theta}{2}\sin\frac{3}{2}\theta\right),\\
\tau_{xz} &= \tau_{yz} = 0,
\end{aligned} \tag{2.20}$$

$$\begin{aligned}
u &= \frac{K_{II}}{G}\sqrt{\frac{r}{2\pi}}\sin\frac{\theta}{2}\left(2-2\nu+\cos^2\frac{\theta}{2}\right),\\
v &= \frac{K_{II}}{G}\sqrt{\frac{r}{2\pi}}\cos\frac{\theta}{2}\left(1-2\nu+\sin^2\frac{\theta}{2}\right), \qquad w=0.
\end{aligned} \tag{2.21}$$

The last of the above-mentioned special cases is connected with antiplane strain in which one surface slides over the other parallel to the leading edge of the crack. In this case $w = w(x, y)$ is the only non-zero displacement component ($u = v = 0$), and the equilibrium equations and Hooke's law assume the following form:

$$\frac{\partial\tau_{xz}}{\partial x}+\frac{\partial\tau_{yz}}{\partial y}=0, \tag{2.22}$$

$$\tau_{xz}=G\gamma_{xz}=G\frac{\partial w}{\partial x}, \quad \tau_{yz}=G\gamma_{yz}=G\frac{\partial w}{\partial y}, \tag{2.23}$$

from which it follows that, upon substitution of (2.23) in (2.22), the displacement satisfies Laplace's equation

$$\Delta w = 0. \tag{2.24}$$

If $w = w(x, y)$ is chosen in the form

$$w=\frac{1}{G}\operatorname{Im} Z_3, \tag{2.25}$$

then from (2.23) we obtain

$$\tau_{xz} = \operatorname{Im} Z_3', \quad \tau_{yz} = \operatorname{Re} Z_3'. \tag{2.26}$$

In the vicinity of the tip of a crack ($y = 0$, $x < 0$) with head at the point $x = y = 0$ the stress function Z_3 is of

the form

$$Z_3|_{|\xi|\to 0} = \frac{K_{III}}{\sqrt{2\pi\xi}}, \quad K_{III} = \lim_{|\xi|\to 0} \sqrt{2\pi\xi}\, Z_3. \tag{2.27}$$

Substituting (2.27) in (2.25) and (2.26), we obtain expressions for displacements and stresses at the crack tip in the case of antiplane strain

$$\tau_{xz} = -\frac{K_{III}}{\sqrt{2\pi r}} \sin\frac{\theta}{2}, \quad \tau_{yz} = \frac{K_{III}}{\sqrt{2\pi r}} \cos\frac{\theta}{2}, \tag{2.28}$$
$$\sigma_x = \sigma_y = \sigma_z = \tau_{xy} = 0;$$

$$w = \frac{K_{III}}{G}\sqrt{\frac{2r}{\pi}} \sin\frac{\theta}{2}, \quad u = v = 0. \tag{2.29}$$

The relations obtained involve three quantities, K_I, K_{II}, K_{III}, termed the stress intensity factors for the three modes of deformation discussed above. These factors play an extremely important role in the mechanics of brittle fracture (see Chap. II).

The stress intensity factors are often designated by the symbol K without a suffix implying that either the mode of deformation is clear from the problem or the factor may apply to any mode.

3. THE GRIFFITH-OROWAN-IRWIN CONCEPT. STABLE AND UNSTABLE CRACK GROWTH

To form a true notion of the strength of a body it is insufficient to have a solution of the theory of elasticity or plasticity for the stress concentration at notches or cracks. It is necessary to have also the so-called strength criteria which establish the moment or the process of exhausting the load-carrying capacity of the material at a point (or alternatively, in other interpretations, of the body as a whole). The formulation of these criteria is such that the corresponding relations necessarily contain some material constants (or, possibly, constants of a specimen together with a testing device) determined experimentally. Among these constants are such well-known mechanical characteristics of materials as the yield strength, the ultimate strength, the true tensile

strength, etc., the procedure for determining of which on smooth specimens is standardized.

The process of fracture is made up of two stages, crack initiation and propagation, each of these stages following its particular laws. It is natural that among the strength criteria there are such which represent the conditions for crack initiation or the conditions for crack propagation. The former are actually the conditions for the occurrence of a dangerous state at a point at the moment under consideration (the classical strength theories referred to in Sec. 1). The latter proceed from the presence of a crack in a body (they are treated in this and the following two sections).

The criterion for the initiation of crack propagation,* which forms the basis of fracture mechanics, does not follow from the equations of equilibrium and motion of continuum mechanics. This is an additional boundary condition in the solution of the problem of the limiting equilibrium for a cracked body. The limiting equilibrium state is said to be reached if a crack-like cut can propagate. The cut then becomes a crack. From the last definition it is seen that a crack is a thin cut (slit) which is capable of propagating (increasing its surface) in the volume of the body under the action of external effects.** Among external effects are mechanical forces, thermal stresses, corrosive and surface-active environmental effects, as well as the time during which the change in material parameters occurs.

After the body reaches the limiting equilibrium state the crack growth may be either stable or unstable.

In a stable state the crack is stationary under constant external load and the crack extension over a small area (or through a small distance) also requires a small increment of the external loading parameter. Consequently, if the relation between the external loading parameter P and the crack length l is found from the fracture criterion, then the following inequality expressions are valid for a stable

* Sometimes termed a fracture criterion in what follows.

** The name, 'crack' is often used to refer to a mathematical cut in a body or a flaw in a metal for which the conditions of limiting equilibrium state are not fulfilled. This is justified only by considerations of shortness and, possibly, convenience.

crack:

$$\frac{dP}{dl} > 0 \quad \text{or} \quad \frac{dK}{dl} < 0. \tag{3.1}$$

In an unstable equilibrium state the crack begins to move after the load reaches the critical value determined from the fracture criterion. In the supercritical range the crack can propagate under constant load. The range of unstable equilibrium states is characterized by the inequality expressions

$$\frac{dP}{dl} < 0 \quad \text{or} \quad \frac{dK}{dl} > 0. \tag{3.2}$$

As far as the prevention of complete fracture is concerned, it is important to know the kind of equilibrium to which the limiting state belongs. If the limiting equilibrium state is stable, there is no danger of immediate complete fracture of a part. If, however, the limiting state is unstable, such a crack is impermissible, at any rate without further more detailed analysis. The choice of the allowable size of an initial crack depends largely on the particular limiting equilibrium state.

Criteria for the initiation of crack propagation can be obtained on the basis of both energy and force considerations. Historically, at first an energy fracture criterion was proposed by A. A. Griffith [104] in 1920 and G. R. Irwin [117] formulated a force criterion in 1957, while at the same time demonstrating the equivalence of the two criteria.

The idea of these approaches consists in the following. Let there be a perfectly elastic body with an initial cut. In order that this cut should begin to propagate increasing its surface, it is necessary to expend an amount of energy equal to that which must be spent to achieve the integrity of the material ahead of the edge of the cut. This energy may be termed fracture energy. Simultaneously with the formation of a new surface free from loads, the deformation in a part of the volume of the body decreases. This leads to a corresponding elastic energy release from the body. Thus, on the basis of the law of conservation of energy, with neglect of other possible energy flows, the following energy condition is fulfilled as the crack spreads by an amount

δS:

$$\delta\Gamma = G\,\delta S. \tag{3.3}$$

Here $\delta\Gamma$ is the amount of fracture energy needed to make a new fracture surface of area δS, G is the energy flow into the crack tip calculated per unit area of the crack, or, in other words, the strain energy release rate.

Griffith supposed that $\delta\Gamma$ represents the surface energy of a solid and is of the same physical nature as it is for a liquid. Subsequently, however, it was established that the expenditure of energy in producing new surfaces during crack extension is mainly connected with the plastic work of deformation in volumes of material ahead of the crack front. If the linear dimensions of these volumes are small compared with the crack length, the elastic energy flow can be calculated as before in accordance with the elastic solution, and the expenditure of energy in fracture is now related to the plastic work of deformation. This is the concept of quasi-brittle fracture due to E. O. Orowan [211] and G. R. Irwin [115]. This concept was a great contribution to the process of transition from the ideal material in Griffith's model to real metallic materials. The benefits of this concept are due to the fact that the fracture of actual structures practically always proceeds by the quasi-brittle mechanism: macrobrittle fracture involves significant residual strains near the fracture surface. Thus, this concept opened the way for application of the Griffith fracture theory to the solution of engineering problems. The energy Γ ensures the existence of a solid as a single unit, and when new surfaces form (from the initial cut) it is customary to assume that the energy Γ is of a surface nature and may therefore be expressed by the relation

$$\delta\Gamma = 2\,\gamma\delta S. \tag{3.4}$$

Here γ is the intensity of the surface energy expended in fracture.

The energy balance (3.3) has the same form irrespective of the manner in which the external load is applied, be it the case of fixed points of application of external forces (grips), the case of a fixed value of external forces or some intermediate case.

If the grips are fixed (do not move), the work done by the external forces is zero, and equality (3.3) follows directly from this. The strain energy W of the body decreases by an amount G which is wholly expended in fracture.

If, as a result of crack growth, the grips are displaced under constant external forces, the right-hand side of equality (3.3) is the difference between the work done by the external forces and the strain energy. This difference is positive and equal to G [83]. The energy balance retains the same form (3.3).

In both extreme cases G is the same and equal to

$$G = \pm \partial W / \partial l. \tag{3.5}$$

Here the plus sign refers to the case of a constant force, and the minus sign to fixed grips. The energy flow into the crack tip can be calculated if on the prolongation of the cut being considered we introduce an imaginary cut whose surfaces are acted on by widely varying stresses produced in a continuous medium near the edge of the cut by the external load. As the cut advances a unit of area, the above-mentioned surfaces of the imaginary cut separate from each other, and the work done by the forces $\sigma_y\, dx$ during the displacements v gives the required energy flow

$$G = -\lim_{\alpha \to 0} \frac{1}{2\alpha} \int_0^\alpha \sigma_y 2v\, dx. \tag{3.6}$$

This advance of the cut is shown schematically in Fig. 3.1.

The asymptotic expression for the stresses and displacements in the vicinity of the end of a stationary cut, as follows from relations (2.17) with $\theta = 0$ and (2.18) with $\theta = \pi$ $(r = \alpha - x)$, is of the form

$$\sigma_y = \frac{K}{\sqrt{2\pi x}}, \qquad v = \frac{4(1-\nu^2)}{E} K \sqrt{\frac{\alpha - x}{2\pi}}. \tag{3.7}$$

Upon substitution and integration we obtain in the case of plane strain

$$G = (1-\nu^2)\frac{K^2}{E}, \tag{3.8}$$

and in the case of plane stress

$$G = \frac{K^2}{E}. \tag{3.9}$$

Note that for a perfectly elastic body K is independent of the degree of constraint to transverse deformation (along

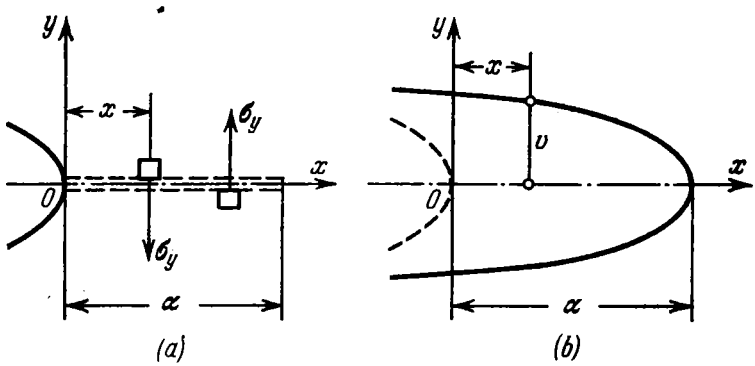

Fig. 3.1. Schematic representation of the tip of a crack before it advances a distance α (*a*) and after advancing (*b*).

the crack front) since the value of G for plane strain (because of smaller displacements) is $(1 - \nu^2)$ times G for plane stress.

We thus come to two equivalent formulations of the fracture criterion. The crack will propagate when

(1) the energy release rate G reaches a critical value $G_c = \delta\Gamma/\delta S$ = constant;

(2) the stress intensity factor K reaches a critical value K_c = constant.

Thus, the energy criterion for crack growth is of the form

$$G = G_c. \tag{3.10}$$

The force criterion is

$$K = K_c. \tag{3.11}$$

These formulations are valid for perfectly elastic fracture (when $\sigma_y \to \infty$ at the crack tip in a linearized statement of an elasticity problem) and, generally speaking, they

exhaust the linear mechanics of crack extension in the proper sense.

Actually, for most real materials, in a small region at the end of a cut because of large stresses there is a zone in which the material displays non-linear properties and the distribution of stress and displacement differs from the elastic one. In the quasi-brittle fracture scheme (Orowan, Irwin) it is taken that the zone of non-linear effects is small compared with the crack length. This enables one to assume that both the size of the given zone and the intensity of plastic strains in it are entirely governed by the stress intensity factor, the yield stress and the work-hardening exponent, and the stress field around the plastic region is described by asymptotic formulas.

Consequently, both formulations of the fracture criterion hold for quasi-brittle fracture. Henceforth, no significant distinction will be made between brittle and quasi-brittle (in the sense indicated) fracture, and the term brittle fracture will be used for both cases.

4. THE INTEGRAL VARIATIONAL PRINCIPLE IN CRACK THEORY

Let us show the possibility of using the energy equilibrium criterion for the solution of crack problems for an elastic-perfectly plastic body [185, 191]. The consideration will be given for the case when the plastic deformation is concentrated in a narrow zone ahead of the crack edge [23, 71, 218]. The thickness of this zone is of the order of elastic displacements (Fig. 4.1*a*). Cracks with a thin plastic zone ahead of the edge are considered for convenience in performing further analysis* in which the problem is reduced to the solution of an elastic problem instead of an elastic-plastic one. This reduction is based on the fact that, in the linearized formulation, a thin plastic zone may be replaced schematically by an additional cut along the faces of which are applied forces replacing the action of the plastically deforming material (Fig. 4.1*b*).

* A more general case is also possible when the plastic zone ahead of a crack tip is not thin (Fig. 4.2). Here, however, this case is not considered.

Attention is drawn to the fact that the region of plastic non-linear effects (of size d, Fig. 4.1a) in the model under consideration varies with the external load and represents

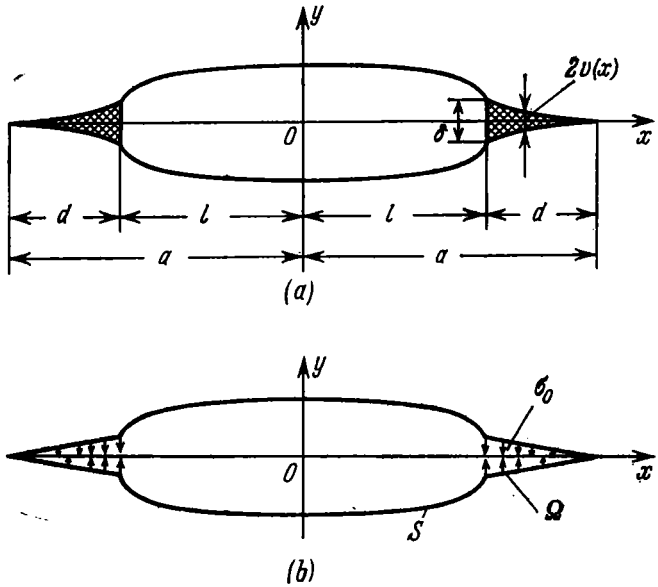

Fig. 4.1. Crack with a plastic zone at its tip in plane stress; (a) elastic-plastic problem, (b) elastic problem.

a plastically deforming material in which the state of stress and strain must be determined from the solution of an elastic-plastic problem. By hypothesis, the thickness of the plastic

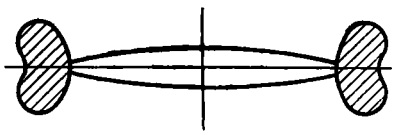

Fig. 4.2. Crack with a plastic zone of different shape than a strip

zone $2v$ (x) in a symmetric problem is small enough to make possible the linearized formulation of the problem, but at the same time it is large compared with the interatomic

spacing. Consequently, the stresses on the surface of the additional cut in this model differ from the cohesive forces of atomic interaction. Thus, the model under consideration is appreciably different from the model presented in [15] at the basis of which is the assumption about the presence (in the region $d \ll l$) of atomic forces of interaction dependent, according to the well-known physical law, on the distance $2v(x)$ comparable with the interatomic spacing. It is then implied that there is no material between the crack surfaces in the region $d \ll l$, and the region d itself does not change with the external load.

The justification of the foregoing statement of the problem lies in the fact that narrow and long plastic zones ($d \cong l$) ahead of the tip of a crack were observed experimentally in cracked plates under tension (see Sec. 17) [139, 157, 282, 301].

The size d of the plastic zone is not restricted to any limits, and when the crack length is sufficiently small the onset of general yielding becomes possible at the given section of the body in which case $d \to \infty$.

For an actual or a possible increment of crack area, the equilibrium criterion, which expresses the law of conservation of energy, may be written as [180, 251]

$$\delta W + \delta \Gamma = \delta A. \tag{4.1}$$

Here δA is the mechanical work done by the external forces, δW is the volume elastic strain energy of the body, $\delta \Gamma$ is the fracture energy. Since the problem under consideration is assumed to be quasi-static, the kinetic energy is taken to be zero. Moreover, condition (4.1) is written on the assumption that there are no heat flows or other forms of energy.

In our case the energy expended in producing new fracture surfaces, i.e., the fracture energy, is virtually determined by the plastic strain energy δW_p, i.e., $\delta \Gamma = \delta W_p$. This fracture energy differs from the fracture energy of an elastic body in that here $\delta \Gamma$ is entirely determined by the energy expended in doing plastic work of deformation, whereas for a brittle body, by definition, $d = 0$. For a brittle body, $\delta \Gamma$ is therefore a part of the internal energy not necessarily associated with the work done by the surface

cohesive forces acting on the faces of the already formed fracture crack and which can be determined in terms of the energy flow at the crack tip defined by the singular elastic solution [251]. Hence, in contrast to a perfectly elastic brittle body, the fracture energy density γ for the model under consideration cannot, in general, be considered a material constant; in this case the quantity $\gamma = \Delta W_p/\Delta S$ (the plastic strain energy per unit area of a newly formed surface) depends on the mode of application of the external loads, on the shape and dimensions of the body, and in particular on the crack size.

To the variational condition (4.1) must be added three additional conditions:

(1) for determining the size d of the plastic zone shead of the crack edge (for example, the smoothness of closure of the boundaries of the plastic zone at its end, or, what amounts to the same thing, the continuity of the stresses at this end);

(2) for determining the stress σ_{0i} on the surface of the additional cut (for example, either the solution of an independent elastic-plastic problem for the vicinity of the crack edge with the use of the well-known plasticity conditions [209], or the assignment of this stress, which may be different, and in particular constant and equal to the yield stress);

(3) for fixing the limiting value of δW_p, which is necessary [99, 209, 294, 295] for the study of cracks capable of propagating, for otherwise we shall have an elastic-plastic problem for a stationary cut (for example, the equality of the maximum separation between the boundaries of the plastic zone and some material constant δ_c).

Let a cracked body be given which is in equilibrium under prescribed loads q_i over the surface of the body Σ and over the surface of a crack S. The work done by the external forces is

$$\delta A = \int_{\Sigma} q_i \delta u_{i1}\, d\sigma + \delta \int_{S} q_i u_{i1}\, d\sigma. \tag{4.2}$$

Here u_i are the components of the displacement vector, the subscript unity indicating the state number introduced below.

Without violating the state of stress and strain in the elastic part of the body, we imagine a cut to be passed along

the plastically deforming region ahead of the crack edge (first state). There remains, then, an elastic body with a cut whose surface includes the crack surface S and the boundary surface of the plastic zone Ω with a uniform stress σ_0 distributed over it. We have [99]

$$\delta W_p = \int_{\Omega} |\sigma_{0i} \delta u_{i1}^* | \, d\sigma. \tag{4.3}$$

Here the displacement u_{i1}^* is determined using the third of the above-mentioned additional conditions.

For the first state we have

$$\delta W = \frac{1}{2} \int_{\Sigma} q_i \delta u_{i1} \, d\sigma + \frac{1}{2} \delta \int_{S} q_i u_{i1} \, d\sigma + \frac{1}{2} \delta \int_{\Omega} \sigma_{0i} u_{i1} \, d\sigma. \tag{4.4}$$

It is convenient, for practical applications, to eliminate the integral over Σ. For this purpose, we introduce, according to [198], a second state, viz. the same body with loads q_i over Σ, with a cut $S + \Omega$ whose surface is acted on by stresses p_i which ensure the deformation of the body as a sound one. The components of the elastic solution relating to this state are marked by the superscript 'circle.' The bodies in both states are identical and elastic, which allows us to write Betti's theorem [257]

$$\frac{1}{2} \int_{\Sigma+S+\Omega} q_{i1} u_i^\circ \, d\sigma = \frac{1}{2} \int_{\Sigma+S+\Omega} q_i^\circ u_{i1} \, d\sigma.$$

From this, noting that $\int_{\Omega} \delta_{0i} u_i^\circ d\sigma = 0$, $q_i = q_{i1} = q_i^\circ$ on Σ and $q_i^\circ = p_i$ on $S + \Omega$, we obtain a useful relation

$$\int_{\Sigma} q_i u_{i1} \, d\sigma = \int_{\Sigma+S} q_i u_i^\circ \, d\sigma - \int_{S+\Omega} p_i u_{i1} \, d\sigma.$$

The varied state represents a body with the former external loads, but with a different length of the basic and the additional cut. The equations of the theory of elasticity hold for this body. By applying again the operation with Betti's theorem and calculating the corresponding differ-

ence of the energies, we obtain

$$\delta \int_{\Sigma} q_i u_{i1}\, d\sigma = \delta \int_{\Sigma+S} p_i u_i^{\circ}\, d\sigma - \delta \int_{S+\Omega} p_i u_{i1}\, d\sigma.$$

This relation is used to reduce formulas (4.2) and (4.4) to an alternative form noting that

$$\int_{S+\Omega} p_i u_i^{\circ}\, d\sigma = 0.$$

On the basis of the superposition principle of the linear theory of elasticity the displacements u_{i1}° may be represented as the sum of the displacement u_i° of an uncracked body subjected to the load q_i on Σ (the body of the second state) and the displacements u_i of a body without the load q_i on Σ but with a crack whose surface is acted on by stresses g_i defined as

$$g_i = \begin{cases} q_i + p_i & \text{on } S, \\ \sigma_{0i} + p_i & \text{on } \Omega. \end{cases}$$

Here the vector p_i has a direction opposite to that in a sound body; hence, in the relation given below the sign before p_i is also reversed.

Substituting expressions (4.2), (4.3), and (4.4) in condition (4.1), we obtain [185]

$$2 \int_{\Omega} |\sigma_{0i} \delta u_i^{*}|\, d\sigma - \delta \int_{S} (p_i + q_i)\, u_i\, d\sigma + \delta \int_{\Omega} (\sigma_{0i} - p_i)\, u_i\, d\sigma -$$
$$- 2\delta \int_{S} q_i u_i^{\circ}\, d\sigma - \int_{\Sigma} q_i \delta u_i^{\circ}\, d\sigma = 0. \qquad (4.5)$$

It will be recalled that the vectors p_i, σ_{0i}, and u_i are mutually opposite in direction, and hence the corresponding terms must be less than zero.

In this form the energy criterion for equilibrium in conjunction with the equations of the theory of elasticity is suitable for the solution of specific crack problems.

We shall mention the following types of problem solvable with the use of condition (4.5).

(1) The determination of the limiting (critical) equilibrium state of a cracked body with varied crack area under

constant external load. The displaced state is not then an equilibrium state in the sense that $\Delta W_p < |-\Delta A + \Delta W|$ for a small but finite ΔS. For a two-dimensional problem

$$\delta = \frac{\partial}{\partial l}\,\delta l \qquad (q_i = \text{const},\ \delta u_i^\circ = 0).$$

(2) The determination of slow subcritical crack growth with increasing load. The varied state coincides with an actual equilibrium state in which the external loads have other values. For a two-dimensional problem

$$\delta = \left[\frac{\partial}{\partial l} + \left(\frac{\partial}{\partial q}\right)\left(\frac{dq}{dl}\right)\right]\delta l$$

[q is the external loading parameter, $q = q(l)$].

(3) The determination of the number of cycles required for a crack to reach the critical state under repeated static loading.

(4) The determination of the relation between the crack length and the number of cycles under repeated static loading.

(5) The possibility of applying approximate methods for calculating the above-mentioned characteristics in bodies of limited dimensions.

The energy criterion for limiting equilibrium in the case of perfectly elastic fracture can be obtained from condition (4.5) assuming $\Omega = 0$ and introducing into (4.1) an experimentally determined value of the surface fracture energy density γ. The first term in Eq. (4.5) then assumes the form $2\gamma\delta\,(S^+ + S^-)$.

It is obvious that in the extreme cases of perfectly soft loading ($\delta q = 0$, $\delta u_i^\circ = \frac{\partial u_i^\circ}{\partial q}\,\delta q$) and perfectly hard loading ($\delta u_i^\circ = 0$) the integral over Σ in expression (4.5) vanishes. Henceforth this term is therefore assumed zero. Moreover, if the load q_i on S is symmetrical, the term $2\delta \int_S q_i u_i^\circ d\sigma$ also vanishes. Hence, for a perfectly elastic body the fracture criterion is of the form [184]

$$\delta \int_S [2\gamma + (p_i + q_i)\,u_i]\,d\sigma = 0. \tag{4.6}$$

Here $p_j = -\sigma_{ij} n_i$ are the components of the stress tensor on planes whose position coincides with the crack surface, σ_{ij} is the stress tensor for a stressed uncracked body, n_i are the direction cosines of the outward normal to the crack surface, u_i are the components of the displacement vector of the points of the crack surface for a body which is loaded on the crack surface by a pressure $p_i + q_i$, q_i is the prescribed symmetrical load on the crack surface.

To determine the critical equilibrium state, the fracture surface area S in condition (4.6) is varied under constant load.

Let us now show how the presence of the plastic zone can be approximately taken into account by using relation (4.6) and introducing a discontinuity in displacement at the crack edge [195].

We write down criterion (4.5) for the case of the symmetrical loading of a plane containing a single straight crack ($y = 0$, $|x| \leqslant l$, $\delta = \left(\frac{\partial}{\partial l}\right) \delta l$):

$$\frac{\partial}{\partial l} \int_0^l (2\gamma - \sigma_y v)\, dx - \frac{\partial}{\partial l} \int_l^a (\sigma_y - \sigma_0)\, v\, dx = 0. \qquad (4.7)$$

Here $\sigma_y = \sigma_y(x)$ is the stress due to the given load developed along the x axis in an uncracked body. This stress enters into (4.7) with an opposite sign. The displacement of the points of the surface of the cut $v = v(x, l)$ is produced (in the y direction) by the crack opening stress σ_y in the region $y = 0$, $|x| \leqslant l$ and by the stress $(\sigma_y - \sigma_0)$ when $l < |x| \leqslant a$. The plastic zone occupies the region $y = 0$, $l \leqslant |x| \leqslant a$, which is replaced by a cut for the solution of the problem.

Upon differentiation Eq. (4.7) becomes

$$2\gamma - \int_0^l \sigma_y \frac{\partial v}{\partial l}\, dx - \sigma_0 v(l, l) - \int_l^a (\sigma_y - \sigma_0) \frac{\partial v}{\partial l}\, dx = 0. \qquad (4.8)$$

We now adopt the condition that the length of the plastic zone $(a - l)$ is small, which is equivalent to assuming that $\sigma_y(x) = \sigma_y(l)$ under the integral between the limits l and a. Moreover, we assume that the shape of the plastic

zone is unchangeable, which is expressed by the self-similarity condition $\frac{\partial v}{\partial l} = -\frac{\partial v}{\partial x}$. We obtain $[v(a, l) = 0]$

$$\int_l^a (\sigma_y - \sigma_0) \frac{\partial v}{\partial l} dx = [\sigma_y(l) - \sigma_0] v(l, l).$$

Substituting this integral in (4.8) gives the relation

$$2\gamma - \sigma_y(l) v(l, l) - \int_0^l \sigma_y \frac{\partial v}{\partial l} dx = 0. \tag{4.9}$$

If the derivative $\partial v/\partial l$ in this equation is determined from the elastic solution, we arrive at an energy criterion of the form

$$\delta \int_0^l (2\gamma - \sigma_y v) dx = 0, \tag{4.10}$$

which is identical in form with condition (4.6). The assumption $v(l, l) \neq 0$ in condition (4.10) reflects, approximately, the existence of the plastic zone at the end of the cut.

The assumptions made are equivalent to the Orowan-Irwin concept of quasi-brittle fracture to the effect that the plastic zone at the tip of a crack may be so small that it has considerable influence only on the quantities (displacements and their derivatives in our case) relating directly to the crack tip and exerts no influence on the elements of the elastic solution in the remainder of the body.

From the comparison of conditions (4.1) and (4.6) we may write a useful expression for the energy flow into the crack tip

$$G = -\frac{\partial}{\partial l}(W - A) = \int_0^l p_i \frac{\partial u_i}{\partial l} d\sigma. \tag{4.11}$$

This relation is valid in the case of elastic fracture.

Let us write down the boundary conditions for internal and surface cracks resulting from Eq. (4.6). Suppose that the equation of the crack surface is written in explicit form $z = z(x, y)$ and is the same for both opposite surfaces of the crack. Assuming that the displacements u_j on them

are equal, we rewrite expression (4.6) in the form (for the case of $q_i = 0$ on S) [92, 179]

$$(p = z_{,x};\quad q = z_{,y};\quad i,\ j = x,\ y,\ z),$$

$$\delta I \equiv \delta \iint_D (2\gamma - p_j u_j)\sqrt{1+p^2+q^2}\,dx\,dy = 0. \quad (4.12)$$

Here D is the projection of the fracture region on the co-ordinate plane xy, C is the contour of the region D; the subscript after the comma denotes partial differentiation with respect to the variable appearing after the comma.

To calculate the variation of the functional I, we vary the co-ordinates of the points on the contour of the fracture region. The integrand depends on the equation of the contour line of the region of integration $\Gamma(x^*, y^*, z^*) = 0$ through some functional $\Psi = \Psi[z(x, y), \Gamma(x^*, y^*, z^*)]$ introduced by us, where the star indicates that the point belongs to the contour of the fracture region. This functional is introduced to describe the dependence of the displacement on the shape of the fracture region, i.e., the displacement on the crack surface can be represented as $u_j = u_j[x, y, z(x, y), \Psi]$.

We write down the variation of the functional

$$(M = (2\gamma - p_j u_j)\sqrt{1+p^2+q^2}),$$

$$\delta I = \iint_D [M_{,u_j} u_{j,\Psi}(\Psi_{,x^*}\delta x^* + \Psi_{,y^*}\delta y^* + \Psi_{,z^*}\overline{\delta z^*})]\,dx\,dy +$$

$$+ \int_C [(M_{,p}\overline{\delta z^*} + M\delta x^*)\,dy^* - (M_{,q}\overline{\delta z^*} + M\delta y^*)\,dx^*]. \quad (4.13)$$

Here the summation over the repeated index j applies, and the bar above δz^* denotes the variation of z^* for the unvaried arguments x^*, y^*. The integral along C in formula (4.13) corresponds to the classical expression of the variation for a variational problem with partial derivatives and a variable region of integration. The appearance of the integral over D is due to the dependence of the integrand in (4.12) on the contour of the region of integration.

The first necessary condition for an extremum takes the form

$$\int_C [M\,dy^*\,\delta x^* - M\,dx^*\,\delta y^* + (M_{,p}\,dy^* - M_{,q}\,dx^*)\,\overline{\delta z^*}] +$$
$$+ \iint_D M_{,u_j} u_{j,\Psi} (\Psi_{,x^*}\,\delta x^* + \Psi_{,y^*}\,\delta y^* + \Psi_{,z^*}\,\overline{\delta z^*})\,dx\,dy = 0. \tag{4.14}$$

This equation serves to establish the limiting loads for a given law of propagation of the fracture region by assigning the variations δx^*, δy^*, $\overline{\delta z^*}$.

The variations of the contour points are, in general, interconnected. To obtain the relations between the variations, we assume that when the crack propagates a point A of the contour moves perpendicular to the tangent to the contour line at that point, remaining at the same time in a plane tangential to some surface S passing through the contour at the point A. This surface may be either the given surface $z(x, y)$ or any other one. In the first case $\overline{\delta z^*} = 0$, and in the second $\overline{\delta z^*} \neq 0$.

Suppose that the equations of the contour line Γ and of the above-mentioned surface S may be represented in parametric form as

$$[z^*(t),\ y^*(t),\ x^*(t)]$$

and

$$[\zeta(u, v),\ \eta(u, v),\ \xi(u, v)],$$

respectively. The displacement of the point A then coincides with a vector formed by the vector product of a unit vector of the tangent to the curve Γ at the point A and a unit vector of the normal to the surface S at the point A. The scalars c_x, c_y, c_z proportional to the projections of the displacement vector of the point A on the co-ordinate axes are

$$c_x = y^*_{,t} b_\zeta - z^*_{,t} b_\eta, \qquad b_\xi = \eta_{,u}\zeta_{,v} - \eta_{,v}\zeta_{,u},$$
$$c_y = z^*_{,t} b_\xi - x^*_{,t} b_\zeta, \qquad b_\eta = \zeta_{,u}\xi_{,v} - \zeta_{,v}\xi_{,u},$$
$$c_z = x^*_{,t} b_\eta - y^*_{,t} b_\xi, \qquad b_\zeta = \xi_{,u}\eta_{,v} - \xi_{,v}\eta_{,u}.$$

The point of the surface S defined by the independent variables u, v coincides with the point A of the line Γ defined by the independent variable t.

The required relation between the variations of the contour points is written in the form [here the surface S is represented as $z = z(x, y)$]

$$\frac{\delta x^*}{c_x} = \frac{\delta y^*}{c_y} = \frac{\overline{\delta z^*} + (z_{,x})^* \, \delta x^* + (z_{,y})^* \, \delta y^*}{c_z}. \qquad (4.15)$$

These relations enable us to express all variations in condition (4.14) in terms of any one variation which may further be considered independent.

The resulting boundary condition (4.14) differs from the known ones in that the variations of the contour points are under two integrals, one integral being taken over the region and the other along the contour. Hence, in order to make use of conditions (4.14), say, for determining the load corresponding to the occurrence of the limiting equilibrium state at some points of the contour, it is necessary to assign a conceivable variation of the contour at these points. Corresponding to each particular kind of variation of the contour there is a definite value of the load.

In particular, let us consider one useful case of the variation of the contour. We rewrite Eq. (4.14) in more compact form

$$\int_C f(s)\, h(s)\, ds + \iint_D F(x, y)\, h(s)\, dx\, dy = 0, \qquad (4.16)$$

where $F(x, y)$ is a continuous function in the region D, and $f(s)$ on the line C enclosing the region D, $h(s)$ is the independent variation of some co-ordinate of the contour points, s is the arc length of the line C.

The particular case of the variation of the contour we are interested in is the following: $h(s) \equiv 0$ on the segment $0 \leqslant s \leqslant \alpha$ of the line C, $h(s)$ increases monotonically from 0 to a value k = constant on the segment $\alpha \leqslant s \leqslant \beta$, $h(s) \equiv k$ on the segment $\beta \leqslant s \leqslant \gamma$, $h(s)$ decreases monotonically from the value k to 0 on the segment $\gamma \leqslant s \leqslant \delta$, and $h(s) \equiv 0$ on the remainder of the interval of integration in (4.16).

The integral in (4.16) may be written as

$$\int_C f(s)\, h(s)\, ds = \int_\alpha^\beta f(s)\, h(s)\, ds + k \int_\beta^\gamma f(s)\, ds + \int_\gamma^\delta f(s)\, h(s)\, ds.$$

By using the mean-value theorem for the integrals on the segments $[\alpha, \beta]$ and $[\gamma, \delta]$ and passing to the limit as these segments are indefinitely diminished, we obtain

$$\lim_{\alpha\to\beta} \int_{\alpha}^{\beta} f(s)\, h(s)\, ds = \lim_{\alpha\to\beta} [(\beta-\alpha) f(s_*) h(s_*)] = 0.$$

Consequently,

$$\int_{C} f(s)\, h(s)\, ds = k \int_{\beta}^{\gamma} f(s)\, ds = k \int_{C_0} f(s)\, ds.$$

Let the abscissas of the ends β and γ be x_* and x_{**}, respectively. Further,

$$\iint_{D} F(x, y)\, h(s)\, dx\, dy =$$

$$= \int_{x_1}^{x_2} h[x, y_2(x), y_1(x)]\, dx \int_{y_1(x)}^{y_2(x)} F(x, y)\, dy =$$

$$= k \int_{x_*}^{x_{**}} dx \int_{y_1(x)}^{y_2(x)} F(x, y)\, dy = k \iint_{D_0} F(x, y)\, dx\, dy.$$

Here $y_1(x)$, $y_2(x)$ are the equations of the corresponding segments of the line C, and x_1, x_2 are their extreme abscissas.

Equality (4.16) thus transforms to

$$\int_{C_0} f(s)\, ds + \iint_{D_0} F(x, y)\, dx\, dy = 0. \tag{4.17}$$

Here the region D_0 represents a part of the region D, and C_0 is a part of the line C bounding D_0. The proposition considered shows the possibility of a stepwise variation of the contour.

By using this expression, we write down condition (4.14) for the case when C_0 is ds near some point $s = s_A$ of the contour C. The region D_0 becomes $[y_2(x) - y_1(x)]\, dx$ with $x = x_A$. At the same time we take into account relation (4.15) and choose, say, δy^* as the independent variation. The condition for the occurrence of the limiting equi-

librium state at the point A of the contour Γ then becomes

$$\Big[My^*_{,x*}\frac{c_x}{c_y}-M+$$
$$+(M_{,p}y^*_{,x*}-M_{,q})\left(\frac{c_z}{c_y}-\frac{c_x}{c_y}(z_{,x})^*-(z_{,y})^*\right)\Big]_{x=x_A}+$$
$$+\int\limits_{y_1(x_A)}^{y_2(x_A)} M_{,u_j}u_{j,\Psi}\Big[\Psi_{,x*}\frac{c_x}{c_y}+\Psi_{,y*}+$$
$$+\Psi_{,z*}\left(\frac{c_z}{c_y}-\frac{c_x}{c_y}(z_{,x})^*-(z_{,y})^*\right)\Big]dy=0. \qquad (4.18)$$

If the load obtained from this is minimized with respect to the arc length of the contour, it is possible to establish the starting point of crack propagation.

If the crack is a line $z(x)$ situated in the co-ordinate plane zx within the limits $B \leqslant x \leqslant A$, then in order to use condition (4.14) it is more convenient to represent the crack as a band of uniform width dy. Assuming that the crack grows at one end, A, we have that C_0 is dy with $x = x_A$, and the region $D_0 = (x_A - x_B)\,dy$. In this case from Eq. (4.14) we obtain

$$[M\,\delta x^*+M_{,p}(\delta z^*-(z_{,x})^*\,\delta x^*)]_{x_A}+$$
$$+\int\limits_{x_B}^{x_A} M_{,u_j}u_{j,\Psi}\left(\Psi_{,x*}\,\delta x^*+\Psi_{,z*}\,\overline{\delta z^*}\right)dx=0. \qquad (4.19)$$

If the crack propagates in the direction of the tangent to the line $z(x)$ at the point A, then $\delta z^* = dz^*$, $\overline{\delta z^*} = 0$, $\delta x^* = dx^*$ and Eq. (4.19) transforms into

$$(2\gamma-p_ju_j)_A-\int\limits_B^A p_j\frac{\partial u_j}{\partial l}\,ds=0. \qquad (4.20)$$

Here l is the crack length between the points A and B.

Thus, it turns out that for linear cracks lying on a flat surface of a body the functional Ψ represents the crack length.

Equation (4.20) may also be rewritten for the case when a crack lies on a curved surface of a body by representing ds in terms of the first quadratic form of the body surface.

The results obtained enable us to formulate the following problems of limiting equilibrium in fracture mechanics.

If the surface of a crack is known, the problem reduces to that of finding a contour of the fracture region corresponding to the equilibrium state of the body under the given load. The contour of the fracture region is then determined from Eq. (4.14) if the variations of the contour points are known.

When the surface and the contour of the fracture region are known, it is possible to find the values of critical loads corresponding to different variations, that interest us, of the co-ordinates of the contour points in (4.14), i.e., when the crack propagates in a prescribed manner (for example, either with all its contour points or some part of the contour up to an infinitesimally small one).

At the same time the above equations must be supplemented by the equations of the theory of elasticity for determining the stresses and displacements involved in (4.14).

5. SOME OTHER MODEL REPRESENTATIONS

The Irwin force criterion for crack extension and the equivalent Griffith energy criterion completely solve the question of the limiting equilibrium state of a cracked continuous elastic body. Nevertheless, there exists a number of other formulations also establishing the limiting equilibrium state of a cracked body (elastic body as a whole). Among these the best known model is that of M. Ya. Leonov and V. V. Panasyuk (1959) [155, 156, 218]. The idea of this model consists in introducing a zone of weakened bonds as a thin layer ahead of the end of an existing cut. The body possesses the following properties: (a) the maximum tensile stress nowhere exceeds the resistance to separation σ_0, (b) the stress-strain relation follows Hooke's law unless the tensile stresses reach the value σ_0, (c) there is no force interaction between the surfaces of the cut, (d) the opposite boundary surfaces of the layer of weakened bonds attract each other with a stress equal to σ_0. Consequently, within

the limits of the layer of weakened bonds Hooke's law is not fulfilled, which allows us to treat this layer either as a region of action of Van der Waals forces in atomic-layer splitting* or as a plastically deforming material. In both interpretations the mathematical formalization of the model is the same; in particular, the following boundary conditions are fulfilled on the line of a crack free from external loads:

$$\begin{aligned} &\sigma_y = 0, \quad 2v(x) > \delta_k && \text{when } |x| < l, \\ &\sigma_y = \sigma_0, \quad \delta_k > 2v(x) \geqslant 0 && \text{when } l < |x| \leqslant a, \\ &\sigma_y < \sigma_0, \quad v(x) = 0 && \text{when } |x| > a. \end{aligned}$$

Here $2l$ is the crack length, $d = a - l$ is the length of the layer of weakened bonds, the y axis is perpendicular to the crack line, and the x axis coincides with it; the origin is at the midpoint of the crack. The layer of weakened bonds is replaced by an additional cut $y = 0$, $l \leqslant |x| \leqslant a$ whose surfaces are acted on by the stresses $\sigma_y = \sigma_0$. The displacement $v(x, y = 0)$ in the y direction taking the value $\delta_k/2$ at the point $x = l$ is called the fracture (or critical) displacement and considered to be a material constant.

The limiting equilibrium state is determined by the condition

$$2v(l) = \delta_k. \tag{5.1}$$

This condition is introduced into the model as a crack extension criterion.

To define the extent of the layer of weakened bonds, it is necessary to introduce one more condition which may be the smoothness of closure of the opposite surfaces of the additional cut at its end.

Despite the identical mathematical expression, the physical significance of the two interpretations is entirely different. In the first case the surfaces of the zone of weakened bonds are planes of atoms, in the second case they are the boundaries of the plastic zone.

Consequently, in the first case there is no material between the surfaces of the additional cut, and in the second case

* The region of the descending branch of the curve of force interaction as the interatomic spacing increases.

this space is filled with a continuous medium which is in a state of plastic flow. It is natural that there is both a fundamental and a quantitative difference in the material characteristic δ_k between the two cases. This distinction is underlined by a different symbol used for the critical crack tip opening displacement due to plastic deformation, namely δ_c is written for δ_k.

It might be well to point out the fundamental difference between the Leonov-Panasyuk crack model and the Irwin model, the difference being that in the latter the length d of the plastic zone (or of the zone of weakened bonds) is exactly equal to zero over the entire range of critical crack lengths. As a consequence, δ_c is also zero. In the Leonov-Panasyuk model the length of the plastic zone tends to zero only when the critical stress tends to zero, or, what is equivalent, when the critical crack length tends to infinity. In this limiting process the results of the calculation on the two models begin to coincide.

The analytic solution shows that the plastic zone in the form of a thin line ahead of the crack tip may exist under plane-stress conditions. The discontinuity in elastic displacement between the opposite boundaries of this zone is interpreted as a neck in a thin sheet (contraction or reduction along the crack line).

Practically simultaneously with M. Ya. Leonov and V. V. Panasyuk, analytic and experimental studies of this kind of plastic zones were carried out by D. S. Dugdale (1960) [71]. He derived and experimentally confirmed the following formula for determining the length of the plastic zone in a plane with a single crack under uniform tension σ:

$$\frac{l}{a} = \cos \frac{\pi\sigma}{2\sigma_y}. \tag{5.2}$$

The crack growth criterion was not, however, introduced.

The plastic crack tip opening displacement δ_c as a material characteristic, entering into the crack growth criterion and having practical significance for assessing the quality of material, was introduced by A. A. Wells (1961) [287, 288]. He also established a relation between the material characteristics G_c and δ_c in the form

$$G_c = \delta_c \sigma_y. \tag{5.3}$$

A similar relation for the surface energy density 2γ of a solid was known before; in particular, M. Ya. Leonov and V. V. Panasyuk wrote it in terms of the parameters of the problem in their formulation as

$$2\gamma = \delta_k \sigma_0. \tag{5.4}$$

The peculiar interpretation of cuts (cracks) as non-trivial equilibrium configurations of elastic bodies with physically non-linear characteristics suggested by V. V. Novozhilov (1969) [205, 206] helps in understanding a possible cause of the formation of slit-like regions or voids. It is known that as the atomic spacing in a solid increases, the interatomic forces increase to a maximum and then fall. The equilibrium of atoms interacting according to the law of the descending branch of this curve is unstable. An atomic layer located between two other fixed layers has one position of unstable equilibrium and two positions of stable equilibrium. Hence, various causes (thermal fluctuations, local crystal imperfections, tensile stresses, say, due to an external load) produce conditions for overcoming the potential barrier in passing (through the maximum of force interaction) from a stable state of equilibrium to an unstable one. The visible display of instability reduces to a jump of an atomic layer (more precisely, of its part) to a new position, which is characteristic of the phenomenon known as the loss of stability in the large.

When an instability occurs, the spacing between layers of atoms becomes so large that one may speak of the formation of a slit-like cavity. The atoms around this cavity are in a stable position of equilibrium and ensure the existence of the body as a whole.

Moreover, V. V. Novozhilov also introduced the strength criterion

$$\bar{\sigma}_n \leqslant \sigma_0. \tag{5.5}$$

It is implied here that for infinitely large stresses and their gradients obtained from solutions of the linear theory of elasticity at some points of a body, the strength-controlling quantity is the averaged stress on a plane within one

interatomic spacing

$$\bar{\sigma}_n = \frac{1}{D^2} \int_D \sigma_n \, d\Omega.$$

The fracture criterion (5.5) is a necessary condition for the separation of one pair of atoms. But since there are neighbouring atoms close by, this criterion alone is inadequate to determine the condition for crack development.

Another fracture criterion worthy of notice is that proposed by F. A. McClintock (1958) [163], which may be written as

$$\gamma = \gamma_k \quad \text{when} \quad r = \rho_s. \tag{5.6}$$

It is supposed here that the propagation of a crack occurs when the strain γ at some distance ρ_s ahead of the crack tip reaches the limiting value γ_k. The structure parameter ρ_s may be determined, say, by the grain size, the distance between inclusions, the lattice parameter for an elastic body, etc. This criterion finds useful application in the case of a fully developed plastic zone ahead of the crack front. In particular, it offers a means of describing the subcritical crack growth for unstable loading conditions of a cracked body in a critical state.

CHAPTER II

STRESS INTENSITY FACTOR

6. INTENSITY FACTOR—BASIC CHARACTERISTIC OF A CRACKED BODY

The design of a body for strength is closely related to the determination of its state of stress. This is necessary not only for the purpose of finding a dangerous point and the components of stress at it but also for assessing the strength of material at this point since most criteria for the occurrence of a dangerous state are expressed in terms of the components of stress. For many practically important shapes of bodies and loading conditions the determination of the state of stress at a dangerous point is reduced to the calculation of stress concentration factors. These factors represent the ratio of the maximum value of any component of the stress tensor to the corresponding nominal value and are thus expressed by non-dimensional numbers. The determination of the state of stress and hence of stress concentration is a subject to which entire branches of continuum mechanics are devoted, such as elasticity theory and plasticity theory, which are presently thoroughly studied.

In the presence of a crack in a body an understanding of the nature of its propagation and thus an understanding of brittle or fatigue strength also require a knowledge of the state of stress. The problem of determining the state of stress near the crack tip differs from the usual problems of determining stress concentration in that the geometrically linearized formulation of boundary conditions and the physically linear theory of elasticity lead to infinite stresses and infinite stress gradients at the end of a thin cut. The concept of the stress concentration factor becomes meaning

less. Of course, one could try to retain the numerical non-dimensional expression for the stress concentration factor by taking into account complex details of the deformation of the material at the end of a cut. For the solution of crack problems, however, it is not at all necessary to go into the detailed processes taking place in a very small vicinity of the end of a cut [183, 190]. It is sufficient to know the nature

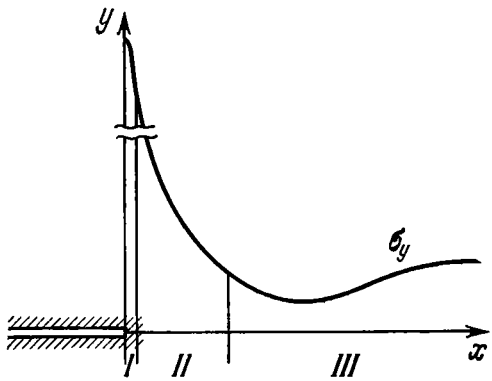

Fig. 6.1. Distribution of stress σ_y ahead of the tip of a brittle crack. *I*, region of non-linear strains and of realization of fracture mechanism; *II*, region of validity of asymptotic formulas, $\sigma_y = K/\sqrt{2\pi x}$; *III*, region of nominal stresses.

and intensity of the state of stress in a region surrounding the end of the cut together with a small volume where the fracture mechanism is concentrated (Fig. 6.1). This means a rejection of the stress concentration factor in favour of the asymptotic representation of the state of stress at the end of the cut. The radial and angular distribution for the asymptotic representation of the state of stress is independent (see Sec. 2) of the crack length, the body shape and the loading conditions. The intensity of this distribution, however, depends only on a single factor K which, in contrast, is independent of the co-ordinates of points near the end of the cut. Consequently, all fracture processes in materials are initiated and governed by the intensity of the stress

field (surrounding the crack end) through the stress intensity factor K. In contrast to the concentration factor, the stress intensity factor is a dimensional quantity (with the dimension kgf/mm$^{3/2}$ in engineering).

Actually, for most real materials there is a more or less developed plastic zone ahead of the crack tip, and even if the extent of this region reaches 20 per cent of the crack length, the stress field around the plastic zone is still determined by the asymptotic formulas. Hence, both the size of the plastic region and the intensity of plastic strains in it are entirely controlled by the stress intensity factor K and the properties of the material. It should only be mentioned that for the principles of the linear mechanics of crack development to be valid, in calculating the factor K the length (or half-length) of the crack must artificially (fictitiously) be increased by half the length of the plastic zone [165]. This procedure is known as Irwin's plastic correction. In plane stress the crack is increased in one way by the amount

$$r_y = K_c^2/2\pi\sigma_{0.2}^2. \tag{6.1}$$

Formula (6.1) is approximate; the exact value of the length of the plastic zone is analytically obtained only for antiplane strain.

From the above discussion one can see the dominant role of the stress intensity factor in fracture mechanics, a fact which accounts for the consideration of the stress intensity factor as the subject of analytic or experimental investigation.

Tables of analytic expressions for stress intensity factors for bodies of various configurations and different loading conditions are given in the books [33, 54, 85]. A major portion of the material presented here is devoted to the study of the influence of this factor on the laws of crack growth and also to the determination of the stress intensity factor in a variety of new problems.

7. BASIC NUMERICAL METHODS FOR CALCULATING THE STRESS INTENSITY FACTOR *

As is known, the study of brittle fracture is connected with the investigation of the laws of crack development at average stresses below the yield point. One of the most fruitful approaches to the assessment of the possibility of brittle fracture is that based on the consideration of the stress intensity factor. For actual structures containing cracks the derivation of analytic solutions involves considerable mathematical difficulties. Hence, the calculation of the stress intensity factor requires the use of numerical methods. At present one of the most general methods having the least limitations is the finite element method.

In the last few years the finite element method has found extremely wide application in the solution of various problems in structural mechanics, elasticity, and other fields. In this connection we considered it advisable to acquaint the reader with basic procedures of realizing the finite element method in computerized design (see Appendix B). Below we shall discuss some of the most interesting works where the finite element method is applied directly to the calculation of the stress intensity factor.

The methods of calculating the stress intensity factor may be divided into methods of calculation using networks of ordinary elements (which will be termed basic) and special elements. In the latter case use is made of finite elements among which there is one or more elements whose structure takes account of a crack. The basic methods of calculating the stress intensity factor may be classified as follows: the direct method, the linear integration method, the flexibility method. Further discussion will be restricted to the case of the plane problem.

1. The direct method of calculating the stress intensity factor. This method is most obvious and is based on the fact that the stress distribution for the elastic solution near the crack tip is defined, as noted above, by a formula whose

* Secs. 7, 8 and Appendices B, C are written with the participation of G. P. Nikishkov.

form is determined from (2.17)

$$\sigma_{ij} = \frac{K}{\sqrt{2\pi r}} f_{ij}(\theta). \tag{7.1}$$

Knowing the stress distribution around the crack tip, we can determine the value of K (similarly, from (2.18) we can determine K having information on the displacement field).

As calculations show, the computation of the factor K by this method requires a very fine network of elements. At the same time the most accurate values of the stress intensity factor are obtained if the elements used for its determination are immediately adjacent to the crack tip. Many questions then arise, however. For example, if displacements are used, then for the same cracked body different values of K are obtained when it is determined from the component u or v. In the work [38] it is shown that more accurate values of the stress intensity factor are obtained if displacements perpendicular to the crack direction are taken. For example, for plane strain the stress intensity factor K_I is determined in this case as follows [see formula (2.18)]:

$$K_I = \frac{\left(\frac{2\pi}{r}\right)^{1/2} Gv}{\sin\frac{\theta}{2}\left[2 - 2\nu - \cos^2\frac{\theta}{2}\right]}. \tag{7.2}$$

Another important point is the choice of a network of elements. How small must the elements be? What should be the nature of the variation of the size of elements with the distance from the crack tip? We shall discuss some works which give suggestions for the solution of these problems.

The author of the work [286] considered the problem of the extension of a rectangular plate with a central crack for which an analytic solution is available. At first use was made of 470 elements for idealization, most of which were rectangular. The network was of finer mesh at the crack tip. The non-dimensional values found for K_I varied from 1.5 to 18.5, its actual value being $K_I = 5.82$. The author indicates that if a stress component is taken for determin-

ing K_{I} and the elements are chosen in the range $0 < \theta < < 90°$, closer approximations to the exact values may be obtained, but still not wholly satisfactory. It is supposed that in determining K_{II} the best results may be reached with the use of τ_{xy}.

In the above-mentioned work [38] the computations were performed in the same way, but the region was automatically divided into elements, which in this case were of much smaller size. The smallest elements at the crack tip were by a factor of 100 to 500 less than in [286]. The authors calculated the factor K_{I} for different values of r in the direction $\theta = \text{constant}$. For the problem considered this relation was practically linear. The value of K_{I} was extrapolated to the case $r = 0$. The results obtained were good (an error of 3 to 5 per cent), but the labour and cost of calculations were considerably augmented. It should be noted that even in this case the question as to which component of stress or displacement is to be taken for calculations remains undecided, particularly in those problems where the exact value of the required quantity is not known.

A similar approach is described in [2]. To determine K_{I}, a displacement field was found and extrapolation was made to the case $r = 0$. Particular emphasis was placed upon the choice of division of the region under investigation. The calculations were carried out for five networks. The interesting thing is that the nature of the variation of the size of elements near the crack tip corresponds to the stress gradient. For triangular elements, this may be illustrated by a simple reasoning. Since the usual triangular element has all components of displacement constant over its area, the size of the elements must be chosen so that the stress curve $(\sigma - r^{-1/2})$ will be best approximated by line segments. To accomplish this, the size of the elements must vary approximately as $r^{1/2}$ (the components of displacement are proportional to the same quantity). This distribution of the size of the elements is obtained automatically if the nodes of the elements are distributed in an arithmetical progression in any direction from the crack tip. For analysis the authors have chosen a network such as shown in Fig. 7.1. The characteristic properties of this network are that the variation of the size of the elements corresponding to the

stress gradient is observed not over the entire network but only in a certain region around the crack tip and, besides, very large structural elements are employed far from the crack tip. The highest accuracy obtained using networks of this type is about 99 per cent.

In [133] the authors applied one more procedure which enabled them to obtain a reasonable accuracy by using the method in question. In this case the solution is carried out twice by the finite element method. The solution is first

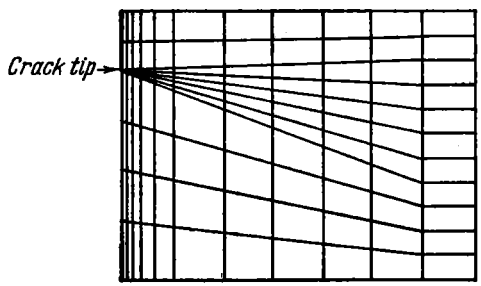

Fig. 7.1. Network of elements whose dimensions correspond to the nature of the stress variation near the crack tip.

constructed with a coarse network of elements, and then a small region around the crack tip is isolated from the body under consideration, which is idealized by finer finite elements. Its analysis is also carried out by the finite element method, with the quantities found in the first solution as the boundary conditions. The authors obtained good agreement with theoretical results in solving the problem of a centrally cracked plate. In this case 339 rectangular elements were used for a coarse network, and 798 elements for a fine network.

2. Linear integration method. J. R. Rice [241] showed that in the elastic range the value of the contour integral

$$J = \int_{\Gamma} \left(W_0\, dy - T \frac{\partial u}{\partial x}\, ds \right) \tag{7.3}$$

is proportional to the square of the stress intensity factor. Here Γ is an arbitrary contour enclosing the crack tip, W_0

is the strain energy density, T and u are the load and displacement vectors, respectively.

For plane stress, J and K are related by the equation

$$K^2 = JE.$$

The data of numerical verifications show that this method provides much the same accuracy as the direct method; it is subject to the same limitations.

3. The energy or flexibility method. The method consists in determining the elastic energy W for two or more equilibrium states of a cracked body. The quantity W may be calculated by the formula following from Clapeyron's theorem

$$W = \frac{1}{2} \sum_i F_i^e u_i. \tag{7.4}$$

Here F_i^e are the generalized external forces, u_i are the corresponding nodal displacements.

Subsequently the elastic energy release rate is calculated by formula (3.5).

The factors G and K are related by the well-known equations (3.8) and (3.9).

The flexibility method was used to determine K in [286] and [2]. In [286] the network consisted of 470 elements. In this case the direct method failed to give acceptable results (with no choice of stresses or extrapolation to $r = 0$), and in the case of applying the flexibility method the error was less than 2 per cent.

The authors of the paper [2] obtained an accuracy of about 99 per cent by the direct method using a very fine network, while the energy method gave an accuracy of better than 99.9 per cent.

Comparison of the foregoing methods of calculating the stress intensity factor gives conclusive evidence of advantages of the flexibility method over the other two. This method is simple in its computational structure, it does not require the introduction of fine elements or the local fineness of the mesh, permits the calculation to be easily carried out for a wide range of crack lengths, and provides a far better accuracy. Even though in [2] it is assumed that if an automatic mesh generation program is available one

can obtain, in the case of the direct method, an accuracy that will even exceed that of the flexibility method, in this case, too, the flexibility method is more convenient and efficient for practical purposes.

4. Special methods for determining the stress intensity factor. As already noted, the special methods of determining K are characterized by the fact that in solving problems with the use of the finite element method the idealization

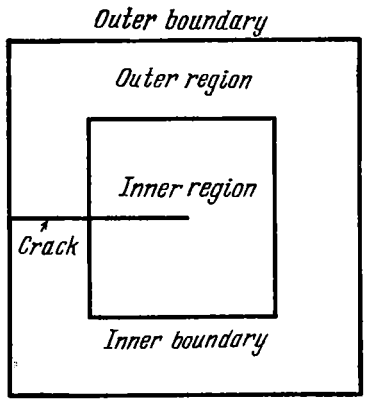

Fig. 7.2. Special element containing the crack tip.

contains at least one special element whose structure takes account of the presence of a crack. A crack represents an infinitely sharp cut, the exact distribution of stress around which cannot be found using a network of usual structural elements. The actual stress distribution may be approximated at the expense of mesh refinement, but the computation time is then considerably augmented.

In [285] a method is proposed which possesses all the advantages of the finite element method in the representation of the structure. A special crack tip element is introduced with a theoretically exact stress field near the crack tip. This domain is then surrounded by a transition region to the usual network of finite elements.

The proposed special element (Fig. 7.2) consists of two regions. In the inner region the distribution of stress and displacement is determined by the usual asymptotic formulas

of fracture mechanics, which involve the stress intensity factors K_{I} and K_{II} as factors of proportionality. The outer region consists of the usual finite elements designed to satisfy the conditions of equilibrium and compatibility at the boundary between the two regions.

We write down an expression for the stiffness matrix of the special element for an isotropic body in plane strain.

The displacements near the crack tip may be expressed by means of relations (2.18) and (2.21). These formulas

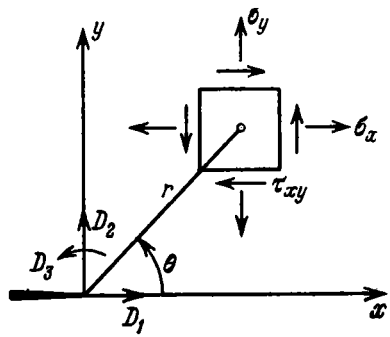

Fig. 7.3. Co-ordinate system near the crack tip.

are given in accordance with the co-ordinate system shown in Fig. 7.3. The displacement of any point in the inner region may be expressed as a function of its position, the stress intensity factors K_{I} and K_{II}, and the components of displacement of the body as a whole D_1, D_2, and D_3*

$$\begin{Bmatrix} u_x \\ u_y \end{Bmatrix} = \begin{bmatrix} u_{x\mathrm{I}} & u_{x\mathrm{II}} & 1 & 0 & -y \\ u_{y\mathrm{I}} & u_{y\mathrm{II}} & 0 & 1 & x \end{bmatrix} \begin{Bmatrix} K_{\mathrm{I}} \\ K_{\mathrm{II}} \\ D_1 \\ D_2 \\ D_3 \end{Bmatrix}$$

or

$$U_{xy} = MU_S. \tag{7.5}$$

* The square brackets indicate a matrix, and the braces a column matrix.

Here u_{xI}, u_{yI} are the displacements of the point for a unit value of K_I from formula (2.18), u_{xII}, u_{yII} are the corresponding values from (2.21). The matrix U_S plays the role of a generalized displacement matrix.

We introduce a generalized force matrix P'_S which corresponds to the matrix U_S. If a matrix S_S is introduced the ijth element of which is calculated as the work done by the stress due to the unit value of the jth component of U_S in the displacement field due to the unit value of the ith component of U_S, P'_S is determined by the expression

$$P'_S = S_S U_S. \tag{7.6}$$

The non-zero elements of S_S are calculated by exact or numerical integration.

For the outer region, the stiffness matrices may be summed to obtain an expression relating the nodal forces P_m and the displacements U_m at the outer and inner boundaries

$$S_m U_m = P_m. \tag{7.7}$$

If there are nodes that lie outside these boundaries, their displacements may be eliminated by Gauss-Jordan partial elimination. The quantities pertaining to the inner boundary will be identified by the subscript i, and those pertaining to the outer boundary by the subscript o; then

$$U_m = \begin{Bmatrix} U_o \\ U_i \end{Bmatrix}, \quad P_m = \begin{Bmatrix} P_o \\ P_i \end{Bmatrix}.$$

The compatibility at the inner boundary is only approximate since the variation of the displacement field at the edge of the inner region differs from that along the boundaries of the outer region. The compatibility conditions may be more accurately satisfied by increasing the number of nodes. If, now, the co-ordinates of the nodes at the inner boundary are substituted successively in Eq. (7.5), the following matrix relation is obtained:

$$U_i = BU_S. \tag{7.8}$$

Here B is the matrix of the transformation from the generalized to the nodal displacements.

Here

$$c_{1,p}=a_{1,p}+ib_{1,p},\quad c_{2,p}=a_{2,p}+ib_{2,p}.$$

The stresses and displacements are determined from the well-known relations (2.5), which may be represented in a slightly modified form as

$$\begin{aligned}\sigma_x+\sigma_y&=2\left[\Phi(z)+\overline{\Phi(z)}\right]=4\,\mathrm{Re}\left[\Phi(z)\right],\\ \sigma_y-i\tau_{xy}&=\Phi(z)+\Omega(\bar z)+(z-\bar z)\overline{\Phi'(z)},\\ u+iv&=\frac{1}{2\mu}\left[\varkappa\varphi(z)-\omega(\bar z)-(z-\bar z)\overline{\Phi(z)}\right].\end{aligned}\tag{7.13}$$

Here the following relations have been introduced (c_3 reflects the displacement of the body as a whole):

$$\omega(z)=\int_0^z\Omega(\zeta)\,d\zeta+c_3,\quad c_3=a_3+ib_3.$$

The stress intensity factors are determined by the following expression:

$$K_{\mathrm{I}}+iK_{\mathrm{II}}=\lim_{x\to0+,\ y=0}\left[\sqrt{2\pi x}\,(\sigma_y+i\tau_{xy})\right]=2\bar c_{1,0}.\tag{7.14}$$

The conditions for the equilibrium of an element are satisfied by the choice of relations (7.12). The condition for compatibility of displacements between the elements with the crack and the usual elements is fulfilled if the displacement field in the latter is chosen in the same form, which, however, is very difficult and inconvenient. It is therefore natural that the compatibility condition is not fulfilled and hence no monotonic convergence of the solution can be expected.

The development of the stiffness matrix is a formidable task when the special element is of complex shape. It is considerably simplified when the element is a regular polygon symmetrical about the crack.

The stress field chosen in the usual elements is the simplest one, i.e., uniform. The simplest special element is a regular triangle symmetrical about the crack and having four nodes.

Limitations of this method are that the stiffness matrix of the special element is very difficult to develop and that

in the analysis of a body with a symmetrical crack it is necessary to make idealization of the whole model and not only of the symmetrical part alone.

5. Determination of stress intensity factors by the boundary collocation method. The boundary collocation method does not provide such a general approach to the solution of problems as the finite element method. The latter method enables one to consider problems with curvilinear cracks, with complex body geometry and various loading conditions.

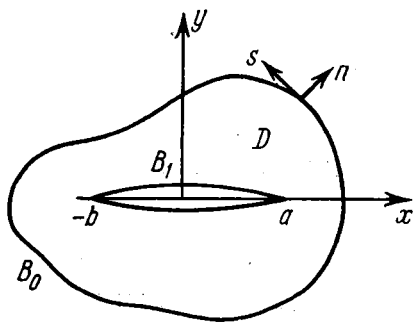

Fig. 7.6. Flat body with a crack in the boundary collocation method.

The boundary collocation method is applicable for a narrower range of problems. But in problems where it can be applied, the boundary collocation method offers undeniable advantages of greater accuracy, less input preparation, and a smaller system of linear equations to be solved.

Consider the boundary collocation method which can be applied for the analysis of arbitrary flat bodies of finite dimensions containing an interior through-thickness straight crack (Fig. 7.6) [293].

As is known [200], the representation of stresses and displacements by two analytic functions, $\Phi(z)$ and $\Psi(z)$, of the complex variable $z = x + iy$ leads to a general method of solving plane problems in elasticity [see relations (2.5)]. If the stresses are chosen in this form, the equilibrium equations are satisfied identically. It remains to satisfy the boundary conditions and supplementary compatibility con-

ditions for a doubly connected body

$$\varkappa \oint \Phi(z)\, dz - \oint \Omega(\bar{z})\, d\bar{z} = 0. \tag{7.15}$$

The complex functions $\Phi(z)$ and $\Omega(z)$ are represented as follows:

$$\Phi(z) = F_1(z)\, G(z) + F_2(z), \quad \Omega(z) = F_1(z)\, G(z) - F_2(z),$$
$$F_1(z) = c_0 + c_1 z + \ldots + c_n z^n, \quad F_2(z) = d_0 + d_1 z + \ldots + d_m z^m,$$
$$G(z) = [(z - a)\,(z + b)]^{-1/2}. \tag{7.16}$$

Here c_i and d_i are arbitrary complex coefficients.

By using the Airy stress function $U(x, y)$ we can write, from (2.4) and (2.5),

$$U = \operatorname{Re}[\bar{z}\varphi(z) + \chi(z)],$$
$$\frac{\partial U}{\partial x} + i\,\frac{\partial U}{\partial y} = \varphi(z) - z\overline{\varphi'(z)} + \psi(z).$$

Here, as always,

$$\chi(z) = \int \psi(z)\, dz,$$
$$\psi(z) = \int \Psi(z)\, dz,$$
$$\Psi(z) = \overline{\Omega}(z) - [z\Phi(z)]'.$$

The Airy stress function is used to obtain an approximate solution in the case of flat plates with an interior straight crack [293]. By suitably selecting the constants involved in this function it is possible to satisfy exactly the supplementary compatibility condition. The boundary conditions on the boundary of the body $B = B_0 + B_1$ are satisfied in an approximate manner, i.e., at a finite number of points on B_0. The approximate solution will approach the exact solution as the number of collocation points is increased if they are properly chosen.

One of the following three conditions may be prescribed on the boundary of the region under consideration:

(a) $\frac{\partial^2 U}{\partial s^2}$ and $\frac{\partial^2 U}{\partial n\, \partial s}$;

(b) $\frac{\partial U}{\partial n}$ and $\frac{\partial U}{\partial s}$;

(c) U and $\frac{\partial U}{\partial n}$

The most accurate results are obtained if conditions are imposed at boundary points on the value of the Airy func-

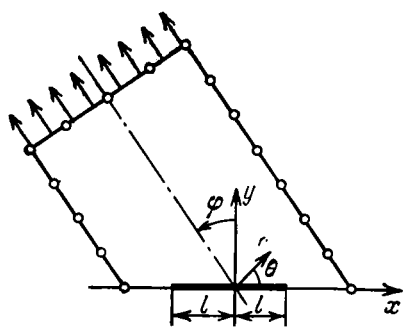

Fig. 7.7. Distribution of collocation points in a strip with an inclined crack under tension.

tion and its normal derivative [case (c)]. The chief advantages of using these boundary conditions are stability, simplicity, and relative independence of results with respect to the number of collocation points.

The stress intensity factors can be obtained from the following relation (z_1 is the co-ordinate of the crack tip):

$$K_{\mathrm{I}} - iK_{\mathrm{II}} = (8\pi)^{1/2} \lim_{z \to z_1} (z - z_1)^{1/2} \Phi(z). \qquad (7.17)$$

For the crack tip located at the point $y = 0$, $x = a$ this relation becomes

$$K_{\mathrm{I}} - iK_{\mathrm{II}} = \left(\frac{8\pi}{a+b} \right)^{1/2} (c_n a^n + c_{n-1} a^{n-1} + \ldots + c_0).$$

The stability of the solution was investigated by considering the extension of a strip with an inclined crack (Fig. 7.7).

Since, by symmetry, the stress distribution has an angular period of π, the following coefficients must be set equal to zero:

$$c_i = 0 \text{ for } i = 0, 2, 4, \ldots,$$

$$d_i = 0 \text{ for } i = 1, 3, 5, \ldots;$$

the upper half of the specimen is considered and collocation points are distributed periodically over the boundary.

If conditions are imposed on U and $\partial U/\partial n$, the result depends only slightly on the number of collocation points. Thus, as the number of collocation points increased from 14 to 28, the change in stress intensity factors was less than 0.5 per cent. When collocating on $\partial U/\partial n$ and $\partial U/\partial s$ the stability is not nearly as good (the maximum deviations from the value obtained are more than 10 per cent), but the average values do not differ greatly from the result of collocation with respect to U and $\partial U/\partial n$. If conditions are imposed on the second derivatives, the stability is even poorer. Thus, in all cases it seems desirable to carry out collocation on the functions U and $\partial U/\partial n$.

8. CALCULATION OF THE STRESS INTENSITY FACTOR FOR DOUBLE CANTILEVER BEAM SPECIMENS BY THE FINITE ELEMENT METHOD

To demonstrate numerical methods for calculating the stress intensity factor, we consider the problem of a double cantilever beam under two types of loading as shown in Fig. 8.1. Based on the considerations which have been outlined in Sec. 7, we use the flexibility method. The idealization (see Appendix B) of the computational scheme is carried out by dividing the symmetrical part of the specimen into equal rectangular elements.

The flexibility method uses the formula due to G. R. Irwin [118] for the calculation of energy release during crack growth

$$G = \frac{P^2}{2} \frac{d\lambda}{dl}. \tag{8.1}$$

Here λ is the flexibility of the specimen defined by the expression $\Delta = \lambda P$, Δ is the displacement of the point of application of the force P,

To calculate the derivative in expression (8.1), it is necessary to know the flexibility for cracks of different length.

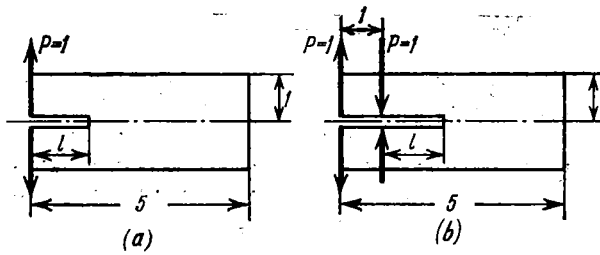

Fig. 8.1. Double cantilever beam specimen loaded by a wedging force (*a*) and a couple (*b*).

The change in crack length was produced by successively inhibiting displacements perpendicular to the crack line.

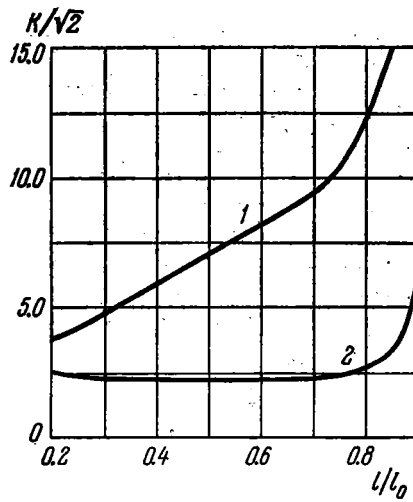

Fig. 8.2. Relation between the stress intensity factor and the crack length for a double cantilever beam specimen. *1*, loading by a wedging force; *2*, loading by a couple ($P = 1$, $t = 1$).

The increment of the crack length is equal to one of the linear dimensions of the element. A direct calculation of λ can be avoided by substituting $\lambda = \Delta/P$ in formula (8.1).

The stress intensity factor is then, by formula (3.8),

$$K=\left(\frac{EG}{1-\nu^2}\right)^{1/2}=\left[\frac{E}{2t(1-\nu^2)}\frac{\partial}{\partial l}\left(\sum P_i u_i\right)\right]^{1/2}. \quad (8.2)$$

Here P_i are the nodal forces, u_i are the corresponding nodal displacements, t is the specimen thickness.

The program realizing this computation is given in Appendix C. The relation between the stress intensity factor and the crack length when the specimen is idealized by 60 elements is shown in Fig. 8.2 ($\nu = 0.3$).

9. THE METHOD OF SECTIONS FOR AN APPROXIMATE CALCULATION OF THE SIRESS INTENSITY FACTOR

As already mentioned, one of the basic problems dealt with in theoretical fracture mechanics in relation to fracture design is the determination of the stress intensity factor.

We shall show the possibility of applying the method of sections, a method well known in structural mechanics, to calculate the stress intensity factor [178, 186]. Consider a plane crack problem. We isolate a part of the body by an imaginary section (which may be a broken one) so that this section passes through the crack tip. We further write down the conditions for the equilibrium of external and internal forces exerted on the remaining part of the body. In setting up these conditions we take into account the asymptotic expressions for stresses (2.17) or (3.7).

The additional force arising at the crack tip from an increase in stresses is equal to

$$\int_0^a \sigma_\theta \, dr,$$

where a can be determined from the condition that σ_θ at $r = a$ is equal to the nominal stress.

Thus, the equilibrium condition expresses the fact that the force not transmitted through the crack line is compensated for by an additional force due to the stress concentration at the crack tip. Below are given examples of the calculation of the intensity factor using the method of sections.

Example 1. The Griffith problem: an infinite plate with a single crack of length $2l$ is extended by a uniformly distributed stress σ perpendicular to the crack line.

The force not transmitted through the crack is $2\sigma l$, and the increased stress at the ends of the crack produces an additional force equal to $2\int_0^a \sigma_\theta dr$. The value of a is found from the condition

$$\sigma_\theta (r = a) = \sigma,$$

i.e.,

$$K/\sqrt{2\pi a} = \sigma,$$

from which

$$a = K^2/2\pi\sigma^2.$$

The equilibrium condition becomes

$$2\sigma l - 2\int_0^a \sigma_\theta \, dr = 0.$$

Substituting the value

$$\sigma_\theta = K/\sqrt{2\pi r},$$

we find the stress intensity factor

$$K = \sigma\sqrt{\pi l}$$

which coincides with its exact value.

Example 2. The extension of a plate of finite width with a central crack. We evaluate the extent of the stress field disturbed by the presence of the crack. For an infinite plate the size of the disturbed zone ahead of the crack tip is $a = l/2$. Consequently, if the width of the plate is $b \geqslant 2l + 2a = 3l$, the finiteness of its width does not affect the intensity factor $K = \sigma\sqrt{\pi l}$.

If $b < 3l$, from the equilibrium condition

$$\sigma b - \sigma (b - 2l) - 2\int_0^a \sigma_\theta \, dr = 0 \quad \left[a = \frac{(b-2l)}{2}\right]$$

we find the intensity factor

$$K=\sigma\sqrt{\pi l}\sqrt{\frac{l}{(b-2l)}}.$$

The well-known formula of G. R. Irwin [118] taking account of the finiteness of the width is of the form*

$$K=\sigma\sqrt{\pi l}\sqrt{(b/\pi l)\tan(\pi l/b)}.$$

These two relations are shown in Fig. 9.1 from which it is seen that the approximate method gives a too high value compared with Irwin's formula.

Example 3. An infinite plate with a crack is loaded by two equal and opposite forces P, the distance between the points

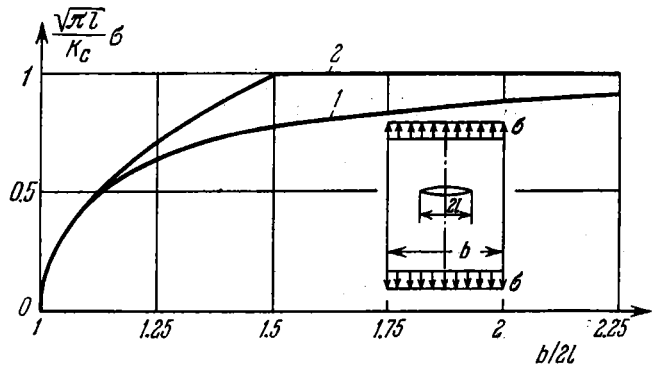

Fig. 9.1. Critical stress in a strip with a central crack under tension. *1*, Irwin's 'tangent' formula; *2*, formula in the method of sections.

of application being $2L$. The straight crack is situated along the line of symmetry. A section is passed through a straight line coincident with the crack line. The equation of equilibrium is

$$\int_{-l}^{l} p(x)\,dx=2\int_{0}^{a}(K/\sqrt{2\pi r})\,dr,$$

$$p(x)=\frac{PL}{2\pi(x^2+L^2)}\left[1-\nu+2(1+\nu)\frac{L^2}{x^2+L^2}\right]. \qquad (9.1)$$

* A comparison of various formulas for the stress intensity factor of a crack in a strip of finite width under tension may be found, for example, in [85].

Here $p(x)$ is the stress at the location of the crack in a sound body [162]. The upper limit of integration is found from the equality $\frac{K}{\sqrt{2\pi a}} = p(l)$. Upon integration we obtain ($c = l/L$)

$$K = \frac{P}{\sqrt{2\pi L}\left(1+\frac{c^2}{4}\right)} \left\{ \left[2\left(1+\frac{c^2}{4}\right) \arctan\frac{c}{2} + \right.\right.$$

$$\left.\left. + (1+\nu)\frac{c}{2} \right] \left[1-\nu+2(1+\nu)\frac{4}{4+c^2} \right] \right\}^{1/2}.$$

The stress intensity factor corresponding to the exact solution is of the form [15]

$$K = \frac{P}{\sqrt{\pi L}\,(4+c^2)^{3/2}} (6+2\nu+c^2)\sqrt{2c}.$$

By comparison of the approximate and exact solutions (Fig. 9.2) it will be seen that the approximate solution gives

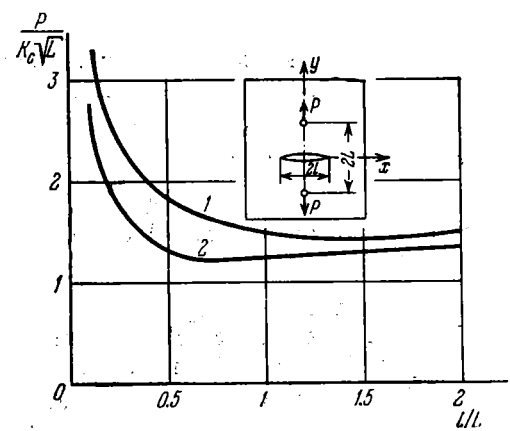

Fig. 9.2. Critical force for a plane loaded in tension by two concentrated forces symmetrically applied on both sides of the crack. *1*, exact solution; *2*, approximate solution by the method of sections.

a too low value for the forces (the result is some 20 per cent lower than the exact value) for a given c, while the qualitative picture is the same: up to a certain value of the length (determined by the minimum of the curve) the equilibrium

state of the cracked body is unstable (the descending branch of the curve), but as c increases, the cracked body passes into a stable state (the ascending branch). The forces for the limiting equilibrium state are obtained from the usual condition $K = K_c$.

Example 4. Find the critical stress for an infinite plane weakened by two cracks situated along the real axis. The lengths of the cracks are $2l_1$ and $2l_2$. The uniform tensile stress is directed perpendicular to the crack line. We pass a section along this line and write down the conditions of equilibrium for each half of the crack separately.

For the outer ends of the cracks we have

$$\sigma l_1 = \int_0^{a_1'} \left(\frac{K'_{(1)}}{\sqrt{2\pi r}}\right) dr, \quad \sigma l_2 = \int_0^{a_2'} \left(\frac{K'_{(2)}}{\sqrt{2\pi r}}\right) dr,$$

$$a_1' = \frac{K_{(1)}^2}{2\pi\sigma^2}. \qquad a_2' = \frac{K_{(2)}^2}{2\pi\sigma^2}.$$

From this we obtain the stress intensity factors

$$K'_{(1)} = \sigma\sqrt{\pi l_1}, \quad K'_{(2)} = \sigma\sqrt{\pi l_2}.$$

For the inner ends of the cracks

$$\sigma l_1 = \int_0^{a_1} \sigma_{\theta(1)}\, dr, \qquad \sigma l_2 = \int_0^{a_2} \sigma_{\theta(2)}\, dr.$$

The stress intensity factor depends on the distance c between the inner ends of the cracks. When $c = a_1 + a_2$, the values of a_1 and a_2 are found from the condition $\sigma_{\theta(1)} = \sigma_{\theta(2)}$ or $K_{(1)}/\sqrt{2\pi a_1} = K_2/\sqrt{2\pi a_2}$. From this we obtain $a_1 = cl_1/(l_1 + l_2)$. The stress intensity factors are then

$$K_{(1)} = \sigma\sqrt{\pi l_1}\sqrt{(l_1+l_2)/2c}, \quad K_{(2)} = \sigma\sqrt{\pi l_2}\sqrt{(l_1+l_2)/2c}.$$

Cracks begin to grow from the tip where the stress intensity factor is the highest.

If the distance between the cracks is great, viz. $c \geqslant 0.5\,(l_1 + l_2)$, the cracks are independent of each other.

When the crack lengths are equal, $l_1 = l_2 = l$, the exact solution gives [34, 218] (a prime corresponds, as before, to the outer ends)

$$K' = \frac{\sigma}{\sqrt{\pi}} \left\{ \frac{\sqrt{\left(\frac{c}{2}+2l\right)\left[\left(\frac{c}{2}+2l\right)^2 - \frac{c^2}{4}\right]}\, F(k)}{\left(\frac{c}{2}+2l\right)^2 [F(k) - E(k)]} \right\}^{-1},$$

$$K = \frac{\sigma}{\sqrt{\pi}} \frac{(c+4l)^2 E(k) - c^2 F(k)}{4\sqrt{c^2 l + 2cl^2}}.$$

Here the modulus of the elliptic integrals of the first and second kind (F, E) is

$$k = \sqrt{\left(\frac{c}{2}+2l\right)^2 - \frac{c^2}{4}} \left(\frac{c^2}{2}+2l\right)^{-1}.$$

Example 5. A beam of rectangular section and unit thickness is bent by a moment M. A crack is on the tension side and perpendicular to the axis of the beam. If the crack is entirely within the tension zone (does not approach the surface or touch the neutral axis), the condition for no longitudinal force is of the form

$$\int_{y_2}^{y_1} \frac{M}{J} y\, dy = \int_{y_1}^{y_1+a} \frac{K_{(1)}\, dy}{\sqrt{2\pi(y-y_1)}} + \int_{y_2-b}^{y_2} \frac{K_{(2)}\, dy}{\sqrt{2\pi(y_2-y)}}.$$

Here y_1 and y_2 are the distances from the neutral axis to the upper and lower ends of the crack, respectively, J is the moment of inertia of the sound cross section of the beam with respect to the neutral axis.

The values of a and b are determined from the conditions

$$\frac{K_{(1)}}{\sqrt{2\pi a}} = \frac{M}{J} y_1, \qquad \frac{K_{(2)}}{\sqrt{2\pi b}} = \frac{M}{J} y_2.$$

The intensity factor at the crack tip nearest to the free surface of the beam is

$$K_{(1)} = \frac{M}{J} \sqrt{\pi l} \sqrt{y_1 y_2/2} \qquad (l = y_1 - y_2).$$

Meanwhile the exact solution is of the form [217]

$$K_{(1)} = \frac{M}{J} \sqrt{\pi l}\, (3y_1 + y_2)/4\sqrt{2}.$$

From these examples it is seen that the proposed method can be applied to the calculation of the strength of bodies with various positions of cracks and applied loads.

Taking into account an increasing demand of modern engineering for an estimation of the strength of cracked bodies, it should be recognized that the complex methods of the mathematical crack theory must be supplemented by simpler, even though less accurate, design procedures in which the lower accuracy of the calculation is warranted by a smaller amount of work involved.

10. SOME MATERIAL CHARACTERISTICS USED FOR THE EVALUATION OF CRACK PROPAGATION RESISTANCE

At present there is a wide variety of experimental methods and corresponding characteristics of a material (more precisely, of a specimen of this material) for a qualitative assessment of the material as to its capacity to arrest the main crack. Here only two characteristics will be considered which are not only of qualitative interest (for the purposes of comparison and selection of materials and technologies), but also of computational interest. The latter means that by using such a characteristic it is possible, on the basis of appropriate fracture criteria, to carry out design calculations involving the determination of the required factors of safety. These characteristics are the critical stress intensity factors K_c and K_{Ic}, respectively in plane stress and in a three-dimensional state of stress in the case of plane strain, the critical crack tip opening displacement (fracture displacement) δ_c.

The fracture toughness G_c (G_{Ic}) is proportional to the critical stress intensity factor K_c (K_{Ic}) [see formulas (3.8) and (3.9)]. Henceforth, G_c (G_{Ic}) will therefore not be discussed as independent characteristics, though it should be recognized that the correspondence between G_c and K_c may not be complete.

These characteristics are determined for specimens with cracks and they supplement the information on the material obtained for smooth specimens.

In perfectly brittle fracture both K and K_c are naturally independent of the characteristics of the material's resis-

tance to plastic deformation. In quasi-brittle fracture the above factors depend on these characteristics. As stated above [see (6.1)], this dependence [85] is reflected analytically in the fact that when calculating K the crack length is artificially increased by an amount r_y (one half the extent of the plastic zone in the crack direction) equal to

$$r_y = K_c^2/2\pi\sigma_{0.2}^2 \text{ (plane stress)},$$

$$r_y = K_{Ic}^2/6\pi\sigma_{0.2}^2 \quad (\text{sometimes } r_y = K_{Ic}^2/4\sqrt{2}\,\sigma_{0.2}^2)$$

(three-dimensional state of stress in plane strain).

With this increased fictitious crack length $l + r_y$, the elements of the elastic and elastic-plastic solutions coincide in the elastic region.

The experimentally determined values of K_c relate to quasi-brittle fracture and hence these values reflect the dependence of K_c on the plastic properties of materials. This must be kept in mind when designing components with cracks, and therefore the crack length (sometimes half-length) in the analytic expression for K should be increased by r_y. The above correction is more important in the case of a single static loading under plane stress conditions and is less important in fatigue, since in the latter case the size of the plastic zone is relatively small. The correction can be neglected in the case of a three-dimensional state of stress under plane strain conditions.

In designing components with cracks (which may be absent, but whose existence is conceivable) it is necessary to have a certain factor of reliability in case of their occurrence. If, for example, we have a material with $K_c = 200$ kgf/mm$^{3/2}$ and it is reliable in operation for a factor of safety $n = \sigma_u/\sigma_{max} = 3$, the use of another material having $K_c = 400$ kgf/mm$^{3/2}$ makes it possible to reduce the factor of safety. The value to which it can be reduced depends on the operating conditions, namely the number of repetitions of loads and their level, the amount of elastic energy stored in the system, the presence of a corrosive environment, and other factors. A quantitative determination of the degree to which the factor of safety can be reduced must be the objective of fracture-design methods a possible variant of which is given in Sec. 25.

In an experimental determination of the value of K_c one can either measure it directly on a test specimen by means of gauges bonded ahead of a growing crack or adjacent to it, or else, after measuring the critical loads and the crack length, use the formula for the value of K in a body having the shape of the test specimen. The latter method is the one most commonly used. It should be added that the experimental determination of K_c usually involves the measurement of the length of a growing central crack in a flat specimen in a subcritical state.

Considerable subcritical crack growth is possible only if the thickness of a flat specimen is sufficiently small compared with its width, the deformation across its thickness is not completely constrained and appreciable plastic deformation takes place in subsurface layers of the specimen during the subcritical fracture. The intensity and extent of this deformation vary greatly with the specimen thickness and in consequence the values of G_c determined on specimens of different thickness will differ considerably even for a given environment and a given temperature.

For a valid experimental determination of K_c (G_c) the plastic deformation must not be excessive. Thus, when the plastic deformation spreads through the whole thickness, the plastically deforming volume at the crack tip is so large that the asymptotic formulas can no longer be used. On the basis of experimental verifications it was found approximately that an allowable plastic strain occurs at the crack tip if the fracture stress at the net section of the specimen does not exceed 0.8 of the yield stress of the material determined on smooth specimens. The critical crack length used for the calculation of K_c is not, in this case, equal to the experimentally determined value, but is somewhat (by the above-mentioned quantity r_y) larger. For the value of K_c to be determined with reasonable accuracy, the length of the plastic zone must not exceed 20 per cent of the crack half-length, otherwise no use can be made of the asymptotic formulas of linear fracture mechanics outside this zone.

Decreasing the plastic strain in subsurface layers by increasing the specimen thickness leads to a reduction in the value of K_c to a certain limit which it asymptotically approaches. This is just the value of K_c for a three-dimen-

sional state of stress in plane strain, for which (owing to sufficient thickness of a given material) the macroplastic deformation ahead of the crack edge is virtually suppressed and failure occurs by "direct" fracture without lateral distortion. This quantity is referred to as the critical stress intensity factor in plane strain and designated K_{Ic} since here the failure occurs in the first mode of deformation, i.e., by separation (Fig. 2.1). This value is much closer to that obtained from a purely elastic problem since the plastically deforming volume is smaller in this case and there is no correction to the crack length to be introduced.

The experimental determination of K_{Ic} does not require any measurements of the length of a growing crack since the crack does not virtually grow and its original length is used for the calculation. Nevertheless, the determination of the K_{Ic} value is more complicated than that of K_c since it is not possible to know in advance for an unknown material whether direct fracture will result for a given thickness. Moreover, the thickness of the available material is often insufficient to permit an evaluation of K_{Ic}. In these cases it is advisable to use the phenomenon of popin of the crack front [33]. The fact is that, as has been observed, the load-displacement diagram for many materials shows a popin step, where the displacement increases abruptly with no increase or even with decrease in load. This popin phenomenon is usually accompanied by an audible "click"* and by the formation of a region of direct fracture in the form of a triangle at the centre of the thickness immediately at the head of the initial fatigue crack. The occurrence of this region of direct fracture is observed under plane strain conditions, which allows the load corresponding to its formation to be taken for determining the stress in the K_{Ic} calculation.

In the last few years, however, another characteristic has found application, viz. δ_c, which is determined by the value of the plastic crack tip opening displacement. A small vicinity of the crack tip is severely overstressed. If a member as a whole is considered to be a multiply statically indeterminate system, its reliability depends largely on the

* This fact forms the basis of acoustic methods of crack analysis.

capacity of the material to redistribute the stresses due to local plastic deformation. Taking into account the possibility of calculating analytically the crack tip opening displacement, the reason for increased attention which is given to the characteristic δ_c becomes apparent.

The value of δ_c may either be measured directly by means of suitable devices or (on the basis of the Leonov-Panasyuk model) be found from the analytic expression for the crack opening displacement δ for a specimen of given shape. The characteristic δ_c is a constant of local plasticity of the material (for its given thickness) at the tip of a stationary crack at the moment when the crack begins to grow.

Note that if the subsequent motion of the crack after determining δ_c is subcritical (slow), then δ_c is a subcritical characteristic [70, 91]. If, however, δ_c is determined at the beginning of rapid crack growth (at the maximum load or at the moment of popin), then the characteristic δ_c is critical. Such a duality of δ_c may complicate the interpretation of the estimate of the material behaviour.

Let us compare the two mechanical characteristics bearing in mind the corresponding fracture criteria.

(1) The material assessment based on K_c assumes perfectly elastic fracture, while δ_c does not assume this. In order to evaluate quasi-brittle fracture using K_c we have to introduce into the elastic solution, as additional assumptions, a region of plastic strains for the purpose of taking into account the properties of the material during plastic flow and its actual behaviour at the crack tip. Meantime, taking into account the plasticity of the material at the crack tip is inherent in the theory of critical crack opening displacement δ_c.

(2) In carrying out calculations on the basis of the two criteria under discussion (for the purpose of determining P_{cr}, l_{cr}) it is found that in the calculation based on K_c the critical load increases indefinitely with decreasing crack length, and this circumstance is responsible for the application of the theory only in the range of sufficiently large crack lengths and low critical stress levels in comparison with $\sigma_{0.2}$, which ensures a small size of the plastic zone. In the calculation based on δ_c, even in the range of small crack lengths the stress may become close to the yield stress

(or, in our opinion, to the ultimate strength, see Sec. 23) and the plastic zone ahead of the crack tip may considerably exceed the crack length.

(3) In Irwin's criterion, the fracture energy intensity 2γ is assumed (for a given material and a given thickness) to be a constant independent of the critical crack length (because of the smallness of the zone of plastic deformation). The calculation of the fracture energy intensity using the Leonov-Panasyuk criterion shows that this quantity varies with the critical crack length, viz. as the crack length decreases, 2γ increases indefinitely, and as the length increases, it approaches $\sigma_0\delta_c$. This follows from the general expression for the fracture energy intensity [99, 187, 294] (see also Sec. 19)

$$2\gamma = 2\sigma_0 \int_l^a \frac{\partial v^*(x, l)}{\partial l}\, dx = 2\frac{\partial}{\partial l} \int_l^a \sigma_0 v^*(x, l)\, dx + \sigma_0\delta_c.$$

Here $v^*(x, l)$ is the displacement of points of the crack surface subject to the condition $2v(l, l) = \delta_c$. The integral term in this formula is due to the variation of the shape and size of the plastic zone with the crack length, i.e., due to the non-self-similarity of the problem. At the same time it is assumed that δ_c is constant with variation of the critical crack length.

(4) The existing formula $G_c = \sigma_0\delta_c$ may be obtained from a comparison of the solutions for the critical stresses in a cracked plane under tension using both criteria. According to Irwin's criterion,

$$\sigma_{cr} = \sqrt{EG_c/\pi l};$$

according to the Leonov-Panasyuk criterion, as $l \to \infty$,

$$\sigma_{cr} = \sqrt{E\sigma_0\delta_c/\pi l}.$$

The above relation between G_c and δ_c is apparent from this, but it is essential that this relation is valid only for $l \to \infty$, i.e., for small critical stresses compared with σ_0; in other words, it is valid for materials for which the determination of G_c is legitimate.

Thus, from the foregoing comparison it follows that for large crack lengths and small local plastic deformations

of the material there is exact coincidence between the results of the calculation by the two criteria. Both characteristics of the material are also completely coincident

$$K_c^2 = EG_c = E\sigma_0\delta_c. \tag{10.1}$$

For small crack lengths the calculation of critical loads by the two criteria leads to a significant discrepancy. Nevertheless, as far as the assessment of the material is concerned, the characteristics K_c and δ_c are, as before, formally equivalent within the framework of the theories considered since, by hypothesis, they are independent of the critical crack length.

The scope of the theory may be broadened by considering plastic zones of different shape. The plastic zone ahead of the crack edge may differ from a thin strip and spread sideways from the crack propagation direction. Such a broadening of the scope will concern the determination of δ_c and not of K_c since the latter is limited only by the linear dimensions of the plastic zone rather than by its shape.

Finally, to understand the difference between the characteristics K_{Ic} and δ_c and their potentialities in material assessment, it is useful to draw the following analogy. Just as σ_u, S_k and δ, ψ* evaluate the strength and ductility of a smooth specimen, so K_c, K_{Ic}, and δ_c evaluate, respectively, the strength and ductility at singular points of a cracked specimen. This analogy helps in understanding the difference in the material behaviour evaluated by K_{Ic} and δ_c.

* S_k is the true tensile strength, δ is the ductility, ψ is the reduction of area [94].

CHAPTER III

CRACKS IN LINEARLY ELASTIC BODIES

11. SOLUTION OF SOME PLANE AND THREE-DIMENSIONAL PROBLEMS

We first present the solution of some plane problems relating to the determination of the crack length corresponding to the critical value of the load when the crack propagation line assumed to be fixed is known.

(1) An infinite plane with a straight crack is subjected to a uniform uniaxial tensile stress σ at infinity. It is required to determine the critical value of the stress σ at which the crack begins to propagate under constant external load (Griffith problem). The crack is situated along the x axis, $|x| \leqslant l$, $y = 0$.

We use relation (4.20) which, for the case under consideration, takes the form

$$2\gamma - p(l)\, v(l, l) - \int_0^l p(x) \frac{\partial v(x, l)}{\partial l} dx = 0. \qquad (11.1)$$

Here, as before, $p(x)$ is the stress on the crack line in a sound body taken with opposite sign, $v = v(x, l)$ is the displacement of points of the crack surface in the y direction caused by the stresses $p(x)$ acting on the crack surface.

In our case

$$p(x) = -\sigma_{ij} n_i = -\sigma(-1) = \sigma,$$

$$v(x, l) = \frac{2(1-\nu^2)\sigma}{E} \sqrt{l^2 - x^2}.$$

From this expression and from (11.1) it follows that the functional Ψ introduced in Sec. 4 is equal in a plane problem

to the crack length. Substituting the values of $p(x)$ and $v(x, l)$ in Eq. (11.1) and setting the displacement $v(l, l)$ equal to zero, we obtain the Griffith formula

$$\sigma = \sqrt{\frac{2E\gamma}{\pi(1-\nu^2)l}}$$

or in non-dimensional form

$$\lambda = (l_*)^{-1/2}. \tag{11.2}$$

Here

$$\lambda = \frac{\sigma}{\sigma_0}, \quad l_* = \frac{\pi(1-\nu^2)\sigma_0^2}{2E\gamma} l.$$

We now fix our attention on the role of the second term in condition (11.1), which, according to the theory of elasticity, is zero and has been rejected in the derivation of expression (11.2). As seen, the adoption of the condition $v(l, l) = 0$ leads to the well-known result on the equilibrium of a cracked body. At the same time numerous experimental and theoretical studies give conclusive evidence of the presence of a non-zero crack tip opening displacement as a result of the plastic flow in the material. The size of the region covered by the plastic flow depends on the material properties and the loading conditions. In this connection, as pointed out above (Sec. 3), there is available the Orowan-Irwin concept of quasi-brittle fracture, one of the simplest consequences of which is that the plastic zone is small compared with the crack length. This concept enables one to assume that the non-zero value of the displacement at the crack tip has an appreciable effect only in the vicinity of the crack tip, the size of this vicinity being of the same order of magnitude as the non-zero crack opening displacement. Outside this small vicinity the strain, displacement, and stress fields are described, as before, by the linear theory of elasticity. Thus, the use of the Orowan-Irwin concept makes it possible, on the one hand, to preserve the solution of elasticity theory and, on the other hand, to obtain new effects which are not revealed when the displacement at the crack tip is zero. The inclusion of the second term in (11.1) ensures a finite value of the strength of a body in the absence of a crack.

Consider two cases. In the first case the jump in the elastic displacement is of constant amount, $2v_* = \delta_c =$ constant. Equation (11.1) then becomes

$$2\gamma - \sigma \frac{\delta_c}{2} - \frac{\pi (1-\nu^2) l\sigma^2}{E} = 0.$$

In the absence of a crack fracture occurs when $\sigma = \sigma_0$; consequently, $\delta_c/2 = 2\gamma/\sigma_0$. From this we obtain the critical stress

$$\lambda = \frac{1}{2l_*} (\sqrt{1+4l_*} - 1). \tag{11.3}$$

In the second case the jump in the elastic displacement is proportional to the stress σ. Equation (11.1) then becomes

$$2\gamma - a\sigma^2 - \pi (1-\nu^2) \frac{l\sigma^2}{E} = 0.$$

Here the coefficient $a = 2\gamma/\sigma_0^2$ is determined from the condition $\sigma = \sigma_0$ when $l = 0$. The critical stress is

$$\lambda = (1 + l_*)^{-1/2}. \tag{11.4}$$

In Fig. 11.1 lines *1*, *2*, *3* correspond to relations (11.2), (11.3), (11.4), respectively.

(2) Consider a plane problem for a body with a straight crack extended by two equal and opposite concentrated forces P (Fig. 11.2) which are symmetrical about the line of the cut [182].

The distribution of stresses $p(x)$ along the crack line in a sound body is given by formula (9.1).

To determine the displacement $v(x, l)$, we assume the stresses $p(x)$ to be applied to the edges of the crack $-l \leqslant x \leqslant l$ so that the crack opens. In this case the solution of the problem of linear relationship gives [200]

$$\Phi(z) = \varphi'(z) = \frac{1}{2\pi i \sqrt{z^2 - l^2}} \int_{-l}^{l} \frac{\sqrt{t^2 - l^2}\, p(t)\, dt}{t - z},$$

$$\varphi(z) = \frac{1}{2\pi i} \int_{-l}^{l} p(t) \ln \frac{\sqrt{(t+l)(z-l)} + \sqrt{(t-l)(z+l)}}{\sqrt{(t+l)(z-l)} - \sqrt{(t-l)(z+l)}}\, dt, \tag{11.5}$$

$$\frac{\partial\varphi}{\partial l}=-\frac{1}{2\pi i}\int_{-l}^{l}\frac{p(t)(tz+l^2)\,dt}{l\sqrt{(l^2-t^2)(l^2-z^2)}}=\frac{Pl[(3+\nu)L^2+2l^2]}{4\pi i\sqrt{l^2-z^2}(L^2+l^2)^{3/2}}.$$

$$\frac{\partial v}{\partial l}=\frac{4(1-\nu^2)}{E}\operatorname{Im}\frac{\partial\varphi}{\partial l}=-\frac{(1-\nu^2)Pl[(3+\nu)L^2+2l^2]}{\pi E\sqrt{l^2-z^2}(L^2+l^2)^{3/2}}.$$

$$\int_0^l p(x)\frac{\partial v(x,l)}{\partial l}\,dx=\frac{(1-\nu^2)P^2l[(3+\nu)L^2+2l^2]^2}{4\pi E(L^2+l^2)^3}. \qquad (11.6)$$

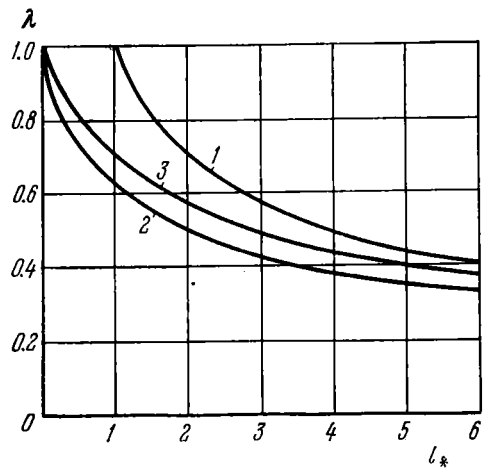

Fig. 11.1. Critical stress in a cracked plane under tension. *1*, Griffith's solution; *2*, crack tip opening displacement is a constant; *3*, crack tip opening displacement is proportional to the critical stress.

Substituting relations (9.1) and (11.6) in (11.1) and putting $v(l, l) = 0$, we obtain

$$\frac{P}{K_c\sqrt{L}}=\left(1+\frac{L^2}{l^2}\right)^{3/2}\frac{2\sqrt{\pi}}{\left[2+(3+\nu)\frac{L^2}{l^2}\right]\sqrt{\frac{L}{l}}}. \qquad (11.7)$$

This result is identical with the solution obtained from the Irwin force criterion (3.11).

From (11.7) it is seen that as $l\to 0$, the force $P\to\infty$. The infinite strength of the material in the absence of a crack indicates that the Irwin criterion (based on the assump-

tion that the stress intensity factor reaches a limiting value) is restricted to ideal elasticity.

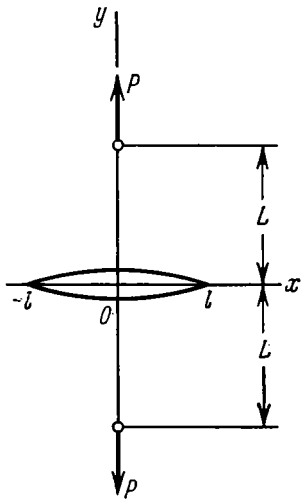

Fig. 11.2. Plane with a crack held open by two concentrated forces.

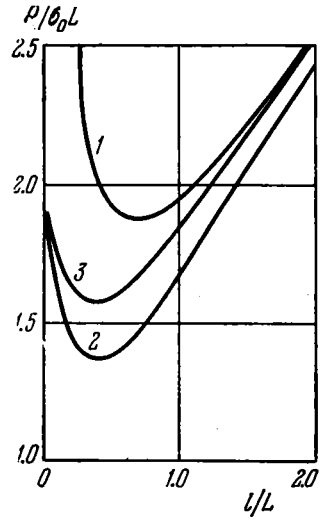

Fig. 11.3. Critical force for a plane loaded in tension by concentrated forces ($c = 1$, $\nu = 0.25$). *1*, solution for a perfectly elastic body; *2*, crack tip opening displacement is a constant; *3*, crack tip opening displacement is proportional to the stress at the location of the crack tip in the sound body.

For further discussion it is convenient to rewrite relation (11.7) as follows:

$$y = (cA)^{-1/2}, \tag{11.8}$$

$$y = \frac{P}{L\sigma_0}, \quad c = \frac{L\sigma_0^2}{2E\gamma}, \quad x = \frac{l}{L},$$

$$A = \frac{1-\nu^2}{4\pi}\,\frac{[(3+\nu)+2x^2]^2\,x}{(1+x^2)^3},$$

where σ_0 is the fracture stress for the sound material. In Fig. 11.3, line *l* corresponds to relation (11.8).

The value $c = 1$ for soda-lime silicate glass with characteristics [218] $\gamma \cong 2.1 \times 10^{-6}$ j/mm^2, $E = 6.7 \times 10^3$ kgf/mm^2, $\sigma_0 \cong 0.36$ kgf/mm^2 corresponds to the distance from the crack to the point of application of the force $L \cong 22$ mm.

From (11.1), which is written as

$$2\gamma - Pf(l)\, v_* - P^2 \int_0^l f(x) \frac{\partial V}{\partial l}\, dx = 0$$

$$\left(p(x) = Pf(x), \quad \frac{\partial v}{\partial l} = P \frac{\partial V}{\partial l} \right), \tag{11.9}$$

it follows that as $l \to 0$ the limiting load remains finite and equal to

$$P|_{l=0} = P_0 = \frac{2\gamma}{v_* f(0)}. \tag{11.10}$$

Further, a comparison with result (11.7) will be made in two directions. First, suppose that v_* is a material constant, $\delta_c/2$. On the basis of the first strength theory we assume that when $l = 0$ the limiting stress is equal to the maximum value σ_1 on the fracture line, i.e., $\sigma_1 = p(0) = P_0 f(0) = \sigma_0$. Then from (11.10) we obtain $v_* = 2\gamma/\sigma_0$, and equality (11.9) gives a relation between the force and the crack length as

$$y = \frac{-B + \sqrt{B^2 + 4cA}}{2cA},$$

$$B = \frac{(1-\nu)(1+x^2) + 2(1+\nu)}{2\pi(1+x^2)^2}. \tag{11.11}$$

Line *2* (Fig. 11.3) corresponding to (11.11) starts on the axis of ordinates from a strength value equal to

$$P_0 = 2\pi L \sigma_0 / (3 + \nu).$$

Second, it may be assumed that v_* is proportional to the stress $p(l)$ normal to the crack line. Hence, $v_* = ap(l)$ and from (11.10) it follows that $a = 2\gamma/\sigma_0^2$. Condition (11.9) is then rewritten as

$$2\gamma - \frac{2\gamma}{\sigma_0^2} [Pf(l)]^2 - P^2 \int_0^l f(x) \frac{\partial V}{\partial l}\, dx = 0.$$

Taking this into account we obtain, for our problem,

$$y = (cA + B^2)^{-1/2}. \tag{11.12}$$

Line *3* (Fig. 11.3) corresponding to (11.12) also indicates that the strength of a flawless material is finite.

As $l \to \infty$, all three lines coincide.

We now present the solution of some three-dimensional problems of determining the contour of a fracture region corresponding to the critical value of the load when the crack surface is known.

(3) We consider the problem of the extension of a space by a uniform stress σ at infinity. Suppose that the crack is flat and has the shape of a circle of radius R in plan (Sack's problem). We use a system of polar co-ordinates r, θ with pole at the centre of the circle. The displacement of points of the crack surface caused by the uniformly distributed pressure σ is given by

$$w = \frac{4(1-\nu^2)\sigma}{\pi E}\sqrt{R^2-r^2}. \tag{11.13}$$

In view of the symmetry of the problem we assume that the crack grows in the radial direction. Relation (4.14) takes the form

$$\int_C [2\gamma - \sigma w(R)](dy^*\delta x^* - dx^*\delta y^*) -$$

$$-\sigma \iint_D \frac{\partial w}{\partial \Psi}\left(\frac{\partial \Psi}{\partial x^*}\delta x^* + \frac{\partial \Psi}{\partial y^*}\delta y^*\right) dx\,dy = 0. \tag{11.14}$$

In our problem D is the region of the crack (here a circle) with contour C; x^*, y^* are the values of x, y on the contour,

$$\Psi = \pi R^2, \quad R^2 = (x^*)^2 + (y^*)^2,$$

$$\delta x^* = \frac{\delta R}{\cos\theta}, \quad \delta y^* = \frac{\delta R}{\sin\theta}, \quad M = 2\gamma - \sigma w(R).$$

The functional Ψ in a three-dimensional problem is the crack area.

From Eq. (11.14), putting $w(R) = 0$, we obtain

$$\sigma^2 = \frac{\pi E\gamma}{2(1-\nu^2)R} = \frac{\pi K_c^2}{4R}. \tag{11.15}$$

This result coincides with that obtained by R. A. Sack [246]. As already noted, however, the relative separation of the opposite faces of the crack $2w(R)$ at its edge is not zero. If this is so, we obtain a finite value for the strength of a sound body. Indeed, we set $M = 2\gamma - \sigma_0 w$ in Eq. (11.14)

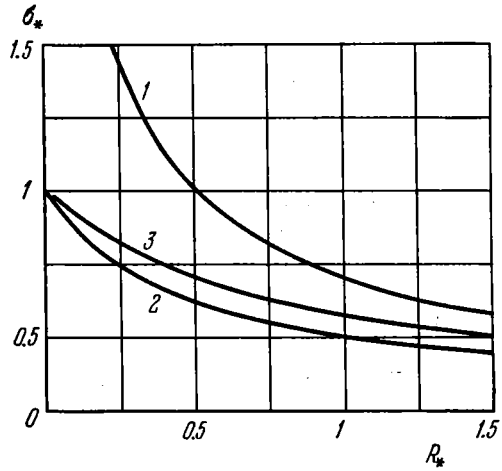

Fig. 11.4. Critical stress in a space with a penny-shaped crack under tension. *1*, Sack's problem; *2*, crack tip opening displacement is a constant; *3*, crack tip opening displacement is proportional to the critical stress.

on the contour, where $w(R) = w_*$ is a constant. The strength of the uncracked body is then determined by the stress $\sigma_0 = 2\gamma/w_*$ (theoretical strength). Equation (11.15) is then rewritten as

$$\sigma^2 = \frac{\pi E(\gamma - \gamma\sigma/\sigma_0)}{2(1-\nu^2)R} = \frac{\pi K_c^2}{4R}\left(1 - \frac{\sigma}{\sigma_0}\right).$$

By solving this equation for $\sigma_* = \sigma/\sigma_0$, we obtain

$$\sigma_* = -\frac{1}{4R_*} + \sqrt{\frac{1}{16R_*^2} + \frac{1}{2R_*}}, \quad R_* = \frac{2\sigma_0^2}{\pi K_c^2} R. \quad (11.16)$$

If we assume that the relative separation of the opposite faces of the crack is proportional to the stress on these planes in a sound body, the strength in the absence of a crack is determined by the stress $\sigma_0 = (2\gamma/c)^{1/2}$, which corresponds

to $M = 2\gamma - c\sigma^2$. Similarly to the above

$$\sigma_* = (1 + 2R_*)^{-1/2}. \tag{11.17}$$

Figure 11.4 shows lines *1*, *2*, *3* corresponding to relations (11.15), (11.16), (11.17), respectively.

(4) We shall use relation (11.14) to derive an equation describing the behaviour of a crack having the shape of an ellipse in plan. The space is weakened by a crack and is subjected to a tensile stress σ normal to the plane of the crack.

The displacement of points of the crack surface due to the uniformly distributed pressure σ is given by [213]

$$w = \frac{2\sigma(1-\nu^2)b}{EE(k)}\sqrt{1-\frac{x^2}{a^2}-\frac{y^2}{b^2}}. \tag{11.18}$$

Here $k^2 = 1 - b^2/a^2$; a, b are the semimajor and semiminor axes of the ellipse situated in the x and y directions respectively; $E(k)$ is the complete elliptic integral of the second kind.

Suppose that the crack propagates in the direction of the minor axis so that the given ellipse is changed into another one (major axis fixed). Then

$$y^* = b\sqrt{1-(x^*/a)^2},$$

$$\delta y^* = \delta b\sqrt{1-(x^*/a)^2},$$

$$\delta x^* = 0, \quad \Psi = \pi ab,$$

$$\frac{\partial\Psi}{\partial y^*} = \frac{\pi a}{\sqrt{1-(x^*/a)^2}},$$

$$\frac{\partial w}{\partial\Psi} = \frac{2\sigma(1-\nu^2)}{E}\left[\frac{a^2-x^2}{\sqrt{1-(x/a)^2-(y/b)^2}}\,\frac{1}{a^2E(k)} - \right.$$

$$\left. -\frac{b^2}{a^2}\,\frac{K(k)-E(k)}{k^2E^2(k)}\sqrt{1-\frac{x^2}{a^2}-\frac{y^2}{b^2}}\right]\frac{1}{\pi a}.$$

Substituting these relations in (11.14), we obtain ($w = 0$ on the contour)

$$\sigma^2 = \frac{3E\gamma k^2E^2(k)}{2(1-\nu^2)b\,[(1+k^2)E(k)-(1-k^2)K(k)]}. \tag{11.19}$$

This critical stress coincides with the result of [213], where, using the Griffith criterion, the nature of the growth

of an elliptical crack corresponded to the variation of the contour adopted here.

In the limit (as $a \to b$) formula (11.19) gives a solution for a circular crack and gives no solution for the Griffith case (as $a \to \infty$).

In [218] it is shown that the ellipse begins to propagate from the end points of the minor axis, and as the load increases the arc of the contour line of the ellipse involved in the motion propagates from the points $x = 0$, $y = \pm b$ in both directions along the contour. Accordingly we may adopt a different way of varying the contour of the ellipse, namely that of varying the contour only at the end points of the minor axis.

In this case relation (4.18) becomes

$$2\gamma - \sigma w_* - \int_0^l \sigma \frac{\partial w}{\partial b}\Big|_{x=0} dy = 0, \tag{11.20}$$

where the second term refers to the crack contour.

From this we obtain

$$\sigma^2 = \frac{4E\gamma k^2 E^2(k)}{\pi(1-\nu^2)\, b\, [(1+k^2)\, E(k) - (1-k^2)\, K(k)]}. \tag{11.21}$$

Here $K(k)$ is the complete elliptic integral of the first kind. Relation (11.21) shows that the critical stress for an ellipse is less than that for a circle of radius $R = a$. In particular, as $a \to \infty$ the critical stress (11.21) approaches Griffith's stress

$$\sigma = \sqrt{\frac{2E\gamma}{\pi(1-\nu^2)\, b}}.$$

Note that the stress given by (11.21) is approximate and in the range $0 < b/a \leqslant 1$ is somewhat different from the expression obtained in [215]

$$\sigma = E(k) \sqrt{\frac{2E\gamma}{\pi(1-\nu^2)\, b}}.$$

This discrepancy is due to the fact that the displacement was obtained for the area enclosed by the ellipse, whereas it should have been found for the area enclosed by the ellipse plus some small additional areas along the minor axis at

the points 0, $\pm b$ resulting from the variation of the area of the ellipse at these points. Hence, when the semiaxis b is varied there is a variation, not taken into account, of the contour at points other than the end points of the minor axis of the ellipse.

Similarly to the foregoing problems we take into consideration the finiteness of the strength of a sound body. In the one case, assuming that the relative separation of the opposite faces of the crack at its tip is a material constant, we have

$$\sigma_* = -\lambda + \sqrt{\lambda^2 + 2\lambda}. \tag{11.22}$$

Here

$$\lambda = \frac{2k^2 E^2(k)}{\pi^2 \varkappa b_*}, \quad b_* = \frac{2\sigma_0^2}{\pi K_c^2} b,$$

$$\varkappa = (1 + k^2) E(k) - (1 - k^2) K(k).$$

In the other case, assuming that the relative separation of the opposite faces of the crack is proportional to the stress in a sound body at the location of the crack, we have

$$\sigma_* = \left(1 + \frac{1}{2}\lambda\right)^{-1/2}. \tag{11.23}$$

As the crack size increases, the stresses given by (11.22) and (11.23) approach that of (11.21).

Thus, the application of the variational principle in crack theory can widen the formulation of problems and offers considerable scope for obtaining solutions of various problems in fracture mechanics, while the foregoing examples give physically more natural results than in the case of application of the theory of linear fracture mechanics [118].

Finally, we shall draw a conclusion regarding a possible value of the crack tip opening displacement. It is clear that for real materials the value of this displacement is greater than zero as a result of plastic flow and may be regarded either as a material constant or as a quantity dependent on the external load. The worked examples show that in both cases the difference between the critical states is insignificant (lines *2* and *3* in Figs. 11.1, 11.3, 11.4). Moreover, beginning with a certain value of the crack size, the assumption of zero opening displacement also leaves the critical state

practically unaltered. From this it may be concluded that the adoption of one or another hypothesis about the degree to which the crack tip opening displacement is assumed constant may be justified rather by convenience in performing calculations than by considerations of accuracy. It may be added that the details of deformation in a small vicinity of the crack tip affecting the opening displacement are strongly dependent on the grain size, anisotropy, inhomogeneity, and other factors, which introduces some uncertainty into experimental crack opening displacement measurements. Hence, the results of direct measurement of small values of crack tip opening displacement should be used with caution [70]. In brittle fracture it is therefore sufficient to know the fracture energy density 2γ measured on specimens with a reasonably large crack and the engineering strength σ_0 of a smooth (uncracked) specimen. These parameters suffice to construct the limiting state region for a body with a crack or with a finite strength when $l = 0$.

12. CONSTRUCTIONAL CRACK ARREST

One of the most important characteristics of fracture toughness of materials is the value of the limiting load associated with the onset of crack extension which is often identified with the concept of complete failure. This is true, however, only in the case of avalanche unstable crack propagation. As experiments [19, 242] and calculations [26, 49, 83, 102, 121, 151, 196, 222, 224] show, in many cases of the interaction of cracks with obstacles or boundaries and also in problems of the interaction between cracks the crack propagation is stable over a considerable range of load. It is obvious that the presence of stable cracks in machines and structures that often operate under specified variations of external loads is much less dangerous and the artificial reinforcement of such structures (by attaching rivets, plates and stringers, by drilling holes in the path of crack propagation, etc.) may considerably prolong their life.

To avoid catastrophic crack extension and structural failure cracks are reinforced by attaching stiffeners, which halt crack propagation (Fig. 12.1). A possible simple sche-

matization of this problem is as follows [196, 224]. An infinite plate with a crack of length $2l$ is extended at infinity by a uniform stress p_0 (Fig. 12.2); the action of the stiffeners

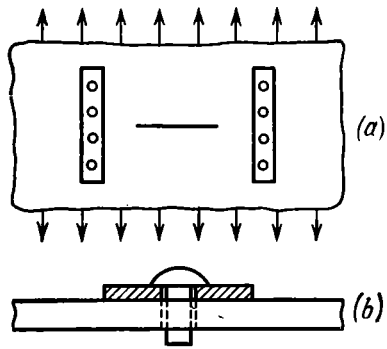

Fig. 12.1. Sheet with stiffeners.

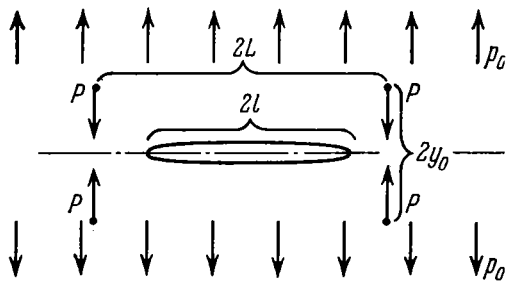

Fig. 12.2. Schematization of the crack problem with stiffeners.

is replaced by four symmetrically situated concentrated forces P applied at the locations of the rivets nearest to the crack; the magnitude of the forces P is assumed to be given. The schematization proposed here may further be complicated since the magnitude of the forces P is fully determined by the elastic and geometrical characteristics of the problem under consideration and by the magnitude of the tensile load p_0. In [49] the value of the forces P is determined as a function of the parameters of the problem. For simplicity, however, similarly to [242] we assume, as a first approximation, that the forces P are given. As estimates show, the

effect of the more distant rivets can be neglected. The same schematization (Fig. 12.2) may also be applied to the problem of a plate reinforced with a pair of wire loops in which there are no initial stresses and which are passed through holes drilled in the plate [17].

We shall give a solution to the problem thus formulated on the assumption of plane strain deformation.

By summing the well-known Boussinesq fundamental solutions [162], we obtain an expression for the distribution of normal stresses in an uncracked body subjected to the given loads

$$p(x) = -\frac{Py_0}{\pi[y_0^2+(x-L)^2]}\left[\frac{3+\nu}{2}-(1+\nu)\frac{(x-L)^2}{y_0^2+(x-L)^2}\right]-$$
$$-\frac{Py_0}{\pi[(x+L)^2+y_0^2]}\left[\frac{3+\nu}{2}-(1+\nu)\frac{(x+L)^2}{y_0^2+(x+L)^2}\right]+p_0=$$
$$=-\frac{Py_0}{2\pi[y_0^2+(x-L)^2]}\left[1-\nu+\frac{2y_0^2(1+\nu)}{y_0^2+(x-L)^2}\right]-$$
$$-\frac{Py_0}{2\pi[y_0^2+(x+L)^2]}\left[1-\nu+\frac{2y_0^2(1+\nu)}{y_0^2+(x+L)^2}\right]+p_0. \quad (12.1)$$

Here $2y_0$ is the distance between the points of application of the concentrated forces along their common line of action, $2L$ is the distance between the points of application of these forces in a direction parallel to the crack.

Because of the symmetry of the problem, we use the following relation for an isolated crack [118, 255]:

$$K=2\sqrt{\frac{l}{\pi}}\int_0^l \frac{p(x)\,dx}{\sqrt{l^2-x^2}}. \quad (12.2)$$

Substituting (12.1) in (12.2) and using Irwin's criterion (3.11), we obtain the following expression [196]:

$$p_0\frac{\pi}{2}-\frac{Py_0}{2}\left[\frac{(1-\nu)L}{A\sqrt{A-B+2L^2}}+\right.$$
$$+\frac{12y_0^2(1+\nu)L^3}{A^2(A+B-2L^2)\sqrt{A-B+2L^2}}=\frac{2(2B-A-4L^2)L(1+\nu)}{A^2\sqrt{A-B+2L^2}}-$$
$$\left.-\frac{l^2(1+\nu)L(B+A)(2B-A-4L^2)}{A^3(A+B-2L^2)\sqrt{A-B+2L^2}}\right]=\frac{\sqrt{\pi}}{2}\frac{K_c}{\sqrt{l}}.$$

Here $B=y_0^2+l^2+L^2$, $A=\sqrt{B^2-4L^2l^2}$.

We reduce this relation to non-dimensional parameters

$$p^\circ = \frac{\sqrt{2}}{\pi} P^\circ \varepsilon \left[\frac{1-\nu}{A\sqrt{A-B+2}} + \frac{12(1+\nu)\varepsilon^2}{A^2(A+B-2)\sqrt{A-B+2}} + \right.$$
$$\left. + \frac{2(1+\nu)(2B-A-4)}{A^2\sqrt{A-B+2}} + \varepsilon^2 \frac{(1+\nu)(B+A)(2B-A-4)}{A^3(A+B-2)\sqrt{A-B+2}} \right] +$$
$$+ \frac{\sqrt{2}}{\pi} \frac{1}{\sqrt{\frac{l}{L}}}. \quad (12.3)$$

Here

$$p^\circ = p^\circ\left(\frac{l}{L}\right) = \frac{p_0\sqrt{2L}}{K_c\sqrt{\pi}}, \quad P^\circ = \frac{P\sqrt{2}}{K_c\sqrt{\pi}\sqrt{L}},$$

$$B = 1 + \varepsilon^2 + \left(\frac{l}{L}\right)^2, \quad A = \sqrt{B^2 - 4\left(\frac{l}{L}\right)^2}, \quad \varepsilon = \frac{y_0}{L}.$$

Figure 12.3 gives the relation $p^\circ = p^\circ(l/L)$ according to (12.3) for $\nu = 0.25$, $P^\circ = 0.2$ and several values of the parameter ε. Here is also plotted Griffith's curve *1* [104] corresponding to the absence of stiffeners. It is obvious that the crack is stable if the stress required to hold it in a mobile equilibrium state increases with increasing crack length. As seen, for every value of the non-dimensional parameter P° characterizing the force exerted by the rivets there is a critical value ε_0 (in our case $\varepsilon_0 \cong 0.45$) of the non-dimensional parameter ε such that when $\varepsilon > \varepsilon_0$ curve (12.3) has no ascending portions so that the crack is always unstable, and when $\varepsilon < \varepsilon_0$ there is an ascending portion in which the crack is stable.

The solution for an infinite row of stiffeners (Fig. 12.4) situated at points $\pm nL$ ($n = 1, 2, \ldots$) is obtained from (12.3) if L is replaced by nL. Figure 12.5 presents curves for two pairs of stiffeners with the same values of P° and ν.

Thus, when the rivets are sufficiently closely spaced ($\varepsilon < \varepsilon_0$), the action of the stiffeners gives rise to a new qualitative effect, viz. crack stabilization.

We make a change of the variable $x = l\xi$ in (12.2) and put $p_0 = \lambda p$ (λ is the non-dimensional loading parameter, p is a constant with the dimensions of stress). Then (12.2)

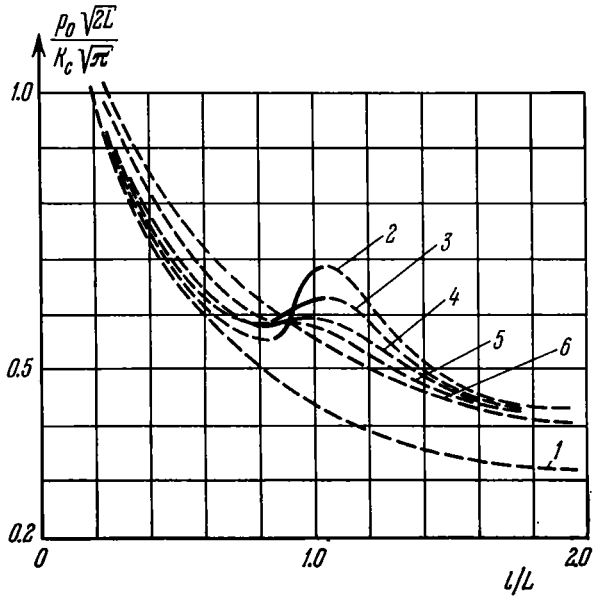

Fig. 12.3. Relation between the critical stress and the crack length for several positions of the points of application of concentrated forces (simulating the action of rivets). Curve *1* corresponds to Griffith's solution. The values of y_0/L are: *2*, 0.15; *3*, 0.25; *4*, 0.4; *5*, 0.5; *6*, 0.75.

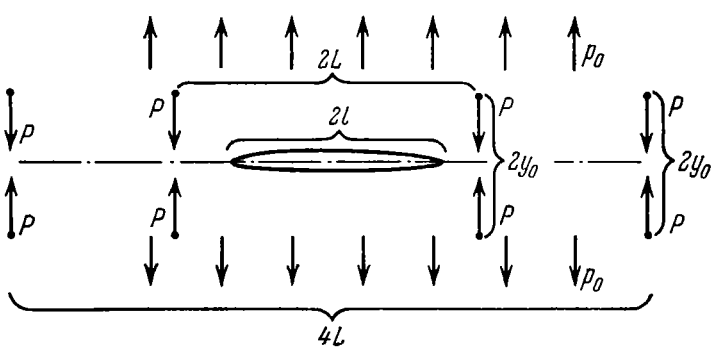

Fig. 12.4. Schematization of the crack problem with two pairs of stiffeners.

is rewritten as

$$\lambda = \varphi(l) = \frac{\sqrt{\pi}\, K_c}{2\sqrt{l}} \left[\int_0^1 \frac{p(l\xi)\, d\xi}{\sqrt{1-\xi^2}} \right]^{-1}. \qquad (12.4)$$

As the parameter λ increases, the propagation of the existing initial crack of length $2l_0$ in the body may follow one of the patterns described below (Fig. 12.6). If the curve

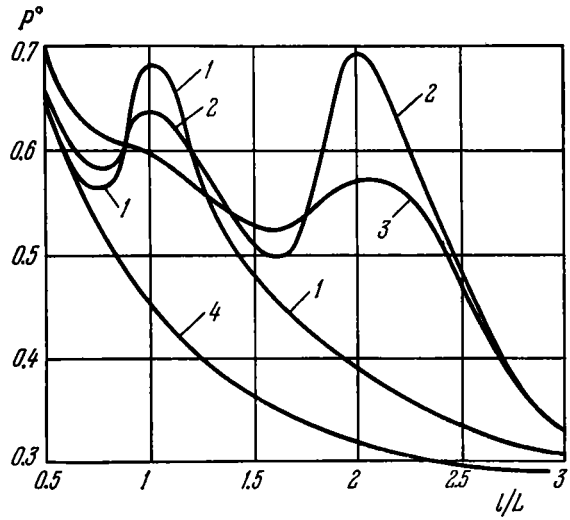

Fig. 12.5. Relation between the critical stress and the crack length for several positions of the points of application of concentrated forces. The values of y_0/L are: *1*, 0.15; *2*, 0.25; *3*, 0.5; *4*, Griffith's solution.

of crack length plotted against applied load has no stable portion (the rivets are widely spaced along the vertical), the crack length $2l_0$ remains unchanged as λ increases, until the crack reaches the critical state of equilibrium. Upon reaching the value of the loading parameter λ corresponding to this state, the crack begins to expand catastrophically and the body fractures (line *1*). For the curve having a stable portion, when $l_0 < l_{min}$ ($\lambda > \lambda_{max}$) and $l_0 > l_{max}$ ($\lambda < \lambda_{max}$), the development of the initial crack proceeds as in the first case (lines *2* and *3*). If $l_{min} < l_0 < l_s$, the crack size is unchanged until the crack reaches the crit-

ical state of equilibrium and then the slightest exceeding of the equilibrium load causes the crack to pass abruptly into another state, a stable state corresponding to the same value of λ, whereupon it develops stably as the loading parameter rises to the value λ_{max}. Thereafter the crack begins to expand catastrophically and the body fractures. The crack development in this case is represented by line *4*. When $l_s < l_0 < l_{max}$, the crack size does not change until

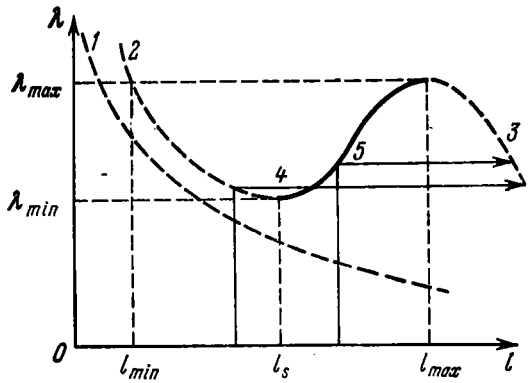

Fig. 12.6. Two kinds of critical fracture diagrams.

the crack reaches the critical state of equilibrium, then, as λ increases, the crack develops stably until the loading parameter reaches the value λ_{max}, whereupon the body fractures (line *5*).

In the last cases, when $\lambda_{min} < \lambda < \lambda_{max}$ condition (12.4) is fulfilled at the crack ends, a condition that determines the crack length as a continuous function of the loading parameter. Here, despite the crack growth, no fracture occurs and the body is capable of sustaining the increased load. The limiting value of the loading parameter λ_{max} determining here the strength of such a structure is the same for all values of the initial crack lengths in the range $l_{min} < l_0 < l_{max}$. Hence, if the initial crack length in an unloaded plate is less than $2l_{max}$ ($l_0 > l_{max}$ means that the crack has run through the stiffeners), the application of a load smaller than $p_0 = \lambda_{max} p$ entails no fracture.

This example is illustrative in that the fracture of a body is determined by the general integral condition for the non-existence of a solution as a whole to the problem of the equilibrium of a cracked body (and not by the local state of stress at specific points of the body). Fracture mechanics enables one to obtain a universal characteristic of structural strength, independent of the initial crack length, which is a useful quantity to introduce into design.

The foregoing analysis of solution can be used for the construction of surfaces of local fracture, instability and complete fracture in the space $\lambda_1, \lambda_2, \ldots, \lambda_n$ (in this space the curve $\lambda_1 = \lambda_1(t)$, $\lambda_2 = \lambda_2(t), \ldots, \lambda_n = \lambda_n(t)$ passing through the origin $\lambda_1 = \lambda_2 = \ldots = 0$ when $t = 0$ determines the loading path for the body) (see also [17, 252]).

For example, the most important strength characteristic, viz. the surface of complete fracture, defining the "fracture-safe" range of loading parameters for which no failure occurs can be determined as follows. The surface of complete fracture is defined as a surface

$$F_{\max}(\lambda_1, \lambda_2, \ldots, \lambda_n) = 0 \tag{12.5}$$

for interior points of which, when approached along any active loading path lying inside this surface, there exists a solution of the problem for a cracked body. For points external to this surface there exists no such solution. For our problem the equation of the surface of complete fracture is

$$\lambda - \lambda_{\max} = 0. \tag{12.6}$$

13. SYSTEM OF CRACKS

Of great interest are the problems of the mutual influence of randomly or orderly oriented cracks since after any prior treatment real materials contain a large number of different kinds of microdefects whose development under the action of external loads gives rise to systems of cracks. In this connection detailed studies have been made of problems involving the interaction of cracks of equal or unequal length situated along a common axis [14, 20, 116, 118, 181]. For example, in the case of a system of cracks of unequal length parallel to a certain direction the most dangerous crack is that whose motion begins first [181]. In all these

cases the mechanism of crack growth is similar to that for a single crack in a plane whose propagation is unstable under uniform tension. Experimental data indicate, however, that for systems of cracks it is possible under certain conditions to have their mutual strengthening [66].

Let us examine this question beginning with the solution of the first fundamental problem of the theory of elasticity for a doubly periodic system of cuts [151].

In the class of doubly periodic problems of the theory of elasticity the investigations have been primarily con-

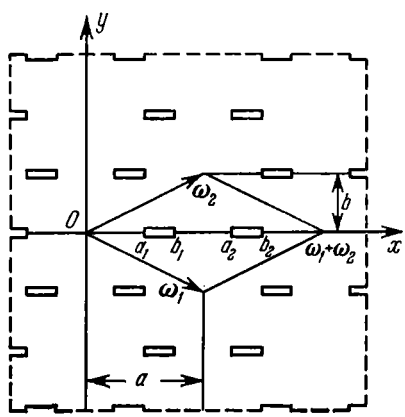

Fig. 13.1. Elastic plane weakened by a doubly periodic system of cuts.

cerned with problems of the equilibrium of plates and shells with circular or elliptical holes (perforated plates and shells). For applications in fracture mechanics, however, of principal interest are analogous problems for straight or arc cuts [222].

1. Consider an infinite elastic plane weakened by a doubly periodic system of cuts parallel to the real axis. Suppose that the primitive period parallelogram has the shape of a rhombus and the primitive periods ω_1 and ω_2 are conjugate complex numbers. There are two cuts of equal length within the parallelogram of periods, which are situated along a diagonal symmetrically about the centre of the rhombus (Fig. 13.1). Let a_1, b_1, a_2, b_2 be the co-ordinates of the ends

of the cuts

$$a_2 = \omega_1 + \omega_2 - b_1, \quad b_2 = \omega_1 + \omega_2 - a_1,$$
$$\omega_1 = a - ib, \qquad \omega_2 = a + ib. \tag{13.1}$$

Suppose that a normal load p is given on the sides of the cuts, and the state of stress in the plane is symmetrical about the x and y axes.

The stress components within the primitive period parallelogram are determined by means of the functions $\Phi(z)$ and $\Omega(z)$ [200] satisfying relations (2.5), (7.13).

By virtue of the very formulation of the problem the functions $\Phi(z)$ and $\Omega(z)$ must satisfy some additional conditions that ensure the doubly periodic nature of the state of stress. From the conditions for the double periodicity of the stress components and from relations (2.5) and (7.13) it follows that $\Phi(z)$ is a doubly periodic function, and $\Omega(z)$ must satisfy the conditions

$$\Omega(z + \omega_1) - \Omega(z) = (\omega_1 - \bar{\omega}_1)\,\bar{\Phi}'(z),$$
$$\Omega(z + \omega_2) - \Omega(z) = (\omega_2 - \bar{\omega}_2)\,\bar{\Phi}'(z). \tag{13.2}$$

Moreover, from the symmetry of the state of stress about the x and y axes we obtain

$$\Phi(z) = \bar{\Phi}(z), \qquad \Omega(z) = \bar{\Omega}(z),$$
$$\Phi(z) = \Phi(-z), \quad \Omega(z) = \Omega(-z). \tag{13.3}$$

On the basis of the second formula of (7.13) the boundary conditions for the functions $\Phi(z)$ and $\Omega(z)$ become

$$[\Phi(t) + \Omega(t)]^+ + [\Phi(t) + \Omega(t)]^- = 2p \quad \text{on } L, \tag{13.4}$$

$$[\Phi(t) - \Omega(t)]^+ - [\Phi(t) - \Omega(t)]^- = 0 \quad \text{on } L. \tag{13.5}$$

Here L is the line of discontinuity in the primitive period parallelogram consisting of the segments a_1b_1 and a_2b_2 of the real axis.*

* Note that the stated problem of the theory of elasticity has already attracted the attention of investigators. In [276] an attempt is made to reduce this problem to the solution of a problem of linear relationship. The author, however, makes a mistake that lies in the fact

In solving the boundary value problems (13.4), (13.5) we make use of the representation of doubly periodic functions in the form of Cauchy-type integrals with doubly periodic kernel [57].

Consider an even doubly periodic function

$$F(z)=\frac{1}{2\pi i}\int_L \frac{P'(t)f(t)\,dt}{P(t)-P(z)}. \tag{13.6}$$

Here $P(z)$ is the Weierstrass function.

Taking into account the well-known relations for Weierstrass functions [304]

$$\zeta(t+z)-\zeta(t)-\zeta(z)=\frac{1}{2}\frac{P'(t)}{P(t)-P(z)}-\frac{1}{2}\frac{P'(z)}{P(t)-P(z)},$$

$$\zeta(t-z)-\zeta(t)+\zeta(z)=\frac{1}{2}\frac{P'(t)}{P(t)-P(z)}+\frac{1}{2}\frac{P'(z)}{P(t)-P(z)},$$

it may be shown that the limiting values of integral (13.6) as the point z approaches the contour L from the left and right are related by equalities similar to the Sokhotskii-Plemelj formulas

$$F^+(\tau)-F^-(\tau)=f(\tau), \tag{13.7}$$

$$F^+(\tau)+F^-(\tau)=\frac{1}{\pi i}\int_L \frac{P'(t)f(t)\,dt}{P(t)-P(\tau)}. \tag{13.8}$$

In exactly the same way it may be proved that for an odd doubly periodic function

$$F_1(z)=\frac{1}{2\pi i}P'(z)\int_L \frac{f_1(t)\,dt}{P(t)-P(z)}$$

the following relations are valid:

$$F_1^+(\tau)-F_1^-(\tau)=f_1(\tau),$$

$$F_1^+(\tau)+F_1^-(\tau)=\frac{1}{\pi i}P'(\tau)\int_L \frac{f_1(t)\,dt}{P(t)-P(\tau)}.$$

---

that the proposed analytic representation does not lead to the problem of linear relationship between analytic functions which he is solving. In principle, an analogous representation and the reduction to the problem of linear relationship are possible, but require an introduction of non-analytic functions.

We shall seek the functions $\Phi(z)$ and $\Omega(z)$ in the form

$$\Phi(z)=\frac{1}{2\pi i}\int_L \frac{f(t)P'(t)\,dt}{P(t)-P(z)}, \tag{13.9}$$

$$\Omega(z)=\Phi(z)+\frac{1}{2\pi i}\int_L f(t)\,k(z,t)\,dt. \tag{13.10}$$

Here

$$k(z,t)=(z-t)P(z-t)-\zeta(z-t)-(z+t)P(z+ \\ +t)+\zeta(z+t)-Q(z-t)+Q(z+t)-2\zeta(t),$$

$\zeta(z)$ is the Riemann zeta function, and $Q(z)$ is a special meromorphic function [201] for which the following relations are valid [105]:

$$Q(z+\omega_1)-Q(z)=\bar{\omega}_1 P(z)+\gamma_1,$$
$$Q(z+\omega_2)-Q(z)=\bar{\omega}_2 P(z)+\gamma_2.$$

On this basis we prove that the following equalities hold for the functions $k(z,t)$:

$$k(z+\omega_1,t)=k(z,t)+(\omega_1-\bar{\omega}_1)P'(z)\frac{P'(t)}{[P(t)-P(z)]^2},$$

$$k(z+\omega_2,t)=k(z,t)+(\omega_2-\bar{\omega}_2)P'(z)\frac{P'(t)}{[P(t)-P(z)]^2},$$

$$k(z,t)=k(-z,t).$$

Thus, conditions (13.2) and (13.3), which must be satisfied by the function $\Omega(z)$, are fulfilled. It is easily seen that the function $k(z,t)$ has no singularities at the points $z=t$ and hence the integral in (13.10) can be continued across the contour L.

Substituting (13.9) and (13.10) in (13.4) and (13.5), we find that condition (13.5) is satisfied identically, and equality (13.4) takes the form

$$\Phi^+(t)+\Phi^-(t)=p-\frac{1}{2\pi i}\int_L f(\tau)\,k(t,\tau)\,d\tau \text{ on } L. \tag{13.11}$$

Assuming the right-hand side of (13.11) to be known, we shall seek the solution of the boundary value problem (13.11) in the class of even doubly periodic functions.

We consider, following [57], the canonical function of the homogeneous boundary value problem (13.11)

$$X_0(z) = \frac{\sigma(z-A_1)\,\sigma(z-A_2)}{\sqrt{\sigma(z-a_1)\,\sigma(z-b_1)\,\sigma(z-a_2)\,\sigma(z-b_2)}}. \quad (13.12)$$

Here $\sigma(u)$ is the Weierstrass sigma function, A_1 and A_2 are real constants lying off the line L and satisfying the relation

$$A_1 + A_2 = \omega_1 + \omega_2. \quad (13.13)$$

It is easily seen that $X_0(z)$ is an even elliptic function having two simple zeros in the parallelogram of periods at the points A_1 and A_2. For the limiting values of $X_0(z)$ on the contour L the following equality is valid:

$$X_0^+(t) + X_0^-(t) = 0 \quad \text{on } L. \quad (13.14)$$

We transform expression (13.12) taking into account (13.13), (13.1) and the following formulas [304]:

$$P(u) - P(v) = -\frac{\sigma(u+v)\,\sigma(u-v)}{\sigma^2(u)\,\sigma^2(v)},$$

$$\sigma(u+\omega_1) = -e^{-\delta_1\left(u+\frac{\omega_1}{2}\right)}\sigma(u),$$

$$\sigma(u+\omega_2) = -e^{-\delta_2\left(u+\frac{\omega_2}{2}\right)}\sigma(u),$$

$$\delta_1 = 2\zeta\left(\frac{\omega_1}{2}\right), \quad \delta_2 = 2\zeta\left(\frac{\omega_2}{2}\right).$$

The result is

$$X_0(z) = \frac{\sigma^2(A_1)\,e^{\frac{1}{2}(2A_1-a_1-b_1)(\delta_1+\delta_2)}\,[P(A_1)-P(z)]}{\sigma(a_1)\,\sigma(b_1)\sqrt{[P(a_1)-P(z)]\,[P(b_1)-P(z)]}}.$$

If we put $A_1 = 0$ and reject the constant factor, the canonical function of the homogeneous boundary value problem (13.11) may be taken in the form

$$X(z) = \{[P(a_1) - P(z)]\,[P(b_1) - P(z)]\}^{-1/2}.$$

The values of $X(z)$ on the upper side of the cut are determined as follows:

$$X^+(x) = i\{[P(a_1) - P(x)]\,[P(x) - P(b_1)]\}^{-1/2}$$
$$(a_1 < x < b_1),$$
$$X^+(x) = -i\{[P(a_1) - P(x)]\,[P(x) - P(b_1)]\}^{-1/2}$$
$$(a_2 < x < b_2).$$

With the use of the canonical function $X(z)$ we find the general solution of the homogeneous problem (13.11) for the even doubly periodic function $\Phi_0(z)$ that satisfies the condition

$$\Phi_0(z) = \bar{\Phi}_0(z) \tag{13.15}$$

and has no poles inside the parallelogram of periods with the cut L. The solution is

$$\Phi_0(z) = X(z)\,[\beta + \beta_1 P(z)].$$

Here β and β_1 are arbitrary constants. By virtue of condition (13.15) and the equality $P(z) = \bar{P}(z)$ the constants β and β_1 are real quantities.

By using (13.14), we write condition (13.11) as follows:

$$\frac{\Phi^+(t)}{X^+(t)} - \frac{\Phi^-(t)}{X^-(t)} = \frac{p}{X^+(t)} - \frac{1}{2\pi i}\,\frac{1}{X^+(t)}\int_L f(\tau)\,k(t,\tau)\,d\tau.$$

On the basis of formulas (13.6) and (13.7) we obtain the solution of this boundary value problem

$$\Phi(z) = \Phi_*(z) - \frac{1}{2\pi i}\,X(z)\int_L \frac{P'(t)}{X^+(t)\,[P(t) - P(z)]}\times$$
$$\times\left[\frac{1}{2\pi i}\int_L f(\tau)\,k(t,\tau)\,d\tau\right]dt. \tag{13.16}$$

Here

$$\Phi_*(z) =$$
$$= \frac{1}{2\pi i}\,X(z)\int_L \frac{pP'(t)\,dt}{X^+(t)\,[P(t) - P(z)]} + \frac{1}{2}\,X(z)\,[\beta + \beta_1 P(z)].$$

In the case of a constant load applied to the sides of the cut we have

$$\Phi_*(z)=\frac{p}{2}-\frac{p}{4}[P(a_1)+P(b_1)-2P(z)]X(z)+$$
$$+\frac{1}{2}[\beta+\beta_1 P(z)]X(z).$$

According to expressions (13.9), (13.6), and (13.7) the boundary values of $\Phi(z)$ assumed on the left and right of L satisfy the relation

$$\Phi^+(t)-\Phi^-(t)=f(t).$$

Substituting the limiting values (13.16) in this relation, we find

$$f(u)=[\Phi_*^+(u)-\Phi_*^-(u)]+$$
$$+\frac{1}{2\pi^2}X^+(u)\int_L\frac{P'(t)}{X^+(t)[P(t)-P(u)]}\left[\int_L f(\tau)k(t,\tau)\,d\tau\right]dt.$$

Because of the continuity of $k(t,\tau)$, the order of integration in the last term on the right-hand side may be interchanged. On interchanging we obtain a Fredholm integral equation for determining the function $f(t)$

$$f(u)=[\Phi_*^+(u)-\Phi_*^-(u)]+\int_L f(\tau)K(u,\tau)\,d\tau.$$

Here

$$K(u,\tau)=\frac{1}{2\pi^2}X^+(u)\int_L\frac{k(t,\tau)P'(t)\,dt}{X^+(t)[P(t)-P(u)]}.$$

By formulas (7.13), (13.9), and (13.10) we determine the stress components on the real axis

$$(\sigma_y-i\tau_{xy})_{y=0}=2\Phi(x)+\frac{1}{2\pi i}\int_L f(t)k(x,t)\,dt. \qquad (13.17)$$

To find the constants β and β_1 we consider the resultant of all forces acting along a certain arc AB joining two congruent points. The expression for the resultant is [200]

$$X+iY=-ig(z)\Big|_A^B=-i[\varphi(z)+(z-\bar{z})\overline{\Phi(z)}+\omega(\bar{z})]_A^B.$$

Here, as usual, $\varphi'(z) = \Phi(z)$, $\omega'(z) = \Omega(z)$. If the external load is self-balanced on each of the cuts, the resultant of all forces along the arc AB is zero, i.e.,

$$g(z+\omega_1) - g(z) = \varphi(z+\omega_1) - \varphi(z) + \omega(\bar{z}+\bar{\omega}_1) - \\ -\omega(\bar{z}) + (\omega_1 - \bar{\omega}_1)\overline{\Phi(z)} = 0, \tag{13.18}$$

$$g(z+\omega_2) - g(z) = \varphi(z+\omega_2) - \varphi(z) + \omega(\bar{z}+\bar{\omega}_2) - \\ -\omega(\bar{z}) + (\omega_2 - \bar{\omega}_2)\overline{\Phi(z)} = 0.$$

Since the function $\Phi(z)$ is even and doubly periodic, the following relations hold for the function $\varphi(z)$:

$$\varphi(z+\omega_1) - \varphi(z) = c_1, \quad \varphi(z+\omega_2) - \varphi(z) = c_2. \tag{13.19}$$

Here

$$c_1 = 2\varphi\left(\frac{\omega_1}{2}\right), \quad c_2 = 2\varphi\left(\frac{\omega_2}{2}\right).$$

Likewise, from equalities (13.2) we obtain the following conditions for the function $\omega(z)$:

$$\omega(z+\omega_1) - \omega(z) = (\omega_1 - \bar{\omega}_1)\Phi(z) + d_1, \\ \omega(z+\omega_2) - \omega(z) = (\omega_2 - \bar{\omega}_2)\Phi(z) + d_2. \tag{13.20}$$

Here

$$d_1 = 2\omega\left(\frac{\omega_1}{2}\right) - (\omega_1 - \omega_2)\Phi\left(\frac{\omega_1}{2}\right),$$

$$d_2 = 2\omega\left(\frac{\omega_2}{2}\right) + (\omega_1 - \omega_2)\Phi\left(\frac{\omega_2}{2}\right).$$

With (13.19) and (13.20) conditions (13.18) take the form

$$c_1 + d_1 = 0, \quad c_2 + d_2 = 0.$$

Substituting the values of the constants c_1, c_2, d_1, and d_2, we find

$$\varphi\left(\frac{\omega_1}{2}\right) + \omega\left(\frac{\omega_1}{2}\right) - \frac{1}{2}(\omega_1 - \omega_2)\Phi\left(\frac{\omega_1}{2}\right) = 0, \\ \varphi\left(\frac{\omega_2}{2}\right) + \omega\left(\frac{\omega_2}{2}\right) + \frac{1}{2}(\omega_1 - \omega_2)\Phi\left(\frac{\omega_2}{2}\right) = 0. \tag{13.21}$$

Consequently, the constants β and β_1 must be chosen so as to fulfil equalities (13.21).

We now present a somewhat different procedure for solving the boundary value problems (13.4) and (13.5). The functions $\Phi(z)$ and $\Omega(z)$ are sought in the form

$$\Phi(z) = \Phi_0(z) + \sum_{j=1}^{\infty} \Phi_j(z), \tag{13.22}$$

$$\Omega(z) = \Phi_0(z) + \sum_{j=1}^{\infty} \left\{ \Phi_j(z) + \right.$$
$$\left. + \frac{1}{2\pi i} \int_L [\Phi_{j-1}^+(t) - \Phi_{j-1}^-(t)]\, k(z, t)\, dt \right\}. \tag{13.23}$$

Here Φ_j ($j = 0, 1, 2, \ldots$) are even doubly periodic functions. Evidently, conditions (13.4) and (13.5) are fulfilled if Φ_j ($j = 0, 1, 2, \ldots$) satisfy the following relations on the contour L:

$$\Phi_0^+(t) + \Phi_0^-(t) = p \text{ on } L,$$

$$\Phi_j^+(t) + \Phi_j^-(t) =$$
$$= -\frac{1}{2\pi i} \int_L [\Phi_{j-1}^+(\tau) - \Phi_{j-1}^-(\tau)]\, k(t, \tau)\, d\tau \text{ on } L$$
$$(j = 1, 2, \ldots).$$

Thus, we have a sequence of boundary value problems for even doubly periodic functions. By determining from this the functions $\Phi_j(z)$ ($j = 0, 1, 2, \ldots$), we obtain, in the case of constant loads along the length of the cut,

$$\Phi_0(z) = \frac{p}{2\pi i} X(z) \int_L \frac{P'(t)\, dt}{X^+(t)\,[P(t) - P(z)]} +$$
$$+ \frac{1}{2} X(z)\, [\beta^{(0)} + \beta_1^{(0)} P(z)],$$

$$\Phi_j(z) = -\frac{1}{2\pi i} X(z) \int_L \frac{P'(t)}{X^+(t)\,[P(t) - P(z)]} \times$$
$$\times \left\{ \frac{1}{2\pi i} \int_L [\Phi_{j-1}^+(\tau) - \Phi_{j-1}^-(\tau)]\, k(t, \tau)\, d\tau \right\} dt +$$
$$+ \frac{1}{2} X(z)\, [\beta^{(j)} + \beta_1^{(j)} P(z)] \quad (j = 1, 2, \ldots).$$

The conditions that the resultant of all forces is zero may be written as

$$\varphi_0\left(\frac{\omega_1}{2}\right)+\omega_0\left(\frac{\omega_1}{2}\right)=0,\quad \varphi_0\left(\frac{\omega_2}{2}\right)+\omega_0\left(\frac{\omega_2}{2}\right)=0,$$

$$\varphi_j\left(\frac{\omega_1}{2}\right)+\omega_j^*\left(\frac{\omega_1}{2}\right)=\frac{1}{2}(\omega_1-\omega_2)\,\Phi_{j-1}\left(\frac{\omega_1}{2}\right),\quad (13.24)$$

$$\varphi_j\left(\frac{\omega_2}{2}\right)+\omega_j^*\left(\frac{\omega_2}{2}\right)=-\frac{1}{2}(\omega_1-\omega_2)\,\Phi_{j-1}\left(\frac{\omega_2}{2}\right)$$

$(j=1,\ 2,\ 3,\ \ldots)$.

Here

$$\varphi_j(z)=\int_0^z \Phi_j(z_1)\,dz_1\quad (j=0,\ 1,\ 2,\ \ldots),$$

$$\omega_0^*(z)=\varphi_0(z),\quad \omega_j^*(z)=\int_0^z \Omega_j(z_1)\,dz_1\quad (j=1,\ 2,\ \ldots),$$

$$\Omega_j(z)=\Phi_j(z)+\frac{1}{2\pi i}\int_L [\Phi_{j-1}^+(t)-\Phi_{j-1}^-(t)]\,k(z,\ t)\,dt.$$

The above relations enable one to determine successively the constants $\beta^{(0)}$, $\beta_1^{(0)}$, $\beta^{(j)}$, and $\beta_1^{(j)}$.

To obtain numerical results, use was made of the approximate solution of the problem taking into account the first terms in expansions (13.22) and (13.23). The normal stresses on the real axis for $x<a_1$ are then determined as follows:

$$\sigma_y\big|_{y=0,\ x<a_1}\cong 2\Phi_0(x)=$$

$$=p-\frac{p}{2}\,\frac{2P(x)-P(a_1)-P(b_1)}{\sqrt{[P(x)-P(a_1)]\,[P(x)-P(b_1)]}}+$$

$$+\frac{\beta^{(0)}+\beta_1^{(0)}P(x)}{\sqrt{[P(x)-P(a_1)]\,[P(x)-P(b_1)]}}.\quad (13.25)$$

From conditions (13.24) we find

$$p\left[\frac{\omega_1}{2}-I_1\left(\frac{\omega_1}{2}\right)\right]+\frac{1}{2}\{p\,[P(a_1)+$$

$$+P(b_1)]+2\beta^{(0)}\}\,I_0\left(\frac{\omega_1}{2}\right)+\beta_1^{(0)}I_1\left(\frac{\omega_1}{2}\right)=0,$$

$$p\left[\frac{\omega_2}{2}-I_1\left(\frac{\omega_2}{2}\right)\right]+\frac{1}{2}\{p\,[P(a_1)+\quad (13.26)$$

$$+P(b_1)]+2\beta^{(0)}\}\,I_0\left(\frac{\omega_2}{2}\right)+\beta_1^{(0)}I_1\left(\frac{\omega_2}{2}\right)=0.$$

Here

$$I_0\left(\frac{\omega_1}{2}\right)=I_0'+iI_0''=\int_0^{\omega_1/2} X(z)\,dz,$$

$$I_1\left(\frac{\omega_1}{2}\right)=I_1'+iI_1''=\int_0^{\omega_1/2} P(z)\,X(z)\,dz,$$

$$I_0\left(\frac{\omega_2}{2}\right)=I_0'-iI_0'',\quad I_1\left(\frac{\omega_2}{2}\right)=I_1'-iI_1''.$$

From Eqs. (13.26) we obtain the values of the constants $\beta^{(0)}$ and $\beta_1^{(0)}$

$$\beta^{(0)}=-\frac{1}{2}p\,[P(a_1)+P(b_1)]+\frac{1}{2}p\,\frac{aI_1''+bI_1'}{I_0''I_1'-I_0'I_1''},$$

$$\beta_1^{(0)}=p-\frac{1}{2}p\,\frac{bI_0'+aI_0''}{I_0''I_1'-I_0'I_1''}.$$

Here

$$a=\frac{1}{2}(\omega_1+\omega_2),$$

$$b=\frac{1}{2i}(\omega_2-\omega_1).$$

In accordance with (13.25) we find an approximate value of the stress intensity factor at the point a_1

$$K=\lim_{x\to a_1}\left[\sqrt{2\pi(a_1-x)}\,\sigma_y(x,0)\right|_{x<a_1}\cong$$

$$\cong-\sqrt{\frac{\pi}{2}}\,\frac{p\,[P(a_1)-P(b_1)]-2\beta^{(0)}-2\beta_1^{(0)}P(a_1)}{\sqrt{-P'(a_1)\,[P(a_1)-P(b_1)]}}. \qquad (13.27)$$

The application of Irwin's fracture condition (3.11) makes it possible to relate the crack length and the applied loads. The calculations by formula (13.27) have been performed for the case $b_1=a_2$ (there is one cut inside the parallelogram of periods; see Fig. 13.2). Figure 13.3 shows the relation between $p^*=p\sqrt{2\pi a}/K_c$ and the relative length of the cut l/a. From the foregoing solution it follows that for some values of the ratio b/a it is possible to have a stable development of the system of cracks (their mutual strengthening).

Thus, the above solution confirms the previously obtained approximate numerical result [222] on a stable development of a system of cracks forming a doubly periodic pattern.

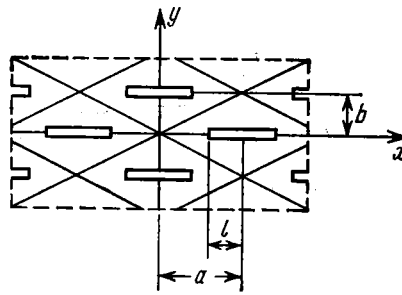

Fig. 13.2. Elastic plane weakened by a doubly periodic system of cuts with $b_1 = a_2$.

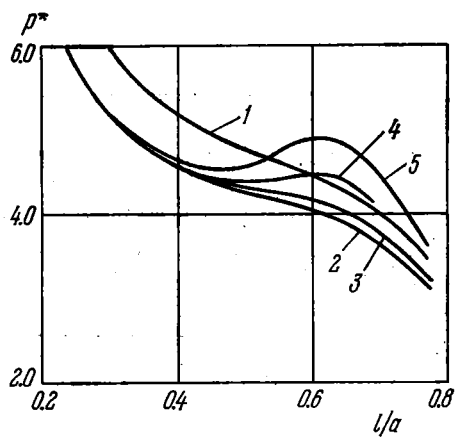

Fig. 13.3. Relation between the critical stress and the crack length. The values of b/a are 0.5, 0.45, 0.4, 0.35, 0.3 for lines *1*, *2*, *3*, *4*, *5*, respectively.

2. Consider one more problem of the interaction of cracks, now parallel to some axis. In the case of a system of cracks of unequal length parallel to some direction the most dangerous crack is that whose motion begins first. We present one

of such problems; its solution can give the answer to the question raised [181].

Consider the problem of the interaction of three cracks situated along the real axis. Let the external load be such

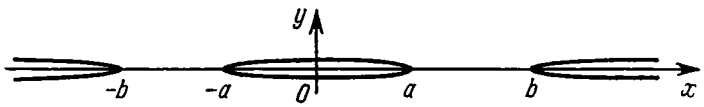

Fig. 13.4. Co-ordinate system for a plane with cuts.

that it reduces to two equal resultant forces P applied at the centre of the sections between the cuts (Fig. 13.4): $y = 0$, $|x| \leqslant a$, $-\infty < x \leqslant -b$, $b \leqslant x < \infty$.

If use is made of the well-known analogy between crack and punch problems, it may be shown that the stress σ_y on both sections between the cracks ($y = 0$) is the same and equal to [247]

$$\sigma_y = \frac{2P\,|x|}{\pi\sqrt{(x^2-a^2)(b^2-x^2)}}. \tag{13.28}$$

In order to determine the critical value of the stress corresponding to crack growth from the points $x = \pm a$ or $x = \pm b$, we use the limiting stress intensity factor condition corrected for a finite strength value in the absence of cracks (see Sec. 11). If the crack grows from the points $x = \pm a$, then

$$\lim_{x\to a} \sqrt{x-a}\,\sigma_y = \frac{1}{\pi}\sqrt{\frac{\pi E\gamma}{2(1-\nu^2)}\left(1-\frac{p^2}{\sigma_0^2}\right)},$$

from which we obtain

$$P_*^a = \sqrt{\pi\lambda}\left(\pi\lambda + \frac{2k}{1-k^2}\right)^{-1/2}. \tag{13.29}$$

Here $P_* = P/\sigma_0$, $\lambda = \gamma\, Gb/\sigma_0^2\,(1-\nu)$, $k = a/b$, σ_0 is the fracture stress in the absence of cracks.

If the crack grows from the points $x = \pm b$, then

$$\lim_{x\to b} \sqrt{b-x}\,\sigma_y = \frac{1}{\pi}\sqrt{\frac{\pi E\gamma}{2(1-\nu^2)}\left(1-\frac{p^2}{\sigma_0^2}\right)},$$

from which we obtain

$$P_*^b = \sqrt{\pi\lambda}\left(\pi\lambda + \frac{2}{1-k^2}\right)^{-1/2}. \qquad (13.30)$$

Relations (13.29) and (13.30) are presented in Fig. 13.5 when $\pi\lambda = 1$, from which it is seen that in this configuration the outer semi-infinite cracks are the first to begin growing.

Let now the external load for the plane with cuts under consideration be such that it reduces to two equal but oppo-

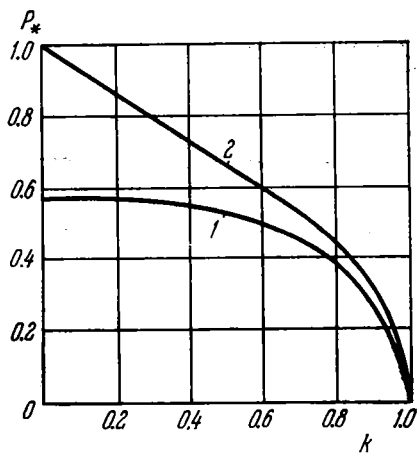

Fig. 13.5. Relation between the limiting load and the relative size of the sections between the cracks. The external load reduces to two equal forces on the uncracked sections. *1*, crack growth starts at the points $x = \pm b$; *2*, crack growth starts at the points $x = \pm a$.

site resultant forces P applied at the centre of the sections. The stress on both uncracked sections in this case [247] is ($y = 0$)

$$\sigma_y = \frac{2P \operatorname{sign} x}{K'(k)\sqrt{(x^2-a^2)(b^2-x^2)}}. \qquad (13.31)$$

Here $K'(k) = K(\sqrt{1-k^2})$ is the complete elliptic integral of the first kind.

If the crack grows from the points $x = \pm a$, the limiting value of the load is obtained, similarly to the case considered

above, as

$$P_*^a = \sqrt{\frac{kc}{1+k}}, \quad c = \frac{2\lambda}{\pi}(1-k^2)(k')^2. \tag{13.32}$$

The crack growth from the points $x = \pm b$ begins when the value of the load is equal to

$$P_*^b = \sqrt{\frac{c}{1+c}}. \tag{13.33}$$

Figure 13.6 presents these relations (for $\lambda = 1$), which show that, in contrast to the preceding case, the inner crack

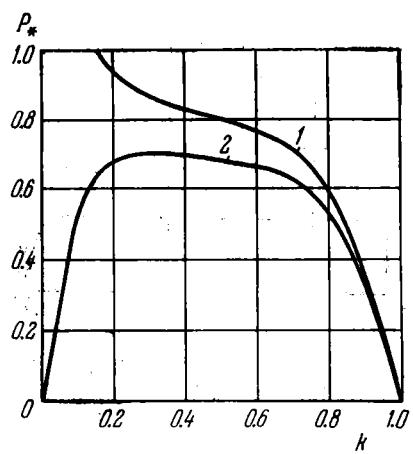

Fig. 13.6. Relation between the limiting load and the relative size of the sections between the cracks. The external load reduces to a couple. *1*, crack growth starts at the points $x = \pm b$; *2*, crack growth starts at the points $x = \pm a$.

begins to grow first. This is natural since here the character of the loading on the sections between the cracks is similar to the action of the shears.

The investigation of the sign of the derivatives $\partial P_*^a/\partial a$ and $\partial P_*^b/\partial b$ supports the conclusion that for the cases considered here the crack growth is unstable.

14. STRESS INTENSITY FACTORS FOR SOME PRACTICALLY IMPORTANT CASES

We now turn to the determination of the state of stress in the vicinity of a circumferential cut on the surface of an infinite solid cylinder and find the stress intensity factor in the case of pure torsion and extension along the axis of the cylinder [152]. The importance of the analysis of the state of stress for a notched circular specimen subjected to combined torsion and tension arises from the fact that the shape of a specimen proves to be essential for standard fracture testing.

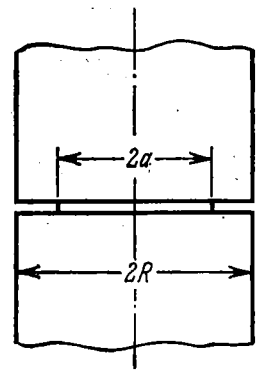

Fig. 14.1. Circular cylinder with an external circumferential cut.

1. Suppose that a solid circular cylinder of unit radius ($R = 1$) having a circumferential notch of inner diameter $2a$ is twisted by couples M (Fig. 14.1). The cylinder is referred to a system of cylindrical co-ordinates (r, θ, z) with origin in the plane of the cut. It is assumed that the lateral surface of the cylinder and the surface of the cut are free from stress.

The shearing stresses in the elementary solution of the torsion problem for a shaft of unit radius are expressed as

$$\tau_{\theta z}^{(0)} = \frac{2M}{\pi} r, \quad \tau_{r\theta}^{(0)} = 0.$$

In order for the surface of the cut to be free from stress, it is necessary to consider an additional state of stress that is independent of the angular co-ordinate θ and is characterized by the only non-zero displacement component $u_\theta = u(r, z)$ satisfying the equilibrium equation

$$\frac{\partial^2 u}{\partial r^2} + \frac{1}{r}\frac{\partial u}{\partial r} - \frac{u}{r^2} + \frac{\partial^2 u}{\partial z^2} = 0. \tag{14.1}$$

The shearing stresses are determined by the formulas

$$\tau_{\theta z}^{(1)} = \mu \frac{\partial u}{\partial z}, \quad \tau_{r\theta}^{(1)} = \mu \left(\frac{\partial u}{\partial r} - \frac{u}{r} \right). \tag{14.2}$$

Consider a semi-infinite cylinder ($z \geqslant 0$) and represent the solution of Eq. (14.1) in the form

$$u(r, z) = 2 \sum_{n=1}^{\infty} \frac{B_n J_1(\lambda_n r)}{\lambda_n} \exp(-\lambda_n z). \tag{14.3}$$

Here $J_1(\lambda_n r)$ is the Bessel function of the first kind, λ_n are the roots of the equation

$$\lambda_n J_1'(\lambda_n) - J_1(\lambda_n) = -\lambda_n J_2(\lambda_n) = 0.$$

The shearing stresses on the lateral surface are zero, and at the end they are determined, according to (14.2) and (14.3), as follows:

$$\tau_{\theta z}^{(1)} = \mu \frac{\partial u}{\partial z} = -2\mu \sum_{n=1}^{\infty} B_n J_1(\lambda_n r) \quad (z = 0). \tag{14.4}$$

The boundary conditions in the plane $z = 0$ are

$$\begin{gathered} \tau_{\theta z}^{(1)}(r, 0) = -\tau_{\theta z}^{(0)}(r, 0) \quad (a < r \leqslant 1), \\ u(r, 0) = 0 \quad (0 \leqslant r < a). \end{gathered} \tag{14.5}$$

By satisfying these boundary conditions and using relations (14.3) and (14.4), we obtain dual series equations

$$\sum_{n=1}^{\infty} B_n (\lambda_n)^{-1} J_1(\lambda_n r) = 0 \quad (0 \leqslant r < a), \tag{14.6}$$

$$\sum_{n=1}^{\infty} B_n J_1(\lambda_n r) = \frac{M}{\pi\mu} r \quad (a < r \leqslant 1). \tag{14.7}$$

Following [264], we assume

$$-\frac{M}{\pi\mu} r + \sum_{n=1}^{\infty} B_n J_1(\lambda_n r) = -\frac{\partial}{\partial r} \int_r^a \frac{g(t)\, dt}{\sqrt{t^2 - r^2}} \quad (r < a). \tag{14.8}$$

On the basis of equalities (14.7) and (14.8) we then find

$$\begin{gathered} B_n = 2 [J_1(\lambda_n)]^{-2} \int_0^a g(u) \sin(\lambda_n u)\, du, \\ -\frac{M}{\pi\mu} = 8 \int_0^a u g(u)\, du. \end{gathered} \tag{14.9}$$

The function $g(u)$ satisfies a Fredholm integral equation of the second kind with a symmetrical kernel [264]

$$g(t)=\int_0^a g(u)K(u,t)\,du+\frac{16t}{\pi}\int_0^a ug(u)\,du,$$

$$K(u,t)=\frac{4}{\pi^2}\int_0^\infty \frac{K_2(y)}{I_2(y)}[8utI_2(y)- \tag{14.10}$$

$$-\sinh(ty)\sinh(uy)]\,dy.$$

Here $I_n(y)$, $K_n(y)$ are modified Bessel functions of the first and second kind, respectively.

By using the power series expansions for the functions $\sinh(ty)$, $\sinh(uy)$, and $I_2(y)$, we represent the kernel of Eq. (14.10) as

$$K(u,t)=-\sum_{k=0}^{\infty} t^{2k+1}b_{2k+1}(u), \tag{14.11}$$

$$b_1(u)=\sum_{n=2}^{\infty}\alpha_n\left[\frac{u^{2n-1}}{(2n-1)!}-\frac{u}{2^{2n-3}(n-1)!\,(n+1)!}\right],$$

$$b_{2k+1}(u)=\frac{1}{(2k+1)!}\sum_{n=2}^{\infty}\frac{\alpha_{n+k-1}u^{2n-3}}{(2n-3)!}\quad(k=1,2,\ldots),$$

$$\alpha_n=\frac{4}{\pi^2}\int_0^\infty\frac{K_2(y)}{I_2(y)}y^{2n}\,dy\quad(n=2,3,\ldots). \tag{14.12}$$

Taking into account expansion (14.11), the solution of the integral equation (14.10) is sought in the form

$$g(t)=C(a)\sum_{m=0}^{\infty}P_{2m+1}t^{2m+1}. \tag{14.13}$$

The constants P_{2m+1} in (14.13) are determined by solving the infinite system of algebraic equations

$$P_{2m+1}=-\sum_{k=0}^{\infty}P_{2k+1}C_{2k+1,\,2m+1}+\delta_m^0\quad(m=0,1,2,\ldots). \tag{14.14}$$

Here

$$C_{2k+1,\,1}=\sum_{n=2}^{\infty}\alpha_n\left[\frac{a^{2k+2n+1}}{(2k+2n+1)\,(2n-1)!}-\right.$$

$$\left.-\frac{a^{2k+3}}{2^{2n-3}\,(2k+3)\,(n-1)!\,(n+1)!}\right],$$

$$C_{2k+1,\,2m+1}=\int_0^a u^{2k+1}b_{2m+1}(u)\,du=$$

$$=\frac{1}{(2m+1)!}\sum_{n=2}^{\infty}\frac{\alpha_{n+m-1}a^{2k+2n-1}}{(2k+2n-1)\,(2n-3)!}$$

$$(k=0,\,1,\,2,\,\ldots,\,m=1,\,2,\,3,\,\ldots);\quad \delta_m^0=\begin{cases}1, & m=0,\\ 0, & m=1,\,2,\,\ldots\end{cases}$$

The constant $C(a)$ is determined from the second equality of (14.19) and expansion (14.13)

$$C(a)\sum_{m=0}^{\infty}P_{2m+1}\frac{a^{2m+3}}{2m+3}=-\frac{M}{8\pi\mu}. \tag{14.15}$$

We shall show that system (14.14) is quasi-regular. We first prove that the functions $b_{2m+1}(u)$ approach zero when $m\to\infty$ and $0\leqslant u<1$. Substituting the expression for the coefficients α_n in the series defining $b_{2m+1}(u)$ and interchanging the order of summation and integration, we obtain

$$b_{2m+1}(u)=\frac{4}{\pi^2\,(2m+1)!}\int_0^{\infty}\frac{K_2(y)}{I_2(y)}\,y^{2m+1}\sinh(uy)\,dy$$

$$(m=1,\,2,\,\ldots).$$

By using the asymptotic expansions for the modified Bessel functions, the following representation may be obtained for large values of m:

$$b_{2m+1}(u)\sim$$

$$\sim\frac{2}{\pi\,(2-u)^{2m+1}}\left[1+\frac{15\,(2-u)}{4\,(2m+1)}+\frac{225\,(2-u)^2}{32\,(2m+1)\,2m}+\ldots\right]-$$

$$-\frac{2}{\pi\,(2+u)^{2m+1}}\left[1+\frac{15\,(2+u)}{4\,(2m+1)}+\frac{225\,(2+u)^2}{32\,(2m+1)\,2m}+\ldots\right].$$

It follows that

$$\lim_{m\to\infty} b_{2m+1}(u)=0 \quad (0\leqslant u<1).$$

Note that the values of α_n for large n can also be determined by the asymptotic formula

$$\alpha_n \sim \frac{(2n)!}{2^{2n-1}\pi}\left[1+\frac{15}{4}\frac{2}{2n}+\frac{225}{32}\frac{2^2}{(2n-1)(2n)}+\dots\right]. \qquad (14.16)$$

Table 14.1 gives values of α_n according to (14.12) (first line) and (14.16) (second line). Comparison shows that when $n\geqslant 5$ the exact values of α_n differ only slightly from the asymptotic ones.

TABLE 14.1

n	α_n		n	α_n	
2	117×10^{-1}	80×10^{-1}	9	235×10^{8}	237×10^{8}
3	297×10^{-1}	274×10^{-1}	10	212×10^{10}	216×10^{10}
4	276	267	11	235×10^{12}	241×10^{12}
5	498×10^{1}	489×10^{1}	12	312×10^{14}	323×10^{14}
6	142×10^{3}	141×10^{3}	13	490×10^{16}	511×10^{16}
7	587×10^{4}	584×10^{4}	14	894×10^{18}	946×10^{18}
8	326×10^{6}	327×10^{6}	15	189×10^{21}	202×10^{21}

By evaluating the coefficients of the infinite system (14.14), we find

$$|C_{2k+1,\,2m+1}|\leqslant|b_{2m+1}(a_1)|\frac{a^{2k+2}}{2k+2} \quad (0\leqslant a_1\leqslant a<1).$$

Consequently,

$$\sum_{k=1}^{\infty}|C_{2k+1,\,2m+1}|\leqslant$$

$$\leqslant|b_{2m+1}(a_1)|\sum_{k=1}^{\infty}\frac{a^{2k+2}}{2k+2}=\frac{1}{2}|b_{2m+1}(a_1)||\ln(1-a^2)+a^2|.$$

From the last relation and (14.16) we deduce that, beginning with a certain number $m=m'$, the following in-

equality holds:

$$S_{2m+1} = \sum_{k=1}^{\infty} |C_{2k+1,\,2m+1}| < 1 \quad (m \geqslant m').$$

Thus, system (14.14) is quasi-regular when $0 \leqslant a < 1$.

To determine the shearing stresses on the prolongation of the cut, we use relations (14.4) and (14.8)

$$\tau_{\theta z}^{(1)}(r, 0) = -\frac{2}{\pi} Mr + 2\mu \frac{\partial}{\partial r} \int_r^a \frac{g(t)\,dt}{\sqrt{t^2 - r^2}} \quad (r < a).$$

If expressions (14.13) and (14.15) are substituted in this, it may be shown that the shearing stress $\tau_{\theta z}^{(1)}$ on the prolongation of the cut has a singularity of the form

$$\tau_{\theta z}^{(1)}(r, 0) = -\frac{2\mu C(a)}{\sqrt{a^2 - r^2}} \sum_{m=0}^{\infty} P_{2m+1} r^{2m+1} + \ldots \quad (r < a). \tag{14.17}$$

Taking into account (14.17), we find the stress intensity factor at the root of the cut

$$K_{\mathrm{III}} = \lim_{r \to a} [\sqrt{2\pi(a - r)}\, \tau_{\theta z}(r, 0)] = -2\mu \sqrt{\frac{\pi}{a}}\, g(a) \quad (r < a). \tag{14.18}$$

By using expansion (14.13), we may write

$$K_{\mathrm{III}} = \frac{M}{4\sqrt{\pi a}} \left(\sum_{m=0}^{\infty} P_{2m+1} a^{2m+1} \right) \left(\sum_{m=0}^{\infty} P_{2m+1} \frac{a^{2m+3}}{(2m+3)} \right)^{-1}. \tag{14.19}$$

In Fig. 14.2 line *1* represents, according to (3.11), the relation between the quantity $M^* = \frac{3}{4} M \pi^{-1/2} R^{-5/2} K_{\mathrm{IIIc}}^{-1}$ and the non-dimensional crack tip radius ($\alpha = a/R$) (R is the radius of the cylinder introduced instead of the unit radius).

It is easily seen that for small values of a (deep circumferential crack) $P_1 \sim 1$, $P_{2k+1} \sim 0$ ($k = 1, 2, \ldots$). From (14.19) it follows then that

$$K_{\mathrm{III}} \sim \frac{3M}{4\sqrt{\pi}} a^{-5/2}. \tag{14.20}$$

This result (line *2* in Fig. 14.2) follows from the well-known Neuber's solution [202] of the torsion problem for a body of revolution containing an external groove.

In contrast, for shallow grooves on the surface of the cylinder we may consider a half-plane with a cut at its boundary under antiplane strain conditions (Fig. 14.3). The boundary conditions in this case are

$$\tau_{zx}=0,\ x=0;\ u=0,$$
$$y=0,\ 1-a\leqslant x;\quad (14.21)$$
$$\tau_{zy}=-\frac{2M}{\pi}(1-x),$$
$$y=0,\quad 0\leqslant x\leqslant 1-a.$$

The last condition corresponds to the choice of stresses (with opposite sign) occurring at the location of a shallow groove in a solid cylinder of unit radius under torsion.

In this case we have

$$\Delta u=0,\quad \tau_{zy}=\mu\frac{\partial u}{\partial y},$$
$$\tau_{zx}=\mu\frac{\partial u}{\partial x}.$$

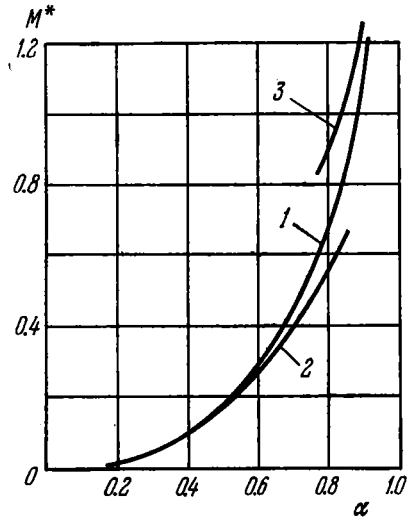

Fig. 14.2. Relation between the critical value of the torque and the distance to the base of a circumferential crack (line *1*); *2*, Neuber's solution of the torsion problem for a body of revolution containing an external groove; *3*, solution for shallow grooves on the surface of a cylinder.

We represent the displacement and stress components as follows:

$$u(x,y)=\int_0^\infty A(\lambda)\,e^{-\lambda y}\cos\lambda x\,d\lambda,$$

$$\tau_{zx}=-\mu\int_0^\infty \lambda A(\lambda)\,e^{-\lambda y}\sin\lambda x\,d\lambda,$$

$$\tau_{zy}=-\mu\int_0^\infty \lambda A(\lambda)\,e^{-\lambda y}\cos\lambda x\,d\lambda.$$

By satisfying the boundary conditions (14.21), we obtain

$$\int_0^\infty \lambda A(\lambda) \cos \lambda x \, d\lambda = \frac{2M}{\pi\mu}(1-x) \quad (0 \leqslant x < 1-a),$$

$$\int_0^\infty A(\lambda) \cos \lambda x \, d\lambda = 0 \quad (x > 1-a);$$

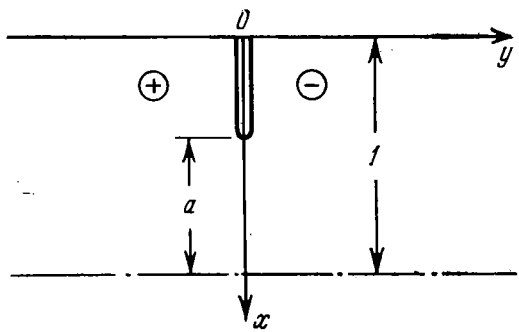

Fig. 14.3. Half-plane with a cut at its boundary.

or upon integration

$$\int_0^\infty A(\lambda) \sin \lambda x \, d\lambda = \frac{2M}{\pi\mu}\left(x - \frac{x^2}{2}\right) \quad (0 \leqslant x < 1-a),$$

$$\int_0^\infty A(\lambda) \cos \lambda x \, d\lambda = 0 \quad (x > 1-a).$$

We introduce a new unknown function $L(t)$

$$A(\lambda) = \int_0^{1-a} L(t) J_0(\lambda t) \, dt.$$

Then

$$\int_0^x \frac{L(t)\,dt}{\sqrt{x^2-t^2}} = \frac{2M}{\pi\mu}\left(x - \frac{x^2}{2}\right), \quad L(t) = \frac{2M}{\pi\mu}\left(t - \frac{2}{\pi}t^2\right),$$

$$\tau_{zy}(x, 0) = -\mu \frac{\partial}{\partial x} \int_0^\infty A(\lambda) \sin \lambda x \, d\lambda =$$

$$= -\mu \frac{\partial}{\partial x} \int_0^{1-a} L(t) \left[\int_0^\infty J_0(\lambda t) \sin \lambda x \, d\lambda \right] dt =$$

$$= -\frac{2M}{\pi}(1-x) - \delta\mu \frac{\partial}{\partial x} \int_0^{1-a} \frac{L(t)\, dt}{\sqrt{x^2-t^2}}$$

$$\delta = \begin{cases} 0, & 0 \leqslant x < 1-a, \\ 1, & x > 1-a. \end{cases}$$

If the last two relations are taken into account, the expression for the shearing stresses on the prolongation of the cut is of the form

$$\tau_{zy}(x, 0) = \frac{2Mx}{\pi\sqrt{x^2-(1-a)^2}} \left[1 - \frac{2(1-a)}{\pi} \right] + \ldots \quad (14.22)$$

$$(x > 1-a).$$

Here we have rejected terms which are bounded when $x \to 1-a$. The stress intensity factor, with (14.22) taken into consideration, is

$$K_{\mathrm{III}} = \lim_{x \to 1-a} \sqrt{2\pi[x-(1-a)]}\, \tau_{zy}(x, 0) =$$

$$= 2M\sqrt{\frac{1-a}{\pi}} \left[1 - \frac{2(1-a)}{\pi} \right]. \quad (14.23)$$

From this and (3.11) we have, in the limiting case,

$$M^* = \frac{3M}{4\sqrt{\pi}K_{\mathrm{III}_c}} = \frac{3}{8\sqrt{1-\alpha}\,[1-2\pi^{-1}(1-\alpha)]} \quad \left(\alpha = \frac{a}{R}\right). \quad (14.24)$$

To relation (14.24) corresponds line *3* in Fig. 14.2.

By combining the three solutions, viz. the exact one (14.18), the solution for the case of a deep cut (14.20), and the solution for a shallow groove (14.23), we represent the stress intensity factor as follows:

$$K_{\mathrm{III}} = \tau_{\max}\sqrt{\pi R}\, F(\alpha). \quad (14.25)$$

Here $\tau_{max} = 2M\pi^{-1}a^{-3}$ is the maximum stress at the net section, $\alpha = a/R$,

$$F(\alpha) = \frac{3}{8}\alpha^3 (M^*)^{-1} \text{ for exact solution,} \tag{14.26}$$

$$F(\alpha) = F_N(\alpha) = \frac{3}{8}\alpha^{1/2} \text{ for deep cut,} \tag{14.27}$$

$$F(\alpha) = F_A(\alpha) = \alpha^3 (1-\alpha)^{1/2}\left[1 - \frac{2}{\pi}(1-\alpha)\right]$$

for shallow groove. (14.28)

Table 14.2 gives values of $F(\alpha)$ according to (14.26), (14.27), and (14.28).

TABLE 14.2

α	$F(\alpha)$	$F_N(\alpha)$	$F_A(\alpha)$
0	0	0	—
0.1	0.119	0.1185	—
0.2	0.167	0.167	—
0.3	0.206	0.205	—
0.4	0.236	0.236	—
0.5	0.264	0.265	—
0.6	0.288	0.29	—
0.7	0.286	0.313	—
0.8	0.274	0.336	—
0.85	0.243	—	0.221
0.9	0.231	—	0.2185
0.95	0.21	—	0.207
1.0	0	—	0

2. Consider the case of a cylinder of unit radius ($R = 1$) with a circumferential cut loaded axially in tension by a force $P = q\pi R^2$ (Fig. 14.1). Let us find an approximate solution of this problem on the assumption that the surface of the cut is free from load, the shearing stresses and radial displacements are zero on the lateral surface of the cylinder. The problem is axially symmetric and the state of stress in the vicinity of the cut can be obtained by considering

a semi-infinite cylinder $z \geqslant 0$ for which the following conditions are fulfilled at the end $z = 0$:

$$\begin{aligned} &\tau_{rz}(r, 0) = 0 && (0 \leqslant r \leqslant 1), \\ &u_z(r, 0) = 0 && (0 \leqslant r < a), \\ &\sigma_z(r, 0) = -q && (a < r \leqslant 1). \end{aligned} \tag{14.29}$$

In this case the displacement and stress components may be expressed in terms of a single harmonic function [257]

$$u_r = z\frac{\partial^2\Psi}{\partial r\,\partial z} + (1-2\nu)\frac{\partial\Psi}{\partial r}, \quad u_z = z\frac{\partial^2\Psi}{\partial z^2} - 2(1-\nu)\frac{\partial\Psi}{\partial z},$$

$$\sigma_z = 2\mu\left(z\frac{\partial^3\Psi}{\partial z^3} - \frac{\partial^2\Psi}{\partial z^2}\right), \qquad \tau_{rz} = 2\mu z\frac{\partial^3\Psi}{\partial r\,\partial z}.$$

Taking into account the conditions as $z \to \infty$, the harmonic axially symmetric function is chosen in the form

$$\Psi(r, z) = \sum_{n=1}^{\infty} \lambda_n^{-2} A_n J_0(\lambda_n r)\exp(-\lambda_n z).$$

Here $J_0(x)$ is the Bessel function of the first kind, λ_n are the roots of the equation $J_0'(\lambda_n) = 0$.

The following conditions must be fulfilled on the lateral surface of the cylinder:

$$\tau_{rz}(1, z) = 0, \quad u_r(1, z) = 0.$$

By satisfying conditions (14.29), we obtain dual series equations of the form

$$\begin{aligned} &\sum_{n=1}^{\infty} \lambda_n^{-1} A_n J_0(\lambda_n r) = 0 && (0 \leqslant r < a), \\ &\sum_{n=1}^{\infty} A_n J_0(\lambda_n r) = q(2\mu)^{-1} && (a < r \leqslant 1). \end{aligned} \tag{14.30}$$

To solve this system we assume [264]

$$-\frac{q}{2\mu} + \sum_{n=1}^{\infty} A_n J_0(\lambda_n r) = -\frac{1}{r}\frac{\partial}{\partial r}\int_r^a \frac{g(t)\,t\,dt}{\sqrt{t^2 - r^2}} \tag{14.31}$$

$$(0 \leqslant r < a).$$

From the second equation of (14.30) and from (14.31) it follows that

$$A_n = \frac{2}{J_0^2(\lambda_n)} \int_0^a g(t) \cos(\lambda_n t)\, dt,$$
$$\int_0^a g(t)\, dt = -\frac{q}{4\mu}. \tag{14.32}$$

Substituting expression (14.32) for the coefficients A_n in the first equation of (14.30) and taking into account the relations obtained in [264], we find

$$g(t) = \int_0^a g(u) K(u, t)\, du + \frac{4}{\pi} \int_0^a g(u)\, du. \tag{14.33}$$

Here

$$K(u, t) = \frac{4}{\pi^2} \int_0^\infty \frac{K_1(y)}{yI_1(y)} [2I_1(y) - y \cosh(uy) \cosh(ty)]\, dy.$$

Thus, equality (14.33) represents a Fredholm integral equation of the second kind for determining the function $g(t)$. To solve this equation we use the representation of the kernel of (14.33) as a power series [258]

$$K(u, t) = \sum_{m=0}^{\infty} b_{2m}(u)\, t^{2m}.$$

Here

$$b_0(u) = \frac{4}{\pi^2} \left[T^* - \sum_{s=1}^{\infty} T_{2s} \frac{u^{2s}}{(2s)!} \right],$$

$$b_{2m}(u) = -\frac{4}{\pi^2} \sum_{s=1}^{\infty} \frac{T_{2m+2s-2} u^{2s-2}}{(2m)!(2s-2)!} \qquad (m = 1, 2, \ldots),$$

$$T^* = \sum_{s=1}^{\infty} \frac{T_{2s}}{2^{2s} s!\,(s+1)!}, \qquad T_n = \int_0^\infty \frac{K_1(y)}{I_1(y)} y^n\, dy$$

and the numerical values of T_n are given in [258].

By seeking the solution of Eq. (14.33) in the form of a series

$$g(t) = C(a) \sum_{m=0}^{\infty} Q_{2m} t^{2m}, \tag{14.34}$$

we obtain an infinite system of algebraic equations for the determination of the coefficients Q_{2m}

$$Q_{2m} = \sum_{k=0}^{\infty} Q_{2k} C_{2k,\,2m} + \delta_m^{\circ} \qquad (m = 0,\ 1,\ 2,\ \ldots). \tag{14.35}$$

Here

$$C_{2k,\,0} = \frac{4}{\pi^2} T^* \frac{a^{2k+2}}{2k+1} - \frac{4}{\pi^2} \sum_{s=1}^{\infty} \frac{T_{2s} a^{2k+2s+1}}{(2s)!\,(2s+2k+1)}$$
$$(k = 0,\ 1,\ 2,\ \ldots),$$

$$C_{2k,\,2m} = -\frac{4}{\pi^2} \sum_{s=1}^{\infty} \frac{T_{2m+2s-2} a^{2k+2s-1}}{(2m)!\,(2s-2)!\,(2k+2s-1)}$$
$$(k = 0,\ 1,\ 2,\ \ldots),$$
$$(m = 1,\ 2,\ 3,\ \ldots).$$

System (14.35) is quasi-regular when $0 \leqslant a < 1$. This follows from the asymptotic expressions for the functions $b_{2m}(u)$ for large values of m

$$b_{2m}(u) \sim$$
$$\sim \frac{2}{\pi (2-u)^{2m+1}} \left[1 + \frac{3}{4} \frac{2-u}{2m} + \frac{9}{32} \frac{(2-u)^2}{(2m-1)\,2m} + \ldots \right] +$$
$$+ \frac{2}{\pi (2+u)^{2m+1}} \left[1 + \frac{3}{4} \frac{2+u}{2m} + \frac{9}{32} \frac{(2+u)^2}{(2m-1)\,2m} + \ldots \right]$$
$$(0 \leqslant u < 1)$$

and from the estimates

$$|C_{2k,\,2m}| \leqslant |b_{2m}(a_1)| \frac{a^{2k+1}}{2k+1} \qquad (0 \leqslant a_1 < a < 1),$$

$$\sum_{k=0}^{\infty} |C_{2k,\,2m}| \leqslant \frac{1}{2} |b_{2m}(a_1)| \ln \frac{1+a}{1-a}.$$

Thus, beginning with a certain number $m = m'$, the following inequality holds:

$$\sum_{k=0}^{\infty} |C_{2k,\,2m}| < 1 \qquad (m > m').$$

We also give an asymptotic formula for determining the coefficients T_n for large values of n

$$T_n \sim \frac{\pi n!}{2^{n+1}} \left[1 + \frac{3}{4}\frac{2}{n} + \frac{9}{32}\frac{2^2}{(n-1)\,n} + \ldots\right].$$

When $n \geqslant 8$, the values of T_n calculated by this formula differ from the exact ones by less than 1.1 per cent.

The constant $C(a)$ is determined so as to fulfil the second condition of (14.32). The result is

$$C(a) = -\frac{q}{\pi G}\left(\sum_{m=0}^{\infty} Q_{2m}\frac{a^{2m+1}}{2m+1}\right)^{-1}. \qquad (14.36)$$

The normal stresses in the plane $z = 0$ on the prolongation of the cut are determined by the formula

$$\sigma_z(r, 0) = -2\mu \sum_{n=1}^{\infty} A_n J_0(\lambda_n r) =$$

$$= -q + \frac{2\mu}{r}\frac{\partial}{\partial r}\int_r^a \frac{g(t)\,t\,dt}{\sqrt{t^2 - r^2}} \qquad (r < a).$$

Substituting (14.34) in this formula and accounting for the stress singularity at the base of the cut, we obtain

$$\sigma_z(r, 0) = -\frac{2GC(a)}{\sqrt{a^2 - r^2}} \sum_{m=0}^{\infty} Q_{2m} r^{2m} + \ldots \qquad (r < a). \quad (14.37)$$

Here we have rejected terms which are bounded when $r \to a$.

Formula (14.37) enables one to determine the stress intensity factor

$$K_{\mathrm{I}} = \sqrt{2\pi}\lim_{r\to a}\left[\sqrt{a - r}\,\sigma_z(r, 0)\right] = -2G\sqrt{\frac{\pi}{a}}\,g(a) \qquad (r < a)$$

(14.38)

and the quantity

$$Q_{\mathrm{I}} = \frac{2q\sqrt{R}}{\sqrt{\pi}\,K_{\mathrm{Ic}}}$$

which is proportional to the critical load.

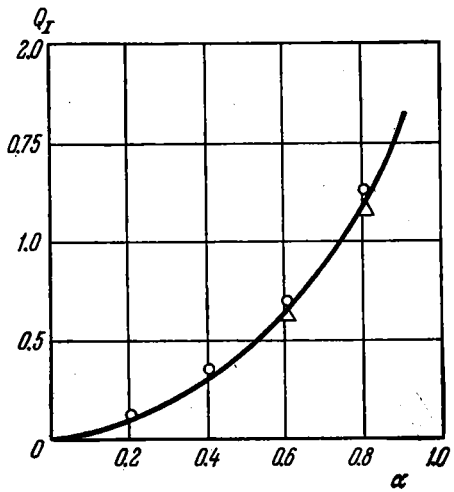

Fig. 14.4. Relation between the critical stress and the distance to the base of a circumferential crack. Circles: Paris' results. Triangles: Bueckner's data.

Taking into account expression (14.36) for the constant $C(a)$, the stress intensity factor in the case of a cylinder of radius R is of the form

$$K_{\mathrm{I}} = \frac{q\sqrt{\pi R}}{2\alpha^{3/2}}\left(\sum_{m=0}^{\infty} Q_{2m}\alpha^{2m}\right)\left(\sum_{m=0}^{\infty} Q_{2m}\frac{\alpha^{2m}}{2m+1}\right)^{-1} \quad \left(\alpha = \frac{a}{R}\right). \tag{14.39}$$

For small values of α, $Q_0 \sim 1$, $Q_{2m} \sim 0$ ($m = 1, 2, \ldots$). From relation (14.39) it follows that

$$K_{\mathrm{I}} \sim \frac{q\sqrt{\pi R}}{2\alpha^{3/2}}.$$

This result follows from Neuber's solution [202] to the problem of the extension of a space with an external slit.

Figure 14.4 gives Q_{I} as a function of the distance ($\alpha = a/R$) to the base of the crack. For comparison, given here are the results of P. C. Paris and H. F. Bueckner [85]. The result obtained by us is intermediate to those of P. C. Paris and H. F. Bueckner.

15. SHELL WITH A CRACK

In view of extensive applications of thin-walled structures the investigation of the state of stress in shells having a through crack is of great practical interest, although the number of works of a theoretical nature devoted to this subject is relatively small.

The problem of stresses in a shallow spherical shell with a straight cut has been previously considered in [81]. Based

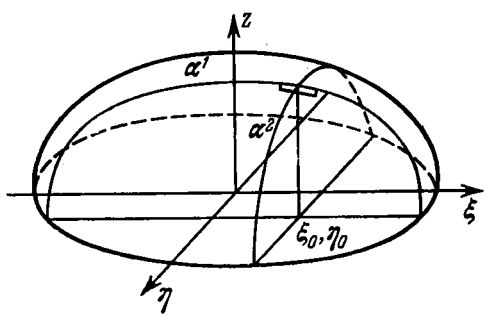

Fig. 15.1. Ellipsoidal shell with a crack.

on this work, further investigations and calculations have been carried out in [248], where the criticism of some results is also contained. A more general result for a shallow shell with a crack situated on a line of curvature is obtained in [302].

We present an approximate procedure for solving problems for an ellipsoidal shell of revolution in the presence of an arbitrarily oriented through-thickness cut, which was proposed by B. A. Kudryavtsev [149].

1. Consider a shell in the form of an ellipsoid of revolution (Fig. 15.1) with semi-axes a, b ($b < a$). Let the middle surface of the shell be referred to curvilinear co-ordinates α^1, α^2.

The radius vector of a point of the middle surface is

$$\mathbf{r}(\alpha^1, a^2) = b\alpha^1\mathbf{i} + b\alpha^2\mathbf{j} + b\sqrt{1-\varepsilon^2\rho^2}\,\mathbf{k},$$
$$\rho^2 = (\alpha^1)^2 + (\alpha^2)^2, \qquad \varepsilon = \frac{b}{a}. \tag{15.1}$$

Clearly, the projection of this co-ordinate network on the equatorial plane is a system of Cartesian co-ordinates. The unit normal vector to the middle surface is determined as

$$\mathbf{n}(\alpha^1, \alpha^2) = [1-(1-\varepsilon^2)\varepsilon^2\rho^2]^{-1/2}[\varepsilon^2\alpha^1\mathbf{i} + \varepsilon^2\alpha^2\mathbf{j} + \\ + \sqrt{1+\varepsilon^2\rho^2}\,\mathbf{k}]. \tag{15.2}$$

To solve the problem we use a simplified system of equations of shell theory expressed in terms of complex forces [56]

$$\nabla_\alpha T^{\alpha j} - \sqrt{-1}\,C b^j_\alpha a^{\alpha\delta}\nabla_\delta T = 0 \qquad (j=1,\ 2),$$
$$T = a^{\gamma\delta}T_{\gamma\delta},$$
$$a^{\alpha\delta}\nabla_\alpha\nabla_\delta T - \frac{\sqrt{-1}}{C}b_{\alpha\delta}T^{\alpha\delta} = q_n\frac{\sqrt{-1}}{C}, \tag{15.3}$$
$$C = \frac{h}{\sqrt{12(1-\nu^2)}}.$$

Here T^{ij} is the complex force tensor, ∇_α is the symbol of the covariant derivative on the surface, h is the thickness of the shell.

The quantities a^{ij} and b_{ij}, which are the components of the twice contravariant metric tensor of the middle surface and the covariant curvature tensor, are easily determined on the basis of expressions (15.1) and (15.2).

The complex displacements may be found from the system of equations [56]

$$\varepsilon_{lk} = \frac{1}{Eh}[T_{lk} - \nu c_{il}c_{jk}T^{ij}],$$
$$\mu_{kl} = \frac{\sqrt{-1}}{EhC}[c_{lk}c_{jl}T^{ij} - c_{lk}c_{jl}T^{ij*}]. \tag{15.4}$$

Here c_{jk} are the components of the antisymmetric discriminant tensor on the surface.

The expressions for μ_{ij} and ε_{ij} are related to the complex displacement components u_i, w ($i = 1, 2$) by the equalities

$$\varepsilon_{ij} = \nabla_i u_j - b_{ij} w - c_{ij}\Omega_n, \quad \mu_{ij} = \nabla_i \vartheta_j - c_{ij} b_i^{\nu}\Omega_n, \tag{15.5}$$

$$\vartheta_i = -\frac{\partial w}{\partial \alpha^i} - b_i^{\alpha} u_{\alpha}, \qquad \Omega_n = \frac{1}{2\sqrt{a}}\left(\frac{\partial u_2}{\partial \alpha^1} - \frac{\partial u_1}{\partial \alpha^2}\right), \tag{15.6}$$

$$a = a_{11}a_{22} - a_{12}^2.$$

We represent the coefficients in Eqs. (15.3) to (15.6) as power series in ε^2 and seek the components of complex force and displacement in the form

$$\begin{aligned} T^{ij} &= T_{(0)}^{ij} + \varepsilon^2 T_{(1)}^{ij} + \ldots, \\ u_i &= u_{i(0)} + \varepsilon^2 u_{i(1)} + \ldots, \\ w &= w_{(0)} + \varepsilon^2 w_{(1)} + \ldots . \end{aligned} \tag{15.7}$$

We introduce the notation

$\alpha^1 = \xi$, $\alpha^2 = \eta$, $\rho^2 = \xi^2 + \eta^2$, $\mathrm{Re}\,(u_1) = u$, $\mathrm{Re}\,(u_2) = v$.

Substituting expansions (15.7) in Eqs. (15.3) to (15.6) and limiting series (15.7) to two terms, we obtain the following system of equations for determining the complex forces and displacements:

$$\begin{gathered} \frac{\partial T_{(0)}^{11}}{\partial \xi} + \frac{\partial T_{(0)}^{21}}{\partial \eta} = 0, \qquad \frac{\partial T_{(0)}^{12}}{\partial \xi} + \frac{\partial T_{(0)}^{22}}{\partial \eta} = 0, \\ \Delta\,(T_{(0)}^{11} + T_{(0)}^{22}) = q_n \frac{\sqrt{-1}}{C}, \qquad \Delta = \frac{\partial^2}{\partial \xi^2} + \frac{\partial^2}{\partial \eta^2}, \end{gathered} \tag{15.8}$$

$$\begin{gathered} \frac{\partial u_{(0)}}{\partial \xi} = \frac{b^4}{Eh}\,\mathrm{Re}\,(T_{(0)}^{11} - \nu T_{(0)}^{22}), \\ \frac{\partial v_{(0)}}{\partial \eta} = \frac{b^4}{Eh}\,\mathrm{Re}\,(T_{(0)}^{22} - \nu T_{(0)}^{11}), \\ \frac{\partial u_{(0)}}{\partial \eta} + \frac{\partial v_{(0)}}{\partial \xi} = \frac{2(1+\nu)}{Eh} b^4\,\mathrm{Re}\,[T_{(0)}^{12}], \end{gathered} \tag{15.9}$$

$$\begin{gathered} \frac{\partial^2 w_{(0)}}{\partial \xi^2} = \frac{b^4}{EhC}\,\mathrm{Im}\,T_{(0)}^{22}, \qquad \frac{\partial^2 w_{(0)}}{\partial \eta^2} = \frac{b^4}{EhC}\,\mathrm{Im}\,T_{(0)}^{11} \\ \frac{\partial^2 w_{(0)}}{\partial \xi\,\partial \eta} = -\frac{b^4}{EhC}\,\mathrm{Im}\,T_{(0)}^{12}, \\ \frac{\partial T_{(1)}^{11}}{\partial \xi} + \frac{\partial T_{(1)}^{21}}{\partial \eta} = -\sqrt{-1}\,\frac{C}{b}\,\frac{\partial}{\partial \xi}\,(T_{(0)}^{11} + T_{(0)}^{22}), \end{gathered} \tag{15.10}$$

$$\frac{\partial T^{12}_{(1)}}{\partial \xi}+\frac{\partial T^{22}_{(1)}}{\partial \eta}=-\sqrt{-1}\,\frac{C}{b}\,\frac{\partial}{b\eta}\,(T^{11}_{(0)}+T^{22}_{(0)}), \tag{15.11}$$

$$\Delta\,(T^{11}_{(1)}+T^{22}_{(1)})=-\sqrt{-1}\,\frac{b}{C}\,(T^{11}_{(0)}+T^{22}_{(0)}),$$

$$\frac{\partial u_{(1)}}{\partial \xi}=-bw_{(0)}+\frac{b^4}{Eh}\,\mathrm{Re}\,(T^{11}_{(1)}-\nu T^{22}_{(1)}),$$

$$\frac{\partial v_{(1)}}{\partial \eta}=-bw_{(0)}+\frac{b^4}{Eh}\,\mathrm{Re}\,(T^{22}_{(1)}-\nu T^{11}_{(1)}), \tag{15.12}$$

$$\frac{\partial u_{(1)}}{\partial \eta}+\frac{\partial v_{(1)}}{\partial \xi}=\frac{b^42\,(1+\nu)}{Eh}\,\mathrm{Re}\,[T^{12}_{(1)}],$$

$$\frac{\partial^2 w_{(1)}}{\partial \xi^2}=\frac{1}{b}\,\frac{\partial u_{(0)}}{\partial \xi}+\frac{b^4}{EhC}\,\mathrm{Im}\,T^{22}_{(1)},$$

$$\frac{\partial^2 w_{(1)}}{\partial \eta^2}=\frac{1}{b}\,\frac{\partial v_{(0)}}{\partial \eta}+\frac{b^4}{EhC}\,\mathrm{Im}\,T^{11}_{(1)}, \tag{15.13}$$

$$\frac{\partial^2 w_{(1)}}{\partial \xi\,\partial \eta}=\frac{1}{2b}\left(\frac{\partial u_{(0)}}{\xi\,\partial \eta}+\frac{\partial v_{(0)}}{\partial \xi}\right)-\frac{b^4}{EhC}\,\mathrm{Im}\,T^{12}_{(1)}.$$

2. We proceed to the formulation of the boundary conditions assuming that the cut is situated on the co-ordinate line $\alpha^1=\xi$ ($\alpha^2=\eta_0=$ constant) and centred at the point ξ_0, η_0. The projection of the cut on the equatorial plane represents a line segment of length $2bl$.

Let $\mathbf{t}$ and $\boldsymbol{\nu}$ be unit tangent and normal vectors to the line $\alpha^2=$ constant. For the determination of the complex boundary quantities on the contour $\alpha^2=\eta_0=$ constant we have the expressions [56]

$$T_{\nu\nu}\cong O_{\nu\nu}=\nu_\alpha\nu_\beta T^{\alpha\beta},$$

$$Q_{\nu t}\cong T_{\nu t}=\nu_\alpha\nu_\beta T^{\alpha\beta},$$

$$M_{\nu\nu}=iC\,[T-T_{\nu\nu}-\nu T'_{\nu\nu}], \tag{15.14}$$

$$Q_{\nu n}=iC\left[\frac{dT}{dS_\nu}-\frac{dT_{\nu t}}{dS_t}-\nu\,\frac{dT'_{\nu t}}{dS_t}\right],$$

$$\frac{d}{dS_\nu}=\nu^\alpha\nabla_\alpha,\qquad \frac{d}{dS_t}=t^\alpha\nabla_\alpha.$$

Here t_α and ν_α are the covariant components of the unit tangent and normal vectors to the co-ordinate line $\alpha^1=\xi$,

$\mathbf{t} = t^\alpha \mathbf{r}_\alpha$, $\mathbf{\nu} = \nu^\alpha \mathbf{r}_\alpha$ [a prime in (15.14) denotes the complex conjugate].

By expanding the components t_α and ν_α in power series of the parameter ε^2 and using expansion (15.7), we find

$$Q_{\nu\nu} \cong b^2 T^{22}_{(0)} + b^2\varepsilon^2 [T^{22}_{(1)} - 2\rho^2 T^{22}_{(0)}] + \ldots,$$

$$Q_{\nu t} \cong -b^2 T^{12}_{(0)} - b^2\varepsilon^2 T^{12}_{(1)} - \ldots,$$

$$M_{\nu\nu} \cong iCb^2 \{(T^{11}_{(0)} - \nu T^{22}_{(0)}) + \\ + \varepsilon^2 [T^{11}_{(1)} - \nu T^{22'}_{(1)} + 2\rho^2 (T^{22}_{(0)} + \nu T^{22'}_{(0)})] + \ldots\}, \quad (15.15)$$

$$Q_{\nu n} \cong -iCb^2 \left\{ \frac{\partial}{\partial\eta}(T^{11}_{(0)} + T^{22}_{(0)}) - \frac{\partial T^{21}_{(0)}}{\partial\xi} - \nu \frac{\partial T^{21'}_{(0)}}{\partial\xi} + \right. \\ \left. + \varepsilon^2 \left[\frac{\partial}{\partial\eta}(T^{11}_{(1)} + T^{22}_{(1)}) - \frac{\partial T^{21}_{(1)}}{\partial\xi} - \nu \frac{\partial T^{21'}_{(1)}}{\partial\xi} \right] + \ldots \right\}.$$

The real parts in expressions (15.15) represent the components of the tangential force, the bending moment, and the generalized shearing force on the boundary element.

For the determination of the components of the displacement vector of the boundary element in the t and ν directions we obtain

$$\begin{aligned} u_\nu &= \mathrm{Re}\,(\nu^\alpha u_\alpha) = -\frac{1}{b}\nu_{(0)} - \varepsilon^2 \frac{1}{b}\nu_{(1)} - \ldots, \\ u_t &= \mathrm{Re}\,(t^\alpha u_\alpha) = \frac{1}{b} u_{(0)} + \varepsilon^2 \frac{1}{b} u_{(1)} + \ldots . \end{aligned} \quad (15.16)$$

Let the following conditions be fulfilled on the sides of the cut:

$$\begin{aligned} &\mathrm{Re}\,[Q_{\nu\nu}(\xi, \eta_0)] = -Q_0, \quad \mathrm{Re}\,[Q_{\nu t}(\xi, \eta_0)] = 0, \\ &\mathrm{Re}\,[M_{\nu\nu}(\xi, \eta_0)] = 0, \qquad \mathrm{Re}\,[Q_{\nu n}(\xi, \eta_0)] = 0 \\ &\qquad (|\xi| < l). \end{aligned} \quad (15.17)$$

Clearly, the components w, u_ν, u_t, $\partial w/\partial\eta$ and quantities (15.15) must be continuous outside the cut.

In solving the problem it is convenient to determine the components of the force tensor of the zero and first ap-

proximations with the help of the complex stress functions

$$T^{11}_{(0)}=\frac{\partial^2\Phi_0}{\partial\eta^2},\quad T^{22}_{(0)}=\frac{\partial^2\Phi_0}{\partial\xi^2},\quad T^{12}_{(0)}=-\frac{\partial^2\Phi_0}{\partial\xi\,\partial\eta},$$

$$\Delta\Delta\Phi_0=\frac{i}{C}q_n,\qquad \Phi_0=\Phi_0'+i\Phi_0'',$$

$$T^{11}_{(1)}=\frac{\partial^2\Phi_1}{\partial\eta^2}-i\frac{C}{b}\Delta\Phi_0,\quad T^{22}_{(1)}=\frac{\partial^2\Phi_1}{\partial\xi^2}+i\frac{C}{b}\Delta\Phi_0,\quad (15.18)$$

$$T^{12}_{(1)}=-\frac{\partial^2\Phi_1}{\partial\xi\,\partial\eta},$$

$$\Delta\Delta\Phi_1=-i\frac{b}{C}\Delta\Phi_0,\quad \Phi_1=\Phi_1'+\Phi_1''.$$

The solution satisfying conditions (15.17) is obtained by using Fourier transforms and the well-known methods of solving the plane problem of elasticity for a half-plane with mixed conditions on the boundary. Without going through intermediate computations we present the final result for the normal stress on the prolongation of the cut

$$\frac{1}{Q_0}\sigma_{\nu\nu}(\xi_1,0)=\frac{1}{h}\left(\frac{|\xi_1|}{\sqrt{\xi_1^2-l^2}}-1\right)+$$
$$+\varepsilon\left[\frac{1}{h}\left(\frac{l^2|\xi_1|-2\xi_1^2|\xi_1|-2\xi_0 l^2\operatorname{sign}\xi_1}{\sqrt{\xi_1^2-l^2}}+2|\xi_1|\sqrt{\xi_1^2-l^2}\right)\pm\right.$$
$$\left.\pm\frac{3}{8}(1+3\nu)\frac{bl^2}{h^2}\left(\frac{|\xi_1|}{\sqrt{\xi_1^2+l^2}}+2\ln\left|\frac{\xi_1}{l}+\sqrt{\frac{\xi_1^2}{l^2}-1}\right|\right)\right].$$
$$(15.19)$$

On the basis of (15.19) we determine the stress intensity factors at the points $(\eta_0,\ \xi_1=l+0)$ and $(\eta_0,\ \xi_1=-l-0)$

$$K^+=\lim_{\xi_1\to l+0}\left[\sqrt{2\pi s_1}\,\sigma_{\nu\nu}(\xi_1,0)\right]=$$
$$=\sqrt{\pi bl}\frac{Q_0}{h}\left\{1+\left(\frac{bl}{a}\right)^2\left[-\left(1+2\frac{\xi_0}{l}\right)\pm\frac{3}{8}(1+3\nu)\frac{b}{h}\right]\right\},$$
$$(15.20)$$

$$K^-=\lim_{\xi_1\to -l-0}\left[\sqrt{2\pi s_1}\,\sigma_{\nu\nu}(\xi_1,0)\right]=$$
$$=\sqrt{\pi bl}\frac{Q_0}{h}\left\{1+\left(\frac{bl}{a}\right)^2\left[-\left(1-2\frac{\xi_0}{l}\right)\pm\frac{3}{8}(1+3\nu)\frac{b}{h}\right]\right\}.$$
$$(15.21)$$

It should be noted that expressions (15.20) and (15.21) involve only one co-ordinate of the centre of the cut.

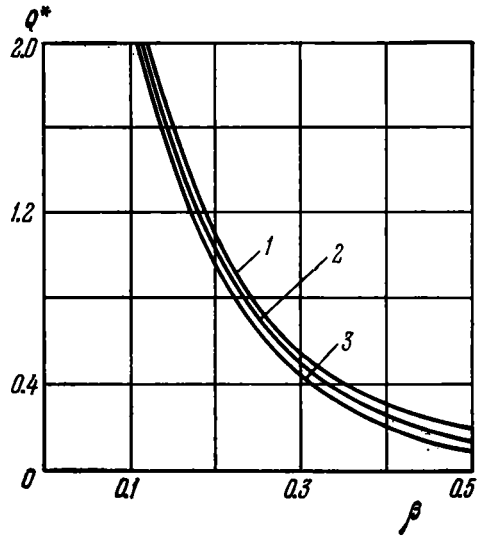

Fig. 15.2. Relation between the critical force on the faces of a crack and its length. Lines *1*, *2*, *3* correspond respectively to the values $\xi_0/l = 2, 4, 6$ ($b/h = 30$).

Figure 15.2 gives $Q^* = Q_0\sqrt{\pi a}/hK_c^-$ as a function of the crack size $\beta = bl/a$.

16. ON A METHOD OF CALCULATING A CRACK TRAJECTORY

We use the variational principle of crack theory formulated in Sec. 4 for finding a crack trajectory. Assuming the surface fracture energy density γ to be constant and the crack length over which the functional is defined to be given, we write down the variational condition for the plane problem as

$$\delta I \equiv \delta\left(\gamma l - \frac{1}{2}\int^{l} p_i u_i\, ds\right) = 0. \qquad (16.1)$$

Here the crack trajectory is varied under some additional conditions. One of these conditions is the requirement that the crack length should be constant. This corresponds to the case of special variations under which the fracture energy $2\int_0^l \gamma\, ds$ is constant. Thus, on the one hand, we obtain the relative extremum problem and, on the other hand, the first term in equality (16.1) may be rejected.

Another additional condition is that the process of crack growth should be equilibrium. In other words, the energy flow due to a possible increment of crack length is entirely expended in fracture. As the external load increases or decreases slowly, the crack propagates slowly and stably along the unknown trajectory. It is essential that the external load should suitably diminish in the region of descending relation between the external load and the crack length in the limiting equilibrium state. This additional condition may thus be represented as $dI/dl = 0$. At the same time, it is known that in the isoperimetric problem of the calculus of variations with a condition of the type $\int_0^l ds = l =$ constant the Lagrangian multiplier λ represents the rate of change of the extreme value of the functional with l, i.e., $\lambda = dI/dl$. By virtue of the second additional condition $\lambda = 0$, which enables us to rewrite equality (16.1) as

$$\delta \int_0^l p_i u_i\, ds = 0. \tag{16.2}$$

At the same time it may be added that, in general, this problem could be considered without introducing the additional conditions. Indeed, the functional I is defined on a line segment of fixed length. The variation of the trajectory changes the magnitude of the integrand over an element of length, but, since the interval of integration remains the same, we obtain a moving-ends problem with "abscissas" of the ends fixed.

Notice the relation between condition (16.2) and Lagrange's variational principle in elasticity. In Sec. 4 it was estab-

lished that

$$-\delta A+\delta W=-\frac{1}{2}\delta\int_0^l p_i u_i\, 2ds$$

(δA is the work done by external forces, δW is the strain energy). The variation of displacement needed in Lagrange's principle ($-\delta A+\delta W=0$) may be realized by varying the trajectory which determines the displacements. Consequently, condition (16.2) is virtually a modified Lagrange's principle.

When σ_{ij} = constant, from (16.2) it follows that the volume occupied by the cavity of the opened crack is stationary on the actual trajectory.

The position of the ends of a crack corresponding to different values of the loading parameter on the known crack trajectory is found from the equation (Sec. 4)

$$\frac{\partial}{\partial l}\left(\gamma l-\frac{1}{2}\int_0^l p_i u_i\, ds\right)=0. \tag{16.3}$$

Thus, the problem of finding a path along which the crack propagates and that of finding a relation connecting the external loading parameter with the crack length are separated.

In order to use Eqs. (16.2) and (16.3), it is necessary to have the values of displacements on the surface of the unknown crack.

To determine the displacements u_j it is convenient to use Muskhelishvili's method with application of a mapping function $\omega(\zeta)$, which transforms the boundary of the crack faces into a circle of unit radius, and the region outside the crack into the outside of the circle.* Suppose that the equation of the trajectory is given by

$$y=f(x). \tag{16.4}$$

Then

$$\omega(\zeta)=P_1(r,\theta)+iP_2(r,\theta)\,(\zeta=re^{i\theta},\ z=\omega(\zeta)=$$
$$=x+iy)$$

* The solution of the problem considered below is due to N. A. Bochkov.

satisfies the conditions

$$r\frac{\partial P_1}{\partial r}=\frac{\partial P_2}{\partial \theta}, \qquad \frac{\partial P_1}{\partial \theta}=-r\frac{\partial P_2}{\partial r},$$
$$\frac{\partial \omega}{\partial \zeta}\neq 0 \qquad (r\geqslant 1), \tag{16.5}$$

$$P_2(r,\ \theta)=f\,[P_1(r,\ \theta)] \qquad (r=1). \tag{16.6}$$

Each point $(r,\ \theta)$ on the circle is transformed into a point $(x,\ y)$ of the trajectory by the relations $x = P_1(r,\ \theta)$, $y = P_2(r,\ \theta)$.

From condition (16.5) it follows that $P_1(r,\ \theta)$ satisfies the Dirichlet problem

$$\Delta^2 P_1(r,\ \theta) = 0,$$
$$P_1(1,\ \theta) = P(\theta), \tag{16.7}$$

whose solution is known [283] for any continuous function $P(\theta)$

$$P_1(r,\ \theta)=\frac{1}{2\pi}\int\limits_0^{2\pi}\frac{(1-r^2)\,P(\varphi)\,d\varphi}{1+r^2-2r\cos(\theta-\varphi)}, \tag{16.8}$$

and $P_2(r,\ \theta)$ is expressed in terms of $P_1(r,\ \theta)$ $(r_0>1)$:

$$P_2(r,\ \theta)=$$
$$=\int\limits_{r_0,\ \theta_0}^{r,\ \theta}\left(\frac{\partial P_1}{\partial r}r+\frac{\partial P_1}{\partial \theta}\tan\theta\right)d\theta+\left(\frac{\partial P_1}{\partial r}\tan\theta-\frac{\partial P_1}{\partial r}\frac{1}{r}\right)dr. \tag{16.9}$$

To make efficient use of numerical methods, we approximate the crack trajectory by a broken line consisting of $2n+1$ segments, every kth segment being characterized by its length l_k and slope α_k to the x axis. The point from which a crack begins to grow in both directions coincides with the origin of co-ordinates xy*

$$y=x\left(-\sum_{p=0}^{k-1}l_p\cos\alpha_p\right)\tan\alpha_k+\sum_{p=0}^{k-1}l_p\sin\alpha_p,$$
$$\sum_{p=0}^{k-1}l_p\cos\alpha_p\leqslant x\leqslant\sum_{p=0}^{k}l_p\cos\alpha_p \tag{16.10}$$
$$(k=0,\ \pm 1,\ \pm 2,\ \ldots).$$

* The choice of the starting point at the centre of the trajectory being sought simplifies the computation in view of a subsequent application of Joukovski's formula.

The function $P(\theta)$ is taken as

$$P(\theta) = L_n(\cos\theta - \cos\theta_{k-1})\cos\alpha_k + \sum_{p=0}^{k-1} l_p \cos\alpha_p,$$

$$\cos\theta_k \geqslant \cos\theta \geqslant \cos\theta_{k-1}, \tag{16.11}$$

$$L_n = \sum_{p=0}^{n} l_p, \qquad \cos\theta_{k-1} = \frac{\sum_{p=0}^{k-1} l_p}{L_n}$$

$$(n \geqslant k).$$

This choice of the function $P(\theta)$ is dictated by the conformal mapping of the crack line onto a straight cut which in turn is mapped onto a unit circle. The mapping of the first inclined segment of the crack when transforming to a cut coinciding with some new axis s gives $x = s\cos\alpha_0$. The mapping of the sides of this cut onto the unit circle by Joukovski's formula gives the relation $s = L_n\cos\theta$. This yields the first line of formula (16.11).

Substituting expression (16.11) in formula (16.8), we find the function $P_1(r, \theta)$, and then from (16.9) we obtain $P_2(r, \theta)$. Thus, the mapping function $\omega(\zeta)$ is determined. It may be shown that it satisfies conditions (16.6), the value of the derivative at the nodal points being equal to the arithmetic mean.

Further the displacement $u_j = u_j(p_j, \alpha_0, \alpha_1, \ldots, \alpha_n, L_n)$ is found by the known methods. Substituting this in the energy functional (16.1), we obtain a function of several variables

$$F(p_j, \alpha_0, \alpha_1, \ldots, \alpha_n, L_n) =$$

$$= \int_S [2\gamma - p_j u_j(p_j, \alpha_0, \alpha_1, \ldots, \alpha_n, L_n)]\, dS. \tag{16.12}$$

The variational problem is thus reduced to that of finding extreme points of a function of several variables, i.e., to the solution of the system of equations

$$\frac{\partial F}{\partial \alpha_j} = 0 \qquad (j = 1, 2, \ldots, n),$$
$$\frac{\partial F}{\partial L_n} = 0. \tag{16.13}$$

Here the last equation is Eq. (16.3). If we use condition (16.2), then

$$F_1 = -\sum_{p=0}^{n} \int_{l_p}^{l_{p+1}} p_j u_j \, dS;$$

all equations of system (16.13), except the last, are unchanged, and the last equation becomes

$$\frac{\partial F_1}{\partial L_n} = \gamma.$$

We restrict ourselves to the case of simple loading for which the relation $p_j = tp_j^0$ is valid (t is the loading parameter, p_j^0 is the given load). The parameter t_n^* characterizing the limiting load under which a new segment n has formed is determined from the last equation of system (16.13). This equation is rewritten as

$$\frac{\partial F}{\partial L_n} = \frac{F(t, \alpha_0, \alpha_1, \ldots, \alpha_n, L_n) - F(t_{n-1}^*, \alpha_0, \alpha_1, \ldots, \alpha_n, L_{n-1})}{l_n}. \tag{16.14}$$

The desired consideration of the variation in stress field with crack growth is accomplished by writing out system (16.13) not simultaneously for the whole set of values of angles α_k, but successively, beginning with the zero value. This takes account of the 'fracture path,' which in contrast to the loading path, may not always be prescribed in advance.

The successive solutions of the problem first for $n = 0$, then for $n = 1$ (with fixed α_0), then for $n = 2$ (with fixed α_0 and α_1), etc., give all values of angles α_n and parameters t_n^*. As a result, we can construct the crack trajectory and the relation between the crack length and the load.

By way of illustration of the method we shall consider the following problem. Let a plate be compressed at infinity by a load of intensity tp_0 parallel to the y axis. The plate has an initial straight crack of length $2l_0$ oriented at an angle α_0 to the x axis. Find the trajectory of a crack developing from the ends of the initial cut and the co-ordinates of the crack ends as a function of the loading parameter t^*.

By solving the problem by the foregoing method, we obtain the function F as

$$F(t, \alpha_0, \alpha_1, \ldots, \alpha_n, L_n) =$$
$$= \sum_{i=0}^{n} \sum_{j=0}^{n} \{(\tau_i\tau_j + N_iN_j)[b_{ij}(1+\varkappa)\cos(\alpha_i - \alpha_j) -$$
$$- a_{ij}(1-\varkappa)\sin(\alpha_i - \alpha_j)] + (\tau_jN_i - \tau_iN_j)[b_{ij}\sin(\alpha_i - \alpha_j) \times$$
$$\times (1+\varkappa) + a_{ij}(1-\varkappa)\cos(\alpha_i - \alpha_j)]\} - \frac{2\pi E\gamma}{(1+0.1n)\, l_0\,(1+\nu)}.$$

Here $\tau_j = -t \sin \alpha_j \cos \alpha_j$, $N_j = -t \cos^2 \alpha_j$. The length of the segment is taken to be $l_k = 0.1\, l_0$. The coefficients in the above expansion are

$$a_{ij} = (\cos\theta_{i-1} - \cos\theta_i)(\sin\theta_{j-1} - \sin\theta_j - \theta_{j-1}\cos\theta_{j-1} +$$
$$+ \theta_j\cos\theta_j) - (\theta_{i-1}\cos\theta_{i-1} - \theta_i\cos\theta_i)(\cos\theta_{j-1} - \cos\theta_j),$$

$$b_{ij} = -\frac{1}{2}(\theta_{i-1} - \theta_i)(\theta_{j-1} - \theta_j) +$$
$$+ \frac{1}{4}[(\sin 2\theta_{j-1} - \sin 2\theta_j)(\theta_{i-1} - \theta_i) +$$
$$+ (\sin 2\theta_{i-1} - \sin 2\theta_i)(\theta_{j-1} - \theta_j)] +$$
$$+ 2\cos_{j-1}\left[(\cos\theta_{j-1} - \cos\theta_{i-1})\ln\left|\sin\frac{\theta_{j-1} - \theta_{i-1}}{2}\right| +\right.$$
$$\left. + (\cos\theta_i - \cos\theta_{j-1})\ln\left|\sin\frac{\theta_{j-1} - \theta_i}{2}\right|\right] +$$
$$+ 2\cos\theta_j\left[(\cos\theta_j - \cos\theta_i)\ln\left|\sin\frac{\theta_j - \theta_i}{2}\right| +\right.$$
$$\left. + (\cos\theta_{i-1} - \cos\theta_j)\ln\left|\sin\frac{\theta_{i-1} - \theta_j}{2}\right|\right] -$$
$$- (\cos\theta_{j-1} - \cos\theta_j)(\cos\theta_{i-1} - \cos\theta_i).$$

The extreme points of the function F will be sought in the region where the values of the normal displacements of the crack faces are positive.

The results of the numerical calculation performed on the M-20 electronic digital computer for several angles of orientation of the initial cut are presented in Figs. 16.1 and 16.2. The problem has been solved for soda-lime silicate

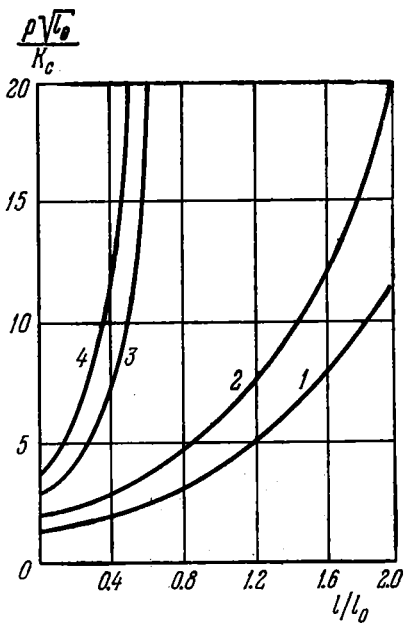

Fig. 16.1. Relation between the compressive stress and the crack length in the limiting equilibrium state for several angles of inclination of the initial cut: *1*, 50°; *2*, 60°; *3*, 70°; *4*, 80°.

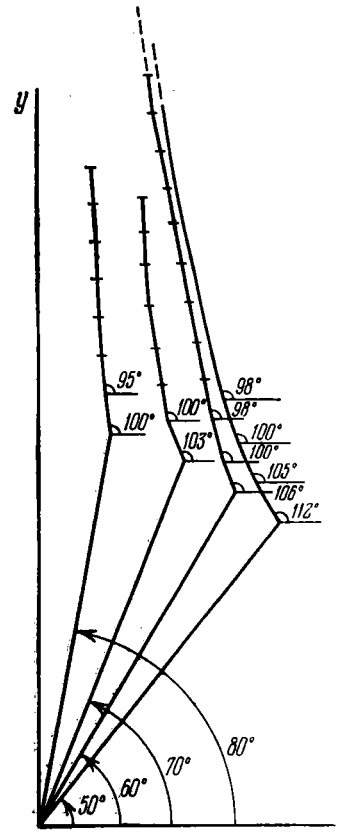

Fig. 16.2. Calculated crack trajectories in a plane under compression for several angles of inclination of the initial cut. The axis of compression is vertical. On the trajectory are marked the angles of inclination α of component segments.

glass on the assumption that the normal displacements of the faces of the initial cut are zero. From the figures it is seen that the propagation of the crack follows a curvilinear path under steadily increasing load. As the crack grows, it tends to straighten out in the direction of the axis

of compression. The minimum load required to propagate a crack occurs for a cut oriented at 45 degrees. This result coincides with the calculations in [218]. As the angle of orientation increases, the limiting load increases and its rate of increase grows to a still greater degree.

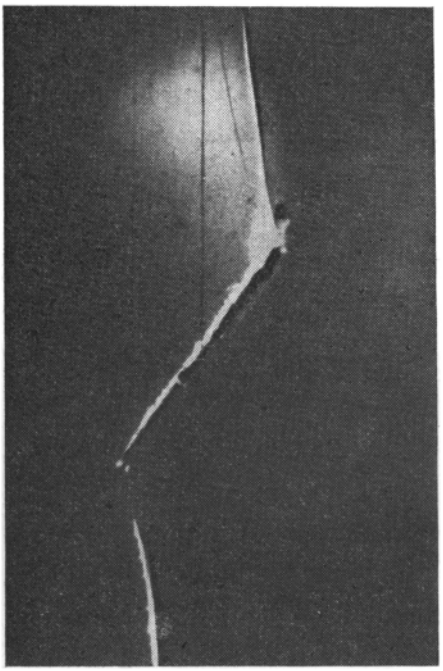

Fig. 16.3. Crack in a compressed glass plate containing an oblique initial cut. The axis of compression is vertical.

The results of the corresponding experiments on specimens of soda-lime silicate glass performed by the authors of [109] show that the loading parameter t_n^* relating to the onset of avalanche crack growth is five times larger than the parameter t_0^* at the moment of crack initiation from the initial cut. From Fig. 16.3 it is seen that the crack trajectory is qualitatively similar to the calculated one. The quantitative discrepancy between the experimental and calculated results can be accounted for by the effect of the specimen boundaries on the stress field around the growing crack.

CHAPTER IV

CRACKS IN ELASTIC-PLASTIC BODIES

17. EXPERIMENTAL INVESTIGATIONS OF THE PLASTIC ZONE AT THE END OF A CUT (CRACK)

The features and details of plastic flow at the end of a cut determine the conditions for its transformation into a crack* and the laws of its further development. It is therefore very important to have a correct idea of the shape and size of the plastic zone, of the strain intensity in it and of the evolution of these quantities during any increment of external load and crack propagation.

The indicated characteristics of the plastic zone at the tip of a crack serve as a basis for introducing some crack models. Such, for example, is the Dugdale-Wells model for plane stress considered above (Sec. 5).

The development of a region of plastic strains can be studied both experimentally and theoretically. A comparison of the results obtained is of some interest and will be made at the end of the next section. We shall now consider the results of experimental observations [106, 243] of plastic zones without going into details of specimen preparation and testing technique.

It is clear that the development of the plastic zone at the end of a cut is affected by many factors, the main of which are the material properties, the shape of a part and the loading conditions.

For an experimental study of plastic zones it is found convenient to use flat specimens of low-carbon steel. By changing their thickness, it is possible to vary the conditions of deformation from plane stress to plane strain.

* In the sense a crack was defined in Sec. 1.

A state of plane strain in a small vicinity of a crack tip is achieved at low stress levels compared with the yield stress. The etching of the polished surface of a specimen shows that the plastic zone spreads in the tension direction (upward and downward) normal to the crack plane (Fig. 17.1).

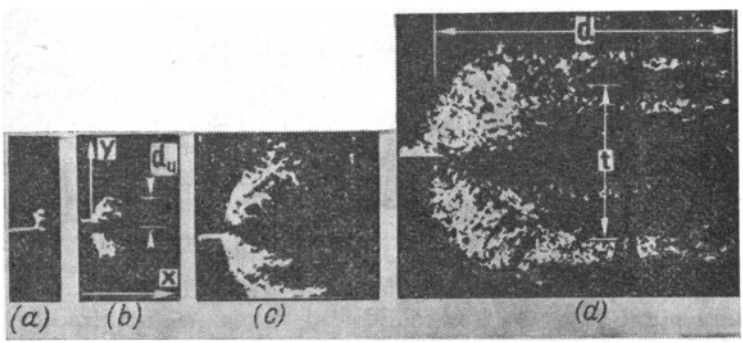

Fig. 17.1. Plastic zone at the end of a cut (0.15 mm clearance) on the surface of a flat steel specimen (0.04% C, 3.31% Si, $\sigma_y = 44$ kgf/mm², $\psi = 70\%$) [243]. Specimen length 200 mm, width 64 mm, thickness $t = 5$ mm, one edge crack of length l, $l/t = 1.3$. The stress level σ/σ_y at the net section is: (*a*) 0.4, (*b*) 0.6, (*c*) 0.8, (*d*) 0.9. In (*b*) is shown the size of the plastic zone d_y, in (*d*) the length of the plastic zone d and the specimen thickness t.

At this stage of the extension of the specimen the length of the plastic zone (on one side of the crack, in the direction of the applied load) is less than the specimen thickness.

The strain normal to the face of the flat specimen is insignificant; if the surface is not etched, the plastic zone is invisible. In the middle part of the specimen thickness, in planes parallel to the face the shape of the plastic zone remains basically unchanged. At the same time there is a marked tendency for the bending of the ends of the plastic zone forward so as to form a kind of a hinge or loop.

As the stress level increases, the conditions for the development of the plastic region approach plane stress. This is assisted by an increase of the size of the plastic zone relative to the thickness.

On the surface of the specimen two narrowing plastic regions begin to develop in the direction of the initial cut from the ends of the vertical plastic regions (formed at an

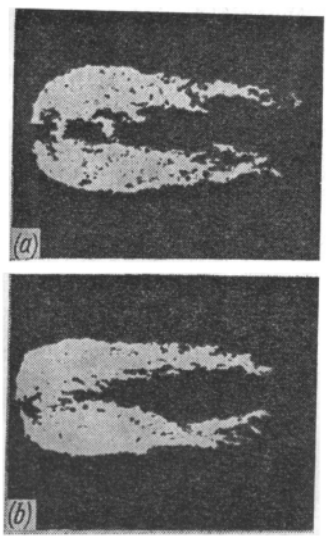

Fig. 17.2. Plastic zone at the surface of a specimen (the steel is the same): (*a*) cut (the notch root radius is approximately 0.07 mm), (*b*) fatigue crack. There is no difference in either the shape or the size of the plastic zone. However, the intensities of plastic strains at the end of the cut and crack must apparently differ greatly.

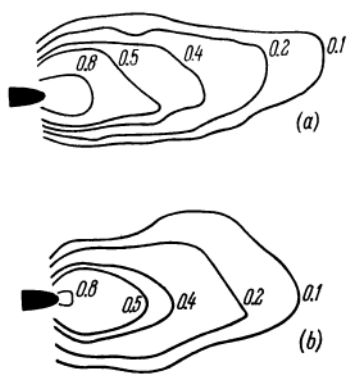

Fig. 17.3. Plastic zone at the surface of steel specimens ($t = 1.52$ mm, $\sigma/\sigma_y = 0.78$) from interferometric data. In the case (*a*) the steel (the same as in the preceding figures) has a yield plateau, in the case (*b*) there is no yield plateau (the steel is the same, tempering at 1200 °C, $\sigma_{0.2} = 38$ kgf/mm²). The difference between these two cases is less than the experimental error. The numbers attached to the lines denote the strain normal to the surface expressed in per cent.

early stage of the loading). The two regions are spaced apart at a distance equal to the specimen thickness (Figs. 17.1 and 17.2). Longitudinal sections of the specimen by planes parallel to the face plane show that these two plastic regions

get closer together and coincide at mid-thickness. From Figs. 17.2 and 17.3 it is seen that the shape of the fully developed plastic zone on the surface of the specimen is independent (within certain limits) of the sharpness of the cut and the presence (or absence) of the yield plateau.

The images at sections passed across the crack direction indicate that the plastic zone takes the form of two inter-

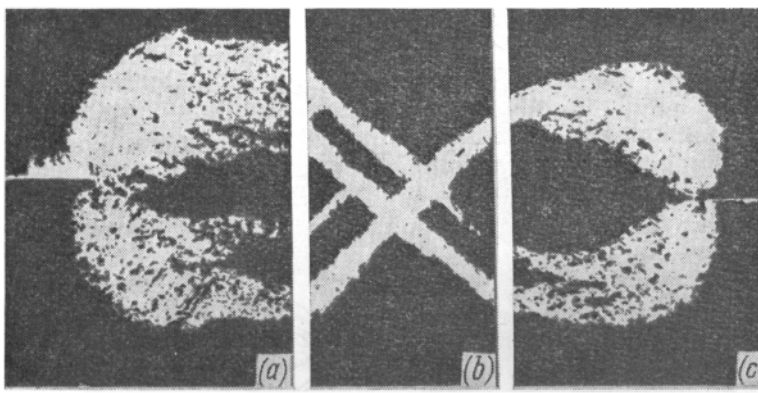

Fig. 17.4. Front view of the plastic zone on the face (*a*), on the cross section (*b*), and the back view of the specimen surface (*c*). The steel is the same, $t = 0.5$ mm, $\sigma/\sigma_y = 0.9$.

secting bands at an angle of 45 degrees to the specimen surface (Fig. 17.4). As is known, this is the direction in which the maximum shearing stresses occur in a thin plate under tension. A considerable strain is observed on the specimen surface in the thickness direction, which appears outwardly as contraction (or necking).

At the same time it might be well to point out the complexity of the configuration of the plastic zone, which is revealed in a more detailed analysis. This complexity lies in the fact that one can simultaneously observe both a configuration in the form of a hinge and a configuration in the form of inclined bands. It might be said that at small stress levels, and in particular for short cracks and thick plates, the hinge form of the plastic zone is predominant. For an appropriate combination of high stress levels, long cracks

and thin plates the inclined bands are the predominant shape of plastic zones.

The transition from plane strain to plane stress takes place permanently and in consequence the line of demarcation is difficult to determine. The hinge form of the plastic zone will apparently predominate in the case of the constrained development of inclined plastic bands when the latter are surrounded by the elastically deforming material. The inclined plastic bands will develop throughout the thickness t of the specimen after the size d_y of the plastic region in the form of a hinge loop on the surface of the specimen reaches the value $0.5t$ on either side of the crack plane. It may be assumed that this is a criterion giving an upper stress bound for the region of plane strain.

The contribution of inclined bands to the volume of the plastic zone is predominant when the band length d exceeds $4t$. This quantity may serve as a lower stress bound for the region of plane stress.

As the stress level increases, both d_y and d also increase. Consequently, the transition from plane strain to plane stress in thick specimens takes place at higher stresses. For example, for a specimen thickness of 0.43 mm the transition from plane strain to plane stress takes place at $\sigma/\sigma_y = 0.4$, and for a thickness of 5 mm at 0.9.

The foregoing investigations enable one to represent schematically a three-dimensional model of the plastic zone (Fig. 17.5). In its initial part the loop-like shape predominates, which is then superseded by one or two inclined bands.

Plastic regions in the form of a layer continuing a crack in a thin sheet (of mild steel) under tension were observed in the experiments of D. S. Dugdale [71] performed by him to verify his crack model.

In [139, 157, 301] the authors also studied plastic regions near the ends of a crack under plane stress in rectangular specimens (200 by 360 mm) with a central cut under tension. The material used was 08 steel ($\sigma_y = 20$ kgf/mm^2) and 3 steel ($\sigma_y = 23.4$ kgf/mm^2) of thickness 1, 1.5, 2, 2.5 mm with the length of the cut 14.8, 18.7, and 29.3 mm. The yield stress was defined here as the ratio of the load to the area of the weakened section when it was brought to a completely plastic state.

In examining the specimen surface the following stages of the development of plastic regions were revealed:

(1) The incubation stage without visible indication of plastic deformation on the specimen surface. It ends at

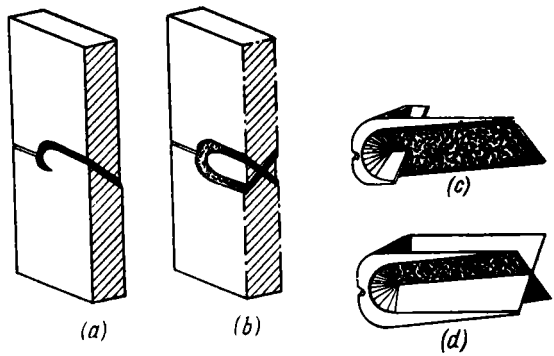

Fig. 17.5. Three-dimensional model of the plastic zone in a flat specimen under tension: (*a*) region of plastic flow for low-carbon steel (0.22% C, 0.36% Mn, $\sigma_y = 25.5$ kgf/mm², $\psi = 63\%$), (*b*) for the steel described in Fig. 17.1, (*c*) and (*d*) three-dimensional models of plastic regions with one and two inclined bands.

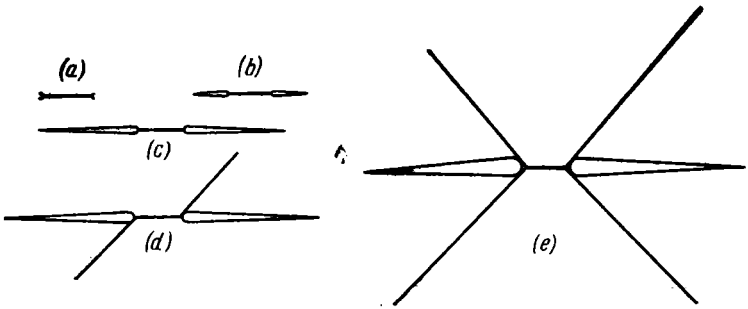

Fig. 17.6. Schematic representation of the process of development of plastic zones detected at the surface of a flat specimen with a central crack under tension: (*a*), (*b*), (*c*) second stage; (*d*), (*e*) third stage.

$\sigma/\sigma_y = 0.37$ for 08 steel and at $\sigma/\sigma_y = 0.51$ for 3 steel (σ is the stress at the weakened section).

(2) There appear dull spots at the ends of the cut (Fig. 17.6*a*) oriented upward and downward from the end of

the horizontal cut (0.5 mm each way). Subsequently they are elongated in the direction of the cut assuming the form of narrow wedge-like bands (Fig. 17.6*b*). At the same time these bands widen reaching a 4 to 6 mm width (Fig. 17.6*c*). The second stage ends at $\sigma/\sigma_y = 0.76$ for 08 steel and at

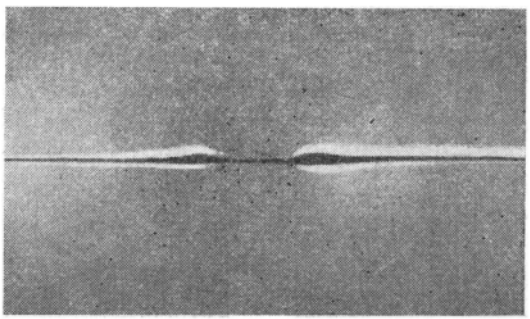

Fig. 17.7. Photograph of a specimen at the end of the second stage. The direction of loading is vertical. It is seen that the length of the plastic zone is about twice as large as the length of the cut.

$\sigma/\sigma_y = 0.92$ for 3 steel.* The appearance of the specimen at this stage is shown in Fig. 17.7.

(3) The third stage begins with a rapid occurrence of thin plastic bands at an angle of 47.5 to 51 degrees to the line of the cut (Fig. 17.6*d*). As the load increases, their number increases to four (two at each end of the crack), their lengths increasing up to the edges of the specimen (Fig. 17.6*e*). The appearance of the end of the cut at this stage is shown in Fig. 17.8.

(4) The bands grow rapidly in width with a simultaneous occurrence of new bands parallel to the original ones. The plastic region assumes a triangular shape (Fig. 17.9). The edges of the crack separate and it begins to grow.

* These and the preceding numerical values for σ/σ_y have been obtained as the arithmetic mean from the data for a large number of specimens. The deviations of individual values from the mean are, however, rather large and depend greatly on the length of the cut, the thickness, etc.

The ranges of loads corresponding to different stages are naturally approximate and vary both from material to material and from part to part for the same material. In particular, for a sufficiently brittle state the fourth, third and even the second of the stages observed may be absent.

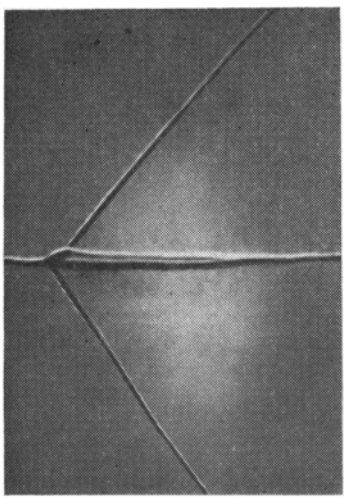

Fig. 17.8. Photograph of the right end of the cut at the third stage. The main plastic zone is much thicker than the initial cut. The inclined plasticity bands show very well.

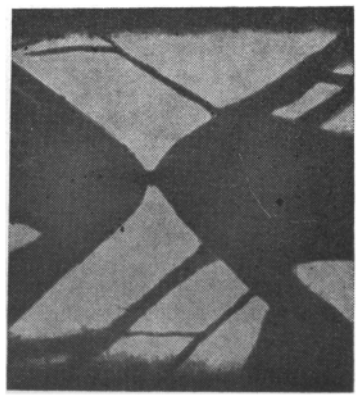

Fig. 17.9. Large triangular regions of plastic strains on both sides of the cut.

It appears from the above that the pictures of the deformation obtained by different authors are consistent: when the lateral elastic strains are constrained, the plastic zones tend to grow across the crack line, and in the absence of this constraint they grow along the crack line.

It should be noted that the end of the main crack in real metallic materials may only schematically and conventionally be approximated by a smooth and a piecewise smooth line following from the elastic or elastic-plastic solution. The degree of correspondence between the results of the

solution obtained by continuum theories and the real situation depends on the degree of locality to which the object is considered. A profound study of the details of the structure of the crack surface and its end will necessarily lead to a rejection of the results of the solution by continuum theories. For this it suffices to look at a series of photographs of cracks detected in various structural elements and occurring for different reasons in service conditions (see, for example, Figs. 17.10 and 17.11). This, however, does not mean that the solutions by continuum theories are wrong. No, they are correct, but for their specific scale, for the corresponding degree of locality to which the object is considered. For example, if the structure of material is taken into account, the range of validity of continuum theories may be determined by means of the structure inhomogeneity diagram of Ya. B. Fridman [90].

Experimental observations show that the tip of a crack need not, in general, be sharp. The crack becomes blunted for different reasons. These may be corrosion (Fig. 17.12), intense plastic deformation, etc. In the case of intense plastic deformation the amount of separation of the faces of a crack at its tip determined at the time of onset of crack growth is taken as a material characteristic [287, 288]. It is assumed that this characteristic estimates local plasticity, and through it the crack sensitivity of the material [70] (see Secs. 5 and 10).

As a result of plastic flow the tip of a crack may even bifurcate. This is how, for example, the process of deformation looks like, from interferometric data, at the tip of a crack on the surface of a flat tensile specimen of Type B95-T1 aluminium alloy [210]. Figure 17.13 shows the tip of a fatigue crack in a specimen taken out of a machine after $42 \times \times 10^3$ cycles ($\sigma = \sigma_m + \sigma_a = 13.5 \pm 11.4$ kgf/mm^2). The interference bands represent equally deepened points of the specimen surface. A considerable permanent deformation is seen at the crack surface, and it may also be noticed that the crack propagates obliquely (not perpendicular to the surface) into the material. This is a consequence of the plastic shear of small volumes of material adjacent to the crack at an angle of 45 degrees to the face of the specimen. The same specimen was then subjected to tension. The interference

patterns are presented in Figs. 17.14 and 17.15. They show a tendency towards blunting and lateral contraction at the crack tip. The crack first propagates in the direction of

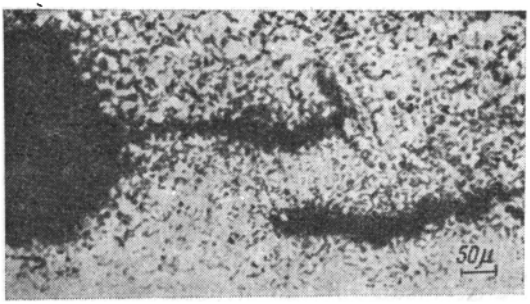

Fig. 17.10. Microphotograph of the surface of a section near the origin of fracture at the inner surface of a rocket body [166]. Two cracks are seen near a corrosion spot.

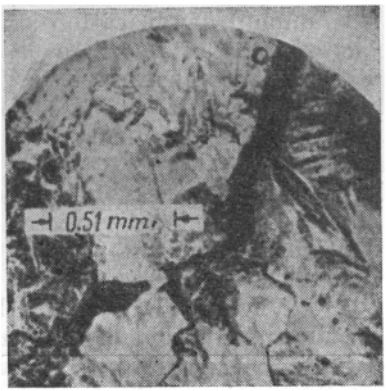

Fig. 17.11. Microphotograph of the tip of a crack in a specimen having the shape of the rim of a turbine wheel [166]. Brittle intergranular fracture under creep.

maximum lateral contraction and then bifurcates. The rapid propagation of the crack occurs in either of these directions. This method was used to reveal that for a fatigue crack the

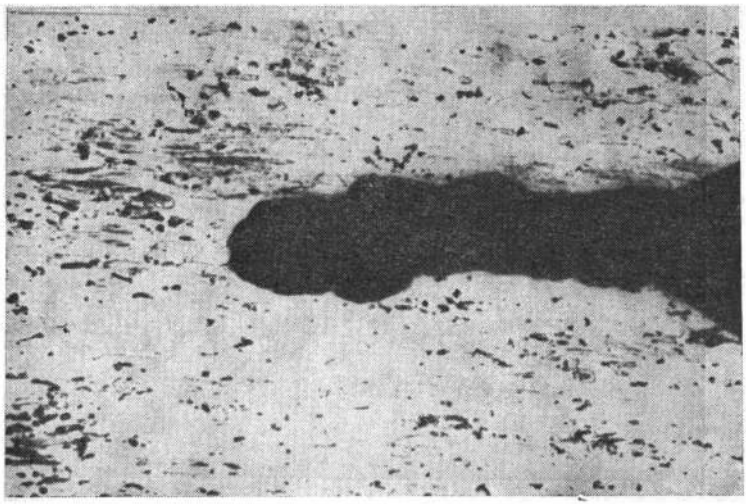

Fig. 17.12. Stress corrosion cracking of Type Д16T aluminium alloy specimen kept in a 3% common salt solution for 1000 hours [61].

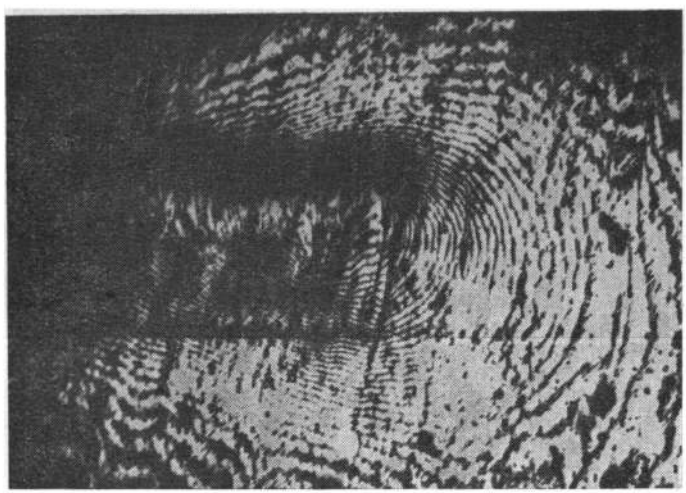

17.13. Residual interference bands at the tip of a fatigue crack. 75 × magnification, reduced by one half in reproduction.

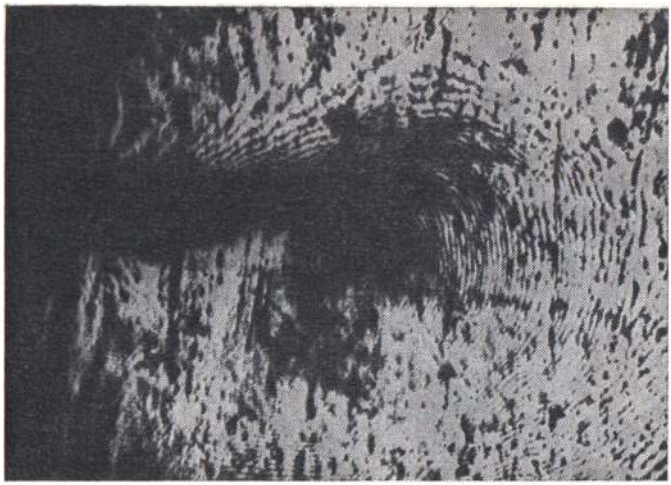

Fig. 17.14. The same crack as in the preceding figure but under a small static tensile load.

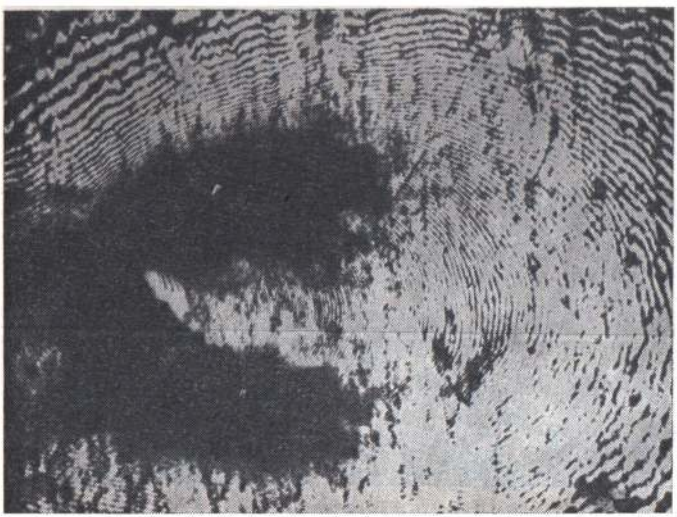

Fig. 17.15. The same crack under a high load before rapid fracture.

lateral contraction (dimple at the crack tip) is constant both in depth and width under constant net stress of the cycle. Under constant load the net stress increases with decreasing section due to the crack growth, with the result that the dimple grows markedly. In this case the depth and width of the dimple at the tip of a fatigue crack may serve as a characteristic of its rate of growth.

18. CALCULATION OF THE PLASTIC ZONE

The material of the preceding section indicates conclusively that in the great majority of cases the fracture is accompanied by the formation of plastic regions. Of considerable interest are therefore the investigations of the laws of crack development in elastic-plastic bodies having certain specific features. First, there is well-known experimental evidence of the presence of a portion of stable crack development in elastic-plastic materials [115, 163]. Second, as theoretical and experimental investigations show [155, 157, 214], the size of the plastic zone depends not only on the kind of loading, but is comparable with the crack length and is a function of it (i.e., of the value of critical loads).

In this connection, of particular importance are such elastic-plastic problems where as part of the solution, besides the determination of the occurring stresses and strains, it is necessary to determine (without any preliminary restrictions) the boundary separating the elastic and plastic zones [108, 145, 146, 158]. The analytic solution in closed form for this class of problems has been obtained only for the case of antiplane strain [40].

1. In order to determine the state of stress and strain in an elastic-perfectly plastic body with a crack we use the deformation theory of plasticity. It is known [124] that the actual displacements u_i corresponding to the equilibrium state realize a minimum of the total energy

$$E = \int \Pi \, dv - A. \tag{18.1}$$

Here Π is the work of deformation, A is the work done by external forces.

Suppose that the relation between the shearing stress intensity

$$T = \left(\frac{1}{2} s_{ij}s_{ij}\right)^{1/2}$$

and the shearing strain intensity

$$\Gamma = (2e_{ij}e_{ij})^{1/2}$$

is determined by

$$T = g(\Gamma)\,\Gamma. \tag{18.2}$$

Here $g(\Gamma)$ is some positive function characteristic of a given material, $s_{ij} = \sigma_{ij} - \delta_{ij}\sigma$ are the components of the stress deviator, $e_{ij} = \varepsilon_{ij} - \frac{1}{3}\delta_{ij}\varepsilon$ are the components of the strain dev ator, $\varepsilon = \varepsilon_{ij}\delta_{ij}$, $\sigma = \frac{1}{3}\sigma_{ij}\delta_{ij}$.

For the case of an elastic-perfectly plastic material we have

$$g(\Gamma) = \begin{cases} \dfrac{\tau_y}{\Gamma} & \text{when } \Gamma > \Gamma_0 = \dfrac{\tau_y}{G}, \\ G & \text{when } \Gamma \leqslant \Gamma_0. \end{cases} \tag{18.3}$$

Assuming $g(\Gamma) = \tau_y/\Gamma$, we obtain von Mises' yield condition. The work of deformation corresponding to expressions (18.2) and (18.3) takes the form

$$\Pi(\varepsilon_{ij}) = \frac{\varepsilon^2}{6k} + \begin{cases} \dfrac{G}{2}\Gamma^2, & \Gamma > \Gamma_0, \\ \tau_y\Gamma - \dfrac{\tau_y^2}{2G}, & \Gamma < \Gamma_0. \end{cases} \tag{18.4}$$

Here $k = \frac{1-2\nu}{E}$ is the bulk modulus.

The differential equations of equilibrium in terms of displacements can be obtained from the system

$$\frac{\partial}{\partial x_i}\left(\frac{\partial \Pi}{\partial \varepsilon_{ij}}\right) = 0; \tag{18.5}$$

they will be different for the elastic state and the state of yielding.

Suppose that the deformed body occupies a volume V bounded by a surface S; in the equilibrium state this volume

consists of an elastic part V_1 and a plastic part V_2 separated by a surface Σ. If the components of displacement, strain and stress are continuous on Σ, the variational principle of the theory of small elastic-plastic deformations may be formulated as [124]

$$\delta\left\{\int_V \frac{\varepsilon^2}{6k}\,dV+\frac{G}{2}\int_{V_1}\Gamma^2\,dV+\tau_y\int_{V_2}\left(\Gamma-\frac{\tau_y}{2G}\right)dV-A\right\}=0; \tag{18.6}$$

the following inequality must then be fulfilled for the region V_2:

$$\Gamma\geqslant\frac{\tau_y}{G}.$$

To analyse the state of stress at the tip of a semi-infinite crack under plane stress or plane strain conditions, we isolate a square of side $2a$ in the xy plane with centre at the point O (Fig. 18.1). In the following discussion we shall assume that the crack is represented by a cut along the positive semi-axis x.

We use the asymptotic expressions (2.17) and (2.18) for the distribution of stress and displacement near the crack tip. In the problem being solved here the loading parameter is the stress intensity factor which assigns the distribution of stress and displacement at the point at infinity. We assign the displacements defined by formulas (2.18) on the boundary of the square under consideration. Since the displacements are subject to variation and their values are given on the boundary, $\delta A = 0$ in expression (18.6). The dimensions of the square are chosen so that the infinite region may be replaced by a finite one and the components of displacement, strain and stress at the crack tip depend only slightly on the boundary conditions now assigned on the sides of the square. Obviously, from the symmetry conditions it follows that we may consider only one half of the square ($-a \leqslant x \leqslant a$, $0 \leqslant y \leqslant a$).

(a) Consider the case of plane stress. Suppose that the material of the body is incompressible ($\nu = 1/2$) and is characterized by Young's modulus E and the yield stress τ_y in pure shear. Noting that the edges of the crack are free

from load and the shearing stresses and displacements along the y axis are zero on the prolongation of the cut, we find

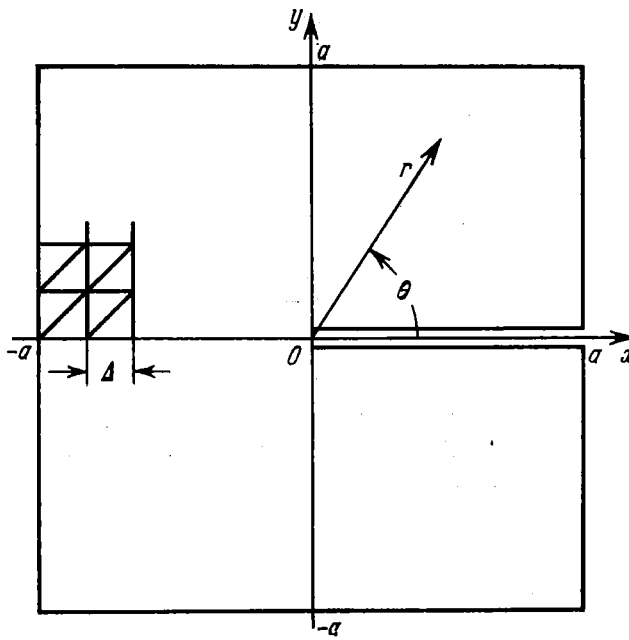

Fig. 18.1. Region in which the solution of the elastic-plastic problem is constructed.

that the actual displacements in the rectangular region S $(-a \leqslant x \leqslant a,\ 0 \leqslant y \leqslant a)$ realize a minimum of the functional

$$I = \frac{1}{6} E \iint\limits_{S_1} \Gamma^2 \, dx \, dy + \tau_y \iint\limits_{S_2} \left(\Gamma - \frac{3\tau_y}{2E} \right) dx \, dy. \qquad (18.7)$$

Here

$$\Gamma = 2 \left(\varepsilon_x^2 + \varepsilon_y^2 + \varepsilon_x \varepsilon_y + \frac{1}{4} \gamma_{xy}^2 \right)^{1/2},$$

$$\varepsilon_x = \frac{\partial u}{\partial x}, \qquad \varepsilon_y = \frac{\partial v}{\partial y}, \qquad \gamma_{xy} = \frac{\partial u}{\partial y} + \frac{\partial v}{\partial x},$$

S_1 is the region of elastic strains, S_2 is the plastic region ($S = S_1 + S_2$).

The boundary C between the regions S_1 and S_2 is determined from the condition

$$\Gamma = \Gamma_0 = \frac{3\tau_y}{E}. \tag{18.8}$$

Displacements (2.18) (for plane stress and a cut along the positive real axis) in the portions of the boundary $x = \pm a$, $0 \leqslant y \leqslant a$ and $y = a$, $-a \leqslant x \leqslant a$ are assumed to be given and in our case ($\nu = 1/2$) are represented by

$$u = -\frac{3}{4}\frac{K}{E}\sqrt{\frac{r}{2\pi}}\left(\frac{7}{3}\sin\frac{\theta}{2} + \sin\frac{3}{2}\theta\right),$$

$$v = \frac{3}{4}\frac{K}{E}\sqrt{\frac{r}{2\pi}}\left(\frac{13}{3}\cos\frac{\theta}{2} + \cos\frac{3}{2}\theta\right), \tag{18.9}$$

$$r = \sqrt{x^2 + y^2}.$$

We introduce non-dimensional quantities

$$\xi = \frac{x}{d}, \quad \eta = \frac{y}{d}, \quad u^* = \frac{u}{d}, \quad v^* = \frac{v}{d}, \quad \rho = \frac{r}{d}, \tag{18.10}$$

where

$$d = \left(\frac{\pi}{4}\frac{K}{\tau_y\sqrt{2\pi}}\right)^2.$$

Functional (18.7) then transforms to

$$I_0 = \frac{I}{Ed^2\tau_0^2} = \frac{1}{6}\iint\limits_{S_1}\left(\frac{\Gamma}{\tau_0}\right)^2 d\xi\, d\eta + \iint\limits_{S_2}\left(\frac{\Gamma}{\tau_0} - \frac{3}{2}\right) d\xi\, d\eta. \tag{18.11}$$

Here

$$\Gamma = 2\left[\left(\frac{\partial u^*}{\partial \xi}\right)^2 + \left(\frac{\partial v^*}{\partial \eta}\right)^2 + \left(\frac{\partial u^*}{\partial \xi}\right)\left(\frac{dv^*}{d\eta}\right) + \right.$$
$$\left. + \frac{1}{4}\left(\frac{\partial u^*}{\partial \eta} + \frac{\partial v^*}{\partial \xi}\right)^2\right]^{1/2}, \quad \tau_0 = \frac{\tau_y}{E}.$$

The boundary separating the plastic and elastic regions is determined from the condition

$$\Gamma = \Gamma_0 = 3\tau_0.$$

The relative magnitudes of displacements in the portions of the boundary $\xi = \pm \frac{a}{d}$, $0 \leqslant \eta \leqslant \frac{a}{d}$ and $\eta = \frac{a}{d}$, $-\frac{a}{d} \leqslant \xi \leqslant \frac{a}{d}$ are found from the equalities

$$\begin{aligned} u^* &= -\frac{3}{\pi}\tau_0\sqrt{\rho}\left(\frac{7}{3}\sin\frac{\theta}{2}+\sin\frac{3}{2}\theta\right), \\ v^* &= \frac{3}{\pi}\tau_0\sqrt{\rho}\left(\frac{13}{3}\cos\frac{\theta}{2}+\cos\frac{3}{2}\theta\right). \end{aligned} \tag{18.12}$$

Thus, in the case of plane stress and material incompressibility the only parameter determining the solution of the problem is the quantity $\tau_0 = \tau_y/E$.

(b) In a similar way, for a state of plane strain we find that to the actual configuration of equilibrium of the region S correspond components of displacement u and v which give a minimum value to the following functional:*

$$I = \frac{1}{6k}\iint_S \varepsilon^2\,dx\,dy + \frac{G}{2}\iint_{S_1}\Gamma^2\,dx\,dy + \\ + \tau_y\iint_{S_2}\left(\Gamma - \frac{\tau_y}{2G}\right)dx\,dy. \tag{18.13}$$

Here

$$\Gamma = \frac{2}{\sqrt{3}}\sqrt{\varepsilon_x^2+\varepsilon_y^2-\varepsilon_x\varepsilon_y+\frac{3}{4}\gamma_{xy}^2},$$
$$\varepsilon = \varepsilon_x + \varepsilon_y, \quad S = S_1 + S_2.$$

The condition $\Gamma = \Gamma_0 = \tau_y/G$ determines the interface between the regions S_1 and S_2.

The minimum of functional (18.13) is sought in the class of functions u, v satisfying, on the boundary of the region,

* To preserve the unique computational scheme of numerical solution for the above-stated problems (a) and (b), the condition of incompressibility of the material is not used in the case of plane strain, and the value for Poisson's ratio is taken to be $\nu = 0{,}46$.

the conditions

$$\tau_{xy} = 0, \quad y = 0, \quad -a \leqslant x \leqslant a;$$
$$v = 0, \quad y = 0, \quad -a \leqslant x < 0;$$
$$\sigma_y = 0, \quad y = 0, \quad 0 < x \leqslant a;$$
$$u = -\frac{K}{4G}\sqrt{\frac{r}{2\pi}}\left[(5-8\nu)\sin\frac{\theta}{2}+\sin\frac{3}{2}\theta\right],$$
$$v = \frac{K}{4G}\sqrt{\frac{r}{2\pi}}\left[(7-8\nu)\cos\frac{\theta}{2}+\cos\frac{3}{2}\theta\right]$$

when $x = \pm a$, $0 \leqslant y \leqslant a$ and $y = a$, $-a \leqslant x \leqslant a$.

Introducing the non-dimensional quantities (18.10) into expression (18.13), we obtain

$$I_0 = \frac{I}{3Gd^2\tau^2} = \frac{1+\nu}{9(1-2\nu)}\iint\limits_S \left(\frac{\varepsilon}{\tau}\right)^2 d\xi\, d\eta + \\ + \frac{1}{6}\iint\limits_{S_1}\left(\frac{\Gamma}{\tau}\right)^2 d\xi\, d\eta + \iint\limits_{S_2}\left(\frac{\Gamma}{\tau}-\frac{3}{2}\right) d\xi\, d\eta. \qquad (18.14)$$

Here

$$\Gamma = \frac{2}{\sqrt{3}}\left[\left(\frac{\partial u^*}{\partial \xi}\right)^2 + \left(\frac{\partial v^*}{\partial \eta}\right)^2 - \left(\frac{\partial u^*}{\partial \xi}\right)\left(\frac{\partial v^*}{\partial \eta}\right) + \\ + \frac{3}{4}\left(\frac{\partial u^*}{\partial \eta}+\frac{\partial v^*}{\partial \xi}\right)^2\right]^{1/2},$$
$$\tau = \frac{\tau_y}{3G}.$$

To the boundary of the plastic region corresponds the value

$$\Gamma = \Gamma_0 = 3\tau.$$

The relative displacements in the portions of the boundary $\xi = \pm\frac{a}{d}$, $0 \leqslant \eta \leqslant \frac{a}{d}$ and $\eta = \frac{a}{d}$, $-\frac{a}{d} \leqslant \xi \leqslant \frac{a}{d}$ are expressed as follows:

$$u^* = -\frac{3}{\pi}\tau\sqrt{\rho}\left[(5-8\nu)\sin\frac{\theta}{2}+\sin\frac{3}{2}\theta\right],$$
$$v^* = \frac{3}{\pi}\tau\sqrt{\rho}\left[(7-8\nu)\cos\frac{\theta}{2}+\cos\frac{3}{2}\theta\right].$$

In this case the desired solution depends on Poisson's ratio ν and the parameter $\tau = \tau_y/3G$.

2. To solve the problems stated above, we use the finite element method [58, 292]. The original region is considered as an assemblage of discrete triangular elements (Fig. 18.2)

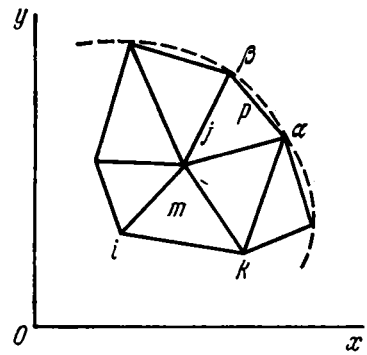

Fig. 18.2. Scheme of dividing the region under consideration into a system of discrete triangular elements.

having a given distribution of displacement and satisfying the compatibility conditions at the nodal points.

Suppose that within the limits of the mth element the displacements $u^*_{(m)}$ and $v^*_{(m)}$ vary linearly

$$\begin{aligned} u^*_{(m)} &= a_1^{(m)} + a_2^{(m)}\xi + a_3^{(m)}\eta, \\ v^*_{(m)} &= a_4^{(m)} + a_5^{(m)}\xi + a_6^{(m)}\eta. \end{aligned} \tag{18.15}$$

For the strain components we then obtain

$$\begin{aligned} \varepsilon_x^{(m)} &= \frac{\partial u^*_{(m)}}{\partial \xi} = a_2^{(m)}, \qquad \varepsilon_y^{(m)} = \frac{\partial v^*_{(m)}}{\partial \eta} = a_6^{(m)}, \\ \gamma_{xy}^{(m)} &= \frac{\partial u^*_{(m)}}{\partial \eta} + \frac{\partial v^*_{(m)}}{\partial \xi} = a_3^{(m)} + a_5^{(m)}. \end{aligned} \tag{18.16}$$

The constants $a_1^{(m)}, \ldots, a_6^{(m)}$ are expressed in terms of the displacements at the vertices of the mth triangular element

$$a_1^{(m)} = \frac{1}{2\omega_m}\left[(\xi_k^{(m)}\eta_j^{(m)} - \xi_j^{(m)}\eta_k^{(m)})\, u^*_{im} + (\xi_i^{(m)}\eta_k^{(m)} - \right.$$
$$\left. - \xi_k^{(m)}\eta_i^{(m)})\, u^*_{jm} + (\xi_j^{(m)}\eta_i^{(m)} - \xi_i^{(m)}\eta_j^{(m)})\, u^*_{km}\right],$$

$$a_2^{(m)}=\frac{1}{2\omega_m}\left[(\eta_k^{(m)}-\eta_j^{(m)})\,u_{im}^*+(\eta_i^{(m)}-\eta_k^{(m)})\,u_{jm}^*+\right.$$
$$\left.+(\eta_j^{(m)}-\eta_i^{(m)})\,u_{km}^*\right],\quad (18.17)$$
$$a_3^{(m)}=\frac{1}{2\omega_m}\left[(\xi_j^{(m)}-\xi_k^{(m)})\,u_{im}^*+(\xi_k^{(m)}-\xi_i^{(m)})\,u_{jm}^*+\right.$$
$$\left.+(\xi_i^{(m)}-\xi_j^{(m)})\,u_{km}^*\right].$$

Here ω_m is the area of the mth triangle, $\xi_i^{(m)}$, $\eta_i^{(m)}$ are the co-ordinates of the ith vertex.

The expressions for the constants $a_4^{(m)}$, $a_5^{(m)}$, $a_6^{(m)}$ may be obtained from (18.17) by replacing $u_{i,j,k,m}^*$ by $v_{i,j,k,m}^*$.

By using representations (18.16) and (18.17), we replace functionals (18.11) and (18.14) by the following expressions:

for plane stress

$$I=\sum_{m=1}^{M}\left[\frac{1}{6}\lambda_{1m}\left(\frac{\Gamma_m}{\tau_0}\right)^2+\lambda_{2m}\left(\frac{\Gamma_m}{\tau_0}-\frac{3}{2}\right)\right]\omega_m,$$
$$\Gamma_m(u_{im}^*,\ldots,u_{km}^*,v_{im}^*,\ldots,v_{km}^*)=$$
$$=2\left[(a_2^{(m)})^2+(a_6^{(m)})^2+a_2^{(m)}a_6^{(m)}+\frac{1}{4}(a_3^{(m)}+a_5^{(m)})^2\right]^{1/2};\quad (18.18)$$

for plane strain

$$I=\sum_{m=1}^{M}\left[\frac{1}{6}\lambda_{1m}\left(\frac{\Gamma_m}{\tau}\right)^2+\lambda_{2m}\left(\frac{\Gamma_m}{\tau}-\frac{3}{2}\right)\right]\omega_m+$$
$$+\frac{1+\nu}{9(1-2\nu)}\sum_{m=1}^{M}\left(\frac{\varepsilon_m}{\tau}\right)^2\omega_m,\quad (18.19)$$
$$\varepsilon_m=a_2^{(m)}+a_6^{(m)},$$
$$\Gamma_m(u_{im}^*,\ldots,u_{km}^*,v_{im}^*,\ldots,v_{km}^*)=$$
$$=\frac{2}{\sqrt{3}}\left[(a_2^{(m)})^2+(a_6^{(m)})^2-a_2^{(m)}a_6^{(m)}+\frac{1}{4}(a_3^{(m)}+a_5^{(m)})^2\right]^{1/2}.$$

The summation in formulas (18.18) and (18.19) is extended over all triangular elements of the region (M is the total number of elements).

The quantities λ_{1m} and λ_{2m} are determined as

$$\lambda_{1m} = 1,\ \lambda_{2m} = 0 \text{ if } \Gamma_m \leqslant \Gamma_0, \qquad (18.20)$$
$$\lambda_{1m} = 0,\ \lambda_{2m} = 1 \text{ if } \Gamma_m > \Gamma_0.$$

The value of Γ_0 is $3\tau_y/E$ for plane stress and τ_y/G for plane strain.

We proceed to the determination of relative displacements at the nodal points, which give a minimum value to the discrete functionals (18.18) and (18.19). We shall use the numerical method of local variations proposed in [55]. A characteristic property of this method is that its application does not require computers with large memory capacity. The application of modern high-speed computers enables one to carry out a numerical analysis on the basis of this method with a large number of unknowns. The algorithm of solution with the use of the method of local variations is as follows. We assign an initial approximation to the displacement components u^* and v^* at all interior nodes of the domain and at those boundary points where the displacements are to be determined. As an initial approximation we may take the distribution of displacements obtained from the solution of the elastic problem. By choosing a sufficiently small step size h, we perform the variation of displacements at all interior points. Note that the variation of displacements at one point produces changes only in some of the terms in sums (18.18) and (18.19), namely in those associated with triangular elements surrounding the given node.

The process of variation is performed as follows. Calculate the part of the discrete analogue of functional (18.18) or (18.19) which is associated with the node under consideration for values of displacements equal to $u_m^* \pm h$, $v_m^* \pm h$. From the given combination choose the values of u_m^*, $u_m^* \pm \pm h$, v_m^*, $v_m^* \pm h$ that lead to a decrease in the indicated sum of terms in (18.18) or (18.19). Thereupon proceed to the variation of the following point. By going round all points in accordance with the given geometric constraints, we obtain the first approximation to the values of displacements at the nodes. If, after completing the nth iteration, it is found that the values of u^* and v^* for all points are the same as for

the preceding approximation, reduce the variation step choosing $h_{n+1} = \alpha h_n$ ($\alpha < 1$). Further the whole process is repeated with a reduced step size. The variation is stopped when h_n becomes less than a certain sufficiently small number. On completion of iterations we obtain approximate values of displacements at the nodal points. The strain components, constant for the mth triangular element, can be determined by formulas (18.16) and (18.17). The strain value at the nodal point may be taken to be the arithmetic mean of these components from all triangles for which the given node is a vertex.

3. For the foregoing algorithm of solving elastic-plastic problems a computer program was written (see Appendix A) for the БЭСМ-6 in Algol 60 by dividing the region under consideration, $-a/d \leqslant \xi \leqslant a/d$, $0 \leqslant \eta \leqslant a/d$, into M right isosceles triangles. The region was divided so that the nodal points formed a regular rectangular pattern with a spacing between the nodes Δ (Fig. 18.1). The values of displacements at the nodal points determined from the elastic solution were taken as an initial approximation, and the initial variation step was equal to $h_0 = 0.5 \times 10^{-4}$. Further reduction of the variation step was effected by the formula $h_n = 0.8h_{n-1}$; the computation process ended after 42 changes of the variation step.

In determining the elastic-plastic interface in the case of plane stress it was found that the shape of the plastic region depends largely on the magnitude of Δ (i.e., on the number of nodes). Figure 18.3 shows a series of lines of equal shearing strain intensity corresponding to $\Gamma/\tau_0 = 3$ with different numbers P of nodal points.

The distribution of lines of equal value of Γ/τ_0 in the whole region is presented in Fig. 18.4. Since increasing the number P of nodes involves an appreciable increase in the machine time, the shape of the boundary was refined by isolating, from the given region, a rectangle of dimensions $-\frac{a}{2d} \leqslant \xi \leqslant \frac{a}{2d}$, $0 \leqslant \eta \leqslant \frac{a}{2d}$, assigning on its sides the displacements obtained from the preceding solution, and then dividing the region into triangular elements whose vertices formed a regular pattern with a spacing between the nodes $\Delta/2$. The shape of the boundary of the plastic

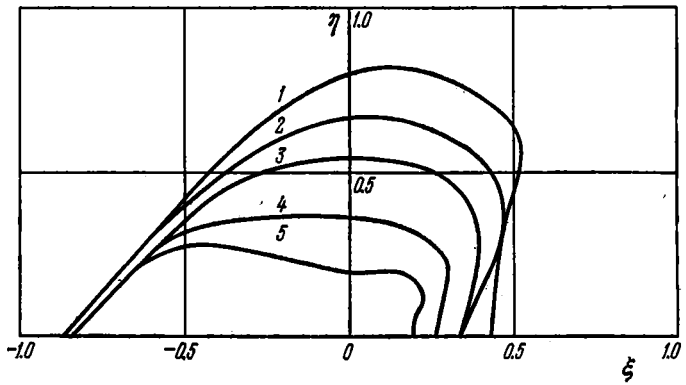

Fig. 18.3. Lines of equal shearing strain intensity near the crack tip for a loading parameter corresponding to $\Gamma/\tau_0 = 3$ (plane stress). Curves *1*, *2*, *3*, *4* are plotted for the number of nodal points 45, 91, 153, 325, respectively. Line *5* is plotted for the region divided into triangular elements with a spacing between the nodes $\Delta/2$.

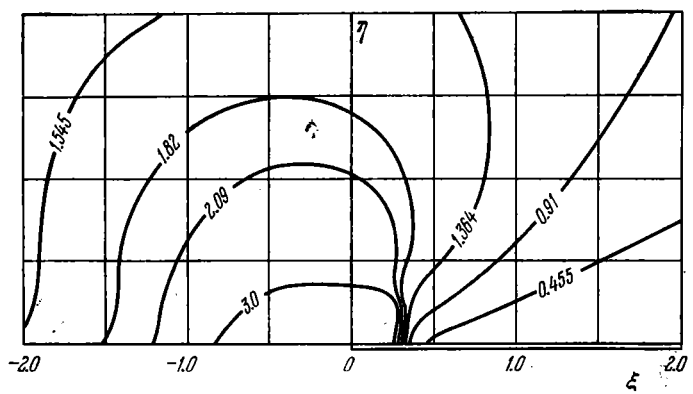

Fig. 18.4. Lines of equal Γ/τ_0 near the crack tip for plane stress with the number of nodal points $P = 325$.

region resulting from this solution is represented by curve *5* in Fig. 18.3*.

The results obtained show that as the number of nodes is increased, the region "contracts" in the η direction, while the characteristic dimension of the region along the ξ axis remains practically unchanged and approximately equal to $0.9d$.

Thus, for plane stress the above calculations suggest the conclusion that the plastic region represents a narrow strip situated on the prolongation of the cut, which supports the well-known Dugdale's hypothesis.

Figures 18.5, 18.6, and 18.7 show the distribution of lines of equal value of ε_x/τ_0, ε_y/τ_0, and γ_{xy}/τ_0 ($P = 325$), respectively.

Figure 18.8 presents the picture of displacements of the region under consideration, and Fig. 18.9 gives the vertical displacement of points of the crack surface (the horizontal displacements are small here).

The corresponding results for plane strain are presented in Figs. 18.10 to 18.18. The shape of the plastic region as influenced by the number of nodes is illustrated in Fig. 18.10. The distribution of lines of equal value of Γ/τ in the whole region for the case of $P = 561$ is shown in Fig. 18.11. Similarly to plane stress, Figs. 18.12, 18.13, 18.14 give the values of ε_x/τ, ε_y/τ, γ_{xy}/τ for the case of plane strain with $P = 561$.

Figures 18.15 and 18.16 show the picture of displacements of the original region for the case of plane strain and the vertical displacement of points of the crack surface. The distribution of normal stress and strain along the real axis on the prolongation of the cut in the case of plane strain is presented in Figs. 18.17 and 18.18, respectively.

4. Let us estimate the error introduced by the linear approximation (18.15) for the displacement components within the limits of one triangular element. Let the approximate expression for the function $u(\xi, \eta)$ be

$$\tilde{u}(\xi, \eta) = a_1 + a_2\xi + a_3\eta.$$

* Note that the influence of the boundary conditions does not appear to have been avoided in the calculation of the refined curve *5* (Fig. 18.3) separating the elastic and plastic zones.

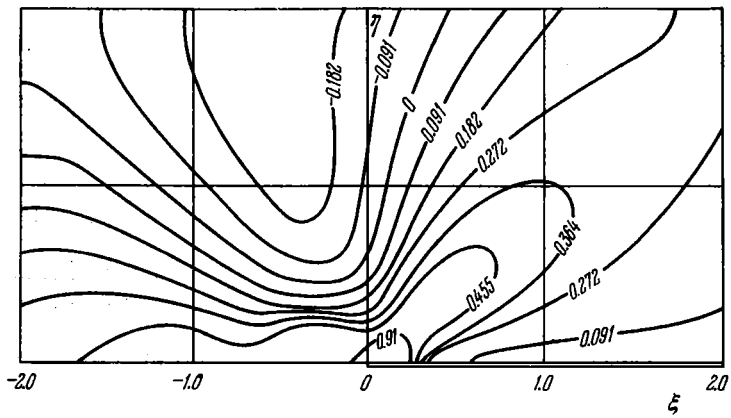

Fig. 18.5. Lines of equal ε_x/τ_0 for plane stress.

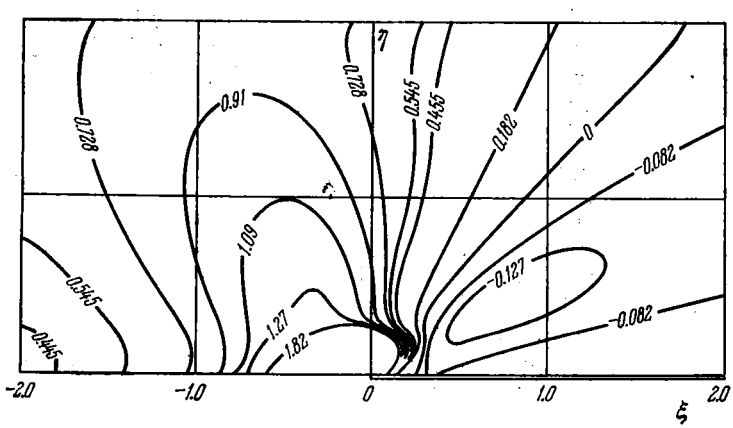

Fig. 18.6. Lines of equal ε_y/τ_0 for plane stress.

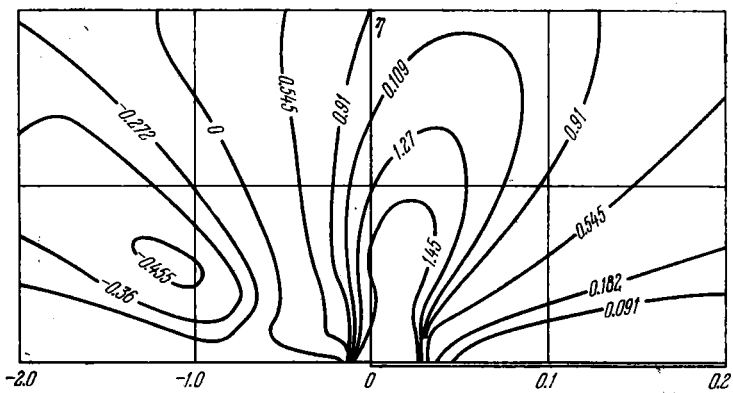

Fig. 18.7. Lines of equal γ_{xy}/τ_0 for plane stress.

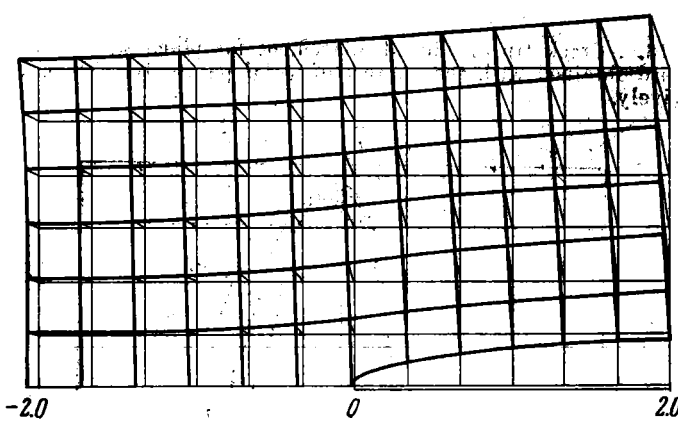

Fig. 18.8. Picture of displacements in the region under consideration for plane stress ($P = 325$).

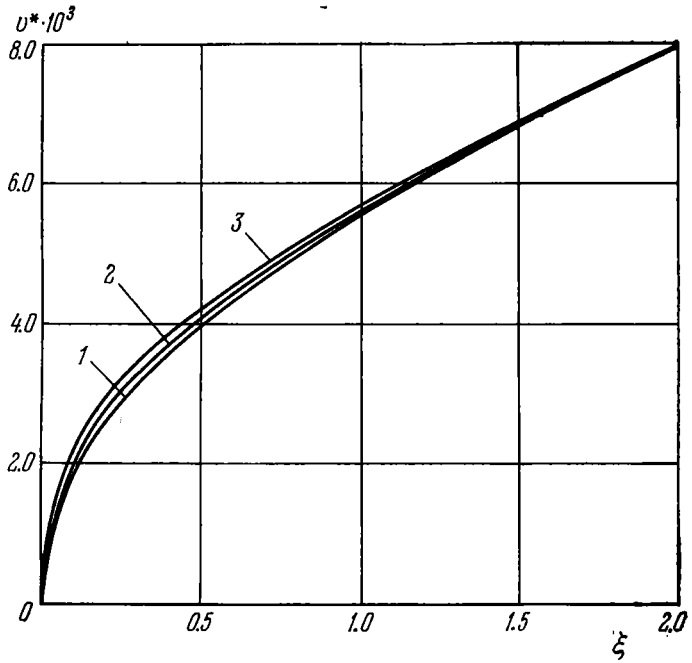

Fig. 18.9. Crack tip opening displacement for plane stress. Lines *1*, *2*, *3* are obtained with the number of nodal points 91, 153, 325, respectively.

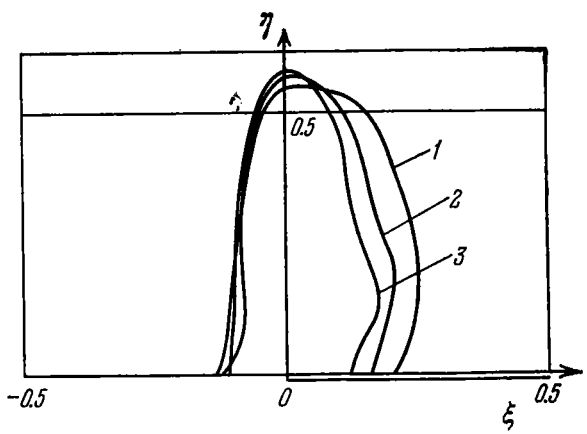

Fig. 18.10. Shape of the plastic zone for plane strain. Lines *1*, *2*, *3* correspond to the number of nodal points 153, 325, 561, respectively.

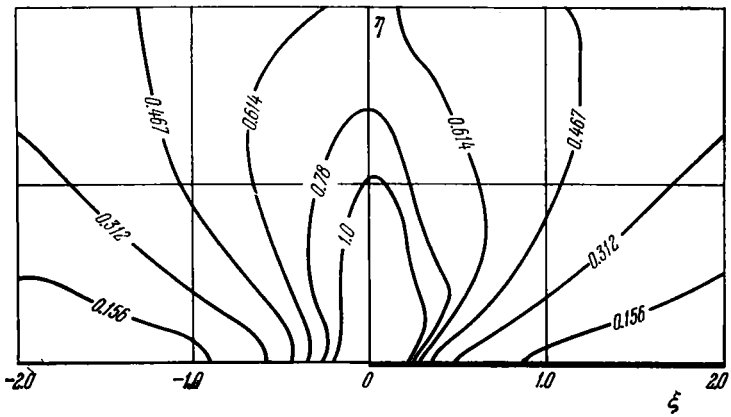

Fig. 18.11. Lines of equal Γ/τ for plane strain ($P = 561$).

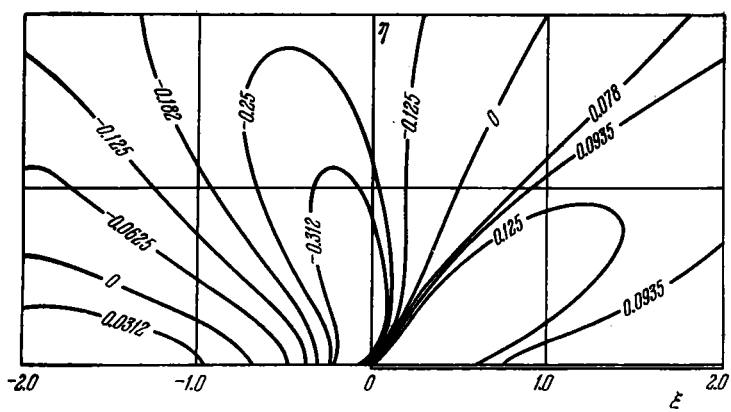

Fig. 18.12. Lines of equal ε_x/τ for plane strain.

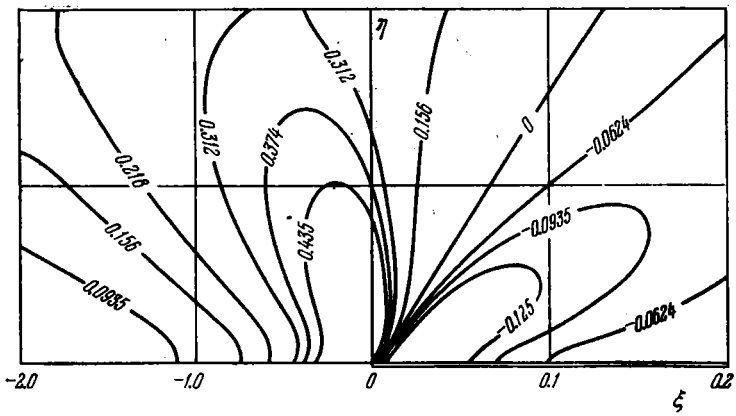

Fig. 18.13. Lines of equal ε_y/τ for plane strain.

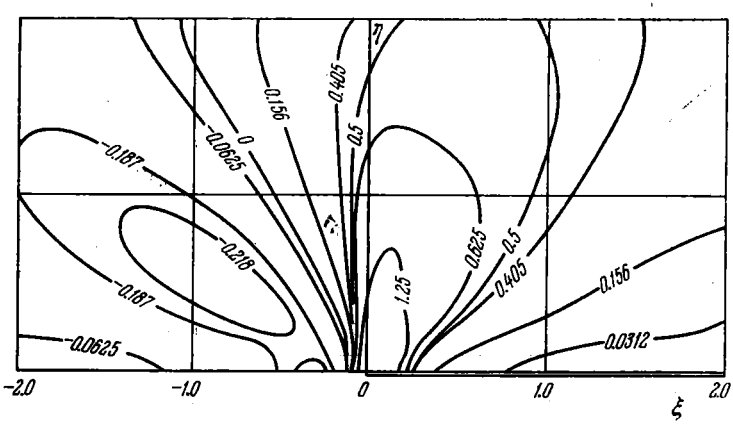

Fig. 18.14. Lines of equal γ_{xy}/τ for plane strain.

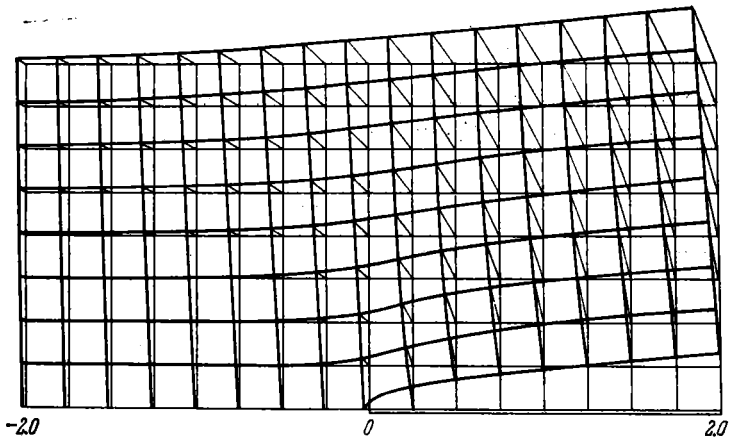

Fig. 18.15. Picture of displacements in the region under consideration for plane strain ($P = 561$).

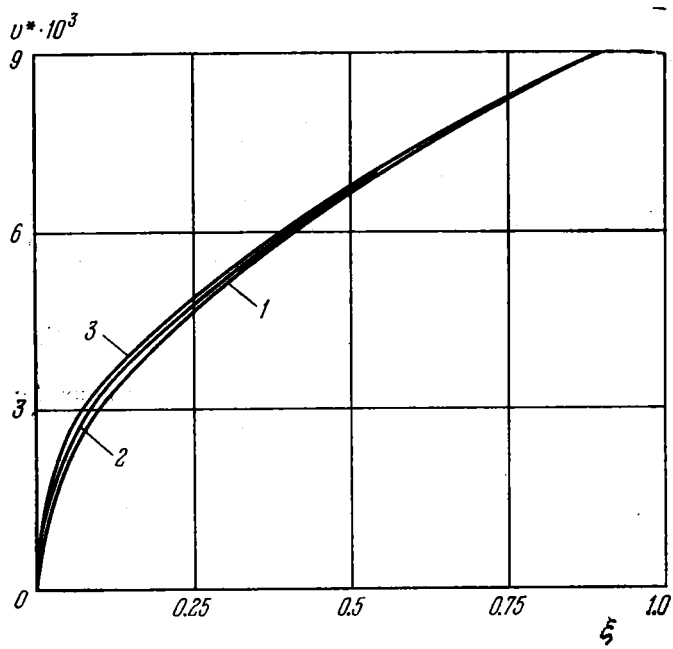

Fig. 18.16. Crack tip opening displacement for plane strain. Lines *1*, *2*, *3* correspond to the number of nodal points 153, 325, 561, respectively.

Here a_1, a_2, a_3 are constants, which are dependent on $\tilde{u}_i = \tilde{u}(\xi_i, \eta_i)$, $\tilde{u}_j = \tilde{u}(\xi_j, \eta_j)$, $\tilde{u}_k = \tilde{u}(\xi_k, \eta_k)$ and are expres-

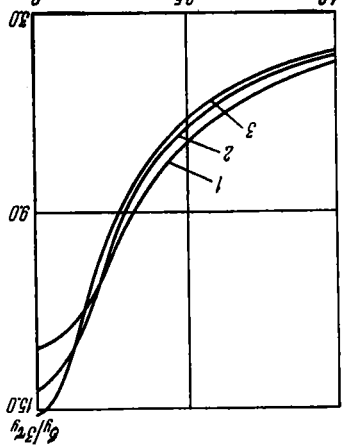

Fig. 18.17. Distribution of stress on the prolongation of the cut for plane strain. Lines *1*, *2*, *3* correspond to the number of nodal points 153, 325, 561, respectively.

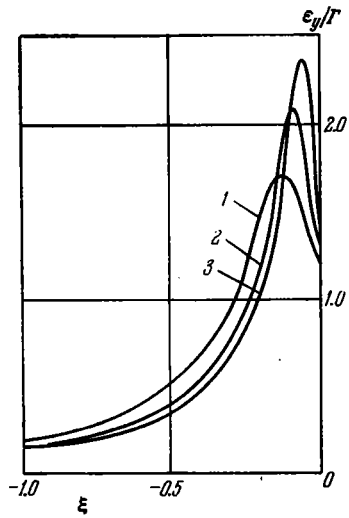

Fig. 18.18. Distribution of strain on the prolongation of the cut for plane strain. Lines *1*, *2*, *3* correspond to the number of points 153, 325, 561, respectively.

sed in terms of the displacements at the vertices of the chosen triangular element (18.17).

Suppose that the function $u(\xi, \eta)$ has continuous derivatives up to the second order. With the use of Taylor's formula we obtain the following expression:

$$\begin{aligned} u(\xi, \eta) = u_0 &+ (\xi - \xi_0)\left(\frac{\partial u}{\partial \xi}\right)_0 + (\eta - \eta_0)\left(\frac{\partial u}{\partial \eta}\right)_0 + \\ &+ \frac{1}{2}\Big[(\xi - \xi_0)^2 \left(\frac{\partial^2 u}{\partial \xi^2}\right)_{\xi=\bar{\xi},\ \eta=\bar{\eta}} + \\ &+ 2(\xi - \xi_0)(\eta - \eta_0)\left(\frac{\partial^2 u}{\partial \xi\, \partial \eta}\right)_{\xi=\bar{\xi},\ \eta=\bar{\eta}} + \\ &+ (\eta - \eta_0)^2 \left(\frac{\partial^2 u}{\partial \eta^2}\right)_{\xi=\bar{\xi},\ \eta=\bar{\eta}}\Big]. \end{aligned} \tag{18.21}$$

Here u_0, $\left(\frac{\partial u}{\partial \xi}\right)_0$, $\left(\frac{\partial u}{\partial \eta}\right)_0$ are the values of the function and its derivatives at some point (ξ_0, η_0) lying within the given triangle $(\bar{\xi} = \xi_0 + \theta(\xi - \xi_0), \bar{\eta} = \eta_0 + \theta(\eta - \eta_0), \theta < 1)$.

Substituting the co-ordinates of points i, j, k in formula (18.21) and noting that

$$\tilde{u}(\xi_i, \eta_i) = u(\xi_i, \eta_i),$$
$$\tilde{u}(\xi_j, \eta_j) = u(\xi_j, \eta_j),$$
$$\tilde{u}(\xi_k, \eta_k) = u(\xi_k, \eta_k),$$

we obtain a system of three equations for the determination of u_0, $\left(\frac{\partial u}{\partial \xi}\right)_0$, $\left(\frac{\partial u}{\partial \eta}\right)_0$.

For the derivatives of displacement, for example, we have

$$\left(\frac{\partial u}{\partial \xi} - \frac{\partial \tilde{u}}{\partial \xi}\right)_0 =$$
$$= -\frac{1}{4\omega}\Big\{[\xi_i^2(\eta_k - \eta_j) + \xi_j^2(\eta_i - \eta_k) + \xi_k^2(\eta_j - \eta_i) -$$
$$- 4\xi_0\omega]\frac{\partial^2 u}{\partial \xi^2} + [2\xi_i\eta_i(\eta_k - \eta_j) + 2\xi_j\eta_j(\eta_i - \eta_k) +$$
$$+ 2\xi_k\eta_k(\eta_j - \eta_i) - 4\eta_0\omega]\frac{\partial^2 u}{\partial \xi\, \partial \eta} +$$
$$+ [\eta_i^2(\eta_k - \eta_j) + \eta_j^2(\eta_i - \eta_k) +$$
$$+ \eta_k^2(\eta_j - \eta_i)]\frac{\partial^2 u}{\partial \eta^2}\Big\}_{\xi=\bar{\xi},\ \eta=\bar{\eta}},$$

$$\left(\frac{\partial u}{\partial \eta} - \frac{\partial \tilde{u}}{\partial \eta}\right)_0 =$$
$$= -\frac{1}{4\omega}\Big\{[\xi_i^2(\xi_j - \xi_k) + \xi_j^2(\xi_k - \xi_i) + \xi_k^2(\xi_i - \xi_j)]\frac{\partial^2 u}{\partial \xi^2} +$$
$$+ [2\xi_i\eta_i(\xi_j - \xi_k) + 2\xi_j\eta_j(\xi_k - \xi_i) + 2\xi_k\eta_k(\xi_i - \xi_j) -$$
$$- 4\xi_0\omega]\frac{\partial^2 u}{\partial \xi\, \partial \eta} + [\eta_i^2(\xi_j - \xi_k) + \eta_j^2(\xi_k - \xi_i) + \eta_k^2(\xi_i - \xi_j) -$$
$$- 4\eta_0\omega]\frac{\partial^2 u}{\partial \eta^2}\Big\}_{\xi=\bar{\xi},\ \eta=\bar{\eta}}. \qquad (18.22)$$

If we denote

$$M_2 = \max\left\{\left|\frac{\partial^2 u}{\partial \xi^2}\right|, \left|\frac{\partial^2 u}{\partial \xi\, \partial \eta}\right|, \left|\frac{\partial^2 u}{\partial \eta^2}\right|\right\},$$

from relations (18.22) we find

$$\left|\frac{\partial u}{\partial \xi} - \frac{\partial \tilde{u}}{\partial \xi}\right|_{\substack{\xi=\xi_0\\ \eta=\eta_0}} \leqslant \frac{M_2}{4\omega} \left| (\xi_i + \eta_i)^2 (\eta_k - \eta_j) + \right.$$
$$\left. + (\xi_i + \eta_j)^2 (\eta_i - \eta_k) + (\xi_k + \eta_k)^2 (\eta_j - \eta_i) - 4(\xi_0 + \eta_0)\,\omega \right|, \tag{18.23}$$

$$\left|\frac{\partial u}{\partial \eta} - \frac{\partial \tilde{u}}{\partial \eta}\right|_{\substack{\xi=\xi_0\\ \eta=\eta_0}} \leqslant \frac{M_2}{4\omega} \left| (\xi_i + \eta_i)^2 (\xi_j - \xi_k) + \right.$$
$$\left. + (\xi_j + \eta_j)^2 (\xi_k - \xi_i) + (\xi_k + \eta_k)^2 (\xi_i - \xi_j) - 4(\xi_0 + \eta_0)\,\omega \right|.$$

For the given division of the region into elements (Figs. 18.1 and 18.2) the following estimates can be obtained according to (18.23):

$$\left|\frac{\partial u}{\partial \xi} - \frac{\partial \tilde{u}}{\partial \xi}\right|_{\substack{\xi=\xi_0\\ \eta=\eta_0}} \leqslant \frac{3}{2} M_2 \Delta, \quad \left|\frac{\partial u}{\partial \eta} - \frac{\partial \tilde{u}}{\partial \eta}\right|_{\substack{\xi=\xi_0\\ \eta=\eta_0}} \leqslant \frac{3}{2} M_2 \Delta. \tag{18.24}$$

In a similar way it may be shown that

$$|u - \tilde{u}|_{\substack{\xi=\xi_0\\ \eta=\eta_0}} \leqslant \frac{M_2}{2} \Delta^2. \tag{18.25}$$

According to (18.18) and (18.19) we ascertain that

$$|\Gamma - \tilde{\Gamma}| \leqslant M\Delta. \tag{18.26}$$

Here M is some constant independent of Δ.

We use Runge's principle [21] for the approximate estimation of the error involved in determining the boundary of the region by the finite element method. Suppose that the region is uniformly divided into triangular elements whose vertices form a square network with an interval Δ (Fig. 18.1). On the basis of (18.26) we then conclude that the error involved in determining the value of Γ at the point (ξ, η) may be approximated by

$$\varepsilon_\Delta(\xi, \eta) = \Gamma - \Gamma_\Delta \cong k(\xi, \eta)\,\Delta.$$

Here Γ_Δ is the value of $\tilde{\Gamma}$ for a division into elements with an interval Δ, and $k(\xi, \eta)$ is independent of Δ.

Let $\Gamma_{\alpha\Delta}$ be a solution obtained with an interval $\alpha\Delta$ ($\alpha < 1$). Then

$$\varepsilon_{\alpha\Delta}(\xi, \eta) = \Gamma - \Gamma_{\alpha\Delta} \cong k(\xi, \eta)\,\alpha\Delta.$$

From the last two relations we find

$$\varepsilon_\Delta(\xi, \eta) \cong \frac{\Gamma_{\alpha\Delta} - \Gamma_\Delta}{1-\alpha}. \tag{18.27}$$

With the help of expression (18.27) we may refine the values of Γ at the nodal points using the formula

$$\Gamma = \frac{\Gamma_{\alpha\Delta} - \alpha\Gamma_\Delta}{1-\alpha}. \tag{18.28}$$

The solid lines in Figs. 18.19 and 18.20 are the refined boundaries of the plastic region plotted according to (18.28)

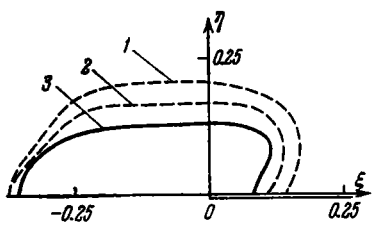

Fig. 18.19. Shape of the plastic region in plane stress. *1*, number of points is 153; *2*, number of points is 325; *3*, refined curve.

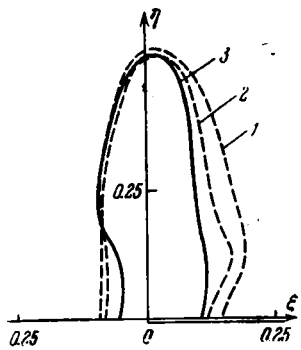

Fig. 18.20. Shape of the plastic region in plane strain. *1*, number of points is 325; *2*, number of points is 561; *3*, refined curve.

with the refined values of Γ at the nodal points, the starting values being taken for the numbers of points indicated in the figures. Figures 18.21 and 18.22 give approximating curves (ρ, θ are the polar co-ordinates)

$$\rho = 0.25\theta + 0.15\cos\frac{3}{2}\theta \text{ (plane stress)}, \tag{18.29}$$

$$\rho = 0.55\sqrt{\cos 14\xi} \text{ (plane strain)}. \tag{18.30}$$

The distance of points of the approximating curve from the boundary of the plastic region ($P_4 = 325$—plane stress, $P_3 = 561$—plane strain) does not exceed the maximum value of the departure of points of the refined curve from this boundary.

Such a detailed experimental and theoretical investigation of plastic zones in Secs. 17 and 18 is accounted for by our

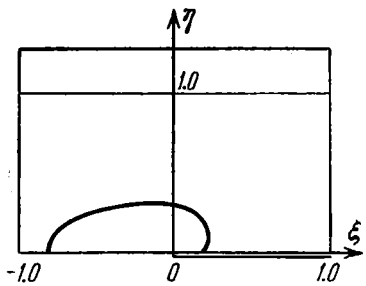

Fig. 18.21. Approximated boundary of the plastic zone for plane stress.

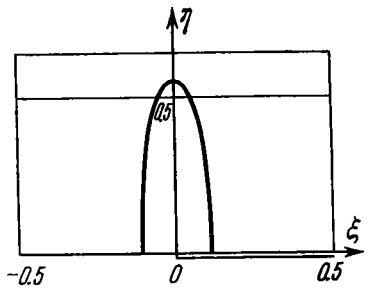

Fig. 18.22. Approximated boundary of the plastic zone for plane strain.

wish to emphasize the role of plastic deformation which involves the accumulation of damages and microfractures preparing the way for macroscopic fracture.

19. CRITICAL STATE OF THE PLANE AND SPACE WITH A CRACK

As already mentioned, the presence of plastic deformation at the tip of a crack involves an increase in the work expended in propagating it. This work must be determined experimentally, but sometimes it can be calculated analytically using some crack model and a small number of experimental data. In particular, as noted above (Sec. 18), for plane stress the plastic zone (in which the plastic work of deformation is identified with the work of fracture) has a convenient shape to calculate, that of a narrow zone ahead of the crack edge. The remaining volume of the body is in an elastic state. We use the energy condition (4.5) for the determination of the critical equilibrium states. Subsequently, this condition

will be used for the calculation of subcritical states (Sec. 21) and of the fatigue life under repeated loading (Sec. 22).

We first present the solution of some plane crack problems using condition (4.5) [187].

1. An infinite plane containing a single straight crack $y = 0$, $|x| \leqslant l$ is subjected to a uniaxial tensile stress p. The plastic zones occupy the segments $y = 0$, $l \leqslant |x| \leqslant a$. Assume that σ_0 is constant and equal to the ultimate strength (this follows from the experiments described below).

The displacement $v(x)$ of the points of the cut $y = 0$, $|x| \leqslant a$ due to the load p for $|x| < l$ and $-\sigma_0 + p$ for $l \leqslant |x| \leqslant a$ is of the form [218]

$$v(x) = \frac{(1-\nu^2)\sigma_0}{\pi E}\left[2\sqrt{a^2-x^2}\left(\pi\frac{p}{\sigma_0} - 2\arccos\frac{l}{a}\right) + \right.$$
$$\left. + (x-l)\Gamma(x, l) - (x+l)\Gamma(x, -l).\right. \qquad (19.1)$$

Here

$$\Gamma(x, l) = \ln\frac{a^2 - xl - \sqrt{(a^2-x^2)(a^2-l^2)}}{a^2 - xl + \sqrt{(a^2-x^2)(a^2-l^2)}}.$$

The size of the plastic zone can be eliminated by means of the well-known relation (5.2) which, in the notation adopted here, takes the form

$$\frac{l}{a} = \cos\frac{\pi p}{2\sigma_0}. \qquad (19.2)$$

This relation follows from the first additional condition (Sec. 4), namely the condition for smooth closure of the boundaries of the cut: $\partial v/\partial x = 0$ when $x = a$.

We introduce non-dimensional quantities

$$\lambda = \frac{p}{\sigma_0}, \quad \rho = \frac{x}{a}, \quad m = \frac{l}{a}, \quad \zeta = \frac{l}{c},$$
$$c = \frac{\pi E \delta_c}{8(1-\nu^2)\sigma_0}.$$

With (19.2) the displacement is

$$v(\rho) = \frac{(1-\nu^2)\sigma_0}{\pi E}\frac{l}{\cos\frac{\pi\lambda}{2}}\left[(\rho - m)\Gamma(\rho, m) - \right.$$
$$\left. - (\rho + m)\Gamma(\rho, -m)\right],$$

where by the symbol m is meant its dependence on λ according to (19.2).

The necessary integrals are

$$\int_0^1 v\,d\rho = \frac{(1-\nu^2)\,\sigma_0}{E}\,l \sin\frac{\pi\lambda}{2},$$

$$\int_m^1 v\,d\rho = \frac{(1-\nu^2)\,\sigma_0}{\pi E}\,l\left[4\cos\frac{\pi\lambda}{2}\ln\cos\frac{\pi\lambda}{2} + \pi\lambda\sin\frac{\pi\lambda}{2}\right].$$

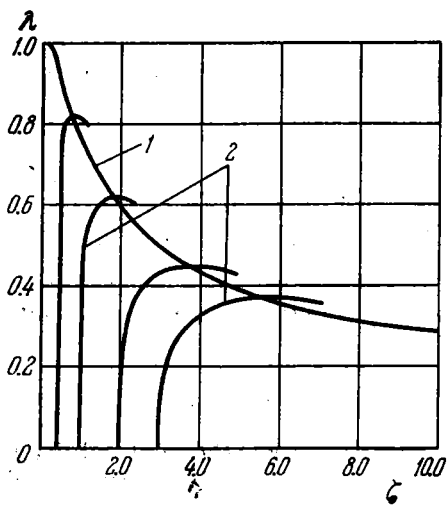

Fig. 19.1. Critical (*1*) and subcritical (*2*) fracture diagrams for the extension of a cracked plane having thin plastic zones.

Taking this into account, condition (4.5) is written as

$$\frac{\pi\lambda}{2}\tan\frac{\pi\lambda}{2} + \ln\cos\frac{\pi\lambda}{2} = \\ = e^{1/\zeta}(\arccos e^{-1/\zeta})\sqrt{1-e^{-2/\zeta}} - \frac{1}{\zeta}. \qquad (19.3)$$

Here λ is the critical value of the non-dimensional stress whose dependence on the non-dimensional length of the crack is illustrated by curve *1* in Fig. 19.1,

The displacement $v^*(x)$ appearing in (4.5) is calculated from the third additional condition (Sec. 4), namely

$$2v(l) = \delta_c. \tag{19.4}$$

Consequently, $v^*(x)$ is the displacement under the load $p = p^*$ determined from (19.4). This load is equal to [218]

$$\lambda^* = \frac{2}{\pi} \arccos e^{-1/\zeta} \tag{19.5}$$

and represents the critical stress by the δ_c-theory. Note that it is identically equal to the critical stress following from the energy condition (19.3).

We present an expression for the fracture energy density in this problem. Since

$$\Delta W_p = 4\sigma_0 \int_l^a \frac{\partial v^*(x)}{\partial l} \Delta l \, dx, \quad \Delta S = 4\Delta l,$$

the value of the fracture energy density is [294]

$$\gamma = \frac{\Delta W_p}{\Delta s} = \sigma_0 \int_l^a \frac{\partial v^*(x)}{\partial l} dx = \frac{\partial}{\partial l} \int_l^a \sigma_0 v^*(x)\, dx + \frac{\sigma_0 \delta_c}{2} \tag{19.6}$$

or, upon integration and substitution of $\lambda = \lambda^*$, we obtain

$$\gamma = \frac{\sigma_0 \delta_k}{2} \left[\zeta e^{1/\zeta} (\arccos e^{-1/\zeta}) \sqrt{1 - e^{-2/\zeta}} - 1\right]. \tag{19.7}$$

From this it is seen that the fracture energy is not a material constant. This is a result of the non-self-similarity of the problem since, as the crack propagates, the contour of its leading edge deforms and does not remain unchanged. The fracture energy density becomes constant and equal to $\gamma = \sigma_0 \delta_c / 2$ for sufficiently small external loads and long cracks, i.e., when $\zeta \to \infty$. Note that with the introduction of γ condition (4.5) in our problem may be written as

$$2\gamma - p \frac{\partial}{\partial l} \int_0^a v\, dx - \sigma_0 \frac{\partial}{\partial l} \int_l^a v\, dx = 0. \tag{19.8}$$

2. An infinite plane is weakened by a single straight crack subjected to internal pressure p.

To solve the problem we must know the displacement $v(x)$ on the crack surface due to the load p for $|x| < l$ and due to σ_0 for $l \leqslant |x| \leqslant a$. This displacement is of the form [218]

$$v(x) = \frac{(1-\nu^2)\sigma_0}{\pi E}\left\{2\sqrt{a^2-x^2}\left[\pi\lambda - 2(1+\lambda)\arccos\frac{l}{a}\right] + \right.$$
$$\left. + (1+\lambda)\left[(x-l)\Gamma(x, l) - (x+l)\Gamma(x, -l)\right]\right\}. \quad (19.9)$$

Similarly to the preceding problem, the size of the plastic zone may be eliminated by means of the relation

$$\frac{l}{a} = \cos\frac{\pi\lambda}{2(1+\lambda)}. \quad (19.10)$$

With the introduction of γ the basic relation (4.5) becomes

$$2\gamma - p\frac{\partial}{\partial l}\int_0^l v\,dx - \sigma_0\frac{\partial}{\partial l}\int_l^a v\,dx = 0$$

or

$$\frac{2\gamma}{\sigma_0} - \frac{1}{\cos\frac{\pi\lambda}{2(1+\lambda)}}\left[\lambda\frac{\partial}{\partial l}\left(l\int_0^m v\,d\rho\right) + \frac{\partial}{\partial l}\left(l\int_m^1 v\,d\rho\right)\right] = 0. \quad (19.11)$$

The integrals involved are

$$\int_0^m v\,d\rho = \frac{1-\nu^2}{\pi E}\sigma_0 l\left[\pi\sin\frac{\pi\lambda}{2(1+\lambda)} - \right.$$
$$\left. - 4(1+\lambda)\cos\frac{\pi\lambda}{2(1+\lambda)}\ln\cos\frac{\pi\lambda}{2(1+\lambda)}\right],$$

$$\int_m^1 v\,d\rho = \frac{1-\nu^2}{\pi E}\sigma_0 l\left[\pi\lambda\sin\frac{\pi\lambda}{2(1+\lambda)} + \right.$$
$$\left. + 4(1+\lambda)\cos\frac{\pi\lambda}{2(1+\lambda)}\ln\cos\frac{\pi\lambda}{2(1+\lambda)}\right],$$

$$\int_0^1 v\,d\rho = \frac{1-\nu^2}{\pi E}\sigma_0 l\left[\pi(1+\lambda)\sin\frac{\pi\lambda}{2)\,1+\lambda)}\right].$$

The fracture energy density is, by formula (19.6),

$$\gamma = \frac{\sigma_0 \delta_c}{2} \left[\zeta \frac{\pi\lambda^*}{2} \tan \frac{\pi\lambda^*}{2(1+\lambda^*)} - 1 \right]. \qquad (19.12)$$

Here λ^* is determined from condition (19.4), which reduces to

$$(1+\lambda^*) \ln \cos \frac{\pi\lambda^*}{2(1+\lambda^*)} = -\frac{1}{\zeta}. \qquad (19.13)$$

This value of λ^* is critical according to the δ_c-theory; it is shown by curve *2* in Fig. 19.2.

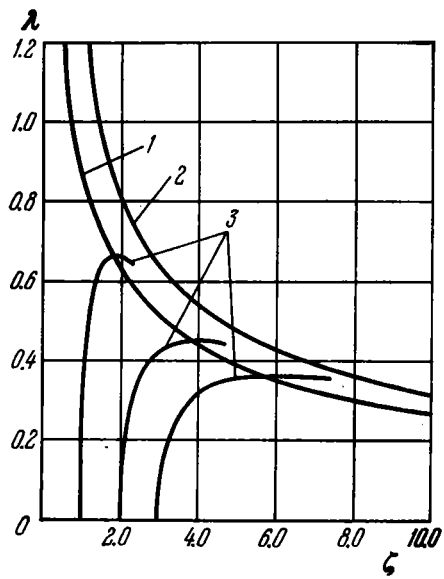

Fig. 19.2. Critical (*1* and *2*) and subcritical (*3*) fracture diagrams for a plane with a pressurized crack. *1*, energy criterion; *2*, δ_c — theory.

The basic relation (19.11) takes the form

$$\frac{\pi\lambda^*}{2} \tan \frac{\pi\lambda^*}{2(1+\lambda^*)} - \frac{1}{\zeta} =$$

$$= \frac{\pi\lambda}{2} \tan \frac{\pi\lambda}{2(1+\lambda)} + (1-\lambda^2) \ln \cos \frac{\pi\lambda}{2(1+\lambda)}. \qquad (19.14)$$

The critical value of λ by (19.14) (obtained with the aid of a computer) is shown by curve *1* in Fig. 19.2.

In this problem the critical stresses by the energy method and the δ_c-theory are not coincident (the critical stress by the δ_c-theory is higher than that based on the energy criterion). The disagreement between the results for different criteria is due to the existence of two kinds of criteria for the occurrence of a critical state, namely necessary and sufficient criteria [166, 205, 294]. To the former belongs the energy criterion, and among the latter criteria are the δ_c-theory and also the theory assuming that the maximum stress (or the average stress over a characteristic interval [206]) at the crack tip reaches the theoretical strength value. It is supposed that for the crack motion it is necessary to have a corresponding redistribution of energy for which the released energy exceeds the energy absorbed in fracture. At the same time this condition may not be sufficient since, for the energy transfer and the crack motion, there must be a corresponding crack opening or the maximum stress at the crack tip must reach its limiting value.

Thus, in some cases the necessary and sufficient conditions give identical results, and in other cases different results, the necessary condition giving a lower value of the critical load than does the sufficient condition.

We now use condition (4.5) to determine the critical load in a three-dimensional axially symmetric problem.

3. Uniaxial (at infinity) extension of a space containing a penny-shaped (flat and circular in plan) crack of radius l. A thin plastic zone occupies the region $y = 0$, $l \leqslant r \leqslant a$ (the y axis is perpendicular to the plane of the crack).

The displacement $v(r)$ of the points of the cut due to the load p for $0 \leqslant r < l$ and due to $-\sigma_0 + p$ for $l \leqslant r \leqslant a$ is of the form [295]

$$v(\rho) = \frac{4(1-\nu^2)\sigma_0}{\pi E}\frac{l}{m}\left[\lambda\sqrt{1-\rho^2} - \sqrt{\frac{1-m^2}{1-\rho^2}} + mE\left(\mu_1, \frac{\rho}{\mu}\right)\right] \quad (0 \leqslant \rho \leqslant m), \tag{19.15}$$

$$v(\rho) = \frac{4(1-\nu^2)\sigma_0}{\pi E}\frac{l}{m}\left[\lambda\sqrt{1-\rho^2} - \sqrt{\frac{1-\rho^2}{1-m^2}} + \frac{m^2-\rho^2}{\rho^2}F\left(\mu_2, \frac{m}{\rho}\right) + \rho E\left(\mu_2, \frac{m}{\rho}\right)\right] \quad (m \leqslant \rho \leqslant 1).$$

Here

$$\lambda = \frac{p}{\sigma_0}, \quad m = \frac{l}{a}, \quad \rho = \frac{r}{a},$$

$$\mu_1 = \arcsin \sqrt{\frac{1-m^2}{1-\rho^2}}, \quad \mu_2 = \arcsin \sqrt{\frac{1-\rho^2}{1-m^2}},$$

$F(\alpha, \beta)$, $E(\alpha, \beta)$ are the elliptic integrals of the first and second kind.

The size of the plastic zone is determined by the relation

$$m = \sqrt{1-\lambda^2} \tag{19.16}$$

which is later taken account of in formula (19.15).

The basic relation (4.5) reduces to

$$2\gamma l - \frac{\partial}{\partial l}\left[p \int_0^l vr\,dr + (\sigma_0 + p) \int_l^a vr\,dr\right] = 0$$

or

$$\frac{2\gamma l}{\sigma_0} - \frac{\lambda}{1-\lambda^2} \frac{\partial}{\partial l}\left(l^2 \int_0^m v\rho\,d\rho\right) -$$

$$- \frac{1}{1-\lambda} \frac{\partial}{\partial l}\left(l^2 \int_m^l v\rho\,d\rho\right) = 0. \tag{19.17}$$

The corresponding integrals are [295]

$$\int_0^m v\rho\,d\rho =$$

$$= \frac{4(1-\nu^2)\sigma_0}{\pi E} \frac{l}{\sqrt{1-\lambda^2}} \frac{1+\lambda}{3} [3\lambda - \lambda^2 - 2 + 2(1-\lambda)\sqrt{1-\lambda^2}],$$

$$\int_m^1 v\rho\,d\rho = \frac{4(1-\nu^2)\sigma_0}{\pi E} l \frac{\sqrt{1-\lambda^2}}{3} (1-\sqrt{1-\lambda^2})^2.$$

The fracture energy density is, by (19.6),

$$\gamma = \frac{\sigma_0}{l} \int_l^a \frac{\partial v^*}{\partial l} r\,dr = \frac{\sigma_0}{l} \frac{1}{1-\lambda^{*2}} \frac{\partial}{\partial l}\left(l^2 \int_m^1 v^*\rho\,d\rho\right) + \frac{\sigma_0 \delta_c}{2}$$

or

$$\gamma = \frac{\sigma_0 \delta_c}{2} \frac{\zeta}{\zeta - 1}. \tag{19.18}$$

Here in calculating the value v^* corresponding to the

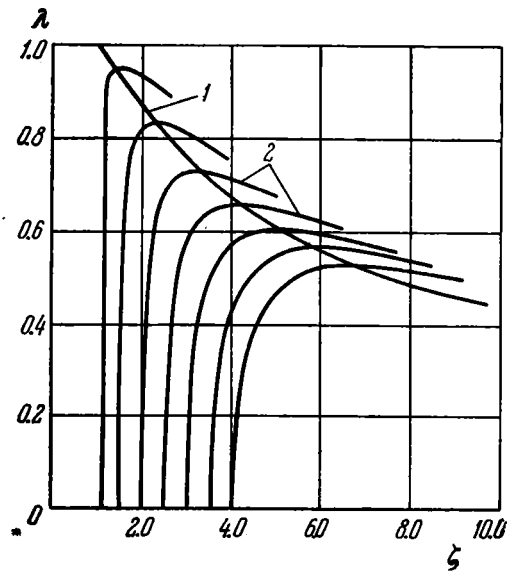

Fig. 19.3. Critical (*1*) and subcritical (*2*) fracture diagrams for a tensioned space with a penny-shaped crack having a thin plastic zone.

limiting crack opening displacement use has been made of condition (19.4) from which it follows that

$$\lambda^* = \frac{\sqrt{2\zeta - 1}}{\zeta}. \tag{19.19}$$

Equation (19.17) reduces to

$$\frac{2\gamma}{\sigma_0} \frac{\pi E}{(1-\nu^2)\,\sigma_0 l} = \frac{2\left(1 - \sqrt{1-\lambda^2}\right)}{\sqrt{1-\lambda^2}}.$$

From this we obtain a condition for the occurrence of a critical state

$$\zeta = \frac{1 + \sqrt{1-\lambda^2}}{\lambda^2} \tag{19.20}$$

which is identical with condition (19.19) following from the δ_c-theory. In Fig. 19.3 curve *1* is plotted by formulas (19.20) and (19.19).

4. A space contains a penny-shaped crack subjected to internal pressure p.

The displacement $v(r)$ due to the load p for $0 \leqslant r < l$ and due to $-\sigma_0$ for $l \leqslant r \leqslant a$ is of the form [294]

$$v(\rho) = \frac{4(1-\nu^2)\sigma_0}{\pi E}\frac{l}{m}\left\{\lambda\sqrt{1-\rho^2} + \right.$$

$$\left. + (1+\lambda)\left[mE\left(\mu_1, \frac{\rho}{m}\right) - \sqrt{\frac{1-m^2}{1-\rho^2}}\right]\right\} \quad (0 \leqslant \rho \leqslant m), \tag{19.21}$$

$$v(\rho) = \frac{4(1-\nu^2)\sigma_0}{\pi E}\frac{l}{m}\left\{\sqrt{1-\rho^2}\left(\lambda - \frac{1+\lambda}{\sqrt{1-m^2}}\right) + \right.$$

$$\left. + (1+\lambda)\left[\frac{m^2-\rho^2}{\rho^2}F\left(\mu_2, \frac{m}{\rho}\right) + \rho E\left(\mu_2, \frac{m}{\rho}\right)\right]\right\}$$

$$(m \leqslant \rho \leqslant 1).$$

The size of the plastic zone is determined by the relation

$$m = \frac{\sqrt{1+2\lambda}}{1+\lambda}. \tag{19.22}$$

The basic equation (4.5) becomes

$$2\gamma l - \frac{\partial}{\partial l}\left(p\int_0^l vr\,dr + \sigma_0\int_l^a vr\,dr\right) = 0. \tag{19.23}$$

The fracture energy density is

$$\gamma = \frac{\sigma_0}{l}\frac{(1+\lambda)^2}{(1+2\lambda)}\frac{\partial}{\partial l}\left(l^2\int_m^1 v\rho\,d\rho\right) + \frac{\sigma_0\delta_c}{2}$$

in the case of the limiting crack opening displacement, i.e., for the load

$$\lambda^* = (1+\sqrt{2\zeta})/\zeta, \tag{19.24}$$

determined from condition (19.4).

The necessary integrals are [294]

$$\int_0^m v\rho\, d\rho = \frac{4(1-\nu^2)\sigma_0}{\pi E}\, l\, \frac{\sqrt{1+2\lambda}}{3}\, \frac{-2-3\lambda+2(1+\lambda)\sqrt{1+2\lambda}}{(1+\lambda)^2},$$

$$\int_m^1 v\rho\, d\rho = \frac{4(1-\nu^2)}{\pi E}\, \frac{l}{3}\, \frac{\sqrt{1+2\lambda}}{(1+\lambda)^2}\,(1+\lambda-\sqrt{1+2\lambda})^2.$$

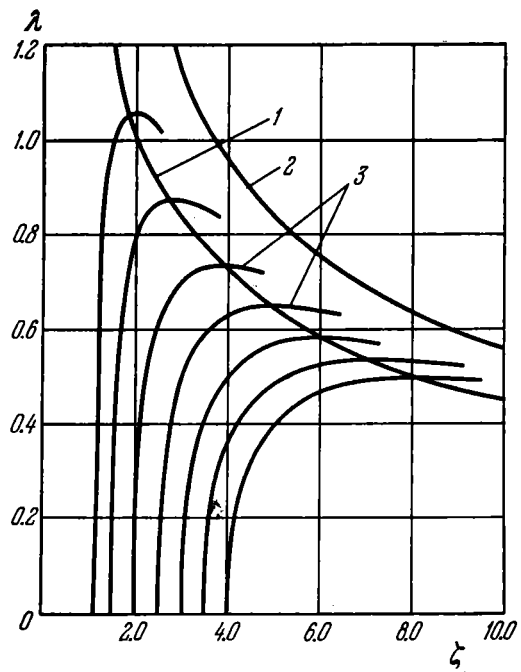

Fig. 19.4. Critical (*1* and *2*) and subcritical (*3*) fracture diagrams for a space with a pressurized penny-shaped crack. *1*, energy criterion; *2*, δ_c-theory.

Consequently,

$$\gamma = \frac{\sigma_0 \delta_c}{2}\left(1 + \frac{1}{\zeta + \sqrt{2\zeta}}\right) \tag{19.25}$$

and the basic equation (19.23) takes the form

$$\frac{1}{\zeta}\,\frac{1+\zeta+\sqrt{2\zeta}}{\zeta+\sqrt{2\zeta}}=\frac{1+\lambda-\lambda^2-(1-\lambda^2)\sqrt{1+2\lambda}}{\sqrt{1+2\lambda}}. \qquad (19.26)$$

The curve for critical loads λ plotted by this equation is shown by line *1* in Fig. 19.4, and the value λ^* by the δ_c-theory [formula (19.24)] is represented by line *2*.

Thus, in the case of a pressure applied in the interior of a crack (in its plane) the critical values of the pressure in both plane and three-dimensional problems are different by the necessary and sufficient conditions. If, however, the external load is not applied to the crack surface, the critical loads based on these criteria coincide in the examples considered.

A comparison of the values of the fracture energy density 2γ in the problems of the extension of a cracked body and of a pressurized crack shows that in the latter case the value of 2γ is less (for a fixed length ζ). Hence, the reduced critical load in the energy criterion as compared with the limiting crack opening displacement criterion in problems of pressurized cavities appears to be natural.

20. THE ELASTIC-PLASTIC PROBLEM FOR A PLANE WITH STRAIGHT SLITS

Consider an elastic-plastic problem [143] where in Dugdale's formulation [71] (the plastic region represents a line of zero thickness on the prolongation of the cut) one can obtain an exact analytic solution. The possibility of applying Dugdale's hypothesis follows not only from the solution obtained in Sec. 18, but is also confirmed by the fact (Sec. 17) that, in general, a state of plane stress in plates of elastic-perfectly plastic material is characterized by the tendency to form plastic regions as thin slip bands (the physical realization is in the form of a slip plane inclined at 45 degrees to the plane of the plate). For example, even in the biaxial extension of a plate of elastic-plastic material with a circular hole [42], when the state of stress at infinity deviates from the uniform one by 0.1 ($\Delta\sigma/\sigma \cong 0.1$), the circular plastic region becomes elongated with an approximate width-length ratio of 1:4.

Suppose that an infinite thin plate is weakened by a periodic system of cuts of length $2l$ situated along the real x axis with centres at the points $x = \pm 2nL$, where n is an integer (Fig. 20.1). The material of the plate is assumed to be elastic-perfectly plastic and satisfying the Tresca-Saint

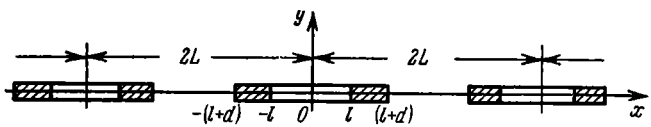

Fig. 20.1. Plane with a periodic system of cuts in the presence of thin plastic zones.

Venant plasticity condition. The sides of the cuts are free from load, and the plate is subjected at infinity to a uniform tensile stress σ

$$\sigma_y = \sigma, \quad \sigma_x = 0, \quad \tau_{xy} = 0 \text{ when } z \to \infty \ (z = x + iy),$$
$$\sigma_y = 0, \quad \tau_{xy} = 0 \text{ when } y = 0, \ |x| < l, \tag{20.1}$$
$$\sigma_y = \sigma_y, \quad \tau_{xy} = 0 \text{ when } l < |x| < l + d.$$

According to the Tresca-Saint Venant condition, the maximum shearing stress at each point of the elastic-plastic body under consideration cannot exceed the yield stress in shear τ_y ($2\tau_y = \sigma_y$, σ_y is the yield stress in tension).

With the help of the transformation

$$w = \sin \frac{\pi z}{2L} \tag{20.2}$$

we transfer from the z plane to the parametric plane of the complex variable w. The region outside the periodic system of the cuts in the z plane is then transformed onto an infinite-sheeted w-Riemann surface with a cut $\left(-\sin\frac{\pi l}{2L}, \sin\frac{\pi l}{2L}\right)$.

We use the well-known Muskhelishvili relations [200] and the results obtained in [45] for the case of a single crack in an infinite plane. With transformation (20.2), the solution

of our problem may then be written as

$$\sigma_x+\sigma_y=4\,\mathrm{Re}\,\Phi(z),\quad \sigma_y-\sigma_x+2i\tau_{xy}=\sigma-4iy\Phi(z),$$
$$2\mu\left(\frac{\partial u}{\partial x}+i\,\frac{\partial v}{\partial x}\right)=\frac{3-\nu}{1+\nu}\Phi(z)-\overline{\Phi(z)}-\frac{1}{2}\sigma-2iy\overline{\Phi'(z)},\tag{20.3}$$

$$\Phi(z)=\frac{\sigma}{4}-\frac{\sigma_y}{2\pi i}\times$$
$$\times\ln\left\{\frac{(\sin\alpha-w)(\sqrt{B-\sin^2\alpha}\,\sqrt{B-w^2}+A+B)}{(\sin\alpha+w)(\sqrt{B-\sin^2\alpha}\,\sqrt{B-w^2}-A+B)}\right\},$$

where $A=w\sin\alpha$, $B=\sin^2\alpha_1$.

Here

$$\alpha=\frac{\pi l}{2L},\quad \alpha_1=\frac{\pi(l+d)}{2L},$$
$$\ln F=\ln|F|+i\arg F\ (-\pi<\arg F<\pi).$$

The function $\sqrt{B-w^2}$ is considered positive on the upper side of the cut $\left(-\sin\frac{\pi l}{2L},\ \sin\frac{\pi l}{2L}\right)$. The plastic region represents a segment of length d on the prolongation of each crack. With (20.2), d is related to the crack length $2l$ and the applied load σ by the following expression:

$$\frac{\sin\alpha}{\sin\alpha_1}=\cos\beta,\quad \beta=\frac{[\pi\sigma]}{2\sigma_y}.\tag{20.4}$$

It may be shown that the principal stresses corresponding to solution (20.3) satisfy the Tresca-Saint Venant condition $-\sigma\leqslant\sigma_{1,\,2}\leqslant\sigma_y$, the equality sign holding only when $y=0$, $l<x-Ln<l+d$, $-l-d<x-Ln<-l$.

We calculate the displacement v when $y=0$ using relations (20.3)

$$v(x,\ l,\ \beta)=\mp\frac{2\sigma_y l}{\pi E}\,\frac{\sin\alpha}{\alpha}\times$$
$$\times\int\limits_{\omega}^{\sec\beta}\ln\left\{\frac{(t-1)(\sin\beta\sqrt{1-t^2\cos^2\beta}+t\cos^2\beta+1)}{(t+1)(\sin\beta\sqrt{1-t^2\cos^2\beta}-t\cos^2\beta+1)}\right\}\times$$
$$\times\frac{dt}{\sqrt{1-t^2\sin^2\alpha}},\tag{20.5}$$

$$\omega=\frac{w}{\sin\alpha}=\frac{\sin\frac{\pi x}{2L}}{\sin\alpha}.$$

Integrating by parts, we obtain

$$v(x, l, \beta) = \pm \frac{2\sigma_y l}{\pi E} \frac{\sin\alpha}{\alpha} \left\{ \frac{\arcsin(\omega \sin\alpha)}{\sin\alpha} \times \right.$$

$$\times \ln \left[\frac{(\omega-1)(\sin\beta \sqrt{1-\omega^2\cos^2\beta} + \omega\cos^2\beta + 1)}{(\omega+1)(\sin\beta\sqrt{1-\omega^2\cos^2\beta} - \omega\cos^2\beta + 1)} \right] +$$

$$\left. + 2\frac{\sin\beta}{\sin\alpha} \int_{\omega}^{\sec\beta} \frac{\arcsin(t\sin\alpha)}{(t^2-1)\sqrt{1-t^2\cos^2\beta}}\, dt \right\}. \qquad (20.6)$$

It is easy to see that the last integral of (20.6) is taken in closed form when $\alpha \to 0$, which corresponds to a single cut [45].

We use the expansion of the function arc sin (t sin α) and transform expression (20.6) to

$$v(x, l, \beta) = \pm \frac{2\sigma_y l}{\pi E} \left\{ \frac{1}{2} \arcsin(\omega\sin\alpha) \times \right.$$

$$\times \ln \left[\frac{(\omega-1)(\sin\beta\sqrt{1-\omega^2\cos^2\beta} + \omega\cos^2\beta + 1)}{(\omega+1)(\sin\beta\sqrt{1-\omega^2\cos^2\beta} - \omega\cos^2\beta + 1)} \right] -$$

$$- \ln(\omega^2-1) + 2\ln(\sin\beta + \sqrt{1-\omega^2\cos^2\beta}) - 2\ln\cos\beta +$$

$$+ \frac{2\sin\beta}{\alpha} \sum_{k=1}^{\infty} \frac{(2k)!\,(\sin\alpha)^{2k+1}}{2^{2k}(k!)^2(2k+1)(\cos\beta)^{2k-2}} \times$$

$$\left. \times \int_0^{\arccos(\omega\cos\beta)} \frac{(\cos^{2k}\xi - \cos^{2k}\beta)}{\cos\xi(\cos^2\xi + \cos^2\beta)}\, d\xi \right\}. \qquad (20.7)$$

Solution (20.3) depends on a single arbitrary parameter l. To establish the relation between the crack length and the applied load, we therefore apply the law of conservation of energy, which, in conjunction with the modified Griffith-Orowan-Irwin physical concepts of fracture energy, may be reduced to the following expression [45]:

$$2\sigma_y \int_l^{l+d} \left(\frac{\partial v}{\partial l} + \frac{\partial v}{\partial \beta}\frac{\partial \beta}{\partial l} \right) dx = 2\gamma. \qquad (20.8)$$

Substituting (20.7) in (20.8), we obtain

$$\zeta^2\left[\beta\sec^2\beta-\left(2-2\frac{\sin\alpha}{\alpha}+\frac{\sin^2\alpha}{\alpha^2}\right)\tan\beta-\right.$$

$$-2\frac{\sin\alpha}{\alpha}\sum_{k=1}^{\infty}\frac{(2k)!\,(\sin\alpha)^{2k}A_k(\beta)}{2^{2k}(k!)^2(2k+1)}+$$

$$\left.+\left(\frac{\sin\alpha}{\alpha}\right)^2\sum_{k=1}^{\infty}\frac{2^{2k}(k!)^2(\sin\alpha)^{2k}B_k(\beta)}{(2k+1)!\,(k+1)}\right]\frac{d\beta}{d\zeta}=$$

$$=1-2\zeta\left[\ln\cos\beta+\beta\tan\beta-\frac{\cos\alpha}{\alpha}\sum_{k=1}^{\infty}\frac{(2k)!\,(\sin\alpha)^{2k}}{2^{2k}(k!)^2}C_k(\beta)+\right.$$

$$\left.+\frac{\sin\alpha}{\alpha}\cos\alpha\sum_{k=1}^{\infty}\frac{2^{2k}(k!)^2(\sin\alpha)^{2k}D_k(\beta)}{(2k+1)!}\right]. \qquad (20.9)$$

Here $2\gamma=\text{constant}$ is the fracture energy

$$\zeta=\frac{2\sigma_y^2 l}{\pi E\gamma},\quad \alpha=\frac{\pi\zeta}{2\zeta_0},\quad \zeta_0=\frac{2\sigma_y^2}{\pi E\gamma}L,$$

$$A_k(\beta)=\sum_{j=1}^{k}\frac{\cos^2\beta+2j\sin^2\beta}{\cos^{2j+1}\beta}\int_0^{\beta}\cos^{2j-1}\xi\,d\xi,$$

$$B_k(\beta)=\sum_{j=1}^{k}\frac{1+2j\sin^2\beta}{\cos^{2j+1}\beta}\int_0^{\beta}\cos^{2j}\xi\,d\xi,$$

$$C_k(\beta)=\sum_{j=1}^{k}\frac{\sin\beta}{\cos^{2j}\beta}\int_0^{\beta}\cos^{2j-1}\xi\,d\xi,$$

$$D_k(\beta)=\sum_{j=1}^{k}\frac{\sin\beta}{\cos^{2j+1}\beta}\int_0^{\beta}\cos^{2j}\xi\,d\xi.$$

The differential equation (20.9) serves to determine the non-dimensional crack length ζ as a function of the non-dimensional load β under monotonic loading.

Figure 20.2 (lines *1*) presents a family of integral curves of Eq. (20.9) obtained by a numerical method using a computer. The integral curves were calculated only in the stable region since the transition to an unstable region involves complete fracture. As seen, the problem under consideration

retains the qualitative features inherent in the process of crack growth in elastic-plastic bodies, such as the presence of a region of stable crack growth. Because of the boundary effect, however, the corresponding values of the limiting loads are less than those in the case of a single crack.

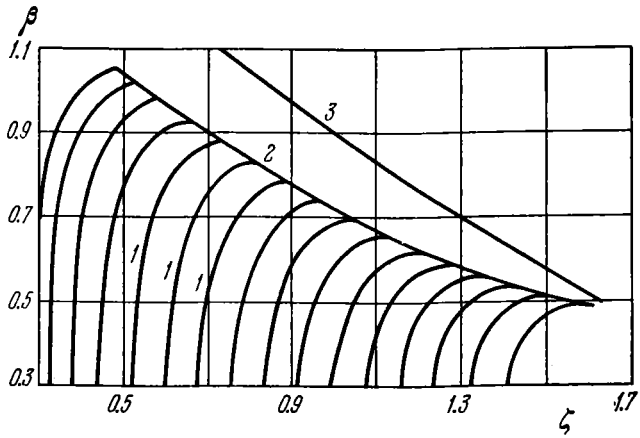

Fig. 20.2. Subcritical (*1*) and critical (*2* and *3*) fracture diagrams for a plane with a periodic system of cuts.

Thus, the crack development in an elastic-plastic material is always stable at the beginning and there is an interface (line *2*) between the stable region $d\beta/d\zeta > 0$ and the instability region in which $d\beta/d\zeta < 0$. It can easily be shown that in the instability region all integral curves for large values of ζ asymptotically approach the Irwin curve (line *3*) [117]

$$\zeta\beta^2 = \frac{\alpha}{\tan\alpha}, \tag{20.10}$$

which represents the solution of the corresponding elastic problem for a system of periodic cracks of equal length.

The resulting pattern is in good agreement with the well-known experimental data on the construction of fracture diagrams [68], which will be discussed in greater detail below.

The basic equation (20.9) may also be used to solve the problem of the development of the cracks in question up to

complete fracture under any path of loading and, in particular, under cyclic loading if the effect of residual stresses is neglected, as has been previously done in the work of F. A. McClintock [164] and P. C. Paris [220]. The crack growth is then observed at each stage of loading, and during

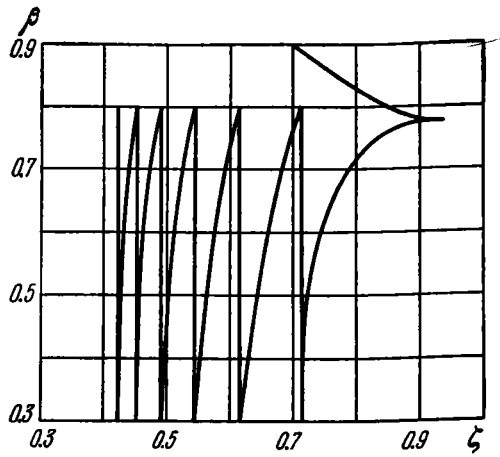

Fig. 20.3. Cyclic crack growth.

unloading the crack length remains constant. Figure 20.3 shows the numerical results for one case of cyclic loading. The availability of a sufficiently dense network of integral curves of Eq. (20.9) also enables a direct graphical determination of the number of cycles to fracture for given characteristics of the cycle.

The results obtained may be regarded as a first approximation in the problem of the extension of a plate of width $2L$ of elastic-perfectly plastic material having a symmetrical central crack of length $2l$.

21. SUBCRITICAL CRACK GROWTH

Experiment shows that just before the occurrence of the critical equilibrium state (when the crack begins to propagate rapidly in an avalanche fashion under constant external

load) a stage of slow stable subcritical crack growth is nearly always observed in centrally through-cracked flat specimens in tension. This slow crack growth well known to experimentors may be rather lengthy, so that the critical crack length l_k exceeds the original length l_0 by 30, 50, or even by 100 per cent, depending on the material properties and the original crack length [93]. The relation between the stress on the sound section of the specimen and the stable crack length is commonly termed the subcritical fracture diagram [68]. To the stage of slow crack growth is attached so much importance that it is reasonable to supplement the stress-strain diagrams by the fracture diagrams in the analysis of the mechanical properties of materials [68].

The subcritical fracture diagram represents a characteristic of the material of given thickness which evaluates the capacity of the material to arrest the crack. This diagram reflects the fracture process, while on the conventional stress-strain diagrams the fracture stage is marked only by the coordinates of the end point. This information is insufficient to assess such an important stage of the process of material resistance to the action of external loads as the fracture stage. At the same time the stage of slow crack growth is not described by Griffith's, Irwin's, Leonov and Panasyuk's theories. We shall briefly discuss the existing theories of subcritical crack growth.

So far as we are aware, the first attempt to describe mathematically subcritical crack growth was made by G. R. Irwin in 1960 [8, 129]. The concept was that the growth of the crack length is accompanied by a change in resistance to this growth in the form of the fracture energy R*.

At each current instant the released energy G in the stable state is equal to the energy R.

The expression for the fracture energy density is [129]

$$R = G_{\mathrm{Ic}} + \left(\frac{l-l'}{l_k-l'}\right)^n (G_c - G_{\mathrm{Ic}}). \qquad (21.1)$$

* The fracture energy R is measured by the work required to advance a crack a distance of unit length in a specimen of given thickness t. It is worth noting that R differs from the well-known fracture energy intensity (or the fracture toughness) $2\gamma = G_c$ since the latter is determined at the time of onset of rapid crack propagation. The following inequality holds: $0 \leqslant R \leqslant 2\gamma t$.

Here the exponent $n < 1$ is determined experimentally; when the crack length reaches the value l', $R = G_{Ic}$, and when $l = l_k$, rapid crack growth occurs and $R = G_c$.

For example, the released energy for a tensioned plate with a central crack is [129], by the well-known tangent formula and with Irwin's plastic correction,

$$G = \frac{\sigma^2 bq}{E} = \frac{\sigma^2 b}{E} \tan\left[\frac{\pi l_0}{b} + \frac{\pi l}{b} + \frac{EG}{2\pi\sigma_{0.2}^2}\right]. \quad (21.2)$$

Here l_0 is the initial half-length of the crack, b is the width of the specimen, q is an unknown factor taking account of slow subcritical crack growth.

At the critical moment ($l = l_k$) the following condition is fulfilled:

$$\frac{dG}{dl} = \frac{dR}{dl}; \quad (21.3)$$

this condition supplies an equation to determine the amount the crack grows

$$2 \arctan q - \frac{q}{1+q^2} = \frac{2\pi l_0}{b} + C + \frac{1}{2}\left(\frac{\sigma}{\sigma_{0.2}}\right)^2 q. \quad (21.4)$$

Here $C = 4.7\,(P - 0.43)\frac{t}{b}$, the exponent $n = 1/2$, P is a fraction of shear lips in a part of the section between lines distant t and $2t$ from the edge of the initial crack.

According to this equation, the authors of [129] restricted their analysis to a calculation of the factor q which allowed slow crack growth to be taken into account without its measurement in the experimental determination of the characteristic G_c. The idea of this procedure was just to eliminate the experimental measurement of the critical crack length, which was not sufficiently reliable methodically at that time.

Further development of this method consisted in assuming [85, 141] that the R-curve is a material characteristic, the shape of the curve depending on the growth of the crack (but not on its initial length). The shape of the experimental R-curve determines the character of subcritical crack growth. Figure 21.1 shows how the subcritical fracture diagram can be obtained from the R-curve, and conversely how the frac-

ture energy density can be obtained as a function of crack growth from the experimentally known fracture diagram.

To each point of the R-curve at which $G(\sigma, l) = R(l - l_0)$ corresponds a point (σ, l) of the fracture diagram. In the critical state condition (21.3) 'cuts' the fracture diagram at the point (σ_k, l_k). At that moment $G = G_c$, $R = G_c = 2\gamma$.

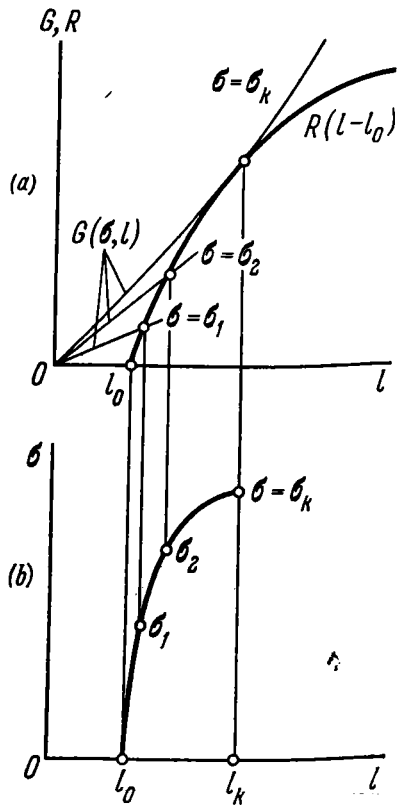

Fig. 21.1. Relation between the R-curve (a) and the subcritical fracture diagram (b).

F. A. McClintock [163] obtained, on the basis of the fracture criterion introduced by him (see Sec. 5), an integral equation whose numerical solution is the subcritical fracture diagram. The mechanical significance of subcritical crack growth is the following. Let the fracture condition (5.6) be satisfied at the point $r = \rho_s$ $(\theta = 0)$ ahead of the crack tip. The crack then advances a small amount dl. In consequence, the stress at the neighbouring point lying at a distance ρ_s from the end of the crack of increased length $l + dl$ rises, but not enough to fulfil criterion (5.6). To satisfy this criterion under which the crack continues to grow, the load must be increased. This leads to stable subcritical crack growth characterized by the subcritical fracture diagram.

G. P. Cherepanov [44, 45] used the local energy criterion for fracture and the Orowan-Irwin hypothesis of quasi-brittle fracture to write down Eq. (20.8) from which one can

obtain the subcritical fracture diagram $p = p(l)$. An example of this calculation was given in the preceding section. The constant on the right-hand side of Eq. (20.8) is the effective fracture energy density.

A similar equation is found in the work of M. P. Wnuk [296] who simultaneously extended it to the case of viscoelastic bodies.

It might be well to point out the characteristic feature of the fracture diagram calculated by Eq. (20.8). The point is that the growth of the crack from the initial to the critical length is very small. For example [299], when the initial non-dimensional length is $\zeta_0 = 10$, the crack length increases by 14.5 per cent, when $\zeta_0 = 1000$, by 0.4 per cent (here $\zeta_0 = l_0/c$, $c = \pi E\delta_c/8(1 - \nu^2)\sigma_0$). So slight crack growth is characteristic of thick specimens with a small plastic region at the crack edge.

The subcritical fracture diagrams can also be calculated with the use of the energy criterion for crack extension (4.5). For this it should be assumed that the varied state is actual and represents a new equilibrium state in which the magnitude of the external load differs from that in the unvaried state. It follows that the variation in condition (4.5) arises from both the increment in length and the increment in external load, i.e., for the two-dimensional problem we have

$$\delta = \frac{\partial}{\partial l}\delta l + \frac{\partial}{\partial p}\delta p.$$

Here $\delta p = (dp/dl)\,\delta l$, p is the external loading parameter; for example, $\sigma_y(x) = pf(x)$.

By using this operator, we obtain from (4.5) an ordinary differential equation of the first order in the function $p = p(l)$ with the boundary condition $l = l_0$ when $p = 0$. In a more general case the boundary conditions may be written as $l = l_0$ when $p = p_0$, where the load p_0 corresponding to the beginning of the motion of the crack tip must be assigned on the basis of experimental data. For example, Eq. (19.8) in this case becomes

$$2\gamma - \left(\frac{\partial}{\partial l} + \frac{\partial}{\partial p}\frac{dp}{dl}\right)\left(\int_0^a pv\,dx + \int_l^a \sigma_0 v\,dx\right) = 0$$

with the value of 2γ determined by relation (19.7). Here, in contrast to criterion (20.8), the fracture energy density 2γ is a variable quantity dependent on the crack length. For $dp/dl = 0$ we have the critical equilibrium state, and the value of p at this moment is equal to the critical value $\left(\text{i.e., to the value obtained from (4.5) with the use of the simpler operator } \delta = \frac{\partial}{\partial l}\delta l\right)$.

We write down the corresponding differential equations for the four cases considered in Sec. 19.

(1) The extension of a cracked plane

$$\frac{d\lambda}{d\zeta} = \frac{8\cos^2\frac{\pi\lambda}{2}}{\pi^2\lambda\zeta}\left[e^{1/\zeta}(\arccos e^{-1/\zeta})\sqrt{1-e^{-2/\zeta}} - \right.$$
$$\left. -\frac{1}{\zeta} - \frac{\pi\lambda}{2}\tan\frac{\pi\lambda}{2} - \ln\cos\frac{\pi\lambda}{2}\right]. \quad (21.5)$$

(2) A plane with a pressurized crack

$$\frac{d\lambda}{d\zeta} = \frac{\frac{\pi\lambda^*}{2}A^* - \frac{1}{\zeta} - \frac{\pi\lambda}{2}A - (1-\lambda^2)\ln\cos\frac{\pi\lambda}{2(1+\lambda)}}{\frac{\zeta}{2}\left[\frac{\pi\lambda}{1+\lambda}A - 2\lambda\ln\cos\frac{\pi\lambda}{2(1+\lambda)} + \frac{\pi^2\lambda}{4(1+\lambda)^2}\frac{1}{\cos^2\frac{\pi\lambda}{2(1+\lambda)}}\right]}, \quad (21.6)$$

where

$$A = \tan\frac{\pi\lambda}{2(1+\lambda)}, \quad A^* = \tan\frac{\pi\lambda^*}{2(1+\lambda^*)}.$$

(3) The extension of a space with a penny-shaped crack

$$\frac{d\lambda}{d\zeta} = \frac{3(1-\lambda^2)\sqrt{1-\lambda^2}}{\lambda\zeta}\left(\frac{1}{\zeta-1} - \frac{1-\sqrt{1-\lambda^2}}{\sqrt{1-\lambda^2}}\right). \quad (21.7)$$

(4) A space with a pressurized penny-shaped crack

$$\frac{d\lambda}{d\zeta} = \frac{3(1+2\lambda)\sqrt{1+2\lambda}}{\zeta[2\lambda(1+2\lambda)\sqrt{1+2\lambda}-\lambda-3\lambda^2]} \times$$
$$\times\left[\frac{1}{\zeta}\frac{1+\zeta+\sqrt{2\zeta}}{\zeta+\sqrt{2\zeta}} - \frac{1+\lambda-\lambda^2-(1-\lambda^2)\sqrt{1+2\lambda}}{\sqrt{1+2\lambda}}\right]. \quad (21.8)$$

The subcritical fracture diagrams plotted by these equations for several initial crack sizes are shown in Figs. 19.1 to 19.4.

Note that when the plastic zone is small (which is the case when $\zeta \gg 1$ and accordingly $\lambda \to 0$) Eq. (21.5) may be written as

$$\frac{d\lambda}{d\zeta} = \frac{(8/\pi^2) - \zeta\lambda^2}{\lambda\zeta^2}.$$

The integral of this equation with the boundary condition $\lambda(\zeta_0) = \lambda_0$ is of the form

$$\lambda = \frac{2}{\pi\zeta}\sqrt{4(\zeta - \zeta_0) + \frac{\pi^2}{4}\zeta_0^2\lambda_0^2}.$$

The expression obtained describes the subcritical fracture diagram. If we assume that the plastic zone is small for the entire range of crack lengths and accordingly 2γ = constant everywhere, we arrive at the generalized Griffith criterion (see the footnote on p. 212). In the critical state $d\lambda/d\zeta = 0$, whence the critical load is

$$\lambda_k = \frac{2}{\pi}\sqrt{\frac{2}{\zeta_k}}$$

and the critical crack length is

$$\zeta_k = 2\zeta_0 - \frac{\pi^2}{8}\zeta_0^2\lambda_0^2.$$

From this it is seen that an increase in the fracture initiation load λ_0 leads to a decrease in subcritical crack growth.

Finally, we may discuss the physical meaning of the size c, which is taken by us as a computing unit to obtain the non-dimensional crack length ζ. When $\zeta \gg 1$, from formula (19.2) (in which $\cos\frac{\pi\lambda}{2}$ is replaced by the first two terms of the corresponding series) it follows that

$$\frac{l}{l+d} = 1 - \frac{\pi^2\lambda^2}{8}.$$

Taking into account the relation $\lambda(\zeta)$ in the critical state, we obtain

$$d = c\,[\zeta/(\zeta - 1)] \cong c.$$

Consequently, the size c is the length of the plastic zone in the case of very long cracks when the critical state occurs at a small stress compared with the yield stress.

Let us express the basic equation (4.5) in terms of the stress intensity factor (195, 261]. For this purpose we take into account the well-known relations (3.9) and (4.11). Assume also that (Sec. 11)

$$\sigma_y(l)\, v(l) = 2\gamma \frac{\sigma_y^2(l)}{\sigma_u^2}.$$

From Eq. (4.5) we then obtain:

for the critical fracture diagram

$$2\gamma\left[1-\frac{\sigma_y^2(l)}{\sigma_u^2}\right]-\frac{K^2}{E}=0, \tag{21.9}$$

for the subcritical fracture diagram

$$\frac{dp}{dl}=\frac{2\gamma\left[1-\frac{\sigma_y^2(l)}{\sigma_u^2}\right]-\frac{K^2}{E}}{\frac{2}{E}\int K\frac{\partial K}{\partial p}\,dl+\frac{4\gamma}{\sigma_u^2}\int \sigma_y(l)\frac{\partial \sigma_y(l)}{\partial p}\,dl}. \tag{21.10}$$

If the expression for the stress intensity factor K is known, relations (21.9) and (21.10) enable one to plot the corresponding fracture diagrams.

Let us reduce Eqs. (21.9) and (21.10) to non-dimensional form (here $\sigma_y(x) = p =$ constant)

$$1-\lambda^2-K_0^2=0, \tag{21.11}$$

$$\frac{d\lambda}{d\zeta}=\frac{1}{2}\,\frac{1-\lambda^2-K_0^2}{\lambda\zeta+\int K_0\frac{\partial K_0}{\partial\lambda}\,d\zeta}. \tag{21.12}$$

Here the following notation has been introduced:

$$\lambda=\frac{p}{\sigma_u},\quad \zeta=\frac{l}{c},\quad K_0=\frac{K}{K_c},\quad c=\frac{\pi K_c^2}{8\sigma_u^2}.$$

Equations (21.11) and (21.12) may be used to calculate the critical and subcritical fracture diagrams for the tension of a strip of finite width containing a central crack. In

this case from [85]

$$K_0 = \pi\lambda \sqrt{\frac{\zeta}{8}} \left(1 + 0.595 \frac{\zeta^2}{\beta^2} + 0.481 \frac{\zeta^4}{\beta^4}\right). \quad (21.13)$$

Here $\beta = b/c$, $2b$ is the width of the strip, $2l$ is the crack length. Figure 21.2 presents relations (21.11) and (21.12) in

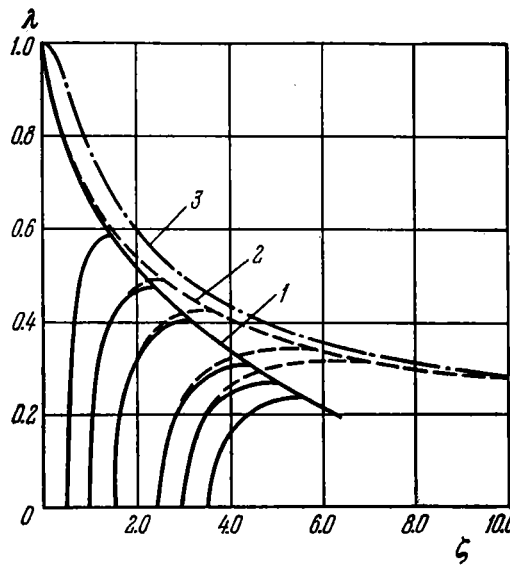

Fig. 21.2. Critical and subcritical fracture diagrams. *1*, centrally-cracked strip ($\beta = 7$); *2*, cracked plane; *3*, critical diagram for the cracked plane by the δ_c-theory [see formulas (19.3) and (19.5)].

which use has been made of expression (21.13). Here are also plotted similar curves for a cracked plane ($K_0 = \pi\lambda\sqrt{\zeta/8}$).

The possibility exists of describing subcritical crack growth by means of a generalization of the well-known δ_c-theory [189].

According to the δ_c-model, as the load increases, the initial crack ($y = 0$, $|x| \leqslant l_0$) opens, with its length remaining unchanged, until the discontinuity in elastic displacement $2v(l_0) = \delta$ at the base of the plastic zone (when $x =$

$= l_0$) attains its limiting value $\delta = \delta_c$, which means that the limiting (critical) state is reached. Only after this does the crack propagation become possible. It is assumed that one of the material characteristics is the curve represented in Fig. 21.3*a*. Thus, the subcritical crack growth is not incorporated in this scheme.

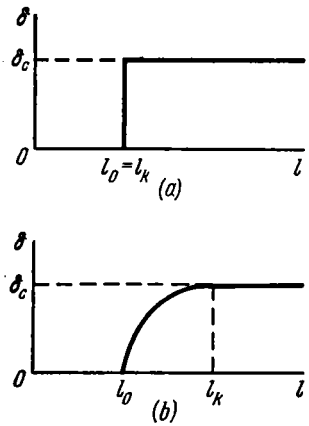

Fig. 21.3. Relation between the crack tip opening displacement and the crack length: (*a*) δ_c-theory, (*b*) its generalization.

Suppose now that the crack opening occurs simultaneously with the crack growth, i.e., the material characteristic is the curve represented in Fig. 21.3*b*. The form of the relation $\delta = \delta(l)$ subject to the conditions $\delta(l_0) = 0$, $\delta(l_k) = \delta_c$, $0 \leqslant \delta \leqslant \delta_c$ must, in general, be determined experimentally. In the absence of experimental data this relation may suitably be approximated on the basis of some general considerations and indirect experimental results.

To illustrate the proposed method, we assume that $\delta(l)$ represents a segment of a parabola

$$\delta = \delta_c \left[1 - \left(\frac{\zeta_k - \zeta}{\zeta_k - \zeta_0}\right)^2\right]. \tag{21.14}$$

Condition (21.14) satisfies the requirement $\partial\delta/\partial\zeta = 0$ when $\zeta = \zeta_k$, which follows from the physical meaning of the problem.

The quantity ζ_k appearing in (21.14) may be found from the following considerations. It is known [165] that as l_0 increases, the amount of crack length change $l_k - l_0$ increases to $l_k - l_0 = l_0$ for very large values of l_0.* Hence, for

* As is known, in the limit when $l_0 \to \infty$ Griffith's theory with a constant (effective) fracture energy density follows from the δ_c-theory. In this case the amount of crack extension is $l_k - l_0 = l_0$. Indeed, considering the subcritical state in which to each value of $p = p(l)$ corresponds a stable equilibrium state, we may write

cracks which encounter no obstacles in their paths we may assume in condition (21.14)

$$\zeta_k = \zeta_0 (2 - e^{-\zeta_0}). \tag{21.15}$$

The equation of the fracture diagram is obtained from the condition

$$2v(l) = \delta. \tag{21.16}$$

Consider special cases.

(1) An infinite plane with a single straight crack is subjected to a stress p perpendicular to the crack line. We make use of the well-known expression for $v(l)$ [218]. Condition (21.16) may be written as

$$\lambda = \frac{2}{\pi} \arccos e^{-\Delta}. \tag{21.17}$$

Her

$$\lambda = \frac{p}{\sigma_0}, \quad \Delta = \frac{1}{\zeta}\left[1 - \left(\frac{\zeta_k - \zeta}{\zeta_k - \zeta_0}\right)^2\right].$$

The fracture diagrams plotted for several values of ζ_0 are shown in Fig. 21.4 by lines *1*. The maxima of these diagrams fall on the line of limiting stress *2*.

(2) An infinite plane with a straight crack under an internal pressure p. The displacement $v(l)$ is determined by the well-known methods. From Eq. (21.16) we then obtain

$$-(1+\lambda) \ln \cos \frac{\pi\lambda}{2(1+\lambda)} = \Delta. \tag{21.18}$$

The fracture diagrams for this case are given in Fig. 21.4 by lines *3*, the limiting loads by line *4*.

(3) An infinite space with a penny-shaped crack (circular in plan) under a field of tensile stress p perpendicular to the plane of the crack. On the basis of equalities (21.14) and

---

(somewhat extending the formulation of Griffith's theory)

$$\left(\frac{\partial}{\partial l} + \frac{\partial}{\partial p}\frac{dp}{dl}\right)\left(2\gamma l - \frac{\pi l^2 p^2}{2E}\right) = 0.$$

From this, provided that $p = 0$ when $l = l_0$, we obtain an analytic expression for the fracture diagram $p = 4\sigma_0 \sqrt{c(l - l_0)/\pi l}$. It is seen that whatever the initial length l_0 the amount of crack extension to a finite length l_k is 100 per cent.

(21.16), using [209], we find

$$1-\sqrt{1-\lambda^2}=\Delta.$$

In Fig. 21.5 lines *1* represent the fracture diagrams, and curve *2*, the limiting stresses.

(4) A space with a pressurized penny-shaped crack [209]. The equation of the fracture diagram (21.16) gives

$$1+\lambda-\sqrt{1+2\lambda}=\Delta.$$

The fracture diagrams are shown in Fig. 21.5 by lines *3*, the limiting pressure by line *4*. Note that the diagrams obtained for the cases (1) and (3) are in fair agreement (on the

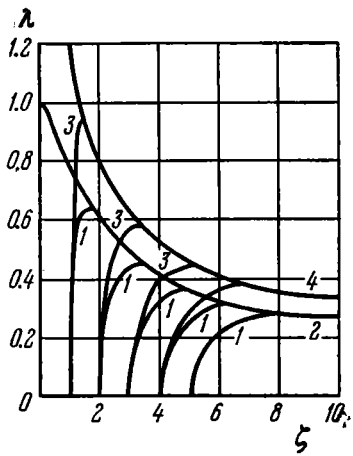

Fig. 21.4. Fracture diagrams by the generalized δ_c-theory. *1* and *2*, extension of a cracked plane; *3* and *4*, the case of a pressurized crack.

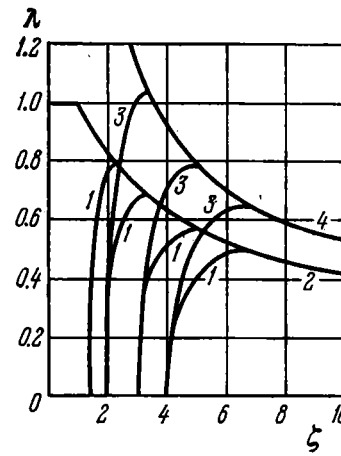

Fig. 21.5. Fracture diagrams by the generalized δ_c-theory. *1* and *2*, extension of a space with a penny-shaped crack; *3* and *4*, the case of a pressurized crack.

chosen scale) with the diagrams following from the variational principle (Figs. 19.1 and 19.3). As already mentioned (Sec. 19), in the cases (2) and (4) the limiting stress curves by the δ_c-theory lie above those corresponding to the variational energy principle since the δ_c-theory represents a sufficient condition for the onset of rapid crack motion, while the

energy criterion represents a necessary condition [166]. At the same time all the foregoing fracture diagrams differ somewhat from those obtained in [45] since the author of the latter work adopted the condition of constant fracture energy density during crack growth, which is not assumed (when cracks are not very long) in either the δ_c-model or the variational energy principle.

We finally turn our attention to the discussion of the possibility of calculating the R-curve from the variational fracture criterion [194]. Of course, the characteristic of a material (specimen) $R = R(l)$ may be obtained with the help of the experimentally determined fracture diagram $p = p(l)$.

We shall demonstrate the possibility of calculating the R-curve from the fracture diagram obtained analytically from the integral variational principle (4.5).

The fracture diagrams for a cracked plane in tension represent the integral curves $\lambda = \lambda(\zeta)$ of Eq. (21.5) with the boundary condition $\lambda(\zeta_0) = 0$.

From the variational principle (4.7) it follows that for the present problem of the extension of a cracked plane the amount of energy released by an elastic body when the crack advances a unit area is equal to

$$G = \frac{\partial}{\partial l}\left[\int_0^l pv\,dx + \int_l^a (\sigma_0 + p)\,v\,dx\right]$$

or, after some manipulation,

$$\frac{G}{\sigma_0\delta_c} = \zeta\left[\frac{\pi\lambda}{2}\tan\frac{\pi\lambda}{2} + \ln\cos\frac{\pi\lambda}{2}\right]. \qquad (21.19)$$

When λ = constant, G is directly proportional to the non-dimensional crack length ζ. To plot the R-curve, we use the condition $G = R$; in this case the values of λ and ζ occurring in (21.19) must be taken from the fracture diagram determined by Eq. (21.5). The graphs of the functions G and R for several initial crack lengths are given in Fig. 21.6. The G lines represent a one-parameter family of curves with parameter p. It will be recalled that the critical value of $R = G_c$ is determined from the condition $\partial G/\partial l = \partial R/\partial l$. The locus of points of contact of the G and R lines (on the

basis of the above-mentioned instability condition) determines the relation between the fracture toughness G_c and the crack length (Fig. 21.6), which is also written as [184]

$$\frac{G_c}{\sigma_0\delta_c} = \frac{2}{\delta_c}\int_l^a \frac{\partial v^*}{\partial l}\,dx = \zeta e^{1/\zeta}\arccos e^{-1/\zeta} \times \sqrt{1-e^{-2/\zeta}} - 1. \quad (21.20)$$

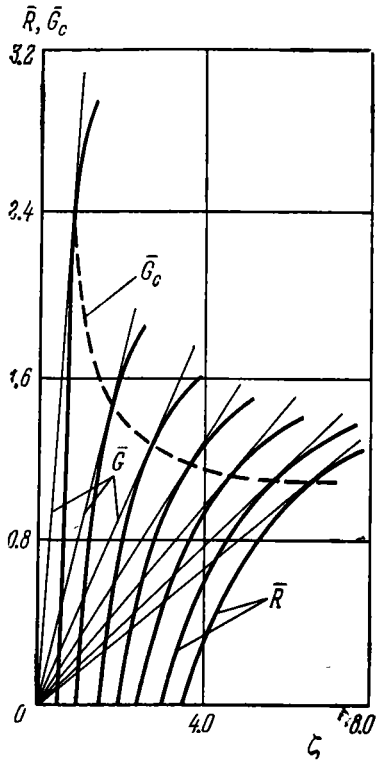

Fig. 21.6. The released energy G and the absorbed energy R in the extension of a plane with a single crack. The G_c line joins the points of contact of the G and R lines ($\bar{G} = G/\sigma_0\delta_c$, $\bar{R} = R/\sigma_0\delta_c$).

When evaluating the integral in (21.20), the displacement $v^*(x)$ was chosen so as to satisfy condition (5.1). As the crack length decreases, G_c increases indefinitely, and for large crack lengths $G_c = \sigma_0\delta_c =$ constant.

The R-curve may serve as a mechanical characteristic of a material assessing its susceptibility to subcritical crack growth. The flatter is the R-curve, the higher is this susceptibility (i.e., the greater is the amount of crack growth $l - l_0$). This characteristic, however, depends not only on the material properties, but also on the specimen geometry, the manner in which the load is applied, and the crack length.

Note a certain inconsistency in the adopted model for crack growth. The point is that in calculating the fracture diagram the fracture energy intensity is taken to be equal to the critical value (21.20), whereas the R-curve points to the gradual growth of the intensity of crack propagation

energy. This is shown up in the fracture diagram following from (21.5) as a decrease in the range of stability of crack growth.

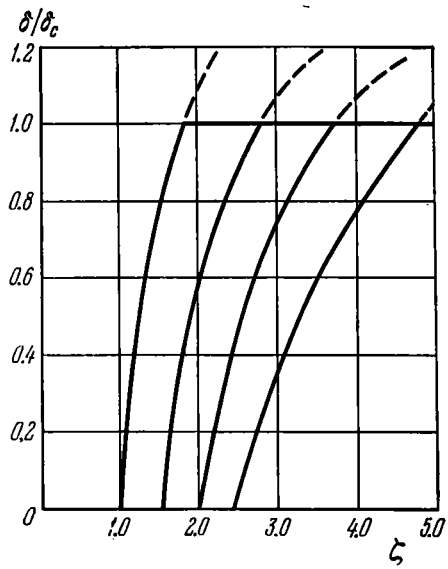

Fig. 21.7. Crack tip opening displacement under steadily growing load.

The expression obtained for the R-curve can be used to calculate the crack opening displacement $\delta = 2v(l)$ when the crack growth is slow. Indeed,

$$R = 2\int_l^a \sigma_0 \frac{\partial v}{\partial l}\,dx = 2\frac{\partial}{\partial l}\int_l^a \sigma_0 v\,dx + \sigma_0\delta$$

and accordingly

$$\delta = \frac{R}{\sigma_0} - 2\frac{\partial}{\partial l}\int_l^a v\,dx. \qquad (21.21)$$

After some manipulation relation (21.21) may be reduced to

$$\frac{\delta}{\delta_c} = \frac{R}{\sigma_0\delta_c} - \zeta\left[\frac{\pi\lambda}{2}\tan\frac{\pi\lambda}{2} + 2\ln\cos\frac{\pi\lambda}{2}\right]. \qquad (21.22)$$

Relation (21.22) for several initial crack lengths is given in Fig. 21.7.

22. LOW-CYCLE FATIGUE LIFE BASED ON THE NUMBER OF CYCLES

Of some interest is the estimation of fatigue life based on the number of stress cycles at the stage of crack growth. This is due to the fact that from a theoretical standpoint a study of the parameters responsible for the process of crack growth and entering into design equations gives a deeper insight into the mechanical nature of the processes occurring in the vicinity of a growing crack. From the practical point of view this interest is supported by possible applications, say, in the prediction of component life.

Empirical formulas estimating the rate of growth of fatigue cracks have long been known for special cases. However, only the inclusion of the stress intensity factor among the parameters affecting crack propagation makes possible a quantitative and qualitative analysis of the laws of crack growth under repeated (cyclic) loading. And this is natural since the growth of fatigue cracks occurs against the background of elastic strains when the fracture mechanics criteria are valid.

Based on this circumstance, numerous relations have been obtained for the rate of crack growth (a review of these results may be found in [60]). All these relations virtually follow from Paris' formula, which is based on the above-mentioned idea that all phenomena at a crack tip and also the rate of crack propagation depend on the stress intensity factor [219]. This formula is written as

$$\frac{dl}{dN} = A\Delta K^n. \tag{22.1}$$

Here A and n are empirical coefficients, $\Delta K = K_{\max} - K_{\min}$ is the range of the intensity factor per stress cycle, N is the number of cycles.

Numerous experimental investigations confirm sufficiently well this formula, the exponent n ranging from 2 to 7 for different materials. The figure most commonly observed is $n = 4$.

G. P. Cherepanov established the following relation [46]:

$$\frac{dl}{dN} = -\beta\left(\frac{K_{\max}^2 - K_{\min}^2}{K_c^2} + \ln\frac{K_c^2 - K_{\max}^2}{K_c^2 - K_{\min}^2}\right), \tag{22.2}$$

where the factor β is determined empirically. In the case when $K_{min} < 0$, it is taken that $K_{min} = 0$ in expression (22.2).

These formulas are employed for both low-cycle fatigue and conventional (high-cycle) fatigue. Of course, it is convenient, but at the same time care is needed in dealing with empirical coefficients. The point is that the laws of the mechanism of the fatigue phenomenon are different for low-cycle and high-cycle fatigue. This difference may even lead to a discontinuity in Wöhler's curve in the range of limited endurance. Also, in the one case the crack extends inside the grain, and in the other along its boundary. From this it is also seen that the fatigue strength characteristics must depend on the material structure. Hence, one should allow for a possible dependence of empirical coefficients on the maximum stress level of the cycle.

From the equations describing the fracture diagrams it is also possible to obtain the endurance characteristics under repeated static loading, or, according to the modern terminology, in low-cycle fatigue. To do this, the fracture diagram for the first cycle is plotted up to the load corresponding to the maximum stress of the cycle σ_{max}. The crack length therewith increases and this new length must be taken as the initial length in the calculation of the subcritical diagram for the next cycle. Consequently, the boundary condition for the calculation of the integral curve of the differential equation of the subcritical fracture diagram for the ith cycle is $\sigma = \sigma_{min}$, $l = l_{i-1}$.

The family of subcritical fracture diagrams in the range of stress from σ_{min} to σ_{max} enables one to calculate the crack length as a function of the number of cycles.

Taking into account the idealization of the model being considered and the occurrence of residual compressive stresses during unloading, it should be assumed that when the load is removed (and the distance between the crack surfaces decreases) the increment of crack length also diminishes. Thus, if the increment of crack length for the ith cycle is, from the subcritical fracture diagram, Δl_i, then the crack length for the $(i + 1)$th cycle is $l_{i+1} = l_i + \alpha \Delta l_i$ (Fig. 22.1). The crack length increment reduction factor α is less than 1 and is determined empirically from the experimental l-N

curves for a particular material of given thickness. It is quite possible that this factor varies with the number of cycles. In the next section it will be shown, on the basis of experiments, that this is in fact true.

During each cycle we obtain a definite increment of crack length, and for a certain specific cycle the fracture diagram

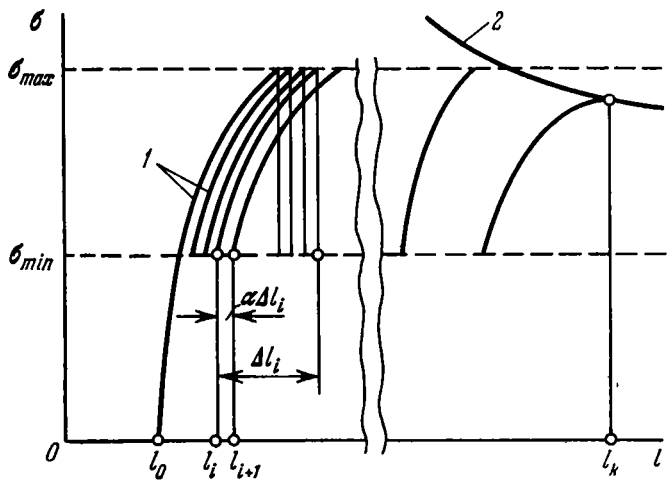

Fig. 22.1. Schematic representation of the crack growth under cyclic loading from the initial length l_0 to the critical length l_k. *1*, subcritical fracture diagrams; *2*, critical fracture diagram.

eventually reaches the limiting load curve, with the result that rapid avalanche fracture occurs under the corresponding constant stress [46, 60, 143].

As an example, Fig. 22.2 shows, according to the results of the computer solution of Eq. (21.5), how the subcritical fracture diagrams look for a cracked plate under repeated static loading. The plate was initially extended with a high maximum stress of the cycle, but then the loading conditions were changed and the maximum stress of the cycle became lower, while the cycle ratio was kept constant. In the first regime the plate worked for three cycles, and for the remaining fourteen cycles to fracture the plate stayed in the second regime passing into the critical state during the fifteenth cy-

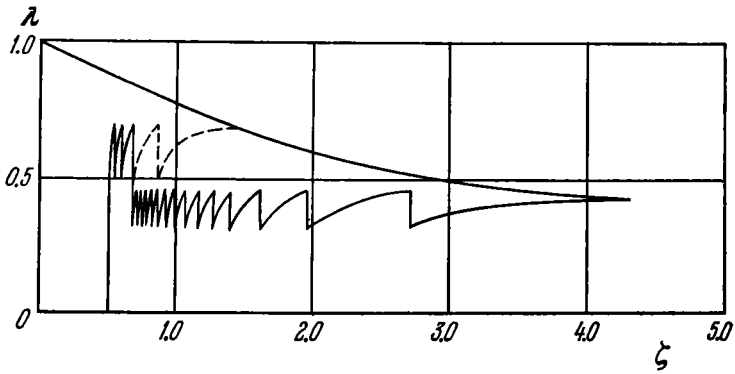

Fig. 22.2. Crack growth in a plate under cyclic tension with cycle ratio $r = \lambda_{min}/\lambda_{max} = 0.7$. In the first loading regime $\lambda_{max} = 0.7$, in the second 0.45. The dashed line shows the behaviour of the cracked plate in the first loading regime alone.

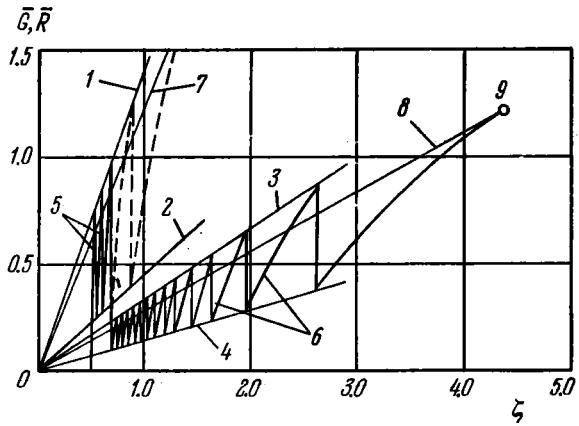

Fig. 22.3. Calculation of crack growth in a plate under cyclic tension (the loading conditions are indicated in Fig. 22.2). *1* and *3*, $\bar{G}$-ζ relations for $\lambda = 0.7$ and 0.45, respectively; *2* and *4*, $\bar{G}$-ζ relations for $\lambda = 0.7 \times 0.7$ and 0.7×0.45, respectively; *5* and *6*, segments of the subcritical fracture diagrams in the given range of load (λ_{max}-λ_{min}) for the first and second regimes, respectively; *7* and *8*, lines of $\bar{G} = \bar{G}_c$ (the dashed lines show possible loading to the critical state in the first regime); *9*, point representing the critical state.

cle. These curves can be replotted by using the crack length and the number of cycles as coordinates, since these are the co-ordinates in which the experimental curves are usually obtained in low-cycle fatigue testing of cracked specimens.

The law of crack propagation in low-cycle fatigue can also be derived with the help of the R-curve [60, 194]. The possibility of determining the crack length as a function of the number of cycles is illustrated in Fig. 22.3. The numerical computation is carried out using a computer. The R-curves for a cracked plane in tension are plotted according to condition (21.19) with the use of relation (21.5). For every ith cycle the crack length increases (in each way) from l_i to l_{i+1}, and this growth continues up to and including the last but one cycle. During the last cycle, at a certain instant the crack reaches the critical size at which the line of generalized force G becomes tangential to the resistance curve (R-curve) and the subsequent crack growth is unstable. By calculating the crack length after each cycle of loading, it is possible to plot it as a function of the number of cycles. This relation determines the number of cycles to fracture and the crack length at which this fracture occurs.

23. EXPERIMENTAL RESULTS FOR SINGLE AND CYCLIC LOADINGS

Let us compare the theoretical data presented in Secs. 19 to 22 for the problem of the extension of a cracked plane subjected to a single loading with the results of the corresponding experiments.*

For an experimental investigation of the process of stable crack propagation the method of automatic recording the crack length was employed using eddy currents [67, 170, 171] and electrical potential differences [172, 261].

Cracks were studied in sheet specimens of Д16Т-1, АК4-1, САП, В-95, ВАД-23 aluminium alloys and ВТ-14 titanium alloy. The chemical composition of these alloys is given

* These investigations were carried out by V. M. Markochev and V. Yu. Gol'tsev at the Moscow Physical-Engineering Institute (MIFI) and B. A. Drozdovskii at the All-Union Scientific-Research Institute of Aviation Materials (VIAM).

TABLE 23.1

Chemical Composition of Materials

Material	Element Content							
	Mg	Mn	Cu	Fe	Zn	Ni	Si	Li
Д16Т-1	1.85	0.77	4.15	0.33	—	—	0.10	—
АК4-1	1.60	0.074	2.00	1.32	—	1.29	0.26	—
В-95	2.90	0.34	1.50	0.35	6.0	—	—	—
САП	—	—	0.008	0.092	—	—	0.12	—
ВАД-23	impur.	0.54	5.0	0.14	—	—	traces	1.0

The Д16Т-1 alloy is quenched and artificially aged 12 hours at 190 °C.

В-95 (A and B) and САП are in the as-rolled condition.

АК4-1 is quenched and artificially aged 12 hours at 190 °C.

ВАД-23 is aged (a) 12 hours at 160 °C, (b) 10 hours at 200 °C, (c) 24 hours at 140 °C.

TABLE 23.2

Mechanical Properties of Materials

Material	σ_y, kgf/mm²	σ_u, kgf/mm²	δ, %	a_k, m-kgf/cm	E, kgf/mm²	K_c, kgf/mm$^{3/2}$	G_c, kgf/cm	$\delta_c \times 10^3$, cm	c, cm
Д16Т-1	37	44.6	7	—	7×10^3	252	90.6	20.3	1.25
АК4-1	36.4	39.9	5.7	0.8	7×10^3	295	124	31.1	2.15
В-95 (A)	48	53.5	7	—	7×10^3	164	38.4	7.2	0.37
В-95 (B)	48	54.7	7	0.36	7×10^3	201	57.8	10.55	0.53
САП	29.2	32.5	5.7	—	7×10^3	245	85.5	26.3	2.22
ВАД-23									
160 °C, 12 hrs	50	55.5	7.6	0.09	7.3×10^3	102	14.24	2.57	0.132
200 °C, 10 hrs	44	49.7	6.25	0.212	7.3×10^3	125	21.4	4.3	0.248
140 °C, 24 hrs	33	49.7	20.7	0.612	7.3×10^3	270	100	20.1	1.16
ВТ-14	119	130	2	1.1	11.5×10^3	200			0.093

in Table 23.1. In the same table are indicated the states of the materials used in the tests. The mechanical properties of smooth specimens in static tension are given in Table 23.2.

The initial crack was obtained as follows: at the centre of a flat specimen a hole of diameter 2 mm was drilled and sawed in each way to obtain a notch of specified length. Then the specimen was subjected to cyclic loading with a frequency of 200 cycles per minute in a ГРМ-1 pulsator until fatigue cracks, each 2 mm long, were obtained at the ends of the notch on both sides. The length of the initial crack was varied from specimen to specimen by changing the length of the initial sawcut. The maximum stress of the cycle in forming the fatigue cracks was 15 kgf/mm^2.

The length of specimens of Д16Т-1, АК4-1, B-95 (lot B) alloys was 500 mm, the width was 200 mm. The thickness of all specimens of the alloys listed above, except specimens of B-95 (B) alloy, was 1.4 mm; the specimens of B-95 (B) alloy were 1.8 mm thick. The width of the specimens of ВАД-23 alloy (aged in three regimes) and of B-95 (A) alloy was 100 mm and the thickness of the specimens was 1.8 mm.

The specimens containing cracks of different initial length were extended in a 50-ton Amsler hydraulic machine. In the tests the load and the increment of crack length (on one side of the specimen axis) were simultaneously registered until the crack reached its critical length. By the critical length in the experiments was meant a crack length on reaching which further fracture of the specimen was produced only by the elastic energy stored in the specimen (and in the loading system).

The experimental results were also used to determine the fracture characteristics K_c, G_c, δ_c, and c, which are given in Table 23.2. The parameter $c = \pi E\delta_c/8\sigma_0$ may be written, by formula (10.1), as $c = \pi K_c^2/8\sigma_0^2$. The critical stress intensity factor K_c was determined from the test results (by the method of successive approximations) using the well-known formula of G. R. Irwin

$$K_c = \sigma \sqrt{b \tan\left[\frac{\pi}{b}\left(l + \frac{K_c^2}{2\pi\sigma_{0.2}^2}\right)\right]}. \qquad (23.1)$$

Here σ is the critical stress at the sound section of the specimen, l is the half-length of the crack, b is the width of

the specimen. The second term under the tangent sign represents Irwin's plastic correction (6.1) (see also Sec. 10).

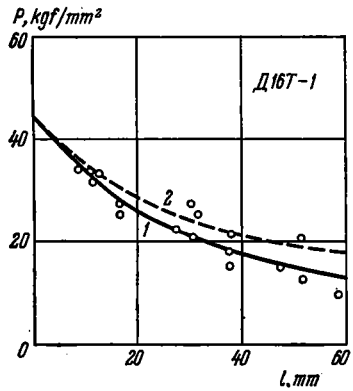

Fig. 23.1. Critical fracture diagram of Д16Т-1 alloy. *1*, strip, $\beta = 16$; *2*, Eq. (19.3).

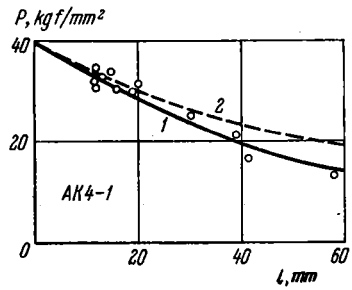

Fig. 23.2. Critical fracture diagram of АК4-1 alloy. *1*, strip, $\beta = 16$; *2*, Eq. (19.3).

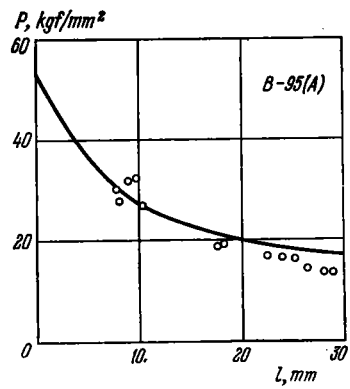

Fig. 23.3. Critical fracture diagram of B-95 alloy (lot A).

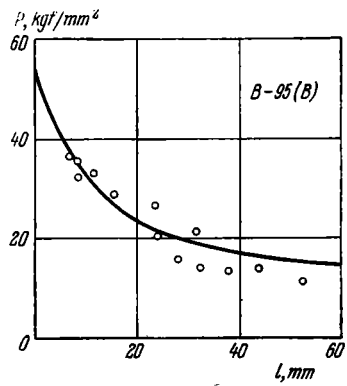

Fig. 23.4. Critical fracture diagram of B-95 alloy (lot B).

In all computational formulas the stress σ_0 was taken to be the ultimate strength σ_u on the basis of the well-known proposition that the stress on the boundary of the plastic zone ahead of the crack tip is higher than the yield stress in

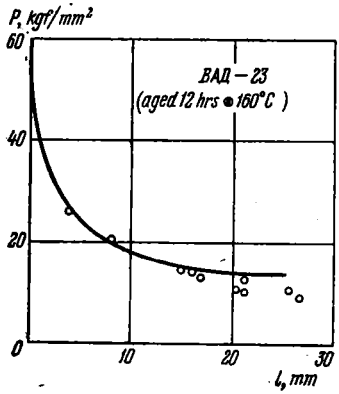

Fig. 23.5. Critical fracture diagram of ВАД-23 alloy (aged 12 hrs at 160 °C).

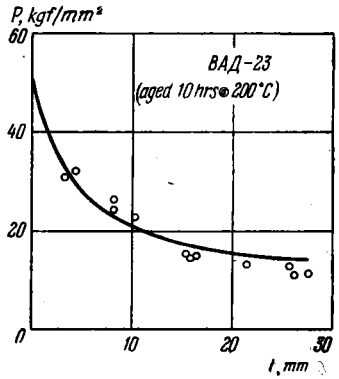

Fig. 23.6. Critical fracture diagram of ВАД-23 alloy (aged 10 hrs at 200 °C).

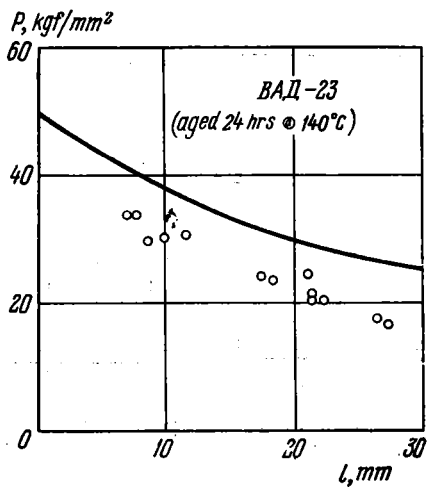

Fig. 23.7. Critical fracture diagram of ВАД-23 alloy (aged 24 hrs at 140 °C)

uniaxial tension, particularly in the presence of lateral constraint and strain-hardening [84, 240, 281].

Figures 23.1 to 23.7 show the critical fracture diagrams plotted by formula (21.11) with the use of (21.13) for the materials indicated in the figures. Each point in the figure is an experimental result obtained on one specimen.

Figures 23.8 to 23.11 show the subcritical fracture diagrams plotted by Eq. (21.12) with the use of (21.13) for the materials indicated in the figures. Each specimen is represented by one fracture diagram.

By comparing the calculated and test data, one can observe that the critical fracture diagrams show a fair agreement between the theoretical analysis and the experimental evidence despite the idealized scheme of the plastic zone ahead of the crack tip adopted in the calculation. The problem of plastic flow ahead of the crack edge under plane-stress conditions is virtually three-dimensional since the planes of maximum shearing stress make an angle of 45 degrees with the tension direction and the face of the plate. Under plane-strain conditions the arising hydrostatic stress tends to increase the stress at the elastic-plastic interface, compared with the yield stress in uniaxial tension [240, 281]. The shape of the plastic zone is different from a narrow strip, and the plastic deformation spreads sideways (upward and downward) from the (horizontal) crack direction (see Sec. 17).

Among the subcritical fracture diagrams the agreement between theory and experiment is not so good. A possible reason for this is a higher sensitivity of the process of slow crack growth to the properties of the material and the features of its structure.

We next compare the experimental data and the theoretical relations obtained in Secs. 21 and 22 and pertaining to the calculation of the crack length as a function of the number of cycles. The same specimens were used in the tests as in the case of static loading.

During testing, the crack length was recorded as a function of the number of cycles. The corresponding experimental curves are shown in Fig. 23.12 by solid lines. The material of the specimens is indicated in the figures. The theoretical curves plotted by Eq. (21.12) with the use of (21.13) for the

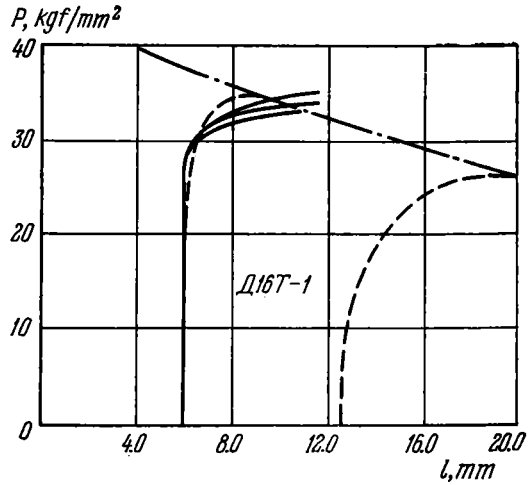

Fig. 23.8. Subcritical fracture diagrams of Д16Т-1 alloy. Solid line: experiment. Dashed line: calculation.

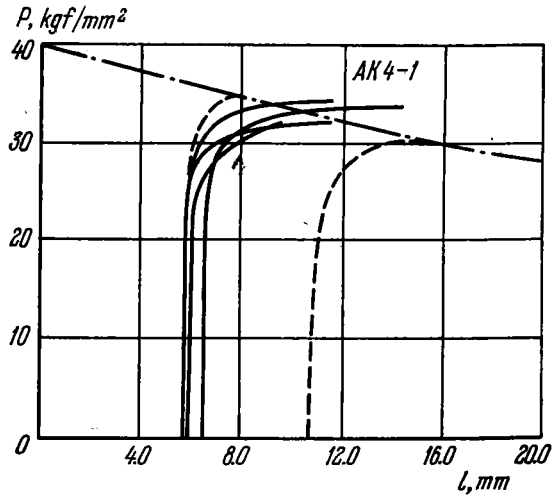

Fig. 23.9. Subcritical fracture diagrams of AK4-1 alloy

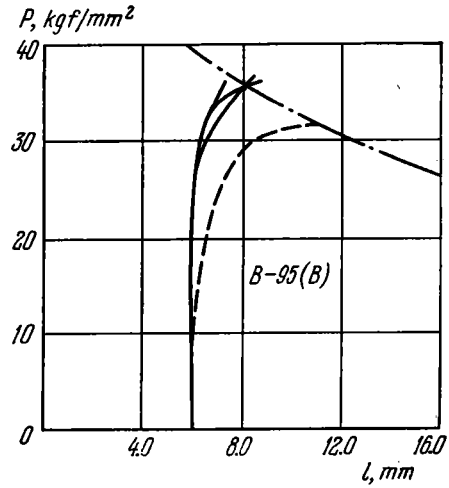

Fig. 23.10. Subcritical fracture diagrams of B-95 alloy (lot B).

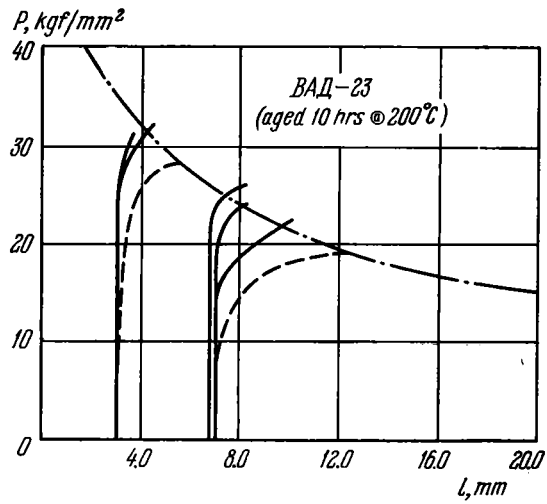

Fig. 23.11. Subcritical fracture diagrams of ВАД-23 alloy (aged 10 hrs at 200 °C).

corresponding material are shown by dashed lines in the same figures.

In plotting the theoretical curves for the crack length as a function of the number of cycles account was taken of the

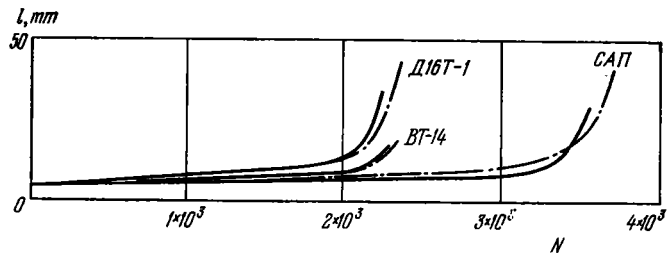

Fig. 23.12. Crack growth under repeated static loading. Solid lines: experiment. Dashed lines: calculation.

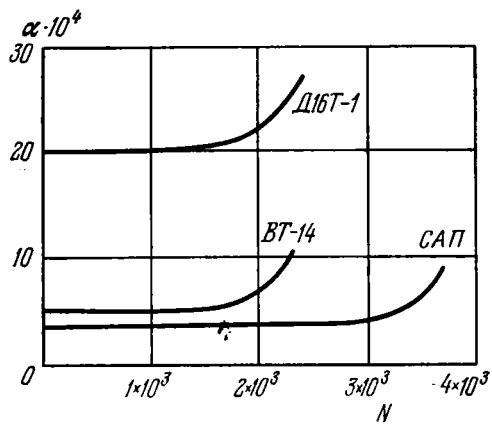

Fig. 23.13. Crack length increment reduction factor as a function of the number of cycles.

fact that during unloading the crack length does not remain constant and the crack partly closes. This phenomenon is allowed for by the crack length increment reduction factor α introduced in the preceding section. It was established by trial and error that the factor varied with the number of cycles as shown in Fig. 23.13. This relation may be regarded as a characteristic of the material of given thickness.

24. THE ULTIMATE FRACTURE STRENGTH

At present there is an urgent need for developing an engineering method of brittle fracture analysis in structural elements containing cracks. The brittle fracture design supplementing the conventional design is summoned to contribute to means for protecting structures against early brittle fracture and to place a tolerance on the safe size of initial cracks.

The existing methods for designing structural elements with cracks based on the well-known fracture criteria have the following disadvantages.

The method of design based on the limiting value of the intensity factor (3.11) is restricted on the part of small crack lengths by the condition imposed on the stress at the weakened section, $\sigma \leqslant 0.8\ \sigma_y$ [9, 269]. This method is unsuitable for cracks of small length, i.e., just in the range that is of particular interest to technologists and designers.

At the same time the method of design based on the limiting value of the plastic crack opening displacement at a crack tip (5.1) becomes very complex in the application to bodies of limited dimensions and complicated shape.

The analytic determination of the crack opening displacement involves greater difficulties than the determination of the intensity factor. Moreover, the experimentally determined value of δ_c depends on the size and the shape of the plastic zone, which is not fixed in any way when measuring δ_c. Hence, there may be variations in the conditions under which the displacement is calculated and measured, giving rise to uncertainty as to the validity of the analysis.

In this connection it is necessary to develop a method of analysis based on such a criterion for the occurrence of the limiting equilibrium state which would combine the relative simplicity of the limiting intensity factor criterion (3.11) with the applicability of the limiting crack opening displacement criterion (5.1) to small crack lengths (to zero lengths in the limit).

These conditions will be satisfied by a criterion based on the approximate consideration of the plastic crack opening displacement at a crack tip (Secs. 4, 11, 19). Let us discuss this possibility.

The equation of the form (11.1) enables one to determine the critical load for the entire range of crack length. In the limiting cases the results obtained for the critical load coincide with those obtained by the above two fracture criteria, namely when the crack length increases indefinitely the results obtained by the three criteria are identical. As the crack length decreases, criterion (3.11) is ruled out, while the other two give, in the limit when $l = 0$, the same result ($_{cr} = \sigma_y$). The proposed fracture criterion represented, for the present, by the equation of the form (11.1) should therefore be regarded as a fortunate possibility of combining the advantages of the two known criteria, with their shortcomings excluded. At the same time in the limit ($l \to 0$, $l \to \infty$) the criterion under consideration rests entirely upon the known criteria.

The behaviour of the proposed criterion in the range of middle crack lengths may be regulated by the relation between a characteristic (ultimate fracture strength) to be introduced below and the corresponding experimental results.

Equation (11.1) [or (4.9)] may be put into a more universal form. To do this, we express the quantities in Eq. (11.1) in terms of the intensity factors. By multiplying the left-hand side of Eq. (11.1) by $E/(1-\nu^2)$ and using relations (3.8), (3.10), and (3.11), we obtain

$$\frac{E}{1-\nu^2}\int_0^l p_i \frac{\partial u_i}{\partial l}\,dx = K_c^2\{1-[p(l)/\sigma_u]^2\}. \qquad (24.1)$$

Here use has been made of the results of Sec. 4 and it has been assumed that the plastic displacement at the crack tip is proportional to the stress (in a sound body at the location of the crack end) $p(l)$ which separates the faces of the crack from each other. Further steps to simplify the computational scheme are as follows. The stress $p(l)$ at the location of the crack end is replaced by the maximum principal stress σ_1 at the dangerous point in the part, remembering that the crack emanates from this point. This replacement gives results on the safe side and may be justified since crack lengths occurring in structural elements are not usually great.

Moreover, if in the region of the future crack the state of stress in a sound body is homogeneous (or close to it), such a

replacement of the stress is of no significance (for example, in a cracked tension specimen). The stress σ_1 is also chosen because the brittle failure at the dangerous point is usually associated with the first strength theory. By taking the square root of both sides of equality (24.1) and using relations (3.8) and (4.11), we obtain

$$K = I. \tag{24.2}$$

Here I is a new mechanical characteristic which, for definiteness, will be termed the ultimate fracture strength.

From the above discussion it follows that the ultimate fracture strength may be expressed analytically in terms of K_c, σ_1, and σ_u as

$$I = K_c \sqrt{1 - \left(\frac{\sigma_1}{\sigma_u}\right)^2}. \tag{24.3}$$

This functional relation may, however, be given a different representation if use is made of the corresponding experimental results. Moreover, for a closer agreement between theory and experiment it is desirable to determine function (24.3) by processing of laboratory test results for specimens of the required materials.

Let us discuss a possible method of deriving the ultimate fracture strength from experimental data. Suppose we have a critical fracture diagram obtained from tensile tests on a series of specimens with different crack lengths (Sec. 23). From the values of the critical stresses σ_{cr} and crack lengths read from this diagram we calculate the limiting intensity factor [for example, by formula (23.1)] for the entire range of crack length, including very small lengths. In calculating K_c it is common to use a standard specimen with a specified crack length [85]. This crack length is specially chosen to ensure the constancy of K_c (for a given specimen thickness). In our case, on the contrary, the calculated limiting intensity factor depends on the crack length, and as the crack length approaches zero, this factor also approaches zero. Although the limiting intensity factor is calculated by the formula for K, the values obtained must not be confused with K_c, since the latter is defined as a material characteristic remaining constant with increasing crack length (from a certain value on) [9].

The calculated values of the limiting intensity factor are represented as a function of σ_{cr}/σ_u, and this is the ultimate fracture strength

$$I = K\,\varphi(\sigma_{cr}/\sigma_u). \tag{24.4}$$

The function $\varphi(\sigma_{cr}/\sigma_u)$ has the following properties: $\varphi = 0$ as $l \to 0$ and $\varphi = 1$ as $l \to \infty$. In the subsequent computations based on the first strength theory we introduce a factor of safety with respect to the ultimate strength, $n = \sigma_u/\sigma_1$. Since σ_{cr} and σ_1 coincide for specimen, we obtain $\varphi = \varphi(1/n)$.

Thus, the following definition may be given. The ultimate fracture strength is a continuous set of values of the limiting intensity factors for the entire range of crack length (from the zero value on) represented as a function of the reciprocal of the factor of safety based on the ultimate strength.

Formula (24.3) must be regarded as a possible approximation to the ultimate fracture strength expressed by the general formula (24.4).

Assume, as is usually done in regard to other mechanical characteristics, that the ultimate fracture strength may be employed in the design of structural elements with geometry and loading conditions different from those contemplated for the specimen used.

25. DESIGN PROCEDURE IN THE PRESENCE OF CRACKS

For designing on the basis of fracture consideration it is necessary to know the stress intensity factor and its limiting value characteristic of the given material and loading conditions. Since the intensity factor may vary with both the load and the crack length, factors of safety must be further introduced to distinguish between the two possible cases. In particular, the conventional factor of safety based on the ultimate strength $n = \sigma_u/\sigma_1$ enters into the analytic expression for the intensity factor K. This means that the factor K is calculated for the service stress level σ_1 due to the given loads. In other words, the loads introduced into design calculations are those obtained from the previously performed ordinary calculations, i.e., are smaller by a factor of n than those satisfying the equality $\sigma_1 = \sigma_u$ for the dangerous point of the part. Consequently, the intensity factor

depends on the factor of safety based on the ultimate strength $K = K(n)$. Since, however, in the presence of a crack we have to establish the allowable and limiting crack lengths, the limiting value of the intensity factor for the given stress level (the ultimate fracture strength) must also be reduced by a certain factor.

At the stage of fracture in the presence of a macroscopic crack the strength-design equation takes the form

$$K(n) = \frac{I(n)}{m}. \tag{25.1}$$

The right-hand side of this equation involves the factor of safety m based on the ultimate fracture strength. When $m = 1$, the crack length occurring in the expression for K is critical for the service stress level. Increasing the factor m leads to a decrease in crack length. To each $m > 1$ corresponds a certain crack length less than the critical one (when $\sigma_1 = \text{constant}$). At some value $m > 1$ the crack length obtained may be considered allowable.

The value of the factor of safety n is established by calculation and on the basis of experience with past practice. The factor m (establishing the allowable crack length) is still not completely studied. After calculating the allowable crack length l_0 with the help of the critical fracture diagram, it is possible to establish the factor of safety based on the critical stress $n_0 = \sigma_{cr}/\sigma_1$ (when $l = l_0$). Since, in general, $n_0 < n$, by establishing the lower limit n_0, we can establish the factor m and thereby l_0.

The factor of safety based on the ultimate fracture strength is a number indicating how many times the stress intensity factor must be increased by increasing the crack length, while holding the loads and the factor of safety constant, to make it (the intensity factor) reach its limiting value for the given factor of safety.

The advantage of the design equation (25.1) lies in the fact that in the absence of a crack this equation transforms into the ordinary strength condition. Indeed, let $l \to 0$, then $K \to 0$ and from Eqs. (25.1) and (24.3) we have $\sigma_1 = \sigma_u$. This condition is identical with the first classical strength theory describing the onset of brittle fracture. To avoid the initiation of fracture, the maximum stress in the ordinary

design calculations is allowed to be σ_u/n. Since this allowable stress is introduced into the intensity factor and the ultimate fracture strength, we obtain a synthesis of the strength conditions by the first theory and in the presence of a crack.

The static design procedure in the presence of a crack under single loading is as follows:

(1) perform the ordinary static stress analysis by the first strength theory to establish a factor of safety and the position of the dangerous point;

(2) calculate the intensity factor for a crack introduced at the dangerous point.

The crack is imagined to emanate from the dangerous point in any direction whatsoever, but it is desirable to choose the one which seems most likely. After calculating the intensity factor, of the crack propagation directions introduced choose the one corresponding to the largest intensity factor. The intensity factor must be represented analytically or graphically as a function of the crack length;

(3) determine the mechanical characteristic—the ultimate fracture strength (Sec. 24). Note that in the experimental determination of the ultimate fracture strength it is desirable that the shape of the specimen should suit the construction of the part being designed;

(4) perform an analysis to determine the allowable crack length and to establish the final factor of safety in the presence of this crack for the given factor of safety based on the ultimate fracture strength.

The stress introduced into the design of a part is that acting perpendicular to the plane of the crack. The other stress components are disregarded.

26. EXAMPLES OF DESIGNING WITH CRACKS

The design procedure will be illustrated by a simple example. The most efficient method of design is a semigraphical one (Fig. 26.1). Consider the extension of a cracked plane. The tensile stress is σ_1. In this case the intensity factor is equal to

$$K = \sigma_1 \sqrt{\pi l} = \frac{\sigma_u}{n} \sqrt{\pi l}.$$

The ultimate fracture strength, from (24.3), is

$$I = K_c \sqrt{1 - \left(\frac{\sigma_1}{\sigma_u}\right)^2} = K_c \sqrt{1 - \frac{1}{n^2}}.$$

Having the value of n and assigning a definite factor of safety m for a crack,* with the help of equality (25.1) we

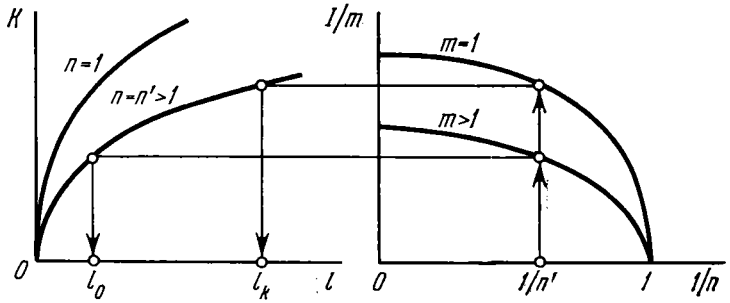

Fig. 26.1. Scheme of the semigraphical method of design with cracks. On the left: stress intensity factor as a function of the crack length for several factors of safety. On the right: ultimate fracture strength.

find the allowable crack length $2l_0$. The critical length is found by setting $m = 1$, as shown in Fig. 26.1.

When $m = 1$, from the condition

$$\frac{\sigma_u}{n} \sqrt{\pi l_k} = K_c \sqrt{1 - \frac{1}{n^2}}$$

we obtain the critical crack length

$$l_k = \frac{1}{\pi} \left(\frac{K_c}{\sigma_u}\right)^2 (n^2 - 1).$$

It appears that the allowable and critical crack lengths are related by the expression $l_0 = l_k/m^2$.

When the crack length is l_0, the factor of safety for the body is less than n, namely $n_0 = \sigma_k/\sigma_1$, where σ_k is the critical stress in the presence of a crack of allowable length l_0 (Fig. 26.2).

* The factor of safety m based on the ultimate fracture strength may also be called a factor of safety for a crack since its value affects the allowable crack size.

For the purpose of determining the value of n_0 we introduce a strength reduction factor α defined by the relation $\alpha = \sigma_u/\sigma_{cr}$. When the fracture stress is equal to σ_{cr}, the allowable crack length becomes critical; hence, the factors

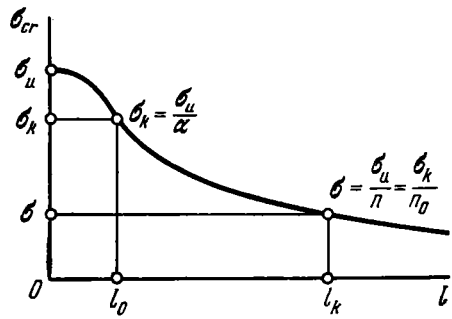

Fig. 26.2. Schematic relation between the fracture stress and the crack length.

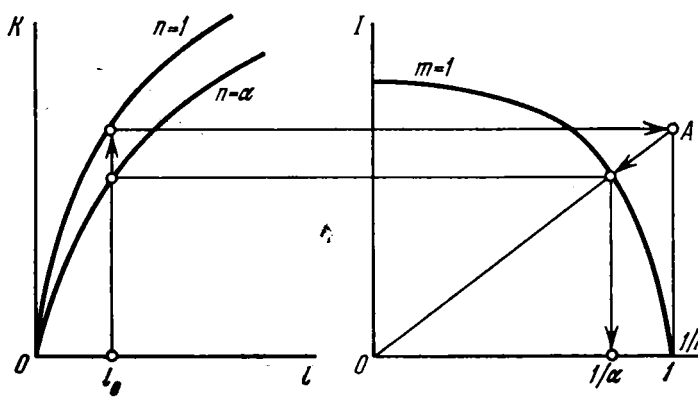

Fig. 26.3. Scheme illustrating the method of determining the strength reduction factor α. The abscissa of the point of intersection of the ray OA and the curve for I when $m = 1$ gives the value of the factor α.

of safety are $n = \alpha$, $m = 1$. The intensity factor is inversely proportional to the number n, hence the line AO (Fig. 26.3) corresponds to this functional relation when $l = l_0 =$ constant. This suggests a graphical procedure for

establishing the factor α, as shown in Fig. 26.3. It is obvious that $\sigma_u/\alpha = \sigma_{cr} = \sigma_u n_0/n$. From this we obtain the required factor of safety based on the critical stress

$$n_0 = \frac{n}{\alpha} \quad (n_0 < n).$$

This is the factor of safety for a body containing a crack of allowable size. It is expressed by a number indicating how many times the external load must be increased for the allowable crack to become critical.

We shall use this design procedure for establishing the allowable crack lengths and factors of safety for some structural elements.

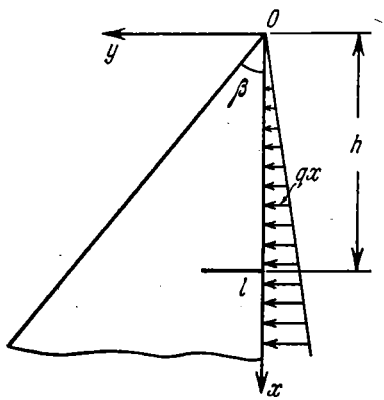

Fig. 26.4. Schematic loading of a cracked wedge.

Example 1. A two-dimensional wedge with a vertex angle β is stressed in its plane by a distributed pressure exerted on one side of the wedge. The load is perpendicular to the side of the wedge and increases from the vertex according to a linear law with a slope q. The co-ordinate system is shown in Fig. 26.4. At a distance h from the vertex of the wedge there is a crack situated perpendicular to the loaded side of the wedge. The wedge is made of B-95 alloy. It is required to establish the allowable crack size under the applied static load.

To determine the stress intensity factor we use the method of sections (Sec. 9). The stresses in the wedge with no crack ($\lambda = \tan\beta$) are

$$\sigma_y = -qx, \quad \sigma_x = -\frac{2q}{\lambda^3}y + \frac{q}{\lambda^2}x, \quad \tau_{xy} = -\frac{q}{\lambda^2}y.$$

Assuming that the crack extends along a straight line normal to the side of the wedge $y = 0$, we set up the force equation

of equilibrium in the x direction for $x = h$

$$\int_0^l \sigma_x\, dy = \int_l^{l+a} \frac{K\, dy}{\sqrt{2\pi (y-l)}}.$$

The size a is determined from the condition

$$-\frac{2q}{\lambda^3} l + \frac{q}{\lambda^2} h = \frac{K}{\sqrt{2\pi a}}.$$

From this we obtain

$$K_* = \frac{1}{\lambda^3} \sqrt{\pi l_* (\lambda - l_*)(\lambda - 2l_*)}. \tag{26.1}$$

Here

$$K_* = \frac{K}{qh^{3/2}}, \quad l_* = \frac{l}{h}.$$

Suppose now that the crack extends along a circular arc $r = h$. Then

$$\sigma_r = \frac{qh}{2\lambda^2}\Big[-\frac{2}{\lambda}\sin\theta\,(1+\cos 2\theta) + (1-\lambda^2)\cos\theta + \\ + (1+\lambda^2)\cos\theta\cos 2\theta\Big]$$

and the equilibrium equation is

$$\int_0^{\theta_k} \sigma_r h\, d\theta = \int_0^a \frac{Kh\, d\varphi}{\sqrt{2\pi\varphi h}}.$$

The value of a is determined from the condition

$$\sigma_r(\theta_k) = \frac{K}{\sqrt{2\pi a h}}.$$

We obtain, finally,

$$K_* = \frac{1}{2\lambda_0^2 n}\sqrt{\pi f_1(l_*) f_2(l_*)},$$

$$f_1(l_*) = -\frac{2}{\lambda_0\sqrt{n}}(1-\cos l_*) + \\ + \frac{1}{3\lambda_0\sqrt{n}}(\cos 3l_* - 3\cos l_* + 2) + (1-\lambda_0^2 n)\sin l_* + \\ + \frac{1+\lambda_0^2 n}{6}(\sin 3l_* + 3\sin l_*), \tag{26.2}$$

$$f_2(l_*) = -\frac{2}{\lambda_0\sqrt{n}}\sin l_*\,(1+\cos 2l_*) + (1-\lambda_0^2 n)\cos l_* + \\ + (1+\lambda_0^2 n)\cos l_*\cos 2l_*, \quad \theta_k = \frac{l}{n}.$$

In this problem q = constant and to change the value of the stress for the purpose of changing the factor of safety n based on the ultimate strength we shall vary the angle at the vertex of the wedge. From the condition

$$\sigma_x = \sigma_u \text{ when } y = 0,\ x = h,\ \lambda = \lambda_0$$

we have $\lambda_0 = \sqrt{qh/\sigma_u}$. This is the value of tan β at which the stress σ_x at the point $y = 0$, $x = h$ in the wedge with no crack reaches its limiting value σ_u. The factor of safety by the first strength theory is

$$n = \frac{\sigma_u}{\sigma_x(h,\ 0)} = \frac{\sigma_u \lambda^2}{qh} = \frac{\lambda^2}{\lambda_0^2}.$$

Consequently, $\lambda = \lambda_0\sqrt{n}$. This is the value of λ that appears in expression (26.2).

By comparing the two values for the intensity factor (26.1) and (26.2), we see that the intensity factor (26.2) for the crack extension along a circular arc is greater than the intensity factor (26.1) for the crack extension along a straight line. We conclude, therefore, that the crack will extend along a circular arc, and use factor (26.2) in the calculation.

The intensity factor (26.2) for two factors of safety, $n = 1$ and $n = 2$, is represented in Fig. 26.5. Shown here is also the ultimate fracture strength ($I_* = I/qh^{3/2}$) for B-95 alloy obtained from the data of [69].

The numerical values used in the calculation are: the external load parameter $q = 0.01$ kgf/mm^3, the position of the dangerous point $h = 215$ cm, the factor of safety based on the ultimate strength $n = 2$.

Consider two variants of the design: the factor of safety for a crack is $m = 2$ and $m = 4$. In the first case ($m = 2$) the allowable crack length determined graphically from Fig. 26.5 is found to be $l_* = 0.07$, or $l = l_* h = 15$ mm.

If the vertex angle of the wedge is decreased until the crack becomes critical, the factor of safety will be less than 2. This final factor of safety n_0 is found with the aid of the strength reduction factor α determined graphically. We obtain $\alpha = 1.35$. The final factor of safety is $n_0 = \frac{n}{\alpha} = \frac{2}{1.35} = 1.48$.

In the second case ($m = 4$) the allowable crack length is found to be $l_* = 0.03$, $l = l_* h = 6.5$ mm.

The strength reduction factor is $\alpha = 1.1$, the final factor of safety based on the critical stress for the allowable crack length is $n_0 = n/\alpha = 1.82$. This number is 9 per cent less than 2. If we choose the last variant, the following conclusion may be drawn. For the given construction of the wedge

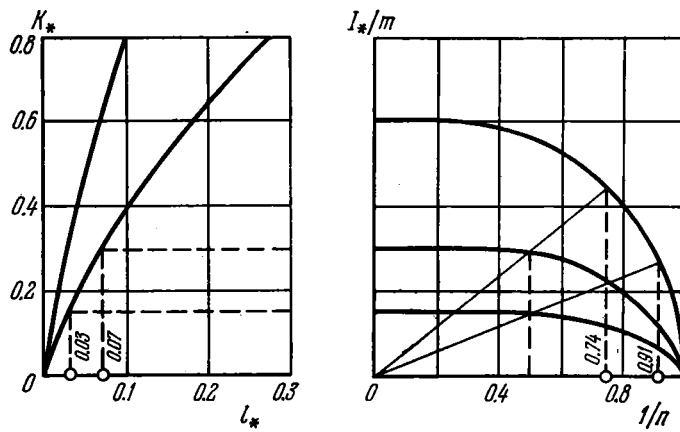

Fig. 26.5. Relation between the stress intensity factor and the crack length for a wedge and the ultimate fracture strength of B-95 alloy.

and the given loading conditions ($\sigma_u = 56$ kgf/mm^2, $\lambda_0 = \sqrt{qh/\sigma_u} = 0.196$), the factor of safety based on the ultimate strength in the absence of a crack is taken to be equal to 2 for the dangerous point located at a distance $h = 215$ mm. If at this location there is a circular arc crack of allowable length 6.5 mm, the factor of safety decreases by 9 per cent.

Example 2. A rotating disk of Д16T-1 alloy with a central hole may contain a radial crack originating at the edge of the hole. The disk rotates with a constant angular velocity ω. The circumferential stresses due to the inertia forces in the disk with no crack are

$$\sigma_\theta = \frac{3+\nu}{8g}\gamma\omega^2\left[R^2 + r^2 - \frac{1+3\nu}{3+\nu}\rho^2 + \frac{R^2 r^2}{\rho^2}\right],$$

where R and r are, respectively, the outer and inner radii of the disk, ρ is the current radius, γ is the specific weight of the material, g is the acceleration of gravity.

The equilibrium condition involved in using the method of sections is

$$\int_r^{r+l} \sigma_\theta \, d\rho = \int_0^a \frac{K\,dx}{\sqrt{2\pi x}},$$

where the size a is determined from the condition

$$\sigma_\theta (\rho = r + a) = \frac{K}{\sqrt{2\pi a}}.$$

The stress intensity factor is

$$K_* = \frac{1}{n}\left[(1+b^2)\, l_* + b^2 \frac{l_*}{1+l_*} - B\frac{(1+l_*)^3-1}{3}\right] \times$$
$$\times \left[1 + b^2 + \frac{b^2}{(1+b_*)^2} - B\,(1+l_*)^2\right]. \qquad (26.3)$$

Here

$$K_* = \frac{8gK}{\sqrt{\pi}\,(3+\nu)\,\gamma\omega_0^2 r^{5/2}}, \quad B = \frac{1+3\nu}{3+\nu}, \quad l_* = \frac{l}{r}, \quad b = \frac{R}{r}.$$

The factor of safety is $n = \sigma_u/\sigma_\theta$ ($\rho = r$); from this we find that the angular velocity for the given factor of safety must be equal to $\omega = \omega_0/\sqrt{n}$, where ω_0 is the angular velocity at which $\sigma_{\theta\max} = \sigma_u$.

Figure 26.6 gives the intensity factor for two values of the factor of safety, $n = 1$ and $n = 2$, when $b = 3$, $\nu = 0.25$, $B = 0.54$. On the right side in Fig. 26.6 is shown the ultimate fracture strength for Д16Т-1 alloy plotted from the data of [69].

The following data are given for the disk: $r = 50$ mm, $\gamma = 2.7$ gf/cm^3, $\sigma_u = 45$ kgf/mm^2, $\omega_0 = 2940$ sec^{-1}.

When the factor of safety for a crack is $m = 2$, the allowable crack length is $l = l_* r = 0.024 \times 50 = 1.2$ mm, $\alpha = 1.25$, the final factor of safety is $n_0 = n/\alpha = 1.6$.

When $m = 4$, the allowable crack length is $l = 0.5$ mm and the final factor of safety in the presence of a radial crack of allowable length (0.5 mm) remains practically the same,

i.e., it is equal, as before, to 2. Consequently, in this case a radial crack of length up to 0.5 mm may be allowed without

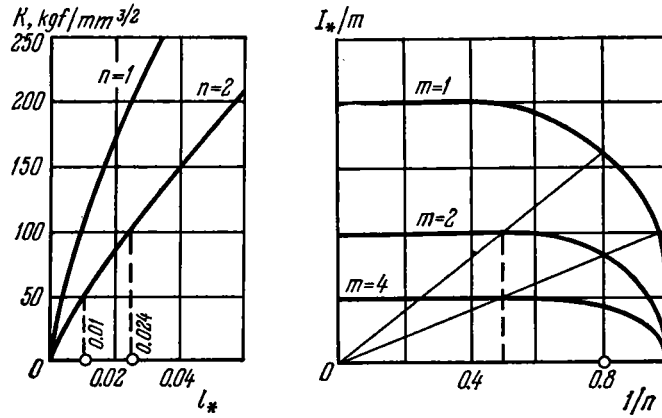

Fig. 26.6. Relation between the stress intensity factor and the crack length for a rotating disk and the ultimate fracture strength of Д16Т-1 alloy.

any marked detriment to the strength properties of the disk (under constant operating conditions and neglecting environmental effects).

Example 3. Consider an axial section of a pipe flange. A crack runs perpendicular to the external surface of the pipe. The acting forces are shown schematically in Fig. 26.7.

It is assumed that the only stresses responsible for crack opening are those acting perpendicular to the plane of the crack. The circumferential and radial stresses are therefore not taken into account; thereby, the problem is reduced to a plane one. The stress intensity factor is determined, as before, by using the method of sections. The nominal stress is

$$\sigma_x = \frac{P}{h}\left(\frac{1}{2} + 24\frac{y}{h}\right)$$

noting that $M = P(L - h/4)$ and assuming $L = 2.25\,h$.

The equation of equilibrium is

$$\int_{h/2-l}^{h/2} \sigma_x\, dy = \int_0^a \frac{K\,dr}{\sqrt{2\pi r}}.$$

The value of a is determined by the condition

$$\sigma_x (y = h/2 - l) = K/\sqrt{2\pi a}.$$

The intensity factor is

$$K_* = \frac{1}{2n}\sqrt{\pi [l_* + 6(1-(1-2l_*)^2)][1+24(1-2l_*)]}. \quad (26.4)$$

Here P_0 is the load corresponding to the stress σ_x reaching the ultimate strength at the point where the crack originates

$$K_* = \frac{K\sqrt{h}}{P_0}, \quad l_* = \frac{l}{h}, \quad P_0 = Pn.$$

The stress intensity factor is presented in Fig. 26.8 for the factors of safety $n = 1$ and $n = 2$. On the right side in the same figure is given the ultimate fracture strength for the pipe material ВЛ1-Д [98].

The numerical values are: $h = 40$ mm, $\sigma_u = 120$ kgf/mm², $P_0 = \sigma_u h/12.5 = 324$ kgf/mm, $K = 60.6K_*$.

For $m = 2$, we obtain graphically the allowable crack length $l = l_* h = 0.032 \times 40 = 1.28$ mm, the strength reduction factor $\alpha = 1.45$, the final factor of safety $n_0 = n/\alpha = 1.38$.

For $m = 4$, the allowable crack length is $l = 0.014 \times 40 = 0.56$ mm, the strength reduction factor is $\alpha = 1.15$, the final factor of safety is $n_0 = 1.74$. Consequently, the presence of a 0.5 mm crack reduces the static factor of safety by 7.7 per cent.

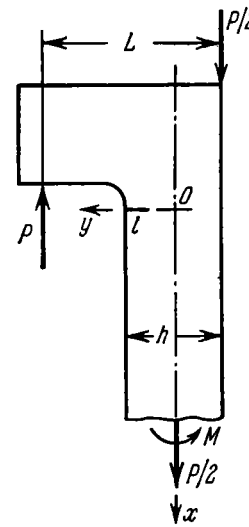

Fig. 26.7. Schematic representation of forces at a longitudinal section of a cracked flange.

Example 4. A welded cylindrical vessel of diameter 508 mm is subjected to internal pressure [37]. The wall thickness is 1.02 mm. The material of the vessel is martempering steel with 20% of nickel. The yield stress is $\sigma_{0.2} = 214.9$ kgf/mm², the ultimate strength is $\sigma_u = 215.6$ kgf/mm². Under a single hydraulic loading, the vessel fractured at a pressure of 59.9 at, which corresponds to the circumferential stress $\sigma_\theta = 134.4$ kgf/mm². The ratio of this stress

to the ultimate strength is 0.62, i.e., the strength of the steel is underused by nearly one half.

From the fractured vessel specimens were cut in the longitudinal and transverse directions, two specimens in each direction, which showed the following values of the critical intensity factors: in the longitudinal direction $K_c = 337$ and

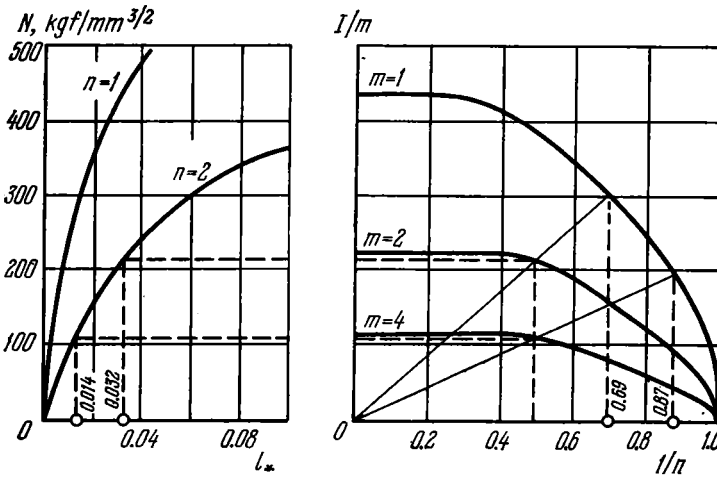

Fig. 26.8. Relation between the stress intensity factor and the crack length for a flange and the ultimate fracture strength of ВЛ1-Д steel.

364 kgf/mm$^{3/2}$, $K_{Ic} = 253$ and 248 kgf/mm$^{3/2}$; in the transverse direction $K_c = 196$ and 145 kgf/mm$^{3/2}$, $K_{Ic} = 178$ and 132 kgf/mm$^{3/2}$.

For the purposes of subsequent investigation, it is useful to recall characteristics for material assessment. The fracture mode may be predicted from the value of the ratio of the plastic zone length d ahead of the crack edge to the thickness h of a plane specimen or a plane structural element. According to Irwin, $d = K_c^2/\pi\sigma_{0.2}^2$ in plane stress.

If $\beta = d/h < 1$, the fracture is predominantly direct (failure occurs by separation); if $\beta > 1$, the fracture is predominantly oblique (failure occurs by shear). If the factor $\alpha_0 = K_c/K_{Ic} < 2$, the material characteristic introduced into the calculation is K_{Ic}; if $\alpha_0 > 2$, the calculation is carried

out with the value of K_c characteristic of the given thickness of the plane part. In our case the parameter β which determines the failure conditions as the direct or oblique mode of fracture is: for the longitudinal direction $\beta = 0.8$, for the transverse direction $\beta = 0.2$ (based on the average values of K_c). Since this ratio is less than unity [120], failure takes place under conditions closely approximating plane strain under a three-dimensional state of stress,* in the plane strain opening mode. In these conditions the structure is sensitive to cracks. The factor α_0 (which shows how much the stress intensity factor in plane stress exceeds its value in triaxial tension) is 1.33 for the longitudinal direction and 1.1 for the transverse direction. Since $\alpha_0 < 2$, the calculation must be carried out with the limiting factor K_{Ic}, and not with K_c.

The inspection of the vessel after fracture revealed the presence of an initial defect in the form of a crack on the external surface orientated perpendicular to the rolling direction in the sheet. This crack was the cause of the reduction in strength of the vessel. Since the length of the crack exceeded its depth l by more than a factor of ten, we use the intensity factor formula for an edge-notched plate [31] $K = 1.1\sigma_\theta\sqrt{\pi l}$.

This formula involves the circumferential stress since the vessel is welded along a helix making a 79° angle with the generator of the cylinder, and the transverse direction of the crack on the sheet is an axial one for the vessel. The crack depth was found to be $l = 0.76$ mm.

Let us determine the fracture crack depth by calculation. The ultimate fracture strength is written in the form of (24.3) where we substitute the average value $K_{Ic} = 251$ kgf/mm$^{3/2}$ for the longitudinal direction. From equality (24.2) with the fracture stress $\sigma_\theta = 134.4$ kgf/mm^2 we find the critical crack depth $l = 0.58$ mm (Fig. 26.9). By comparing this value with the experimental value 0.76 mm, we conclude that the calculation gives conservative values (on the safe side) of the critical crack size.

Let us perform a similar calculation for which the ultimate fracture strength is taken in an alternate form. Suppose

* See the preface by Ya. B. Fridman and B. A. Drozdovskii to [85] (Russian edition).

that the function expressing the ultimate fracture strength is represented by a broken line one segment of which is defined by the equation $I = K_{Ic}$ (when $0 \leqslant 1/n \leqslant 1$), and the other by $0 \leqslant I \leqslant K_{Ic}$ (when $n = 1$) (Fig. 26.9). For the calculation of the critical crack depth condition (24.2) then gives a relation of the form $K = K_{Ic}$, which is at present virtually the only formula used in the design of cracked parts. From this relation we obtain $l = 0.91$ mm, which

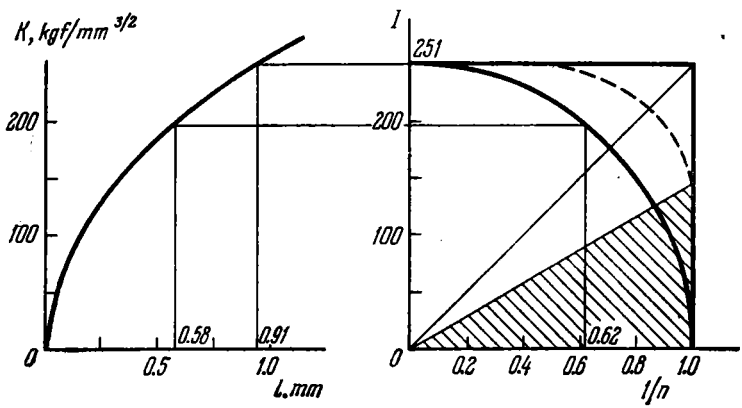

Fig. 26.9. Relation between the stress intensity factor and the crack length ($K = 1.1 \times 134.4 \sqrt{\pi l}$) and the ultimate fracture strength.

exceeds the experimental value by 20 per cent. Consequently, the foregoing simplified relation underestimates the material susceptibility to early brittle fracture.

The actual factor of safety in the presence of a crack is $n_0 = \sigma_k/\sigma_1$. As already stated, it can be determined with the aid of the strength reduction factor $\alpha = \sigma_u/\sigma_k$ by means of the relation $n_0 = n/\alpha$. In the graph of the ultimate fracture strength the factor α is determined by a straight line emanating from the origin and terminating at a point of given co-ordinates (I/m, $1/n$). The co-ordinate of the point of intersection of this straight line and the graph of the ultimate fracture strength when $m = 1$ determines the value of α.

We shall show by the use of this example what the factor of safety for a crack m should be if, for a given factor of

safety n, there is to be no reduction in strength of the vessel because of the early brittle fracture. If a ray is drawn from the origin in the graph of I to a point of co-ordinates $I = K_{Ic}$, $n = 1$, the triangular region below the ray corresponds to values of m and n such that $\alpha = 1$, and hence $n_0 = n$. In this region $m \geqslant n$, which follows from the equation of the ray $K_{Ic}/m = K_{Ic}/n$.

Thus, if the condition $m > n$ is fulfilled, the actual factor of safety in the presence of a crack is equal to the original value and there is no reduction in strength of the vessel because of the existing crack.

However, this conclusion holds only for the case when the factor K_{Ic} (or K_c) remains constant as the critical stress varies up to the ultimate strength. Actually K_c depends on the critical crack length and, beginning with some value of the stress, it decreases considerably. This means that the shape of the graph of the ultimate fracture strength is not rectangular (dashed line in Fig. 26.9) and the ray defining the factor α crosses the curve for the ultimate fracture strength at a point $\alpha > 1$, and hence $n_0 < n$.

If the graph of the ultimate fracture strength has a vertical portion ($n = 1$), the line connecting the top of this vertical portion to the origin cuts off the lower triangular region (shaded in Fig. 26.9) of values m and n for which there is no reduction in strength of the vessel because of the presence of a crack.

Let us determine the range of the actual factor of safety n_0 and of the factor of safety for a crack m for fixed values of the ordinary factor of safety n and of the ultimate fracture strength expressed by function (24.3). In the case under consideration the critical crack length for a given number n is determined, according to equality (24.2), as

$$1.1\left(\frac{\sigma_u}{n}\right)\sqrt{\pi l_k} = K_c\sqrt{1-\left(\frac{1}{n}\right)^2}.$$

In accordance with condition (25.1) the allowable crack length is found from the equation

$$1.1\left(\frac{\sigma_u}{n}\right)\sqrt{\pi l_0} = \left(\frac{K_c}{m}\right)\sqrt{1-\left(\frac{1}{n}\right)^2}.$$

On the other hand, this allowable crack length l_0 is critical if $n = \alpha$, and hence it also satisfies the equation

$$1.1\left(\frac{\sigma_u}{\alpha}\right)\sqrt{\pi l_0} = K_c\sqrt{1-\left(\frac{1}{\alpha}\right)^2}.$$

From these three equations we find the desired relation among the quantities n, m, and $n_0 = n/\alpha$

$$\frac{m^2}{n_0^2} = \frac{n^2-1}{n^2-n_0^2}.$$

The curves plotted by this formula are presented in Fig. 26.10. It is seen that a small reduction in the factor of

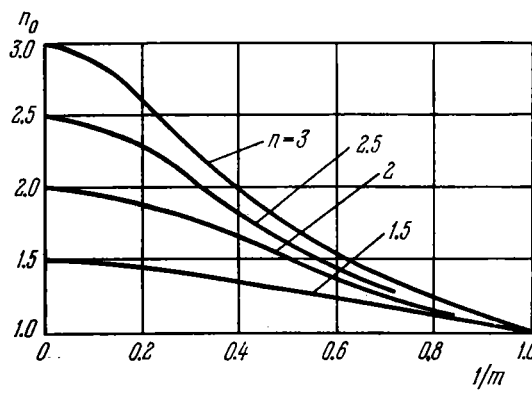

Fig. 26.10. Relation between the factor of safety n_0 based on the critical stress (in the presence of a crack) and the factor of safety m based on the ultimate fracture strength for a given factor of safety n.

safety is achieved at the expense of large factors of safety for a crack.

We also give the values of the actual factor of safety n_0 for some chosen values of the number m

n	1.5	2	2.5	3
n_0 $(m=n)$	1.2	1.51	1.85	2.18
n_0 $(m=n^2)$	1.36	1.84	2.38	2.88

Pressure vessels, tanks, and containers of various functions are among the most common engineering structural elements. Sometimes their operating conditions are such that

the occurrence and development of plastic deformation are constrained. This may be due to different causes among which we may mention irradiation hardening and hydrogen embrittlement typical of reactor technology. As a result of the suppression of the ability of a material to deform plastically there is no possibility for a favourable redistribution of stress and strain in the volume of the body and between its individual structural components. This gives rise to local overstresses, initial microcracks, which have a tendency to develop progressively until macroscopic brittle fracture occurs. As already mentioned, the danger of brittle fracture lies not only in its apparent suddenness, but also in the fact that it may occur at stresses lower than the design ones. This means that the actual factor of safety is lower than that established by the ordinary design procedures neglecting cracks.

The proposed method of design enables one to determine the degree of underusing the strength of a vessel, i.e., to establish the actual (final) factor of safety in the case of brittle fracture. At the same time a safe crack size is established, which does not entail an immediate fracture of a part. Thus, the design procedure taking account of existing cracks and based on proper experiments provides assurance that the structure is prevented from failing by catastrophic brittle fracture.

Of course, the proposed method of design with due allowance for cracks cannot be recognized as universal. The accumulation of the appropriate experience in practice and designing will naturally assist its improvement and adoption in the practical work of design organizations.

CHAPTER V

CRACKS IN LINEARLY VISCOELASTIC MEDIA

27. THE VISCOELASTIC ANALOGUE OF THE GRIFFITH AND SACK PROBLEMS

Let us examine the possibility of using the fracture criteria (Sec. 4) for the solution of crack problems for linearly viscoelastic media. The solutions given below are based on Volterra's principle whose validity for steadily growing cracks is demonstrated in [125].

Suppose that the medium is linearly viscoelastic at all of its points and no plastic deformation occurs at the crack edges. Then, according to [48, 140], there is no slow subcritical crack growth under constant external loads for perfectly brittle fracture. The critical state (the onset of rapid crack growth) occurs at a certain time t^* after application of the load, and the larger the applied load, the shorter is the time t^* to brittle fracture initiation.

To study the growth of cracks in media of such rheology, we use, for example, the integral variational principle for an elastic body (4.10).

As an example let us consider the problem of the extension, by a stress p, of a plane with a single straight crack $y = 0$, $|x| \leqslant l$ and of a space with a penny-shaped crack (circular in plan) of radius l. The load is applied along the y axis perpendicular to the crack surface.

In our case for plane stress

$$v = 2\bar{E}^{-1} p \sqrt{l^2 - x^2}, \quad \bar{E}^{-1} f = \frac{1}{E_0}\left[f + \int_0^t K(t-\tau) f(\tau)\, d\tau\right].$$

Here $\bar{E}^{-1}$ is the linear time operator with the creep kernel $K(t-\tau)$ [235].

The solution of Eq. (4.10) for the stress p (after first integrating with respect to x and varying with respect to l) leads to the following relation [193]:

$$\left(\frac{p}{p_0}\right)^2 = \frac{1}{1+\int\limits_0^{t^*} K(t^*-\tau)\,d\tau} = 1 - \int\limits_0^{t^*} \Gamma(t^*-\tau)\,d\tau. \qquad (27.1)$$

Here $\Gamma(t-\tau)$ is the relaxation kernel, $p_0 = \sqrt{2E_0\gamma/\pi l}$ is the Griffith critical stress with the instantaneous modulus of elasticity E_0.

For the extension of the space with a penny-shaped crack (when $\bar{\nu} = \nu = 0.5$), from (4.10) we obtain a relation similar to (27.1)

$$\left(\frac{p}{p^0}\right)^2 = 1 - \int\limits_0^{t^*} \Gamma(t^*-\tau)\,d\tau. \qquad (27.2)$$

Here $p^0 = \sqrt{\pi E_0\gamma/2(1-\nu^2)\,l}$ is the Sack critical stress.

From Eqs. (27.1) and (27.2) we can obtain the time to brittle fracture for each value of the external load. Fracture delay may be interpreted here as the time of reduction in the critical stress corresponding to a given crack length due to a decrease in the modulus of elasticity. Also, as time goes on the crack opens (without an increase in its length).

Equations similar to Eqs. (27.1) and (27.2) have been derived in [297, 298]. Note that the solution of problems relating to the limiting equilibrium of linearly viscoelastic bodies with cracks may be obtained from the elastic solution for the limiting (critical) load by merely replacing the elastic characteristics of the material by the corresponding time operators.

It is known that the theory of elastic-hereditary media with exponential kernels of fractional order is suitable for describing viscoelastic deformations of some materials. By using this, we represent (27.1) as [235, 245]

$$\left(\frac{p}{p_0}\right)^2 = 1 - \frac{\varkappa}{\beta}\left[1 - \exp\left(-\omega\beta(t^*)^{1+\alpha}\right)\right]. \qquad (27.3)$$

Here $\omega = (1+\alpha)^{1+\alpha}$, and α, β, $\varkappa$ are the parameters characterizing the rheological properties of the material.

Note that the following relations are valid for the parameters β and $\varkappa$ [245]:

$$\beta = T^{1-\alpha}, \quad \varkappa = \frac{E_0 - E_\infty}{E_0} T^{1-\alpha}.$$

Here E_0 and E_∞ are the instantaneous and steady-state moduli of elasticity, T is the relaxation time.

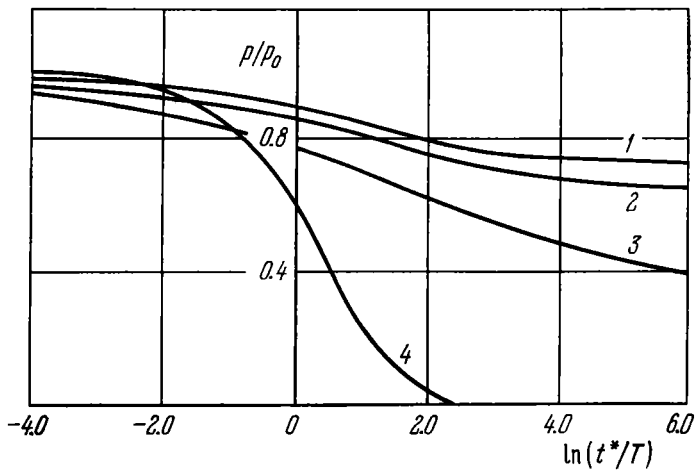

Fig. 27.1. Relation between the lifetime of a cracked plane and the stress level for several materials. *1*, polymer; *2*, copper; *3*, steel; *4*, Maxwell body.

For a Maxwell body ($\alpha = 0$, $\beta = \varkappa = 1/T$) from (27.3)

$$(p/p_0)^2 = \exp(-t^*/T).$$

For copper at $t = 165$ °C [245]

$$(p/p_0)^2 = 1 - 0.58\,[1 - \exp(-0.697\,(t^*/T)^{0.3})].$$

For steel (C = 0.35%) at $t = 454$ °C [245]

$$(p/p_0)^2 = 1 - 0.851\,[1 - \exp(-0.697\,(t^*/T)^{0.3})].$$

For thermoreactive polymer [280]

$$(p/p_0)^2 = 1 - 0.434\,[1 - \exp(-0.707\,(t^*/T)^{0.5})].$$

These relations are presented in Fig. 27.1. From this it is seen that for real materials, in contrast to a Maxwell body,

there exists a value of the load below which the crack does not open with time, and the critical state does not occur. This stress can be determined from (27.3) when $t^* \to \infty$.

The fracture criterion in the integral form (4.10) is convenient for use since it does not require a detailed analysis of stresses at a crack tip, gives the wanted result for the elastic energy difference during a small quasi-static increment of crack length, and thereby the effects accounting for crack growth are automatically included.

28. THE VISCOELASTIC-PLASTIC ANALOGUE OF THE GRIFFITH AND SACK PROBLEMS

Suppose that a crack is propagating in a linearly viscoelastic medium in the presence of a thin plastic zone ahead of the crack edge. This plastic zone is replaced in what follows by an additional cut whose surface is acted on by stresses σ_0.

The integral variational principle for an elastic-plastic body (Sec. 4), as applied to the problem of the extension of a cracked plane, may be written down as [187, 193]

$$2\gamma \dot{l} \delta t - \delta \left[\int_0^l pv\,dx + \int_l^a (\sigma_0 + p)\, v\,dx \right] = 0, \qquad (28.1)$$

where $a - l$ is the extent of the plastic zone ahead of the crack edge and the remaining notation is the same as before (Sec. 4), with the exception of the variation operation.

Here the fracture energy is time dependent, and hence the rapid avalanche growth of a crack is preceded by its slow subcritical growth $[l = l(t)]$, in contrast to the case considered in Sec. 27. To determine the function $l = l(t)$, we vary the time in condition (28.1), i.e.,

$$\delta = \frac{d}{dt}\,\delta t = \left(\frac{\partial}{\partial t} + \frac{\partial}{\partial l}\,\dot{l} \right) \delta t.$$

The displacements on the surface of the crack and of the additional cut are expressed as follows [218]:

$$v(x) = \frac{\sigma_0}{\pi}\,\bar{E}^{-1}\,[(x-l)\,\Gamma(x, l) - (x+l)\,\Gamma(x, -l)],$$

$$\Gamma(x, l) = \ln \frac{a^2 - xl - \sqrt{(a^2-x^2)(a^2-l^2)}}{a^2 - xl + \sqrt{(a^2-x^2)(a^2-l^2)}}.$$

To calculate the fracture energy density, we use the first equality of (21.20). We then obtain

$$\frac{2\gamma}{\sigma_0\delta_c}=\frac{2}{\delta_c}\int\limits_l^a \frac{\partial v^*}{\partial l}\,dx=\Phi(\lambda^*)\left[\zeta+\int\limits_0^t K(t-\tau)\,\zeta(\tau)\,d\tau\right]. \quad (28.2)$$

Here

$$\lambda^*=\frac{2}{\pi}\arccos\exp\left[-1\Big/\left(\zeta+\int\limits_0^t K(t-\tau)\,\zeta(\tau)\,d\tau\right)\right],$$

$$\Phi(\lambda)=\frac{\pi\lambda}{2}\tan\frac{\pi\lambda}{2}+\ln\cos\frac{\pi\lambda}{2},$$

$$\lambda=\frac{p}{\sigma_0},\quad \zeta=\frac{l}{c},\quad c=\frac{\pi E_0\delta_c}{8\sigma_0}.$$

The symbol λ^* represents the limiting load by the δ_c-theory for a viscoelastic medium.

Further transformation of Eq. (28.1), taking into account (28.2), leads to the following relation:

$$\dot{\zeta}=\frac{1}{2}\,\frac{\Phi(\lambda)\left[\int\limits_0^t \dot{K}(t-\tau)\,\zeta^2(\tau)\,d\tau+K(0)\,\zeta^2\right]}{\Phi(\lambda^*)\left[\zeta+\int\limits_0^t K(t-\tau)\,\zeta(\tau)\,d\tau\right]-\zeta\Phi(\lambda)}. \quad (28.3)$$

Equation (28.3) enables one to calculate the crack length and the crack tip velocity as a function of time under constant load. The life t_0^* of a cracked body is determined by the time in which the crack tip velocity reaches infinity. This moment corresponds to the critical state, i.e., the crack length increases to a value for which the given load is critical in the viscoelastic medium (surrounding the crack together with the plastic zone) with the instantaneous modulus of elasticity.

We may write down an asymptotic solution of Eq. (28.3) for small values of time (the initial stage of crack propagation)

$$\zeta=\zeta_0+qt,\quad q=\frac{K(0)}{2}\,\frac{\zeta_0\Phi(\lambda)}{\Phi(\lambda^*)-\Phi(\lambda)}.$$

Here q is the initial velocity of crack propagation dependent on the magnitude of the load, the initial crack length, and the material properties.

Since the solution of Eq. (28.3) for large values of time presents certain difficulties, as a first approximation we may

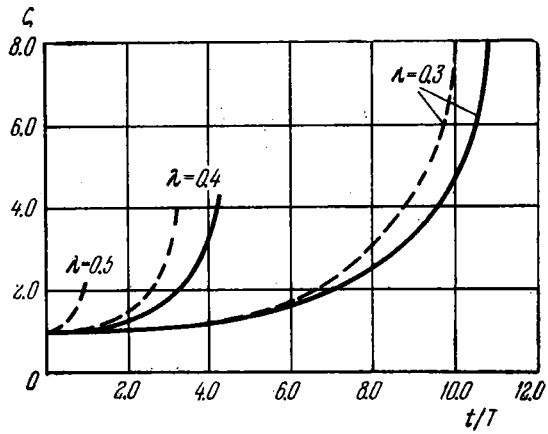

Fig. 28.1. Crack growth with time in a cracked plane under tension (Maxwell body). Solid line: Eq. (28.3). Dashed line: Eq. (28.5).

use the solution obtained on the assumption that the fracture energy density is a constant, $\gamma = \sigma_0\delta_c/2$. In this case Eq. (28.3) becomes

$$\dot{l} - \frac{4\sigma_0}{\pi\delta_c}\Phi(\lambda)\frac{d}{dt}\bar{E}^{-1}l^2 = 0. \tag{28.4}$$

The solution of this equation takes a simpler form

$$\dot{\zeta} = \frac{1}{2}\frac{\Phi(\lambda)\left[\int_0^t \dot{K}(t-\tau)\zeta^2(\tau)\,d\tau + K(0)\zeta^2\right]}{1-\zeta\Phi(\lambda)}. \tag{28.5}$$

The degree of difference in the solutions by Eqs. (28.3) and (28.5) will be illustrated by the example of crack growth in a Maxwell body (Fig. 28.1) for various stress levels.

In the problem of the extension of a space containing a penny-shaped crack of radius l with a thin plastic zone $l \leqslant r \leqslant a$ we obtain an equation from (28.1) and (28.2)

for the determination of the law of crack growth with time

$$\dot{\zeta}=\frac{1}{3}\frac{\Phi_1(\lambda)\left[\int\limits_0^t \dot{K}(t-\tau)\,\zeta^3(\tau)\,d\tau+K(0)\,\zeta^3\right]}{\Phi_1(\lambda)\left[\zeta^2+\int\limits_0^t K(t-\tau)\,\zeta^2(\tau)\,d\tau\right]-\zeta^2\Phi_1(\lambda)}. \qquad (28.6)$$

Here

$$\Phi_1(\lambda)=\frac{1-\sqrt{1-\lambda^2}}{\sqrt{1-\lambda^2}}$$

and the critical load λ^* by the δ_c-theory for the viscoelastic medium is determined by the equation

$$1-\sqrt{1-(\lambda^*)^2}=1\Big/\left[\zeta+\int\limits_0^t K(t-\tau)\,\zeta(\tau)\,d\tau\right].$$

Relation (28.6) determines the crack radius as a function of time. As a first approximation (similarly to the problem of the extension of a cracked plane) it is advisable to use the solution obtained on the assumption that the fracture energy density is constant.

29. ALLOWANCE FOR MATERIAL SENSITIVITY TO THE RATE AND FREQUENCY OF LOADING

The rheological characteristics of a material determine its response to the rate of strain. In order to obtain a general insight into this subject it is very useful to take advantage of the division of the resistance of a material into an elastic and a dissipative component, a division introduced by Ya. B. Fridman [91]. The latter component in turn is the sum of two terms associated with the rate of strain (viscous resistance) and the value of permanent strain (plastic resistance). An infinitesimally slow application of an external load leads to its equilibrium with the elastic resistance force of the specimen. As the external load increases, the elastic resistance force gradually changes to an elastic-plastic one. In this case even if the material possesses viscous resistance, it does not manifest itself.

A high rate of loading accounts for the fact that part of the external load is taken by viscous resistance forces. For qualitative estimates these forces may be assumed proportional to the rate of strain. This phenomenon is illustrated by the well-known fact that the yield point and the ultimate strength on tensile test diagrams rise as the loading rate increases.

The larger is the fraction of the resistance of the material that falls on the dissipative part, the more sensitive is the material to the rate and duration of loading. All kinematic characteristics of the material, the time dependence of its strength and plasticity are entirely determined by the viscous resistance forces of the material which depend on its structure, constitution, and peculiarities. The absence of viscous resistance forces leads to a lack of sensitivity of the material to the loading rate and time effects.

From the standpoint of fracture mechanics the rate sensitivity of a material was evaluated by J. M. Krafft [142], and J. M. Krafft and G. R. Irwin [85]. They obtained a simple relation that holds over some distance ahead of the crack edge among K_{Ic} in tests with increasing load, the strain-hardening exponent n (in the power-law representation of the stress-strain diagram) and the strain rate $\dot{\varepsilon}$

$$\frac{\dot{K}}{K_{Ic}} = \frac{\dot{\varepsilon}}{n}.$$

One should also bear in mind the equivalence between the rate of strain in the material ahead of the crack edge for a propagating crack (under constant load) and the rate of strain due to an increase in the loading rate (at a constant crack length).

These arguments help in establishing a mutual correspondence between the critical stress intensity factors determined by two methods, viz. in arresting a fast running crack and at the onset of the rapid motion of a crack in tests with increasing load.

M. P. Wnuk [299, 300] proposed an equation describing the subcritical fracture diagram

$$M\left(\sigma, l, \frac{d\sigma}{dl}\right) + G(\sigma, l) = G_c. \qquad (29.1)$$

Here M is the slow crack growth operator, which becomes zero at the critical moment (when $d\sigma/dl = 0$). Equation (29.1) then reduces to Irwin's condition $G = G_c$.

For the plane Dugdale model of the crack tip plastic zone we can write [299] (v_* is the displacement at the tip)

$$M = 2\sigma_y \frac{d\sigma}{dl} \frac{\partial}{\partial l} \int_l^a v(x, \sigma, l)\, dx,$$
$$G = 2\sigma_y v_* + \sigma_y \frac{\partial}{\partial l} \int_l^a v(x, \sigma, l)\, dx. \tag{29.2}$$

The boundary condition is written as $\sigma = \sigma_0$ when $l = l_0$.

We apply Eqs. (29.1) and (29.2) to the problem of the extension of a cracked plane in the case of a small plastic zone. This is accomplished by expanding the left-hand side of Eq. (29.1) in a Maclaurin's series in the vicinity of $\sigma = 0$. We obtain

$$\frac{d\beta}{d\zeta} = \frac{3}{2} \frac{2 - \zeta\beta^2}{\zeta^2\beta^3}. \tag{29.3}$$

Here

$$\beta = \frac{\pi\sigma}{2\sigma_y}, \quad \zeta = \frac{l}{c}, \quad c = \frac{\pi K_c^2}{8\sigma_y^2}.$$

If the crack together with a small plastic zone is in a viscoelastic matrix, then, according to M. P. Wnuk, the displacements (and their derivatives) occurring in the expressions for M and G can be represented as the product of the displacements corresponding to the elastic solution $v^0(x, \sigma, l)$ and the 'creep function' $\psi(t)$

$$v(x, \sigma, l) \cong v^0(x, \sigma, l)\, \psi(\delta t),$$
$$\delta v(x, \sigma, l) \cong \delta v^0(x, \sigma, l)\, \psi(\delta t).$$

Here $\delta t = \Delta/\dot{l}$ is the time required for the crack tip to traverse a region of length Δ. The time interval δt is sufficiently small for the function ψ not to vary greatly during this time. The present theory therefore applies to cracks with a small plastic zone, and the rate of strain is properly limited. The extent of the 'internal rupture' Δ is considered as a material

characteristic and, because of the smallness of δt, must be much less than the characteristic length c. These simplifying assumptions enable one to write down Eq. (29.1) in the form

$$2\sigma_y \frac{d\sigma}{dl} \frac{\partial}{\partial \sigma} \int_l^a v^0(x, \sigma, l)\, dx + 2\sigma_y v_*^0 = \frac{G_c}{\psi\left(\frac{\Delta}{\dot{l}}\right)}. \qquad (29.4)$$

If the body contains no plastic zone ($a - l = 0$) or if the critical state is reached ($d\sigma/dl = 0$), then Irwin's criterion holds, $G = \frac{G_c}{\psi(\Delta/\dot{l})}$, extended to a viscoelastic body.

We next expand the function $\psi(\delta t)$ in a Taylor's series in the vicinity of the point $\delta t = 0$ assuming that $\dot{l} > 0$, i.e., the crack is moving, and hence the applied load is higher than the initial one. We have

$$\psi(\delta t \to 0) = 1 + B\delta t + \ldots, \quad \left(B \equiv \frac{d\psi(\delta t)}{d(\delta t)}\bigg|_{\delta t=0}\right).$$

Since $\delta t = \frac{\Delta}{\dot{l}} = \left(\frac{\Delta}{\dot{\sigma}}\right)(d\sigma/dl)$, we can write

$$\psi(\delta t) = 1 + B\frac{\Delta}{\dot{\sigma}}\frac{d\sigma}{dl}.$$

Substituting the well-known elastic solution for displacements in (29.4), we obtain [299]

$$G(\sigma, l)\left\{1 + \frac{\pi E}{12\eta\sigma_y^2}\frac{\partial G}{\partial \sigma}\left[1 + B\frac{\Delta}{\dot{\sigma}}\frac{d\sigma}{dl}\right]\frac{d\sigma}{dl}\right\} = \frac{G_c}{1 + B\frac{\Delta}{\dot{\sigma}}\frac{d\sigma}{dl}}.$$

Here $\eta = 1$ for plane stress and $\eta = 1 - \nu^2$ for plane strain.

The resulting equation may be linearized by neglecting terms containing $(d\sigma/dl)^2$ and $(d\sigma/dl)^3$ in comparison with those involving $d\sigma/dl$. We then obtain

$$1 + \left(\frac{\pi\eta l\sigma^2}{E} + B\frac{\Delta}{\dot{\sigma}}\right)\frac{d\sigma}{dl} = \frac{G_c}{G(\sigma, l)}.$$

Taking into account that $G = \pi\eta l\sigma^2/E$ for a cracked plane and transforming to non-dimensional quantities, we finally

obtain

$$\left(\frac{2}{3}\zeta\beta+\frac{C}{\dot{\beta}}\right)\frac{d\beta}{d\zeta}=\frac{2-\zeta\beta^2}{\zeta\beta^2}. \tag{29.5}$$

Here $C=\dot{\psi}\,|_{t=0}\,\frac{\Delta}{c}$ is the strain-rate sensitivity characteristic of the material. The constant Δ is determined experimentally.

From Eq. (29.5) we obtain two extreme situations. For the material that is not sensitive to the loading rate, $C=0$ and Eq. (29.5) transforms into Eq. (29.3). In contrast, for a material which is highly sensitive to the loading rate, Eq. (29.5) may be reduced to

$$\frac{C}{\dot{\beta}}\frac{d\beta}{d\zeta}=\frac{2}{\zeta\beta^2}\quad\text{or}\quad\frac{d\zeta}{dt}=\frac{C\zeta\beta^2}{2}=C\frac{K^2(\sigma,\,l)}{K_c^2}.$$

The last equation is easily integrated for a given loading history $\beta\,(t)$ and leads to the corresponding law of crack propagation in time.

Figure 29.1 shows the subcritical fracture diagrams obtained by Eq. (29.5) on an analogue computer. It is seen that an increase in the loading-rate sensitivity (an increase in the value of $C/\dot{\beta}$) involves an increase in the slow crack growth in the subcritical state.

The law of crack propagation under cyclic loading is obtained from Eq. (29.5) by successively plotting a series of subcritical diagrams in the given range of load with a new initial crack length for each cycle. By integrating the right-hand and left-hand sides of Eq. (29.5) with respect to β between the limits β_{min} and β_{max} (assuming ζ constant during the cycle), we obtain

$$\frac{d\zeta}{dN}=\frac{2}{3}\zeta^2\int\limits_{\beta_{min}}^{\beta_{max}}\frac{\beta^3\,d\beta}{2-\zeta\beta^2}+\frac{C}{\langle\dot{\beta}\rangle}\zeta\int\limits_{\beta_{min}}^{\beta_{max}}\frac{\beta^2\,d\beta}{2-\zeta\beta^2}.$$

Here $\langle\dot{\beta}\rangle$ is the average rate of loading per cycle. Note that the critical state for the plane occurs when $\zeta\beta^2=2$. In the initial stage of high-cycle fatigue the crack length is much less than the critical value, and hence $\zeta\beta^2$ may be neglected in the integrals in comparison with 2. Consequently,

the last equation may be rewritten as

$$\frac{d\zeta}{dN} = \frac{1}{12}\zeta^2(\beta^4_{\max} - \beta^4_0) + \frac{C\zeta}{6\langle\dot{\beta}\rangle}(\beta^3_{\max} - \beta^3_0). \qquad (29.6)$$

The first term on the right-hand side of this formula represents the well-known Paris relation (22.1) in which the

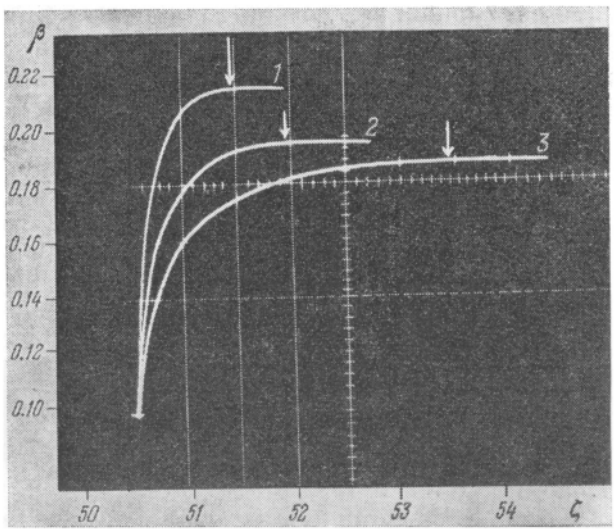

Fig. 29.1. Subcritical crack growth on the screen of an analogue machine. The intial conditions are: $\zeta_0 = 50.5$, $\beta_0 = 0.1$. The arrows mark the maxima of the curves, i.e., the points corresponding to the critical state. *1*, $C/\dot{\beta} = 0$; *2*, $C/\dot{\beta} = 1$; *3*, $C/\dot{\beta} = 2$.

stress intensity factor occurs to the fourth power. The second term represents an additional contribution to the crack growth rate because of the loading-rate sensitivity of the material. The average rate of loading per cycle may be expressed in terms of the cyclic frequency f

$$\langle\dot{\beta}\rangle = 2f\Delta\beta.$$

Here $\Delta\beta = \beta_{\max}$ with $\beta_{\min} = \beta_0 = 0$ for a pulsating cycle. Taking into account that $2(\Delta K/K_c)^2 = (\Delta\beta)^2\zeta$, Eq. (29.6)

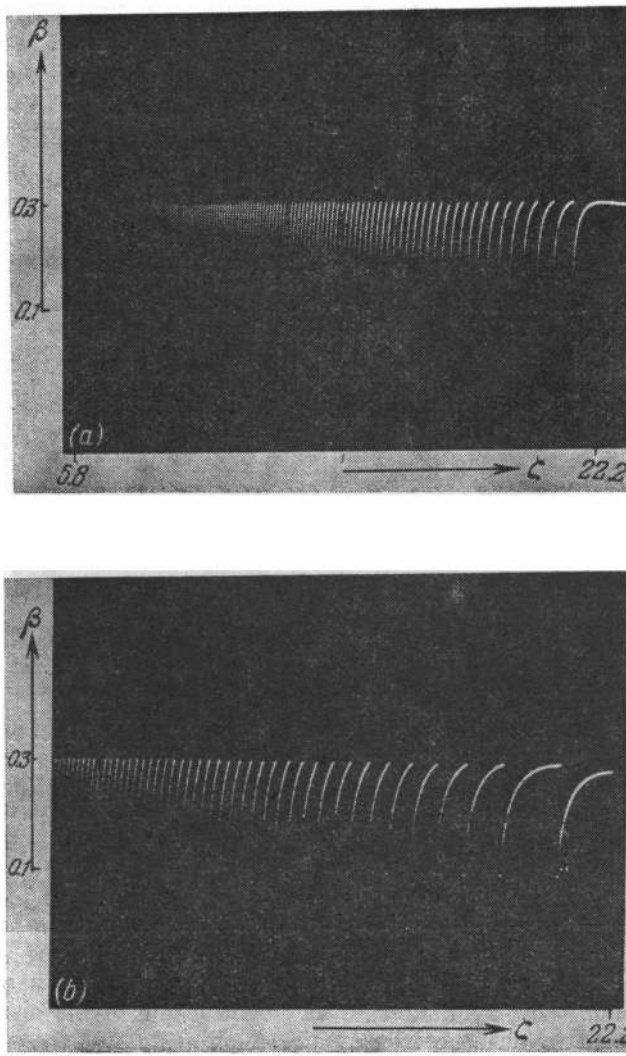

Fig. 29.2. Crack growth under cyclic loading on the screen of an analogue machine (final stage). Initial crack length $\xi_0 = 1$, range of load $0.1 \leqslant \beta \leqslant 0.3$, critical crack length $\zeta_k = 22.2$. (*a*) $C/\langle\dot{\beta}\rangle = 0$, $N = 426$; (*b*) $C/\langle\dot{\beta}\rangle = 2.5$, $N = 132$.

may be rewritten as

$$\frac{dl}{dN}=\frac{c}{3}\left(\frac{\Delta R}{K_c}\right)^4+\frac{Cc}{12}\frac{1}{f}\left(\frac{\Delta K}{K_c}\right)^2. \qquad (29.7)$$

From this equation it follows that as the range of load $\Delta\beta$ and the loading-rate sensitivity of the material $\dot{C}/\langle\beta\rangle$ increase, the number of cycles to complete fracture decreases. For example, for a cycle of $\beta_{max} = 0.2$, $\beta_{min} = 0.1$ and the

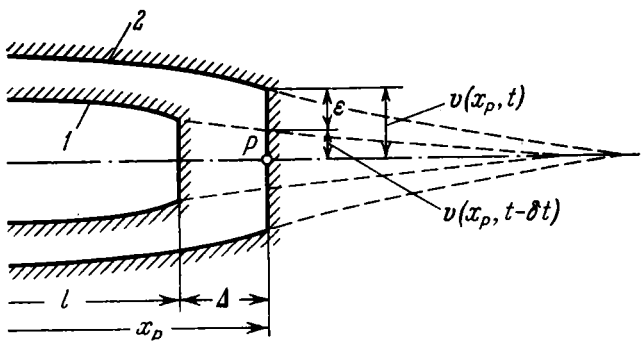

Fig. 29.3. Schematic representation of the fracture process according to the 'final stretch' criterion. *1*, crack contour at the time $t - \delta t$; *2*, crack contour at the time t. The dashed lines show the boundaries of plastic zones.

sensitivity factor $C/\langle\dot{\beta}\rangle = 0$, 0.5, 1, and 1.5, the lifetime based on the number of cycles is, respectively, 6471, 2301, 1423, and 1040.

Figure 29.2 illustrates the effect of increasing of the crack growth rate with increasing $C/\langle\dot{\beta}\rangle$, i.e., with increasing loading-rate sensitivity of the material or decreasing cyclic frequency.

A very promising criterion is the "final stretch" criterion proposed by M. P. Wnuk [300]. It is formulated as follows: the strain increment at a certain point P ahead of the crack tip retains the same value during the slow stable stage of crack growth, i.e.,

$$v(x_P, t) - v(x_P, t - \delta t) = \varepsilon_{,} \cdot \delta t = \Delta/l. \qquad (29.8)$$

Here x_P is the abscissa of the control point P, δt is an element of time in which the material fractures over a length Δ ahead of the crack tip. It is assumed that the characteristic length Δ is a material constant and is less than the length of the plastic zone (Fig. 29.3). The displacements on the left-hand side of Eq. (29.8) may be referred to points on the boundary of the plastic zone in Dugdale's model. In this case the right-hand side of the equation is expressed in terms of the known material constants and Δ. This criterion differs from the limiting crack opening displacement criterion (5.1) since here a restriction is imposed not on the displacement, but on the difference of displacements. The proposed criterion is found to be efficient for the calculation of the R-curve and the subcritical crack growth both in elastic-plastic and viscoelastic materials.

CHAPTER VI

THERMAL PROBLEMS IN FRACTURE MECHANICS

30. CRACKS UNDER THERMAL LOADING

As is known, thermal problems involving steady heat flow are reduced by the use of Muskhelishvili's method [200] to the solution of ordinary plane problems of elasticity. In solving problems relating to stationary thermal distribution it is therefore possible to give the answer to one of the main questions of fracture mechanics, to the question of the nature of singular thermal stresses at a crack tip. The object of such an investigation is to ascertain whether the Griffith-Irwin-Orowan concept is applicable to cracks under thermal loading.

G. C. Sih [253] has shown that the equations for the thermal stress field near a crack tip are identical with the equations of G. R. Irwin [117] for the elastic stress field when only boundary forces are acting. It follows that the concept of a stress intensity factor is basically preserved for problems concerned with crack development under a thermal stress field. It may be assumed *a priori* that the local nature of thermal stresses at a crack tip is the same as in the problem with mechanical stresses (i.e., of the type $r^{-1/2}$) since the presence of heat flow involves no additional singular characteristics. A singularity of the type $r^{-1/2}$ appears to be inherent in the very nature of the stresses arising at a crack tip in an elastic state.

The investigations in this direction were originated with A. L. Florence and J. N. Goodier [79, 80]. They investigated thermal stresses arising in the presence of cavities (a spherical cavity and a circular hole) and then considered the case

of uniform heat flow in a plate with a constant gradient at a certain angle to a crack, the latter acting as an insulator.

G. C. Sih [253] obtained an expression for the stress intensity factors for a plate with equal crack surface temperature, which is important, for example, in the design of vessels when the gas issues through a crack. In the same work the author obtained a solution for a clamped plate with a temperature gradient across the thickness.

The thermoelastic stress distribution in an infinite body containing an axially symmetric crack was determined by N. M. Borodachev [28], while J. N. Goodier and A. L. Florence [100] obtained expressions for the stress intensity factors in the case of an infinite body with an insulated penny-shaped crack.

G. S. Kit and Ya. S. Podstrigach [130] found the steady-state thermal stress distribution in the vicinity of a heat-resisting slit with a given uniform heat flow at infinity. A more general formulation of this kind of problems is given by Ya. S. Podstrigach and G. S. Kit in [229], where, for a plane containing an arbitrary number of heat-conducting cracks whose opposite faces are not in ideal thermal contact, a method is proposed which enables one to determine a steady-state temperature field.

An illustration of this method is provided by the steady-state temperature field and stresses found by G. S. Kit and Yu. S. Frenchko [131] in an infinite plane with a thermally insulated circular-arc crack subjected to a fixed uniform heat flow at infinity. The resulting stress distribution in the vicinity of the crack ends and the limiting value of heat flow enable one to determine the onset of crack propagation in a brittle material.

A. A. Dorosh and G. S. Kit [65] considered the problem of determining a steady-state temperature field and stresses set up in an infinite elastic plane with two equal circular-arc thermally insulated cracks subjected to a given uniform heat flow at infinity. They investigated the limiting equilibrium of this plane under combined temperature field and all-round tension.

Investigations of the state of stress and strain in the vicinity of an opening-mode crack in a stationary temperature field were made by I. V. Gaivas' [95] and by G. S. Kit and

O. V. Poberezhnyi [132]. In the first case the author considered a non-homogeneous plane with a circular-arc cut, and in the second case the authors determined the state of stress in a heated material having internal defects of the circular crack type.

An axially symmetric uncoupled thermal problem of the theory of elasticity for a space with two parallel coaxial penny-shaped cracks was considered by M. K. Kassir and A. Bregman [127]. The external effects are a heat flow parallel to the axis of symmetry and a constant temperature on the crack surface. In solving the problem the authors determine the stress intensity factors for separation and in-plane shear, as well as the difference of the potential energies of the uncracked and cracked bodies.

The work of K. N. Srivastava and R. L. Mahajan [265] is concerned with the thermoelastic problem for a space containing a spherical cavity and a cut situated in a diametrical plane of the cavity and representing the outside of a circle of larger radius than the radius of the cavity. The temperature on the surface of the cavity is given to be zero, while the temperature on the surfaces of the cut is given as a function of the radial co-ordinate. The surfaces of the cavity and cut are free from stress. The authors determine the temperature, stresses, displacements, and stress intensity factor at the edge of the cut. If there is no cavity, the temperature and stresses in the uncracked portion increase. Further the authors consider the thermoplastic problem for the case when, according to Dugdale's model, there is a thin plastic zone ahead of the edge of the cut. It is shown that in some cases the radial extent of the plastic zone increases with increasing temperature.

All the results mentioned above relate to the solution of static thermal problems of fracture mechanics. However, the trend of today towards a stepwise increase in operating temperatures of various machines and engines, the development of such branches of modern mechanical engineering as gas turbine building, reactor building, motor building, rocket technology, and many others call for the solution of quasi-static and dynamic thermal problems of fracture mechanics. The investigation of the laws of crack growth under stepwise temperature changes is of great importance in the

development of theoretical foundations of electric welding, the strength of welded joints.

In the last few years V. Z. Parton [227], B. A. Kudryavtsev and V. Z. Parton [147], B. A. Kudryavtsev [148] obtained solutions of quasi-static thermal problems concerning the development of cracks of fixed trajectory, over part of whose surface the temperature arising at the initial moment is held constant. In the next sections we shall present examples of the solution of static and quasi-static problems of the mechanics of brittle fracture worked out by B. A. Kudryavtsev [148, 150].

31. THE AXIALLY SYMMETRIC THERMOELASTIC PROBLEM FOR A CYLINDER WITH A CUT

1. Consider a system of cylindrical co-ordinates r, φ, z the z axis of which is coincident with the longitudinal axis

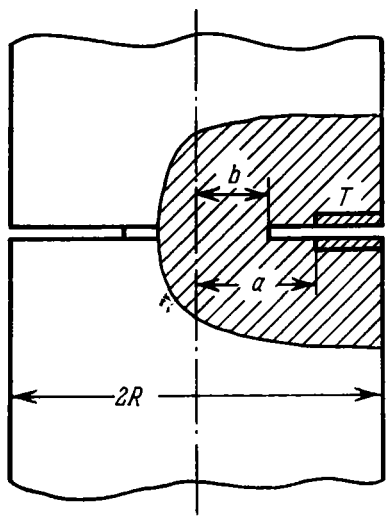

Fig. 31.1. Cylinder with an external circumferential cut.

of an infinite solid cylinder with an external circumferential cut ($b \leqslant r \leqslant R$) in the plane $z = 0$ (Fig. 31.1). Suppose that uniformly distributed heat sources of intensity q are

acting over part of the surface of the cut ($a \leqslant r \leqslant R$, $a > b$). It is assumed that the lateral surface of the cylinder is thermally insulated, free from shearing stress and fixed so that its points undergo no radial displacements.

Taking into account the symmetry conditions with respect to the plane $z = 0$, we consider the effect of heat sources uniformly distributed over the annular region $a \leqslant r \leqslant R$, $z = 0$. In this case the temperature satisfying the condition

$$\left.\frac{\partial T}{\partial r}\right|_{r=R} = 0 \tag{31.1}$$

is the solution of the equation

$$\Delta T = -\frac{q}{\lambda}\,\delta(z)\,\eta(r-a), \quad \left(\Delta = \frac{\partial^2}{\partial r^2} + \frac{1}{r}\frac{\partial}{\partial r} + \frac{\partial^2}{\partial z^2}\right). \tag{31.2}$$

Here λ is the thermal conductivity coefficient, $\delta(z)$ is the δ-function,

$$\eta(r-a) = 1 \quad (r > a), \quad \eta(r-a) = 0 \quad (r < a).$$

By using the integral representation of the δ-function

$$\delta(z) = \frac{1}{\pi}\int_0^\infty \cos\lambda z\, d\lambda$$

and the expansion in Bessel functions

$$\eta(r-a) = -2\frac{a}{R}\sum_{n=1}^{\infty}\frac{J_1(\lambda_n a/R)\,J_0(\lambda_n r/R)}{\lambda_n J_0^2(\lambda_n)}, \tag{31.3}$$

we find the solution of Eq. (31.2) as

$$T(r, z) = -\frac{q}{\lambda}\alpha R\sum_{n=1}^{\infty}\frac{J_1(\lambda_n\alpha)\,J_0(\lambda_n\rho)}{\lambda_n^2 J_0^2(\lambda_n)}\,e^{-\lambda_n\xi}. \tag{31.4}$$

Here $\alpha = a/R$, $\rho = r/R$, $\xi = z/R$, λ_n ($n = 1, 2, 3, \ldots$) are the positive roots of the equation $J_0'(\lambda_n) = 0$ in the order of increasing value.

The stresses $\sigma_{ij}^{(1)}$ and the displacements $u_i^{(1)}$ in a semi-infinite cylinder $0 \leqslant z < \infty$, $0 \leqslant r \leqslant R$ due to the given temperature field (31.4) can be found by using a thermoelastic

potential Φ satisfying the equation [207]

$$\Delta\Phi = mT\left(m = \frac{1+\nu}{1-\nu}\alpha_T\right), \tag{31.5}$$

where α_T is the linear coefficient of expansion of the material. Taking into account (31.4), we write down the solution of Eq. (31.5) as

$$\Phi(r, z) = \frac{mqR^3}{2\lambda}\alpha\sum_{n=1}^{\infty}\frac{J_1(\lambda_n\alpha)J_0(\lambda_n\rho)}{\lambda_n^4 J_0^2(\lambda_n)}e^{-\lambda_n\xi}(1+\lambda_n\xi). \tag{31.6}$$

The components of stress and displacement corresponding to the thermoelastic potential (31.6) satisfy the following conditions on the lateral surface $r = R$ and at the end $z = 0$ of the cylinder:

$$\sigma_{rz}^{(1)}(R, z) = 0,$$
$$u_r^{(1)}(R, z) = 0 \text{ when } 0 \leqslant z < \infty, \tag{31.7}$$
$$\sigma_{rz}^{(1)}(r, 0) = 0,$$
$$\sigma_{zz}^{(1)}(r, 0) = -\mu mT(r, 0) \text{ when } 0 \leqslant r \leqslant R. \tag{31.8}$$

For the sides of the circumferential cut $b \leqslant r \leqslant R$, $z = 0$ to be free from load, it is necessary to superimpose on the state of stress and strain $\sigma_{ij}^{(1)}$, $u_i^{(1)}$ a state with components $\sigma_{ij}^{(2)}$, $u_j^{(2)}$ which satisfy the conditions

$$\sigma_{zz}^{(2)}(r, 0) = -\sigma_{zz}^{(1)}(r, 0) \ (b \leqslant r < R),$$
$$u_z^{(2)}(r, 0) = 0 \ (0 \leqslant r < b), \tag{31.9}$$
$$\sigma_{rz}^{(2)}(r, 0) = 0 \ (0 \leqslant r \leqslant R), \tag{31.10}$$
$$\sigma_{rz}^{(2)}(R, z) = 0, \ u_r^{(2)}(R, z) = 0 \ (0 \leqslant z < \infty). \tag{31.11}$$

Since the shearing stresses $\sigma_{rz}^{(2)}$ are zero in the plane $z = 0$, the displacements and stresses may be expressed in terms of a single harmonic axially symmetric function $\varphi(r, z)$ [257] (μ is the shearing modulus)

$$u_r^{(2)} = z\frac{\partial^2\varphi}{\partial r\,\partial z} + (1-2\nu)\frac{\partial\varphi}{\partial r}, \quad \sigma_{rz}^{(2)} = 2\mu z\frac{\partial^3\varphi}{\partial r\,\partial z^2}. \tag{31.12}$$

By choosing the harmonic function $\varphi(r, z)$ as

$$\varphi(r, z) = \frac{R^2}{2(1-\nu)}\sum_{n=1}^{\infty}\frac{1}{\lambda_n}B_n J_0(\lambda_0\rho)e^{-\lambda_n\xi}, \tag{31.13}$$

we find that conditions (31.10) and (31.11) are fulfilled identically. By satisfying conditions (31.9), we obtain dual series equations

$$\sum_{n=1}^{\infty} \frac{1}{\lambda_n} B_n J_n(\lambda_n \rho) = 0 \quad \left(0 \leqslant \rho < \beta,\ \beta = \frac{b}{R}\right), \tag{31.14}$$

$$\sum_{n=1}^{\infty} B_n J_n(\lambda_n \rho) = (1-\nu)\, m \frac{qa}{\lambda} \sum_{n=1}^{\infty} \frac{J_1(\lambda_n \alpha) J_0(\lambda_n \rho)}{\lambda_n^2 J_0^2(\lambda_n)}$$

$$(\beta < \rho < 1). \tag{31.15}$$

2. The solution of dual equations of the form of (31.14) and (31.15) has been obtained in [258, 264]. The problem of the indentation of the end of a semi-infinite cylinder by a punch [29] is reduced to similar equations.

By using the relation

$$B_n = (1-\nu) \frac{mqa}{\lambda} \frac{J_1(\lambda_n \alpha)}{\lambda_n^2 J_0^2(\lambda_n)} + B_n^*, \tag{31.16}$$

we represent Eqs. (31.14) and (31.15) in the form

$$\sum_{n=1}^{\infty} \frac{1}{\lambda_n} B_n^* J_n(\lambda_n \rho) =$$

$$= -(1-\nu) \frac{mqa}{\lambda} \sum_{n=1}^{\infty} \frac{J_1(\lambda_n \alpha) J_0(\lambda_n \rho)}{\lambda_n^3 J_0^2(\lambda_n)}, \tag{31.17}$$

$$\sum_{n=1}^{\infty} B_n^* J_0(\lambda_n \rho) = 0 \quad (\beta < \rho \leqslant 1). \tag{31.18}$$

Following [264], we assume

$$\sum_{n=1}^{\infty} B_n^* J_0(\lambda_n \rho) =$$

$$= -\frac{1}{\rho} \frac{d}{d\rho} \int_{\rho}^{\beta} \frac{g(t)\, t\, dt}{\sqrt{t^2 - \rho^2}} \quad (0 \leqslant \rho < \beta). \tag{31.19}$$

By the formula defining the coefficients of a Dini expansion we find

$$B_n^* = \frac{2}{J_0^2(\lambda_n)} \int_0^\beta g(t) \cos(\lambda_n t)\, dt. \tag{31.20}$$

Substituting the expression for B_n^* in Eq. (31.17) and taking into account [264]

$$2 \sum_{n=1}^{\infty} \frac{J_0(\lambda_n \rho) \cos(\lambda_n t)}{\lambda_n J_0^2(\lambda_n)} =$$

$$= -L(t, \rho) + \begin{cases} 0, & \rho < t, \\ (\rho^2 - t^2)^{-1/2}, & \rho > t, \end{cases} \tag{31.21}$$

$$L(t, \rho) = 2\sqrt{1-t^2} +$$

$$+ \frac{2}{\pi} \int_0^\infty \frac{K_1(\xi)}{\xi I_1(\xi)} \cosh(t\xi) [2I_1(\xi) - \xi I_0(\rho\xi)]\, d\xi,$$

we obtain, after appropriate transformations [264], an integral Fredholm equation of the second kind for the determination of the function $g(t)$

$$g(t) = \int_0^\beta g(u) K(u, t)\, du -$$

$$-(1-\nu) m \frac{\alpha}{\lambda} \frac{2}{\pi} \sum_{n=1}^{\infty} \frac{J_1(\lambda_n \alpha) \cos \lambda_n t}{\lambda_n^3 J_0^2(\lambda_n)}, \tag{31.22}$$

$$K(u, t) = \frac{2}{\pi} \frac{d}{dt} \int_0^t \frac{\rho L(u, \rho)}{\sqrt{t^2 - \rho^2}}\, d\rho =$$

$$= \frac{4}{\pi} + \frac{4}{\pi^2} \int_0^\infty \frac{K_1(\xi)}{\xi I_1(\xi)} [2I_1(\xi) - \xi \cosh(t\xi) \cosh(u\xi)]\, d\xi.$$

Here $I_1(\xi)$ and $K_1(\xi)$ are the modified Bessel functions of the first and second kind, respectively.

To calculate the sum appearing on the right-hand side of Eq. (31.22), we multiply equality (31.3) by $\rho(t^2 - \rho^2)^{-1/2}$

and integrate with respect to ρ between the limits 0 and t. We obtain

$$2\alpha \sum_{n=1}^{\infty} \frac{J_1(\lambda_n \alpha) \sin \lambda_n t}{\lambda_n^2 J_0^2(\lambda_n)} = \begin{cases} \sqrt{t^2-\alpha^2}, & t > \alpha, \\ t, & t < \alpha. \end{cases}$$

By integrating the last expression with respect to t, we find

$$2\alpha \sum_{n=1}^{\infty} \frac{J_1(\lambda_n \alpha) \cos \lambda_n t}{\lambda_n^3 J_0^2(\lambda_n)} = A(\alpha) - \frac{t^2}{2},$$
$$A(\alpha) = 2\alpha \sum_{n=1}^{\infty} \frac{J_1(\lambda_n \alpha)}{\lambda_n^3 J_0^2(\lambda_n)}. \tag{31.23}$$

Hence, Eq. (31.22) takes the form

$$g(t) = \int_0^\beta g(u) K(u, t)\, du - (1-\nu) \frac{qR}{\pi\lambda} \left[A(\alpha) - \frac{t^2}{2} \right]. \tag{31.24}$$

The kernel $K(u, t)$ of Eq. (31.24) may be represented in the form

$$K(u, t) = \sum_{m=0}^{\infty} b_{2m}(u) t^{2m}, \quad b_0(u) = \frac{4}{\pi} + \frac{4}{\pi^2} \left[T^* - \sum_{s=1}^{\infty} \frac{T_{2s} u^{2s}}{(2s)!} \right],$$

$$b_{2m}(u) = -\frac{4}{\pi^2} \sum_{s=1}^{\infty} \frac{T_{2m+2s-2} u^{2s-2}}{(2m)!\,(2s-2)!} \quad (m = 1, 2, \ldots), \tag{31.25}$$

$$T^* = \sum_{s=1}^{\infty} \frac{T_{2s}}{2^{2s} s!\,(s+1)!}, \quad T_n = \int_0^\infty \frac{K_1(\xi)}{I_1(\xi)} \xi^n\, d\xi.$$

The numerical values of the coefficients T_n are given in [258].

Taking into account expansion (31.25), the solution of the integral equation (31.24) may be sought in the form

$$g(t) = \sum_{m=0}^{\infty} Q_{2m} t^{2m}, \tag{31.26}$$

where the coefficients Q_{2m} are determined from the infinite system

$$Q_{2m}=\sum_{k=0}^{\infty} Q_{2k}C_{2k,\,2m}-(1-\nu)\,m\,\frac{qR}{\pi\lambda}\left[A(\alpha)\,\delta_m^0-\frac{1}{2}\,\delta_m^1\right]$$

$$(m=0,\,1,\,2,\,\ldots),$$

$$C_{2k,\,0}=\frac{4}{\pi}\left(1+\frac{T^*}{\pi}\right)\frac{\beta^{2k+1}}{2k+1}-$$

$$-\frac{4}{\pi^2}\sum_{s=1}^{\infty}\frac{T_{2s}\beta^{2s+2k+1}}{(2s)!\,(2s+2k+1)}\qquad(k=0,\,1,\,2,\,\ldots),\qquad(31.27)$$

$$C_{2k,\,2m}=-\frac{4}{\pi^2}\sum_{s=1}^{\infty}\frac{T_{2m+2s-2}\beta^{2k+2s-1}}{(2m)!\,(2s-2)\,(2k+2s-1)}$$

$$(k=0,\,1,\,2,\,\ldots,\;m=1,\,2,\,\ldots),$$

$$\delta_m^j=\begin{cases}1, & m=j,\\ 0, & m\neq j.\end{cases}$$

By using formulas (31.12), (31.16), and (31.19), we find the normal stresses in the plane $z=0$

$$\sigma_{zz}^{(2)}(r,\,0)=\mu mT(\rho,\,0)+$$

$$+\frac{\mu}{1-\nu}\,\frac{1}{\rho}\,\frac{d}{d\rho}\int_{\rho}^{\beta}\frac{g(t)\,t\,dt}{\sqrt{t^2-\rho^2}}\qquad(0\leqslant\rho<\beta).\qquad(31.28)$$

With the help of expressions (31.8), (31.26), and (31.28) we determine the stress intensity factor for the circumferential cut

$$K^*=\sqrt{2\pi}\lim_{\rho\to\beta}\left[\sqrt{R(\beta-\rho)}\,\sigma_{zz}(\rho,\,0)\right]=$$

$$=-\frac{\mu}{1-\nu}\left(\frac{\pi R}{2\beta}\right)^{1/2}\sum_{m=0}^{\infty}Q_{2m}\beta^{2m},\qquad(31.29)$$

$$K^*=\frac{K\lambda\sqrt{\pi}}{\mu mqR^{3/2}}.$$

Here

$$\sigma_{zz}(\rho,\,0)=\sigma_{zz}^{(1)}(\rho,\,0)+\sigma_{zz}^{(2)}(\rho,\,0).$$

Figure 31.2 shows the K^*-β relation for several values of α. The results indicate that for certain combinations of α

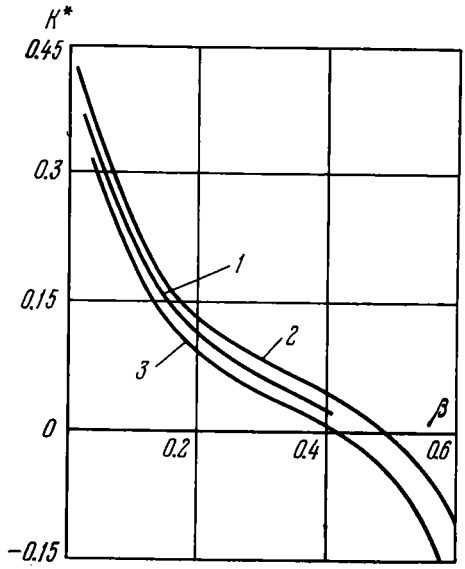

Fig. 31.2. Relation between the stress intensity factor and the radius of the uncracked portion for several values of the extent of the heating region. *1*, $\alpha = 0.4$; *2*, $\alpha = 0.6$; *3*, $\alpha = 0.8$.

and β there may be compressive ($K^* < 0$) normal stresses on the prolongation of the circumferential cut.

32. THE QUASI-STATIONARY THERMOELASTIC PROBLEM FOR A PLANE WITH A SEMI-INFINITE CUT

As is known, in real structural materials there are various kinds of defects, such as cracks, non-metallic inclusions, unwelded areas (for welded structures), which are subjected to temperatures non-uniformly distributed over the volume of a body. It is of interest, therefore, to determine the nature of the state of stress in the vicinity of a crack-type defect in the case of a non-stationary temperature field.

1. Consider an infinite plane with a semi-infinite cut along the real semiaxis (Fig. 32.1). Suppose that the sides of the cut are free from external load. Let the xy plane be sub-

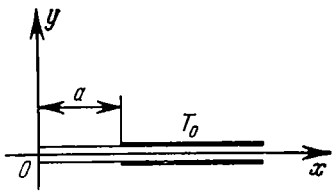

Fig. 32.1. Plane with a semi-infinite cut on part of which a temperature arises instantaneously.

jected to a non-stationary temperature field satisfying the following conditions on the axis $y = 0$ $(a \geqslant 0)$:

$$T(x, 0, t) = T_0 = \text{constant when } x > a,\ t > 0, \tag{32.1}$$

$$\left.\frac{\partial T}{\partial y}\right|_{y=0} = 0 \quad \text{when } x < a,\ t > 0. \tag{32.2}$$

We determine the unsteady temperature field and the resulting thermoelastic quasi-stationary state of an infinite plane containing no cut with the boundary conditions (32.1) and (32.2) and homogeneous initial conditions. Consider an instantaneous point heat source of intensity q acting at the point $x = \xi$, $y = 0$. In this case the temperature $T(x, y, t)$ and the quasi-static stress distribution in the plane are determined by the formulas [207]

$$T(x, y, t) = \frac{q}{4\pi\varkappa t} e^{-\frac{r^2}{4\varkappa t}}, \tag{32.3}$$

$$\bar{\sigma}_x(x, y, t) = -\frac{\mu m}{\pi}\frac{1}{r^2}\left\{\left(1 - e^{-\frac{r^2}{4\varkappa t}}\right)\left(1 - \frac{2y^2}{r^2}\right) + \frac{y^2}{2\varkappa t} e^{-\frac{r^2}{4\varkappa t}}\right\},$$

$$\bar{\sigma}_y(x, y, t) = -\frac{\mu m}{\pi}\frac{1}{r^2}\left\{\left(1 - e^{-\frac{r^2}{4\varkappa t}}\right)\left(1 - \frac{2(x-\xi)^2}{r^2}\right) + \frac{(x-\xi)^2}{2\varkappa t} e^{-\frac{r^2}{4\varkappa t}}\right\}, \tag{32.4}$$

$$\bar{\tau}_{xy}(x, y, t) = \frac{2\mu m}{\pi}\frac{(x-\xi)\,y}{r^2}\left\{\frac{e^{-\frac{r^2}{4\varkappa t}}}{4\varkappa t} - \frac{1}{r^2}\left(1 - e^{-\frac{r^2}{4\varkappa t}}\right)\right\}.$$

Here $\varkappa$ is the temperature conductivity coefficient,

$r=\sqrt{(x-\xi)^2+y^2}$,

$$m=\begin{cases}\dfrac{1+\nu}{1-\nu}\alpha_T, & \text{plane strain;}\\ (1+\nu)\alpha_T, & \text{plane stress.}\end{cases}$$

With the use of expressions (32.3) and (32.4) it is possible to determine the temperature and stresses for sources $q(\xi, \tau)$ distributed along the axis $y = 0$, $x > a$ with a time-varying intensity. For the temperature function we obtain [207]

$T(x, y, t)=$

$$=\int_0^\infty d\xi\int_0^t\left\{\frac{q(\xi,\tau)}{4\pi\varkappa(t-\tau)}\exp\left[-\frac{(x-a-\xi)^2+y^2}{4\varkappa(t-\tau)}\right]\right\}d\tau. \quad (32.5)$$

The stress components are found by the formulas

$$\sigma_x'=\int_0^\infty d\xi\int_0^t q(\xi,\tau)\,\bar{\sigma}_x(x-a-\xi, y, t-\tau)\,d\tau,$$

$$\sigma_y'=\int_0^\infty d\xi\int_0^t q(\xi,\tau)\,\bar{\sigma}_y(x-a-\xi, y, t-\tau)\,d\tau, \quad (32.6)$$

$$\tau_{xy}'=\int_0^\infty d\xi\int_0^t q(\xi,\tau)\,\bar{\tau}_{xy}(x-a-\xi, y, t-\tau)\,d\tau.$$

The temperature determined by formula (32.5) satisfies condition (32.2). To fulfil condition (32.1), the density $q(\xi, \tau)$ must be the solution of the equation

$$\int_0^\infty d\xi\int_0^t\left\{\frac{q(\xi,\tau)}{4\pi\varkappa(t-\tau)}\exp\left[-\frac{(x_1-\xi)^2}{4\varkappa(t-\tau)}\right]\right\}d\tau=T_0 \quad (32.7)$$

$$(x_1 = x - a > 0).$$

By applying the Laplace-Carson transformation on t to Eq. (32.7) and using the convolution theorem, we obtain

$$\int_0^\infty \tilde{q}(\xi, p)\,K_0\left(|x_1-\xi|\sqrt{\frac{p}{\varkappa}}\right)d\xi=2\pi\varkappa T_0 \quad (x_1>0). \quad (32.8)$$

Here $\tilde{q}(\xi, p)$ is the Laplace-Carson transform of the density of heat sources distributed along the axis $y = 0$, $x > a$, $K_0(x)$ is a modified Bessel function of the second kind.

The solution of the integral equation (32.8) is known [203] and may be represented as

$$\tilde{q}(\xi, p) = \\ = 2\varkappa T_0 \left\{ \sqrt{\frac{p}{\varkappa}} \operatorname{erf}\left[\left(\frac{p}{\varkappa}\right)^{1/4} \sqrt{\xi}\right] + \frac{1}{\sqrt{\pi}} \left(\frac{p}{\varkappa}\right)^{1/4} \frac{e^{-\xi\sqrt{\frac{p}{\varkappa}}}}{\sqrt{\xi}} \right\}, \tag{32.9}$$

where

$$\operatorname{erf}(z) = \frac{2}{\sqrt{\pi}} \int_0^z e^{-u^2} du, \quad \operatorname{erfc}(z) = 1 - \operatorname{erf}(z).$$

Substituting (32.9) into the left side of equality (32.8) and performing the integration for $x_1 < 0$, we obtain an expression for the Laplace-Carson transform of the temperature function on the axis $y = 0$

$$T(x, 0, p) = T_0 \begin{cases} 1, & x_1 > 0, \\ \operatorname{erfc}\left(\sqrt{|x_1|}\left(\frac{p}{\varkappa}\right)^{1/4}\right), & x_1 < 0. \end{cases} \tag{32.10}$$

To calculate the original of (32.10) we use the well-known formula of operational calculus [64]

$$\tilde{f}(\sqrt{p}) \div \frac{1}{\sqrt{\pi t}} \int_0^\infty e^{-\frac{u^2}{4t}} f(u)\, du \tag{32.11}$$

and the relation

$$\operatorname{erfc}\sqrt{\alpha p} \div \begin{cases} \frac{2}{\pi} \arctan \sqrt{\frac{t}{\alpha} - 1}, & t > \alpha, \\ 0, & t < \alpha. \end{cases} \tag{32.12}$$

On the basis of (32.10) to (32.12) we obtain

$$T(x, 0, t) = \\ = T_0 \begin{cases} 1, & x_1 > 0, \\ \dfrac{2}{\pi} \dfrac{|x_1|}{\sqrt{\pi t \varkappa}} \displaystyle\int_0^\infty e^{-\frac{|x_1|^2 \tau^2}{4\varkappa t}} \arctan \sqrt{\tau - 1}\, d\tau, & x_1 < 0. \end{cases} \tag{32.13}$$

By integrating by parts, we transform equality (32.13) to

$$T(x, 0, t) = \\ = T_0 \begin{cases} 1, & x_1 > 0, \\ \dfrac{1}{\pi} \displaystyle\int_1^\infty \operatorname{erfc}\left[\frac{\tau |x_1|}{2\sqrt{\varkappa t}}\right] \frac{d\tau}{\tau \sqrt{\tau - 1}}, & x_1 < 0. \end{cases} \tag{32.14}$$

The components of stress determined by (32.6) satisfy the following conditions on the boundary $y = 0$:

$$\tau'_{xy}(x, 0, t) = 0, \tag{32.15}$$

$$\sigma'_y(x, 0, t) = \\ = \frac{\mu m}{\pi} \int_0^\infty d\xi \int_0^t q(\xi, \tau) \frac{1 - \exp\left[-\frac{(x - a - \xi)^2}{4\varkappa (t - \tau)}\right]}{(x_1 - \xi)^2} d\tau - \\ - \frac{\mu m}{\pi} \int_0^\infty d\xi \int_0^t q(\xi, \tau) \frac{\exp\left[-\frac{(x - a - \xi)^2}{4\varkappa (t - \tau)}\right]}{2\varkappa (t - \tau)} d\tau. \tag{32.16}$$

Taking into account expression (32.5) and the equality

$$\frac{1}{4\varkappa (t - \tau)} \int_0^1 \exp\left[-\frac{(x - a - \xi)^2}{4\varkappa (t - \tau)} \alpha\right] d\alpha = \frac{1 - \exp\left[-\frac{(x - a - \xi)^2}{4\varkappa (t - \tau)}\right]}{(x - a - \xi)^2},$$

we write down (32.16) in the form

$$\sigma'_y(x, 0, t) = \mu m \int_0^1 T\left(x_1, 0, \frac{t}{\alpha}\right) d\alpha - 2\mu m T(x_1, 0, t). \tag{32.17}$$

Obviously, the state of stress in the plane remains unchanged if the function $T(x, y, t)$ is replaced by the expression $T(x, y, t) - T_0$ since the stress components corresponding to uniform heating of the plane and vanishing at infinity are identically zero. Formula (32.17) may therefore be written as

$$\sigma_y'(x, 0, t) = \\ = \mu m T_0 + \mu m \int_0^1 T\left(x_1, 0, \frac{t}{\alpha}\right) d\alpha - 2\mu m T(x_1, 0, t). \quad (32.18)$$

Substituting (32.14) in (32.18), we obtain

$$\sigma_y'(x, 0, t)|_{x<a} = \\ = \mu m T_0 - \frac{\mu m T_0}{\pi} \int_0^\infty \frac{d\tau}{\tau\sqrt{\tau-1}} \left\{ \operatorname{erfc}\left[\frac{(a-x)\tau}{2\sqrt{\varkappa t}}\right] + \right. \\ \left. + \frac{2}{\sqrt{\pi}} \frac{\sqrt{\varkappa t}}{(a-x)\tau} e^{\frac{(a-x)^2\tau^2}{4\varkappa t}} - \frac{2\varkappa t}{(a-x)^2\tau^2} \operatorname{erf}\left[\frac{(a-x)\tau}{2\sqrt{\varkappa t}}\right] \right\}, \quad (32.19)$$

$$\sigma_y'(x, 0, t)|_{x>a} = 0. \quad (32.20)$$

2. For the sides of the semi-infinite cut to be free from stress, we consider a state of stress with components σ_x'', σ_y'', τ_{xy}'' chosen so as to satisfy the conditions

$$\tau_{xy}''(x, 0, t) = 0, \\ \sigma_y'(x, 0, t) + \sigma_y''(x, 0, t) = 0 \quad (x > 0). \quad (32.21)$$

This solution can be determined according to [200]. For the normal stress σ_y'' on the prolongation of the cut we obtain the expression

$$\sigma_y''(x, 0, t) = \frac{1}{\pi\sqrt{|x|}} \int_0^\infty \frac{\sqrt{u}\,\sigma_y'(u, 0, t)}{u-x} du \quad (x < 0). \quad (32.22)$$

On the basis of (32.19) and (32.22) we find the stress intensity factor for the semi-infinite cut

$$K = \lim_{x\to 0} [\sqrt{2\pi(-x)}\,\sigma_y(x, 0, t)] = 2\sqrt{\frac{2}{\pi}}\,\mu m T_0 \sqrt{a} -$$

$$-\sqrt{\frac{2}{\pi}}\,\mu m T_0 \sqrt{a}\,\frac{1}{\pi}\int_1^\infty \frac{d\tau}{\tau\sqrt{\tau-1}}\left\{\int_0^1 \operatorname{erfc}\left(\frac{\tau}{t_*}\xi\right)\frac{d\xi}{\sqrt{1-\xi}} + \right.$$

$$\left. + \frac{1}{\sqrt{\pi}}\,\frac{t_*}{\tau}\int_0^1 \left[e^{-\frac{\tau^2\xi^2}{t_*^2}} - \frac{\sqrt{\pi}}{2}\,\frac{t_*}{\tau\xi}\operatorname{erf}\left(\frac{\tau\xi}{t_*}\right)\right]\frac{d\xi}{\xi\sqrt{1-\xi}}\right\}. \tag{32.23}$$

Here $t_* = \dfrac{2\sqrt{\varkappa t}}{a}$, $\sigma_y(x, 0, t) = \sigma_y'(x, 0, t) + \sigma_y''(x, 0, t)$.

Figure 32.2 shows the relation between $K^* = \dfrac{K\sqrt{\pi}}{2\sqrt{2}\,\mu m T_0 \sqrt{a}}$ and t_*. As seen from the graph, the initial instants are

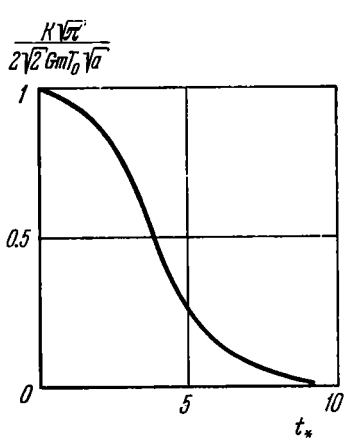

Fig. 32.2. Time dependence of the stress intensity factor ($G \equiv \mu$).

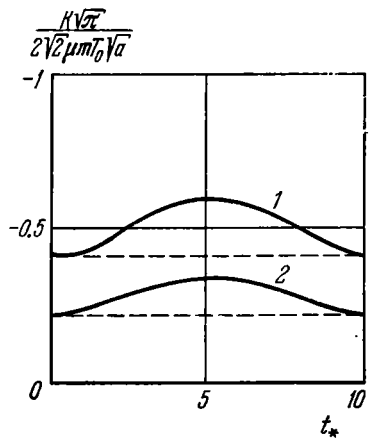

Fig. 32.3. Time dependence of the stress intensity factor. *1*, $\lambda=0.5$; *2*, $\lambda = 1$.

the most dangerous from the viewpoint of crack propagation.

Consider the case when the plane with a semi-infinite cut $y = 0$, $x > 0$ is subjected to a temperature field satisfying

the following conditions on the axis $y = 0$:

$$\begin{gathered} T(x, 0, t) = T_0 \text{ when } a < x < a + l, \\ T(x, 0, t) = 0 \text{ when } x > a + l, \\ \left.\frac{\partial T}{\partial y}\right|_{y=0} = 0 \quad \text{when} \quad x < a. \end{gathered} \tag{32.24}$$

In this case the expression for the temperature can be obtained as follows. To solution (32.5), (32.14) is added a term of a similar type with T_0 replaced by $(-T_0)$ and a by $a + l$. For the temperature on the axis $y = 0$ we thus obtain

$$T(x, 0, t) = \\ = T_0 \begin{cases} 1, \ a < x < a + l, \\ \dfrac{1}{\pi} \displaystyle\int_1^\infty \left\{ \operatorname{erfc}\left[\frac{|x-a|\tau}{2\sqrt{\varkappa t}}\right] - \operatorname{erfc}\left[\frac{|x-a-l|\tau}{2\sqrt{\varkappa t}}\right]\right\} \frac{d\tau}{\tau\sqrt{\tau-1}}, \end{cases} \tag{32.25}$$

$$T(x, 0, t) = 0, \quad x > a + l.$$

For the stress intensity factor corresponding to the given temperature field we obtain the expression

$$K = \sqrt{\frac{2}{\pi}}\, 2\mu m T_0 \sqrt{a}\, [1 - \sqrt{1+\lambda} + F(t_*, \lambda) - F(t_*, 0)]. \tag{32.26}$$

Here $\lambda = \dfrac{l}{a}$,

$$F(t_*, \lambda) = \\ = \frac{1}{2\pi} \int_1^\infty \left\{ \int_0^1 \operatorname{erfc}\left[\frac{\tau}{t_*}(\lambda+\xi)\right] \frac{d\xi}{\sqrt{1-\xi}} + \frac{1}{\sqrt{\pi}} \frac{t_*}{\tau} \int_0^1 \left\{ e^{-\frac{(\lambda+\xi)^2\tau^2}{t_*^2}} - \right.\right. \\ \left.\left. - \frac{\sqrt{\pi}}{2} \frac{t_*}{\tau(\lambda+\xi)} \operatorname{erf}\left[\frac{\tau}{t_*}(\lambda+\xi)\right]\right\} \frac{d\xi}{(\lambda+\xi)\sqrt{1-\xi}} \right\} \frac{d\tau}{\tau\sqrt{\tau-1}}.$$

The relation between $K^* = \dfrac{K\sqrt{\pi}}{2\sqrt{2}\mu m T_0 \sqrt{a}}$ and t_* is given in Fig. 32.3. The temperature field satisfying conditions (32.24) gives rise to compressive normal stresses on the prolongation of the cut.

33. PROCEDURE FOR SOLVING CRACK AND PUNCH PROBLEMS

In solving contact problems in the case of a semi-infinite body or (mathematically) equivalent problems of cuts in an infinite two-dimensional body the application of Fourier transformations reduces the problem to that of finding the solutions of dual integral equations [256, 257]. In the classical theory of elasticity the solution of such a system was found by I. W. Busbridge [35]. The formulation of analogous problems in thermoelasticity, of contact problems in the mechanics of deformation of porous viscoelastic media, of problems of crack growth in the couple-stress theory of elasticity shows that the resulting system of dual integral equations contains closely similar kernels. However, the method applied by I. W. Busbridge for the construction of the solution in the classical theory of elasticity is not useful in these cases since it is associated with a specific form of the kernel ($K(\xi)=\xi^{\alpha}$), which enables one to employ the inverse Mellin transformation for the construction of the solution. Below, by way of example, the plane problem of the couple-stress theory of elasticity for an infinite plane with a cut (or the corresponding contact problem for a half-plane) is reduced by means of Fourier transforms to dual integral equations for which a simple approximate solution is obtained in [226]. A similar approach was applied to the solution of problems in thermoelasticity [147, 227] and of contact problems for porous viscoelastic media [225].

1. The solution of the plane problem of the couple-stress theory of elasticity for the case when small rigid-body rotations of a medium are completely defined by the displacement vector is reduced to finding functions U and F satisfying the equations [176]

$$\nabla^2\nabla^2 U=0, \quad \nabla^2(F-l^2\nabla^2 F)=0, \tag{33.1}$$

$$\begin{aligned} \frac{\partial}{\partial x}(F-l^2\nabla^2 F) &= -2(1-\nu)\, l^2 \frac{\partial}{\partial y}\nabla^2 U, \\ \frac{\partial}{\partial y}(F-l^2\nabla^2 F) &= 2(1-\nu)\, l^2 \frac{\partial}{\partial x}\nabla^2 U. \end{aligned} \tag{33.2}$$

Here $l^2=\eta/\mu$, η is the flexural-torsional modulus, μ is the shearing modulus.

The force and couple stresses and the displacements are determined in terms of the functions U and F by the formulas

$$\sigma_x = \frac{\partial^2 U}{\partial y^2} - \frac{\partial^2 F}{\partial x\, \partial y}, \qquad \sigma_y = \frac{\partial^2 U}{\partial x^2} + \frac{\partial^2 F}{\partial x\, \partial y},$$

$$\tau_{xy} = -\frac{\partial^2 U}{\partial x\, \partial y} - \frac{\partial^2 F}{\partial y^2}, \qquad \tau_{yx} = -\frac{\partial^2 U}{\partial x\, \partial y} + \frac{\partial^2 F}{\partial x^2}, \tag{33.3}$$

$$\mu_x = \frac{\partial F}{\partial x}, \qquad \mu_y = \frac{\partial F}{\partial y},$$

$$u = \frac{1}{2\mu}\left(-\frac{\partial U}{\partial x} + (1-\nu)\int \nabla^2 U\, dx - \frac{\partial F}{\partial y}\right),$$

$$v = \frac{1}{2\mu}\left(-\frac{\partial U}{\partial y} + (1-\nu)\int \nabla^2 U\, dy + \frac{\partial F}{\partial y}\right). \tag{33.4}$$

Consider an infinite plane with a cut of length $2a$ along the real axis to the sides of which is applied a constant normal load q. Because of the symmetry of the state of stress we consider the upper half-plane on the boundary of which the following simplifying conditions are fulfilled (for a rigorous formulation of the boundary conditions in such problems see the end of the section):

$$\mu_y(x, 0) = \tau_{yx}(x, 0) = 0 \quad (-\infty < x < \infty), \tag{33.5}$$

$$\sigma_y(x, 0) = -q \text{ when } |x| < a, \tag{33.6}$$

$$v(x, 0) = 0 \text{ when } |x| > a.$$

By applying the Fourier transformation to Eqs. (33.1), we represent the functions U and F as

$$U(x, y) = \int_0^\infty [A(\lambda) + yB(\lambda)]\, e^{-\lambda y} \cos(\lambda x)\, d\lambda,$$

$$F(x, y) = \int_0^\infty \left[C(\lambda) \exp\left(-y\sqrt{\frac{1}{l^2} + \lambda^2}\right) + D(\lambda)\, e^{-\lambda y}\right] \sin \lambda x\, d\lambda. \tag{33.7}$$

Substituting expressions (33.7) in equality (33.2), we obtain

$$D(\lambda) = -4(1-\nu)\, l^2 \lambda B(\lambda). \tag{33.8}$$

By satisfying the boundary conditions (33.5) and (33.6), we have

$$C(\lambda)=4(1-\nu)\,l\,\frac{\lambda^2\beta(\lambda)}{\sqrt{1+\lambda^2l^2}},$$
$$A(\lambda)=\frac{1}{\lambda}\left[1+4(1-\nu)\,l^2\lambda^2\left(1-\frac{\lambda l}{\sqrt{1+\lambda^2l^2}}\right)\right]B(\lambda). \tag{33.9}$$

The function $B(\lambda)$ is the solution of the dual integral equations

$$\int_0^\infty \lambda\left[1+4(1-\nu)\,l^2\lambda^2\left(1-\frac{\lambda l}{\sqrt{1+\lambda^2l^2}}\right)\right]B(\lambda)\cos(\lambda x)\,d\lambda=q$$
$$(x\leqslant a), \tag{33.10}$$
$$\int_0^\infty B(\lambda)\cos(\lambda x)\,d\lambda=0 \qquad (x>a).$$

On the basis of relations (33.7) to (33.9) the expression for the stresses σ_y, for example, is written down as

$$\sigma_y(x,y)=-\int_0^\infty\left\{\lambda\left[1+4(1-\nu)\,l^2\lambda^2\left(1-\frac{\lambda l}{\sqrt{1+\lambda^2l^2}}\right)\right]+\right.$$
$$\left.+\lambda^2\left[y-4(1-\nu)\,l^2\right]\right\}e^{-\lambda y}B(\lambda)\cos\lambda x\,d\lambda-$$
$$-4(1-\nu)\frac{1}{l}\int_0^\infty\lambda^2\exp\left(-\frac{y}{l}\sqrt{1+\lambda^2l^2}\right)B(\lambda)\cos(\lambda x)\,d\lambda$$

and on the prolongation of the cut

$$\sigma_y(x,0)=$$
$$=-\int_0^\infty\lambda\left[1+4(1-\nu)\,l^2\lambda^2\left(1-\frac{\lambda l}{\sqrt{1+\lambda^2l^2}}\right)\right]B(\lambda)\cos\lambda x\,d\lambda. \tag{33.11}$$

2. We write down the integral equations (33.10)

$$\int_0^\infty \xi \left\{1+\omega\left[\xi^2\left(1-\frac{\xi}{\sqrt{1+\xi^2}}\right)-\frac{1}{2}\right]\right\} \times$$

$$\times B(\xi)\cos\left(\xi\frac{x}{l}\right)d\xi = q^* l^2 \quad (x \leqslant a), \qquad (33.12)$$

$$\int_0^\infty B(\xi)\cos\left(\xi\frac{x}{l}\right)d\xi = 0 \quad (x > a).$$

Here

$$\xi = \lambda l, \quad q^* = \frac{q}{3-2\nu}, \quad \omega = \frac{4(1-\nu)}{3-2\nu}.$$

In the first equation of (33.12) we set (Fig. 33.1)

$$\xi^2\left(1-\frac{\xi}{\sqrt{1+\xi^2}}\right)-\frac{1}{2} \cong \frac{A_0}{\xi^2+c^2}. \qquad (33.13)$$

If we assume, for example, $A_0 = -\frac{3}{8}$, $c^2 = \frac{3}{4}$, the relative error introduced by approximation (33.13) does not exceed 3 per cent for $0 \leqslant \xi < \infty$.

Closely similar ideas associated with the construction of approximate solutions by approximating kernels have also been developed by W. T. Koiter [134].

Taking into account equality (33.13), we write down Eqs. (33.12)

$$\int_0^\infty \xi\left[1+\frac{\omega A_0}{\xi^2+c^2}\right]B(\xi)\cos\left(\xi\frac{x}{l}\right)d\xi = q^* l^2 \quad (x \leqslant a), \qquad (33.14)$$

$$\int_0^\infty B(\xi)\cos\left(\xi\frac{x}{l}\right)d\xi = 0 \quad (x > a).$$

The solution of the dual equations (33.14) is sought in the form

$$B(\xi) = \int_0^a L(t)\, J_0\left(\xi\frac{t}{l}\right)dt. \qquad (33.15)$$

We substitute expression (33.15) in the second equation of (33.14) and interchange the order of integration. Taking into account the value of the integral [101]

$$\int_0^\infty J_0\left(\xi\frac{t}{l}\right)\cos\left(\xi\frac{x}{l}\right)d\xi=0, \quad (x>t),$$

it may be concluded that in assuming $B(\xi)$ in the form of (33.15) the second equation of (33.14) is satisfied identically.

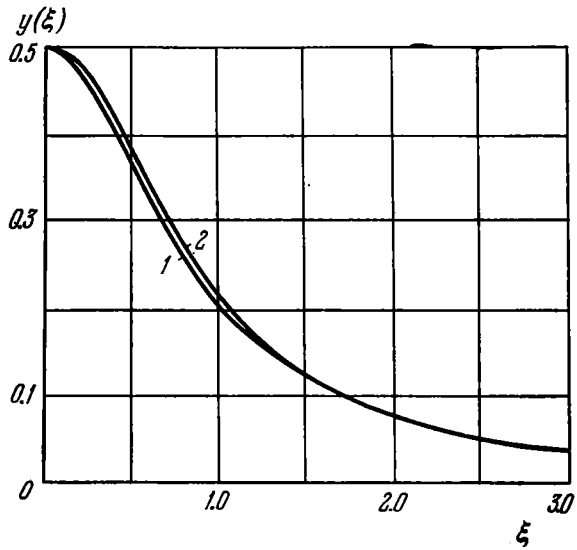

Fig. 33.1. True kernel (*1*) of Eq. (33.12) and its approximation (*2*). *1*, $y(\xi)=\frac{1}{2}-\xi^2\left(1-\frac{\xi}{\sqrt{1+\xi^2}}\right)$; *2*, $y(\xi)=\frac{3/8}{\xi^2+3/4}$.

We substitute expression (33.15) in the first equation of (33.14) and integrate it with respect to x. Taking into account the value of the discontinuous integral [101]

$$\int_0^\infty J_0\left(\xi\frac{t}{l}\right)\sin\left(\xi\frac{x}{l}\right)d\xi=\begin{cases}0, & t>x,\\ \dfrac{l}{\sqrt{x^2-t^2}}, & t<x,\end{cases}$$

we find

$$\int_0^x \frac{L(t)\,dt}{\sqrt{x^2-t^2}} =$$

$$= -\frac{\omega A_0}{l}\int_0^a L(t)\left[\int_0^\infty \frac{J_0\left(\xi\frac{t}{l}\right)\sin\left(\xi\frac{x}{l}\right)}{\xi^2+c^2}\,d\xi\right]dt + q^*x. \quad (33.16)$$

Considering (33.16) as a Schloemilch integral equation, we write down its solution in the form [291]

$$L(t) = q^*t - t\frac{\omega A_0}{l^2}\int_0^a L(\tau)\left[\int_0^\infty \frac{\xi J_0\left(\xi\frac{\tau}{l}\right)J_0\left(\xi\frac{t}{l}\right)}{\xi^2+c^2}\,d\xi\right]d\tau. \quad (33.17)$$

The value of the inner integral on the right-hand side of Eq. (33.17) is known [101]

$$\int_0^\infty \frac{\xi J_0\left(\xi\frac{\tau}{l}\right)J_0\left(\xi\frac{t}{l}\right)}{\xi^2+c^2}\,d\xi =$$

$$= \begin{cases} I_0\left(\frac{c}{l}t\right)K_0\left(\frac{c}{l}\tau\right), & t<\tau, \\ I_0\left(\frac{c}{l}\tau\right)K_0\left(\frac{c}{l}t\right), & t>\tau. \end{cases} \quad (33.18)$$

Here $I_0(z)$ and $K_0(z)$ are modified Bessel functions of the first and second kind, respectively.

With relations (33.18), equality (33.17) is written as follows:

$$L(t) = q^*t - \frac{\omega A_0}{l^2}t\left[K_0\left(\frac{c}{l}t\right)\int_0^t L(\tau)I_0\left(\frac{c}{l}\tau\right)d\tau + \right.$$

$$\left. + I_0\left(\frac{c}{l}t\right)\int_t^a L(\tau)K_0\left(\frac{c}{l}\tau\right)d\tau\right]. \quad (33.19)$$

Differentiating expressions (33.19) twice with respect to t, it can be verified that the function $L(t)$ satisfies the second-

order differential equation

$$L''(t)-\frac{1}{t}L'(t)+\left(\frac{1}{t^2}-\frac{k^2}{l^2}\right)L(t)=-q^*\frac{c^2}{l^2}t, \qquad (33.20)$$

$$k=\sqrt{c^2+\omega A_0}.$$

The solution of (33.20) is of the form

$$L(t)=C_0tI_0\left(\frac{k}{l}t\right)+D_0tK_0\left(\frac{k}{l}t\right)+q^*\frac{c^2}{k^2}t, \qquad (33.21)$$

where C_0 and D_0 are integration constants.

Substituting expression (33.21) in Eq. (33.15), we find

$$B(\lambda)=$$

$$=C_0\frac{al^2}{k^2+\lambda^2l^2}\left[I_0\left(\frac{k}{l}a\right)\lambda I_1(\lambda a)+\frac{k}{l}I_1\left(\frac{k}{l}a\right)J_0(\lambda a)\right]+$$

$$+D_0\frac{al^2}{k^2+\lambda^2l^2}\left[K_0\left(\frac{k}{l}a\right)\lambda J_1(\lambda a)-\frac{k}{l}K_1\left(\frac{k}{l}a\right)J_0(\lambda a)\right]+$$

$$+q^*\frac{c^2}{k^2}\frac{a}{\lambda}J_1(\lambda a). \qquad (33.22)$$

To determine the constants C_0 and D_0, we substitute relation (33.22) in the original equations (33.14) and evaluate the integrals involved. As a result we find that expression (33.22) is the solution of the dual equations (33.14) if the constants are

$$C_0=q^*\frac{\omega A_0}{k^2}c\frac{K_1\left(\frac{c}{l}a\right)}{\left[cI_0\left(\frac{k}{l}a\right)K_1\left(\frac{c}{l}a\right)+kI_1\left(\frac{k}{l}a\right)K_0\left(\frac{c}{l}a\right)\right]},$$

$$D_0=0. \qquad (33.23)$$

We determine the distribution of stress σ_y on the prolongation of the cut. By using relations (33.11), (33.13), and (33.22), we obtain

$$\sigma_y(x,\ 0)=$$

$$=(3-2\nu)C_0a\left[I_0\left(\frac{k}{l}a\right)G_1(a,\ x)+\frac{k}{l}I_1\left(\frac{k}{l}a\right)G(a,\ x)\right]+$$

$$+qa\int_0^\infty J_1(\lambda a)\cos(\lambda x)\,d\lambda-qa\frac{\omega A_0}{k^2}G_1(a,\ x). \qquad (33.24)$$

Here

$$\int_0^\infty J_1(\lambda a)\cos(\lambda x)\,d\lambda = \frac{x}{a\sqrt{x^2-a^2}} - \frac{1}{a} \quad (x > a > 0),$$

$$G(a,\ x) = \int_0^\infty \frac{\lambda J_0(\lambda a)\cos(\lambda x)}{\lambda^2 + \frac{c^2}{l^2}}\,d\lambda \quad (x > a), \tag{33.25}$$

$$G_1(a,\ x) = \int_0^\infty \frac{\lambda^2 J_1(\lambda a)\cos(\lambda x)}{\lambda^2 + \frac{c^2}{l^2}}\,d\lambda \quad (x > a).$$

To calculate $G(a,\ x)$ for $x > a$, we apply the Laplace-Carson transformation on the variable x

$$\overline{G}(a,\ p) = p^2 \int_0^\infty \frac{\lambda J_0(\lambda a)\,d\lambda}{(\lambda^2+p^2)\left(\lambda^2+\frac{c^2}{l^2}\right)} =$$

$$= \frac{p^2}{p^2-\frac{c^2}{l^2}} K_0\left(\frac{c}{l}a\right) - \frac{p^2}{p^2-\frac{c^2}{l^2}} K_0(ap). \tag{33.26}$$

The first term on the right-hand side of equality (33.26) represents the transform of the function

$$\cosh\left(\frac{c}{l}x\right) K_0\left(\frac{c}{l}a\right). \tag{33.27}$$

The second term on the right-hand side is written as the product $\frac{1}{p} f_1(p) f_2(p)$, where

$$f_1(p) = \frac{p^2}{p^2-\frac{c^2}{l^2}}, \qquad f_2(p) = pK_0(ap).$$

By using the convolution theorem [64], we obtain

$$\frac{p^2 K_0(ap)}{p^2-\frac{c^2}{l^2}} \overset{\cdot}{\leftrightarrow} \begin{cases} \displaystyle\int_0^x \frac{\cosh\frac{c}{l}(x-t)}{\sqrt{t^2-a^2}}\,dt & \text{when } x > a, \\ 0 & \text{when } x < a. \end{cases} \tag{33.28}$$

Returning to the original, we find, according to (33.27) and (33.28),

$$G(a, x) = \cosh\left(\frac{c}{l}x\right) K_0\left(\frac{c}{l}a\right) - \\ - \int_a^x \frac{\cosh\left[\frac{c}{l}(x-t)\right]}{\sqrt{t^2-a^2}}\, dt \quad (x > a). \quad (33.29)$$

In a similar way it may be shown that

$$G_1(x, a) = \frac{c}{l}\cosh\left(\frac{c}{l}x\right) K_1\left(\frac{c}{l}a\right) - \\ - \frac{c}{la}\int_a^x \frac{t\cosh\left[\frac{c}{l}(x-t)\right]}{\sqrt{t^2-a^2}}\, dt \quad (x > a). \quad (33.30)$$

Taking into account expression (33.24), we now apply Irwin's condition (3.11) at the crack tip. We find that in the limiting state

$$K_c = \lim_{x \to a} [\sqrt{2\pi(x-a)}\,\sigma_y(x, 0)] = q\sqrt{\pi a},$$

which agrees with the well-known result of Griffith. Whereas the stresses in the couple-stress theory of elasticity are different from the ordinary elastic stresses according to Eqs. (33.24), (33.25), (33.29), and (33.30), the value of the stress intensity factor is the same.

There are investigations of P. S. Paris and G. C. Sih [221], D. E. Setzer*, G. R. Tiwari [271] which confirm our conclusion that the stress intensity factor is the same in the couple-stress and the ordinary theory of elasticity. In the work of E. Sternberg and R. Muki [266], however, other than (33.5) and (33.6) boundary conditions were assigned. In our notation they take the following form ($y = 0$):

$$\begin{aligned} &\tau_{yx} = 0 \ (-\infty < x < \infty), \\ &\mu_y(x, 0) = 0 \qquad (|x| < a), \\ &\omega(x, 0) = 0 \qquad (|x| > a), \\ &\sigma_y(x, 0) = -q \quad (|x| < a), \\ &v(x, 0) = 0 \qquad (|x| > a). \end{aligned} \quad (33.31)$$

* Setzer D. E., *A Plane Elastostatic Couple-stress Problem: Extension of an Elastic Body Containing a Cut of Finite Length*, Ph. D. Dissertation, Lehigh University, 1964.

Here $\omega(x, y)$ is the rotation in the couple-stress theory of elasticity.

In this formulation (assigning a kind of mixed boundary conditions in couple-stresses and rotations), the result obtained in solving the problem of a plane with a circular hole agrees with the solution in the case of the boundary conditions (33.5) and (33.6). In the case of a cut, however, the stress intensity factor is dependent on Poisson's ratio.

CHAPTER VII

DYNAMIC PROBLEMS IN FRACTURE MECHANICS

34. VELOCITY OF SUPERCRITICAL CRACK PROPAGATION

Here is formulated an energy variational condition which, in conjunction with the equations of the theory of elasticity, determines the law of motion of the crack edge during its rapid unstable propagation or in the case of a dynamic load acting on a cracked body.

Suppose there is an elastic body containing a moving crack under constant or time-varying external load. At the initial instant the crack occupies a region S_0. This region is either an original stationary cut or a crack at the critical value of the external load at the initial instant. It is required to determine the kinematic characteristics of the crack edge moving along a given surface.

To solve this problem we use the Hamilton-Ostrogradsky principle in the form [230]

$$\int_{t_0}^{t_1} \delta L \, dt = 0. \tag{34.1}$$

Here $t_1 - t_0$ is a fixed interval of time between two different states of a body with a growing crack. The Lagrange function may be taken as [180]

$$\delta L = \delta \Gamma + \delta W - \delta A. \tag{34.2}$$

Here use has been made of the notation of Sec. 4.

The specific form of writing expression (34.2) will be sought by using the procedure given in [184, 188].

Consider the (first) state of this body at a certain instant (Fig. 34.1). The body in this state is not in equilibrium, but

further formal transformations on the basis of d'Alembert's principle can be effected in the same way as for the equilibrium state by adding the mass inertia forces $-\rho\ddot{u}_{i1}$ to each elementary volume of the body. The numeral suffix indicates the state number. The external load $q_i(t)$ is pre-

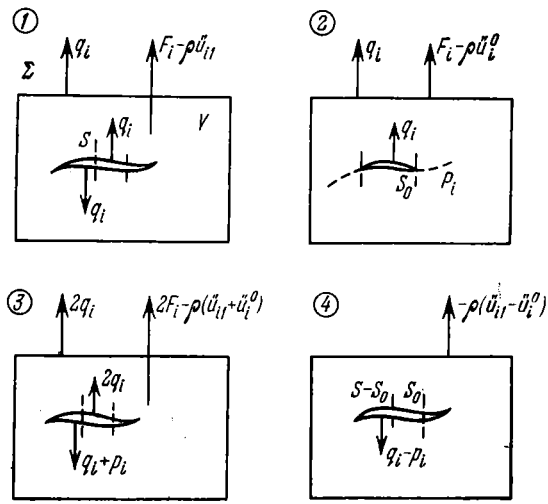

Fig. 34.1. States of a body with a moving crack at a certain instant. *1*, state under investigation; *2*, state of the body with the initial crack, but for loads corresponding to the time considered; *3*, 'sum' state; *4*, 'difference' state.

scribed over the surface of the body Σ, over the surface of the initial crack S_0, and over the crack surface made by the time considered $S - S_0$. A mass force $F_i(x, y, z, t)$ is given in the volume V of the body.

We introduce a second state, viz. the same body but with an initial crack S_0. The external loads are the same as in the first state and relate to the same instant. To the mass forces are added the inertia forces $-\rho\ddot{u}_i^0$ which arise if the external load is time dependent. Finally, it may be assumed that the body in the second state contains the same cut $S - S_0$ (as in the first state) on whose surface are applied stresses $p_i(t)$

which eliminate the discontinuity in displacement on $S - S_0$. (Consequently, these are the stresses on planes coinciding with $S - S_0$ at the given instant, which are determined from the solution of the dynamic problem of the theory of elasticity for a body with an initial cut S_0.)

The work done by the external forces when these latter stresses are removed (i.e., as one passes from the second to the first state at the same instant) is

$$A_{1-2} = \int\limits_{\Sigma+S} q_i (u_{i1} - u_i^0)\, d\sigma + \int\limits_V F_i (u_{i1} - u_i^0)\, dV - \\ - \frac{1}{2} \int\limits_V \rho (\ddot{u}_{i1} + \ddot{u}_i^0)(u_{i1} - u_i^0)\, dV. \quad (34.3)$$

The corresponding change in volume strain energy is

$$W_{1-2} = \frac{1}{2} \int\limits_V (\sigma_{ij1}\varepsilon_{ij1} - \sigma_{ij}^0 \varepsilon_{ij}^0)\, dV = \\ = \frac{1}{2} \int\limits_V (\sigma_{ij1} + \sigma_{ij}^0)(\varepsilon_{ij1} - \varepsilon_{ij}^0)\, dV. \quad (34.4)$$

The last equality has been obtained by using Betti's theorem

$$\int\limits_V \sigma_{ij}\varepsilon_{ij}^0\, dV = \int\limits_V \sigma_{ij}^0 \varepsilon_{ij}\, dV$$

which holds in the case under consideration since the bodies in both states are elastic and identical in the undeformed state*.

We introduce two more auxiliary states: a third state in which the stresses are $\sigma_{ij3} = \sigma_{ij1} + \sigma_{ij}^0$, the strains $\varepsilon_{ij3} = \varepsilon_{ij1} + \varepsilon_{ij}^0$, the displacements $u_{i3} = u_{i1} + u_i^0$. Consequently, in the third state the external loads $2q_i$ are acting on $\Sigma + S_0$, $q_i + p_i$ on $S - S_0$, and $2F_i - \rho(\ddot{u}_{i1} + \ddot{u}_i^0)$ in the volume of the body V.

A fourth state has the stresses $\sigma_{ij} = \sigma_{ij1} - \sigma_{ij}^0$, the strains $\varepsilon_{ij} = \varepsilon_{ij1} - \varepsilon_{ij}^0$, the displacements $u_i = u_{ij} - u_i^0$. Consequently, in the fourth state there are no external loads on

* Betti's theorem is also valid in the presence of inertia forces incorporated in the given mass forces (see, for example, [25]).

$\Sigma + S_0$, the crack surface $S - S_0$ is acted on by the stresses $q_i - p_i$, the mass forces $-\rho(\ddot{u}_{i1} - \ddot{u}_i^0) = -\rho\ddot{u}_i$ are acting in the volume of the body.

By passing from internal to external forces, the last integral in expression (34.4) can be rewritten as

$$W_{1-2} = \frac{1}{2}\int_V \sigma_{ij3}\varepsilon_{ij}\,dV =$$

$$= \int_{\Sigma+S_0} q_i u_i\,d\sigma + \int_V F_i u_i\,dV - \frac{1}{2}\int_V \rho(\ddot{u}_{i1} + \ddot{u}_i^0)\,u_i\,dV +$$

$$+ \frac{1}{2}\int_{S-S_0} (q_i + p_i)\,u_i\,d\sigma. \quad (34.5)$$

From formulas (34.3) to (34.5) we obtain the change in energy of the system when passing from the second to the first state

$$-A_{1-2} + W_{1-2} = -\frac{1}{2}\int_{S-S_0} q_i u_i\,d\sigma + \frac{1}{2}\int_{S-S_0} p_i u_i\,d\sigma. \quad (34.6)$$

Consider the first state in which the varied parameters are those determining the contour line of the fracture region. Since the variation of the crack size is isochronous*, the external loads remain invariant. We find that the variation of functional (34.6) represents the required variation $-\delta A + \delta W$ of the first state under consideration. By supplementing this expression by the fracture energy, we obtain, according to (34.2), the variation of the Lagrange function [188]

$$\delta L = \delta\int_{S-S_0} \gamma\,d\sigma - \frac{1}{2}\delta\int_{S-S_0} (q_i + p_i)\,u_i\,d\sigma. \quad (34.7)$$

Here q_i are given external forces on $S - S_0$, p_i are surface stresses corresponding to the surface $S - S_0$ in the body with the crack S_0. These stresses entering into (34.7) with opposite sign are produced by the given surface loads q_i on $\Sigma + S_0$ and the mass forces $F_i - \rho\ddot{u}_i^0$ acting on the body containing the initial crack S_0 (if the crack propagates under

* In the Hamilton-Ostrogradsky principle the time is not subject to the variation [230].

constant external loads, the term $-\rho\ddot{u}_i^0$ is absent, then $\ddot{u}_{i1} = \ddot{u}_i$).

The displacements u_i on the crack surface are produced by the surface forces $q_i + p_i$ on $S - S_0$ and the mass forces $-\rho\ddot{u}_i$ in the volume of the body; these are the displacements for a moving crack whose law of motion is to be determined from the condition (34.8) given below.

All values in (34.7) relate to a certain instant, and the calculation of the corresponding stresses and displacements is carried out for the "frozen" state at that instant.

Thus, the Hamilton-Ostrogradsky principle (34.1) assumes a specific form suitable for the solution of problems in fracture mechanics

$$\int_0^{t_1} \left[\delta \int_{S-S_0} (2\gamma - (p_i + q_i)\, u_i)\, d\sigma \right] dt = 0. \qquad (34.8)$$

Here $t = 0$ and t_1 are fixed instants corresponding to the transition of the crack from the given position S_0 to another position S_1.

We shall use the resulting condition to establish the kinematic characteristics of a propagating crack in the supercritical state. In this case the integral over $S - S_0$ in (34.8) must be taken between the limits l_0 and $l(t)$. The law of motion of the crack ends is to be determined as part of the solution of the problem.

The solution of the elastodynamic problem concerning the determination of displacements on the surface of a cut propagating with a velocity not known in advance appears to be very complicated. Hence, as a possible method of solution we may suggest the following iterative process: first determine displacements by assigning some constant (subsonic) velocity of crack growth, $\dot{l}(t) = c =$ constant. Next, from condition (34.8) find a velocity $c(t) \neq$ constant, which represents a second approximation. This value of the velocity may in turn be used to calculate displacements, and again from condition (34.8) we find a velocity, the next approximation, etc.

For example, in [41] the crack velocity initially assumed constant, after being determined with the use of the limiting stress intensity factor criterion for fracture and the law

of conservation of energy, naturally turned out to be variable, this latter velocity being in better agreement with the physical meaning of the problem than the initially assumed constant velocity.

Consider another possible approach [192]. Let an infinite plane be uniformly extended by a stress p in the y direction. The plane contains a crack $y = 0$, $|x| \leqslant l(t)$.

At the time $t = 0$ the crack length has the critical size $2l_0$, and the crack begins to propagate rapidly at a constant value of the external stress which is determined by the Griffith formula $p^2 = 2E\gamma/\pi(1-\nu^2)\,l_0$. It is required to establish the kinematic characteristics of the propagating crack in the supercritical state.

The problem of this type of crack growth with the energy balance incorporating the kinetic energy of some region around the crack tip was first solved by N. F. Mott [197]. He obtained the following formula relating the crack velocity and its length:

$$\dot{l} = c_m \sqrt{1 - \frac{l_0}{l}}, \tag{34.9}$$

where c_m is the maximum velocity of crack propagation.

Subsequently formula (34.9) was found to be wrong. The error lay in the tacit assumption $d\dot{l}/dl = 0$, which is approximately justified only at velocities close to the limiting values. The correct formula is as follows [22, 23]:

$$\dot{l} = c_m \left(1 - \frac{l_0}{l}\right). \tag{34.10}$$

We solve this problem starting from the Euler-Lagrange equation corresponding to the variational condition (34.8) and then using the relation

$$\frac{\partial L}{\partial l} = \text{constant}. \tag{34.11}$$

The last relation was derived for stationary isothermal cracks [177, 180], and the case under consideration will be referred to this type of crack.*

* The term 'stationarity is used here in the thermodynamic sense, i.e., the change in entropy and in quantity of heat for a body as a whole is zero. Condition (34.11) was obtained from Prigogine's principle [232] of minimum entropy production per unit time due to irreversible changes within the system.

Assume that the Lagrange function is of the form

$$L = \int_0^l (2\gamma - pv)\, dx. \tag{34.12}$$

It is supposed for ease of calculation that $l_0 = 0$.* The displacement v of the points of the crack surface produced by the pressure p acting on the crack faces must be determined using the fact that the crack ends move along the x axis with a certain velocity $\dot{l}$. The unknowns are the velocity of the crack ends and the relation between the displacement and this velocity.

To determine the relation between the displacement and the velocity of crack propagation, we assume, on the basis of the solution of K. B. Broberg [32], that the required displacement may be written as $v = v_0 F(\dot{l})$, where $v_0 = 2(1 - \nu^2) p\sqrt{l^2 - x^2}/E$ is the displacement for a stationary crack of length l, and $F(0) = 1$.

Since the Lagrange function does not depend explicitly on the time, the Euler-Lagrange equation admits of lowering the order, and its first integral is written as

$$L - \dot{l}\frac{\partial L}{\partial \dot{l}} = C. \tag{34.13}$$

After substituting the appropriate quantities this equation takes the form

$$\frac{\partial F}{\partial \alpha} - \frac{1}{\alpha} F = \frac{1}{\alpha a^2}\left(\frac{c}{\gamma l_0} - 2a\right). \tag{34.14}$$

Here $\alpha = \dot{l}/c_m$, $a = l/l_0$ are the non-dimensional velocity and crack length, respectively.

The general solution of Eq. (34.14) is

$$F = A(a)\,\alpha - \frac{1}{a^2}\left(\frac{c}{\gamma l_0} - 2a\right).$$

* Assuming $l_0 \neq 0$ in expression (34.12) only complicates the Euler-Lagrange equation and changes the magnitude of the integration constants without introducing any changes into the form of the relation between the velocity and the crack length. Henceforth, $l_0 = 0$ throughout.

The constant c is equal to γl_0 and is determined from the condition $F = 1$ when $\alpha = 0$ and $a = 1$. Consequently,

$$F = \alpha A(a) + \frac{1}{a^2}(2a - 1). \tag{34.15}$$

We now use condition (34.11), which here assumes the form

$$2\gamma - \frac{\pi(1-\nu^2)p^2}{E} lF = \text{constant}. \tag{34.16}$$

From the Griffith criterion

$$2\gamma - \frac{\pi(1-\nu^2)p^2}{E} l_0 = 0$$

it follows that the right-hand side of equality (34.16) is zero when $a = 1$ and $\alpha = 0$. Substituting now expression (34.15) in Eq. (34.16), we obtain

$$\alpha = \frac{1-a}{a^2 A(a)}. \tag{34.17}$$

The function $A(a)$ is determined from the condition that the crack velocity reaches its maximum value as the crack length increases indefinitely, i.e., $\alpha = 1$ as $a \to \infty$. From this we find $A(a) = -1/a$ and, upon substitution in expression (34.17), we ascertain that the crack velocity is determined by formula (34.10).

This value of the crack velocity satisfies identically Eq. (34.13).

Note that we can now write out the relation between the function F and α, which was not expanded explicitly in the course of the solution. From expression (34.15), using $a = 1/(1-\alpha)$, we find $F = 1 - \alpha$.

It might be well to point out that this is approximately the same qualitative relation as that given by the expression for $F(\alpha)$ obtained in a different way in [32] for a given constant crack velocity.

In the foregoing solution the constant c_m remains undetermined. It may be assumed, however, that the maximum velocity of crack propagation c_m depends on the critical stress p corresponding to the Griffith initial length l_0. This relation was obtained in [16] by equating the stress intensity factor of a moving crack (Broberg's solution) to a constant. The crack velocity c_m was found to increase with increasing critical stress p.

35. THE DYNAMIC PROBLEM FOR A PLANE WITH A CUT

Until recently, primary emphasis has been placed on static problems in fracture mechanics. However, the development of new fields demands not only the application of advanced materials with complex and non-equilibrium structure, but also the consideration of the non-uniformity of loading in time. Modern machines and structures having crack-like defects often operate under conditions of multiple static and cyclic loading and vibratory loads. In considering this kind of phenomena it is important to examine purely inertia effects in crack propagation. If the external load is applied off the sides of a cut, its action on the crack is not completely transmitted because of stress relaxation, and somewhat lags behind in time. Hence, in considering, for example, problems involving steady-state vibrations for bodies containing cracks we shall assign a normal load directly on the sides of a cut.

Consider a steady-state wave process assuming that the time dependence of all quantities is expressed by the factor $\exp(-i\omega t)$, where ω is the frequency of vibration and t is the time.

Suppose that a normal load $q(\theta)\, e^{-i\omega t}$ is applied to the sides of a cut and introduce a system of elliptical co-ordinates

$$x + iy = l \cosh(\rho + i\theta).$$

The contour of the cut is defined by $\rho = 0$ $(0 \leqslant \theta \leqslant 2\pi)$.

The equations of motion and the relations of elasticity for the amplitude values of stresses and displacements in the chosen system of co-ordinates are

$$\frac{\partial}{\partial\rho}(H\sigma_\rho) + \frac{\partial}{\partial\theta}(H\sigma_{\rho\theta}) + \frac{\partial H}{\partial\theta}\sigma_{\rho\theta} - \frac{\partial H}{\partial\rho}\sigma_\theta = -H^2\rho_0\omega^2 u_\rho,$$

$$\frac{\partial}{\partial\theta}(H\sigma_\theta) + \frac{\partial}{\partial\rho}(H\sigma_{\rho\theta}) + \frac{\partial H}{\partial\rho}\sigma_{\rho\theta} - \frac{\partial H}{\partial\theta}\sigma_\rho = -H^2\rho_0\omega^2 u_\theta, \tag{35.1}$$

$$\sigma_\rho = 2\mu\left(\frac{1}{H}\frac{\partial u_\rho}{\partial\rho} + \frac{1}{H^2}\frac{\partial H}{\partial\theta}u_\theta\right) + \\ + \lambda\frac{1}{H^2}\left[\frac{\partial}{\partial\rho}(Hu_\rho) + \frac{\partial}{\partial\theta}(Hu_\theta)\right],$$

$$\sigma_{\rho\theta} = \mu\left[\frac{\partial}{\partial\rho}\left(\frac{u_\theta}{H}\right) + \frac{\partial}{\partial\theta}\left(\frac{u_\rho}{H}\right)\right], \tag{35.2}$$

$$\sigma_\theta = 2\mu\left(\frac{1}{H}\frac{\partial u_\theta}{\partial\theta} + \frac{1}{H^2}\frac{\partial H}{\partial\rho}u_\rho\right) + \\ + \lambda\frac{1}{H^2}\left[\frac{\partial}{\partial\rho}(Hu_\rho) + \frac{\partial}{\partial\theta}(Hu_\theta)\right].$$

Here $H^2 = \frac{1}{2}l^2(\cosh 2\rho - \cos 2\theta)$, ρ_0 is the density of the material, ω is the circular frequency, λ and μ are Lamé's constants.

We express, as usual, the displacement and stress components in terms of two functions (potentials), φ and ψ,

$$u_\rho = \frac{1}{H}\frac{\partial\varphi}{\partial\rho} + \frac{1}{H}\frac{\partial\psi}{\partial\theta}, \quad u_\theta = \frac{1}{H}\frac{\partial\varphi}{\partial\theta} - \frac{1}{H}\frac{\partial\psi}{\partial\rho}.$$

Here φ and ψ are the solutions of the equations

$$\nabla^2\varphi + 2k_1(\cosh 2\rho - \cos 2\theta)\varphi = 0 \quad \left(\nabla^2 = \frac{\partial^2}{\partial\rho^2} + \frac{\partial^2}{\partial\theta^2}\right), \tag{35.3}$$
$$\nabla^2\psi + 2k_2(\cosh 2\rho - \cos 2\theta)\psi = 0.$$

Here $k_1 = \frac{\omega^2 l^2}{4c_1^2}$, $k_2 = \frac{\omega^2 l^2}{4c_2^2}$ are non-dimensional quantities, $c_1 = \left(\frac{\lambda + 2\mu}{\rho_0}\right)^{1/2}$, $c_2 = \left(\frac{\mu}{\rho_0}\right)^{1/2}$ are the velocities of longitudinal and transverse waves.

With this representation, Eqs. (35.2) become

$$\frac{1}{2\mu}\sigma_{\rho\theta} = \frac{1}{H}\frac{\partial}{\partial\theta}\left(\frac{1}{H}\frac{\partial\varphi}{\partial\rho} + \frac{1}{H}\frac{\partial\psi}{\partial\theta}\right) - \\ - \frac{1}{H^3}\frac{\partial H}{\partial\rho}\left(\frac{\partial\varphi}{\partial\theta} - \frac{\partial\psi}{\partial\rho}\right) + \frac{\omega^2}{2c_2^2}\psi,$$
$$\frac{1}{2\mu}\sigma_\rho = -\frac{1}{H}\frac{\partial}{\partial\theta}\left(\frac{1}{H}\frac{\partial\varphi}{\partial\theta} - \frac{1}{H}\frac{\partial\psi}{\partial\rho}\right) - \\ - \frac{1}{H^3}\frac{\partial H}{\partial\rho}\left(\frac{\partial\varphi}{\partial\rho} + \frac{\partial\psi}{\partial\theta}\right) - \frac{\omega^2}{2c_2^2}\varphi, \tag{35.4}$$
$$\frac{1}{2\mu}\sigma_\theta = \frac{1}{H}\frac{\partial}{\partial\theta}\left(\frac{1}{H}\frac{\partial\varphi}{\partial\theta} - \frac{1}{H}\frac{\partial\psi}{\partial\rho}\right) + \\ + \frac{1}{H^3}\frac{\partial H}{\partial\rho}\left(\frac{\partial\varphi}{\partial\rho} + \frac{\partial\psi}{\partial\theta}\right) - \frac{\lambda}{2\mu}\frac{\omega^2}{c_1^2}\varphi.$$

By separating the variables in Eqs. (35.3), we obtain ordinary differential equations whose solutions are Mathieu functions [167].

Suppose that stresses $\sigma_\rho^{(0)}$ and $\sigma_{\rho\theta}^{(0)} = 0$ are given on the contour of the slit $\rho = 0$ $(-\pi \leqslant \theta \leqslant \pi)$; from the first two equalities of (35.4), with $\left.\frac{\partial H}{\partial \rho}\right|_{\rho=0} = 0$, $H|_{\rho=0} = l \sin\theta$, we then obtain

$$\left(\frac{\partial\varphi}{\partial\theta} - \frac{\partial\psi}{\partial\rho}\right)_{\rho=0} =$$

$$= -2k_2 \sin\theta \int_{\pi/2}^{\theta} \sin\theta \cdot \varphi|_{\rho=0}\, d\theta - \frac{l^2}{2\mu} \sin\theta \int_{\pi/2}^{\theta} \sin\theta \cdot \sigma_\rho^{(0)}|_{\rho=0}\, d\theta, \tag{35.5}$$

$$\left(\frac{\partial\varphi}{\partial\rho} + \frac{\partial\psi}{\partial\theta}\right)_{\rho=0} = -2k_2 \sin\theta \int_0^{\theta} \sin\theta \cdot \psi|_{\rho=0}\, d\theta.$$

Relations (35.5) have been derived with the help of the obvious equalities

$$u_\rho|_{\rho=0,\,\theta=0} = 0, \quad u_\theta|_{\rho=0,\,\theta=\pi/2} = 0.$$

By using the symmetry of the state of stress and the conditions at infinity, we represent the solutions of (35.3) as

$$\begin{aligned} \varphi(\rho, \theta) &= \sum_{m=0}^{\infty} C_m \operatorname{Fek}_{2m}(\rho, k_1) \operatorname{ce}_{2m}(\theta, k_1). \\ \psi(\rho, \theta) &= \sum_{m=0}^{\infty} D_m \operatorname{Gek}_{2m}(\rho, k_2) \operatorname{se}_{2m+2}(\theta, k_2). \end{aligned} \tag{35.6}$$

Here C_m, D_m are constants, $\operatorname{ce}_{2m}(\theta, k_1)$, $\operatorname{se}_{2m+2}(\theta, k_2)$ are periodic Mathieu solutions, $\operatorname{Fek}_{2m}(\rho, k_1)$, $\operatorname{Gek}_{2m}(\rho, k_2)$ are the second solutions of Mathieu's equation.

The periodic Mathieu functions may be represented as series [167]

$$\operatorname{ce}_{2m}(\theta, k_1) = \sum_{r=0}^{\infty} A_{2r}^{(2m)} \cos 2r\theta,$$

$$\operatorname{se}_{2m+2}(\theta, k_2) = \sum_{r=0}^{\infty} B_{2r+2}^{(2m+2)} \sin(2r+2)\theta.$$

In these series $A_{2r}^{(2m)}$, $B_{2r+2}^{(2m+2)}$ are functions of k_1 and k_2, the method of their calculation is indicated in [167].

Note the behaviour of the functions $\mathrm{Fek}_{2m}(\rho, k_1)$ and $\mathrm{Gek}_{2m+2}(\rho, k_2)$ for large values of ρ. When $\rho \to \infty$ we have [$H_{2m}^{(1)}(x)$ is a Hankel function] [167]

$$\mathrm{Fek}_{2m}(\rho, k_1) \to \frac{i}{2}(-1)^m p_{2m} H_{2m}^{(1)}\left(\frac{2}{l}\sqrt{k_1}r\right), \quad \frac{1}{2} l e^{\rho} \to r, \tag{35.7}$$

$$\mathrm{Gek}_{2m+2}(\rho, k_2) \to \frac{i}{2}(-1)^{m+1} s_{2m+2} H_{2m+2}^{(1)}\left(\frac{2}{l}\sqrt{k_2}r\right),$$

$$p_{2m} = \frac{\mathrm{ce}_{2m}(0, k_1)\,\mathrm{ce}_{2m}\left(\frac{\pi}{2}, k_1\right)}{A_0^{(2m)}},$$

$$s_{2m+2} = \frac{\mathrm{se}'_{2m+2}(0, k_2)\,\mathrm{se}'_{2m+2}\left(\frac{\pi}{2}, k_2\right)}{k_2 B_2^{(2m+2)}}. \tag{35.8}$$

With (35.7), the potentials φ and ψ defined by relations (35.6) satisfy the well-known radiation conditions

$$\lim_{r\to\infty} \sqrt{r}\left(\frac{\partial\varphi}{\partial r} - i\frac{2\sqrt{k_1}}{l}\varphi\right) = 0, \quad \varphi = O\left(\frac{1}{\sqrt{r}}\right),$$

$$\lim_{r\to\infty} \sqrt{r}\left(\frac{\partial\psi}{\partial r} - i\frac{2\sqrt{k_2}}{l}\psi\right) = 0, \quad \psi = O\left(\frac{1}{\sqrt{r}}\right).$$

In the general case the functions $\mathrm{Fek}_{2m}(\rho, k_1)$ and $\mathrm{Gek}_{2m+2}(\rho, k_2)$ are complex functions and may be represented as [167]

$$\mathrm{Fek}_{2m}(\rho, k_1) = -\frac{1}{2}\mathrm{Fey}_{2m}(\rho, k_1) + \frac{i}{2}\mathrm{Ce}_{2m}(\rho, k_1),$$

$$\mathrm{Gek}_{2m+2}(\rho, k_2) = -\frac{1}{2}\mathrm{Gey}_{2m+2}(\rho, k_2) + \frac{i}{2}\mathrm{Se}_{2m+2}(\rho, k_2), \tag{35.9}$$

$$\mathrm{Ce}_{2m}(\rho, k_1) = \sum_{r=0}^{\infty} A_{2r}^{(2m)} \cosh 2r\rho,$$

$$\mathrm{Se}_{2m+2}(\rho, k_2) = \sum_{r=0}^{\infty} B_{2r+2}^{(2m+2)} \sinh(2r+2)\rho,$$

$$\mathrm{Fey}_{2m}(\rho, k_1) = \frac{\mathrm{ce}_{2m}\left(\frac{\pi}{2}, k_1\right)}{A_0^{(2m)}} \sum_{r=0}^{\infty} (-1)^r A_{2r}^{(2m)} Y_{2r}(2k_1 \cosh\rho),$$

$$\mathrm{Gey}_{2m+2}(\rho, k_2) =$$

$$= -\frac{s_{2m+2}}{B_2^{(2m+2)}} \sum_{r=0}^{\infty} (-1)^r B_{2r+2}^{(2m+2)} [J_r(e^{-\rho}\sqrt{k_2}) Y_{r+2}(e^{\rho}\sqrt{k_2}) -$$

$$- J_{r+2}(e^{-\rho}\sqrt{k_2}) Y_r(e^{\rho}\sqrt{k_2})]. \quad (35.10)$$

Here $\mathrm{Ce}_{2m}(\rho, k_1)$, $\mathrm{Se}_{2m+2}(\rho, k_2)$ are modified Mathieu functions of the first kind, J_{2r} and Y_{2r} are the Bessel functions of the first and second kind.

Substituting (35.6) in the boundary conditions (35.5), we obtain

$$\sum_{m=0}^{\infty} C_m \mathrm{Fek}_{2m}(0, k_1) \mathrm{ce}'_{2m}(\theta, k_1) -$$

$$- \sum_{n=0}^{\infty} D_n \mathrm{Gek}'_{2n+2}(0, k_2) \mathrm{se}_{2n+2}(\theta, k_2) =$$

$$= -2k_2 \sum_{m=0}^{\infty} C_m \mathrm{Fek}_{2m}(0, k_1) \left[\sin\theta \int_{\pi/2}^{\theta} \sin\theta \, \mathrm{ce}_{2m}(\theta, k_1) \, d\theta\right] -$$

$$- \frac{l^2}{2\mu} \sin\theta \int_{\pi/2}^{\theta} \sin\theta \cdot \sigma_\rho |_{\rho=0} \, d\theta, \quad (35.11)$$

$$\sum_{n=0}^{\infty} C_n \mathrm{Fek}'_{2n}(0, k_1) \mathrm{ce}_{2n}(\theta, k_1) +$$

$$+ \sum_{m=0}^{\infty} D_m \mathrm{Gek}_{2m+2}(0, k_2) \mathrm{se}'_{2m+2}(0, k_2) =$$

$$= -2k_2 \sum_{m=0}^{\infty} D_m \mathrm{Gek}_{2m+2}(0, k_2) \times$$

$$\times \left[\sin\theta \int_0^{\theta} \sin\theta \, \mathrm{se}_{2m+2}(\theta, k_2) \, d\theta\right]. \quad (35.12)$$

By multiplying equality (35.11) by $\mathrm{se}_{2n+2}(\theta, k_2)$ and equality (35.12) by $\mathrm{ce}_{2n}(\theta, k_1)$ and integrating with respect

to θ between the limits 0 and 2π, we obtain, using the orthogonality of periodic Mathieu solutions, two infinite systems of equations for the determination of C_m and D_m

$$C_n \operatorname{Fek}'_{2n}(0, k_1) + \sum_{m=0}^{\infty} D_m \operatorname{Gek}_{2m+2}(0, k_2)\, \alpha_{mn} = 0, \tag{35.13}$$

$$\sum_{m=0}^{\infty} C_m \operatorname{Fek}_{2m}(0, k_1)\, \beta_{nm} - D_n \operatorname{Gek}'_{2n+2}(0, k_2) = -\frac{l^2}{2\mu} \sum_{m=0}^{\infty} f_{nm} q_m. \tag{35.14}$$

Here q_m are the coefficients in the expansion of the normal stresses on the contour in even Mathieu functions

$$q_m = \frac{1}{\pi} \int_0^{2\pi} \sigma_\rho |_{\rho=0} \operatorname{ce}_{2m}(\theta, k_1)\, d\theta,$$

$$\sigma_\rho |_{\rho=0} = \sum_{m=0}^{\infty} q_m \operatorname{ce}_{2m}(\theta, k_1),$$

$$\alpha_{nm} = \frac{1}{\pi} \int_0^{2\pi} \operatorname{se}'_{2m+2}(\theta, k_2) \operatorname{ce}_{2n}(\theta, k_1)\, d\theta + \frac{2k_2}{\pi} \int_0^{2\pi} \left[\sin\theta \operatorname{ce}_{2n}(\theta, k_1) \int_0^{\theta} \sin\theta_1 \operatorname{se}_{2m+2}(\theta_1, k_2)\, d\theta_1 \right] d\theta,$$

$$f_{nm} = \frac{1}{\pi} \int_0^{2\pi} \left[\sin\theta \operatorname{se}_{2n+2}(\theta, k_2) \int_{\pi/2}^{\theta} \sin\theta_1 \operatorname{ce}_{2m}(\theta_1, k_1)\, d\theta_1 \right] d\theta, \tag{35.15}$$

$$\beta_{nm} = \frac{1}{\pi} \int_0^{2\pi} \operatorname{ce}'_{2m}(\theta, k_1) \operatorname{se}_{2n+2}(\theta, k_2)\, d\theta + \frac{2k_2}{\pi} \int_0^{2\pi} \left[\sin\theta \operatorname{se}_{2n+2}(\theta, k_2) \int_{\pi/2}^{\theta} \sin\theta_1 \operatorname{ce}_{2m}(\theta_1, k_1)\, d\theta_1 \right] d\theta.$$

Thus, α_{nm}, β_{nm}, f_{nm} are the coefficients in the following expansions:

$$\mathrm{ce}'_{2m}(\theta, k_1) + 2k_2 \sin\theta \int_{\pi/2}^{\theta} \sin\theta\, \mathrm{ce}_{2m}(\theta, k_1)\, d\theta = \sum_{n=0}^{\infty} \beta_{nm}\, \mathrm{se}_{2n+2}(\theta, k_2),$$

$$\mathrm{se}'_{2m+2}(\theta, k_2) + 2k_2 \sin\theta \int_{0}^{\theta} \sin\theta\, \mathrm{se}_{2m+2}(\theta, k_2)\, d\theta = \sum_{n=0}^{\infty} \alpha_{nm}\, \mathrm{ce}_{2n}(\theta, k_1),$$

$$\sin\theta \int_{\pi/2}^{\theta} \sin\theta\, \mathrm{ce}_{2m}(\theta, k_1)\, d\theta = \sum_{n=0}^{\infty} f_{nm}\, \mathrm{se}_{2n+2}(\theta, k_2).$$

By using the expansions in Fourier series for the functions $\mathrm{ce}_{2n}(\theta, k_1)$ and $\mathrm{se}_{2n+2}(\theta, k_2)$, it may be shown that

$$\alpha_{nm} = \sum_{r=0}^{\infty} 2rA_{2r}^{(2n)} B_{2r}^{(2m+2)} + \frac{k_2}{2} \sum_{r=0}^{\infty} \frac{B_{2r+2}^{(2m+2)}}{(2r+1)(2r+3)} \times$$
$$\times [(2r+3) A_{2r}^{(2n)} + (2r+1) A_{2r+3}^{(2n)} - 4(r+1) A_{2r+2}^{(2n)}],$$

$$\beta_{nm} = -\alpha_{mn},$$

$$f_{nm} = -\frac{1}{2} A_0^{(2m)} B_2^{(2n+2)} +$$
$$+ \frac{1}{4} \sum_{r=1}^{\infty} \frac{A_{2r}^{(2m)}}{4r^2-1} [4rB_{2r}^{(2n+2)} - (2r-1) B_{2r+2}^{(2n+2)} -$$
$$- (2r+1) B_{2r-2}^{(2n+2)}].$$

Thus, our problem involving a given normal load on the contour of a cut is reduced to that of determining the constants C_n, D_n ($n = 0, 1, \ldots$) from two infinite systems (35.13) and (35.14).

Let us determine the normal stresses at points of the real axis on the prolongation of the cut

$$\sigma_\theta|_{\theta=0} = \frac{2\mu}{l^2 \sinh^3 \rho}\left[\sinh\rho\left(\frac{\partial^2\varphi}{\partial\theta^2} - \frac{\partial^2\psi}{\partial\rho\,\partial\theta}\right)_{\theta=0} + \right.$$
$$\left. + \cosh\rho\left(\frac{\partial\varphi}{\partial\rho} + \frac{\partial\psi}{\partial\theta}\right)_{\theta=0}\right] - \frac{\lambda\rho\omega^2\varphi}{\lambda+2\mu}\Big|_{\theta=0}. \quad (35.16)$$

With (35.16), the stress intensity factor K is $\left(\sqrt{S} = \sqrt{2l}\sinh\frac{\rho}{2}\right)$

$$K = \lim_{S\to 0}\left[\sqrt{2\pi S}\,\sigma_\theta|_{\theta=0}\right] = \frac{\mu\sqrt{\pi l}}{l^2}\lim_{\rho\to 0}\left(\frac{\partial^3\varphi}{\partial\rho\,\partial\theta^2} - \frac{\partial^3\psi}{\partial\rho^2\,\partial\theta}\right)_{\theta=0}.$$

Substituting the expressions for φ and ψ and passing to the limit, we obtain

$$K = \frac{\mu\sqrt{\pi l}}{l^2}\sum_{m=0}^{\infty}\left[C_m \operatorname{Fek}'_{2m}(0, k_1)\operatorname{ce}''_{2m}(0, k_1) - \right.$$
$$\left. - D_m \operatorname{Gek}''_{2m+2}(0, k_2)\operatorname{se}'_{2m+2}(0, k_2)\right]. \quad (35.17)$$

Taking into account the relations [167]

$$\operatorname{ce}''_{2m}(0, k_1) = (2k_1 - a_{2m})\operatorname{ce}_{2m}(0, k_1),$$
$$\operatorname{Gek}''_{2m+2}(0, k_2) = (b_{2m+2} - 2k_2)\operatorname{Gek}_{2m+2}(0, k_2),$$

expression (35.17) may be written as

$$K = \frac{\mu\sqrt{\pi l}}{l^2}\sum_{m=0}^{\infty}\left[C_m \operatorname{Fek}'_{2m}(0, k_1)(2k_1 - a_{2m})\operatorname{ce}_{2m}(0, k_1) - \right.$$
$$\left. - D_m \operatorname{Gek}_{2m+2}(0, k_2)(b_{2m+2} - 2k)\operatorname{se}'_{2m+2}(0, k_2)\right]. \quad (35.18)$$

Here a_{2m}, b_{2m+2} are the eigenvalues of the Mathieu functions $\operatorname{ce}_{2m}(\theta, k_1)$, $\operatorname{se}_{2m+2}(\theta, k_2)$, respectively.

In calculating, for example, the stress intensity factor according to (35.18) the main difficulty lies in solving systems (35.13) and (35.14). However, for small values of k_1 and k_2 the solution is simplified [223].

For real materials the values of the arguments k_1 and k_2 of the Mathieu functions in terms of which the solution is

represented are as follows:

$$k_1 = \frac{\omega^2 l^2 \rho_0}{4(\lambda + 2\mu)} \sim 0.74 \times 10^{-12} (\omega l)^2,$$

$$k_2 = \frac{\omega^2 l^2 \rho_0}{4\mu} \sim 2.5 \times 10^{-12} (\omega l)^2.$$

Thus, notwithstanding the requirement that k_1 and k_2 should be small, it is possible to investigate a wide, and the most important (in contrast to diffraction problems), range of frequency considered here (at least up to $\omega l \sim 10^5$).

For small values of k_1 and k_2 use can be made of the asymptotic formulas for calculating the Mathieu functions and of the well-known relations

$$\mathrm{Fek}'_{2m}(0, k_1) = -\frac{1}{2}\mathrm{Fey}'_{2m}(0, k_1) = -\frac{1}{\pi}\frac{p_{2m}}{A_0^{(2m)}}\mathrm{ce}_{2m}\left(\frac{\pi}{2}, k_1\right),$$

$$\mathrm{Gek}_{2m+2}(0, k_2) = -\frac{1}{2}\mathrm{Gey}_{2m+2}(0, k_2) = \frac{1}{\pi}\frac{s_{2m+2}\,\mathrm{se}'_{2m+2}\left(\frac{\pi}{2}, k_2\right)}{k_2 B_2^{(2m+2)}},$$

$$\mathrm{Fek}_0(0, k_1) \cong -\frac{\sqrt{2}}{4\pi}\ln k_1,$$

$$\mathrm{Fek}_{2m}(0, k_1) = -\frac{1}{2}\mathrm{Fey}_{2m}(0, k_1) + \frac{i}{2}\mathrm{ce}_{2m}(0, k_1) \cong -\frac{1}{2\pi}2^{4m-1}(2m-1)!\,(2m)!\,\frac{1}{k_1^{2m}} + \frac{i}{2}\mathrm{ce}_{2m}(0, k_1),$$

$$\mathrm{Gek}'_{2m+2}(0, k_2) = -\frac{1}{2}\mathrm{Gey}'_{2m+3}(0, k_2) + \frac{i}{2}\mathrm{se}'_{2m+2}(0, k_2) \cong -\frac{1}{2\pi}2^{4m+3}[(2m+2)!]^2\frac{1}{k_2^{2m}} + \frac{i}{2}\mathrm{se}'_{2m+2}(0, k_2).$$

The results of the numerical calculation of the non-dimensional quantity $\left|\frac{K}{q\sqrt{l}}\right|$ as a function of $\omega l/c_1$ are presented in Fig. 35.1 for $q(\theta) = q =$ constant.

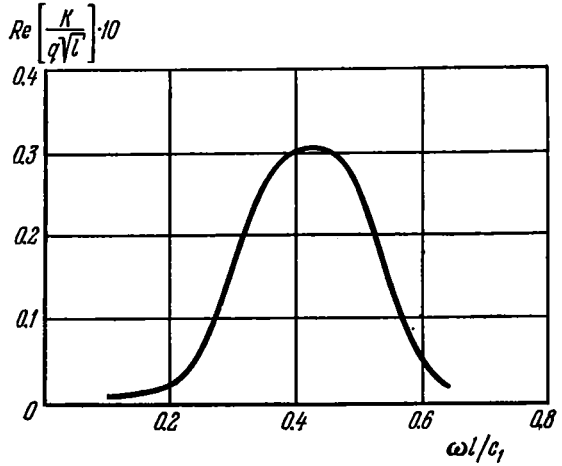

Fig. 35.1. Relation between the stress intensity factor K and the wave number $\omega l/c_1$ for $\nu = 0.3$.

The result obtained here is supported by the analysis of G. C. Sih and J. F. Loeber [254].

36. THE DYNAMIC PROBLEM FOR A LONGITUDINAL SHEAR CRACK

Consider an elastic isotropic infinite body with a thin internal 'tunnel' crack (Fig. 36.1) subjected to dynamic shearing forces $\tau(x)\, e^{i\omega t}$. In this case shear occurs in a direction perpendicular to a possible crack propagation. In accordance with the classification given in Sec. 2 the case being studied belongs to mode III, which is also called pure shear or antiplane strain. A demand for a thorough analytic study of this kind of crack was indicated, for example, in [165].

We present the solution of this problem found by N. M. Borodachev [30] in elliptic co-ordinates and repre-

sentable, as in the preceding sections, in series in Mathieu functions.

The solution of the static problem for an infinite body with a crack of this kind is known [221].

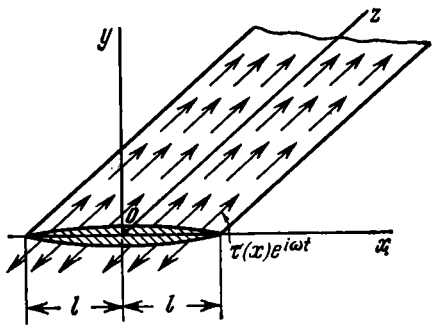

Fig. 36.1. Loading scheme for an infinite body with a crack.

Suppose that a shearing force $\tau(x)\, e^{i\omega t}$ is applied to the faces of a crack $|x| \leqslant l$, $y = 0$. To simplify the problem we assume that $\tau(x)$ is an even function of x.

In the case of pure shear

$$u = v = 0, \quad w = w(x, y, t). \tag{36.1}$$

Here, as usual, u, v, and w are the projections of the displacement vector on the x, y, and z axes, respectively.

In the absence of body forces the displacement w satisfies the differential equation

$$\frac{\partial^2 w}{\partial x^2} + \frac{\partial^2 w}{\partial y^2} = \frac{1}{c_2^2}\frac{\partial^2 w}{\partial t^2}, \tag{36.2}$$

where $c_2 = (G/\rho)^{1/2}$ is the velocity of shear wave.

In this case the non-vanishing components of the stress tensor are given by

$$\tau_{xz} = \mu\frac{\partial w}{\partial x}, \qquad \tau_{yz} = \mu\frac{\partial w}{\partial y}. \tag{36.3}$$

By considering steady-state periodic vibrations with circular frequency ω, we assume

$$w(x, y, t) = w^*(x, y)\, e^{i\omega t}.$$

Equation (36.2) then becomes

$$\frac{\partial^2 w^*}{\partial x^2}+\frac{\partial^2 w^*}{\partial y^2}+k_2^2 w^*=0, \quad k_2^2=\frac{\omega^2}{c_2^2}. \tag{36.4}$$

The boundary conditions when $y = 0$ are as follows:

(1) $\tau_{zy}^*(x, 0) = -\tau(x), \ |x| < l; \ w^*(x, 0) = 0,$

$$|x| > l; \tag{36.5}$$

(2) $\tau_{zy}(x, y, t) = \tau_{zy}^*(x, y)\, e^{i\omega t}$.

In addition to conditions (36.5) we must also satisfy the conditions for radiation (the conditions at infinity), which, as is known, require that the (displacement, stress) field at infinity should represent a diverging wave.

Thus, the problem under consideration is reduced to that of finding the solution of Eq. (36.4) satisfying the boundary conditions (36.5) and the condition for radiation.

We introduce elliptic co-ordinates defined by the relation

$$x + iy = l \cosh(\xi + i\eta).$$

In elliptic co-ordinates the crack ($|x| < l$, $y = 0$) is characterized by the fact that $\xi = 0$ for it. Equation (36.4) in these co-ordinates is of the form

$$\frac{\partial^2 w^*}{\partial \xi^2}+\frac{\partial^2 w^*}{\partial \eta^2}+2k^2(\cosh 2\xi-\cos 2\eta)\, w^*=0,$$

$$2k=k_2 l. \tag{36.6}$$

The solution of Eq. (36.6) is sought in the form

$$w^*(\xi, \eta)=\sum_{n=0}^{\infty} C_n \operatorname{Ne}_{2n+1}^{(2)}(\xi, q)\, \operatorname{se}_{2n+1}(\eta, q). \tag{36.7}$$

Here $q = k^2$, $\operatorname{se}_{2n+1}(\eta, q)$ are periodic Mathieu functions of integral order, $\operatorname{Ne}_{2n+1}^{(2)}(\xi, q)$ are modified Mathieu functions [167], C_n are constants.

By using the properties of Mathieu functions [167], we verify that solution (36.7) satisfies the differential equation (36.6), the conditions for radiation, and the second boundary condition of (36.5). Moreover, it satisfies the symmetry and periodicity conditions. The first condition of (36.5) in elliptic co-ordinates is

$$\tau_{zy}^* = -\tau(l \cos \eta) \text{ when } \xi = 0. \tag{36.8}$$

With the use of formula (36.7) for the determination of displacements at any point we can also calculate the stresses τ_{zy} at any point of the body. In particular, when $\xi = 0$ we have

$$\tau_{zy}^*(0, \eta) = \frac{\mu}{l \sin \eta} \sum_{n=0}^{\infty} C_n \operatorname{Ne}_{2n+1}^{(2)\prime}(0, q) \operatorname{se}_{2n+1}(\eta, q). \tag{36.9}$$

We can now satisfy the boundary condition (36.8). Since the function $\tau_{zy}^*(0, \eta)$ is known, we write down the following expansion:

$$\sin \eta \tau_{zy}^*(0, \eta) = \sum_{n=0}^{\infty} \tau_n \operatorname{se}_{2n+1}(\eta, q). \tag{36.10}$$

Here

$$\tau_n = \frac{1}{\pi} \int_0^{2\pi} \sin \eta \tau_{zy}^*(0, \eta) \operatorname{se}_{2n+1}(\eta, q)\, d\eta. \tag{36.11}$$

By comparing (36.9) and (36.10), we find

$$C_n = \frac{\tau_n l}{\mu \operatorname{Ne}_{2n+1}^{(2)\prime}(0, q)}.$$

With this relation, formula (36.7) takes the form

$$w^*(\xi, \eta) = \frac{l}{\mu} \sum_{n=0}^{\infty} \frac{\tau_n}{\operatorname{Ne}_{2n+1}^{(2)\prime}(0, q)} \operatorname{Ne}_{2n+1}^{(2)}(\xi, q) \operatorname{se}_{2n+1}(\eta, q). \tag{36.12}$$

Further we shall need the expression for τ_{zy}^* when $\eta = 0$. By using (36.12), we obtain

$$\tau_{zy}^*(\xi, 0) = \frac{1}{\sinh \xi} \sum_{n=0}^{\infty} \tau_n \frac{\operatorname{se}_{2n+1}'(0, q)}{\operatorname{Ne}_{2n+1}^{(2)\prime}(0, q)} \operatorname{Ne}_{2n+1}^{(2)}(\xi, q). \tag{36.13}$$

The stress intensity factor in the case of pure shear is

$$K_{\mathrm{III}}(t) = \lim_{x \to l+0} \sqrt{2\pi(x-l)}\, \tau_{zy}(x, 0, t).$$

In the case of steady-state periodic vibrations

$$K_{\mathrm{III}}(t) = K_{\mathrm{III}}^* e^{i\omega t},$$

where K^*_{III} is the complex amplitude of the stress intensity factor.

Since the distance from the crack tip (along the x axis) is

$$x|_{\eta=0} - l = l\cosh\xi - l = 2l\sinh^2\frac{\xi}{2},$$

we have

$$K^*_{III} = 2\sqrt{\pi l}\lim_{\xi\to 0}\left[\sinh\frac{\xi}{2}\tau^*_{zy}(\xi, 0)\right]. \qquad (36.14)$$

Substituting the expression for $\tau^*_{zy}(\xi, 0)$ from (36.13) in (36.14) and opening the indeterminacy, we obtain

$$K^*_{III} = 2i\pi^{-1/2}l^{1/2}\sum_{n=0}^{\infty}\tau_n\frac{s^2_{2n+1}}{\mathrm{Ne}^{(2)\prime}_{2n+1}(0, q)}. \qquad (36.15)$$

Here

$$s_{2n+1} = \frac{\mathrm{se}'_{2n+1}(0, q)\,\mathrm{se}_{2n+1}(\pi/2, q)}{q^{1/2}B_1^{(2n+1)}},$$

where $B_1^{(2n+1)}$ is the coefficient of the first term in the sine-series expansion of the function $\mathrm{se}_{2n+1}(\eta, q)$.

Since K^* is a complex quantity, we assume

$$K^*_{III} = K^{(1)}_{III} + iK^{(2)}_{III} = K_0 e^{-i\delta}, \qquad (36.16)$$

where

$$K_0 = \sqrt{(K^{(1)}_{III})^2 + (K^{(2)}_{III})^2}, \quad \delta = -\arctan\frac{K^{(2)}_{III}}{K^{(1)}_{III}}.$$

Thus,

$$K_{III}(t) = K_0 e^{i(\omega t - \delta)}. \qquad (36.17)$$

With the help of the last formula one can determine the stress intensity factor for an infinite elastic body with a crack of the kind considered here in the case of steady-state vibrations. If shearing forces $\tau(x)\cos\omega t$ are applied to the faces of the crack, the stress intensity factor is $K_0\cos(\omega t - \delta)$.

Taking into account that

$$\mathrm{Ne}^{(2)}_{2n+1}(\xi, q) = \mathrm{Se}_{2n+1}(\xi, q) - i\,\mathrm{Gey}_{2n+1}(\xi, q)$$

and using (36.15) and (36.16), we find

$$K_{\mathrm{III}}^{(1)} = -2\left(\frac{l}{\pi}\right)^{1/2} \sum_{n=0}^{\infty} \frac{\tau_n s_{2n+1}^2 \operatorname{Gey}'_{2n+1}(0, q)}{\Omega_{2n+1}(q)},$$

$$K_{\mathrm{III}}^{(2)} = 2\left(\frac{l}{\pi}\right)^{1/2} \sum_{n=0}^{\infty} \frac{\tau_n s_{2n+1}^2 \operatorname{Se}'_{2n+1}(0, q)}{\Omega_{2n+1}(q)}. \tag{36.18}$$

Here

$$\Omega_{2n+1}(q) = [\operatorname{Se}'_{2n+1}(0, q)]^2 + [\operatorname{Gey}'_{2n+1}(0, q)]^2.$$

In performing calculations by these formulas it is necessary to use tables for evaluating Mathieu functions [268].

Consider a numerical example illustrating the results obtained. Let

$$\tau(x) = \tau = \text{constant when } |x| < l,$$

i.e., the shearing forces are uniformly distributed over the faces of the crack. In this case

$$\tau_{zy}^*(0, \eta) = -\tau = \text{constant when } 0 < \eta < 2\pi$$

and on the basis of (36.11)

$$\tau_n = -\frac{\tau}{\pi} \int_0^{2\pi} \sin\eta \operatorname{se}_{2n+1}(\eta, q)\, d\eta.$$

By evaluating the above integral, we find

$$\tau_n = -\tau B_1^{(2n+1)}.$$

Formulas (36.18) become, in this case,

$$K_{\mathrm{III}}^{(1)} = 2\tau\left(\frac{l}{\pi}\right)^{1/2} \sum_{n=0}^{\infty} \frac{B_1^{(2n+1)} s_{2n+1}^2 \operatorname{Gey}'_{2n+1}(0, q)}{\Omega_{2n+1}(q)},$$

$$K_{\mathrm{III}}^{(2)} = -2\tau\left(\frac{l}{\pi}\right)^{1/2} \sum_{n=0}^{\infty} \frac{B_1^{(2n+1)} s_{2n+1}^2 \operatorname{Se}'_{2n+1}(0, q)}{\Omega_{2n+1}(q)}.$$

These formulas were used to calculate $K_{\mathrm{III}}^{(1)}$ and $K_{\mathrm{III}}^{(2)}$ for several values of the non-dimensional parameter $q = \omega^2 l^2/4c_2^2$. (As noted, in practice $0 \leqslant q < 2$.) Then the values of K_0 and δ were found by formulas (36.16). In this case it is advisable to represent the formula for K_0 as

$$K_0 = \alpha\tau\sqrt{\pi l}.$$

Figure 36.2 shows the α-q and δ-q relations (the values of δ are given in radians). As $\omega \to 0$ and hence $q \to 0$, we obtain the well-known results relating to the static problem.

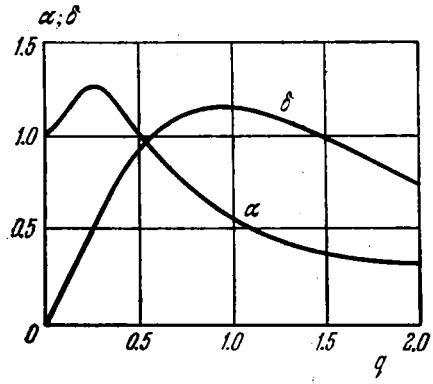

Fig. 36.2. Variation of the parameters α and δ with q.

37. THE PLANE PROBLEM OF STEADY-STATE VIBRATIONS FOR A STRIP WITH A CUT

1. Consider now, following [228], a strip $-\infty < y < \infty$, $|x| \leqslant L$ with a cut of length $2l$ along the real axis which is symmetrical about the y axis. The sides of the cut are acted on by a time-periodic normal load $p = q \exp(i\omega t)$, $q =$ constant when $|x| \leqslant l$.

The amplitude values of displacements and stresses in the system of Cartesian co-ordinates x, y are determined with the help of the functions φ and ψ by the formulas [257]

$$
\begin{gathered}
u = \frac{\partial\varphi}{\partial x} + \frac{\partial\psi}{\partial y}, \qquad v = \frac{\partial\varphi}{\partial y} - \frac{\partial\psi}{\partial x}, \\
\sigma_x = 2\mu \frac{\partial}{\partial x}\left(\frac{\partial\varphi}{\partial x} + \frac{\partial\psi}{\partial y}\right) - \lambda \frac{\omega^2}{c_1^2}\varphi, \\
\sigma_y = -2\mu \frac{\partial}{\partial x}\left(\frac{\partial\varphi}{\partial x} + \frac{\partial\psi}{\partial y}\right) - (\lambda + 2\mu)\frac{\omega^2}{c_1^2}\varphi, \\
\tau_{xy} = 2\mu \frac{\partial}{\partial x}\left(\frac{\partial\varphi}{\partial y} - \frac{\partial\psi}{\partial x}\right) - \mu \frac{\omega^2}{c_2^2}\psi.
\end{gathered}
\tag{37.1}
$$

Here c_1 and c_2 are, as before, the velocities of longitudinal and transverse waves, respectively. The functions φ and ψ

satisfy the equations

$$\nabla^2\varphi+\frac{\omega^2}{c_1^2}\varphi=0,\quad \nabla^2\psi+\frac{\omega^2}{c_2^2}\psi=0,\quad \nabla^2=\frac{\partial^2}{\partial x^2}+\frac{\partial^2}{\partial y^2}. \tag{37.2}$$

By using the symmetry of the state of stress and the conditions at infinity, we represent the functions φ and ψ as

$$\varphi(x,\ y)=\sum_{n=1}^{\infty} A_n \exp\left(-\sqrt{\alpha_n^2-\frac{\omega^2}{c_1^2}}\,y\right)\cos\alpha_n x,$$

$$\alpha_n=\frac{(2n-1)\pi}{2L}, \tag{37.3}$$

$$\psi(x,\ y)=\sum_{n=1}^{\infty} B_n \exp\left(-\sqrt{\alpha_n^2-\frac{\omega^2}{c_2^2}}\,y\right)\sin\alpha_n x.$$

The following conditions are fulfilled on the straight boundaries of the strip:

$$\begin{gathered}\sigma_x(\pm L,\ y)=0,\ \tau_{xy}(\pm L,\ y)\neq 0,\\ v(\pm L,\ y)=0,\ u(\pm L,\ y)\neq 0,\ -\infty<y<\infty;\end{gathered} \tag{37.4}$$

these conditions are realized if the edges of the strip are reinforced with inextensible stiffener of zero bending stiffness. Similar conditions arise in solving the problem of a punch acting on a strip when the size of the contact area is not small compared with the strip width [29].

The coefficients A_n and B_n in expansions (37.3) are found from the boundary conditions on the contour of the cut

$$\begin{gathered}\tau_{xy}(x,\ 0)=0,\ \sigma_y(x,\ 0)=-q,\ \text{when } |x|<l,\\ v(x,\ 0)=0 \text{ when } l<|x|<L.\end{gathered} \tag{37.5}$$

By satisfying (37.5), we obtain

$$A_n=-B_n\frac{\left(2\alpha_n^2-\frac{\omega^2}{c_2^2}\right)}{2\alpha_n\sqrt{\alpha_n^2-\frac{\omega^2}{c_1^2}}}, \tag{37.6}$$

$$\sigma_y(x,\ 0)=2\mu\sum_{n=1}^{\infty} B_n\left[\sqrt{1-\frac{\omega^2}{\alpha_n^2c_2^2}}-\frac{\left(1-\frac{\omega^2}{2\alpha_n^2c_2^2}\right)^2}{\sqrt{1-\frac{\omega^2}{\alpha_n^2c_1^2}}}\right]\times$$

$$\times\alpha_n^2\cos\alpha_n x=-q\quad (x<l),$$

$$v(x, 0) = -\frac{\omega^2}{2c_2^2} \sum_{n=1}^{\infty} \frac{B_n}{\alpha_n} \cos \alpha_n x = 0 \quad (l < x < L). \tag{37.7}$$

Suppose that the frequency of the applied load is such that the following conditions are fulfilled:

$$\frac{\omega^2}{\alpha_n^2 c_1^2} < 1, \quad \frac{\omega^2}{\alpha_n^2 c_2^2} < 1 \quad (n = 1, 2, \ldots);$$

hence, the following expansions hold:

$$\sqrt{1 - \frac{\omega^2}{\alpha_n^2 c_1^2}} = \sum_{k=0}^{\infty} d_k \left(\frac{\omega^2}{\alpha_n^2 c_1^2}\right)^k,$$

$$\sqrt{1 - \frac{\omega^2}{\alpha_n^2 c_2^2}} = \sum_{k=0}^{\infty} d_k \left(\frac{\omega^2}{\alpha_n^2 c_2^2}\right)^k \quad (d_0 = 1), \tag{37.8}$$

$$\sqrt{1 - \frac{\omega^2}{\alpha_n^2 c_2^2}} - \frac{\left(1 - \frac{\omega^2}{2\alpha_n^2 c_2^2}\right)^2}{\sqrt{1 - \frac{\omega^2}{\alpha_n^2 c_1^2}}} = -\sum_{k=1}^{\infty} D_k \left(\frac{\omega^2}{\alpha_n^2 c_1^2}\right)^k,$$

where

$$D_k = d_k \left(\frac{c_1^2}{c_2^2}\right)^k + 2(k+1) d_{k+1} - 2k d_k \left(\frac{c_1^2}{c_2^2}\right) + \\ + \frac{1}{2}(k-1) d_{k-1} \left(\frac{c_1^2}{c_2^2}\right)^2.$$

With (37.8), equalities (37.7) are written as

$$\sum_{n=1}^{\infty} \sum_{k=1}^{\infty} D_n \left(\frac{\omega^2}{\alpha_n^2 c_1^2}\right)^{k-1} \alpha_n B_n^* \cos \alpha_n x = \frac{q}{2\mu} \frac{c_1^2}{\omega^2} \quad (0 \leqslant x < l),$$

$$\sum_{n=1}^{\infty} B_n^* \cos \alpha_n x = 0 \quad (l < x < L). \tag{37.9}$$

Here $B_n^* = B_n/\alpha_n$.

The coefficients B_n^* are sought in the form of a series

$$B_n^* = B_{n(-1)}^* \left(\frac{c_1^2}{\omega^2}\right) + B_{n(0)}^* + B_{n(1)}^* \left(\frac{\omega^2}{c_1^2}\right) + \ldots \tag{37.10}$$

Substituting (37.10) in (37.9) and comparing the coefficients of like powers of ω^2/c_1^2, we obtain a sequence of dual trigonometric series for finding $B^*_{n(-1)}$, $B^*_{n(0)}$, $B^*_{n(1)}$, . . .

$$\sum_{n=1}^{\infty} (2n-1)\, B^*_{n(-1)} \cos (2n-1) \frac{\xi}{2} = \left(\frac{2L}{\pi}\right) \frac{q}{2\mu D_1}$$

$$(0 \leqslant \xi < \xi_0), \tag{37.11}$$

$$\sum_{n=1}^{\infty} B^*_{n(-1)} \cos (2n-1) \frac{\xi}{2} = 0 \quad (\xi_0 < \xi < \pi),$$

$$\sum_{n=1}^{\infty} (2n-1)\, B^*_{n(0)} \cos (2n-1) \frac{\xi}{2} =$$

$$= -\frac{D_2}{D_1} \left(\frac{2L}{\pi}\right)^2 \sum_{n=1}^{\infty} B^*_{n(-1)} \frac{\cos \frac{1}{2} (2n-1) \xi}{2n-1} \quad (0 \leqslant \xi < \xi_0),$$

$$\tag{37.12}$$

$$\sum_{n=1}^{\infty} B^*_{n(0)} \cos \frac{1}{2} (2n-1) \xi = 0 \quad (\xi_0 < \xi < \pi),$$

$$\sum_{n=1}^{\infty} (2n-1)\, B^*_{n(1)} \cos \frac{1}{2} (2n-1) \xi =$$

$$= -\frac{D_2}{D_1} \left(\frac{2L}{\pi}\right)^2 \sum_{n=0}^{\infty} B^*_{n(0)} \frac{\cos \frac{1}{2} (2n-1) \xi}{2n-1} -$$

$$-\frac{D_3}{D_1} \left(\frac{2L}{\pi}\right)^4 \sum_{n=1}^{\infty} B^*_{n(-1)} \frac{\cos \frac{1}{2} (2n-1) \xi}{(2n-1)^3} \quad 0 \leqslant \xi < \xi_0, \tag{37.13}$$

$$\sum_{n=1}^{\infty} B^*_{n(1)} \cos \frac{1}{2} (2n-1) \xi = 0 \quad (\xi_0 < \xi < \pi),$$

. . . . . .

Here

$$\xi = \frac{\pi x}{L}, \quad \xi_0 = \frac{\pi l}{L}.$$

In the following discussion we limit series (37.10) to three terms. According to (37.7), (37.8), and (37.10) the normal stresses on the prolongation of the cut are then determined by the formula

$$\frac{1}{2\mu}\sigma_y(x, 0) = -D_1\left(\frac{\pi}{2L}\right)\sum_{n=1}^{\infty} B^*_{n(-1)}(2n-1)\cos\frac{1}{2}\times$$
$$\times(2n-1)\xi - \left(\frac{\omega^2}{c_1^2}\right)\sum_{n=1}^{\infty}\left[D_2\left(\frac{2L}{\pi}\right)\frac{B^*_{n(-1)}}{(2n-1)} + \right.$$
$$\left. + D_1\left(\frac{\pi}{2L}\right)B^*_{n(0)}(2n-1)\right]\cos\frac{1}{2}(2n-1)\xi -$$
$$-\left(\frac{\omega^2}{c_1^2}\right)^2\sum_{n=1}^{\infty}\left[D_3\left(\frac{2L}{\pi}\right)^3\frac{B^*_{n(-1)}}{(2n-1)^3} + D_2\left(\frac{2L}{\pi}\right)\frac{B^*_{n(0)}}{(2n-1)} + \right.$$
$$\left. + D_1\left(\frac{\pi}{2L}\right)B^*_{n(1)}(2n-1)\right]\cos\frac{1}{2}(2n-1)\xi - \ldots \quad (37.14)$$

2. Consider dual trigonometric series of the form

$$\sum_{n=1}^{\infty}(2n-1)B^*_{n(j)}\cos\frac{1}{2}(2n-1)\xi = f_j(\xi)$$
$$(0 \leqslant \xi \leqslant \xi_0),$$
$$\sum_{n=1}^{\infty} B^*_{n(j)}\cos\frac{1}{2}(2n-1)\xi = 0 \quad (37.15)$$
$$(\xi_0 \leqslant \xi \leqslant \pi, \quad j = -1, 0, 1, 2, \ldots).$$

According to [273], the coefficients $B^*_{n(j)}$ are determined as follows:

$$B^*_{n(j)} = 2\sin\frac{\xi_0}{2}\int_0^1 F\left(n, 1-n; 1; s^2\sin^2\frac{\xi_0}{2}\right)X_j(s)\,ds. \quad (37.16)$$

Here $F(n, 1-n; 1; x)$ is a hypergeometric function,

$$X_j(s) = \frac{2}{\pi}\sin\frac{\xi_0}{2}s\int_0^s \frac{f_j\left[2\arcsin\left(\rho\sin\frac{\xi_0}{2}\right)\right]d\rho}{(s^2-\rho^2)^{1/2}\left(1-\rho^2\sin^2\frac{\xi_0}{2}\right)^{1/2}}. \quad (37.17)$$

In order to find the value of the sum of the first of series (37.15) for $\xi > \xi_0$, we proceed as follows. According to [273],

$$\sum_{n=1}^{\infty} F\left(n,\ 1-n;\ 1;\ s^2 \sin^2 \frac{\xi_0}{2}\right) \sin \frac{1}{2}(2n-1)\xi =$$

$$= \begin{cases} 0, & \sin\frac{\xi}{2} < s \sin\frac{\xi_0}{2}, \\ \left(\sin^2\frac{\xi}{2} - s^2 \sin^2\frac{\xi_0}{2}\right)^{1/2}, & \sin\frac{\xi}{2} > s\sin\frac{\xi_0}{2}. \end{cases} \tag{37.18}$$

We now differentiate (37.18) with respect to ξ, multiply the result obtained by $X_j(s)$ and integrate with respect to s between the limits 0 and 1. Then

$$\sum_{n=1}^{\infty} (2n-1) B^*_{n(j)} \cos \frac{1}{2}(2n-1)\xi =$$

$$= \begin{cases} f_j(\xi), & 0 \leqslant \xi < \xi_0, \\ -\frac{1}{2}\sin\frac{\xi_0}{2}\sin\xi \int\limits_0^1 \dfrac{X_j(s)\,ds}{\left(\sin^2\frac{\xi}{2} - s^2\sin^2\frac{\xi_0}{2}\right)^{1/2}}, & \\ & \xi_0 < \xi < \pi. \end{cases} \tag{37.19}$$

From this equality it follows that the sum of series (37.19) has, as $\xi \to \xi_0 + 0$, a singularity of the form

$$\left[\sum_{n=1}^{\infty} (2n-1) B^*_{n(j)} \cos \frac{1}{2}(2n-1)\xi\right]_{\xi > \xi_0} =$$

$$= -\frac{1}{2} \frac{\sin\xi}{\sin\frac{\xi_0}{2}} \frac{X_{(j)}(1)}{\left(\sin^2\frac{\xi}{2} - \sin^2\frac{\xi_0}{2}\right)^{1/2}}. \tag{37.20}$$

Taking into account that the series

$$\sum_{n=1}^{\infty} \frac{B^*_{n(j)}}{(2n-1)^k} \cos \frac{1}{2}(2n-1)\xi \quad (k = 1, 2, 3, \ldots) \tag{37.21}$$

are continuous functions when $\xi = \xi_0$, we find, according to (37.14) and (37.20), the following expression for the

stress intensity factor:

$$K = \lim_{x \to l} \sqrt{2\pi (x - l)}\, \sigma_y (x, 0) =$$

$$= \mu D_1 (4L \sin \xi_0)^{1/2} \frac{1}{\sin \frac{\xi_0}{2}} \left(\frac{\pi}{2L}\right) \sum_{j=0}^{\infty} \left(\frac{\omega^2}{c_1^2}\right)^j X_{j-1}(1). \quad (37.22)$$

The coefficients $X_j(1)$ $(j = -1, 0, 1, 2, \ldots)$ are successively determined by formula (37.17), where $f_j(\xi)$ is the right-hand side of the corresponding dual series (37.11) to (37.13). The series of the form of (37.21), which enter into the expressions for $f_0(\xi)$, $f_1(\xi)$, ..., can be summed on the basis of equality (37.19). For example, the value of the sum of series (37.21) with $k = 1$ is found by integrating (37.19) with respect to ξ first from 0 to ξ and then from π to ξ.

We present the final expression for the stress intensity factor at the point $\xi = \xi_0$ with three terms in expansion (37.22)

$$K = \frac{q}{\pi} (4L \sin \xi_0)^{1/2} \left\{ N\left(\sin \frac{\xi_0}{2}\right) + \right.$$

$$+ \left(\frac{\omega 2L}{\pi c_1}\right)^2 \frac{D_2}{D_1} \left[\frac{1}{8} G_2(1, \xi_0) - a_0 N\left(\sin \frac{\xi_0}{2}\right)\right] +$$

$$+ \left(\frac{\omega 2L}{\pi c_1}\right)^4 \left[\left(\frac{D_2^2}{D_1^2} a_0^2 - \frac{D_2}{D_1} a_1 - \frac{D_3}{D_1} b_0\right) N\left(\sin \frac{\xi_0}{2}\right) + \right.$$

$$\left. + \left(\frac{D_2^2}{D_1^2} + \frac{D_3}{D_1}\right) \frac{1}{8} a_0 G_2(1, \xi_0) - \frac{1}{384} G_4(1, \xi_0)\right]. \quad (37.23)$$

Here use has been made of the notation $\left[F(\varphi, x)\right.$ is the elliptic integral of the first kind, $\left.F(x) = F\left(\frac{\pi}{2}, x\right)\right]$

$$G_{2k} = \int_0^s \frac{\left[2 \arcsin\left(\rho \sin \frac{\xi_0}{2}\right)\right]^{2k} d\rho}{(s^2 - \rho^2)^{1/2} \left(1 - \rho^2 \sin^2 \frac{\xi_0}{2}\right)^{1/2}} \quad (k = 1, 2),$$

$$a_0 = \frac{1}{4}\left[M(\xi_0, \xi_0) - (\pi - \xi_0) N(\xi_0) + \frac{1}{2} \xi_0 (2\pi - \xi_0)\right],$$

$$a_1 = \frac{1}{32}\left[M_1(\xi_0, \xi_0) - (\pi - \xi_0) N_1(\xi_0) + \frac{1}{12} \xi_0^2 (4\pi - 3\xi_0)\right],$$

$$b_0 = \frac{1}{16}\left[\frac{1}{2}\xi_0(2\pi - \xi_0) M(\xi_0, \xi_0) - \frac{1}{6}(\xi_0^3 - 3\pi\xi_0^2 + \right.$$

$$\left. + 2\pi^2) N(\xi_0) + \frac{1}{24}\xi_0(\xi_0^3 - 4\xi_0^2\pi + 8\pi^3) - \int_\pi^{\xi_0} d\xi \int_{\xi_0}^{\xi} M(\xi, \xi_0)\, d\xi,\right.$$

$$N(\xi_0) = \frac{4}{\pi}\sin\frac{\xi_0}{2}\int_0^1 \frac{sN\left(s\sin\frac{\xi_0}{2}\right) ds}{(1-s^2)^{1/2}},$$

$$N_1(\xi_0) = \frac{4}{\pi}\sin\frac{\xi_0}{2}\int_0^1 \frac{sG_2(s, \xi_0)\, ds}{(1+s^2)^{1/2}},$$

$$M(\xi, \xi_0) = \frac{8}{\pi}\sin\frac{\xi_0}{2}\int_0^1 sF[a(s), b(s)]\, N\left(s\sin\frac{\xi_0}{2}\right) ds,$$

$$a(s) = \arcsin\frac{\cos\frac{\xi}{2}}{\sqrt{1 - s^2\sin^2\frac{\xi_0}{2}}},$$

$$M_1(\xi, \xi_0) = \frac{8}{\pi}\sin\frac{\xi_0}{2}\int_0^1 sF[a(s), b(s)]\, G_2(s, \xi_0)\, ds,$$

$$b(s) = \sqrt{1 - s^2\sin^2\frac{\xi_0}{2}}.$$

With (37.23), from the condition of limiting equilibrium (3.11), which is preserved in the case of dynamic loads [47], we obtain the relation between the crack length and the applied load. Figure 37.1 presents curves showing this relation for several frequencies $\left[\omega^* = \frac{\omega}{c_1}\left(\frac{2L}{\pi}\right)\right]$ of the external load ($\nu = 1/3$). Line *1* corresponds to the static case $\omega^* = 0$. The solution developed above shows that over a wide frequency range the inertia effect acts to reduce the value of the fracture load for a given crack length. It is easy to see from (37.23) that as $l/L \to 1$, $\frac{2}{\pi}\frac{q}{K_c}\sqrt{L} \to 0$, which corresponds to a complete fracture of the strip.

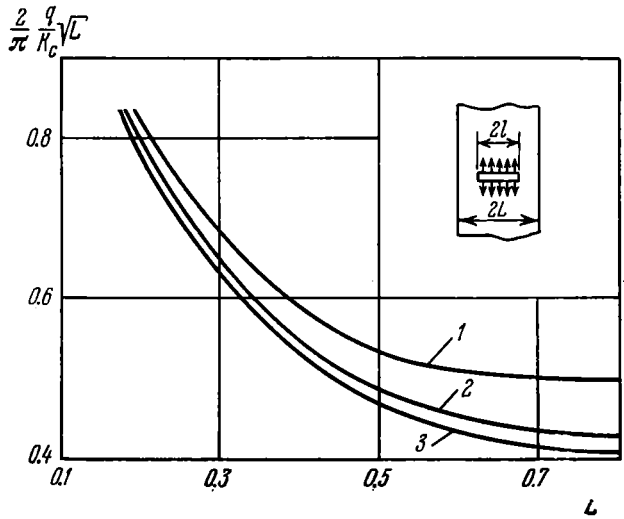

Fig. 37.1. Relation between the load amplitude and the crack length for several frequencies. *1*, $\omega^* = 0$ (static case); *2*, $\omega^* = 0.274$; *3*, $\omega^* = 0.316$.

38. STEADY-STATE VIBRATIONS OF AN INFINITE PLANE WITH A PERIODIC SYSTEM OF CUTS ALONG AN AXIS

Before proceeding to the formulation of the problem indicated in the heading, we shall consider one class of dual trigonometric series to which it is usual to reduce some of the static and dynamic problems of slits and punches [144]. The possibility of obtaining the solution was indicated by C. J. Tranter [274]. Here a different method of solution is proposed, which is better suited to applications and provides a means for obtaining asymptotic expressions that will subsequently be needed, for series with isolated singularities at points of discontinuity in the boundary conditions.

1. Consider dual trigonometric series of the form

$$\begin{gathered}\sum_{n=1}^{\infty} nB_n^* \cos n\xi = f(\xi) \quad (0 \leqslant \xi \leqslant \xi_0),\\ \sum_{n=1}^{\infty} B_n^* \cos n\xi = 0 \quad (\xi_0 \leqslant \xi \leqslant \pi).\end{gathered} \tag{38.1}$$

Following C. J. Tranter [273], we represent the coefficients B_n^* as

$$B_n^* = \frac{2}{\pi} \int_0^{\xi_0} V(\xi) \cos n\xi \, d\xi, \tag{38.2}$$

$$V(\xi) = \cos\frac{\xi}{2} \int_x^1 \frac{\chi(s)\, ds}{\left(s^2 - \sin^2\frac{\xi}{2} \operatorname{cosec}\frac{\xi_0}{2}\right)^{1/2}},$$

$$x = \sin\frac{\xi}{2} \operatorname{cosec}\frac{\xi_0}{2}. \tag{38.3}$$

Substituting (38.3) in (38.2) and interchanging the order of integration, we obtain

$$B_n^* = 2\sin\frac{\xi_0}{2} \int_0^1 F\left(n, -n;\ 1;\ s^2 \sin^2\frac{\xi_0}{2}\right) X(s)\, ds. \tag{38.4}$$

Here $F\left(n, -n;\ 1;\ s^2 \sin^2\frac{\xi_0}{2}\right)$ is a hypergeometric function.

Integrating the first of Eqs. (38.1) between the limits 0 and ξ, multiplying the result obtained by $\sin\frac{\xi}{2}$ and again integrating between the same limits, we find

$$\sum_{n=1}^{\infty} B_n^* \left[\frac{\sin\frac{1}{2}(2n-1)\xi}{2n-1} - \frac{\sin\frac{1}{2}(2n+1)\xi}{2n+1}\right] = I_c(\rho). \tag{38.5}$$

Here

$$\frac{\xi}{2} = \arcsin\left(\rho \sin\frac{\xi_0}{2}\right), \quad I_c(\rho) = \int_0^{\xi} G(\xi) \sin\frac{\xi}{2}\, d\xi,$$

$$G(\xi) = \int_0^{\xi} f(\xi)\, d\xi.$$

By replacing the bracketed expression in (38.5) by the corresponding hypergeometric series [101] and substituting (38.4) in (38.5), we obtain an equation for the determination

of the function $X(s)$

$$\int_0^1 X(s)\, S_1(s, \rho, \xi_0)\, ds = \frac{3I_c(\rho)}{8\rho^3 \sin^4 \frac{\xi_0}{2}} \quad (0<\rho<1). \tag{38.6}$$

Here

$$S_1(s, \rho, \xi_0) = \sum_{n=1}^{\infty} nF\left(n, -n; 1; s^2 \sin^2 \frac{\xi_0}{2}\right) \times$$

$$\times F\left(1+n, 1-n; \frac{5}{2}; \rho^2 \sin \frac{\xi_0}{2}\right). \tag{38.7}$$

This series can be summed [273]

$$S_1 = 0 \ (\rho < s), \quad S_1 = \frac{3(\rho^2 - s^2)^{1/2}}{4\rho^3 \sin^2 \frac{\xi_0}{2}} \ (\rho > s). \tag{38.8}$$

Substituting (38.8) in (38.6), we obtain

$$\int_0^s X(s)(\rho^2 - s^2)^{1/2} ds = \frac{1}{2\sin^2 \frac{\xi_0}{2}} I_c(\rho). \tag{38.9}$$

It can easily be shown that the solution of (38.9) is of the form

$$X(s) = \frac{2}{\pi} \frac{1}{2\sin^2 \frac{\xi_0}{2}} \frac{d}{ds} \int_0^s \frac{\hat{I}_c'(\rho)\, d\rho}{(s^2 - \rho^2)^{1/2}} =$$

$$= \frac{2}{\pi} \frac{d}{ds} \int_0^s \frac{\rho G(\xi)\, d\rho}{\sqrt{(s^2 - \rho^2)\left(1 - \rho^2 \sin^2 \frac{\xi_0}{2}\right)}}, \tag{38.10}$$

which, together with relations (38.2) and (38.3), gives the final solution.

For applications it is useful to find an asymptotic expression for the series as $\xi \to \xi_0 + 0$. By differentiating equal-

ity (38.8) twice with respect to ξ and using the expression [101]

$$\frac{\sin\frac{1}{2}(2n-1)\xi}{2n-1}-\frac{\sin\frac{1}{2}(2n+1)\xi}{2n+1}=$$

$$=\frac{4}{3}\sin^3\frac{\xi}{2}\,nF\left(1+n,\ 1-n;\ \frac{5}{2};\ \sin^2\frac{\xi}{2}\right),$$

we find

$$S_2=\sum_{n=1}^{\infty} nF\left(n,\ -n;\ 1;\ s^2\sin^2\frac{\xi_0}{2}\right)\cos n\xi=0,$$

$$\sin\frac{\xi}{2}<s\sin\frac{\xi_0}{2},$$

$$S_2=-\frac{\sin\frac{\xi}{2}\left(1-s^2\sin^2\frac{\xi_0}{2}\right)}{4\left(\sin^2\frac{\xi}{2}-s^2\sin^2\frac{\xi_0}{2}\right)^{3/2}},$$

$$\sin\frac{\xi}{2}>s\sin\frac{\xi_0}{2}. \tag{38.11}$$

Relation (38.11) is multiplied by $2\sin\frac{\xi_0}{2}X(s)$ and integrated with respect to s from zero to unity. Taking into account (38.1) and (38.4), we then obtain

$$S_3=\sum_{n=1}^{\infty} nB_n^*\cos n\xi=f(\xi),\qquad (\xi<\xi_0),$$

$$S_3=-\frac{1}{2}\sin\frac{\xi_0}{2}\sin\frac{\xi}{2}\int_0^1\frac{\left(1-s^2\sin^2\frac{\xi_0}{2}\right)X(s)\,ds}{\left(\sin^2\frac{\xi}{2}-s^2\sin^2\frac{\xi_0}{2}\right)^{3/2}} \tag{38.12}$$

$$(\xi>\xi_0).$$

By integration by parts, it may be shown that (38.12) has the following singularity as $\xi\to\xi_0+0$:

$$S_3=-\frac{1}{2}\sin\frac{\xi}{2}\cot\frac{\xi_0}{2}\cos\frac{\xi_0}{2}\frac{X(1)}{\left(\sin^2\frac{\xi}{2}-\sin^2\frac{\xi_0}{2}\right)^{1/2}}+\ldots$$

$$(\xi>\xi_0). \tag{38.13}$$

Here the terms that are bounded as $\xi \to \xi_0$ have been rejected.

2. Consider the problem of steady-state vibrations of an infinite plane with a periodic system of cuts of length $2l$

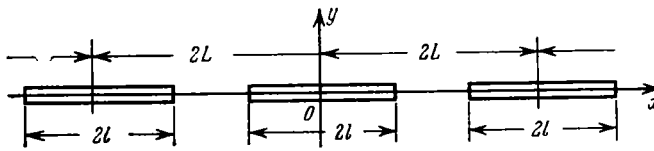

Fig. 38.1. Plane with a periodic system of cuts of equal length.

along the real axis (the spacing between the centres of the cuts is $2L$) (Fig. 38.1). The sides of the cuts are acted on by a normal load $p = q \cos \omega t$.

The amplitude values of displacements and stresses are determined, as before, with the help of the functions φ and ψ by relations (37.1); the functions φ and ψ are the solutions of Eqs. (37.2) and are representable in the form (considering the behaviour at infinity and the symmetry of the state of stress)

$$\varphi(x, y) = \sum_{n=1}^{\infty} A_n e^{-\alpha_n \Omega_1 y} \cos \alpha_n x, \quad \alpha_n = \frac{\pi n}{L},$$

$$\omega_1 = \frac{\omega}{\alpha_n c_1}, \quad \Omega_1 = \sqrt{1 - \omega_1^2},$$

$$\psi(x, y) = \sum_{n=1}^{\infty} B_n e^{-\alpha_n \Omega_2 y} \sin \alpha_n x, \quad \omega_2 = \frac{\omega}{\alpha_n c_2}, \tag{38.14}$$

$$\Omega_2 = \sqrt{1 - \omega_2^2}.$$

The coefficients A_n and B_n in expansions (38.14) must be determined from the following conditions:

$$\begin{aligned} \tau_{xy}(x, 0) &= 0 && (|x| < \infty), \\ \sigma_y(x, 0) &= -q && (0 \leqslant x \leqslant l), \\ v(x, 0) &= 0 && (l \leqslant x \leqslant L). \end{aligned} \tag{38.15}$$

From (38.15) we find

$$A_n = -B_n \frac{1-\frac{1}{2}\omega_2^2}{\Omega_1},$$

$$2\mu \sum_{n=1}^{\infty} B_n \left[\Omega_2 - \frac{\left(1-\frac{1}{2}\omega_2^2\right)^2}{\Omega_1}\right] \alpha_n^2 \cos \alpha_n x = -q \quad (38.16)$$

$$(0 \leqslant x \leqslant l),$$

$$\frac{1}{2} \sum_{n=1}^{\infty} \alpha_n \omega_2 B_n \cos \alpha_n x = 0 \quad (l \leqslant x \leqslant L). \quad (38.17)$$

In determining the coefficients B_n satisfying the dual trigonometric series, we assume

$$\omega_1^2 = \frac{\omega^2}{\alpha_n^2 c_1^2} < 1, \quad \omega_2^2 = \frac{\omega^2}{\alpha_n^2 c_1^2} < 1 \quad (n = 1, 2, \ldots).$$

Thus, the following expansions hold:

$$\Omega_1 = \sum_{k=0}^{\infty} d_k \omega_1^{2k}, \quad \Omega_2 = \sum_{k=0}^{\infty} d_k \omega_2^{2k},$$

$$\Omega_2 - \frac{\left(1-\frac{1}{2}\omega_2^2\right)^2}{\Omega_1} = -\sum_{k=1}^{\infty} D_k \omega_1^{2k}. \quad (38.18)$$

Here

$$d_0 = 1, \quad d_1 = \frac{1}{2}, \ldots,$$

$$D_k = d_k \left(\frac{c_1^2}{c_2^2}\right)^k + 2(k+1) d_{k+1} - 2k d_k \left(\frac{c_1^2}{c_2^2}\right) + \\ + \frac{1}{2}(k-1) d_{k-1} \left(\frac{c_1^2}{c_2^2}\right)^2$$

With (38.18), relations (38.17) are rewritten as

$$\sum_{n=1}^{\infty} \sum_{k=1}^{\infty} D_k \omega_1^{2k-2} \alpha_n B_n^* \cos \alpha_n x = \frac{q}{2\mu} \frac{c_1^2}{\omega^2}$$

$$(0 \leqslant x \leqslant l), \quad (38.19)$$

$$\sum_{n=1}^{\infty} B_n^* \cos \alpha_n x = 0, \quad l \leqslant x \leqslant L \quad \left(B_n^* = \frac{B_n}{\alpha_n}\right).$$

The coefficients B_n^* are sought in the form of a series

$$B_n^* = B_{n,-1}^* \left(\frac{c_1^2}{\omega^2}\right) + B_{n,0}^* + B_{n,1}^* \left(\frac{\omega^2}{c_1^2}\right) + B_{n,2}^* \left(\frac{\omega^2}{c_1^2}\right)^2 + \ldots \tag{38.20}$$

Substituting (38.20) in (38.19) and comparing the coefficients of like powers of ω^2/c_1^2, we obtain the following sequence of dual trigonometric series for finding $B_{n,j}$ ($j = -1, 0, 1, 2, \ldots$):

$$\begin{gathered}\sum_{n=1}^{\infty} nB_{n,-1}^* \cos n\xi = \frac{L}{\pi}\frac{q}{2\mu D_1} \quad (0 \leqslant \xi \leqslant \xi_0),\\ \sum_{n=1}^{\infty} B_{n,-1}^* \cos n\xi = 0 \quad (\xi_0 \leqslant \xi \leqslant \pi),\end{gathered} \tag{38.21}$$

$$\begin{gathered}\sum_{n=1}^{\infty} nB_{n,0}^* \cos n\xi = \\ = -\frac{D_2}{D_1}\left(\frac{L}{\pi}\right)^2 \sum_{n=1}^{\infty} \frac{B_{n,-1}^*}{n} \cos n\xi \quad (0 \leqslant \xi \leqslant \xi_0),\\ \sum_{n=1}^{\infty} B_{n,0}^* \cos n\xi = 0 \quad (\xi_0 \leqslant \xi \leqslant \pi),\end{gathered} \tag{38.22}$$

$$\begin{gathered}\sum_{n=1}^{\infty} nB_{n,1}^* \cos n\xi = -\frac{D_2}{D_1}\left(\frac{L}{\pi}\right)^2 \sum_{n=1}^{\infty} \frac{B_{n,0}^*}{n} \cos n\xi - \\ - \frac{D_3}{D_1}\left(\frac{L}{\pi}\right)^4 \sum_{n=1}^{\infty} \frac{B_{n,-1}^*}{n^3} \cos n\xi \quad (0 \leqslant \xi \leqslant \xi_0),\\ \sum_{n=1}^{\infty} B_{n,1}^* \cos n\xi = 0 \quad (\xi_0 \leqslant \xi \leqslant \pi),\end{gathered} \tag{38.23}$$

$$\xi = \frac{\pi x}{L}, \quad \xi_0 = \frac{\pi l}{L}.$$

In the subsequent discussion (as calculations show) it is sufficient to limit expansion (38.20) to three terms, in which case the normal stresses on the prolongation of the cut are

determined by the following relation:

$$\frac{1}{2\mu}\sigma_y(x, 0) = -D_1\left(\frac{\pi}{L}\right)\sum_{n=1}^{\infty} nB^*_{n,-1}\cos n\xi -$$

$$-\left(\frac{\omega^2}{c_1^2}\right)\sum_{n=1}^{\infty}\left[\frac{L}{\pi}D_2\frac{B^*_{n,-1}}{n} + \frac{\pi}{L}D_1 B^*_{n,0}\, n\right]\cos n\xi -$$

$$-\left(\frac{\omega^2}{c_1^2}\right)^2\sum_{n=1}^{\infty}\left[D_3\left(\frac{L}{\pi}\right)^3\frac{B^*_{n,-1}}{n^3} + D_2\left(\frac{L}{\pi}\right)\frac{B^*_{n,0}}{n} + \right. \tag{38.24}$$

$$\left. + D_1\left(\frac{\pi}{L}\right)B^*_{n,1}\, n\right]\cos n\xi \qquad (\xi_0 \leqslant \xi \leqslant \pi).$$

Noting that series of the form

$$\sum_{n=1}^{\infty}\frac{B^*_{n,j}}{n^k}\cos n\xi \qquad (k = 1, 3, 5, \ldots)$$

are continuous functions when $\xi = \xi_0$, we obtain, with (38.23) and (38.24), from the condition of limiting equilibrium (3.11)*

$$K_c = \lim_{x\to l}\sqrt{2\pi(x-l)}\,\sigma_y(x, 0) =$$

$$= \mu D_1\cos\frac{\xi_0}{2}\left(\frac{L}{\pi}\tan\frac{\xi_0}{2}\right)^{-1/2}\sum_{j=0}^{\infty}\left(\frac{\omega^2}{c_1^2}\right)^j X_{j-1}(1). \tag{38.35}$$

By determining successively $X_{j-1}(1)$ ($j = 0, 1, 2$) from (38.20) and (38.21) to (38.23), we obtain

$$X_{-1}(1) = \left(\frac{L}{\pi}\right)\frac{q}{\mu D_1}\frac{\tan\frac{\xi_0}{2}}{\cos\frac{\xi_0}{2}},$$

$$X_0(1) = \left(\frac{L}{\pi}\right)^3\frac{q}{\mu D_1}\left(\frac{D_2}{D_1}\right)[N^1_{-1}(\xi_0) + M_0(1, \xi_0)]\frac{\tan\frac{\xi_0}{2}}{\cos\frac{\xi_0}{2}},$$

* As mentioned in Sec. 37, the condition of limiting equilibrium retains the same form (which is based on considerations of invariance [47]) in the case of dynamic loads.

$$X_1(1)=\left(\frac{L}{\pi}\right)^5\frac{q}{\mu D_1}\left\{\left(\frac{D_2}{D_1}\right)^2[N_0^1(\xi_0)+M_1(1,\ \xi_0)]+\right.$$

$$\left.+\frac{D_3}{D_1}[N_{-1}^3(\xi_0)-N_{-1}^1(\xi_0)\,M_0(1,\ \xi_0)]\right\}\frac{\tan\frac{\xi_0}{2}}{\cos\frac{\xi_0}{2}},$$

$$N_{-1}^1(\xi_0)=-4\sin^2\frac{\xi_0}{2}\times$$

$$\times\int_0^1\left[\sum_{n=1}^{\infty}\frac{1}{n}F\left(n,\ -n;\ 1;\ s^2\sin^2\frac{\xi_0}{2}\right)\right]\frac{s\,ds}{1-s^2\sin^2\frac{\xi_0}{2}}=$$

$$=4\sin^2\frac{\xi_0}{2}\int_0^1\ln\left(s\sin\frac{\xi_0}{2}\right)\frac{s\,ds}{1-s^2\sin\frac{\xi_0}{2}},$$

$$N_{-1}^3(\xi_0)=-4\sin^2\frac{\xi_0}{2}\int_0^1\left[\sum_{n=1}^{\infty}\frac{1}{n^3}F\times\right.$$

$$\left.\times\left(n,\ -n;\ 1;\ s^2\sin^2\frac{\xi_0}{2}\right)\right]\frac{s\,ds}{1-s^2\sin^2\frac{\xi_0}{2}},$$

$$M_0(s,\ \xi_0)=\frac{1}{6}\pi\frac{\cos^2\frac{\xi_0}{2}}{\sin\frac{\xi_0}{2}}\frac{d}{ds}\int_0^s\frac{\rho\xi^3\,d\rho}{\sqrt{(s^2-\rho^2)\left(1-\rho^2\sin^2\frac{\xi_0}{2}\right)}},$$

$$N_0^1(\xi_0)=[N_{-1}^1(\xi_0)]^2+4\tan^2\frac{\xi_0}{2}\int_0^1\ln\left(s\sin\frac{\xi_0}{2}\right)M_0(s,\ \xi_0)\,ds,$$

$$M_1(s,\ \xi_0)=\frac{1}{120}\pi\frac{\cos^2\frac{\xi_0}{2}}{\sin\frac{\xi_0}{2}}\frac{d}{ds}\int_0^s\frac{\rho\xi^5\,d\rho}{\sqrt{(s^2-\rho^2)\left(1-\rho^2\sin^2\frac{\xi_0}{2}\right)}}.$$

By limiting series (38.25) to three terms, we obtain the final expression

$$\frac{K_c}{\sqrt{2\pi}}=q\left(\frac{L}{\pi}\tan\frac{\xi_0}{2}\right)^{1/2}\left\{1+\left(\frac{\omega L}{\pi c_1}\right)^2\left(\frac{D_2}{D_1}\right)[N_{-1}^1(\xi_0)+\right.$$

$$+M_0(1,\ \xi_0)]+\left(\frac{\omega L}{\pi c_1}\right)^4\left[\left(\frac{D_2}{D_1}\right)^2(N_0^1(\xi_0)+M_1(1,\ \xi_0))+\right.$$

$$\left.\left.+\left(\frac{D_3}{D_1}\right)(N_{-1}^3(\xi_0)-N_{-1}^1(\xi_0)\,M(1,\xi_0))\right]\right\}.\quad(38.26)$$

From (38.26) with $\omega = 0$ we obtain the well-known solution [14] of the problem for a plane with a periodic system

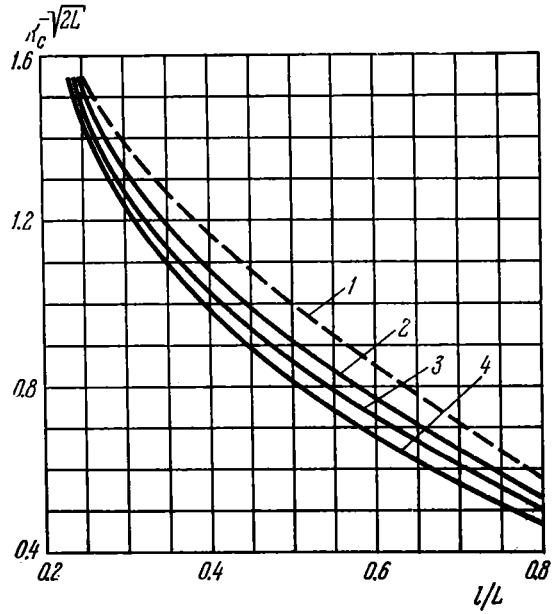

Fig. 38.2. Relation between the load amplitude and the crack length for several frequencies. *1*, $\omega = 0$ (static case); *2*, $\alpha = 0.214$; *3*, $\alpha = 0.224$; *4*, $\alpha = 0.316$ ($\nu = 1/3$, $(c_1/c_2)^2 = 4$).

of cuts along the x axis when the sides of the cuts are acted on by a static normal load q constant along the length of the cut.

Figure 38.2 presents curves showing relation (38.26) for several frequencies of the external load

$$q^* = \frac{q}{K_c}\sqrt{2L} \quad \left(\alpha = \frac{\omega L}{\pi c_1}\right).$$

The expression developed above again shows that the inertia effect in this frequency range acts to reduce the value of the fracture load for a given crack length.

Relation (38.26) may also be used to determine the crack length in a strip of width $2L$ under a normal load $p = q \cos \omega t$ applied to the sides of the cut.

39. STEADY-STATE VIBRATIONS OF AN INFINITE PLANE WITH A PERIODIC SYSTEM OF CUTS ALONG AN AXIS (CONTINUED)

We revert to the problem of an infinite row of collinear cracks of equal length $2l$ spaced a distance 2π apart under a low-frequency cyclic load. Below is presented an elegant solution of this problem suggested by M. A. Hussain and S. L. Pu [110], where use is made of a simple perturbation procedure based on the possibility of obtaining the solution of the corresponding system of zero order (static case). The static problem for collinear cracks was studied by many investigators [73, 135, 259, 290]. A wide review of the literature on this problem may be found in the book of J. N. Sneddon and M. Lowengrub [260]. The method applied below is based on the solution of a system of zero order using a certain artificial transformation proposed by J. Schwinger [159] for problems of wave propagation. In contrast to the conventional schemes of perturbation of the exact solution [1], this procedure requires no solution of a succession of systems. For some fixed order of perturbation one must solve only dual series. The method possesses sufficient generality and may be used in other problems of mathematical physics, which reduce to dual trigonometric series.

The dynamic stress intensity factor in the given problem obtained on the basis of this method may be expressed in terms of the static stress intensity factor multiplied by a certain factor which depends on the material constants, the crack length, and the frequency of the cyclic load. This multiplying factor is determined from a matrix of the Nth order. By increasing N this multiplier can be made as close to the exact value as desired ($N \to \infty$). Numerical calculation shows that reasonable accuracy may be obtained for small values of N.

This method is extremely simple, but has not yet received the recognition it deserves. It offers a means of comparing the results of this section and the preceding one.

Let each of the cracks be acted on by the load $\sigma_y = -qe^{-i\omega t}$. Suppose that ω is small compared with the velocities of longitudinal and transverse waves, c_1 and c_2, and that the edges of each crack are separated from each

other by superimposing constant tensile stresses so that they cannot touch under cyclic loading. This assumption was discussed in [168]. In view of the symmetry about the real axis we consider the semi-infinite plane $y \leqslant 0$.

Let $\mathbf{u} = \mathbf{i}u + \mathbf{j}v$ be the displacement vector. The plane strain equations are written as

$$(\lambda + \mu)\nabla\nabla\mathbf{u} + \mu\nabla^2\mathbf{u} = \rho\ddot{\mathbf{u}}. \tag{39.1}$$

The boundary conditions in the plane $y = 0$, $t > 0$ ($k = \pm 1, \pm 2, \ldots$) are

$$\begin{gathered}\tau_{xy}(x, 0, t) = \tau_{xy}(x + 2k\pi, 0, t) = 0 \quad (0 \leqslant |x| \leqslant \pi),\\ \sigma_y(x, 0, t) = \sigma_y(x + 2k\pi, 0, t) = -qe^{-i\omega t}\\ (0 \leqslant |x| \leqslant l),\\ v(x, 0, t) = v(x + 2k\pi, 0, t) = 0 \quad (l \leqslant |x| \leqslant \pi).\end{gathered} \tag{39.2}$$

For the stationary solution we obtain

$$\mathbf{u}(x, y, t) = \mathbf{u}^*(x, y)\, e^{-i\omega t}, \tag{39.3}$$

and the amplitude values u^*, v^* then satisfy the equations

$$\begin{gathered}\frac{2(1-\nu)}{1-2\nu}\frac{\partial^2 u^*}{\partial x^2} + \frac{\partial^2 u^*}{\partial y^2} + \frac{1}{1-2\nu}\frac{\partial^2 v^*}{\partial x\,\partial y} = -\frac{\omega^2}{c_1^2}u^*,\\ \frac{2(1-\nu)}{1-2\nu}\frac{\partial^2 v^*}{\partial y^2} + \frac{\partial^2 v^*}{\partial x^2} + \frac{1}{1-2\nu}\frac{\partial^2 u^*}{\partial x\,\partial y} = -\frac{\omega^2}{c_2^2}v^*.\end{gathered} \tag{39.4}$$

By introducing the Fourier finite transformation

$$\begin{gathered}U = U(n, y) = \int_0^\pi u^*(x, y)\sin nx\,dx,\\ V = V(n, y) = \int_0^\pi v^*(x, y)\cos nx\,dx,\end{gathered} \tag{39.5}$$

Eqs. (39.4) are reduced to the ordinary equations

$$\begin{gathered}U'' + n^2\left[\omega_2^2 - \frac{2(1-\nu)}{1-2\nu}\right]U = \frac{n}{1-2\nu}V',\\ V'' - n^2\frac{1-2\nu}{2(1-\nu)}(1-\omega_2^2)V = -\frac{n}{2(1-\nu)}U'.\end{gathered} \tag{39.6}$$

Here

$$\omega_i = \omega (nc_i)^{-1} \qquad (i = 1, 2),$$

$$c_1^2 = \frac{\lambda + 2\mu}{\rho}, \qquad c_2^2 = \frac{\mu}{\rho},$$

$$\left(\frac{c_2}{c_1}\right)^2 = \frac{\mu}{\lambda + 2\mu} = \frac{1 - 2\nu}{2(1 - \nu)}.$$

Equations (39.6) may be represented as

$$\left[\frac{\partial^2}{\partial y^2} - \left(n^2 - \frac{\omega^2}{c_1^2}\right)\right]\left[\frac{\partial^2}{\partial y^2} - \left(n^2 - \frac{\omega^2}{c_2^2}\right)\right]\left\{\begin{matrix} U(n, y) \\ V(n, y) \end{matrix}\right\} = 0.$$

The solution is

$$U(n, y) = a_{n1} e^{n\Omega_1 y} + a_{n2} e^{n\Omega_2 y},$$

$$V(n, y) = a_{01} \cos\frac{\omega y}{c_1} + a_{02} \sin\frac{\omega y}{c_1} - a_{n1}\Omega_1 e^{n\Omega_1 y} - a_{n2}\Omega_2^{-1} e^{n\Omega_2 y},$$

where a_{n1} and a_{n2} are constants and

$$\Omega_i = (1 - \omega_i^2)^{1/2} \qquad (i = 1, 2).$$

Inverting (39.5) gives

$$U^*(x, y) = \frac{2}{\pi} \sum_{n=1}^{\infty} (a_{n1} e^{n\Omega_1 y} + a_{n2} e^{n\Omega_2 y}) \sin nx,$$

$$V^*(x, y) = \frac{1}{\pi}\left[a_{01} \cos\left(\frac{\omega y}{c_1}\right) + a_{02} \sin\left(\frac{\omega y}{c_1}\right)\right] +$$

$$+ \frac{2}{\pi} \sum_{n=1}^{\infty} (-a_{n1}\Omega_1 e^{n\Omega_1 y} - a_{n2}\Omega_2^{-1} e^{n\Omega_2 y}).$$

The amplitude values of the stresses are

$$\frac{1 - 2\nu}{2\mu} \sigma_x^* = \frac{\nu}{\pi}\left(-\frac{\omega a_{01}}{c_1} \sin\frac{\omega y}{c_1} + \frac{\omega a_{02}}{c_1} \cos\frac{\omega y}{c_1}\right) +$$

$$+ \frac{2}{\pi} \sum_{n=1}^{\infty} \{[1 - \nu) - \nu\Omega_1^2] a_{n1} e^{n\Omega_1 y} + (1 - 2\nu) a_{n2} e^{n\Omega_2 y}\} n \cos nx, \tag{39.7}$$

$$\frac{1-2\nu}{2\mu}\sigma_y^* = \frac{1-\nu}{\pi}\left(-\frac{\omega a_{01}}{c_1}\sin\frac{\omega y}{c_1} + \frac{\omega a_{02}}{c_1}\cos\frac{\omega y}{c_1}\right) +$$

$$+\frac{2}{\pi}\sum_{n=1}^{\infty}\{[-(1-\nu)\Omega_1^2+\nu]\,a_{n1}e^{n\Omega_1 y} +$$

$$+(-1+2\nu)\,a_{n2}e^{n\Omega_2 y}\}\,n\cos nx,$$

$$\frac{1}{\mu}\tau_{xy}^* = \frac{2}{\pi}\sum_{n=1}^{\infty}\left[2\Omega_1 a_{n1}e^{n\Omega_1 y} + \left(\frac{1}{\Omega^2}+\Omega_2\right)a_{n2}e^{n\Omega_2 y}\right]n\sin nx.$$

From conditions (39.2) and (39.7) we obtain

$$a_{n1}\Omega_1\Omega_2 = -a_{n2}\left(1-\frac{1}{2}\omega_2^2\right). \tag{39.8}$$

By using (39.8) and (39.7) and letting $y \to 0$, we obtain the boundary conditions for the normal stresses and displacements

$$\begin{gathered}\sigma_y^*(x,\,0) = \frac{2(1-\nu)\mu\omega}{(1-2\nu)\pi c_1}a_{02} + \frac{2\mu}{\pi}\sum_{n=1}^{\infty}d_nF_n\cos nx,\\ \pi V^*(x,\,0) = a_{01} + \sum_{n=1}^{\infty}d_n\cos nx,\end{gathered} \tag{39.9}$$

where

$$d_n = -a_{n2}\omega_2^2\Omega_2^{-1},$$

$$F_n = \frac{2n}{\omega_2^2}\left[\Omega_2 - \Omega_1^{-1}\left(1-\frac{1}{2}\omega_2^2\right)^2\right] \quad \text{for } n \geqslant 1. \tag{39.10}$$

By satisfying the mixed conditions (39.2), we obtain dual series for finding the unknowns d_n $(n \geqslant 1)$, a_{02}, and a_{01}

$$\begin{gathered}\frac{2(1-\nu)\mu\omega}{(1-2\nu)\pi c_1}a_{02} + q + \frac{2\mu}{\pi}\sum_{n=1}^{\infty}d_nF_n\cos nx = 0 \quad (0 \leqslant |x| \leqslant l),\\ a_{01} + \sum_{n=1}^{\infty}d_n\cos nx = 0 \quad (l \leqslant |x| \leqslant \pi).\end{gathered} \tag{39.11}$$

Because of the complex nature of F_n these series cannot be solved in the general case in closed form. When $\omega \to 0$, we obtain the static case, and the problem can be solved exactly.

Simple manipulations show that the conditions for boundedness of displacements are satisfied if $\omega \neq \alpha$, where α is the velocity of Rayleigh waves. By expanding F_n in powers of $\omega^2/n^2c_1^2$ and $\omega^2/n^2c_2^2$, we obtain

$$F_n \cong \frac{1}{2(1-\nu)} n + O\left(\frac{1}{n}\right). \tag{39.12}$$

Consequently,

$$F_n = \frac{1}{2(1-\nu)} n(1+\rho_n). \tag{39.13}$$

In the static case $\rho_n \to 0$.

Let us find the solution for the static case by Schwinger's method and use this method to establish a perturbation procedure. It should be noted that in (39.12) we use the expansion of F_n to obtain the zero approximation (statics). The perturbation procedure will not require any further expansions of F_n or ρ_n, as was necessary in [144] (Sec. 38).

When $\rho_n = 0$, we have

$$\begin{gathered} \frac{(1-\nu)\pi}{\mu} q + \sum_{n=1}^{\infty} n d_n \cos nx = 0 \qquad (0 \leqslant |x| \leqslant l), \\ a_{01} + \sum_{n=1}^{\infty} d_n \cos nx = 0 \qquad (l \leqslant |x| \leqslant \pi). \end{gathered} \tag{39.14}$$

Let

$$\frac{(1-\nu)\pi}{\mu} q + \sum_{n=1}^{\infty} n d_n \cos nx = h_0(x) \qquad (l \leqslant |x| \leqslant \pi), \tag{39.15}$$

where $\frac{\mu}{(1-\nu)\pi} h_0(x) - q$ is an unknown function of the stresses $\sigma_y^*(x, 0)$ in the segment $l \leqslant |x| \leqslant \pi$.

Inverting (39.15) gives

$$\frac{(1-\nu)\pi}{\mu} q = \frac{1}{\pi} \int_l^{\pi} h_0(t)\, dt, \tag{39.16}$$

$$d_n = \frac{2}{\pi\mu} \int_l^{\pi} h_0(t) \cos nt\, dt. \tag{39.17}$$

Substituting (39.17) in (39.14) and interchanging the summation and integration give the following integral equation for $h_0(t)$:

$$a_{01}+\frac{2}{\pi}\int_l^{\pi} h_0(t)\sum_{n=1}^{\infty}\frac{\cos nx\cos nt}{n}\,dt=0 \qquad (l\leqslant|x|\leqslant\pi). \tag{39.18}$$

The kernel of this equation may be summed

$$\sum_{n=1}^{\infty}\frac{\cos nx\cos nt}{n}=-\frac{1}{2}\ln 2\,|\cos x-\cos t|. \tag{39.19}$$

Equation (39.18) is a singular integral equation with the logarithmic kernel (39.19) and can be solved in the usual way [199]. In the general case of the given problem the corresponding integral equation cannot be reduced to such a simple form. We therefore use Schwinger's method [159]. The advantages of this method will appear at a later stage.

Let

$$\cos x = b + b'\cos\xi,$$
$$\cos t = b + b'\cos\zeta. \tag{39.20}$$

Here b and b' are constants such that the new variables ξ and ζ vary in the range from 0 to π when x and t vary from l to π. Consequently,

$$b = (\cos l - 1)/2,\ b' = (\cos l + 1)/2.$$

Substituting (39.20) in (39.19), we obtain

$$\sum_{n=1}^{\infty}\frac{\cos nx\cos nt}{n}=-\frac{1}{2}\ln b'+\sum_{n=1}^{\infty}\frac{\cos n\xi\cos n\zeta}{n}. \tag{39.21}$$

From (39.20) we have

$$\frac{dt}{d\zeta}=\frac{1}{\sqrt{2}}\frac{(\cos l-\cos t)^{1/2}}{\sin(t/2)}. \tag{39.22}$$

The unknown stresses have a singularity of order 1/2 as $t\to l$. Consequently, from (39.22) it follows that $h_0(t(\zeta))\times$ $\times(dt/d\zeta)$ satisfies Dirichlet's conditions in the range $0\leqslant$

$\leqslant \zeta \leqslant \pi$; because of the symmetry of the problem we may write [256]

$$h_0(t)\frac{dt}{d\zeta}=\sum_{m=1}^{\infty}\alpha_m\cos(m-1)\zeta \qquad (0\leqslant\zeta\leqslant\pi). \quad (39.23)$$

Substituting (39.21) and (39.23) in the integral equation (39.18), we obtain

$$a_{01}+\frac{2}{\pi}\int_0^{\pi}\left(\sum_{m=1}^{\infty}\alpha_m\cos(m-1)\zeta\right)\left(-\frac{1}{2}\ln b'+\right.$$

$$\left.+\sum_{n=1}^{\infty}\frac{1}{n}\cos n\xi\cos n\zeta\right)d\zeta=0 \qquad (0\leqslant\xi\leqslant n). \quad (39.24)$$

By using the orthogonality conditions, we reduce (39.24) to

$$a_{01}-\alpha_1\ln b'+\sum_{n=1}^{\infty}\alpha_{n+1}\frac{\cos n\xi}{n}=0 \qquad (0\leqslant\xi\leqslant\pi). \quad (39.25)$$

Consequently,

$$\alpha_1=\frac{a_{01}}{\ln b'}, \quad \alpha_{n+1}=0 \quad (n\geqslant 1). \quad (39.26)$$

Substituting (39.22) and (39.26) in (39.23) gives

$$h_0(t)=\frac{a_{01}}{\ln b'}\frac{\sqrt{2}\sin(t/2)}{(\cos l-\cos t)^{1/2}} \qquad (l\leqslant t\leqslant\pi). \quad (39.27)$$

The unknown coefficient a_{01} is determined by substituting (39.27) in (39.16)

$$a_{01}=\frac{(1-\nu)\pi\ln b'}{\mu}q.$$

For the normal stresses we obtain

$$\sigma_y^*(x,0)=q\left[\frac{\sqrt{2}\sin(x/2)}{\sqrt{\cos l-\cos x}}-1\right] \qquad (l\leqslant|x|\leqslant\pi). \quad (39.28)$$

The stress intensity factor is

$$K_{\mathrm{I}}=\lim_{x\to l}\sqrt{2\pi(x-l)}\,\sigma_y^*(x,0)=q\sqrt{2\pi\tan(l/2)}. \quad (39.29)$$

This is the well-known result.

In the foregoing method the solutions of dual series are obtained by reducing them to an algebraic equation. The simplicity of this method becomes obvious when it is compared with Tranter's method [144, 273].

From (39.12) and (39.13) it is clear that $\rho_n \cong O(1/n^2)$ for large n and the series $\sum_l^\infty nd_n\rho_n \cos nx$ may be regarded as a perturbation of the exact solution developed above. Retaining the first N terms in the first equation of (39.11) for the perturbed series, we obtain

$$\frac{\pi(1-\nu)}{\mu}\left[\frac{2(1-\nu)\mu\omega}{(1-2\nu)\pi c_1}a_{02}+q\right]+\sum_{n=1}^{\infty} nd_n \cos nx+$$
$$+\sum_{n=1}^{N} nd_n\rho_n \cos nx=0 \qquad (0\leqslant x\leqslant l). \tag{39.30}$$

The solution of dual equations, viz., (39.30) and the second equation of (39.11), is an Nth approximation to the solution of Eqs. (39.11). By increasing N the approximate solution can be made arbitrarily close to the exact one. As before, the left-hand side of series (39.30) is denoted by an unknown function $h_N(x)$ for $l \leqslant |x| \leqslant \pi$. The equilibrium condition gives

$$\frac{\pi(1-\nu)}{\mu}q=\frac{1}{\pi}\int_l^\pi h_N(x)\,dx. \tag{39.31}$$

The coefficient a_{02} must be zero from comparison between Eq. (39.31) and the inversion of (39.30). Inverting (39.30) gives

$$\begin{aligned} d_n &= \frac{1}{\pi n}\int_l^\pi h_N(t)\cos nt\,dt \qquad (n>N),\\ d_n &= \left(1-\frac{\rho_n}{1+\rho_n}\right)\frac{2}{\pi n}\int_l^\pi h_N(t)\cos nt\,dt \\ &\qquad\qquad (n=1,\,2,\,\ldots,N). \end{aligned} \tag{39.32}$$

Substituting (39.31) and (39.32) in the second equation of (39.11), we obtain an integral equation for the unknown function $h_N(x)$

$$a_{01}+\frac{2}{\pi}\int_l^{\pi} h_N(t)\sum_{n=1}^{\infty}\frac{\cos nx\cos nt}{n}\,dt-$$

$$-\sum_{n=1}^{N}\frac{\rho_n}{1+\rho_n}\frac{\cos nx}{n}\frac{2}{\pi}\int_l^{\pi} h_N(t)\cos nt\,dt=0 \qquad (39.33)$$

$$(l\leqslant|x|\leqslant\pi).$$

We use the same variables, defined by (39.20), and replace $\cos nx$ in the finite series of (39.33) by

$$\cos nx(\xi)=\sum_{k=1}^{n+1}\beta_k^{(n)}\cos(k-1)\xi,$$
$$\cos nt(\zeta)=\sum_{k=1}^{n+1}\beta_k^{(n)}\cos(k-1)\zeta. \qquad (39.34)$$

Assume

$$h_N(t)\frac{dt}{d\zeta}=\sum_{m=1}^{\infty}\alpha_m^{(N)}\cos(k-1)\zeta. \qquad (39.35)$$

Substituting (39.35) and (39.34) in the integral equation (39.33) and using the procedure applied above [see (39.24) and (39.25)], we obtain

$$a_{01}-\sum_{k=1}^{\infty}B_k\alpha_k^{(N)}\cos(k-1)\xi-$$

$$-\sum_{n=1}^{N}\frac{\rho_n}{1+\rho_n}\frac{1}{n}\left(\sum_{i=1}^{n+1}\beta_i^{(n)}\cos(i-1)\xi\sum_{j=1}^{n+1}\delta_j\beta_j^{(n)}\alpha_j^{(N)}\right)=0$$

$$(0\leqslant\xi\leqslant\pi), \qquad (39.36)$$

where

$$B_1=\ln b',\quad \delta_1=2,\quad B_k=-\frac{1}{k-1},\quad \delta_k=1,\quad k=2,3,\ldots$$

Since the left-hand side of (39.36) is zero for all values of ξ in the interval $(0,\ \pi)$, each coefficient of $\cos k\xi$ for

$k = 0, 1, 2, \ldots$ in (39.36) must be zero. Consequently,

$$\alpha_m^{(N)} = 0 \quad \text{for} \quad m > N+1 \tag{39.37}$$

and $\alpha_m^{(N)}$ for $m = 1, 2, \ldots, N+1$ can be determined from the following $(N+1)$ ordinary equations:

$$\sum_{j=1}^{N+1} (B_i \delta_{ij} + A_{ij}) \alpha_j^{(N)} = R_i \qquad (i = 1, 2, \ldots, N+1), \tag{39.38}$$

where δ_{ij} is the Kronecker symbol and

$$R_1 = a_{01}, \quad R_i = 0 \quad (i > 1),$$

$$A_{ij} = \delta_j \sum_{n=1}^{N} \beta_i^{(n)} \beta_j^{(n)} \frac{1}{n} \frac{\rho_n}{1+\rho_n}. \tag{39.39}$$

From (39.34) we obviously have

$$\beta_k^{(n)} = 0 \qquad (k > n+1).$$

Substituting $\alpha_m^{(N)}$ from (38.37) and (39.38) in (39.35) determines the unknown function

$$h_N[x(\xi)] = \sum_{m=1}^{N+1} \alpha_m^{(N)} \cos(m-1)\xi \frac{d\xi}{dx}, \tag{39.40}$$

where

$$\frac{d\xi}{dx} = \sqrt{\frac{4-(1+\cos l)(1+\cos\xi)}{(1+\cos l)(1-\cos\xi)}}.$$

The normal stresses on the boundary $y = 0$ may be written as

$$\sigma_y^*[x(\xi), 0] = \frac{\mu}{\pi(1-\nu)} h_N[x(\xi)] - q =$$

$$= -q + q\left(\sum_{m=1}^{N+1} \alpha_m^{(N)} \cos(m-1)\xi\right)(\alpha_1^{(N)})^{-1} \frac{d\xi}{dx} \tag{39.41}$$

$$(l \leqslant |x| \leqslant \pi).$$

In (39.41) use has been made of the following relation:

$$\frac{q\pi(1-\nu)}{\mu} = \frac{1}{\pi}\int_l^{\pi} h_N(t)\,dt = \frac{1}{\pi}\int_0^{\pi} h_N(t)\frac{dt}{d\xi}\,d\xi = \alpha_1^{(N)}. \tag{39.42}$$

The dynamic intensity factor is

$$D_{\mathrm{I}} = \lim_{x \to l} \sqrt{2\pi (x-l)}\, \sigma_y^*(x, 0), \tag{39.43}$$

$$\frac{D_{\mathrm{I}}}{\sqrt{2\pi}\, q} = \sqrt{\tan \frac{l}{2}}\, (\alpha_1^{(N)})^{-1} \sum_{m=1}^{N+1} \alpha_m^{(N)} \tag{39.44}$$

or

$$\frac{D_{\mathrm{I}}}{K_{\mathrm{I}}} = (\alpha_1^{(N)})^{-1} \sum_{m=1}^{N+1} \alpha_m^{(N)}.$$

We now turn our attention to numerical calculations. As a first approximation, we consider one term in the 'perturbed' series. By comparing (39.34) and (39.20), we find

$$\beta_1^{(1)} = b, \quad \beta_2^{(1)} = b'. \tag{39.45}$$

The coefficient $\alpha_1^{(1)}$ is known from (39.42); the remaining two unknown coefficients, $\alpha_2^{(1)}$ and a_{01}, are determined from the equations

$$\begin{bmatrix} \ln b' + 2b\rho_1/(1+\rho_1) & bb'\rho_1/(1+\rho_1) \\ 2bb'\rho_1/(1+\rho_1) & -1+(b')^2\rho_1/(1+\rho_1) \end{bmatrix} \begin{bmatrix} \alpha_1^{(1)} \\ \alpha_2^{(2)} \end{bmatrix} = \begin{bmatrix} a_{01} \\ 0 \end{bmatrix}, \tag{39.46}$$

where ρ_1 is given by (39.13) and (39.10) with $n = 1$. From (39.46) and (39.44) we can obtain the numerical values of the dynamic stress intensity factor for given ν, ω, l. For comparison we choose $\omega/c_1 = 0.214$, 0.224, and 0.316, $\nu = 1/3$. The numerical results are in good agreement with the data obtained in the preceding section.

By increasing the number of terms in the series, we find a second, a third, and a fourth approximation. We limit ourselves to $N = 4$. For $N = 4$ the five unknown coefficients, a_{01} and $\alpha_i^{(4)}$ $(i = 2, 3, 4, 5)$, are found from the equations

$$\sum_{j=1}^{5} m_{ij}\alpha_j^{(4)} = R_i \qquad (i = 1, 2, \ldots, 5), \tag{39.47}$$

where the matrix elements m_{ij} are determined from (39.38) and (39.39)

$$m_{11} = \ln b' + 2\beta_1^{(1)}\beta_1^{(1)} \frac{\rho_1}{1+\rho_1} + \beta_1^{(2)}\beta_1^{(2)} \frac{\rho_2}{1+\rho_2} + \\ + \frac{2}{3}\beta_1^{(3)}\beta_1^{(3)} \frac{\rho_3}{1+\rho_3} + \frac{1}{2}\beta_1^{(4)}\beta_1^{(4)} \frac{\rho_4}{1+\rho_4}.$$

$$m_{12} = \beta_1^{(1)}\beta_2^{(1)} \frac{\rho_1}{1+\rho_1} + \frac{1}{2}\beta_1^{(2)}\beta_2^{(2)} \frac{\rho_2}{1+\rho_2} + \\ + \frac{1}{3}\beta_1^{(3)}\beta_2^{(3)} \frac{\rho_3}{1+\rho_3} + \frac{1}{4}\beta_1^{(4)}\beta_2^{(4)} \frac{\rho_4}{1+\rho_4},$$

$$m_{22} = -1 + \beta_2^{(1)}\beta_2^{(1)} \frac{\rho_1}{1+\rho_1} + \frac{1}{2}\beta_2^{(2)}\beta_2^{(2)} \frac{\rho_2}{1+\rho_2} + \\ + \frac{1}{3}\beta_2^{(3)}\beta_2^{(3)} \frac{\rho_3}{1+\rho_3} + \frac{1}{4}\beta_2^{(4)}\beta_2^{(4)} \frac{\rho_4}{1+\rho_4}, \quad \text{etc.}$$

$$\beta_1^{(2)} = 2b^2 + b'^2 - 1, \quad \beta_2^{(2)} = 4bb', \quad \beta_3^{(2)} = b'^2,$$
$$\beta_1^{(3)} = 4b^3 - 3b + 6bb'^2, \quad \beta_2^{(3)} = 3b'(4b^2 + b'^2 - 1),$$
$$\beta_3^{(3)} = 6bb'^2, \quad \beta_4^{(3)} = b'^3,$$
$$\beta_1^{(4)} = 8b^4 - 8b^2 + 1 + 4b'^2(8b^2 - 1) + 3b'^4,$$
$$\beta_2^{(4)} = 8bb'(4b^2 - 2 + 3b'^2),$$
$$\beta_3^{(4)} = 4b'^2(8b^2 + b'^2 - 1), \quad \beta_4^{(4)} = 8bb'^3, \quad \beta_5^{(4)} = b'^4.$$

Figure 39.1 shows the numerical results obtained from (39.47) and (39.44) for the case of plane strain with $\nu = 1/3$, $\omega = 0.316\, c_1$. Also shown in the same figure are the results for $N = 0$ (statics), $N = 1$ and 4, as well as the results of the preceding section.

The dynamic stress intensity factor increases with increasing frequency of loading. The ratio of the dynamic and static intensity factors as a function of ω/c_2 is shown in Fig. 39.2 for several crack lengths. This ratio increases monotonically with increasing ω/c_2. When $l/\pi = 0.6$, the inertia effect attains a maximum. The influence of Poisson's ratio ν on the dynamic intensity factor is shown in Fig. 39.3.

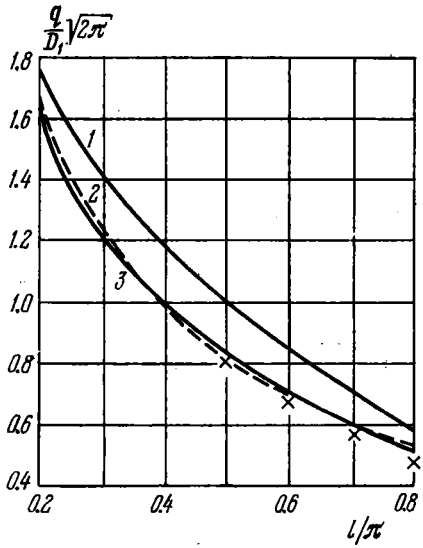

Fig. 39.1. Dynamic stress intensity factor as a function of the relative crack length. *1*, $N = 0$; *2*, $N = 1$; *3*, $N = 4$; the crosses mark points of curve *4* from Fig. 38.2.

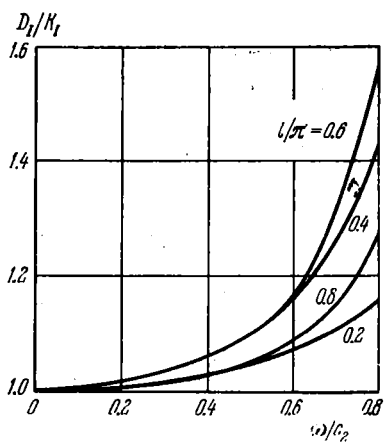

Fig. 39.2. Relation between the ratio of the dynamic and static stress intensity factors and the frequency of loading for several relative crack lengths.

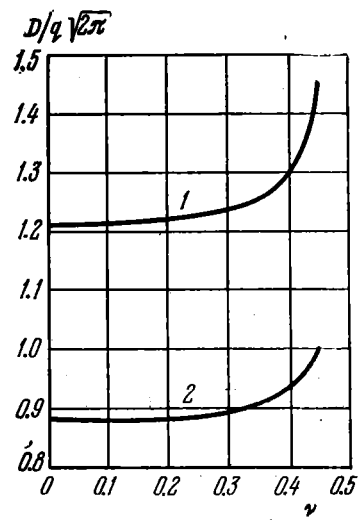

Fig. 39.3. Relation between the dynamic stress intensity factor and Poisson's ratio ($\omega = 0.2c_1$). *1*, $l/\pi = 0.6$; *2*, $l/\pi = 0.4$.

40. THE ACTION OF A SHEAR WAVE ON A PERIODIC SYSTEM OF CRACKS

The investigations of problems dealing with the diffraction of elastic waves by cuts were originated with A. Sommerfeld [262] and A. W. Maue [173, 174]. The first author considered the problem of diffraction by a semi-infinite straight cut in the stationary case of longitudinal shear (more precisely, an equivalent mathematical problem of the optical diffraction of waves by a screen) and in [173, 174] the author presented an analysis of a similar problem in the case of plane strain*. Further investigations of this problem are concerned with a semi-infinite cut and a crack of finite length [4, 39, 53, 88, 89, 161, 254].

1. Consider an infinite elastic isotropic body containing a periodic system of equal length cuts situated along the real axis (Fig. 38.1).

In the system of Cartesian co-ordinates x, y, z the plane of the cracks coincides with the xz plane and their edges are parallel to the z axis.

Consider the case of so-called antiplane strain in which the only non-zero displacement is that along the z axis. The non-zero components of the stress tensor are

$$\tau_{xz} = \mu \frac{\partial W}{\partial x}, \quad \tau_{yz} = \mu \frac{\partial W}{\partial y}. \tag{40.1}$$

Here μ is the shearing modulus, W is the displacement component satisfying the wave equation, c is the velocity of propagation of shear waves, γ_1 is the density of the material,

$$\frac{\partial^2 W}{\partial x^2} + \frac{\partial^2 W}{\partial y^2} = \frac{1}{c_2^2} \frac{\partial^2 W}{\partial t^2}, \quad c = \sqrt{\frac{\mu}{\rho}}. \tag{40.2}$$

Suppose that the strains in the body are produced by harmonic transverse waves (SH-waves) $W^{(1)}$ coming from infinity

$$W^{(1)} = w^{(1)} e^{-i\omega t}. \tag{40.3}$$

Here $w^{(1)} = w_0 e^{-i\lambda y}$, $\lambda = \omega/c$, w_0 is the wave amplitude, ω is the circular frequency.

The solution of Eq. (40.2) is sought in the form

$$W = \operatorname{Re}\left[w(x, y)\, e^{-i\omega t}\right]. \tag{40.4}$$

* As follows from [52], this result corresponds to an incorrect static solution.

Substituting (40.4) in (40.2), we obtain Helmholtz' equation in $w(x, y)$

$$\frac{\partial^2 w}{\partial x^2}+\frac{\partial^2 w}{\partial y^2}+\lambda^2 w=0. \tag{40.5}$$

The function w is represented as the sum of two functions

$$w=w^{(1)}+w^{(2)}, \quad w \to w^{(1)} \text{ as } y \to \infty; \tag{40.6}$$

$w^{(2)}$ corresponds to the disturbed wave field and satisfies Eq. (40.5).

For the shearing stresses we obtain

$$\tau_{yz}=\operatorname{Re}\left[(\sigma_{yz}^{(1)}+\sigma_{yz}^{(2)})\, e^{-i\omega t}\right]=\operatorname{Re}(\sigma_{yz}e^{-i\omega t}).$$

Here

$$\sigma_{yz}^{(1)}=\mu\frac{\partial w^{(1)}}{\partial y}=-i\mu w_0\lambda e^{-i\lambda y},$$

$$\sigma_{yz}^{(2)}=\mu\frac{\partial w^{(2)}}{\partial y}, \quad \sigma_{yz}=\sigma_{yz}^{(1)}+\sigma_{yz}^{(2)}=\mu\frac{\partial w}{\partial y}.$$

The disturbance field $w^{(2)}$ is sought under the condition that the crack surface is free from stress and $w^{(2)}$ is an odd function in y.

In view of the periodicity of the state of stress in x and condition (40.6) we represent the unknown function $w^{(2)}$ in the form of a series

$$w^{(2)}=\pm\sum_{n=1}^{\infty} A_n \cos n\xi \exp\left(\pm\sqrt{n^2-\alpha^2}\,\eta\right). \tag{40.7}$$

Here

$$\alpha^2=\frac{L^2\omega^2}{\pi^2 c^2}, \quad \eta=\frac{\pi y}{L}, \quad \xi=\frac{\pi x}{L}.$$

The upper signs in expression (40.7) correspond to $y \geqslant 0$.

Satisfying the condition

$$\sigma_{yz}^{(2)}(x, 0)+\sigma_{yz}^{(1)}(x, 0)=0 \qquad (0<x<l)$$

and taking into account the continuity of w when $y = 0$, $l < x < L$, we obtain the following dual series equations:

$$\sum_{n=1}^{\infty} \sqrt{n^2-\alpha^2}\, A_n \cos n\xi = -\frac{L}{\pi\mu} i\tau_0 \quad (0 \leqslant \xi < \xi_0),$$
$$\sum_{n=1}^{\infty} A_n \cos n\xi = 0 \quad \left(\xi_0 < \xi \leqslant \pi,\ \tau_0 = \mu w_0 \lambda,\ \xi_0 = \frac{\pi l}{L}\right). \tag{40.8}$$

2. We proceed to the solution of the dual equations (40.8), first writing them down as

$$\sum_{n=1}^{\infty} [n - F(n)]\, A_n \cos n\xi = -\frac{L}{\pi\mu} i\tau_0 \quad (0 \leqslant \xi < \xi_0),$$
$$\sum_{n=1}^{\infty} A_n \cos n\xi = 0 \quad (\xi_0 < \xi \leqslant \pi). \tag{40.9}$$

Here

$$F(n) = n - \sqrt{n^2-\alpha^2} = \frac{\alpha^2}{n+\sqrt{n^2-\alpha^2}} = \\ = \frac{\alpha^2}{2n} + \frac{\alpha^4}{2n\,(n+\sqrt{n^2-\alpha^2})^2}.$$

Following [264], we assume

$$\sum_{n=1}^{\infty} A_n \cos n\xi = \cos\frac{\xi}{2} \int_{\xi}^{\xi_0} \frac{g(t)\,dt}{\sqrt{\cos\xi - \cos t}} \quad (0 \leqslant \xi < \xi_0). \tag{40.10}$$

The coefficients A_n are then determined by the formula

$$A_n = \frac{1}{\sqrt{2}} \int_0^{\xi_0} g(t)\, y_n(\cos t)\, dt. \tag{40.11}$$

Here $y_n(\cos t) = P_n(\cos t) + P_{n-1}(\cos t)$, $P_n(x)$ is a Legendre polynomial.

Integrating the first of Eqs. (40.9) with respect to ξ between the limits 0 and ξ and substituting expression (40.11),

we obtain

$$\int_0^{\xi_0} g(t)\left[\frac{1}{2}\sum_{n=1}^{\infty} y_n(\cos t)\sin n\xi\right]dt=$$

$$=\int_0^{\xi_0} g(t)\left[\frac{1}{\sqrt{2}}\sum_{n=1}^{\infty}\frac{F(n)}{n}y_n(\cos t)\sin n\xi\right]dt-$$

$$-\frac{L}{\pi\mu}i\tau_0\xi \quad (0\leqslant\xi<\xi_0). \qquad (40.12)$$

By using the expansion [11, 264]

$$\frac{1}{\sqrt{2}}\sum_{n=1}^{\infty} y_n(\cos t)\sin n\xi=\frac{\cos\frac{\xi}{2}H(\xi-t)}{\sqrt{\cos t-\cos\xi}},$$

$$H(\xi-t)=\begin{cases}1, & t<\xi,\\ 0, & t>\xi,\end{cases}$$

equality (40.12) may be written as

$$\cos\frac{\xi}{2}\int_0^{\xi}\frac{g(t)\,dt}{\sqrt{\cos t-\cos x}}=$$

$$=\int_0^{\xi_0} g(t)\left[\frac{1}{\sqrt{2}}\sum_{n=1}^{\infty}\frac{F(n)}{n}y_n(\cos t)\sin n\xi\right]dt-\frac{L}{\pi\mu}i\tau_0\xi. \qquad (40.13)$$

Assuming the right-hand side of (40.13) to be known, we solve this equation for $g(t)$

$$g(t)=\frac{1}{2}\tan\frac{t}{2}\int_0^{\xi_0} g(\tau)\left[\sum_{n=1}^{\infty}F(n)\,y_n(\cos\tau)\,y_n(\cos t)\right]d\tau-$$

$$-\frac{L}{\pi\mu}i\tau_0\sqrt{2}\tan\frac{t}{2}. \qquad (40.14)$$

Denote

$$\int_0^{\xi_0} g(\tau)\,y_n(\cos\tau)\,d\tau=a_n.$$

We then obtain

$$g(t)=\frac{1}{2}\tan\frac{t}{2}\sum_{n=1}^{\infty}F(n)\,a_n y_n(\cos t)-\frac{L}{\pi\mu}i\tau_0\sqrt{2}\tan\frac{t}{2}. \tag{40.15}$$

In [11] it is shown that the functions $y_n(\cos t)$ are orthogonal in the interval $0\leqslant t\leqslant\pi$ with weight $\tan\frac{t}{2}$ and form a complete system in the class $L_2(0,\pi)$, i.e., any function belonging to $L_2(0,\pi)$ may be represented in the form of a series

$$f(t)=\tan\frac{t}{2}\sum_{n=1}^{\infty}C_n y_n(\cos t),$$

$$C_n=\frac{n}{2}\int_0^{\pi}f(t)\,y_n(\cos t)\,dt.$$

By writing such a series expansion for the function

$$G(t)=\begin{cases} g(t), & 0\leqslant t<\xi_0,\\ 0, & \xi_0<t<\pi,\end{cases}$$

we obtain an infinite system of equations

$$a_n=\sum_{m=1}^{\infty}a_m C_{mn}-\frac{L}{\pi\mu}i\tau_0\sqrt{2}\,b_n. \tag{40.16}$$

Here

$$C_{mn}=\frac{1}{2}F(m)\,I_{mn}(\xi_0)\qquad(n\neq m),$$

$$I_{mn}(\xi_0)=\int_0^{\xi_0}\tan\frac{t}{2}\,y_n(\cos t)\,y_m(\cos t)\,dt=$$

$$=\frac{n y_m(\cos\xi_0)\,z_n(\cos\xi_0)-m y_n(\cos\xi_0)\,z_m(\cos\xi_0)}{n^2-m^2},$$

$$I_{mn}(\xi_0)=\frac{1}{2}\Big\{2+P_{n-1}^2(\cos\xi_0)-$$

$$-P_n^2(\cos\xi_0)-4\cos\xi_0+2P_n(\cos\xi_0)\,P_{n-1}(\cos\xi_0)+$$

$$+4\sum_{k=1}^{n-1}P_k(\cos\xi_0)\,[P_{k-1}(\cos\xi_0)-\cos\xi_0 P_k(\cos\xi_0)]\Big\},$$

$$z_n(\cos\xi_0) = P_{n-1}(\cos\xi_0) - P_n(\cos\xi_0),$$

$$b_n = \int_0^{\xi_0} \tan\frac{t}{2}\, y_n(\cos t)\, dt = \frac{1}{n} z_n(\cos\xi_0).$$

Following [11], it may be shown that system (40.16) is quasi-completely regular, i.e., beginning with a certain number, the following inequality holds:

$$\sum_{m=1}^{\infty} |C_{mn}| < 1 - \varepsilon \qquad (n > n_0).$$

3. We shall indicate an alternate method of solving the dual equations (40.9), which is more efficient from the point of view of the labour involved in computational work. After integrating the first equation of (40.9) with respect to ξ, we write system (40.9) as

$$\sum_{n=1}^{\infty} \left(1 - \frac{\alpha^2}{2n^2}\right) A_n \sin n\xi =$$

$$= -\frac{L}{\pi\mu} i\tau_0\xi + \frac{\alpha^4}{2} \sum_{n=1}^{\infty} \frac{A_n \sin n\xi}{n^2 (n + \sqrt{n^2 - \alpha^2})^2} \qquad (0 \leqslant \xi < \xi_0), \tag{40.17}$$

$$\sum_{n=1}^{\infty} A_n \cos n\xi = 0 \qquad (\xi_0 < \xi \leqslant \pi).$$

Assume

$$\sum_{n=1}^{\infty} A_n \cos n\xi = \cos\frac{\xi}{2} \int_{\xi}^{\xi_0} \frac{g(t)\, dt}{\sqrt{\cos\xi - \cos t}} -$$

$$- \frac{\alpha^2}{2} \int_{\xi}^{\xi_0} d\xi_1 \int_{\xi_1}^{\xi_0} \cos\frac{\xi_2}{2} \int_{\xi_2}^{\xi_0} \frac{g(t)\, dt}{\sqrt{\cos\xi_2 - \cos t}}\, d\xi_2 \qquad (0 \leqslant \xi < \xi_0).$$

On the basis of this equality and the second equation of (40.17) the coefficients A_n are determined by the formula

$$A_n = \frac{1}{\sqrt{2}} \left(1 + \frac{\alpha^2}{2n^2}\right) \int_0^{\xi_0} g(t)\, y_n(\cos t)\, dt - \frac{\alpha^2}{\sqrt{2}\, n^2} \int_0^{\xi_0} g(t)\, dt. \tag{40.18}$$

Substituting (40.18) in the first equality of (40.17), we obtain

$$\int_0^{\xi_0} g(t)\left[\frac{1}{\sqrt{2}}\sum_{n=1}^{\infty} y_n(\cos t)\sin n\xi\right]dt =$$

$$=\frac{\alpha^4}{4}\int_0^{\xi_0} g(t)\left[\frac{1}{\sqrt{2}}\sum_{n=1}^{\infty}\frac{F_1(n)}{n}y_n(\cos t)\sin n\xi\right]dt+$$

$$+\frac{\alpha^2}{\sqrt{2}}\sum_{n=1}^{\infty}F_2(n)\frac{\sin n\xi}{n}\int_0^{\xi_0} g(t)\,dt-\frac{L}{\pi\mu}i\tau_0\xi. \quad (40.19)$$

Here

$$F_1'(n)=\frac{1}{n^3}+2\frac{\left(1+\frac{\alpha^2}{2n^2}\right)}{n\left(n+\sqrt{n^2-\alpha^2}\right)^2},$$

$$F_2(n)=\frac{1}{n}-\frac{\alpha^2}{2n^3}-\frac{\alpha^4}{2n^3\left(n+\sqrt{n^2-\alpha^2}\right)^2}.$$

By carrying out the same transformations as indicated above, from equalities (40.19) we obtain a Fredholm integral equation of the second kind for the determination of the function $g(t)$

$$g(t)=\frac{\alpha^4}{8}\int_0^{\xi_0} g(\tau)K(t,\tau)\,d\tau+$$

$$+\frac{\alpha^2}{2}a_0\tan\frac{t}{2}\sum_{n=1}^{\infty}F_2(n)y_n(\cos t)-\frac{L}{\pi\mu}i\tau_0\sqrt{2}\tan\frac{t}{2}, \quad (40.20)$$

$$a_0=\int_0^{\xi_0} g(t)\,dt,$$

$$K(t,\tau)=\tan\frac{t}{2}\sum_{n=1}^{\infty}F_1(n)y_n(\cos t)\,y_n(\cos\tau). \quad (40.21)$$

Since $F_1(n)$ approaches zero as $O\left(\frac{1}{n^3}\right)$ when $n \to \infty$ and, moreover, for large n

$$|y_n(x)| < \frac{2}{\sqrt{n}} \quad \text{when} \quad |x| < 1-\varepsilon,$$

series (40.21) converges rapidly, and hence the kernel of expression (40.21) may be replaced by a degenerate one by retaining a certain number N of terms

$$K_N(t, \tau) = \tan\frac{t}{2} \sum_{n=1}^{N} F_1(n)\, y_n(\cos t)\, y_n(\cos \tau). \quad (40.22)$$

By applying the well-known procedure of solving integral equations with a degenerate kernel [21], we obtain the following expression for the function $g(t)$:

$$g(t) = \frac{\alpha^4}{4} \tan\frac{t}{2} \sum_{n=1}^{N} a_n F_1(n)\, y_n(\cos t) + \\ + \frac{\alpha^2}{2} a_0 \varphi(t) - \frac{Li\tau_0}{\pi\mu} \sqrt{2} \tan\frac{t}{2}. \quad (40.23)$$

Here

$$\varphi(t) = \tan\frac{t}{2} \sum_{n=1}^{\infty} F_2(n)\, y_n(\cos t) = -2\tan\frac{t}{2} \ln\sin\frac{t}{2} - \\ - \frac{\alpha^2}{2} \tan\frac{t}{2} \sum_{n=1}^{\infty} \left(\frac{1}{n^3} + \frac{\alpha^2}{n^3 (n+\sqrt{n^2-\alpha^2})^2}\right) y_n(\cos t),$$

$$a_n = \int_0^{\xi_0} g(\tau)\, y_n(\cos \tau)\, d\tau.$$

The constants a_n ($n = 0, 1, 2, \ldots$) are determined by solving a system of $N + 1$ equations of the form

$$a_0 = \frac{\alpha^2}{2} p_0 a_0 + \frac{\alpha^4}{8} \sum_{n=1}^{N} \frac{F_1(n)}{n} z_n(\cos \xi_0)\, a_n + \\ + \frac{L}{\pi\mu} i\tau_0 2\sqrt{2} \ln\left(\cos\frac{\xi_0}{2}\right), \quad (40.24)$$

$$a_m = \frac{\alpha^2}{2} p_m a_0 + \frac{\alpha^4}{8} \sum_{n=1}^{N} F_1(n) I_{nm}(\xi_0) a_n -$$

$$- \frac{L}{\pi\mu} i\tau_0 \sqrt{2} \frac{z_m(\cos\xi_0)}{m} \qquad (m = 1, 2, \ldots, N). \quad (40.25)$$

Here

$$p_0 = \sum_{n=1}^{\infty} \frac{F_2(n)}{n} z_n(\cos\xi_0),$$
$$p_m = \sum_{n=1}^{\infty} F_2(n) I_{mn}(\xi_0). \quad (40.26)$$

Let us find the amplitude values of the shearing stresses on the axis $y = 0$. With (40.7), we obtain

$$\sigma_{yz|y=0} = -i\mu w_0 \lambda - \mu \frac{\pi}{L} \sum_{n=1}^{\infty} \gamma_n A_n \cos n\xi, \quad (40.27)$$

$$\gamma_n = \sqrt{n^2 - \alpha^2}.$$

To determine the stress intensity factor it is necessary to find from this an expression with an isolated singularity at the base of the cut as $\xi \to \xi_0 +$. By using (40.18) it may be shown that

$$\left(\sum_{n=1}^{\infty} \gamma_n A_n \cos n\xi\right)_{\xi>\xi_0} = \frac{d}{d\xi} \left\{ \sum_{n=1}^{\infty} \left(1 - \frac{F(n)}{n}\right) A_n \sin\xi \right\}_{\xi>\xi_0} =$$

$$= \frac{d}{d\xi} \left\{ \cos\frac{\xi}{2} \int_0^{\xi_0} \frac{g(t)\,dt}{\sqrt{\cos t - \cos\xi}} \right\}_{\xi>\xi_0} -$$

$$- \frac{\alpha^4}{4} \int_0^{\xi_0} g(t) \left[\frac{1}{\sqrt{2}} \sum_{n=1}^{\infty} F_1(n) y_n(\cos t) \cos n\xi \right] dt -$$

$$- \frac{\alpha^2}{2} a_0 \sum_{n=1}^{\infty} F_2(n) \cos n\xi.$$

By isolating the singularity of this expression as $\xi \to \xi_0 +$, we obtain

$$\sigma_{yz|y=0} = \frac{\pi\mu}{L} g(\xi_0) \frac{\sin\xi \cos\frac{\xi}{2}}{\sin\xi_0 \sqrt{\cos\xi_0 - \cos\xi}} + \ldots \quad (40.28)$$

Here the terms bounded as $\xi \to \xi_0$ have been rejected.

Taking into account the last relation, we find the stress intensity factor

$$K(t) = \lim_{x \to x_0} [\sqrt{2\pi(x - x_0)}\, \tau_{yz}|_{y=0}] =$$

$$= \frac{\pi\mu}{L} \sqrt{L \cot\frac{\xi_0}{2}}\, \mathrm{Re}\,[g(\xi_0) e^{-i\omega t}] =$$

$$= \frac{\pi\mu}{\sqrt{L \tan\frac{\xi_0}{2}}}\, \mathrm{Re}\,[g(\xi_0, \alpha) e^{-i\alpha t^*}].$$

Here $t^* = \pi c t/L$ is the non-dimensional time, $\alpha = L\omega/\pi c$ is, as before, the non-dimensional wave number.

The last expression may be written as

$$K(t^*) = \pi \left(\frac{\mu w_0}{\sqrt{L}}\right) \frac{\alpha}{\sqrt{\tan\frac{\xi_0}{2}}}\, \mathrm{Re}\left[g(\xi_0, \alpha) \left(\frac{\pi\mu}{L\tau_0}\right) e^{-i\alpha t^*}\right],$$

which, after some obvious substitutions leads to the expression

$$\frac{K\sqrt{L}}{\pi\mu w_0} = \frac{1}{\sqrt{\tan\frac{\xi_0}{2}}}\, \mathrm{Re}\left[\frac{g(\xi_0, \alpha)}{w_0} e^{-i\alpha t^*}\right]. \quad (40.29)$$

To perform numerical calculations, it is necessary first to determine p_0 and p_m by formulas (40.26), for which it is useful to isolate slowly convergent series

$$p_0 = \sum_{n=1}^{\infty} \frac{F_2(n)}{n} z_n(\cos\xi_0) = p_0^0 - \sum_{n=1}^{\infty} F_3(n) \frac{z_n(\cos\xi_0)}{n},$$

$$p_m = \sum_{n=1}^{\infty} F_2(n) I_{mn}(\xi_0) = p_m^0 - \sum_{n=1}^{\infty} F_3(n) I_{mn}(\xi_0),$$

$$F_3(n) = \frac{\alpha^2}{2n^3} + \frac{\alpha^4}{2n^3(n+\sqrt{n^2-\alpha^2})^2},$$

$$p_0^0 = \sum_{n=1}^{\infty} \frac{z_n(\cos\xi_0)}{n^2}, \qquad p_m^0 = \sum_{n=1}^{\infty} \frac{I_{mn}(\xi_0)}{n}.$$

We shall indicate the following equalities:

$$\int \frac{y_n(x)\,dx}{1+x} = -\frac{z_n(x)}{n},$$

$$\int y_n(\cos t)\tan\frac{t}{2}\,dt = \frac{1}{n} z_n(\cos t),$$

$$\int \frac{z_n(x)\,dx}{1-x} = \frac{y_n(x)}{n},$$

$$\int z_n(\cos t)\cot\frac{t}{2}\,dt = -\frac{1}{n} y_n(\cos t).$$

Consequently,

$$\int_0^{\xi_0} \tan\frac{t}{2}\, y_n(\cos t)\,dt = \frac{1}{n} z_n(\cos\xi_0),$$

$$\int_0^{\xi_0} \cot\frac{t}{2}\, z_n(\cos t)\,dt = \frac{1}{n}[2 - y_n(\cos\xi_0)].$$

We calculate expressions needed in what follows

$$y_n(1) = 2, \quad z_n(1) = 0, \quad \sum_{n=1}^{\infty} \frac{y_n(\cos t)}{n} = -2\ln\left|\sin\frac{t}{2}\right|,$$

$$p_m^0 = \sum_{n=1}^{\infty} \frac{I_{mn}(\xi_0)}{n} = \int_0^{\xi_0} \tan\frac{t}{2}\, y_m(\cos t)\left[\sum_{n=1}^{\infty} \frac{1}{n} y_n(\cos t)\right] dt =$$

$$= -2\int_0^{\xi_0} \tan\frac{t}{2}\ln\left|\sin\frac{t}{2}\right| y_m(\cos t)\,dt =$$

$$= -\frac{2}{m}\int_0^{\xi_0} \ln\left|\sin\frac{t}{2}\right| \frac{d}{dt}[z_m(\cos t)]\,dt =$$

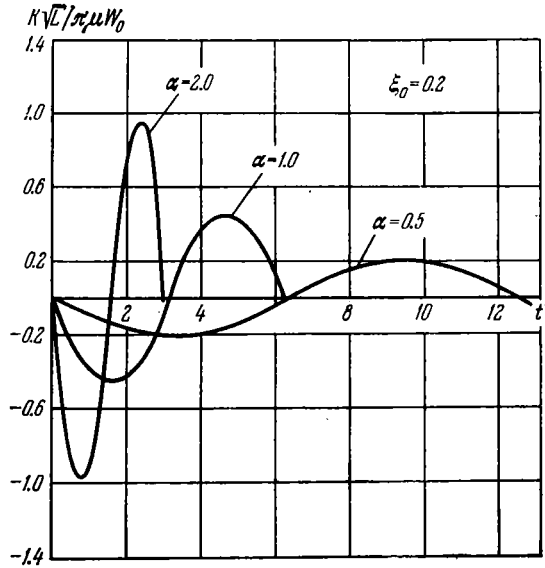

Fig. 40.1. Stress intensity factor as a function of time for several values of the wave number α ($\xi_0 = \pi l/L = 0.2$).

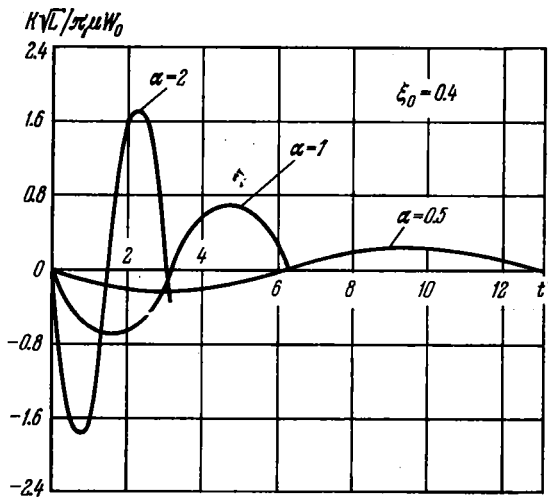

Fig. 40.2. Stress intensity factor as a function of time for several values of the wave number α ($\xi_0 = \pi l/L = 0.4$).

$$= -\frac{2}{m}\ln\left|\sin\frac{\xi_0}{2}\right| z_m(\cos\xi_0) + \frac{1}{m}\int_0^{\xi_0}\cot\frac{t}{2}\, z_m(\cos t)\, dt =$$

$$= -\frac{2}{m}\ln\left|\sin\frac{\xi_0}{2}\right| z_m(\cos\xi_0) + \frac{1}{m^2}\left[2 - y_m(\cos\xi_0)\right],$$

$$p_0^0 = \sum_{n=1}^{\infty}\frac{z_n(\cos\xi_0)}{n^2} = \int_0^{\xi_0}\tan\frac{t}{2}\left[\sum_{n=1}^{\infty}\frac{y_n(\cos t)}{n}\right]dt =$$

$$= -2\ln\left|\sin\frac{\xi_0}{2}\right|\ln\left(1+\sin^2\frac{\xi_0}{2}\right) +$$

$$+\sum_{k=1}^{\infty}(-1)^{k-1}\frac{\left(\sin^2\frac{\xi_0}{2}\right)^k}{k^2}.$$

Figures 40.1 and 40.2 give, using these relations, the stress intensity factor as a function of time for several values of the non-dimensional wave number α.

41. ON SOME PROSPECTIVE PROBLEMS IN FRACTURE MECHANICS

Characteristic of theoretical fracture mechanics is the tendency to describe the main features of the fracture phenomenon within the framework of rigorously formulated and sufficiently general models. At the same time there is a number of practically important fracture phenomena which have not yet received their mechanical interpretation and represent an interesting field of action for future theoretical investigations. We shall first of all mention the problem of irradiation effects on the strength and fracture of solids (neutron and proton beams, powerful photoradiation, high-frequency electric and magnetic fields, etc.). In connection with the demands of rocket and space technology the fracture of solid propellants is gaining in importance, the fracture occurring in complex combustion conditions and being often the cause of the transition of the engine to unstable operation. Some problems involving new technological processes also arise in the study of already known phenomena (fracture of liquids, the effect of residual stresses, etc.).

Of fundamental importance to fracture mechanics and its numerous applications is the investigation of the strength of ideal crystal lattices and lattices with (structure) defects. The very first estimates of theoretical strength produced an enormous effect on the development of the physics of strength and fracture mechanics. Further progress in this direction can apparently be achieved by using quantum-mechanical concepts. Here we can expect considerable advances not only in a more profound and precise investigation of the theoretical strength of already known crystal structures, but also in the discovery of new ones possessing, for example, higher strength.

We shall discuss briefly some of the above-mentioned problems.

1. The effect of radioactive irradiation on the strength and fracture of solids. Numerous experiments on radioactive irradiation show an appreciable change in both chemical and mechanical properties of materials, the changes being irreversible in many cases and remaining for a long time (see, for example, [208]). This circumstance demanded not only the development of technological measures against detrimental effects, but also the working out of new methods of designing structural elements exposed to radioactive irradiation (nuclear reactors, artificial satellites, space ships, and stations).

One of the methods of experimental investigation of the effect of irradiation on the mechanical properties of materials is to determine the natural-frequency spectrum of a specimen and the change in logarithmic decrement. A great body of experimental data show only a slight change in the elastic modulus and a high radiation sensitivity of strength characteristics and of the resistance to plastic deformation. Typical of metals under irradiation are the lack of homogeneity of elastic-plastic properties, the shift "upward and to the left" of the tensile test diagram, the tendency towards embrittlement.

Of particular interest is the effect of irradiation on high-molecular substances. Under moderate radiation doses, some plastics (for example, polyethylene) strengthen, while others tend to lose strength, becoming brittle, up to reducing to powder. Under large radiation doses, how-

ever, nearly all plastics fracture, which puts in the forefront the problem of strengthening plastics and developing radiation-resistant polymers.

From a theoretical point of view, of some interest is the generalization of the theory of small elastic-plastic deformations to the case of inhomogeneity of a medium induced by non-uniform radioactive irradiation, proposed by V. S. Lenskii [154].

The neutron irradiation of a substance produces a number of complex structural changes and transformations. The primary effects are the displacement of atoms from lattice points and also the excitation of atoms without displacement, and nuclear transformations; the secondary effect is ionization.

The internal stresses may arise in a body from different physical processes, such as a non-uniform volume expansion of the body.

In [238] the author examined the relation between stresses and small strains in a crystalline solid under volume expansion produced by heavy-particle irradiation, and proposed a number of hypotheses to determine this expansion. The consideration was concerned with neutron irradiation since a bombarding neutron passing through a crystal lattice does not interact with atoms with Coulomb forces and produces the largest disturbance. It was assumed that as a result of the irradiation the mechanical properties of the material could change while the isotropy of the material remained unaltered. A. A. Il'yushin and P. M. Ogibalov [113] proposed a method for designing thick-walled cylinders and hollow shells. As in [238], it is taken that the decrease in neutron flux is proportional to the layer thickness, and the material properties at a given point depend on the radiation dose at that point.

In determining the state of stress and strain in light metals under irradiation, in addition to the assumption of the absence of nuclear reactions and the fulfilment of the two hypotheses mentioned above, in [303] the author neglected the inhomogeneity of elastic properties produced in a body. This is justified by the experimental evidence of only a slight change in elastic properties compared

with a change in plasticity and strength characteristics, which makes it possible to use the ordinary equations of the theory of elasticity for the calculation of stresses and strains.

The achievements of atomic energetics also pose new problems before the science of strength. Among these is, for example, the swelling of fissile materials arising from the fact that the volume of (solid and gaseous) fission products exceeds the volume of the fissioned material. A suitable introduction of a computational scheme describing the specific structure of such a material allowed Yu. I. Likhachev to solve a number of problems of the non-uniform swelling of heat-generating elements of nuclear reactors under a non-uniform temperature field [160]. Besides, in high-power reactors the radiation doses reach such values as to cause the volume swelling of structural materials. The coefficient of linear expansion involved in this kind of swelling is one order higher than the temperature coefficient. Such phenomena require a careful analysis of the whole complex of phenomena accompanying the deformation of structures.

2. Fracture under powerful photoradiation. New possibilities of investigating the strength and fracture of solids are opened up by the application of quantum generators capable of producing high-power laser rays. The investigations of the state of stress during the passage of a laser ray were first conducted on transparent polymers [7, 18, 231, 284]. The process of passage of a laser ray is accompanied by complex physical phenomena and, at a certain specific power of the pulse, causes the fracture of a transparent material. Until the present time relatively few physicomechanical investigations of this phenomenon have been made. In this connection the problems of determining the basic parameters affecting fracture as well as those of finding the laws governing the transfer of electromagnetic energy into a mechanical stress are far from their solution.

In one of the first works [7] the authors established the formation of plane circular cracks situated at an angle of approximately 45 degrees to the ray axis. Cracks also occur in the path of the laser ray reflected from the body

boundary when the ray has a complete internal reflection. It should be noted that the crack formation involves an extremely high energy concentration comparable, in general, with energy concentration in nuclear explosion. The authors of the above-mentioned work are of the opinion that the fracture is caused by the coherent hypersound generated by the laser. The fracture of the material at an angle of 45 degrees is produced by longitudinal and transverse phonons directly generated by a light wave.

At the same time in other works it is pointed out that the main effect in these processes is heat generation.

Moreover, hypotheses were advanced that at the initial moment of fracture dynamic stresses are produced by heating and hypersound in the region of the canal. The occurrence of these stresses gives rise to minute shear defects in the planes of maximum shearing stresses inclined at an angle of 45 degrees to the ray axis. The appearance of these defects is accompanied by the absorption of light energy, giving rise to gas bubbles with high internal pressure and temperature, which predetermines further crack development.

Note that the fracture of transparent dielectrics under powerful laser radiation proceeds for times of the order of 10^{-5} to 10^{-8} second. The fracture is initiated at local inhomogeneities and depends on both the power and the energy of a light wave.

3. Fracture under high-frequency electric and magnetic fields. In the last few years both in the Soviet Union and abroad intensive investigations of electrophysical methods of fracturing various materials have been conducted requiring a detailed study of electrophysical and other properties of materials subjected to electromagnetic fields and electric discharges. The first investigations in this direction are concerned with electrothermal fracture of dielectric materials under the action of dielectric heating. In the forties [62] the behaviour of dielectrics in high-frequency electric fields between plane electrodes was studied with reference to rocks. It was shown that the high-intensity electric fields produced under electrodes cause the heating of areas adjacent to the elec-

trodes and give rise to thermal stresses (for rocks this leads to cleavage of large blocks and to breakage of rock from the massif). The efficiency of fracturing depends largely on the correlation of the parameters of a generator oscillatory circuit with the material properties. Moreover, a suitably formed electric field can produce cleavage in materials along a specified cleavage line ('directional high-frequency fracturing'). The directional high-frequency fracturing may be of particular importance in such problems as, for example, dielectric heating of rocks containing precious inclusions, requiring selective fracturing of empty rocks and preservation of precious rocks.

Attempts to intensify the fracture process in relation to simple dielectric heating have led to a discovery of the phenomenon of high-frequency thermal break-down and electrical rupture.

The theory of high-frequency thermal break-down and electrical rupture must correlate the physical properties of materials subjected to comminution with the field parameters defining the conditions for thermal break-down and rupture. The phenomenon of thermal break-down consists in the following. Impressing the voltage across the electrodes gives rise to intensive heating of portions of material directly under the electrodes. As a result of the material heating the conductance of the heated portion increases; the zones of increased conductance gradually get closer together and finally form a conducting channel. After the conducting channel (break-down) is formed, the material is heated by Joule heat sources. The thermal break-down in the vicinity of the conducting channel gives rise to high thermal stresses, which may produce fracture in the material.

The distribution of temperature and thermal stress in thermal break-down was investigated in [277], where the author considered a quasi-stationary axially symmetric state of stress in an infinitely long cylinder with heat sources distributed in the conducting channel. Since the radius of a conducting channel is usually small compared with the mean radius of the material being fractured, it was assumed in [277] that the heat sources of given

specific intensity are uniformly distributed along the geometric axis of the cylinder under consideration. Further attempts were made to develop the theory for rocks [62], but because of the complexity of the structure of rocks and anisotropy, the variability of properties and their dependence on the temperature, on the field intensity and frequency for different specimens, they led only to some qualitative results.

In recent years, in connection with advances in the field of power electronics [126], which made it possible to create powerful ultrahigh-frequency generators, waveguides and radiators, some investigations of the fracture of materials by ultrahigh-frequency (U.H.F.) radio waves were initiated.

In the fifties [62] it was shown that an U.H.F. radio wave (of the order of 3000 megacycles) incident on sandstone causes spallation of thin plates off its surface. With a power of the magnetron of 5 kilowatts the spallation occurs in pulses with intervals of tens of seconds, a threefold increase of the magnetron power increasing the rate of fracturing by a factor of 6. The depth and distribution of electromagnetic energy flow in the material depend on the length of electromagnetic waves, their mode of delivering and the electrophysical properties of the material. When electromagnetic waves are acting at a distance, it is possible to have their focusing at some depth, and this may lead to spallation in the material at that place ('radio wave breakage'). The experimental evidence of this phenomenon was obtained on a specimen of granite [62].

The thermal effect is the cause of fracture not only in the case of the action of heat flow (reactive burner or plasmatron), but also in the case of fracture by radio waves. However, the radio-wave heating occurs throughout the volume penetrated by the electromagnetic flow whereas during thermal heating the heat spreads inwards mainly due to heat conduction.

Of particular importance in the mining science are the investigations of intergranular transformation, which leads to a reduction in strength up to complete fracture of material grains or to a decrease in intercrystalline bonds,

under the action of high-frequency electromagnetic fields, and also of the effect of cleavage in mica in high-frequency electric fields. A search for the most efficient methods of comminution of rocks brought forth problems of fracture by power current (thermal break-down, electric arc technique, and rock melting) and by impulsive electric discharges of a dynamic, explosive type.

4. Fracture of burning solid fuels. Peculiar problems of fracture mechanics, closely related to physical chemistry and gas dynamics, arise in the study of some aspects of combustion instability of solid fuels, which are of particular importance in rocket technology [263].

One of the possible causes of the off-design starting operation of a rocket engine is the presence of too large crack-like defects in a solid propellant, which may lead to unstable combustion. The instability mechanism consists in the following. As the combustion front approaches the edge of a crack-like cavity, the combustion rapidly spreads all over the cavity surface since the pressure in the chamber is much higher than the initial pressure in the cavity. Because of the impeded gas offtake the local pressure and temperature may increase abruptly (particularly in the end part of the cavity). Moreover, because of the specific structure of solid propellants in the indicated end region, there may occur volume combustion which, in conjunction with the fracture mechanism in this region, may cause burn-through or even explosion. With the help of the methods of fracture mechanics it will evidently be possible in the future to predict allowable crack-like cavities formed mainly during technological processes. The first attempts to describe theoretically these phenomena were made in [51, 153].

5. Fracture of liquids. The upper bound of the volume strength of a liquid is taken to be the absolute value of the maximum negative pressure that can be applied to the liquid. The upper bound of volume strength varies over a wide range for different liquids. For example, at 20 °C its value for mercury is 24,500 kgf/cm^2, for water 3250 kgf/cm^2, and for ethyl ester 600 kgf/cm^2. These figures correspond to the concept of fracture or decay of a liquid occurring simultaneously throughout the volume.

In actuality, however, the fracture mechanism of liquids is far more complicated. The fracture of a liquid always begins with the "weakest" link (this may, for example, be a gas bubble contained in the volume of liquid). When the liquid is subjected to tension, the radius of the bubble and the surface energy of the liquid increase, while the gas pressure in the bubble drops. A simple calculation shows that the relation between the applied tensile stress p and the radius R of the bubble is of the form

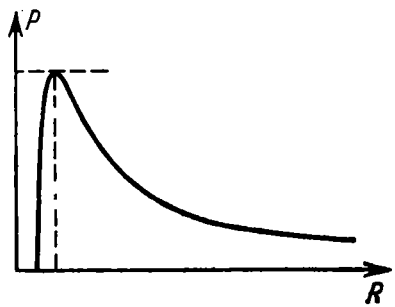

Fig. 41.1. Relation between the tensile stress and the bubble radius.

represented in Fig. 41.1. Thus, as long as the hydrostatic pressure does not reach its maximum value, the gas bubble is stable. The instability occurs at the moment when the hydrodynamic pressure attains a maximum. The qualitative picture of the fracture of liquids represented in Fig. 41.1 is similar to the rupture of interatomic bonds during the fracture of crystals.

The investigation of the strength of a liquid shows that it decreases with increasing bubble radius. Consequently, the most dangerous gas bubble is that having the largest radius among all those existing prior to extension. These considerations find experimental confirmation in an appreciable increase of the strength of a liquid upon the removal of gas bubbles by applying considerable pressures [107].

However, the existence of small gas bubbles is impeded because of their dissolubility in the surrounding liquid, and in consequence we have to consider gas bubbles occur-

ring in a liquid under favourable fluctuations. Such a bubble grows if the elasticity of liquid vapour p_v is greater than the external pressure p (the sum of the hydrostatic pressure and the surface tension σ), and otherwise decreases. The critical size of the bubble is

$$R^* = \frac{2\sigma}{|p_v - p|}.$$

Thus, the fracture of a liquid subjected to the pressure $p_v - p$ takes place at the moment of occurrence of vapour bubbles of radius $R > R^*$.

Experimental verifications show that the strength of liquids is 5 or 6 orders of magnitude lower the theoretical strength. One of the causes of this discrepancy is the fact that the fracture of liquids occurs not in the volume, but at the interface between the liquid and some solid surface (suspended particles in the liquid, the vessel walls, etc.).

The calculation of the fracture strength of a vapour bubble at the solid-liquid interface was carried out by Ya. I. Frenkel' [87] who introduced into consideration the magnitude of the angle of contact (wetting angle). As calculations show, the surface strength decreases with increasing angle of contact and becomes much lower than the volume strength.

The volume strength of liquids decreases steadily with increasing temperature and vanishes near the critical temperature, a fact fairly well confirmed experimentally for most liquids, with the exception of water for which the maximum volume strength is reached at 6 °C. The phenomenological similarity of the fracture mechanisms of liquids and solids promoted a series of experiments which showed that at sufficiently high rates of strain a liquid behaves as a sclid capable of fracturing in a brittle manner.

These data follow from a series of original tests [138] on a mixture of rosin and transformer oil, the desired viscosity of the mixture being reached by varying the rosin concentration. The rupture of a jet flowing out through the bottom of a vessel was produced by a rotating impact machine. The experiments showed that the deform-

ation of the jet at low velocities was viscous (laminar), while at an impact velocity of about 23 m/sec the fracture of the jet becomes brittle, the phenomenon of brittle fracture being observable at viscosities of the order of 10^3 P, i. e., in substances conventionally considered liquid.

We shall also mention some interesting features of an unstable flow of polymeric systems leading, under certain conditions, to brittle fracture.

Experiments carried out on different polymeric materials (polymer solutions and melts, elastomers, rubber stocks, etc.) extruded through smooth dies show that depending on the flow rate the surface of the jet may vary from slight haze (roughness) to complete rupture of the jet into separate pieces of irregular shape. To describe this phenomenon, various terms are employed in the literature in an effort to emphasize the peculiar behaviour of the jet surface in this particular case ('shark skin', 'orange rind', 'elastic turbulence' or 'unstable flow', 'fracture' or 'comminution' of a melt). By the fracture of a melt is meant the occurrence of sharp oscillations of flow at the inlet of the capillary resulting in severe defectiveness. The study of the melt fracture is of great importance in technological processes, for example in the manufacture of products from polymeric materials, where the defectiveness of a jet considerably slows down the efficiency of such processes as the extrusion of fibres, sheets, cable insulation, etc.

In the experimental investigations the flow was realized mostly in isothermal conditions with a constant volume flow rate or pressure drop, and the required quantities were the shearing stress and the rate of shear. The time of occurrence of unstable flow conditions corresponded to some critical values of the rate of shear and the shearing stress.

In theoretical treatments of this phenomenon consideration was given to a large number of experimental facts which show that the unstable flow of polymers is associated in many cases with their elasticity. The assumption of the leading role of high elasticity in the onset of unstable flow was first made by J. P. Tordella [272] and E. B. Bagley [12].

In [169], without considering the detailed mechanism of instability, it was suggested that the condition for the onset of instability should be taken as the fulfilment of a definite relation between the elastic and viscous forces in the flow. For a system with one relaxation time, this criterion represents the product of the characteristic relaxation time and the rate of shear, and in the simplest case it is equal to the critical value of the elastic strain. The experimental investigations carried out for different polymeric systems show that the onset of instability is satisfactorily described by this criterion. Thus, the highly elastic strain stored in the stream determines the critical flow conditions.

Note that under certain conditions an analogy was observed between the fracture phenomenon of brittle bodies and the onset of flow instability.

J. F. Hatton [111, 112] proposed a criterion for the onset of flow instability similar to Griffith's criterion. In [13], however, this proposal was criticized since Griffith's criterion does not take into account energy dissipation in irreversible deformation processes, which plays a significant part in viscoelastic media.

6. The effect of residual stresses on the strength of solids.

As is known, residual (or internal) stresses exist in a body irrespective of external actions (forces and temperatures) and arise from the inhomogeneity of linear or volume strains in adjacent volumes of material. According to the size of the latter, these stresses are defined as macro-, micro- or submicroscopic (stresses of the first, second or third kind). The first studies on residual stresses are due to T. J. Rodman (1857), N. A. Umov (1871), and N. V. Kalakutskii (1887) who were the first to suggest a method for measuring residual stresses [270]. These works, however, remained unnoticed for a long time, and it was not until the twenties of this century that due attention was given to the study of questions associated with residual stresses.

The most complete and exact classification of residual stresses was proposed by N. N. Davidenkov [63] and improved by B. M. Rovinskii [244]. The subject of 'the classification and nomenclature of internal stresses' was

treated in the paper by E. Orowan [212] presented at the Symposium on Internal Stresses in Metals and Alloys (London, 1948), in which the definition of internal stresses corresponded to the concept of 'internal stress' introduced by N. V. Kalakutskii. Without touching upon the analysis of these problems, the residual stresses may be conventionally divided into macrostresses and microstresses, depending on the rate of change of stresses with respect to the spatial co-ordinate. For example, macrostresses do not change appreciably within grain size.

We now turn our attention to the discussion of some questions associated with the effect of residual stresses on the strength and deformation of parts taking into account the action of macroscopic stresses.

A necessary condition for the occurrence of residual stresses may be taken to be the appearance of inhomogeneity of strain at different points of a body without external load. This inhomogeneity may be due to widely different causes such as inhomogeneous thermal expansion or compression during non-uniform heating or cooling of a body, phase transformations resulting in inhomogeneous volume changes (quenching, hardening, cooling after welding, etc.), inhomogeneous plastic deformation, etc.

The complexity of the study of the laws governing the occurrence of residual stresses arises from the necessity of taking into account mechanical, thermal, and physicochemical factors affecting the course of the technological process.

The problem of determining residual stresses arising during the technological process is very complicated since its solution requires theoretical investigations of the relevant physicochemical processes. Promising investigations in this direction were begun by Ya. S. Podstrigach. Service residual stresses can in general be calculated within the framework of the corresponding mechanical models of a continuous medium with irreversible reaction [10, 24].

Let us consider the effect of residual stresses on strength under static and repeated loads. Numerous experimental data point to the great effect of residual stresses on the reliability and life of machines and structures. The frac-

ture of the latter (frequently at the beginning of service) at a sufficiently low stress level is sometimes accounted for by an unfavourable distribution of residual stresses. As experiments show, for materials in a ductile condition the residual stresses have little effect on the value of the fracture force, and the plastic strain produced by a single application of external load leads to a decrease or even a complete relief of the residual stresses.

The investigation of the effect of residual stresses on the static strength of a material in a brittle condition shows that the value of the fracture load is usually lower than that in the absence of residual stresses. The small plastic strains produced before fracture do not eliminate residual stresses, and if the material is susceptible to brittle fracture the effect of residual stresses may be very appreciable.

To reduce residual stresses and to lessen their adverse effect on brittle strength, the parts usually need special heat treatment.

In service different parts are often subjected to repeated stresses.

As is known, the residual stresses can change under cyclic loads. If the sum of the residual and alternating stresses is greater than the elastic limit of the material, plastic strains occur under cyclic loading which reduce the residual stresses. Moreover, in the case when the plastic strain due to the alternating stresses exceeds the value of the original residual strains, there may be a change in the sign of the residual stresses.

In the case when the overall stresses (the residual and alternating stresses) are less than the elastic limit of the material, the residual stresses do not change appreciably under repeated loads.

As experimental investigations show, if a reduction in residual stresses takes place, this occurs in surface layers, which are weaker by their physical nature. To produce useful residual stresses, the surface layers are subjected to work hardening and shot peening, which give rise to compressive residual stresses and improve the fatigue strength of parts. The increase in fatigue strength due to compressive residual stresses at the surface of a part

is more pronounced for less ductile materials and in the presence of stress concentration.

7. The effect of the rate of loading on the strength of solids. In design it is often necessary to take into account the rate of loading since in actual conditions the deformation processes occur at widely different rates ranging from extremely small (for example, under conditions of long-term creep) to very high rates (for example, in cases where the processes of plastic deformation and fracture terminate in infinitesimal fractions of a second). A major portion of the work in this direction is concerned with the experimental determination of the mechanical properties of dynamically deformed materials. The methods for the experimental study of rapidly growing cracks are presented in [78].

The effect of increasing the rate of loading is, in general, an increase in the resistance to plastic deformation, with the fracture becoming more brittle.

The effect of the rate of loading is best studied for carbon steels. Two (upper and lower) yield points are then introduced, and it is found that the upper yield point is more sensitive to the change in loading rate. In order to have an idea of the amount of this effect, we note that increasing the rate of loading by one order of magnitude increases the upper yield point of carbon steels by about 4 kgf/mm^2. Thus, if the rate of loading is increased by five orders of magnitude, which approximately corresponds to the transition from static to impact loading, the upper yield point increases by 20 kgf/mm^2. It is clear that for mild (low-carbon) steels this effect is very appreciable, while for high-strength (high-carbon) steels it can be neglected. A review of experimental works on delayed yielding in steels is given in [267]. At the same time Yu. N. Rabotnov proposed [236] a general three-dimensional model of an elastic-plastic medium with delayed yielding. Within the framework of this model Yu. N. Rabotnov (in conjunction with Yu. V. Suvorova) solved several specific dynamic problems [236].

In contrast to metallic alloys, characteristic of polymers is the greater effect on deformation and fracture of such factors as strain rate, temperature, and time.

In [128] it was shown with reference to rubber and polyvinyl that the dynamic stress-strain curves closely approximating straight lines lie above the static ones, and in the region of stresses close to zero the permanent strains due to dynamic loads may be three times as large as the static strains.

The investigation of various plastics [122] revealed a widely differing dependence of strength on the loading rate at different temperatures (increasing the loading rate by a factor of 10^7 at elevated temperatures leads to an increase in strength by a factor of 3 to 6, whereas at a temperature of 196 °C with the same increase in the loading rate the strength increases only by 25 per cent).

42. CONCLUSION

The material presented in this book shows that a considerable period of investigations in fracture mechanics is associated with the development of empirical estimates of mechanical properties and methods of analysis of fractures. However, the theoretical foundations of the fracture process are still far from their completion at all scale levels—both at the microscopic (fracture physics) and the macroscopic level (fracture mechanics). Moreover, the definition itself of the degree of scale for the phenomenon involved needs refinement, to say nothing of the fact that the relationship between fracture physics and fracture mechanics is practically lacking. It is this relationship that must to a considerable extent contribute to the achievement of desired progress in the development of the science of fracture, progress which will lead to the formulation of theoretical foundations for the design of materials with preassigned properties. Only after the solution of this cardinal problem will it be possible to speak of the relative completion of the science of strength and fracture of materials.

At the same time one should bear in mind the complex 'material-part-structure-environment-loading conditions'. This is a second, and no less complicated, direction for investigations in which much experimental, but little generalizing theoretical, work has been done. In this

direction it is desirable to develop a perfect method for designing a structure at all stages of deformation. In particular, this method must promote the solution of problems of residual strength, long-term prediction, and simulation.

It is natural that the solution of all the above problems is possible only in the case of proper interpretation of the mechanical properties of materials and specimens and the standardization of testing methods. Without the development of experimental techniques and methodology it is apparently impossible to imagine the future of the science of strength, and in particular of fracture mechanics.

APPENDIX A

A PROCEDURE FOR SOLVING THE PLANE ELASTIC-PLASTIC PROBLEM FOR A SEMI-INFINITE SLIT IN ALGOL 60

The procedure parameters:

$h > 0$	—plane stress,
$h < 0$	—plane strain,
n	—number of nodes in horizontal direction,
m	—number of nodes in vertical direction,
$x1$	—Young's modulus E,
$x2$	—yield stress in simple shear τ_y,
$x3$	—stress intensity factor K,
xm	—Poisson's ratio ν,
b	—spacing between nodes (leg of triangle),
du	—initial variation step,
$du \times du2$	—last variation step,
$ux - u_x$, $uy - u_y$	arrays.

The nodal values of u_x, u_y, and nn_i (the arrays ux, uy, nn) are stored in the course of the solution.

nn_i = **true** means that the values of displacements at a given node changed in the preceding pass-around.

nn_i = **false** means that the values of displacements did not change.

In triangles (Fig. 18.2), the values of $\varepsilon_x \cdot b$, $\varepsilon_y \cdot b$, $\gamma_{xy} \cdot b$ (the arrays $b1$, $b2$, $b3$) are stored.

The arrays kk, kn are introduced to select the necessary values from the arrays ux, uy, nn, $b1$, $b2$, $b3$ in view of the fact that the last arrays in the procedure are one-dimensional.

The variation involves the computation of the quantities (see also the table below)

$$\Delta\,(\varepsilon_x \times b) = \Delta u_x \cdot \xi_x,$$

$$\Delta\,(\varepsilon_y \times b) = \Delta u_y \cdot \xi_y,$$

$$\Delta\,(\gamma_{xy} \times b) = \Delta u_y \cdot \xi_x + \Delta u_x \cdot \xi_y.$$

In the block 'Pass' (here and below the word 'block' is employed not in the Algol sense, but to denote a sequence of operators combined

by the function) the nodes are passed around. The variation of the values of displacements at a node is performed in the case when at least one of the values of the array *nn* corresponding to the node itself and adjacent nodes is **true.**

	1	2	3	4	5	6	In procedure array
ξ_x	0	−1	−1	0]	1	1	*km*1
ξ_y	−1	0	1	1	0	−1	*km*2

In this block the variation step is changed and the completion of variation is controlled. The variation terminates when the step

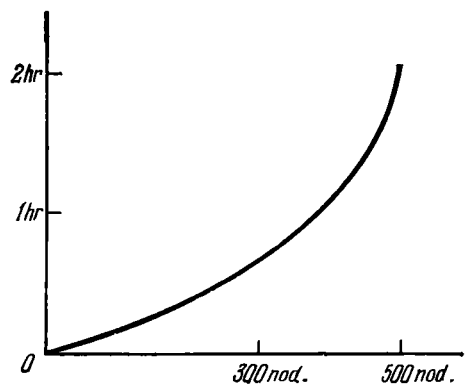

Fig. A.1

size becomes less than a preassigned value. The exit from the procedure takes place when in the first ten pass-arounds no changes occur in displacements at any of the nodes.

In the block 'Variation' the variation of the values of displacements is performed for a given node. A return to the block 'Pass' is effected the moment values of displacements are found which reduce the magnitude of the 'functional' compared with the initial values of displacements.

Figure A.1 shows the approximate computing time on the БЭСМ-6 if the procedure given here is used.

```
procedure plane problem (h, n, m, x1, x2, x3, xm, b, du, du2, ux,
uy);
        value h, n, m, b, x1, x2, x3, xm, du, du2;
        real b, x1, x2, x3, xm, du, du2; integer h, n, m;
        array ux, uy;
begin real a1, a2, a3, d1, d2, d3, g, g1, g2, pi, t1, t2, t3, t4,
t5, du1;
        integer i, i1, i2, i5, j, j1, j2, j3, j4, r1, r2, m3, k, k1, k2,
        k3, k4, m1, n1, n3, n4, n5; boolean p, p1, p2, p3, p4, p5,
        p6, p7;
        array b1, b2, b3 [1 : 2 × (n − 1) × (m − 1)];
        integer array kk, km1, km2, kn [1 : 9];
        boolean array nn [1 : n × m];
        switch wb := w21, w22, w23, w24, w25, w26, w27, w28, w29;
        switch wa := w41, w42, w43;
calculation of constants:
        n1 := n − 1; m1 := m − 1; b := b/m1;
        n4 := n × m; n5 := 2 × (n − 1) × (m − 1);
        x1 := x1/(2 × (1 + xm));
        p4 := if h > 0 then true else false;
        pi := 2 × arcsin (1); t4 := (x2 + b/2) ↑ 2/x1;
        t1 := x1; t3 := x2 × b; t2 := (x2/x1) ↑ 2 × b ↑ 2/4;
        n3 := (n − 1)/2 + 1;
        if ¬ p4 then
            begin
                t5 := x1 × (1 + xm)/(6 × (1 − 2 × xm));
                t1 := t1/3; t2 := t2 × 3; t3 := t3/sqrt (3);
            end;
        kn [2] := km2 [3] := km2 [4] := km1 [5] := km1 [6] := 1;
        kn [5] := km2 [6] := km2 [1] := km1 [2] := km1 [3] := − 1;
        kn [8] := km2 [9] := 1; km1 [8] := km1 [9] := km2 [7] := −1;
        kn [3] := kn [9] := n; kn [6] := −n; kn [1] := kn [7] :=1−n;
        kn [4] := n − 1;
        km1 [1] := km1 [7] := km2 [2] := km2 [8] := km1 [4] :=
        km2 [5] := 0;
        i1 := −4 × n; i2 := −2 × n; m3 := 2 × n − 2;
        kk [1] := kk [7] := i1 + 3; kk [2] := kk [8] := i1 + 4;
        kk [3] := kk [9] := i2 + 1; kk [4] := i2; kk [5] := i2 − 1;
        kk [6] := i1 + 2;
calculation of other displacements at nodes:
        d1 := x3/(4 × x1);
        d3 := if p4 then 2 × (3 − xm)/(1 + xm) else 2 × (3 − 4×xm);
        i1 := n × m1 + 1; i2 := n × m1 + n3; ux [i2] := 0;
        for i := i1 step 1 until i2 do uy [i] := 0;
        k := 0;
        for j := 1 step 1 until m do
            for i := 1 step 1 until n do
                begin k := k + 1;
                    if i = n3 ∧ j = m then go to w92;
                    d2 := sqrt (sqrt ((m − j) ↑ 2 + (n3 − i) ↑ 2) × 2);
                    if i = n3 then begin a2 := pi/4; go to w91 end;
```

```
                a1 := arctan ((m — j)/(i — n3));
                a2 := if  a1 ≤ 0  then  abs (a1)/2  else  (pi — a1)/2;
                if j = m ∧ i > n3 then a2 := pi/2;
w91:
                a3 := 3 × a2;
                ux [k] := d1 × d2 × (cos (a3) — (d3 — 1) × cos (a2));
                if i < n3 ∧ j = m then go to w92;
                uy [k] := d1 × d2 ((d3 + 1) × sin (a2) — sin (a3));
w92:
            end;
        k := k1 := 0;
        for j := 1 step 1 until m1 do
            begin k := k + 1;
                for i := 2 step 1 until n do
                    begin  k := k + 1;  k1 := k1 + 1;
                        i1 := k — 1; i2 := i1 + n;
                        b1 [k1] := ux [i1] — ux [i2];  b2 [k1] := uy [k] —
                        — uy [i1];
                        b3 [k1] := uy [i1] — uy [i2] + ux [k] — ux [i1];
                        k1 := k1 + 1;  i1 := k + n;
                        b1 [k1] := ux [i1] — ux [i2];  b2 [k1] := uy [k]—
                        — uy [i1];
                        b3 [k1] := uy [i1] — uy [i2] + ux [k] — ux [i1];
                    end.
            end:
pass:
        du1 := du × du2;
        for i := 1 step 1 until n4 do nn [i] := false;
        p6 := true;  r1 := 0;
w11:
        r1 := r1 + 1;  k := n — 1;
        for j := 2 step 1 until m do
            begin k := k + 2;
                for i := 2 step 1 until n1 do
                    begin  k := k + 1;
                        nn [k] := true;
                    end;
            end;
        r2 := 0;
w12:
        r2 := r2 + 1;  p3 := true;
        k1 := 1;  k2 := 6;  p1 := false;
        k := n + 1;  i5 := 1;
        for j := 2 step 1 until m1 do
            begin
                for i := 2 step 1 until n1 do
                    begin k := k + 1;
                        if nn [k] then go to w; go to w45;
w41:
                    end;
                k := k + 2;
```

```
        end;
    p1 := true; k1 := 6; k2 := 8;
    i5 := 2; j := m;
    for i := 2 step 1 until n3 do
        begin k := k + 1;
            if nn [k] ∨ nn [k − 1] then go to w; go to w45;
w42:
        end;
    p1 := false; i5 := 3;
    for i := n3 + 1 step 1 until n1 do
        begin k := k + 1;
            if nn [k] ∨ nn [k − 1] then go to w; go to w45;
w43:
        end;
    if p3 then
        begin du := 0.8 × du;
            if p6 then du 1 := du × du2;
            x1 := du × (r2 − 1)/0.8;
            if p6 ∧ r1 > 10 then go to w61;
            if du < du1 then go to w61; go to w11;
        end;
    p6 := false; go to w12;
w45:
    for i1 := k1 step 1 until k2 do
        if nn [k + kn [i]] then go to w;
    go to wa [i5];
variation:
w:
    p5 := true; k4 := m3 × j + 2 × i;
    for j3 := 0, 1, −1 do
        begin d1 := j3 × du;
            for j4 := 0, 1, −1 do
                begin d2 := j4 × du; g := 0;
                    for i1 := k1 step 1 until k2 do
                        begin k3 := k4 + kk [i1];
                            x1 := b1 [k3] + km1 [i1] × d1;
                            x2 := b2 [k3] + km2 [i1] × d2;
                            x3 := b3 [k3] + km2 [i1] × d1 × km1[i1] ×
                            × d2;
                            g1 := if p4 then (x1 ↑ 2 + x2 ↑ 2 + x1 ×
                            × x2 + x3 ↑ 2/4) else
                                (x1 ↑ 2 + x2 ↑ 2 − x1 × x2 + 3 ×
                                × x3 ↑ 2/4);
                            g2 := if g1 ≤ t2 then t1 × g1 else
                                (t3 × sqrt (g1) − t4);
                            if ¬ p4 then g2 := g2 + (x1 + x2) ↑ 2 ×
                            × t5;
                            g:= g − g2;
                        end;
                    if p5 then
                        begin a1 := g, p5 := false;
```

```
                    a2 := if g < 10—9 then 10—15 else abs
                    (g × 10—7);
                    go to w71;
                  end;
              x1 := g — a1;
              if x1 > a2 then
                begin nn [k] := true; p3 := false;
                  ux [k] := ux [k] + d1; uy [k] := uy [k] +
                  + d2;
                  for i1 := k1 step 1 until k2 do
                    begin k3 := k4 + kk [i1];
                      b1 [k3] := b1 [k3] + km1 [i1]×d1;
                      b2 [k3] := b2 [k3] + km2 [i1]×d2;
                      b3 [k3] := b3 [k3] + km2 [i1] ×
                      × d1 + km1 [i1] × d2;
                    end;
                  go to wa [i5];
                end;
w71:
              if p1 then go to w72;
            end;
w72:
        end;
      nn [k] := false; go to wa [i5];
w61:
end plane problem
```

APPENDIX B

THE FINITE ELEMENT METHOD IN THE SOLUTION OF ELASTICITY PROBLEMS

1. BASIC CONCEPTS OF THE FINITE ELEMENT METHOD

In less than two decades the finite element method has become one of the most popular and general numerical methods of structural analysis. It is difficult to determine the time of the first application of the method, particularly if it is remembered that some ideas of this method, used in the analysis of framed structures, were substantiated by J. C. Maxwell and A. Castigliano back in the last century. Nevertheless the beginning of the extensive development and application of the finite element method may be dated from the middle of the fifties for two reasons. First, at that time electronic computers came into use, and without these the realization of the method is impracticable as it involves large systems of algebraic linear equations. Second, at that time the necessary results of particular problems of continuum mechanics became known since the analytic relationships between nodal forces and displacements were formulated for simple structural elements, namely a triangle [275] and a rectangle [5]. Thus, the finite element method appears to be a bridge between strength of materials and elasticity theory.

We shall briefly consider the basic ideas and trends in the development of the finite element method using the approach known as the displacement formulation. The basis of the method is the assumption that every body may be represented as an assemblage of finite elements. For each element an analytic relationship may be obtained between nodal forces and displacements, which involves the stiffness matrix. The stiffness matrices of the individual elements are assembled into the matrix of the system of linear algebraic equations, which expresses the conditions of equilibrium of the body.

This system is of the form

$$\{P\} = [K]\ \{u\} + \{P^T\}. \tag{1.1}$$

Here $\{P\}$ is the nodal force vector, $\{u\}$ is the nodal displacement vector, $[K]$ is the matrix of the system of equilibrium equations of the body, $\{P^T\}$ are 'the thermal forces' due to thermal effects.

The most important feature of the finite element method is that it can be realized by using a highly automatized program which can be applied to a wide range of practical problems. The usual flow chart of such a program is represented in Fig. B.1. The input data consist of a geometrical description of the structure, the material properties, the specification of load and temperature, and the definition of elements by which the given body may be represented. The library must contain a sufficient set of various elements to permit a correct representation of the region under consideration.

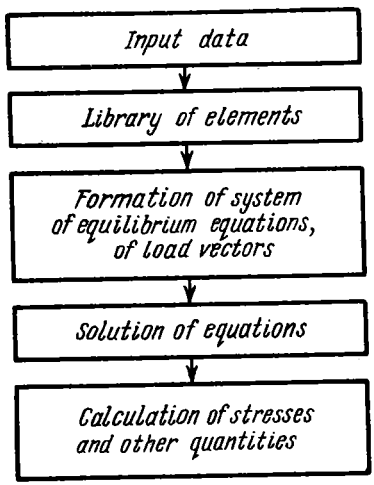

Fig. B.1

The formulation of analytic relationships between nodal forces and displacements for various types of element is the corner-stone of the finite element method. This is a very important aspect of the method since the resulting solution and the potentialities of the method depend very much on the structural elements used. The basic types of element for the plane problem are triangles and rectangles. The rectangles provide a far greater accuracy of the calculation with the same number of nodes than do the triangles. However, they are inconvenient for describing complex geometries and for a local finer mesh of elements. Sometimes use is made of elements in the form of trapezoids, parallelograms, arbitrary quadrilaterals. For these types of element, however, the development of the stiffness matrix becomes considerably complicated, though they provide basically the same accuracy as do the rectangles.

For a three-dimensional analysis the following elements are usually employed: a tetrahedron, a ring of triangular section, a right-angle prism. The ring element of triangular section was described in [36, 59, 278]. It is designed for analysis of axially symmetric bodies. The basic element shape for complex unsymmetrical bodies is an element in the form of a tetrahedron. Elements in the form of a tetrahedron and a parallelepiped were first suggested in [97, 175]. In these works the displacement functions are taken to be linear.

The formulation of force-displacement relationships is based on the methods of elasticity theory, which define these relationships fairly accurately, but, in spite of this, the error involved in the solution is sometimes very large. This may occur, for example, because of the application of too coarse a network or due to the elements being excessively long and narrow. The determination of allowable element

proportions is a problem awaiting further research. For the three-dimensional problem there are practically no available data whatsoever because of the difficulties involved in the computation process.

Further development of the method is the application of elements with a higher order of the functional relationship between nodal forces and displacements and of isoparametric elements. In order to obtain a higher order of the force-displacement relationship, it is necessary to introduce additional nodes (at the middles of the element edges), so that the number of degrees of freedom becomes larger than the minimum possible number for the particular element. This idea of using higher order representations originated at the very beginning of the development of the finite element method, but, until now, there has been no conclusive evidence that the considerable difficulties involved in the evaluation of higher order stiffness matrices are justified by a gain in accuracy. At the same time the results presented in [77] point to the advantage of such elements.

Isoparametric elements (with curved edges) were first described in [74, 75], and later were considered in [6]. The use of isoparametric elements permits curved boundaries to be represented by a small number of elements. The accuracy of computations can be improved by introducing additional nodes. In constructing the stiffness matrix of each element it is necessary to use numerical integration (because of the complexity of the expressions). The development of the stiffness matrix for an isoparametric element must also be clearly founded and, what is more, it is necessary to check the applicability of various algorithms for numerical integration.

In its computational structure the finite element method is closest to grid methods. The underlying assumption of this method, namely that every body may be represented as an assemblage of individual elements connected together, leads to the fact that this kind of approximation has an obvious physical nature (as distinct from the finite difference method where the differential equations describing the behaviour of the whole body are approximated). Hence, once the scheme of division of the region into elements has been chosen, the finite element method may be regarded as an exact method requiring no estimates of errors and of the stability of the computational scheme, if it is considered, of course, that all arithmetic operations are carried out exactly.

The finite element analysis may be subdivided into a different number of stages (depending on the approach, imagination, etc.). We assume the analysis to consist of four stages.

(1) Idealization of the medium under consideration.

(2) Assessment of element properties, i.e., the matrix representation of the elastic and geometrical characteristics of the medium and also of the load characteristics. Since it is assumed that the elements are connected at a limited number of nodal points, a relationship is introduced between the forces applied at the nodal points and the displacements caused by them. This relationship is represented by the element stiffness matrix.

(3) Formulation of a system of canonical equilibrium equations expressing the relationship between the nodal forces appliced to the body and the resulting displacements.

(4) Solution of the system of equations, i.e., the determination of displacements; the calculation of the other required quantities.

Let us now consider all these stages in succession with some emphasis on a formulation suitable for digital computers.

2. IDEALIZATION

By idealization are meant a division of the body under consideration into a finite number of regions (discrete elements) and a description of the geometrical and physical properties of the elements. Idealization is virtually a generation of the geometrical and physical initial data which include the following.

(1) Node numbers and their co-ordinates.

(2) Element numbers and for each element the node numbers in the appropriate order. The order of the node numbers depends on the

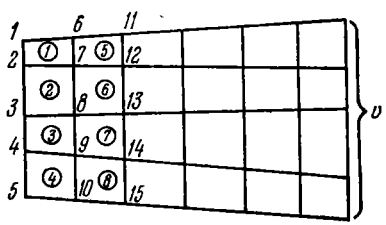

Fig. B.2

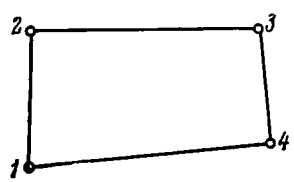

Fig. B.3

notation of these nodes in the derivation of the element stiffness matrix. We thereby indicate how the element in question is connected to others.

(3) A material specification number for each element.

Hand idealization of complex-shaped regions by a large number of elements involves considerable difficulties. This may be demonstrated by the following example. It requires about four minutes on the IBM 360/75 computer to calculate the stresses in a mesh consisting of 1000 triangular elements and 600 nodes whereas it may take weeks to produce and check the same mesh. It is therefore natural to try to reduce the part of manual effort involved in the preparation of initial data.

In this connection we consider the following example illustrating how a quadrilateral two-dimensional region composed of the same material can be divided into quadrilateral elements.

Figure B.2 shows the representation of the region by a network of straight lines. In the direction of the numbering of the nodes the network has v elements. Suppose that in evaluating the element stiffness matrix the nodes are numbered in the order shown in Fig. B.3. The calculation of the array of node numbers np [1 : 4] for the ith element

can then be described by the following algorithm (the Algol 60 language):

$$np\ [1] := i + (i - 1) \div v + 1;$$
$$np\ [2] := np\ [1] - 1;$$
$$np\ [3] := np\ [1] + v;$$
$$np\ [4] := np\ [3] + 1.$$

The calculation of the co-ordinates of the nodes presents no difficulties in this case either. To do this, it is sufficient to specify the co-ordinates of the nodes at the boundary of the region. It is also easy to write down the algorithm for dividing each quadrilateral element into two triangles.

Unfortunately, regions are far from always of such a simple shape Moreover, it is necessary to have irregular networks (a finer mesh of

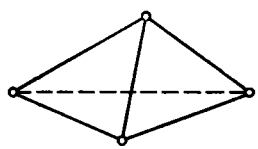

Fig. B.4

triangles at those places where a large stress gradient is expected), and the above algorithm is very inconvenient to provide such mesh refinement.

The following principles may be proposed for developing a program of automatic division into triangular elements [305].

(1) The region under consideration is divided into parts by straight lines (not necessarily parallel) or arcs of circles (not necessarily concentric) or both.

(2) Each straight line is defined by specifying the co-ordinates of its ends. To define the circular arc, it is necessary to specify the co-ordinates of three points.

(3) Each of the specified lines is then divided into segments. If the segments are of equal length, only the number of segments is specified into which the line is to be divided. If unequal segments are required, the irregularity coefficient is introduced.

(4) The number of segments in adjacent lines may be equal or differ by one. This ensures the simplicity of the algorithm of constructing a network. The non-observance of this rule results in considerable complication of the program.

(5) The numbering of nodal points along the specified lines follows a definite sequence, i.e., line after line and starting at the same end every time.

(6) In constructing triangles, four nodal points are considered every time. It is obvious that two triangles can be formed between them. It is essential that the triangles constructed be closest in shape to equilateral ones (Fig. B.4).

This is accomplished as follows: the lengths of both diagonals of the quadrilateral are computed and the shorter one is chosen to form the triangles.

An example of the operation of the program developed on these principles is the division of a region represented in Fig. B.5.

At present there are more advanced methods available for idealization. Consider one of the approaches to this problem outlined in [86].

The authors propose a method of discretizing an irregular and inhomogeneous two-dimensional region into triangular elements. The method consists of a graphical and a computational part. In performing the graphical part use is made of a magnetic 'pen' to record nodal point data and of a digitizer to record material specifications. The fulfilment of the graphical part saves the researcher from the tedium in the preparation of initial data, minimizes the information on carriers such as punched cards, punched tapes, etc. The computational part generates all the information about the elements.

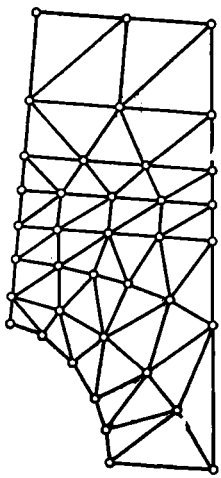

Fig. B.5

To perform the graphical part use is made of an electromagnetic information carrier on which the co-ordinates of nodal points are indicated. If a model is composed of several materials, an additional register is used. In recording a point, it is set manually to the required specification number. For points lying on boundaries between regions made of different materials the register is set to zero. More points are marked at those places where it is necessary to have a finer mesh. Of some interest is the approach in [86] to the question of the identification of boundaries. The point is that if the model is not a convex polygon, a situation may arise in which the boundary will not be correctly interpreted by the program since the program tends to form

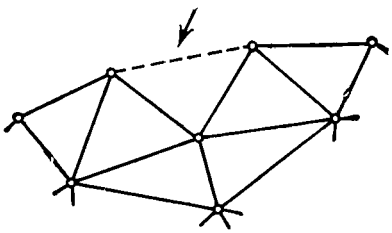

Fig. B.6

the largest number of triangles close in shape to equilateral ones as it is with such triangles that the computation provides the highest accuracy. This case is represented in Fig. B.6. To avoid this, provision

is made for marking ghost points along the boundaries after all true points have been marked. These ghost points must be placed so as to make it advantageous for the program to form a triangle with

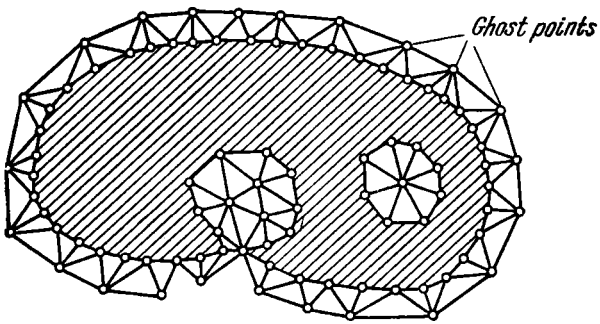

Fig. B7

a side lying on the boundary and with one of the vertices at a ghost point (and not a triangle between three boundary points where in actuality the body is absent) (Fig. B.7).

The points placed along the convex boundaries thus play a passive role and serve only to identify the boundaries.

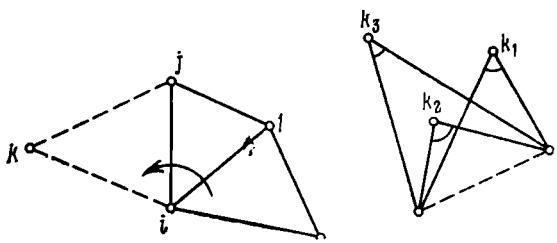

Fig. B.8

The function of the computational part, i.e., of the program proper, is to interconnect the points to form triangular elements in such a way that no elements overlap and the entire structure is defined.

The method is based on the principle of fully surrounded points. Starting with point *1*, each node is surrounded in turn with triangular elements (Fig. B.8). When a node is being surrounded, new triangles are only formed with nodes of a larger node number. This ensures that triangles do not overlap. The process starts with selecting the nearest point to node *1*, and thus a side *1j* is constructed.

When surrounding another point, say i, a check is first made to see whether the point i is already part of an existing triangle. If this is the case, the already existing side is taken as the starting side. Suppose the triangle $1ji$ already exists. Then ij is used to seek a node k such that the angle ikj is a maximum and ijk is an anticlockwise sequence. If a node k is found such that the triangle ikl already exists, it is omitted and l becomes the new point i. The process stops when a triangle contains the side with which the process began, and the point is thus completely surrounded. When seeking a new point k, it is not necessary to consider all the points in the mesh. If the bandwidth of the matrix of the system of equilibrium equations of the body is given to be h, it is necessary to consider true points with nodal numbers such that $(h + a) > k > i$, where a is equal to i or j. It is also necessary to consider all the ghost points.

As to the parameter h we remark, for the present, that its value depends on the maximum difference in nodal numbers in any element. If we have n elements and to the ith element corresponds an array of node numbers $np\ [i,\ 1 : p]$, where p is the number of nodal points of the element, then h can be evaluated as follows (provided there are no zero node numbers):

```
h := 0;
for i := 1 step 1 until n do
begin min := np [i, 1]; max := 0;
      for j := 1 step 1 until p do
      begin if np [i, j] < min then min := np [i, j];
         if np [i, j] > max then max := np [i, j];
      end;
      if max-min > h then h := max-min;
end;
h := 2 × (h + 1)
```

The last expression involves the number 2 since the problem considered is a plane one. In general, this number is equal to the number of degrees of freedom of the nodal point.

In the present case the bandwidth h is not known in advance; it is therefore approximately estimated and specified when numbering the nodes.

The program is written so that ghost points are vertices of triangles. When the generation process has been completed, the program deletes those triangles which have at least one ghost point as a vertex. Only after this has been done, are the elements numbered.

In the foregoing discussion of idealization use has been made of the concepts of a node and node numbers as a result of idealization. In developing a system of equilibrium equations, however, it is necessary to have information in the form of nodal displacement numbers. The displacement numbers of a given element constitute a line of code numbers.

A line of code numbers of an element is defined as the displacement numbers associated with this element and written in the order in which they are arranged when evaluating the element stiffness

matrix. It is obvious that the transformation from nodal numbers to displacement numbers is made in an elementary way.

In the idealization, one must try to number the nodes so that the bandwidth h will be a minimum. There is no rigorous rule available for the minimization of h in the general case. However, in some special cases such as shown, for example, in Fig. B.2 this rule can easily be established. In the foregoing example the nodes must be numbered consecutively along straight lines in a direction where the number of elements is minimum.

An alternative approach to this problem may also be suggested. First, number the nodes arbitrarily, generate the matrix of the system of equilibrium equations in accordance with this numbering, and then minimize the bandwidth of the symmetric part of the matrix by interchanging rows and columns.

3. THE EVALUATION OF THE ELEMENT STIFFNESS MATRIX

In the preceding section we outlined some methods for the idealization of a model. The next step in the determination of the matrix of the system of equilibrium equations is the evaluation of stiffness matrices for all elements of which the given structure is composed. It should be noted that this step, from the standpoint of realization on a computer, is the simplest since in evaluating the stiffness matrix of each element we deal with limited information the amount of which is clearly fixed for the given class of problems. On the other hand, the majority of theoretical investigations are presently concerned with this step because here the method has enormous latent possibilities which will make the analysis more accurate, simpler, etc. It may be said that the evaluation of the element stiffness matrix is the fundamental step in the realization of the method.

A number of alternative methods are available for the calculation of the force-displacement relationship which is described by the element stiffness matrix. The following methods can be used:

(1) unit-displacement method,
(2) Castigliano's theorem,
(3) solution of differential equations for element displacements,
(4) inversion of the displacement-force relationship.

By way of example we consider the first of the above listed methods [233].

The unit-displacement theorem. This theorem is used to determine the force P_r necessary to maintain equilibrium in a region for which the stress distribution is known.

Consider a region in which the stresses $\{\sigma\}$ are known. If a virtual displacement δu_r is applied at the point of application and in the direction of P_r, virtual strains $\delta\{e_r\}$ are produced in the region. Here e_{ij} are the elastic strains which ensure the continuity of displacements produced by external forces, thermal and initial strains. By equating the virtual work to the virtual elastic energy, we obtain

$$P_r \delta u_r = \int_V \{\sigma\}^T \delta\{e_r\}\, dV. \tag{3.1}$$

In an elastic region $\delta\{e_r\}$ are proportional to δu_r

$$\delta\{e_r\} = \{\underline{e}_r\}\,\delta u_r, \tag{3.2}$$

where $\{\underline{e}_r\}$ represents the distribution of strains due to a unit displacement δu_r which are compatible only with themselves.

By combining expressions (3.1) and (3.2), we obtain the formulation of the unit-displacement theorem

$$P_r = \int_V \{\sigma\}^T \{\underline{e}_r\}\, dV. \tag{3.3}$$

The evaluation of the element stiffness matrix by the unit-displacement method. Consider an elastic element such as represented in

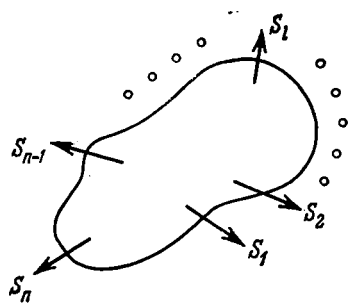

Fig. B.9

Fig. B.9. The element is subjected to n forces $\{S\} = \{S_1, S_2, \ldots, S_n\}$ and some temperature distribution $T = T(x, y, z)$. The displacements corresponding to the forces $\{S\}$ are denoted by the column matrix $\{u\} = \{u_1, u_2, \ldots, u_n\}$.

To determine the force S_i, we apply the unit-displacement theorem

$$S_i = \int_V \{\underline{e}_i\}^T \{\sigma\}\, dV. \tag{3.4}$$

Here $\{\underline{e}_i\}$ is the matrix of compatible strains due to $u_i = 1$, $\{\sigma\}$ is the stress matrix due to the forces $\{S\}$ and the temperature field T. By combining n formulas of the type of (3.4), we obtain

$$\begin{gathered} \{S\} = \int_V [\underline{e}]^T \{\sigma\}\, dV, \\ [\underline{e}] = [\{\underline{e}_1\}\,\{\underline{e}_2\} \cdots \{\underline{e}_n\}]. \end{gathered} \tag{3.5}$$

In an elastic region the total strain distribution $\{\varepsilon\}$ can be represented by the following relation:

$$\{\varepsilon\} = [b]\ \{u\}, \tag{3.6}$$

where $[b]$ is the matrix of exact strains due to unit displacements $\{u\}$. The matrix $\{\sigma\}$ in the case under consideration is expressed as

$$\{\sigma\} = [\varkappa]\ [b]\ \{u\} + \{\varkappa_T\}\,\alpha T. \tag{3.7}$$

Consequently,

$$\{S\} = \int_V [\underline{e}]^T [\varkappa]\ [b]\ dV\ \{u\} + \int_V [\underline{e}]^T [\varkappa_T]\ \alpha T\ dV \tag{3.8}$$

or

$$\{S\} = [k]\ \{u\} + \{Q\}.$$

Here

$$[k] = \int_V [\underline{e}]^T [\varkappa]\ [b]\ dV \tag{3.9}$$

is the element stiffness matrix, $\{Q\}$ are the thermal forces.

If T = constant, then

$$\{Q\} = \{h\}\ \alpha T. \tag{3.10}$$

Here

$$\{h\} = \int_V [\underline{e}]^T \{\varkappa_T\}\ dV \tag{3.11}$$

is the thermal element stiffness matrix.

The matrix $[\underline{e}]$ representing strains compatible only with themselves can easily be evaluated even for complex structural elements. However, the evaluation of the matrix $[b]$ representing the exact strain distribution involves considerable difficulties, and in many cases is not feasible at all. It is usual therefore to replace the matrix $[b]$ by $[\underline{b}] = [\underline{e}]$ in (3.9). In this case we obtain the following approximate relation for the element stiffness matrix:

$$[k] = \int_V [\underline{b}]^T [\varkappa]\ [\underline{b}]\ dV. \tag{3.12}$$

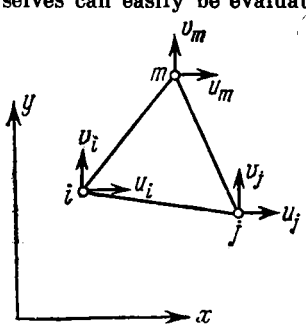

Fig. B.10

The evaluation of the stiffness matrix of the triangular element. Suppose we have a triangular element as shown in Fig. B.10 [305]. We assume that displacements are linear functions of the co-ordinates

$$\begin{aligned} u &= \alpha_1 + \alpha_2 x + \alpha_3 y, \\ v &= \alpha_4 + \alpha_5 x + \alpha_6 y. \end{aligned} \tag{3.13}$$

The boundary conditions at the nodes of the element for these functions are

$$\begin{aligned} u &= u_i, \quad v = v_i \quad \text{when} \quad x = x_i, \quad y = y_i, \\ u &= u_j, \quad v = v_j \quad \text{when} \quad x = x_j, \quad y = y_j, \\ u &= u_m, \quad v = v_m \quad \text{when} \quad x = x_m, \quad y = y_m. \end{aligned} \tag{3.14}$$

This system of equations enables one to express $\alpha_1, \alpha_2, \ldots, \alpha_6$ in terms of $\{u\} = \{u_i v_i u_j v_j u_m v_m\}$. The functions u and v can then be represented as

$$\begin{aligned} u &= \frac{1}{2\Delta}[(A_i + B_i x + C_i y)\, u_i + (A_j + B_j x + C_j y)\, u_j + \\ &\qquad + (A_m + B_m x + C_m y)\, u_m], \\ v &= \frac{1}{2\Delta}[(A_i + B_i x + C_i y)\, v_i + (A_j + B_j x + C_j y)\, v_j + \\ &\qquad + (A_m + B_m x + C_m y)\, v_m]. \end{aligned} \tag{3.15}$$

In (3.15) we have introduced the notation (Δ is the element area)

$$\begin{aligned} A_i &= x_j y_m - x_m y_j, \\ B_i &= y_j - y_m = y_{jm}, \\ C_i &= x_m - x_j = x_{mj}, \end{aligned} \qquad \Delta = \frac{1}{2}\begin{vmatrix} 1 & x_i & y_i \\ 1 & x_j & y_j \\ 1 & x_m & y_m \end{vmatrix}.$$

The matrix $[\underline{b}]$ is found by substituting for u and v in the formulas of the theory of elasticity

$$\varepsilon_x = \frac{\partial u}{\partial x}, \quad \varepsilon_y = \frac{\partial v}{\partial y}, \quad \varepsilon_{xy} = \frac{\partial u}{\partial y} + \frac{\partial v}{\partial x},$$

$$[\underline{b}] = \frac{1}{2\Delta}\begin{bmatrix} B_i & 0 & B_j & 0 & B_m & 0 \\ 0 & C_i & 0 & C_j & 0 & C_m \\ C_i & B_i & C_j & B_j & C_m & B_m \end{bmatrix}. \tag{3.16}$$

The matrix $[\varkappa]$ in relation (3.7) is:
for plane stress

$$[\varkappa] = \frac{E}{1-\nu^2}\begin{bmatrix} 1 & \nu & 0 \\ \nu & 1 & 0 \\ 0 & 0 & \dfrac{1-\nu}{2} \end{bmatrix}, \tag{3.17}$$

for plane strain

$$[\varkappa] = \frac{F}{(1+\nu)(1-2\nu)}\begin{bmatrix} 1-\nu & \nu & 0 \\ \nu & 1-\nu & 0 \\ 0 & 0 & \dfrac{1-2\nu}{2} \end{bmatrix}. \tag{3.18}$$

Substituting for $[\varkappa]$ and $[\underline{b}]$ in (3.12) and taking into account their constancy, we obtain the element stiffness matrix

$$[k] = [\underline{b}]^T [\varkappa] [\underline{b}] \, t\Delta, \tag{3.19}$$

where t is the element thickness.

We shall indicate one more representation of $[k]$, which is sometimes useful in calculations. If the matrix $[\underline{b}]$ is partitioned into three submatrices

$$[\underline{b}] = [\underline{b}_i \ \underline{b}_j \ \underline{b}_m],$$

$$[\underline{b}_i] = \frac{1}{2\Delta} \begin{bmatrix} B_i & 0 \\ 0 & C_i \\ C_i & B_i \end{bmatrix},$$

the matrix $[k]$ will be composed of submatrices $[k_{rs}]$

$$[k] = \begin{bmatrix} k_{ii} & k_{ij} & k_{im} \\ k_{ji} & k_{jj} & k_{jm} \\ k_{mi} & k_{mj} & k_{mm} \end{bmatrix},$$

$$[k_{rs}] = [\underline{b}_r]^T [\varkappa] [\underline{b}_s] \, t\Delta.$$

The evaluation of the stiffness matrix of the rectangular element. Consider a rectangle such as shown in Fig. B.11 in a local system

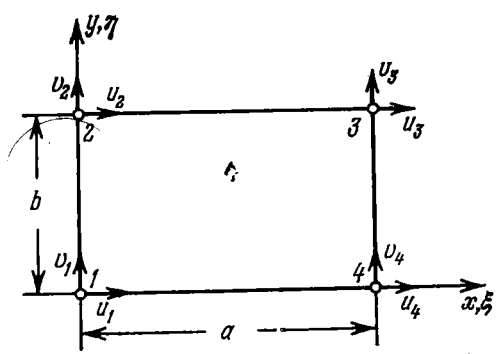

Fig. B.11

of non-dimensional co-ordinates $\xi = x/a$, $\eta = y/b$ [233]. The displacement functions are taken to be polynomials

$$\begin{aligned} u &= \alpha_1\xi + \alpha_2\xi\eta + \alpha_3\eta + \alpha_4, \\ v &= \alpha_5\xi + \alpha_6\xi\eta + \alpha_7\eta + \alpha_8. \end{aligned} \tag{3.20}$$

To determine $\alpha_1, \ldots, \alpha_8$, we use the following boundary conditions:

$$\begin{aligned} u &= u_1, \quad v = v_1 \quad \text{when} \quad \xi = 0, \quad \eta = 0, \\ u &= u_2, \quad v = v_2 \quad \text{when} \quad \xi = 0, \quad \eta = 1, \\ u &= u_3, \quad v = v_3 \quad \text{when} \quad \xi = 1, \quad \eta = 1, \\ u &= u_4, \quad v = v_4 \quad \text{when} \quad \xi = 1, \quad \eta = 0. \end{aligned}$$

By solving the system of equations, we determine the unknowns $\alpha_1, \ldots, \alpha_8$. Substituting them in (3.20), we obtain

$$\begin{aligned} u &= (1-\xi)(1-\eta)u_1 + (1-\xi)\eta u_2 + \xi\eta u_3 + \xi(1-\eta)u_4, \\ v &= (1-\xi)(1-\eta)v_1 + (1-\xi)\eta v_2 + \xi\eta v_3 + \xi(1-\eta)v_4. \end{aligned} \tag{3.21}$$

The displacement distribution along any side is linear and depends only on the displacements of two nodal points lying on this side.

The total strains are obtained by differentiation

$$\varepsilon_x = \frac{1}{a}\frac{\partial u}{\partial \xi}, \quad \varepsilon_y = \frac{1}{b}\frac{\partial v}{\partial \eta}, \quad \varepsilon_{xy} = \frac{1}{b}\frac{\partial u}{\partial \eta} + \frac{1}{a}\frac{\partial v}{\partial \xi}.$$

Assuming that $\{u\} = \{u_1 v_1 u_2 v_2 u_3 v_3 u_4 v_4\}$, we write the matrix $\underline{\{b\}}$ as

$$[\underline{b}] = \begin{bmatrix} -\frac{1-\eta}{a} & 0 & -\frac{\eta}{a} & 0 & -\frac{\eta}{a} & 0 & \frac{1-\eta}{a} & 0 \\ 0 & -\frac{1-\xi}{b} & 0 & \frac{1-\xi}{b} & 0 & \frac{\xi}{b} & 0 & -\frac{\xi}{b} \\ -\frac{1-\xi}{b} & -\frac{1-\eta}{a} & \frac{1-\xi}{b} & -\frac{\eta}{a} & \frac{\xi}{b} & \frac{\eta}{a} & -\frac{\xi}{b} & \frac{1-\eta}{a} \end{bmatrix}. \tag{3.22}$$

Substituting this matrix in (3.12) and integrating, we obtain the element stiffness matrix. For plane strain, for example, it is equal to ($\alpha = a/b$, $\beta = b/a$)

$$\frac{Et}{12(1+\nu)(1-2\nu)} \times$$

$$\times \begin{bmatrix} A & & & & & & & \\ \frac{3}{2} & \overline{A} & & & & & & \\ B & -C & A & & & & & \\ C & \overline{D} & -\frac{3}{2} & \overline{A} & \text{Symmetric} & & & \\ -\frac{A}{2} & -\frac{3}{2} & D & -C & A & & & \\ -\frac{3}{2} & -\frac{\overline{A}}{2} & C & \overline{B} & \frac{3}{2} & \overline{A} & & \\ D & C & -\frac{A}{2} & \frac{3}{2} & B & -C & A & \\ -C & \overline{B} & \frac{3}{2} & -\frac{\overline{A}}{2} & C & \overline{D} & -\frac{3}{2} & \overline{A} \end{bmatrix}$$

Here

$$A = 4(1-\nu)\beta + 2(1-2\nu)\alpha, \quad \overline{A} = 4(1-\nu)\alpha + 2(1-2\nu)\beta,$$

$$B = 2(1-\nu)\beta - 2(1-2\nu)\alpha, \quad \overline{B} = 2(1-\nu)\alpha - 2(1-2\nu)\beta,$$

$$C = \frac{3}{2}(1-4\nu), \quad D = -4(1-\nu)\beta + (1-2\nu)\alpha,$$

$$\overline{D} = -4(1-\nu)\alpha + (1-2\nu)\beta.$$

4. THE FORMATION OF A SYSTEM OF LINEAR ALGEBRAIC EQUILIBRIUM EQUATIONS

With the use of the stiffness matrices $\{k_i\}$ for S individual elements we write the matrix $[k]$ of the disconnected elements as a quasi-diagonal matrix $[k] = \lrcorner [k_1]\,[k_2] \ldots [k_s] \lrcorner$ of order $[1 : m \times S,\ 1 : m \times S]$, where m is the number of degrees of freedom of the element.

To obtain the matrix of the system of equilibrium equations, it is necessary to carry out the following transformation:

$$[K] = [C]^T [k]\,[C]. \tag{4.1}$$

Here the matrix $C\,[1 : m \times S,\ 1 : n]$ expresses the relation between the independent displacements of the individual elements and the displacements of the assembled structure, n is the number of degrees of freedom of the structure under consideration. It is obvious that $[C]$ is a sparse matrix. If the directions of the nodal displacements are chosen the same for the region under consideration and the individual elements, the non-zero elements of $[C]$ will be equal to unity. The matrix $[C]$ is an information matrix indicating the address at which the corresponding elements of the matrices $[k_i]$ must be placed.

Matrix formation of $[K]$. Let the matrix $[C]$ be partitioned into S submatrices of order $[1 : m,\ 1 : n]$

$$[C] = \begin{bmatrix} C_1 \\ C_2 \\ \vdots \\ C_S \end{bmatrix}.$$

Transformation (4.1) can then be written as

$$[K] = \sum_{i=1}^{S} [C_i]^T [k_i]\,[C_i]. \tag{4.2}$$

Since $[C]$ is a sparse matrix, it is not advantageous to enter the complete matrices $[C_i]$ into the computer memory. A variety of procedures may be applied to avoid this difficulty. For example, ignoring the zeros, one can indicate only the positions of the unit elements in $[C_i]$. By allotting one location to each unit element, we divide it into two parts and indicate therein the row and column numbers where the unit element in question is situated.

The resulting matrix of the system of equilibrium equations $[K]$ is of order $[1:n,\ 1:n]$. It is also sparse and, with the proper numbering of the displacements of the region under consideration, has a symmetric band structure. All non-zero elements group around the principal diagonal as a band of width h. One can therefore enter into the memory only the symmetric part of the band together with the elements of the principal diagonal.

The code number method. The matrix multiplication, which must be performed to produce the matrix of the system of equilibrium equations, may be replaced by direct addition of the matrices of structural elements.

Suppose we have S elements, correspondingly S lines of code numbers written as a two-dimensional array $cn\,[1:S,\ 1:m]$ (m is the

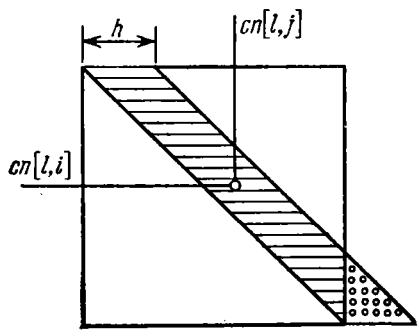

Fig. B.12

number of degrees of freedom of the element), and S stiffness matrices of structural elements written as a three-dimensional array $k\,[1:S,\ 1:m,\ 1:m]$. The algorithm of evaluating the matrix of the system of equilibrium equations K is then written as

for i := 1 **step** 1 **until** n **do**
for j := 1 **step** 1 **until** n **do** $K\,[i,\ j]$:= 0;
for l := 1 **step** 1 **until** S **do**
for i := 1 **step** 1 **until** m **do**
for j := 1 **step** 1 **until** m **do**
$K\,[cn\,[l,\ i],\ cn\,[l,\ j]]$:= $K\,[cn\,[l,\ i],\ cn\,[l,\ j]] + k\,[l,\ i,\ j]$.

As already mentioned, the matrix K has a symmetric band structure and it is sufficient to enter the symmetric part of the band into the computer memory (Fig. B.12). By supplementing the band by a dummy triangle of zeros, $[K]$ may be completely assigned by rows as a one-dimensional array $a\,[1:n \times h]$, which is obtained as follows:

for i := 1 **step** 1 **until** $n \times h$ **do** $a\,[i]$:= 0;
for l := 1 **step** 1 **until** S **do**
for i := 1 **step** 1 **until** m **do**

```
for j := 1 step 1 until m do
begin if cn [l, j] < cn [l, i] then go to m 1;
        t := (cn [l, i] − 1) × h + cn [l, j] − cn [l, i] + 1;
          a [t] := a [t] + k [l, i, j];
m1:
end j
```

If it is necessary to economize on computer storage, the matrix may be assigned as an array $a\,[n \times h - h \times (h - 1) \div 2]$ without supplementing the band by a dummy triangle of zeros. To do this, the following addition must be introduced into the algorithm:

```
if cn [l, i] > n − h + 2 then
t := t − (cn [l, i] − n + h − 1) × (cn [l, i] − n + h − 2) ÷ 2.
```

To obtain better accuracy requires a larger number of elements. Therefore, a demand arises for generating large matrices the symmetric part of whose band cannot be completely stored in the rapid-access

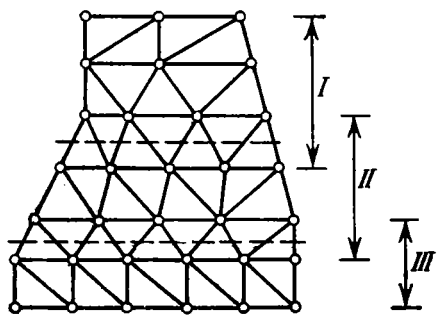

Fig. B.13

storage. Hence, the matrix a must be evaluated by parts and overwritten in the external storages. If, in the idealization, the nodes are numbered in the same direction from line to line, the region under consideration can be divided into parts as shown in Fig. B.13. This will result in the partitioning of the matrix of the system of equilibrium equations. Not more than one partitioning line can pass through an element. The elements through which a partitioning line has passed must be considered twice. For example, in order to form the matrix of the region shown in Fig. B.13, it is necessary to consider successively the groups of elements I, II, and III.

Consider the question of regularization of a general matrix of the system of equilibrium equations. If, in constructing this matrix, all degrees of freedom are taken into account, including those which must be inhibited, the matrix K, or a, comes out singular.

It is clear from physical considerations that values of at least three displacements must be prescribed (in the plane problem). In the case of rigid fixing these displacements must be set equal to zero.

This is accomplished as follows. If the ith displacement is to be inhibited, one must replace the elements of the ith row and ith column of the matrix by zeros and set the iith element equal to unity. It is essential, as a rule, to store the unity because the algorithms commonly used in the solution do not admit the presence of zero elements on the principal diagonal.

An alternative method of inhibiting displacements is that of eliminating the displacements which are inhibited from the list of unknowns. If the particular displacement does not exist, the value zero stands for it in the line of code numbers, the remaining displacements are numbered with no consideration of the inhibited ones.

For rigorousness, we must also consider the question of 'conditioning' of the matrix of the system of equilibrium equations. But since this question is far from being simple, and the matrices involved in the solution of plane problems are usually well conditioned, we shall not discuss this problem.

5. THE SOLUTION OF A SYSTEM OF LINEAR EQUATIONS

The methods for the solution of systems of linear equations may be divided into two groups: (1) exact methods representing finite algorithms for calculating the roots of a system (for example, Cramer's rule, Gauss method, square-root method, Cholesky's method, etc.); (2) iterative methods, which allow the roots of a system to be obtained with preassigned accuracy by means of convergent infinite processes (iteration method, Seidel method, relaxation method, etc.).

Because of inevitable rounding the results of even exact methods are approximate, and the estimation of the error in the roots is, in general, rather troublesome.

There is no need to present the solution algorithms for the general case, they may be found in the books devoted to the foundations of computational mathematics (see, for example, [82]). We shall apply just one of the algorithms to the solution of symmetric band systems since programs for solving such systems do not enter into the standard mathematical facilities of computers and are rarely given elsewhere.

Let us consider, in this connection, the Gauss method [123]. The solution of a linear system is reduced to successive elimination of the unknowns, i.e., to the construction of an equivalent system having a triangular matrix. The process of finding the coefficients of the triangular matrix is called the forward elimination, and the process of obtaining the values of the unknowns is called the back substitution.

For simplicity, we consider a 'tridiagonal' matrix such as shown n Fig. B.14.

$$\begin{bmatrix} a_1 & b_2 & & & & & \\ b_2 & a_2 & b_3 & & & & \\ & b_3 & a_3 & b_4 & & & \\ & & b_4 & a_4 & b_5 & & \\ & & & \ddots & \ddots & \ddots & \\ & & & & \ddots & \ddots & b_n \\ & & & & & b_n & a_n \end{bmatrix} \begin{Bmatrix} x_1 \\ x_2 \\ x_3 \\ x_4 \\ \vdots \\ \vdots \\ x_n \end{Bmatrix} = \begin{Bmatrix} c_1 \\ c_2 \\ c_3 \\ c_4 \\ \vdots \\ \vdots \\ c_n \end{Bmatrix}$$

Fig. B.14

The algorithm for the solution of the system may briefly be written as

$$\bar{a}_1 = a_1$$
$$\bar{c}_1 = c_1$$
$$\left.\begin{aligned} \bar{a}_i &= a_i - b_i^2/\bar{a}_{i-1} \\ \bar{c}_i &= c_i - b_i\bar{c}_{i-1}/\bar{a}_{i-1} \end{aligned}\right\} \quad i = 2, \ldots, n$$
$$x_n = \bar{c}_n/\bar{a}_n$$
$$x_i = \bar{c}_i/\bar{a}_i - b_{i+1}x_{i+1}/\bar{a}_i \qquad i = (n-1), \ldots, 1$$

If the full matrix can be stored in the rapid-access storage (for the M-220 computer the number of terms in the matrix is 3000 to 3300), the solution presents no difficulties and is carried out by algorithms similar to that just described. If, however, the matrix of the system cannot be completely stored in the internal memory and is stored in the external storages, then it must be read and processed by parts. In this case it is advantageous to store the matrix by rows together with free terms written next to the given row. We shall describe the idea of the solution in this case.

The matrix together with free terms partitioned into arrays shown in Fig. B.15 is stored in the external memories. The variables n_i indicate the number of rows in each array. For example, the first array contains $n_1 \times (h + q)$ elements. The solution by the Gauss method requires that $n_1 = h - 1$. The arrays n_1 and n_2 must be stored simultaneously in the useful internal memory. Denoting the capacity of the useful internal storage by z, we find n_2

$$n_2 = z/(h + q) - h + 1, \tag{5.1}$$

where q is the number of columns of free terms.

The solution proceeds as follows. The array n_1 and the first array of n_2 are read in the rapid-access storage. To this total array is applied the subroutine 'forward elimination'. Then the arrays are shifted by n_2 rows since the first n_2 unknowns have already been eliminated (before the shift the first n_2 rows are again overwritten in the external

memory, the second array of n_2 is read in to fill the space left free, the subroutine 'forward elimination' is in operation, and so on) After the array n_{20} is handled, the back substitution is performed in a similar way to obtain the values of the unknowns.

The application of programs taking account of the matrix structure considerably widens the possibilities of the investigator. The standard mathematical facilities of computers incorporate programs for solving

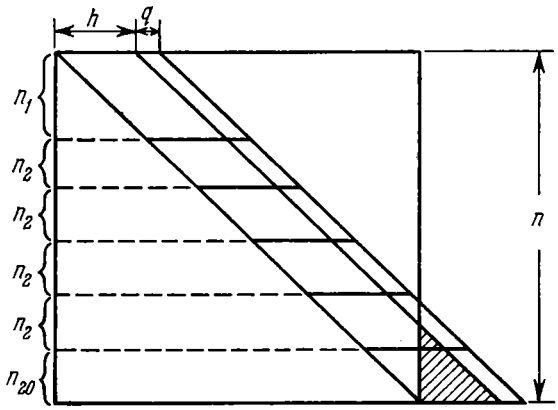

Fig. B.15

systems of linear equations without reference to the matrix structure. They enable one to solve systems of orders up to 60. A great number of programs are described in the literature (see, for example, [3, 204]) which handle the matrix by rows and enable one to solve systems of orders up to 114, but they require large working files. (Everything that was said above about the order of systems which can be solved refers to computers with 4096 words of internal memory.)

Programs that take account of the band structure do not impose any limits on the order of systems at all, they only restrict the bandwidth. Setting n_2 and q equal to unity in (5.1), we find the maximum bandwidth for systems with one right-hand side,

$$h_{\max} = \frac{1+\sqrt{1+4z}}{2}. \tag{5.2}$$

For the M-220, $h_{\max} = 58$ or 59 if it is considered that the usefu memory for storing the array is left after subtracting the space occupied by the interpretative system and program. The second considerable advantage of 'band' programs is saving of time. Imagine a computer with the speed of the M-220 and an internal memory which would store an array $n \times (n+1)$. Suppose we have a band system of order 1000 with $h = 50$. Then it would take about 14 hours to solve the system on the hypothetical computer without taking advantage of the band structure. On the M-220M with complete drum memory the band program will execute the solution in 12 minutes.

APPENDIX C

A SAMPLE PROGRAM FOR THE CALCULATION OF THE STRESS INTENSITY FACTOR BY THE FINITE ELEMENT METHOD

As an illustration of the procedures outlined in Appendix B we present one of the simplest programs for the calculation of the stress intensity factor using the finite element method with digital computer.

The program is written in the input language of the TA-2M translator (the type M-20 computer). It is designed for the calculation of the stress intensity factor for rectangular specimens with a crack propagating along the axis of symmetry. The calculation is carried out for one of the symmetric parts of the specimen, which is divided automatically into rectangular elements. The symmetric part of the band of the matrix of the system of equilibrium equations is formed by the code number method without supplementing by a dummy triangle of zeros. The inhibition of displacements for the regularization of the matrix of the system of equilibrium equations is effected by eliminating the corresponding displacements from the list of unknowns. An algorithm chosen for solving the system of equations is the Gauss method. The change in crack length is simulated by successively inhibiting displacements perpendicular to the crack. The differentiation of the expression for the elastic energy with respect to the crack length is performed so that in evaluating the derivative at a given point account is taken of the values of the energy at two points with smaller crack lengths and at two points with larger crack lengths.

The input data necessary for the operation of the program include the following:

hor, *ver* —number of elements along the length and across the width of the symmetric part of specimen, with $ver \leqslant hor$,
q —number of nodal forces,
w —number of displacements inhibited for regularization of the matrix of system of equilibrium equations,
cr —number of crack lengths to be considered,
stress—stress = 1 for plane stress, any number for plane strain,
e —elastic modulus,
nu —Poisson's ratio,
th —specimen thickness.

hi —size of crack length increment (equal to length or width of element according to how the elements are placed),
fpn —array of degrees-of-freedom numbers in which directions the forces are applied,
fpp —array of magnitudes of forces,
ndn —array of displacement numbers inhibited for regularization of the matrix of system (arranged in the order of decreasing),
u —array of displacement numbers inhibited for variation of the crack length (arranged in the order of increasing crack length). Since the number of these displacements is less by one than the number of crack lengths to be considered, the array is supplemented by an arbitrary figure,
mk —stiffness matrix of rectangular element.

In the idealization, the program numbers the nodal displacements consecutively from node to node, first the displacement in the *ver* direction, then in the *hor* direction. The nodes are considered row after row in the *ver* direction, always starting at the same end. All displacement numbers indicated in the input data must correspond to this numbering. In evaluating the element stiffness matrix the nodal displacements must be numbered as shown in Fig. B.11.

During the operation the program prints out the displacement fields for each crack length in the order of decreasing crack length (they can be used to check the validity of the solution procedure), the arrays of values of the elastic energy and the stress intensity factors for all crack lengths being considered, in the order of their increasing.

```
begin integer i, j, n, ks, s, m, m1, h1, d, d1, d2, b, r, nq, hor, ver,
q, w, cr. stress, h;
      real e, nu, th, hi;
      inout ('r10—2', hor, ver, q, w, cr, stress, e, nu, th, hi);
      h := (ver + 3) × 2; n := (hor + 1) × (ver + 1) × 2 — w;
      ks := n × h — h × (h — 1) ÷ 2;
      begin integer array cn [1 : 8], fpn [1 : q], ndn [1 : w];
         array a [1 : ks], a1 [1 : n], fpp [1 : q], u [1 : cr], si (1 : cr];
         comment do fpn, 10, ndn, 10, a, 2300, moz, a1, 200, moz,
         fpp, 10, u, 30, si, 30;
         inout ('r10 — 2', fpn, fpp, ndn, u);
         begin array mk [1 : 8, 1 : 8];
            inout ('r', mk);
formation of the symmetric part of band:
            for i := 1 step 1 until ks do a [i] := 0;
            for i := 1 step 1 until hor × ver do
            begin cn [1] := (i + (i — 1) ÷ ver + 1) × 2;
               cn [2] := cn [1] — 1; cn [3] := cn [2] — 1;
               cn [4] := cn [3] — 1; cn [5] := cn [1] + ver × 2;
               cn [6] := cn [5] — 1; cn [7] := cn [5] + 2;
               cn [8] := cn [5] + 1;
elimination of unknowns with inhibited displacement numbers:
            for j := 1 step 1 until w do
```

```
                for m := 1 step 1 until 8 do
                begin if cn [m] = ndn [j] then cn [m] := 0;
                    if cn [m] > ndn [j] then cn [m] := cn [m] — 1;
                end;
                for j := 1 step 1 until 8 do
                for m := 1 step 1 until 8 do
                begin if cn [j] × cn [m] = 0 then go to S0;
                    if cn [m] < cn [j] then go to S0;
                    s := (cn [j] — 1) × h + cn [m] — cn [j] + 1;
                    if ch [j] > n — h + 2 then s := s — (cn[j]— n+
                    h — 1) × (cn [j] — n + h — 2) ÷ 2;
                    a [s] := a [s] + mk [j, m];
                end;
S0          end;
        end mk;
        inout ('lc', '412,000', a);
renumbering of displacements inhibited for variation of the crack
length:
        for j := 1 step 1 until w do
        for i := 1 step 1 until cr do
        if u [i] > ndn [j] then u [i] := u [i] — 1;
renumbering of nodal forces and formation of the load vector:
        for i := 1 step 1 until w do
        for m := 1 step 1 until q do
S1:     if fpn [m] > ndn [i] then fpn [m] := fpn [m] — 1;
        for i := 1 step 1 until n do a1 [i] := 0;
        for i := 1 step until q do a1 [fpn [i]] := fpp [i];
solution of the system of equilibrium equations:
        b := 0;
forward elimination:
m0:     h1 : h; d2 := 1;
        for i := 0 step 1 until n — 2 do
        begin
m2:         j := 0; d1 := d2;
            for m1 := 1 step 1 until h1 — 1 do
            begin
m3:             if b = 0 then go to m4;
                a1 [i + 1 + m1] := a1 [i + 1 + m1] — a [d2+m1]×
                a1 [i + 1]/a [d2];
                go to m5;
m4:             d1 := d1 + h1 — j;
                    for m := 0 step 1 until h1 — m1 — 1 do
                    a [d1 + m] := a [d1 + m] — a [d2 + m1] ×
                    a [d2 + m1 + m]/a [d2];
m5:             if n — h1 ≤ m1 + i — 1 then j := j + 1;
            end m1;
            d2 := d2 + h1;
            if n — h1 ≤ i then h1 := h1 — 1;
        end i;
        if b ≠ 0 then go to m7;
```

```
        b := 1;
m6:     go to m0;
back substitution:
m7:     r := n;
m8:     a1 [r] := a1 [r]/a [d2];
        if d2 = 1 then go to m9;
        if h > h1 then h1 := h1 + 1;
        d2 := d2 - h1; r := r - 1;
        for m := 1 step 1 until h1 - 1 do
        a1 [r] := a1 [r] - a [d2 + m] × a1 [r + m];
        go to m8;
m9:     inout ('pb2 - 10', a1);
calculation of the elastic energy:
        j := cr - s + 1; u [j] := 0;
        for i := 1 step 1 until q do  u [j] := u [j] + fpp [i] × a1
        [fpn [i]];
        if s > cr then go to S4;
        s := s + 1; nq := u [j - 1];
        inout ('cl', '412,000', a);
variation of the crack length:
        if nq > n - h + 1 then go to S2; if nq < h
        then d1 := nq - 1 else d1 := h - 1; d := h × (nq -1)+1;
        for i := d step 1 until d + h - 1 do a [i] := 0;
        for i := d step -h + 1 until d - (h - 1) × d1 do
        a [i] := 0;
        go to S3;
S2:     d := (nq - 1) × h + 1 - (nq - n + h - 1) × (nq -
        n + h - 2) ÷ 2;
        for i := d step 1 until d + n - nq do a [i] := 0;
        j := n - nq; d1 = d;
        for i := 1 step 1 until h do
        begin a [d1] := 0; if j < h - 1 then j := j + 1;
        d1 := d1 - j;
        end;
S3:     a [d] := 1.0;
        inout ('lc', '412,000', a);
        go to S1;
calculation of the stress intensity factor:
S4:
        for i := 3 step 1 until cr - 2 do
        begin if i := 3 then
            begin si [1] := (-25 × u [1] + 48 × u [2] - 36×u[3]
                +16 × u [4] - 3 × u [5])/(12 × hi);
                si [2] := (-3 × u [1] -10×u [2] + 18× u [3] - 6
                × u [4] + u [5]/(12 × hi);
            end;
            si [i] := (u [i - 2] - 8 × u [i - 1] + 8 × u [i + 1] -
            u [i + 2])/(12 × hi);
            if i := cr - 2 then
            begin si [i + 1] := (-u [i - 2] + 6 × u [i - 1] - 18
                × u [i] + 10 × u [i + 1] + 3 × u [i + 2])/(12×hi);
```

```
                si [i + 2] := (−3 × u [i − 2] − 16 × u [i−1]+36
                × u [i] − 48 × u [i + 1] + 25 × u [i+2])/(12×hi);
            end;
        end;
        if stress = 1 then d := 1 else d := 1 − nu ↑ 2;
        for i := 1 step 1 until cr do si [i] := sqrt (abs(e × si [i]/
        (th × d)));
        inout ('p2 − 10', u, si);
    end;
end
```

REFERENCES

1. Ames W. F., "Nonlinear Partial Differential Equations in Engineering," Acad. Press, New York-London, 1965.
2. Anderson G. P., Ruggles V. L., Stibor G. S., Use of Finite Element Computer Programs in Fracture Mechanics, *Int. J. Fract. Mech.*, 7(1), 63-76 (1971).
3. Andreeva L. P., A Standard Program for the Solution of Higher-order Systems of Linear Algebraic Equations by a Modified Jordan Method with Row Pivoting, Sb. Rabot Vychisl. Tsentra Mosk. Univ., Vyp. 3, 14 pp., 1965 (in Russian).
4. Ang D. D., Knopoff L., Diffraction of Vector Elastic Waves by a Finite Crack, *Proc. Nat. Acad. Sci. U.S.A.*, 52(4), 1075-1081 (1964).
5. Argyris J. H., Kelsey S., "Energy Theorems and Structural Analysis," Butterworths Scientific Publ., London, 1960.
6. Argyris J. H., The LUMINA Element for the Matrix Displacement Method, *Aeronaut. J.*, 72(690), 514-517 (1968).
7. Ashkinadze B. M., Vladimirov V. I., Likhachev V. A., Ryvkin S. M., Salmanov V. M., Yaroshetskii I. D., On the Fracture of Transparent Dielectrics Induced by a Laser Beam, *Doklady Akad. Nauk SSSR*, 169(5), 1041-1043 (1966) (in Russian).
8. ASTM Committee on Fracture Testing of High-strength Metallic Materials, Fracture Testing of High-strength Sheet Materials: A Report of a Special ASTM Committee, *ASTM Bulletin*, No. 243, January, 1960, pp. 29-40; No. 244, February, 1960, pp. 18-28.
9. ASTM Committee on Fracture Testing of High-strength Metallic Materials, Progress in Measuring Fracture Toughness and Using Fracture Mechanics, Fifth Report, *Materials Research and Standards*, 4(3), 107-119 (1964).
10. Babichev M. A., "Methods of Determining Internal Stresses in Machine Parts," Izd. Akad. Nauk SSSR, Moscow, 1955 (in Russian).
11. Babloyan A. A., Solution of Some Dual Equations Encountered in Elasticity Problems, *Prikl. Matem. i Mekhan.*, 31(4), 678-689 (1967) (in Russian).

12. Bagley E. B., The Separation of Elastic and Viscous Effects in Polymer Flow, *Trans. Soc. Rheol.*, 5, 355-368 (1961).
13. Bagley E. B., Rudin A., Schreiber H. P., Fracture of Liquids in Shear, *Nature*, 203(4941), 175-177 (1964).
14. Barenblatt G. I., Cherepanov G. P., On the Influence of the Body Boundaries on the Development of Brittle Fracture Cracks, *Izv. Akad. Nauk SSSR. Otd. Tekhn. Nauk. Mekhan. i Mashinostr.*, No. 3, 79-88 (1960) (in Russian).
15. Barenblatt G. I., The Mathematical Theory of Equilibrium Cracks in Brittle Fracture, *Zh. Prikl. Mekhan. i Tekhn. Fiz.*, No. 4, 3-56 (1961) (in Russian). Transl.—Advances Appl. Mech., Vol. 7, Acad. Press, New York-London, 1962, pp. 55-129.
16. Barenblatt G. I., Salganik R. L., Cherepanov G. P., On Unstable Crack Propagation, *Prikl. Matem. i Mekhan.*, 26(2), 328-334 (1962) (in Russian).
17. Barenblatt G. I., On Some General Considerations in the Mathematical Theory of Brittle Fracture, *Prikl. Matem. i Mekhan.*, 28(4), 630-643 (1964) (in Russian).
18. Barenblatt G. I., Vsevolodov N. N., Mirkin L. I., Pilipetskii N. F., Raizer Yu. P., On the Fracture of Transparent Materials Under Laser Radiation. The Formation of Gas Bubbles and the Wedging of Materials by Gas Pressure, *Pis'ma v Zh. Eksperim. i Teor. Fiz.*, 5(3), 85-87 (1967) (in Russian).
19. Benbow J. J., Cone Cracks in Fused Silica, *Proc. Phys. Soc.*, 75(5), 697-699 (1960).
20. Berezhnitskii L. T., On the Limiting Equilibrium of a Plate Weakened by a System of Cracks Situated Along a Straight Line at an Angle to the Tension Direction, in "Kontsentratsiya Napryazhenii" (Stress Concentration), Vyp. 1, Naukova Dumka, Kiev, 1965, pp. 46-52 (in Russian).
21. Berezin I. S., Zhidkov N. P., "Computational Methods," 2nd ed., Vol. 2, Fizmatgiz, Moscow, 1962 (in Russian).
22. Berry J. P., Some Kinetic Considerations of the Griffith Criterion for Fracture, *J. Mech. and Phys. Solids*, 8(3), 194-216 (1960).
23. Bilby B. A., Cottrell A. H., Swinden K. H., The Spread of Plastic Yield from a Notch, *Proc. Roy. Soc. London. Ser. A*, 272(1350), 300-314 (1963).
24. Birger I. A., "Residual Stresses," Mashgiz, Moscow, 1963 (in Russian).
25. Blokh V. I., "Theory of Elasticity," Izd. Khar'k. Univ., Khar'kov, 1964 (in Russian).
26. Bloom J. M., Sanders J. L., Jr., The Effect of a Riveted Stringer on the Stress in a Cracked Sheet, *Trans. ASME. Ser. E*, 33(3), 561-570 (1966).
27. Borodachev N. M., A Plane Contact Problem for an Elastic Body of Finite Width, *Izv. Akad. Nauk SSSR. Otd. Tekhn. Nauk. Mekhan. i Mashinostr.*, No. 6, 170-172 (1962) (in Russian).
28. Borodachev N. M., A Thermoelastic Problem for an Infinite Body with an Axially Symmetric Crack, *Prikl. Mekhanika*, 2(2), 91-99 (1966) (in Russian).

29. Borodachev N. M., On the Indentation of the End of a Semi-infinite Elastic Cylinder by a Punch, *Prikl. Mekhanika*, 3(9), 83-89 (1967) (in Russian).
30. Borodachev N. M., A Dynamic Crack Problem in the Case of Longitudinal Shear Deformation, *Probl. Prochnosti*, No. 4, 23-25 (1973) (in Russian).
31. Bowie O. L., Rectangular Tensile Sheet with Symmetric Edge Cracks, *Trans. ASME. Ser. E*, 31(2), 208-212 (1964).
32. Broberg K. B., The Propagation of a Brittle Crack, *Arkiv fys.*, 18(2), 159-192 (1960).
33. Brown W. F., Jr., Srawley J. E., Plane Strain Crack Toughness Testing of High Strength Metallic Materials, *ASTM Special Techn. Publ.* No. 410, Amer. Society for Testing and Materials, Philadelphia, 1967.
34. Buina E. V., Determination of the Critical Force Value for a Brittle Plate with Two Equal Length Cracks, in "Voprosy Mekhaniki Real'nogo Tverdogo Tela" (Problems in the Mechanics of Real Solids), Vyp. 2, Naukova Dumka, Kiev, 1964, pp. 64-70 (in Russian).
35. Busbridge I. W., Dual Integral Equations, *Proc. London Math. Soc. Ser. 2*, 44, Part 2, 115-129 (1938).
36. Byskov E., The Calculation of Stress Intensity Factors Using the Finite Element Method with Cracked Elements, *Int. J. Fract. Mech.*, 6(2), 159-167 (1970).
37. Carman C. M., Armiento D. F., Markus H., Fracture Toughness and Pressure Vessel Performance, *Trans. ASME. Ser. A*, 86(4), 465-471 (1964).
38. Chan S. K., Tuba I. S., Wilson W. K., On the Finite Element Method in Linear Fracture Mechanics, *Eng. Fract. Mech.*, 2(1), 1-17 (1970).
39. Chang Shih-Jung, Diffraction of Plane Dilatational Waves by a Finite Crack, *Quart. J. Mech. and Appl. Math.*, 24, Part 4, 423-443 (1971).
40. Cherepanov G. P., An Elastic-plastic Problem Under Conditions of Antiplane Strain, *Prikl. Matem. i Mekhan.*, 26(4), 697-708 (1962) (in Russian).
41. Cherepanov G. P., On the Effect of Pulses on the Development of Initial Cracks, *Zh. Prikl. Mekhan. i Tekhn. Fiz.*, No. 1, 97-103 (1963) (in Russian).
42. Cherepanov G. P., On a Method of Solving the Elastic-plastic Problem, *Prikl. Matem. i Mekhan.*, 27(3), 428-435 (1963) (in Russian).
43. Cherepanov G. P., On the Strength of Composites, *Zh. Prikl. Mekhan. i Tekhn. Fiz.*, No. 2, 77-79 (1967) (in Russian).
44. Cherepanov G. P., On Crack Propagation in a Continuous Medium, *Prikl. Matem. i Mekhan.*, 31(3), 476-488 (1967) (in Russian).
45. Cherepanov G. P., On Quasi-brittle Fracture, *Prikl. Matem. i Mekhan.*, 32(6), 1034-1042 (1968) (in Russian).
46. Cherepanov G. P., On Crack Growth Under Cyclic Loading, *Zh. Prikl. Mekhan. i Tekhn. Fiz.*, No. 6, 64-75 (1968) (in Russian).
47. Cherepanov G. P., Cracks in Solids, *Int. J. Solids and Struct.*, 4(8), 811-831 (1968).

48. Cherepanov G. P., On Crack Development in Viscous Bodies, *Izv. Akad. Nauk SSSR. Mekhan. Tverd. Tela*, No. 1, 122-127 (1969) (in Russian).
49. Cherepanov G. P., Mirsalimov V. M., On the Effect of Stiffeners on Crack Development, *Izv. Akad. Nauk AzerbSSR. Ser. Fiz.-tekhn. i Matem. Nauk*, No. 1, 7-11 (1969) (in Russian).
50. Cherepanov G. P., The Brittle Strength of Pressure Vessels, *Zh. Prikl. Mekhan. i Tekhn. Fiz.*, No. 6, 90-101 (1969) (in Russian).
51. Cherepanov G. P., On Combustion in Narrow Cavities, *Zh. Prikl. Mekhan. i Tekhn. Fiz.*, No. 2, 90-95 (1970) (in Russian).
52. Cherepanov G. P., On Singular Solutions in Elasticity Theory, in "Problemy Mekhaniki Tverdogo Deformiruemogo Tela" (Problems in the Mechanics of Deformable Solids), Sudostroenie, Leningrad, 1970, pp. 467-479 (in Russian).
53. Cherepanov G. P., Diffraction of Elastic Waves by a Cut, in "Mekhanika Sploshnoi Sredy i Rodstvennye Problemy Analiza" (Continuum Mechanics and Related Problems of Analysis—Contrib. in Honour of the 80th Birthday of Acad. N. I. Muskhelishvili), Nauka, Moscow, 1972, pp. 615-622 (in Russian).
54. Cherepanov G. P., "Mechanics of Brittle Fracture," Nauka, Moscow, 1974 (in Russian).
55. Chernous'ko F. L., The Method of Local Variations for the Numerical Solution of Variational Problems, *Zh. Vychisl. Matem. i Matem. Fiz.*, 5(4), 749-754 (1965) (in Russian).
56. Chernykh K. F., "A Linear Theory of Shells," Part 2, Some Problems of the Theory, Izd. Leningr. Univ., Leningrad, 1964 (in Russian).
57. Chibrikova L. I., On the Riemann Boundary Value Problem for Automorphic Functions, *Uchenye Zapiski Kazan. Univ.*, No. 4, 59-110 (1956) (in Russian).
58. Clough R. W., The Finite Element Method in Plane Stress Analysis, in "Proceedings of the Second Conference on Electronic Computation," American Society of Civil Engineers, Pittsburgh, Pa., 1960, pp. 345-378.
59. Clough R. W., Rashid Y., Finite Element Analysis of Axisymmetric Solids, *J. Eng. Mech. Div. Proc. Amer. Soc. Civ. Eng.*, 91(1), Part 1, 71-85 (1965).
60. Cotterell B., An Interpretation of the Mechanics of Crack Growth by Fatigue, *Trans. ASME. Ser. D*, 87(1), 230-236 (1965).
61. Creager M., Paris P. C., Elastic Field Equations for Blunt Cracks with Reference to Stress Corrosion Cracking, *Int. J. Fract. Mech.*, 3(4), 247-252 (1967).
62. "Current Status of Mining Science in the USSR," Nauka, Moscow, 1968 (in Russian).
63. Davidenkov N. N., "Dynamic Testing of Metals," 2nd ed., *ONTI*, Leningrad-Moscow, 1936 (in Russian).
64. Ditkin V. A., Prudnikov A. P., "Handbook of Operational Calculus," Vysshaya Shkola, Moscow, 1965 (in Russian).
65. Dorosh N. A., Kit G. S., A Thermoelastic State of a Plane with Two Equal Arc Cracks, *Izv. Akad. Nauk SSSR. Mekhan. Tverd. Tela*, No. 5, 115-119 (1969) (in Russian).

66. Drozdovskii B. A., Fridman Ya. B., "The Effect of Cracks on the Mechanical Properties of Structural Steels," Metallurgizdat, Moscow, 1960 (in Russian).
67. Drozdovskii B. A., Markochev V. M., Fridman Ya. B., A Procedure for Estimating the Critical Crack Length in Single Tension, *Zavodsk. Labor.*, 32(7), 859-863 (1966) (in Russian).
68. Drozdovskii B. A., Markochev V. M., Fridman Ya. B., Fracture Diagrams of Solids, *Doklady Akad. Nauk SSSR*, 174(4), 807-810 (1967) (in Russian).
69. Drozdovskii B. A., Markochev V. M., Investigation of the Fracture Kinetics of Sheet Magnetic Materials by the Ferrograph Technique, *Zavodsk. Labor.*, 34(2), 209-212 (1968) (in Russian).
70. Drozdovskii B. A., Morozov E. M., On Two Mechanical Characteristics Giving an Estimate of Fracture Resistance, *Zavodsk. Labor.*, 37(1), 78-89 (1971) (in Russian).
71. Dugdale D. S., Yielding of Steel Sheets Containing Slits, *J. Mech. and Phys. Solids*, 8(2), 100-104 (1960).
72. Dulaney E. N., Brace W. F., Velocity Behavior of a Growing Crack, *J. Appl. Phys.* 31(12), 2233-2236 (1960).
73. England A. H., Green A. E., Some Two-dimensional Punch and Crack Problems in Classical Elasticity, *Proc. Cambridge Philos. Soc.*, 59(2), 489-500 (1963).
74. Ergatoudis J., Irons B. M., Zienkiewicz O. C., Curved, Isoparametric Quadrilateral Elements for Finite Element Analysis, *Int. J. Solids and Struct.*, 4(1), 31-42 (1968).
75. Ergatoudis J., Irons B. M., Zienkiewicz O. C., Three-dimensional Stress Analysis of Arch Dams and Their Foundations, in "Proceedings of the Symposium on Arch Dams," Institution of Civil Engineers, London, 1968.
76. Eshelby J. D., The Continuum Theory of Lattice Defects, in "Solid State Physics" (Advances in Research and Applications), Vol. 3 (Frederick Seitz and David Turnbull, eds.), Acad. Press, New York, 1956, pp. 79-144.
77. Felippa C. A., Refined Finite Element Analysis of Linear and Non-linear Two-dimensional Structures, SESM Rept. 66-22, University of California, Dept. of Civil Engineering, Berkeley, California, 1966.
78. Finkel' V. M., "Physics of Fracture. Crack Growth in Solids," Metallurgiya, Moscow, 1970 (in Russian).
79. Florence A. L., Goodier J. N., Thermal Stress at Spherical Cavities and Circular Holes in Uniform Heat Flow, *Trans. ASME. Ser. E*, 26(2), 293-294 (1959).
80. Florence A. L., Goodier J. N., Thermal Stresses Due to Disturbance of Uniform Heat Flow by an Insulated Ovaloid Hole, *Trans. ASME. Ser. E*, 27(4), 635-639 (1960).
81. Folias E. S., An Axial Crack in a Pressurized Cylindrical Shell, *Int. J. Franct. Mech.*, 1(2), 104-113 (1965).
82. Forsythe G. E., Moler C. B., "Computer Solution of Linear Algebraic Systems," Englewood Cliffs, 1967.
83. "Fracture. An Advanced Treatise, Vol. 2, Mathematical Fundamentals" (H. Liebowitz, ed.), Acad. Press, New York-London, 1969.

84. "Fracture 1969," (Proceedings of the Second International Conference on Fracture, Brighton, April 1969), Chapman and Hall, London, 1969.
85. Fracture Toughness Testing and Its Applications, *ASTM Special Techn. Publ.* No. 381, Amer. Society for Testing and Materials, Philadelphia, 1965.
86. Frederick C. O., Wong Y. C., Edge F. W., Two-dimensional Automatic Mesh Generation for Structural Analysis, *Int. J. Numer. Methods Eng.*, 2(1), 133-144 (1970).
87. Frenkel' Ya. I., "The Kinetic Theory of Liquids," Izd. Akad. Nauk SSSR, Moscow-Leningrad, 1945 (in Russian).
88. Freund L. B., Achenbach J. D., Diffraction of a Plane Pulse by a Closed Crack at the Interface of Elastic Solids, *Z. angew. Math. und Mech.*, 48(3), 173-185 (1968).
89. Freund L. B., The Oblique Reflection of a Rayleigh Wave from a Crack Tip, *Int. J. Solids and Struct.*, 7(9), 1199-1210 (1971).
90. Fridman Ya. B., The Relative Structure Inhomogeneity Diagram of Materials, *Doklady Akad. Nauk SSSR*, 106(2), 258-261 (1956) (in Russian).
91. Fridman Ya. B., The Kinetics of Deformation and Fracture, *Acta techn. Acad. sci. hung.*, 35-36, 83-114 (1961) (in Russian).
92. Fridman Ya. B., Morozov E. M., On the Application of Variational Principles for a Study of Fracture Processes, in "Mekhanizm Plasticheskoi Deformatsii Materialov" (The Mechanism of Plastic Deformation of Materials), Naukova Dumka, Kiev, 1965, pp. 73-82 (in Russian).
93. Fridman Ya. B., Zilova T. K., Drozdovskii B. A., Gordeeva T. A., Material Assessment Relative to Fracture Arrest Capability, *Zavodsk. Labor.*, 33(10), 1316-1328 (1967) (in Russian).
94. Fridman Ya. B., "Mechanical Properties of Metals," 3rd ed., Parts 1, 2, Mashinostroenie, Moscow, 1974 (in Russian).
95. Gaivas' I. V., A Steady Thermoelastic State of a Non-homogeneous Plane with a Circular Arc Cut, *Fiz.-khim. Mekhan. Materialov*, 5(3), 351-356 (1969) (in Russian).
96. Galin L. A., Fridman Ya. B., Cherepanov G. P., Morozov E.M., Parton V. Z., On the Condition at a Crack Tip, *Doklady Akad. Nauk SSSR*, 187(4), 754-757 (1969) (in Russian).
97. Gallagher R. H., Padlog J., Bijlaard P. P., Stress Analysis of Heated Complex Shapes, *ARS Journal*, 32(5), 700-707 (1962).
98. Gol'tsev V. Yu., Fracture Arrest Capability of Thin Steel Sheets Under Single and Repeated Loads, M. Sc. Thesis, Moscow Physical-Engineering Institute, 1968 (in Russian).
99. Goodier J. N., Field F. A., Plastic Energy Dissipation in Crack Propagation, in "Fracture of Solids" (D. C. Drucker and J. J. Gilman, eds.), Interscience Publ., New York, 1963, pp. 103-118.
100. Goodier J. N., Florence A. L., Localized Thermal Stress at Holes, Cavities, and Inclusions Disturbing Uniform Heat Flow. Thermal Crack Propagation, in "Proceedings of the Eleventh International Congress for Applied Mechanics, Munich, 1964" (Henry Gortler, ed.), Springer-Verlag, Berlin, 1966, pp. 562-568.

101. Gradshtein I. S., Ryzhik I. M., "Tables of Integrals, Sums, Series, and Products," Nauka, Moscow, 1971 (in Russian).
102. Greif R., Sanders J. L., Jr., The Effect of a Stringer on the Stress in a Cracked Sheet, *Trans. ASME. Ser. E*, **32**(1), 59-66 (1965).
103. Griffith A. A., The Theory of Rupture, in "Proceedings of the First International Congress for Applied Mechanics, Delft, 1924" (C. B. Biezeno and J. M. Burgers, eds.), Waltman, Delft, 1925, pp. 55-63.
104. Griffith A. A., The Phenomena of Rupture and Flow in Solids, *Philos. Trans. Roy. Soc. London. Ser. A*, **221**, 163-198 (1920).
105. Grigolyuk E. I., Fil'shtinskii L. A., "Perforated Plates and Shells," Nauka, Moscow, 1970 (in Russian).
106. Hahn G. T., Rosenfield A. R., Local Yielding and Extension of a Crack Under Plane Stress, Acta metallurgica, **13**(3), 293-306 (1965).
107. Harvey E. N., McElroy Wm. D., Whiteley A. H., On Cavity Formation in Water, *J. Appl. Phys.*, **18**(2), 162-172 (1947).
108. Hilton P. D., Hutchinson J. W., Plastic Intensity Factors for Cracked Plates, *Eng. Fract. Mech.*, **3**(4), 435-451 (1971).
109. Hoek E., Bieniawski Z. T., Brittle Fracture Propagation in Rock Under Compression, *Int. J. Fract. Mech.*, **1**(3), 137-155 (1965).
110. Hussain M. A., Pu S. L., Dynamic Stress Intensity Factor for an Unbounded Plate Having Collinear Cracks, *Eng. Fract. Mech.*, **4**(4), 865-876 (1972).
111. Hutton J. F., Fracture of Liquids in Shear, *Nature*, **200**(4907), 646-648 (1963).
112. Hutton J. F., The Fracture of Liquids in Shear: The Effects of Size and Shape, *Proc. Roy. Soc. London. Ser. A*, **287**(1409), 222-239 (1965).
113. Il'yushin A. A., Ogibalov P. M., On the Strength of the Casings of a Thick-walled Cylinder and a Hollow Sphere Exposed to Irradiation, *Inzhenernyi Sbornik*, **28**, 134-144 (1960) (in Russian).
114. Ioffe A. F., Kirpicheva M. V., Levitskaya M. A., Deformation and Strength of Crystals, *Zh. Russkogo Fiz.-khim. Obshchestva. Chast' Fiz.*, **56**, Vyp. 5-6, 489-504 (1924) (in Russian).
115. Irwin G. R., Fracture Dynamics, in "Fracturing of Metals" (A Seminar on the Fracturing of Metals), Amer. Society for Metals, Cleveland, 1948, pp. 147-166.
116. Irwin G. R., Relation of Stresses Near a Crack to the Crack Extension Force, in "Actes. IX Congr. internat. mécan. appl.," T. 8, University Bruxelles, Bruxelles, 1957, pp. 245-251.
117. Irwin G. R., Analysis of Stresses and Strains Near the End of a Crack Traversing a Plate, *J. Appl. Mech.*, **24**(3), 361-364 (1957). Discussion—*J. Appl. Mech.*, **25**(2), 299-301 (1958).
118. Irwin G. R., Fracture, in "Encyclopedia of Physics, Vol. VI, Elasticity and Plasticity" (S. Flügge, ed.), Springer-Verlag, Berlin, 1958, pp. 551-590.
119. Irwin G. R., Plastic Zone Near a Crack and Fracture Toughness, in "Proceedings of the Seventh Sagamore Ordnance Materials

Research Conference" (Rept. No. Met. E 661-611/F), Syracuse University Research Institute, 1960, pp. IV-63 to IV-78.
120. Irwin G. R., Crack-toughness Testing of Strain-rate Sensitive Materials, *Trans. ASME. Ser. A*, 86(4), 444-450 (1964).
121. Isida M., Stress-intensity Factors for the Tension of an Eccentrically Cracked Strip, *Trans. ASME. Ser. E*, 33(3), 674-675 (1966).
122. Ivanov N. P., Stepanov V. A., Measurement of the Strength of Plastics Under High-velocity Compression, *Mekhan. Polimerov*, No. 5, 34-38 (1965) (in Russian).
123. Jenkins W. M., "Matrix and Digital Computer Methods in Structural Analysis," McGraw-Hill Book Co., London, 1969.
124. Kachanov L. M., "Fundamentals of the Theory of Plasticity," 2nd ed., Nauka, Moscow, 1969 (in Russian). Transl.—Mir Publishers, Moscow, 1974; "Foundations of the Theory of Plasticity," North-Holland Publ. Co., Amsterdam, 1971.
125. Kaminskii A. A., Rushitskii Ya. Ya., On the Applicability of Volterra's Principle in the Analysis of Crack Motion in Elastic-hereditary Media, *Prikl. Mekhanika*, 5(4), 102-108 (1969) (in Russian).
126. Kapitsa P. L., Power Electronics, *Uspekhi Fiz. Nauk*, 78(2), 181-265 (1962) (in Russian).
127. Kassir M. K., Bregman A., Thermal Stresses in a Solid Containing Parallel Circular Cracks, *Appl. Sci. Res.*, 25(3-4), 262-280 (1971).
128. Kerimov K. A., On Methods for a Theoretical and Experimental Analysis of the Dynamic Laws of the Deformation of Materials, in "Issledovaniya po Teorii Differentsial'nykh Uravnenii i Teorii Funktsii" (Investigations on the Theory of Differential Equations and Function Theory), Akad. Nauk AzerbSSR, Baku, 1965, pp. 76-91 (in Russian).
129. Kies J. A., Romine H., Smith H. L., Bernstein H., Minimum Toughness Requirements for High Strength Sheet Steel, *Trans. ASME. Ser. D*, 83(1), 1-9 (1961).
130. Kit G. S., Podstrigach Ya. S., Determination of a Stationary Temperature Field and Stresses in the Vicinity of a Heat-resisting Slit, *Fiz.-khim. Mekhan. Materialov*, 2(3), 247-252 (1966) (in Russian).
131. Kit G. S., Frenchko Yu. S., Thermal Stresses in an Elastic Plane with a Thermally Insulated Arc Crack, 4(9), 16-22 (1968) (in Russian).
132. Kit G. S., Poberezhnyi O. V., On the State of Stress in a Heated Material Having Circular Crack Type Internal Defects, *Fiz.-khim. Mekhan. Materialov*, 5(3), 345-350 (1969) (in Russian).
133. Kobayashi A. S., Maiden D. E., Simon B. J., Iida S., Application of Finite Element Analysis Method to Two-dimensional Problems in Fracture Mechanics, *Paper Amer. Soc. Mech Eng.*, No. WA/PVP-12, 1969.
134. Koiter W. T., Approximate Solution of Wiener-Hopf Type Integral Equations with Applications, *Proc. Koninkl. nederl. akad. wetensch.*, 57(5), 558-579 (1954).

135. Koiter W. T., An Infinite Row of Collinear Cracks in an Infinite Elastic Sheet, *Ing.-Arch.*, 28, 168-172 (1959).
136. Koiter W. T., Stress Distribution in an Infinite Elastic Sheet with a Doubly-periodic Set of Equal Holes, in "Boundary Problems in Differential Equations" (R. E. Langer, ed.), University Wisconsin Press, Madison, 1960, pp. 191-213.
137. Kolosov G. V., "On One Application of Complex Function Theory to the Plane Problem of the Mathematical Theory of Elasticity," Ur'ev, 1909 (in Russian).
138. Kornfel'd M. O., Ryvkin I. M., Brittleness of Liquids, *Zh. Eksperim. i Teor. Fiz.*, 9(5), 595-596 (1939) (in Russian).
139. Kornilov G. I., Yarema S. Ya., Plate Specimens with a Crack-like Stress Raiser for an Experimental Investigation of Plasticity Bands, in "Voprosy Mekhaniki Real'nogo Tverdogo Tela" (Problems in the Mechanics of Real Solids), Vyp. 1, Izd. Akad. Nauk USSR, Kiev, 1962, pp. 29-36 (in Russian).
140. Kostrov B. V., Nikitin L. V., Flitman L. M., Brittle Fracture Mechanics, *Izv. Akad. Nauk SSSR. Mekhan. Tverd. Tela*, No. 3, 112-125 (1969) (in Russian).
141. Krafft J. M., Sullivan A. M., Boyle R. W., Effect of Dimensions on Fast Fracture Instability of Notched Sheets, in "Proceedings of the Crack Propagation Symposium," Vol. I, College of Aeronautics and the Royal Aeronautical Society, Cranfield (England), 1961, pp. 8-28.
142. Krafft J. M., Correlation of Plane Strain Crack Toughness with Strain Hardening Characteristics of a Low, a Medium, and a High Strength Steel, *Appl. Mater. Res.*, 3(2), 88-101 (1964).
143. Kudryavtsev B. A., Parton V. Z., Cherepanov G. P., An Elastic-plastic Problem for a Plane with Straight Slits, *Izv. Akad. Nauk SSSR. Mekhan. Tverd. Tela*, No. 3, 174-176, (1969) (in Russian).
144. Kudryavtsev B. A., Parton V. Z., Dual Trigonometric Series in Slit and Punch Problems, *Prikl. Matem. i Mekhan.*, 33(5), 844-849 (1969) (in Russian).
145. Kudryavtsev B. A., Parton V. Z., Peskov Yu. A., Cherepanov G. P., On the Local Plastic Zone Near the End of a Slit, *Izv. Akad. Nauk SSSR. Mekhan. Tverd. Tela*, No. 1, 61-64 (1970) (in Russian).
146. Kudryavtsev B. A., Parton V. Z., Peskov Yu. A., Cherepanov G. P., On the Local Plastic Zone Near the End of a Slit (Plane Strain), *Izv. Akad. Nauk SSSR. Mekhan. Tverd. Tela*, No. 5, 132-138 (1970) (in Russian).
147. Kudryavtsev B. A., Parton V. Z., A Quasi-static Thermal Problem for a Plane with a Cut, *Probl. Prochnosti*, No. 2, 46-51 (1970) (in Russian).
148. Kudryavtsev B. A., A Quasi-stationary Thermoelastic Problem for a Plane with a Semi-infinite Cut, in "Dinamika Sploshnoi Sredy" (Continuum Dynamics), Vyp. 6, Novosibirsk, 1970, pp. 24-31 (in Russian).
149. Kudryavtsev B. A., The Stresses in an Ellipsoidal Shell with an Arbitrarily Oriented Crack, *Izv. Akad. Nauk SSSR. Mekhan. Tverd. Tela*, No. 2, 81-85 (1971) (in Russian).

150. Kudryavtsev B. A., An Axially Symmetric Thermoelastic Problem for a Cylinder with a Cut, *Zh. Prikl. Mekhan. i Tekhn. Fiz.*, No. 6, 154-158 (1971) (in Russian).
151. Kudryavtsev B. A., Parton V. Z., The First Fundamental Problem of Elasticity for a Doubly Periodic System of Cuts, in "Mekhanika Sploshnoi Sredy i Rodstvennye Problemy Analiza" (Continuum Mechanics and Related Problems of Analysis—Contrib. in Honour of the 80th Birthday of Acad. N. I. Muskhelishvili), Nauka, Moscow, 1972, pp. 251-258 (in Russian).
152. Kudryavtsev B. A., Parton V. Z., Torsion and Tension [of a Cylinder with an External Circumferential Cut, *Prikl. Matem. i Mekhan.*, 37(2), 316-325 (1973) (in Russian).
153. Leipunskii O. I., Kirsanova Z. V., The Mechanical Stability of Burning Cracks in Powder, in "Pervyi Vsesoyuznyi Simpozium po Goreniyu i Vzryvu, 19-24 fevralya 1968. Tezisy Dokladov" (First All-Union Symposium on Combustion and Explosion, February 19-24, 1968. Abstracts of Papers), Nauka, Moscow, 1968, pp. 53-55 (in Russian).
154. Lenskii V. S., The Effect of Atomic Irradiation on the Mechanical Properties of Solids, *Inzhenernyi Sbornik*, 28, 97-133 (1960) (in Russian).
155. Leonov M. Ya., Panasyuk V. V., Development of Minute Cracks in Solids, *Prikl. Mekhanika*, 5(4), 391-401 (1959) (in Ukrainian).
156. Leonov M. Ya., Elements of the Theory of Brittle Fracture, *Zh. Prikl. Mekhan. i Tekhn. Fiz.*, No. 3, 85-92 (1961) (in Russian).
157. Leonov M. Ya., Vitvitskii P. M., Yarema S. Ya., Plasticity Bands in Plates with Crack-like Stress Raisers Under Tension, *Doklady Akad. Nauk SSSR*, 148(3), 541-544 (1963) (in Russian).
158. Levy N., Mareal P. V., Ostergren W. J., Rice J. R., Small Scale Yielding Near a Crack in Plane Strain: A Finite Element Analysis, *Int. J. Fract. Mech.*, 7(2), 143-156 (1971).
159. Lewin L., "Advanced Theory of Waveguides," Iliffe, London, 1951.
160. Likhachev Yu. I., Zvonarev V. P., Swelling of Fissile Materials in Non-uniform Temperature and Neutron Fields, in "Prochnost' i Deformatsiya Materialov v Neravnomernykh Fizicheskikh Polyakh" (Strength and Deformation of Materials in Non-uniform Physical Fields), Vyp. 2, Atomizdat, Moscow, 1968, pp. 105-126 (in Russian).
161. Loeber J. F., Sih G. C., Diffraction of Antiplane Shear Waves by a Finite Crack, *J. Acoust. Soc. Amer.*, 44(1), 90-98 (1968).
162. Love A. E. H., "A Treatise on the Mathematical Theory of Elasticity," 4th ed., Cambridge University Press, Cambridge, 1927.
163. McClintock F. A., Ductile Fracture Instability in Shear, *J. Appl. Mech.*, 25(4), 582-588 (1958).
164. McClintock F. A., On the Plasticity of the Growth of Fatigue Cracks, in "Fracture of Solids" (D. C. Drucker and J. J. Gilman, eds.), Interscience Publ., New York, 1963, pp. 65-102.
165. McClintock F. A., Irwin G. R., Plasticity Aspects of Fracture Mechanics, in "Fracture Toughness Testing and Its Applications"

(*ASTM Special Techn. Publ.* No. 381), Amer. Society for Testing and Materials, Philadelphia, 1965, pp. 84-113.
166. McClintock F. A., Argon A. S., "Mechanical Behavior of Materials," Addison Wesley Publ. Co., Reading, Mass., 1966.
167. McLachlan N. W., "Theory and Application of Mathieu Functions," Clarendon Press, Oxford, 1947.
168. Mal A. K., Interaction of Elastic Waves with a Penny-shaped Crack, *Int. J. Eng. Sci.*, 8(5), 381-388 (1970).
169. Malkin A. Ya., Leonov A. I., On Criteria for the Instability of the Shear Deformation Behaviour of Viscoelastic Polymeric Systems, *Doklady Akad. Nauk SSSR*, 151(2), 380-383 (1963) (in Russian).
170. Markochev V. M., Drozdovskii B. A., A Procedure for Estimating the Velocity of Crack Propagation and for Producing the Specified Stress Under Repeated Loading, *Zavodsk. Labor.*, No. 31(3), 345-349 (1965) (in Russian).
171. Markochev V. M., A Procedure and a Study of Macrofracture Kinetics in Sheet Materials Under Single and Repeated Loading, M. Sc. Thesis, Moscow Physical-Engineering Institute, 1966 (in Russian).
172. Markochev V. M., Gol'tsev V. Yu., Bobrinskii A. P., A Simplified Procedure for Crack Length Measurement in Sheet Specimens Using an Electrical Potential Method, *Zavodsk. Labor.*, 37(5), 598-600 (1971) (in Russian).
173. Maue A. W., Die Beugung elastischer Wellen an der Halbebene, *Z. angew. Math. und Mech.*, 33(1-2) 1-10 (1953).
174. Maue A. W., Die Entspannungswelle bei plötzlichem Einschnitt eines gespannten elastischen Körpers, *Z. angew. Math. und Mech.*, 34(1-2), 1-12 (1954).
175. Melosh R. J., Structural Analysis of Solids, *J. Struct. Div. Proc. Amer. Soc. Civ. Eng.*, 89(ST4), August, 205-223 (1963).
176. Mindlin R. D., Influence of Couple-stresses on Stress Concentrations, *Experim. Mech.*, 3(4), 1-7 (1963).
177. Morozov E. M., Polak L. S., Fridman Ya. B., On the Variational Principles of Crack Development in Solids, *Doklady Akad. Nauk SSSR*, 156(3), 537-540 (1964) (in Russian).
178. Morozov E. M., Fridman Ya. B., Crack Analysis as a Method of Estimating Fracture Characteristics, *Zavodsk. Labor.*, 32(8), 977-984 (1966) (in Russian).
179. Morozov E. M., Fridman Ya. B., Some Laws in Crack Theory, in "Prochnost' i Deformatsiya Materialov v Neravnomernykh Fizicheskikh Polyakh" (Strength and Deformation of Materials in Non-uniform Physical Fields), Vyp. 2, Atomizdat, Moscow, 1968, pp. 216-253 (in Russian).
180. Morozov E. M., Polak L. S., On Energy Criteria of Fracture, in "Prochnost' i Deformatsiya Materialov v Neravnomernykh Fizicheskikh Polyakh" (Strength and Deformation of Materials in Non-uniform Physical Fields), Vyp. 2, Atomizdat, Moscow, 1968, pp. 254-259 (in Russian).
181. Morozov E. M., Parton V. Z., Some Problems in Fracture Mechanics for a Plane with Cuts, in "Prochnost' i Deformatsiya

Materialov v Neravnomernykh Fizicheskikh Polyakh" (Strength and Deformation of Materials in Non-uniform Physical Fields), Vyp. 2, Atomizdat, Moscow, 1968, pp. 272-275 (in Russian).
182. Morozov E. M., Parton V. Z., Application of the Variational Principle in Crack Problems, *Inzhenernyi Zh. Mekhan. Tverd. Tela*, No. 2, 173-177 (1968) (in Russian).
183. Morozov E. M., Parton V. Z., On a Justification of Irwin's Criterion at a Crack Tip, *Inzhenernyi Zh. Mekhan. Tverd. Tela*, No. 6, 147-152 (1968) (in Russian).
184. Morozov E. M., The Variational Principle in Fracture Mechanics, *Doklady Akad. Nauk SSSR*, 184(6), 1308-1311 (1969) (in Russian).
185. Morozov E. M., The Energy Condition for Crack Growth in Elastic-plastic Bodies, *Doklady Akad. Nauk SSSR*, 187(1), 57-60 (1969) (in Russian).
186. Morozov E. M., The Method of Sections in Crack Theory, *Izv. Vyssh. Uchebn. Zavedenii. Stroit. i Arkhitekt.*, No. 12, 57-63 (1969) (in Russian).
187. Morozov E. M., Sapunov V. T., Crack Development in Elastic-plastic Bodies, in "Deformatsiya i Razrushenie pri Termicheskikh i Mekhanicheskikh Vozdeistviyakh" (Deformation and Fracture Due to Thermal and Mechanical Effects), Vyp. 3, Atomizdat, Moscow, 1969, pp. 49-58 (in Russian).
188. Morozov E. M., Some Methods of Solution of Dynamic Crack Problems, in "Deformatsiya i Razrushenie pri Termicheskikh i Mekhanicheskikh Vozdeistviyakh" (Deformation and Fracture Due to Thermal and Mechanical Effects), Vyp. 3, Atomizdat, Moscow, 1969, pp. 141-147 (in Russian).
189. Morozov E. M., On a Generalization of the δ_c-Crack Theory, *Prikl. Mekhanika*, 6(4), 128-131 (1970) (in Russian).
190. Morozov E. M., On the Correspondence Between the Energy Fracture Criterion and the Mathematical Simulation of Deformation Phenomena at the End of a Cut (Crack), *Prikl. Matem. i Mekhan.*, 34(4), 768-777 (1970) (in Russian).
191. Morozov E. M., The Energy Fracture Criterion for Elastic-plastic Bodies, in "Kontsentratsiya Napryazhenii" (Stress Concentration), Vyp. 3, Naukova Dumka, Kiev, 1971, pp. 85-90 (in Russian).
192. Morozov E. M., Parton V. Z., On the Velocity of Supercritical Crack Propagation, *Izv. Akad. Nauk SSSR. Mekhan. Tverd. Tela*, No. 4, 174-176 (1971) (in Russian).
193. Morozov E. M., Sapunov V. T., Application of the Variational Principle to the Solution of Crack Problems in Viscoelastic Media, *Prikl. Mekhanika*, 8(6), 33-38 (1972) (in Russian).
194. Morozov E. M., Sapunov V. T., On Fracture Resistance Curves, *Fiz.-khim. Mekhan. Materialov*, 8(4), 71-74 (1972) (in Russian).
195. Morozov E. M., Sapunov V. T., On the Calculation of Fracture Diagrams, *Zh. Prikl. Mekhan. i Tekhn. Fiz.*, No. 2, 172-176 (1973) (in Russian).
196. Morozova E. A., Parton V. Z., On the Effect of Stiffeners on Crack Propagation, *Zh. Prikl. Mekhan. i Tekhn. Fiz.*, No. 5, 112-114 (1961) (in Russian).

197. Mott N. F., Fracture of Metals: Theoretical Considerations, *Engineering*, **165**(4275), 16-18 (1948).
198. Murrell S. A. F., The Theory of the Propagation of Elliptical Griffith Cracks Under Various Conditions of Plane Strain or Plane Stress, *Brit. J. Appl. Phys.*, **15**(10), 1195-1223 (1964).
199. Muskhelishvili N. I., "Singular Integral Equations; Boundary Problems of Function Theory and Their Application to Mathematical Physics," 2nd ed., Fizmatgiz, Moscow, 1962 (in Russian). Transl.—P. Noordhoff, Groningen, 1963 (Translation of the 1st ed., Gostekhizdat, Moscow, 1946).
200. Muskhelishvili N. I., "Some Basic Problems of the Mathematical Theory of Elasticity; Fundamental Equations, Plane Theory of Elasticity, Torsion and Bending," 5th ed., Nauka, Moscow, 1966 (in Russian). Transl.— P. Noordhoff, Groningen, 1953 (Translation of the 3rd ed., Izd. Akad. Nauk SSSR, Moscow-Leningrad, 1949).
201. Natanzon V. Ya., On the Stresses in a Tensile Plate Weakened by Equal Holes Arranged in Checker Order, *Matem. Sbornik*, **42**(5), 617-636 (1935) (in Russian).
202. Neuber H., "Kerbspannungslehre. Grundlagen für genaue Spannungsrechnung," Springer-Verlag, Berlin, 1937.
203. Noble B., "Methods Based on the Wiener-Hopf Technique for the Solution of Partial Differential Equations," Pergamon Press, London, 1958.
204. Novikova I. V., A Standard Program for the Solution of Higher-order Systems of Linear Algebraic Equations by the Bordering Method, *Sb. Rabot Vychisl. Tsentra Mosk. Univ.*, Vyp. 4, 15 pp., 1965 (in Russian).
205. Novozhilov V. V., On a Necessary and Sufficient Criterion for Brittle Strength, *Prikl. Matem. i Mekhan.*, **33**(2), 212-222 (1969) (in Russian).
206. Novozhilov V. V., On the Foundations of the Theory of Equilibrium Cracks in Elastic Bodies, *Prikl. Matem. i Mekhan.*, **33**(5), 797-812 (1969) (in Russian).
207. Nowacki W., "Problems of Thermoelasticity," Izd. Akad. Nauk SSSR, Moscow, 1962 (in Russian) (Revised translation by the author of the Polish edition of "Zagadnienia termosprężystości," Państwowe Wydawn. Naukowe, Warszawa, 1960). Transl.— "Thermoelasticity," Pergamon Press, Oxford, 1962.
208. Ogibalov P. M., Kiiko I. A., "An Essay on the Mechanics of High Parameters," Izd. Mosk. Univ., Moscow, 1966 (in Russian).
209. Olesiak Z., Wnuk M., Plastic Energy Dissipation Due to a Penny-shaped Crack, *Rozpr. inż.*, **14**(3), 441-477 (1966) (in Polish); *Int. J. Fract. Mech.*, **4**(4), 383-396 (1968).
210. Oppel G. U., Hill P. W., Strain Measurements at the Root of Cracks and Notches, *Experim. Mech.*, **4**(7), 206-211 (1964).
211. Orowan E. O., Notch Brittleness and the Strength of Metals, *Trans. Inst. Eng. and Shipbuild. Scotland*, **89**, Part 3, 165-204, Part 4, 205-215 (1946).
212. Orowan E. O., Discussion. Session III—Effects Associated with Internal Stresses: (a) Effects on a Microscopic and Submicrosco-

pic Scale, in "Symposium on Internal Stresses in Metals and Alloys," The Institute of Metals, London, 1948, pp. 451-453.
213. Panasyuk V. V., Development of Cracks of Elliptical Shape in Plan, *Prikl. Mekhanika*, 6(1), 14-19 (1960) (in Ukrainian).
214. Panasyuk V. V., On the Theory of Crack Extension During the Deformation of a Brittle Body, *Doklady Akad. Nauk USSR*, No. 9, 1185-1189 (1960) (in Ukrainian).
215. Panasyuk V. V., On a Three-dimensional Problem in the Theory of Elasticity for an Isotropic Body with an Elliptical Crack, *Prikl. Mekhanika*, 8(3), 248-257 (1962) (in Ukrainian).
216. Panasyuk V. V., Lozovoi B. L., Determination of the Limiting Stresses in an Elastic Plane with Two Unequal Cracks Under Tension, in "Voprosy Mekhaniki Real'nogo Tverdogo Tela" (Problems in the Mechanics of Real Solids), Vyp. 1, Izd. Akad. Nauk USSR, Kiev, 1962, pp. 37-56 (in Russian).
217. Panasyuk V. V., Lozovoi B. L., Determination of the Limiting Load for a Strip with Two Unequal Cracks Under Bending, in "Voprosy Mekhaniki Real'nogo Tverdogo Tela" (Problems in the Mechanics of Real Solids), Vyp. 2, Naukova Dumka, Kiev, 1964, pp. 49-58 (in Russian).
218. Panasyuk V. V., "The Limiting Equilibrium of Cracked Brittle Bodies," Naukova Dumka, Kiev, 1968 (in Russian).
219. Paris P. C., A Note on the Variables Affecting the Rate of Crack Growth Due to Cyclic Loading, The Boeing Co., Document No. D-17867, Addendum N, 1957.
220. Paris P. C., The Fracture Mechanics Approach to Fatigue, in "Fatigue—Interdisciplinary Approach" (Proceedings of the Tenth Sagamore Army Materials Research Conference), Syracuse University Press, 1964, pp. 107-127.
221. Paris P. C., Sih, G. C., Stress Analysis of Cracks, in "Fracture Toughness Testing and Its Applications" (*ASTM Special Techn. Publ.*, No. 381), Amer. Society for Testing and Materials, Philadelphia, 1965, pp. 30-83.
222. Parton V. Z., On an Estimate of the Mutual Strengthening of Cracks Arranged in Checker Order, *Zh. Prikl. Mekhan. i Tekhn. Fiz.*, No. 5, 94-97 (1965) (in Russian).
223. Parton V. Z., Kudryavtsev B. A., A Dynamic Problem for a Plane with a Cut, *Doklady Akad. Nauk SSSR*, 185(3), 541-544 (1969) (in Russian).
224. Parton V. Z., Interaction Problems and Inertia Effects in Fracture Mechanics, *Probl. Prochnosti*, No. 1, 56-63 (1970) (in Russian).
225. Parton V. Z., Kudryavtsev B. A., A Contact Problem in the Mechanics of Deformation of Porous Viscoelastic Media, in "Problemy Mekhaniki Tverdogo Deformiruemogo Tela" (Problems in the Mechanics of Deformable Solids), Sudostroenie, Leningrad, 1970, pp. 329-339 (in Russian).
226. Parton V. Z., Kudryavtsev B. A., On a Procedure for Solving Crack and Punch Problems in the Couple-stress Theory of Elasticity, *Probl. Prochnosti*, No. 3, 78-81 (1971) (in Russian).

227. Parton V. Z., An Axially Symmetric Thermal Problem for a Space with a Penny-shaped Crack, *Prikl. Matem. i Mekhan.*, 36(1), 117-124 (1972) (in Russian).
228. Parton V. Z., The Plane Problem of Steady-state Vibrations for a Strip with a Cut, *Trudy Mosk. Inst. Khim. Mashinostr.*, 84-92 (1972) (in Russian).
229. Podstrigach Ya. S., Kit G. S., Determination of Temperature Fields and Stresses in the Vicinity of Heat-conducting Cracks, in "Teplovye Napryazheniya v Elementakh Konstruktsii" (Thermal Stresses in Structural Elements), Vyp. 7, Naukova Dumka, Kiev, 1967, pp. 194-201 (in Russian).
230. Polak L. S., "Variational Principles of Mechanics, Their Development and Application in Physics, "Fizmatgiz, Moscow, 1960 (in Russian).
231. Ponomarenko B. F., Samoilov V. I., Ulyakov P. I., Photoelastic Analysis of the Fracture of Transparent Dielectrics by Laser Radiation, *Zh. Eksperim. i Teor. Fiz.*, 54(3), 776-784 (1968) (in Russian).
232. Prigogine I., "Introduction to Thermodynamics of Irreversible Processes," Thomas, Springfield, 1955.
233. Przemieniecki J. S., "Theory of Matrix Structural Analysis," McGraw-Hill Book Co., New York, 1968.
234. Rabotnov Yu. N., Solid Mechanics and the Paths of Its Development, *Izv. Akad. Nauk SSSR. Otd. Tekhn. Nauk. Mekhan. i Mashinostr.*, No. 2, 3-10 (1962) (in Russian).
235. Rabotnov Yu. N., "Creep Problems in Structural Members," Nauka, Moscow, 1966 (in Russian). Transl.—North-Holland Publ. Co., Amsterdam, 1969.
236. Rabotnov Yu. N., A Model of an Elastic-plastic Medium with Delayed Yielding, *Zh. Prikl. Mekhan. i Tekhn. Fiz.*, No. 3, 45-54 (1968) (in Russian).
237. Rabotnov Yu. N., Suvorova Yu. V., The Dynamics of a Rigid-plastic Beam with Delayed Yielding, *Inzhenernyi Zh. Mekhan. Tverd. Tela*, No. 6, 78-86 (1968) (in Russian).
238. Remnev Yu. I., On the Effect of Radiation on Stresses and Small Strains in Solids, *Doklady Akad. Nauk SSSR*, 124(3), 540-541 (1959) (in Russian).
239. Rice J. R., An Examination of the Fracture Mechanics Energy Balance from the Point of View of Continuum Mechanics, in "Proceedings of the First International Conference on Fracture, Sendai, Japan," Vol. 1, 1965, p. 309.
240. Rice J. R., The Elastic-plastic Mechanics of Crack Extension, *Int. J. Fract. Mech.*, 4(1), 41-49 (1968).
241. Rice J. R., A Path Independent Integral and the Approximate Analysis of Strain Concentration by Notches and Cracks, *Trans. ASME. Ser. E*, 35(2), 379-386 (1968).
242. Romualdi J. P., Sanders P. H., Fracture Arrest by Riveted Stiffeners, in "Proceedings of the Fourth Midwestern Conference on Solid Mechanics," University Texas Press, 1959/1960, pp. 74-90.
243. Rosenfield A. R., Dai P. K., Hahn G. T., Crack Extension and Propagation Under Plane Stress, in "Proceedings of the First

International Conference on Fracture, Sendai, Japan," Vol. 1, 1965, pp. 223-258.
244. Rovinskii B. M., On the Occurrence of Stresses of the Second Kind During Plastic Deformation, *Zh. Tekhn. Fiz.*, 18(10), 1273-1281 (1948) (in Russian).
245. Rozovskii M. I., On Some Features of Elastic-hereditary Media, *Izv. Akad. Nauk SSSR. Otd. Tekhn. Nauk. Mekhan. i Mashinostr.*, No. 2, 30-36 (1961) (in Russian).
246. Sack R. A., Extension of Griffith's Theory of Rupture of Three Dimensions, *Proc. Phys. Soc.*, 58, Part 6, No. 330, 729-736 (1946).
247. Sadowsky M., Stress Concentration Caused by Multiple Punches and Cracks, *J. Appl. Mech.*, 23(1), 80-84 (1956).
248. Sapunov V. T., Morozov E. M., Analysis of the State of Stress in a Spherical Shell with a Crack, in "Prochnost' i Deformatsiya Materialov v Neravnomernykh Fizicheskikh Polyakh" (Strength and Deformation of Materials in Non-uniform Physical Fields), Vyp. 2, Atomizdat, Moscow, 1968, pp. 260-271 (in Russian).
249. Sedov L. I., Eglit M. E., Construction of Non-holonomic Models of Continuous Media Considering the Finiteness of Deformations and Some Physicochemical Effects, *Doklady Akad. Nauk SSSR*, 142(1), 54-57 (1962) (in Russian).
250. Sedov L. I., Models of Continuous Media with Internal Degrees of Freedom, *Prikl. Matem. i Mekhan.*, 32(5), 771-785 (1968) (in Russian).
251. Sedov L. I., "A Course in Continuum Mechanics," Vol. 2, Nauka, Moscow, 1970 (in Russian).
252. Sih G. C., Paris P. C., Erdogan F., Crack-tip, Stress-intensity Factors for Plane Extension and Plate Bending Problems, *Trans. ASME. Ser. E*, 29(2), 306-312 (1962).
253. Sih G. C., On the Singular Character of Thermal Stresses Near a Crack Tip, *Trans. ASME. Ser. E*, 29(3), 587-589 (1962).
254. Sih G. C., Loeber J. F., Wave Propagation in an Elastic Solid with a Line of Discontinuity or Finite Crack, *Quart. Appl. Math.*, 27(2), 193-213 (1969).
255. Sneddon I. N., The Distribution of Stress in the Neighbourhood of a Crack in an Elastic Solid, *Proc. Roy. Soc. London. Ser. A*, 187(1009), 229-260 (1946).
256. Sneddon I. N., "Fourier Transforms," McGraw-Hill Book Co., New York, 1951.
257. Sneddon I. N., Berry D. S., The Classical Theory of Elasticity, in "Encyclopedia of Physics, Vol. VI, Elasticity and Plasticity" (S. Flügge, ed.), Springer-Verlag, Berlin, 1958, pp. 1-126.
258. Sneddon I. N., Tait R. J., The Effect of a Penny-shaped Crack on the Distribution of Stress in a Long Circular Cylinder, *Int. J. Eng. Sci.*, 1(3), 391-409 (1963).
259. Sneddon I. N., Srivastav R. P., The Stress in the Vicinity of an Infinite Row of Collinear Cracks in an Elastic Body, *Proc. Roy. Soc. Edinburgh. Ser. A*, 67(1), 39-49 (1963-1965).
260. Sneddon I. N., Lowengrub M., "Crack Problems in the Classical Theory of Elasticity," Wiley, New York, 1969.

261. Sobolev N. D., Morozov E. M., Markochev V. M., Gol'tsev V. Yu., Sapunov V. T., Bobrinskii A. P., Experimental and Theoretical Study of the Fracture of Sheet Materials with Cracks, *Probl. Prochnosti*, No. 7, 45-49 (1972) (in Russian).
262. Sommerfeld A., "Vorlesungen über theoretische Physik, Bd. 4, Optik," Dieterich, Wiesbaden, 1950. Transl.—"Lectures on Theoretical Physics, Vol. 4, Optics," Acad. Press, New York, 1954.
263. Sorkin R. E., "Gas Thermodynamics of Solid Propellant Rocket Motors," Nauka, Moscow, 1967 (in Russian).
264. Srivastav R. P., Dual Series Relations. II, Dual Relations Involving Dini Series, *Proc. Roy. Soc. Edinburgh. Ser. A*, 66(3), 161-172 (1962-1963).
265. Srivastava K. N., Mahajan R. L., Thermal Stresses in a Solid Containing a Spherical Cavity and an External Crack, *Z. angew. Math. und Mech.*, 51(6), 433-444 (1971).
266. Sternberg E., Muki R., The Effect of Couple Stresses on the Stress Concentration Around a Crack, *Int. J. Solids and Struct.*, 3(1), 69-95 (1967).
267. Suvorova Yu. V., Delayed Yielding in Shells (a Survey of Experimental Results), *Zh. Prikl. Mekhan. i Tekhn. Fiz.*, No. 3, 55-62 (1968) (in Russian).
268. "Tables Relating to Mathieu Functions," Columbia University Press, New York, 1951.
269. Tetelman A. S., McEvily A. J., "Fracture of Structural Materials," Wiley, New York, 1967.
270. Timoshenko S., "History of Strength of Materials, with a Brief Account of the History of Theory of Elasticity and Theory of Structures," McGraw-Hill Book Co., New York, 1953.
271. Tiwari G. R., Effects of Couple-stresses on Stress Intensity Factor and Energy in Griffith Crack, *J. Indian Math. Soc.*, 34(1-2), 67-77 (1970).
272. Tordella J. P., Capillary Flow of Molten Polyethylene—A Photographic Study of Melt Fracture, *Trans. Soc. Rheol.*, 1, 203-212 (1957).
273. Tranter C. J., Dual Trigonometrical Series, *Proc. Glasgow Math. Assoc.*, 4, 49-57 (1959).
274. Tranter C. J., A Further Note on Dual Trigonometrical Series, *Proc. Glasgow Math. Assoc.*, 4, 198-200 (1960).
275. Turner M. J., Clough R. W., Martin H. C., Topp L. J., Stiffness and Deflection Analysis of Complex Structures, *J. Aeronaut. Sci.*, 23(9), 805-823 (1956).
276. Tusupov M. T., On the Solution of the Second Fundamental Problem of the Theory of Elasticity, *Trudy Inst. Matem. i Mekhan. Akad. Nauk KazSSR*, 1, 157-160 (1970) (in Russian).
277. Ustinov V. V., Temperature and Stress Fields in Fracture by Thermal Breakdown in Materials, *Inzh.-fiz. Zh.*, 5(10), 40-46 (1962) (in Russian).
278. Utku S., Explicit Expressions for Triangular Torus Element Stiffness Matrix, *AIAA Journal*, 6(6), 1174-1176 (1968).
279. Vainberg D. V., Gorodetskii A. S., Kirichevskii V. V., Sakharov A. S., The Finite Element Method in the Mechanics of Deformable Bodies, *Prikl. Mekhanika*, 8(8), 3-28 (1972) (in Russian).

280. Van Fo Fy G. A., Ozerov V. I., Viscoelastic Behaviour of Some Thermosetting Polymers, *Prikl. Mekhanika*, 1(8), 100-105 (1965) (in Russian).
281. Vikker I. V., Sobolev N. D., Schapov N. P., The Effect of Stress Concentration on the Yield Stress of Metals, *Zh. Tekhn. Fiz.*, 23(4), 613-618 (1953) (in Russian).
282. Vitvitskii P. M., Leonov M. Ya., Slip Bands in a Plate Under Non-uniform Deformation, in "Voprosy Mekhaniki Real'nogo Tverdogo Tela" (Problems in the Mechanics of Real Solids), Vyp. 1, Izd. Akad. Nauk USSR, Kiev, 1962, pp. 13-28 (in Russian).
283. Vladimirov V. S., "The Equations of Mathematical Physics," 2nd ed., Nauka, Moscow, 1971 (in Russian).
284. Volkova N. V., Likhachev V. A., Ryvkin S. M., Salmanov V. M., Stepanov M. I., Shestopalov L. M., Yaroshetskii I. D., On the Mechanism of Optical Destruction of Transparent Polymers, *Fiz. Tverd. Tela*, 9(7), 1868-1873 (1967) (in Russian).
285. Walsh P. F., The Computation of Stress Intensity Factors by a Special Finite Element Technique, *Int. J. Solids and Struct.*, 7(10), 1333-1342 (1971).
286. Watwood V. B., Jr., The Finite Element Method for Prediction of Crack Behavior, *Nuck. Eng. and Des.*, 11(2), 323-332 (1969).
287. Wells A. A., Unstable Crack Propagation in Metals: Cleavage and Fast Fracture, in "Proceedings of the Crack Propagation Symposium," Vol. I, College of Aeronautics and the Royal Aeronautical Society, Cranfield (England), 1961, pp. 210-230.
288. Wells A. A., Application of Fracture Mechanics at and beyond General Yielding, *Brit. Weld. J.*, 10(11), 563-570 (1963).
289. Westergaard H. M., Stresses at a Crack, Size of the Crack, and the Bending of Reinforced Concrete, *J. Amer. Concr. Inst.*, 5(2), Nov./Dec., 93-102 (1933).
290. Westergaard H. M., Bearing Pressures and Cracks, *J. Appl. Mech.*, 6(2), A-49 to A-53 (1939).
291. Whittaker E. T., Watson G. N., "A Course of Modern Analysis," 4th ed., Cambridge University Press, Cambridge, 1927.
292. Wilson E. L., Structural Analysis of Axisymmetric Solids, *AIAA Journal*, 3(12), 2269-2274 (1965).
293. Wilson W. K., Numerical Method for Determining Stress Intensity Factors of an Interior Crack in a Finite Plate, *Trans. ASME. Ser. D*, 93(4), 685-690 (1971).
294. Wnuk M. P., Criteria of Ductile Fracture Initiated by a Pressurized Penny-shaped Crack, *Trans. ASME. Ser. F*, 90(1), 56-64 (1968).
295. Wnuk M. P., The Nature of Fracture in Relation to the Total Potential Energy, *J. Phys. D: Appl. Phys.*, 1(2), 217-236 (1968).
296. Wnuk M. P., Energy Criterion for Initiation and Spread of Fracture in Viscoelastic Solids, South Dakota State University, Brookings, Engineering Experiment Station, Bulletin 7, April 1968.
297. Wnuk M. P., Effects of Time and Plasticity on Fracture, *J. Phys. D: Appl. Phys.*, 2(9), 1245-1259 (1969).

298. Wnuk M. P., Knauss W. G., Delayed Fracture in Viscoelastic-plastic Solids, Intern. J. Solids and Structures, v. 6, No. 7, 1970.
299. Wnuk M. P., Prior-to-failure Extension of Flaws Under Monotonic and Pulsating Loadings, Annual Progress Report Prepared for NASA at the South Dakota State University, NGR 42-003-006, May 1971; also *Eng. Fract. Mech.*, 5(2), 379-396 (1973).
300. Wnuk M. P., Sih G. C., Slow and Fast Motion of Cracks in Inelastic Solids, Annual Progress Report Prepared for NASA at the South Dakota State University, NGR 42-003-006, August 1972.
301. Yarema S. Ya., Investigation of Plasticity Bands in Plates with Stress Raisers Under Tension, in "Voprosy Mekhaniki Real'nogo Tverdogo Tela" (Problems in the Mechanics of Real Solids), Vyp. 2, Naukova Dumka, Kiev, 1964, pp. 177-190 (in Russian).
302. Yarema S. Ya., Savruk M. P., The State of Stress in a Shallow Shell with a Crack Under Symmetric Loading, *Doklady Akad. Nauk USSR. Ser. A*, No. 1, 55-58 (1969) (in Russian).
303. Zhuravlev A. G., On the Determination of the State of Stress and Strain in Light Metals Under Neutron Irradiation, *Vestnik Mosk. Univ. Matem., Mekhan.*, No. 6, 54-58 (1961) (in Russian).
304. Zhuravskii A. M., "Handbook of Elliptic Functions," Izd. Akad. Nauk SSSR, Moscow-Leningrad, 1941 (in Russian).
305. Zienkiewicz O. C., Cheung Y. K., "The Finite Element Method in Structural and Continuum Mechanics," McGraw-Hill Book Co., London, 1967.

TO THE READER

Mir Publishers welcome your comments on the content, translation and design of this book.

We would also be pleased to receive any proposals you care to make about our future publications.

Our address is:
USSR, 129820, Moscow I-110, GSP
Pervy Rizhsky Pereulok, 2
Mir Publishers

Printed in the Union of Soviet Socialist Republics

OTHER BOOKS FOR YOUR LIBRARY

MACHINE DESIGN

D. RESHETOV, D.Sc.

This book has been written to provide an up-to-date textbook from which to teach the fundamentals of machine design. The material has been arranged for the especial convenience of the instructor and the student.

Contents. General Considerations. History. Basic Criteria of the Working Capacity and Design and Machine Parts. Engineering Materials. Producibility of Machine Parts. Fits and Tolerances. Design Procedure. Joints. Riveted Joints. Welded Joints. Interference Fit Joints. Screw Joints. Cutter and Pin Joints Key, Spline and Shaped Joints. Drives. Friction Drives. Belt Drives. Toothed Gearing. Wormed Gearing. Chained Drives. Power Screws. Shafts and Axles. Sleeve Bearings. Ball and Roller Bearings. Lubricating Devices. Couplings and Clutches. Coil and Leaf Springs. Beds, Baseplates and Housings. Linear Bearings.

MECHANICS

S. STRELKOV, D.Sc.

This general course of mechanics by late professor S. Strelkov is meant for students of physical and mathematical departments of universities and pedagogical colleges. It is based on the material of the seminars and lectures given by the author for many years at the physical department of the Lomonosov State University of Moscow.

Contents. The book covers the traditional branches of mechanics (kinematics of particle, fundamentals of particle dynamics, motion of a rigid body, mechanics of deformable body, fluid and gas dynamics, oscillations and waves) and also treats of some modern topics such as space-craft flight, motion with supersonic velocity and elements of special relativity theory.

THE THEORY OF FUNCTIONS OF A COMPLEX VARIABLE

A. SVESHNIKOV, D.Sc. and A. TIKHONOV,
Mem. USSR Acad. sci.

This textbook is intended for students of physicomathematical departments of colleges and universities; can be used as a reference book by post-graduate students and research workers.

Contents. The Complex Variable and Functions of a Complex Variable. Series of Analytic Functions. Analytic Continuation. Elementary Functions of a Complex Variable. The Laurent Series and Isolated Singular Points. Conformal Mapping. Analytic Functions in the Solution of Boundary-Value Problems. Fundamentals of Operational Calculus. Saddle-Point Method. The Wiener-Hopf Method· Bibliography. Name Index. Subject Index.